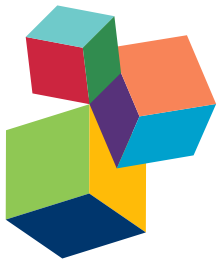


# INTERACTION OF NANOMATERIALS WITH THE IMMUNE SYSTEM: ROLE IN NANOSAFETY AND NANOMEDICINE

EDITED BY: Paola Italiani, Diana Boraschi, Lucio R. C. Castellano,

Paulo Bonan and Eliton S. Medeiros

PUBLISHED IN: Frontiers in Immunology



# frontiers

## **Frontiers Copyright Statement**

© Copyright 2007-2018 Frontiers Media SA. All rights reserved.

All content included on this site, such as text, graphics, logos, button icons, images, video/audio clips, downloads, data compilations and software, is the property of or is licensed to Frontiers Media SA ("Frontiers") or its licensees and/or subcontractors. The copyright in the text of individual articles is the property of their respective authors, subject to a license granted to Frontiers.

The compilation of articles constituting this e-book, wherever published, as well as the compilation of all other content on this site, is the exclusive property of Frontiers. For the conditions for downloading and copying of e-books from Frontiers' website, please see the Terms for Website Use. If purchasing Frontiers e-books from other websites or sources, the conditions of the website concerned apply.

Images and graphics not forming part of user-contributed materials may not be downloaded or copied without permission.

Individual articles may be downloaded and reproduced in accordance with the principles of the CC-BY licence subject to any copyright or other notices. They may not be re-sold as an e-book.

As author or other contributor you grant a CC-BY licence to others to reproduce your articles, including any graphics and third-party materials supplied by you, in accordance with the Conditions for Website Use and subject to any copyright notices which you include in connection with your articles and materials.

All copyright, and all rights therein, are protected by national and international copyright laws.

The above represents a summary only. For the full conditions see the Conditions for Authors and the Conditions for Website Use.

**ISSN 1664-8714**

**ISBN 978-2-88945-387-0**

**DOI 10.3389/978-2-88945-387-0**

## **About Frontiers**

Frontiers is more than just an open-access publisher of scholarly articles: it is a pioneering approach to the world of academia, radically improving the way scholarly research is managed. The grand vision of Frontiers is a world where all people have an equal opportunity to seek, share and generate knowledge. Frontiers provides immediate and permanent online open access to all its publications, but this alone is not enough to realize our grand goals.

## **Frontiers Journal Series**

The Frontiers Journal Series is a multi-tier and interdisciplinary set of open-access, online journals, promising a paradigm shift from the current review, selection and dissemination processes in academic publishing. All Frontiers journals are driven by researchers for researchers; therefore, they constitute a service to the scholarly community. At the same time, the Frontiers Journal Series operates on a revolutionary invention, the tiered publishing system, initially addressing specific communities of scholars, and gradually climbing up to broader public understanding, thus serving the interests of the lay society, too.

## **Dedication to quality**

Each Frontiers article is a landmark of the highest quality, thanks to genuinely collaborative interactions between authors and review editors, who include some of the world's best academicians. Research must be certified by peers before entering a stream of knowledge that may eventually reach the public - and shape society; therefore, Frontiers only applies the most rigorous and unbiased reviews.

Frontiers revolutionizes research publishing by freely delivering the most outstanding research, evaluated with no bias from both the academic and social point of view.

By applying the most advanced information technologies, Frontiers is catapulting scholarly publishing into a new generation.

## **What are Frontiers Research Topics?**

Frontiers Research Topics are very popular trademarks of the Frontiers Journals Series: they are collections of at least ten articles, all centered on a particular subject. With their unique mix of varied contributions from Original Research to Review Articles, Frontiers Research Topics unify the most influential researchers, the latest key findings and historical advances in a hot research area! Find out more on how to host your own Frontiers Research Topic or contribute to one as an author by contacting the Frontiers Editorial Office: [researchtopics@frontiersin.org](mailto:researchtopics@frontiersin.org)

# INTERACTION OF NANOMATERIALS WITH THE IMMUNE SYSTEM: ROLE IN NANOSAFETY AND NANOMEDICINE

Topic Editors:

**Paola Italiani**, Institute of Protein Biochemistry, National Research Council, Italy

**Diana Boraschi**, Institute of Protein Biochemistry, National Research Council, Italy

**Lucio R. C. Castellano**, Federal University of Paraíba, Brazil

**Paulo Bonan**, Federal University of Paraíba, Brazil

**Eliton S. Medeiros**, Federal University of Paraíba, Brazil



Engineered nanoparticles can greatly differ in chemical composition, size, and surface coating/charge, and these characteristics determine their interaction with immune cells. Image: Vasilij Kandinskij, "Several circles" 1926, Solomon R. Guggenheim Museum.

The immune system has the double role of maintaining tissue integrity and homeostasis and of protecting the organism from possible dangers, from invading pathogens to environmentally-borne dangerous chemicals. New chemicals recognisable by the immune system are engineered nanomaterials/nanoparticles, new agents in our environment that are becoming common due to their presence in many products, from constructions and building material (e.g., solar cells, pigments and paints, tiles and masonry materials) to daily products (e.g., food packaging, cosmetics, and cigarettes). Human beings can be accidentally exposed to engineered nanomaterials when these are released from products containing them or during production in workplaces. Furthermore, intentional exposure occurs in medicine, as engineered nanoparticles are used as tools for improving delivery of drugs and vaccines, vaccine adjuvants and contrast agents in therapeutic, preventive and diagnostic strategies.

Nanoparticles that come in contact with the immune system after unintentional exposure need to be eliminated from the organism as they represent a potential threat. In this case, however, due to their peculiar characteristics of size, shape, surface charge and persistence, nanoparticles may elicit undesirable reactions and have detrimental effects on the immune system, such as cytotoxicity, inflammation, anaphylaxis, immunosuppression. Conversely, nanomedicines need to escape immune recognition/elimination and must persist in the organism long enough for

reaching their target and exerting their beneficial effects. Immune cells and molecules at the body surface (airway and digestive mucosae, skin) are the first that come in contact with nanomaterials upon accidental exposure, while immune effectors in blood are those that more easily come in contact with nanomedical products. Thus, evaluating the interaction of the immune system with nanoparticles/nanomaterials is a topic of key importance both in nanotoxicology and in nanomedicine.

Immuno-nanosafety studies consider both accidental exposure to nanoparticles, which may occur by skin contact, ingestion or inhalation (at doses and with a frequency that are not known), and medical exposure, which takes place with a defined administration schedule (route, dose, frequency). Many studies focus on the interaction between the immune system and nanoparticles that, for medical purposes, have been specifically modified to stimulate immunity or to avoid immune recognition, as in the case of vaccine carriers/adjuvants or drug delivery systems, respectively.

The aims of this Research Topic is to provide an overview of recent strategies:

1. for assessing the immunosafety of engineered nanomaterials/nanoparticles, in particular in terms of activation of inflammatory responses, such as complement activation and allergic reactions, based on the nanomaterial intrinsic characteristics and on the possible carry-over of bioactive contaminants such as LPS. Production of new nanoparticles taking into account their effects on immune responses, in order to avoid undesirable effects on one hand, and to design particles with desirable effects for medical applications on the other hand;
2. for designing more effective nanomedicines by either avoiding or exploiting their interaction with the immune systems, with particular focus on cancer diagnosis and therapy, and vaccination.

This collection of articles gives a comprehensive view of the state-of-the-art of the interaction of nanoparticles with the immune system from the two perspectives of safety and medical use, and aims at providing immunologists with the relevant knowledge for designing improved strategies for immunologically safe nanomaterial applications.

**Citation:** Italiani, P., Boraschi, D., Castellano, L. R. C., Bonan, P., Medeiros, E. S., eds. (2018). Interaction of Nanomaterials with the Immune System: Role in Nanosafety and Nanomedicine. Lausanne: Frontiers Media. doi: 10.3389/978-2-88945-387-0

# Table of Contents

- 06 Editorial: Interaction of Nanomaterials with the Immune System: Role in Nanosafety and Nanomedicine**  
Diana Boraschi, Lucio R. C. Castellano and Paola Italiani
- Section 1: Interaction of Nanomaterials with the Immune System:  
Safety Aspects**
- 08 Why the Immune System Should Be Concerned by Nanomaterials?**  
Marc J. Pallardy, Isabelle Turbica and Armelle Biola-Vidamment
- 14 Graphene and the Immune System: A Romance of Many Dimensions**  
Sourav P. Mukherjee, Massimo Bottini and Bengt Fadeel
- 25 Intrinsic and Extrinsic Properties Affecting Innate Immune Responses to Nanoparticles: The Case of Cerium Oxide**  
Eudald Casals, Muriel F. Gusta, Jordi Piella, Gregori Casals, Wladimiro Jiménez and Victor Puntes
- 32 Endotoxin Contamination in Nanomaterials Leads to the Misinterpretation of Immunosafety Results**  
Yang Li, Mayumi Fujita and Diana Boraschi
- 39 Lipopolysaccharide Adsorbed to the Bio-Corona of  $TiO_2$  Nanoparticles Powerfully Activates Selected Pro-inflammatory Transduction Pathways**  
Massimiliano G. Bianchi, Manfredi Allegri, Martina Chiu, Anna L. Costa, Magda Blosi, Simona Ortelli, Ovidio Bussolati and Enrico Bergamaschi
- 51 In Vitro and In Vivo Differences in Murine Third Complement Component (C3) Opsonization and Macrophage/Leukocyte Responses to Antibody-Functionalized Iron Oxide Nanoworms**  
Guankui Wang, James I. Griffin, Swetha Inturi, Barbara Brenneman, Nirmal K. Banda, V. Michael Holers, Seyed Moein Moghimi and Dmitri Simberg
- 60 Activation of Human Complement System by Dextran-Coated Iron Oxide Nanoparticles Is Not Affected by Dextran/Fe Ratio, Hydroxyl Modifications, and Crosslinking**  
Guankui Wang, Fangfang Chen, Nirmal K. Banda, V. Michael Holers, LinPing Wu, S. Moein Moghimi and Dmitri Simberg
- 68 Allergic Responses Induced by the Immunomodulatory Effects of Nanomaterials upon Skin Exposure**  
Yasuo Yoshioka, Etsushi Kuroda, Toshiro Hirai, Yasuo Tsutsumi and Ken J. Ishii

- 79 Nanomaterials in the Context of Type 2 Immune Responses—Fears and Potentials**  
Martin Himly, Robert Mills-Goodlet, Mark Geppert and Albert Duschl
- 91 Nanoparticle Interactions with the Immune System: Clinical Implications for Liposome-Based Cancer Chemotherapy**  
Ninh M. La-Beck and Alberto A. Gabizon
- Section 2: Exploiting the Interaction of Nanomaterials with the Immune System**
- 97 Advanced Strategies in Immune Modulation of Cancer Using Lipid-Based Nanoparticles**  
Shoshy Mizrahy, Inbal Hazan-Halevy, Dalit Landesman-Milo, Brandon D. Ng and Dan Peer
- 104 Nanoparticle-Based Magnetic Resonance Imaging on Tumor-Associated Macrophages and Inflammation**  
Natalie J. Serkova
- 111 Macrophage Polarization Contributes to the Anti-Tumoral Efficacy of Mesoporous Nanovectors Loaded with Albumin-Bound Paclitaxel**  
Fransisca Leonard, Louis T. Curtis, Matthew James Ware, Taraz Nosrat, Xuewu Liu, Kenji Yokoi, Hermann B. Frieboes and Biana Godin
- 125 Ameliorating Amyloid- $\beta$  Fibrils Triggered Inflammation via Curcumin-Loaded Polymeric Nanoconstructs**  
Andrea Ameruoso, Roberto Palomba, Anna Lisa Palange, Antonio Cervadoro, Aeju Lee, Daniele Di Mascolo and Paolo Decuzzi
- 136 Role of Metallic Nanoparticles in Vaccinology: Implications for Infectious Disease Vaccine Development**  
Lázaro Moreira Marques Neto, André Kipnis and Ana Paula Junqueira-Kipnis
- 146 Co-delivery of Dual Toll-Like Receptor Agonists and Antigen in Poly(Lactic-Co-Glycolic) Acid/Polyethylenimine Cationic Hybrid Nanoparticles Promote Efficient In Vivo Immune Responses**  
Mahboubeh Ebrahimian, Maryam Hashemi, Mohsen Maleki, Gholamreza Hashemitabar, Khalil Abnous, Mohammad Ramezani and Alireza Haghparast
- 158 Human Scavenger Receptor A1-Mediated Inflammatory Response to Silica Particle Exposure Is Size Specific**  
Nobuo Nishijima, Toshiro Hirai, Kazuki Misato, Michihiko Aoyama, Etsushi Kuroda, Ken J. Ishii, Kazuma Higashisaka, Yasuo Yoshioka and Yasuo Tsutsumi
- 170 Induction of Innate Immune Memory by Engineered Nanoparticles: A Hypothesis That May Become True**  
Paola Italiani and Diana Boraschi



# Editorial: Interaction of Nanomaterials with the Immune System: Role in Nanosafety and Nanomedicine

Diana Boraschi<sup>1\*</sup>, Lucio R. C. Castellano<sup>2</sup> and Paola Italiani<sup>1</sup>

<sup>1</sup> Institute of Protein Biochemistry, National Research Council, Napoli, Italy, <sup>2</sup> Federal University of Paraíba, João Pessoa, Brazil

**Keywords:** nanoparticles, immune system, innate immunity, inflammation, nanomedicine, nanovaccination

## Editorial on the Research Topic

### Interaction of Nanomaterials with the Immune System: Role in Nanosafety and Nanomedicine

In the past 20 years, engineered nanomaterials/nanoparticles (ENMs/ENPs) have become an increasingly common presence in our environment and everyday life. These new materials are included in a variety of products, such as solar cells, pigments and paints, tiles and masonry materials, and consumer products such as food packaging, cosmetics, and cigarettes. The long-term effects of exposure of human beings and environment to ENM are unknown, and concern is raising that ENM may have a detrimental impact on human health. In this perspective, it is of major importance assessing the interaction between ENM and the immune system, since in all living organisms the immune system is deputed to defending and maintaining the integrity of the body, and its failure is cause of damage and disease (1).

Engineered nanoparticles are being developed also for improving delivery of drugs, contrast agents, and antigens in therapeutic, diagnostic, and vaccination strategies. Such strategies aim at exploiting the unprecedented flexibility of design of ENP for tailoring them as efficient vehicles for delivering payloads to specific organs and locations, thereby increasing efficacy and minimizing side effects. Also in the case of nanomedicines, the interaction between the ENP and the host's immune system is central, because nanomedicines need to avoid immune recognition and elimination. On the other hand, ENP can be used for targeting the immune system and stimulating its effectiveness in combating infections, cancer, and other diseases (1).

The Research Topic "Interaction of nanoparticles with the immune system: role in nanosafety and nanomedicine" intends to provide a snapshot of the latest trends in nanosafety and nanomedicine that take into consideration the interaction between ENM and the immune system.

Living organisms have encountered particles of different size since the very beginning of life on earth, thus the immune system of plants, invertebrates, and vertebrates is able to recognize particles (e.g., volcano ashes, viruses, and bacteria) and react to them by mounting a defensive response. ENM and ENP are new foreign agents for the immune system of both environmental species and human beings. Although we do not expect the immune system to have problems in dealing with ENM, similarly to other particles, nanoimmunosafety is becoming a matter of growing concern. In fact, ENM are produced in such a variety of chemical compositions, shapes, and sizes that predicting their interaction with immunity and the result of such interaction is very difficult. The review by Pallardy et al. specifically addresses this issue, underlying how and in which circumstances ENM and other nanoparticles can trigger immune responses that may represent a threat for human health. Other contributions address the interaction of specific ENM with the immune system. The group of Bengt Fadeel has examined graphene ENM and the mechanisms by which the innate immune system, in particular phagocytic cells, work for eliminating them (Mukherjee et al.). On the other

## OPEN ACCESS

### Edited and Reviewed by:

Pietro Ghezzi,  
Brighton and Sussex Medical School, United Kingdom

### \*Correspondence:

Diana Boraschi  
*d.boraschi@ibp.cnr.it*

### Specialty section:

This article was submitted  
to Inflammation,  
a section of the journal  
*Frontiers in Immunology*

**Received:** 13 November 2017

**Accepted:** 16 November 2017

**Published:** 28 November 2017

### Citation:

Boraschi D, Castellano LRC and Italiani P (2017) Editorial: Interaction of Nanomaterials with the Immune System: Role in Nanosafety and Nanomedicine. *Front. Immunol.* 8:1688.  
doi: 10.3389/fimmu.2017.01688

hand, the review of the group of Victor Puntes underlines the need of a very accurate evaluation of the ENM characteristics in order to understand the variability of the effects on the immune system and the consequent possible safety concerns, taking as an example the case of cerium oxide ENP (Casals et al.). On the same line, two groups address more specifically the issue of endotoxin contamination in ENM as source of variability and misinterpretation of results: Li et al. review the topic and provide suggestions of how to test the presence of contamination, while Bianchi et al. show how titania ENP can adsorb LPS thereby becoming able to induce inflammation. A major issue in nanosafety is the capacity of ENM to activate complement and induce complement-mediated damage. Two contributions of the group of Dmitri Simberg and Moein Moghimi show how surface coating and surface functionalization with antibodies can significantly change the ability of iron oxide nanoworms to activate complement (Wang et al.; Wang et al.). Eventually, the group of Ken Ishii reviews the possibility of allergic reactions induced by skin exposure to EMN (Yoshioka et al.), while the group of Albert Duschl examines the role of ENM in type 2 immune responses and, together with the possible detrimental effects, proposes possible exploitation for therapeutic purposes (Himly et al.).

In nanomedicine, in order to deliver their therapeutic cargo, ENMs are designed so as to escape immune recognition and to penetrate defensive barriers, a strategy that increases targeted delivery and therapeutic efficacy. However, we should take great care in ensuring that nanomedicines do not interfere with immune surveillance and effectiveness, because a failing immune system will leave the body defenseless. On the other hand, nano-medical approaches can exploit the interaction of ENM with the immune system to obtain targeted delivery and targeted immune modulation. The review of La-Beck and Gabizon addresses the critical issue of efficacy of liposome-based anti-cancer therapies, which is most likely hampered by the interaction of administered liposomes with the host immune system. The group of Dan Peer provides important insights on the possibility of using lipid-based ENP, targeting the immune system, as immunotherapeutic agents that stimulate the host immune response against tumors (Mizrahy et al.). Along the very important strategy of targeting immune cells with ENM, Serkova shows how tumor-associated macrophages (TAM) can be specifically visualized with MRI using superparamagnetic iron oxide ENP, while the group of Biana Godin shows that drug-loaded ENP can actually modulate TAM polarization and shift it toward antitumor activation (Leonard et al.). Besides anti-cancer therapy, the use of ENM can be beneficial in other inflammation-based diseases such as neurodegenerative conditions, as suggested by the group of

Paolo Decuzzi that shows decrease of amyloid  $\beta$  fibril-induced inflammation by delivering anti-inflammatory compounds to macrophages via ENP (Ameruoso et al.).

The last topic addressed is the use of ENM in vaccination. Indeed, particles have been included in vaccine formulations since ages, for increasing antigen persistence and for helping inducing and amplifying the protective adaptive immunity, but more recent studies plan to use ENM for a better control both of the antigen delivery and of the inflammation-based adjuvant effect (2). The group of Ana Paula Junquiera-Kipnis reviews the possibility of using metal ENP as adjuvants in vaccination (Moreira Marques Neto et al.), while the group of Alireza Haghparast designed polymeric ENP simultaneously carrying an antigen and two TLR agonists, which were very effective as vaccine in mice (Ebrahimian et al.). A very important issue, in designing ENP for inducing controlled NLRP3-dependent inflammation in vaccine adjuvanticity, is the issue addressed by the group of Yasuo Tsutsumi, i.e., that the control of ENP size is required in order to obtain the desired effect, as particles of the “wrong” size can lose their efficacy (Nishijima et al.). Finally, Italiani and Boraschi propose an original concept for the modulating immune responses with ENM, i.e., the personalized induction of innate memory, which in each individual subject can achieve controlled stimulation (as adjuvant in vaccination and in cancer therapy), or reduction of responses (for approaches in chronic inflammatory and autoimmune diseases).

In conclusion, this Research Topic provides a comprehensive vision of the state-of-the-art of the interaction of ENM with the immune system, its possible threats for human health and the very promising exploitation strategies. Numerous challenges are still outstanding, before we have a complete knowledge of such interaction, in particular in immunologically frail or compromised individuals, but the recent advancements make us believe that we will be soon able to use ENM effectively and safely.

## AUTHOR CONTRIBUTIONS

DB and PI wrote the manuscript. LRCC assisted them.

## FUNDING

This work was supported by the EU Commission project PANDORA (H2020 grant n. 671881), the Italian Ministry of Education, University and Research (MIUR) Cluster project Medintech (CTN01\_00177\_96), and the MIUR-CNR Flagship project InterOmics.

**Conflict of Interest Statement:** The authors declare that they have no financial or non-financial competing interests.

Copyright © 2017 Boraschi, Castellano and Italiani. This is an open-access article distributed under the terms of the Creative Commons Attribution License (CC BY). The use, distribution or reproduction in other forums is permitted, provided the original author(s) or licensor are credited and that the original publication in this journal is cited, in accordance with accepted academic practice. No use, distribution or reproduction is permitted which does not comply with these terms.

## REFERENCES

1. Boraschi D, Italiani P, Palomba R, Decuzzi P, Duschl A, Fadelle B, et al. Nanoparticles and innate immunity: new perspectives on host defence. *Semin Immunol* (2017). doi:10.1016/j.smim.2017.08.013
2. Kuroda E, Coban C, Ishii KJ. Particulate adjuvant and innate immunity: past achievements, present findings, and future prospects. *Int Rev Immunol* (2013) 32:209–20. doi:10.3109/08830185.2013.773326



# Why the Immune System Should Be Concerned by Nanomaterials?

**Marc J. Pallardy\***, **Isabelle Turbica** and **Armelle Biola-Vidamment**

*"Inflammation, Chimiokines and Immunopathology", INSERM UMR 996, Univ Paris-Sud, Université Paris-Saclay, Châtenay-Malabry, France*

Particles possess huge specific surface area and therefore nanomaterials exhibit unique characteristics, such as special physical properties and chemical hyper-reactivity, which make them particularly attractive but also raise numerous questions concerning their safety. Interactions of nanomaterials with the immune system can potentially lead to immunosuppression, hypersensitivity (allergy), immunogenicity and autoimmunity, involving both innate and adaptive immune responses. Inherent physical and chemical NP characteristics may influence their immunotoxicity, i.e., the adverse effects that can result from exposure. This review will focus on the possible interaction of nanomaterials including protein aggregates with the innate immune system with specific emphasis on antigen-presenting cells, i.e., dendritic cells, macrophages and monocytes.

## OPEN ACCESS

### Edited by:

Diana Boraschi,  
Consiglio Nazionale Delle Ricerche  
(CNR), Italy

### Reviewed by:

Francesca Granucci,  
University of Milano-Bicocca, Italy  
Giorgia Fantuzzi,  
University of Illinois at Chicago, USA

### \*Correspondence:

Marc J. Pallardy  
marc.pallardy@u-psud.fr

### Specialty section:

This article was submitted  
to Inflammation,  
a section of the journal  
*Frontiers in Immunology*

**Received:** 29 March 2017

**Accepted:** 24 April 2017

**Published:** 15 May 2017

### Citation:

Pallardy MJ, Turbica I and Biola-Vidamment A (2017) Why the Immune System Should Be Concerned by Nanomaterials? *Front. Immunol.* 8:544.  
doi: 10.3389/fimmu.2017.00544

## INTRODUCTION

Nanoparticles (NP) are defined as structures with at least one dimension in the range of 1–100 nm. At this nanoscale, particles possess huge specific surface area. Nanomaterials therefore exhibit unique characteristics, such as special physical properties and chemical hyper-reactivity, which make them particularly attractive but also raise numerous questions concerning their safety. Nanomaterial interactions with the body include accidental exposure (environmental and industrial NP) and therapeutic exposure (vaccination, drug delivery). Virtually, all the possible routes of exposure (inhalation, ingestion, dermal contact, systemic injection) have to be considered.

The main objective of the immune system is to avoid harmful effects due to contamination by microbes and also to maintain an immune tolerance to environmental antigens. To distinguish between harmful and non-harmful antigens, the dendritic cells (DCs) play a major role by sensing the environment and adapting their phenotype to the most appropriate type of response: immunogenic vs. tolerogenic. Interactions of NP with the immune system can potentially lead to immunosuppression, hypersensitivity (allergy), immunogenicity and autoimmunity, involving both innate and adaptive immune responses. Inherent physical and chemical NP characteristics may influence their immunotoxicity, i.e., the adverse effects that can result from exposure. This review will focus on the possible interaction of nanomaterials, including protein aggregates, with the innate immune system with specific emphasis on antigen-presenting cells, i.e., DCs, macrophages and monocytes.

## NP INTERACTION WITH INNATE IMMUNE CELLS

In host, the mononuclear phagocytic system plays a major role in the exposure to nanomaterials. Macrophages are in charge of nanomaterials recognition, uptake, processing, and clearance (1). Several *in vivo* studies have demonstrated high NPs macrophage sequestration, particularly

in clearance organs such as liver, spleen, and kidney. In these organs, fenestrated capillary beds, competent to capture particles, are associated with specialized macrophages populations (1). In mice injected with non-degradable silica NPs, a high accumulation in the liver and in the spleen was observed, in majority in the macrophages but also in neutrophils (2). This property could be responsible for organ-specific toxicity, especially in the liver, of some NPs.

Nanoparticles uptake can occur through phagocytosis, macropinocytosis, as well as clathrin-, caveolae-, and scavenger receptor-mediated endocytic pathways. These internalization processes are deeply dependent on nanomaterials properties such as size, shape, surface coating, and on the cellular environment (3). Phagocytosis is carried out by professional phagocytes such as macrophages, neutrophils, DCs, or monocytes. Due to their actin-based cytoskeleton rearrangement capacities, these cells can entrap the material through membrane dynamics in a zipper model fashion (1). The best characterized opsonin-dependent phagocytosis receptors are the Fc $\gamma$  receptor and the complement receptor CR3, which appear to play a significant role in the detection of opsonized nanomaterials and in the rate of uptake (1). It was demonstrated that the small gold colloid NPs (30 nm) use several internalization routes (including scavenger receptor-, clathrin-, and caveolin-mediated pathways), in contrast to the larger materials of 150 nm which appear to be preferentially taken up via the scavenger receptor pathway (4). The scavenger receptor MARCO has been involved in the ingestion of unopsonized inhaled TiO<sub>2</sub> and Fe<sub>2</sub>O<sub>3</sub> particles in the lung (5). Moreover, the recognition of silica NPs by macrophages scavenger A receptor could induce the release of cytokines responsible for pulmonary inflammation (6). The mechanisms for NP uptake by DCs are poorly understood. However, according to Vallhov et al. (7), an active mechanism such as endocytosis may be involved in the amorphous silica nanoparticle (aSNP) uptake by DCs (7). Winter et al. (8) additionally suggested that it would be at least partly mediated by an actin-dependent mechanism (8).

Nanomaterials can affect the polarization and the reprogramming of macrophages, mostly depending on chemical composition, size, and surface modification (9). The pro-inflammatory M1 or anti-inflammatory M2 phenotypes have been shown to display distinct uptake capacity for nanomaterials. In particular, silica NPs uptake is enhanced in M2-polarized primary human monocyte-derived macrophages or in the macrophage-like THP-1 cell line as compared with M1 cells (10).

*In vivo*, upon exposure to biological fluids, NPs do not stay “naked” but become coated by biomolecules, primarily proteins but also sugars, lipids, or nucleic acids, forming a “corona” (11). This corona is “what the cell sees” and displays a highly dynamic nature: changes in the composition occur over time, in a continuous flux of desorption/adsorption of proteins. If the “hard” corona is tightly bound with a long exchange time, the “soft” corona, presented as a second layer, is submitted to fast exchanges (12, 13). Interestingly, this process could be compared to the opsonization of pathogens (14) and affects the efficiency of NPs uptake by macrophages. Kapralov et al. demonstrated that single-walled carbon nanotubes (SWCNTs) selectively adsorbed phosphatidylcholines and phosphatidylglycerols from lung surfactant. The

presence of this coating noticeably enhanced the *in vitro* uptake of SWCNTs by macrophages (15). Moreover, proteins may undergo conformational changes, such as unfolding, leading to the possible exposition of cryptic epitopes recognized by immune cells (14). This unfolding was demonstrated with fibrinogen coated on negatively charged poly(acrylic acid) gold NPs, leading to MAC-1 receptor activation and pro-inflammatory cytokines secretion through NF-κB signaling (16). Interestingly, only the negatively charged NPs induced TNF-α and IL-8 release by THP-1 cells, whereas both positively and negatively charged particles could bind fibrinogen with high affinity (17). This protein corona is essential for scavenger receptor-efficient internalization of synthetic-layered silicate NPs by THP-1 cells (18). When bound to these NPs, albumin undergoes unfolding, comparable to heat denaturation, revealing a cryptic sequence allowing recognition of serum albumin by this family of receptors and nanomaterial recognition by macrophages (18).

## DCs AND NANOMATERIALS AS EXOGENOUS DANGER SIGNALS

Dendritic cells are professional antigen-presenting cells that bridge the innate and adaptive immune response. Immature DCs reside in non-lymphoid tissues in an antigen-capturing state. In the presence of various stimuli, such as allergens, inflammation, pro-inflammatory cytokines, bacterial products, or diverse danger signals, DCs undergo a maturation process. This process results in antigen-processing and upregulation of major histocompatibility complex (MHC), co-stimulatory molecules, chemokine, and cytokine receptors, and production of cytokines and chemokines. Mature DCs then migrate to regional lymph nodes and activate naïve T-lymphocytes. Consequently, NP impact on these cells raises growing concerns.

The size of the NP may determine the modulation of DC functions. For example, *in vivo*, 20 nm polystyrene (PS) particles are more frequently captured by lung DCs than 1,000 nm PS particles (19). If the 20 nm PS particle *in vitro* treatment did not affect murine bone marrow-derived dendritic cells (BM-DCs) cell viability, maturation markers expression, and antigen uptake, these particles significantly downregulated antigen degradation in a size-dependent manner, in association with accumulation in lysosomes but without altering T-cell proliferation (19). Moreover, NPs and materials traffic to the draining lymph nodes also appear to be size-dependent. Indeed, only small particles (20–200 nm) are able to drain freely to the lymph nodes (20).

In murine BM-DCs, carbon black NPs upregulate the expression of the cell surface molecules CD86, and slightly CD80 and MHC-II molecules, associated with enhancement of alloigenic-mixed lymphocyte reaction (21). TiO<sub>2</sub> NPs were also demonstrated to increase the expression of CD86, CD80, MHC-II, and TNF-α in murine BM-DCs (22). In murine BM-DCs and in the murine DC line DC 2.4, ultrafine silica NPs decreased cell viability, induced slight phenotypic changes but significantly increased TNF-α production in a size-dependent manner (23). Interestingly, these effects were correlated with inflammatory response *in vivo* in C57BL/6 mice injected subcutaneously with liquid matrigel

containing silica NPs (23). Winter et al. (8) studied the effects of aSNPs on murine BM-DCs. Amorphous SNPs were able to affect cell viability through apoptosis and induced partial maturation of BM-DCs as evidenced by enhanced expression of MHC-II and co-stimulatory molecules at the cell surface. Activation of the NLRP3 inflammasome was also reported (8). Taken together, these observations suggest that certain NP may promote DC maturation and activation, thereby leading to T-lymphocytes activation (**Figure 1**).

## THE “DANGER HYPOTHESIS” APPLIED TO EXOGENOUS PARTICLES AND NANOMATERIALS

Danger signals of endogenous or exogenous origin activate DCs and stimulate both the innate and adaptative immune responses. As proposed by Gallo and Gallucci, “classic,” “homeostatic,” and “emerging” danger signals can be distinguished (24). Classic danger signals are derived from pathogens and released during infections (pathogen-associated molecular patterns) or result from tissue damage, released by necrotic dying cells (damage-associated molecular patterns or “alarmins”) (25). Homeostatic danger signals are endogenous molecules released during cellular stresses such as hypoxia, acidity, or osmolality perturbations. Chemical sensitizers involved in contact allergy have recently been found to modify the cutaneous microenvironment and/or directly activate DCs resulting in DC phenotype modifications necessary for immune sensitization to these chemicals (26). Emerging danger signals are newly man-made materials,

including nanomaterials, and may either directly activate DCs or indirectly by inducing tissue damage. Thus, it is postulated that immune cells could sense nanomaterials, which could be designated as nanoparticles-associated molecular patterns (**Figure 1**) as described for pathogens (14, 24). Sensing of damage signals can be associated with the constitution of inflammasomes, acting as a multiprotein platform to activate caspase-1 and to stimulate the processing of pro-IL-1 $\beta$ . An increase in reactive oxygen species (ROS) production by nanomaterials has been described as an initiating step in the activation of the inflammasome. Interestingly, TiO<sub>2</sub> NPs, associated with the generation of ROS in human DCs, promoted cells maturation and pro-inflammatory cytokine release, whereas CeO<sub>2</sub> NPs, possessing antioxidant properties, triggered human DCs toward an anti-inflammatory profile with IL-10 production (27). Inflammasome activation can also occur through destabilization and rupture of the lysosome following phagocytosis. Indeed, the lysosome compartment is the most described intracellular site of NP sequestration following endocytosis (28). Morishige et al. (29) demonstrated in THP-1 cells that aSNP could induce ROS production, triggered endosomal rupture followed by the activation of NLRP3 inflammasome, and subsequent IL-1- $\beta$  production (29). These authors therefore established a direct relationship between oxidative stress and IL-1- $\beta$  secretion. Nano TiO<sub>2</sub> and nano SiO<sub>2</sub> particles activate the NLRP3 inflammasome in THP-1 cells, correlated with induction of lung inflammation *in vivo* requiring IL-1 receptor expression (30). Inflammasome activation by nano TiO<sub>2</sub> and nano SiO<sub>2</sub> particles would occur through ATP release and adenosine receptor signaling (30, 31). Moreover, 30 nm silica NPs can induce intracellular ATP release and P2X7 receptors purinergic signaling, leading to

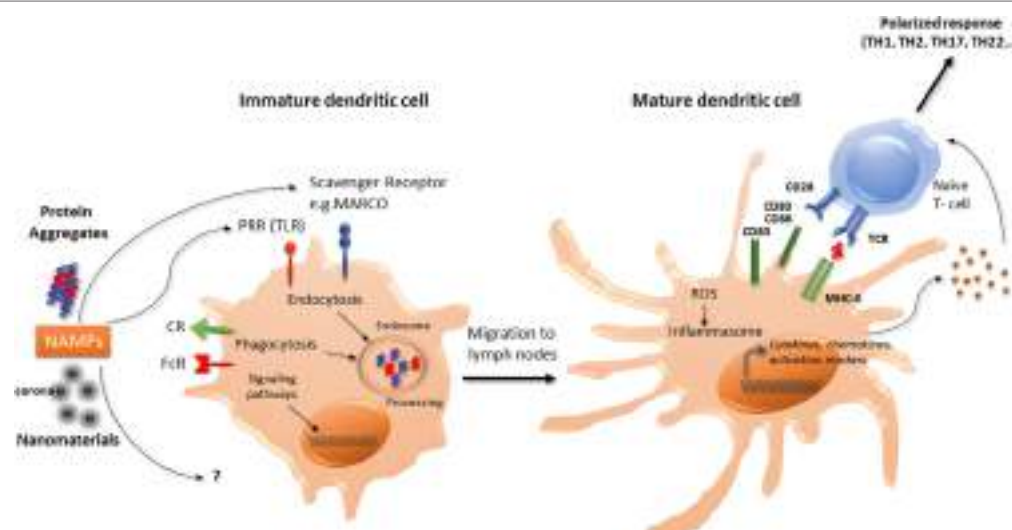


**FIGURE 1 | Interaction of nanomaterials and aggregates with DCs.** Nanomaterials and aggregates can be internalized by several receptors present at immature DCs membrane, either by endocytic or phagocytic pathways. Protein aggregates will then be processed by DCs, leading to peptide presentation associated with MHC class II molecules to naive T-lymphocytes. Both nanomaterials coated with a corona or protein aggregates may also be seen as NAMPs and interact with PRR. This interaction can act as a danger signal that induces a signaling cascade leading to the transcription of maturation genes. Mature DC will then be able to express co-stimulation molecules and to produce cytokines and chemokines that will trigger naïve T-cells activation and polarization. These products can also increase ROS production and initiate the inflammasome activation. CR, complement receptor; DCs, dendritic cells; FcR, immunoglobulin constant fragment receptor; MHC, major histocompatibility complex; NAMP, nanoparticles-associated molecular patterns; PRR, pattern recognition receptors; ROS, reactive oxygen species; Scavenger R, scavenger receptor; TLR, toll-like receptor.

ROS production, inflammasome activation and stimulating the production of IL-1 $\beta$  and IL-18 in LPS-matured murine BM-DC (32).

## PROTEIN AGGREGATES, AS NPs, CAN DRIVE IMMUNE RESPONSES

Beyond the strict definition of NPs, we should also consider nanomaterials in a broader sense of the term, since other structures than those derived from nanotechnologies could interact with the immune system (33). The example of protein aggregates is deeply studied as therapeutic bioproducts (BP) have a propensity to form oligomeric structures that could be assimilated to NPs. It is now well accepted that aggregation of therapeutic proteins is associated with increased potential for immunogenicity in patients, leading to the development of anti-drug antibodies (34, 35). While the aggregation process is strictly followed and controlled during BP manufacturing process, using orthogonal analysis methods (36), this is no more the case over transportation, storage, and administration procedures. Several studies have shown that under accelerated stress conditions, proteins can give mixtures of soluble aggregates that are submicron species including oligomers or multimers, mostly detected with dynamic light scattering method, and insoluble aggregates that are above the micrometer range (37). This was the case for human growth hormone submitted to a stir stress that gave homogenous aggregates around 892 nm (38), or antibody preparations that underwent stir stress (39), or thermal stress (40, 41). Another study showed the appearance of nanosized antibody aggregates upon heat or pH-shift stress that persisted when preparations were diluted in human serum, highlighting the interactions of aggregated proteins with biological fluids (42). A classification scheme was proposed for antibodies aggregates, based on several biophysical characterizations, in which nanosized particles were present in most of the depicted classes (43), although they were more represented in the subclass showing “small, partially folded and partially reversible” aggregates (43). Moreover, protein aggregation can be promoted by the presence of some other nanosized particles, such as glass (44), tungsten (45), or leaching from vial stoppers, as hypothesized in the early 2000s, regarding the episode of increased pure red-cell aplasia cases in patients treated with epoietin alpha (46). Such cases were shown to be mediated by anti-erythropoietin antibodies cross-reacting with the endogenous protein. Several models highlighting protein interactions and aggregation promoted by shedding particles from administration materials have been described (47–49).

The effect of protein aggregates on the immune system can be evaluated using *in vivo* models, such as immune-tolerant transgenic mice that can be treated with the human native or aggregated recombinant protein. Immunogenicity is then assessed following IgG titers developed against the administrated component. Such transgenic mice models have been developed for interferons (50, 51), and a recent paper showed that recombinant interferon beta aggregates induced a break of immune tolerance in transgenic mice, related with the size and structure of the generated aggregates (52). Using a conventional murine model,

another study highlighted that oligomeric antibody aggregates were more immunogenic than larger highly aggregated particles (41), suggesting that protein aggregation that maintains some native epitopes is more immunogenic. However, the use of *in vitro* models is more convenient to test the effect of aggregated proteins on immune cells. Thus, antibody aggregates have the potential to increase the production of inflammatory cytokines by human PBMC (53). Testing these aggregates by size showed that nanosized particles induced a lower response than micro-sized particles (54). The current hypothesis is that aggregates could behave as danger signals and may have mainly an effect on antigen-presenting cells, such as monocytes or DC (Figure 1). This hypothesis was objectivized demonstrating that aggregates interaction with PBMC or primary monocytes is partly mediated by toll-like receptors (TLR2 and TLR4), although other receptors such as Fc or complement receptors are also involved (53, 55). DCs are innate immune cells in first line upon therapeutic protein administration, either by intramuscular, intravenous, or subcutaneous administration, as proteins and aggregates rapidly transit in lymph nodes and interact with resident DCs. Also, cutaneous DCs that are present in the point of injection area could be recruited and migrate to peripheral lymph nodes (56). As therapeutic proteins can be processed by DCs to be presented to T cells, aggregates can interact with pattern recognition receptors, and then induce DCs activation. Indeed, several studies have shown that antibodies or growth hormone (GH) aggregates have the capacity to induce monocyte-derived dendritic cells maturation, evidenced by an increase in phenotypic markers expression, as well as cytokine or chemokine production (38, 57, 58). Both GH and antibodies aggregates could induce the production of IL-6, IL-8, IL-12p40, and CXCL10 whereas CCL2, CCL3, CCL4 production was only seen with GH aggregates (38). These observations could be extended using the monocytic cell line THP-1, that secreted inflammatory cytokines upon incubation with aggregated intravenous immunoglobulin preparations (55). Antibody aggregates are able to induce an increase in CD4+ T-cell proliferation and to drive T-cell polarization, compared to native counterparts through DCs phenotype modifications (38, 53, 57, 58). Cellular mechanisms by which protein aggregates induce DCs maturation remain to be clarified; however, a few elements are available. It was determined that DCs in contact with aggregates presented a higher number and different class II HLA-associated peptides than native counterparts, suggesting different processing and presentation, and thus neo-epitopes presentation (57). Although internalization in DCs lysosomal compartment of aggregated antibodies has been evidenced (58), the exact mechanism, either phagocytosis or macropinocytosis remains to be elucidated. Both certainly take place, depending on the size of the particles (20, 59, 60).

## CONCLUSION

Why the immune system should be concerned by nanomaterials? From the literature, it is now clear that exposure to environmental particles can exacerbate or participate to allergic manifestations such as asthma or rhinitis. Diesel exhaust particles and, more

recently, products generated through the use of nanotechnology have been shown to have detrimental effects on the respiratory systems, with an exacerbation rate of asthma (61). Nanomaterials can alter *in vitro* and *in vivo* responses of the immune system to allergens and can also play a role in allergen sensitization. Mimicking danger signals can lead to a direct effect of DCs phenotype (Figure 1) having consequences on the adaptive immune system response and recognition of allergens. The recent advances in nanotechnology could also lead to unforeseen adverse health effects mediated by the immune system, nanoimmunosafety, in exposed human subjects (62).

## REFERENCES

- Gustafson HH, Holt-Casper D, Grainger DW, Ghandehari H. Nanoparticle uptake: the phagocyte problem. *Nano Today* (2015) 10(4):487–510. doi:10.1016/j.nantod.2015.06.006
- Herd HL, Bartlett KT, Gustafson JA, McGill LD, Ghandehari H. Macrophage silica nanoparticle response is phenotypically dependent. *Biomaterials* (2015) 53:574–82. doi:10.1016/j.biomaterials.2015.02.070
- Kuhn DA, Vanhecke D, Michen B, Blank F, Gehr P, Petri-Fink A, et al. Different endocytotic uptake mechanisms for nanoparticles in epithelial cells and macrophages. *Beilstein J Nanotechnol* (2014) 5:1625–36. doi:10.3762/bjnano.5.174
- Franca A, Aggarwal P, Barsov EV, Kozlov SV, Dobrovolskaia MA, Gonzalez-Fernandez A. Macrophage scavenger receptor A mediates the uptake of gold colloids by macrophages *in vitro*. *Nanomedicine (Lond)* (2011) 6(7):1175–88. doi:10.2217/nmm.11.41
- Palecanda A, Paulauskis J, Al-Mutairi E, Imrich A, Qin G, Suzuki H, et al. Role of the scavenger receptor MARCO in alveolar macrophage binding of unopsonized environmental particles. *J Exp Med* (1999) 189(9):1497–506. doi:10.1084/jem.189.9.1497
- Orr GA, Chrisler WB, Cassens KJ, Tan R, Tarasevich BJ, Markillie LM, et al. Cellular recognition and trafficking of amorphous silica nanoparticles by macrophage scavenger receptor A. *Nanotoxicology* (2011) 5(3):296–311. doi:10.3109/17435390.2010.513836
- Vallhov H, Gabrielsson S, Stromme M, Scheynius A, Garcia-Bennett AE. Mesoporous silica particles induce size dependent effects on human dendritic cells. *Nano Lett* (2007) 7(12):3576–82. doi:10.1021/nl0714785
- Winter M, Beer HD, Hornung V, Kramer U, Schins RP, Forster I. Activation of the inflammasome by amorphous silica and TiO<sub>2</sub> nanoparticles in murine dendritic cells. *Nanotoxicology* (2011) 5(3):326–40. doi:10.3109/17435390.2010.506957
- Miao X, Leng X, Zhang Q. The current state of nanoparticle-induced macrophage polarization and reprogramming research. *Int J Mol Sci* (2017) 18(2):E336. doi:10.3390/ijms18020336
- Hoppstädter J, Seif M, Dembek A, Cavelius C, Huwer H, Kraegeloh A, et al. M2 polarization enhances silica nanoparticle uptake by macrophages. *Front Pharmacol* (2015) 6:55. doi:10.3389/fphar.2015.00055
- Monopoli MP, Aberg C, Salvati A, Dawson KA. Biomolecular coronas provide the biological identity of nanosized materials. *Nat Nanotechnol* (2012) 7(12):779–86. doi:10.1038/nnano.2012.207
- Corbo C, Molinaro R, Parodi A, Toledano Furman NE, Salvatore F, Tasciotti E. The impact of nanoparticle protein corona on cytotoxicity, immunotoxicity and target drug delivery. *Nanomedicine (Lond)* (2016) 11(1):81–100. doi:10.2217/nmm.15.188
- Neagu M, Piperigkou Z, Karamanou K, Engin AB, Docea AO, Constantin C, et al. Protein bio-corona: critical issue in immune nanotoxicology. *Arch Toxicol* (2017) 91(3):1031–48. doi:10.1007/s00204-016-1797-5
- Farrera C, Fadeel B. It takes two to tango: understanding the interactions between engineered nanomaterials and the immune system. *Eur J Pharm Biopharm* (2015) 95(Pt A):3–12. doi:10.1016/j.ejpb.2015.03.007
- Kapralov AA, Feng WH, Amoscato AA, Yanamala N, Balasubramanian K, Winnica DE, et al. Adsorption of surfactant lipids by single-walled carbon nanotubes in mouse lung upon pharyngeal aspiration. *ACS Nano* (2012) 6(5):4147–56. doi:10.1021/nn300626q
- Deng ZJ, Liang M, Monteiro M, Toth I, Minchin RF. Nanoparticle-induced unfolding of fibrinogen promotes Mac-1 receptor activation and inflammation. *Nat Nanotechnol* (2011) 6(1):39–44. doi:10.1038/nnano.2010.250
- Deng ZJ, Liang M, Toth I, Monteiro M, Minchin RF. Plasma protein binding of positively and negatively charged polymer-coated gold nanoparticles elicits different biological responses. *Nanotoxicology* (2013) 7(3):314–22. doi:10.3109/17435390.2012.655342
- Mortimer GM, Butcher NJ, Musumeci AW, Deng ZJ, Martin DJ, Minchin RF. Cryptic epitopes of albumin determine mononuclear phagocyte system clearance of nanomaterials. *ACS Nano* (2014) 8(4):3357–66. doi:10.1021/nn405830g
- Seydoux E, Rothen-Rutishauser B, Nita IM, Balog S, Gazdar A, Stumbles PA, et al. Size-dependent accumulation of particles in lysosomes modulates dendritic cell function through impaired antigen degradation. *Int J Nanomedicine* (2014) 9:3885–902. doi:10.2147/IJNN.S64353
- Manolova V, Flace A, Bauer M, Schwarz K, Saudan P, Bachmann MF. Nanoparticles target distinct dendritic cell populations according to their size. *Eur J Immunol* (2008) 38(5):1404–13. doi:10.1002/eji.200737984
- Koike E, Takano H, Inoue K, Yanagisawa R, Kobayashi T. Carbon black nanoparticles promote the maturation and function of mouse bone marrow-derived dendritic cells. *Chemosphere* (2008) 73(3):371–6. doi:10.1016/j.chemosphere.2008.05.054
- Zhu R, Zhu Y, Zhang M, Xiao Y, Du X, Liu H, et al. The induction of maturation on dendritic cells by TiO<sub>2</sub> and Fe(3)O(4)@TiO(2) nanoparticles via NF-κB signaling pathway. *Mater Sci Eng C Mater Biol Appl* (2014) 39:305–14. doi:10.1016/j.msec.2014.03.005
- Kang K, Lim JS. Induction of functional changes of dendritic cells by silica nanoparticles. *Immune Netw* (2012) 12(3):104–12. doi:10.4110/in.2012.12.3.104
- Gallo PM, Gallucci S. The dendritic cell response to classic, emerging, and homeostatic danger signals. Implications for autoimmunity. *Front Immunol* (2013) 4:138. doi:10.3389/fimmu.2013.00138
- Pradeu T, Cooper EL. The danger theory: 20 years later. *Front Immunol* (2012) 3:287. doi:10.3389/fimmu.2012.00287
- Magdal C, Botton J, El Ali Z, Azoury ME, Guldemann J, Gimenez-Arnau E, et al. Reactivity of chemical sensitizers toward amino acids in cellulo plays a role in the activation of the Nrf2-ARE pathway in human monocyte dendritic cells and the THP-1 cell line. *Toxicol Sci* (2013) 133(2):259–74. doi:10.1093/toxsci/kft075
- Schanen BC, Das S, Reilly CM, Warren WL, Self WT, Seal S, et al. Immunomodulation and T helper TH(1)/TH(2) response polarization by CeO(2) and TiO(2) nanoparticles. *PLoS One* (2013) 8(5):e62816. doi:10.1371/journal.pone.0062816
- Stern ST, Adiseshaiah PP, Crist RM. Autophagy and lysosomal dysfunction as emerging mechanisms of nanomaterial toxicity. *Part Fibre Toxicol* (2012) 9:20. doi:10.1186/1743-8977-9-20
- Morishige T, Yoshioka Y, Tanabe A, Yao X, Tsunoda S, Tsutsumi Y, et al. Titanium dioxide induces different levels of IL-1β production dependent on its particle characteristics through caspase-1 activation mediated by reactive oxygen species and cathepsin B. *Biochem Biophys Res Commun* (2010) 392(2):160–5. doi:10.1016/j.bbrc.2009.12.178
- Yazdi AS, Guarda G, Riteau N, Drexler SK, Tardivel A, Couillin I, et al. Nanoparticles activate the NLR pyrin domain containing 3 (Nlrp3) inflammasome and cause pulmonary inflammation through release of IL-1α and

## AUTHOR CONTRIBUTIONS

MP organized the manuscript and wrote the general part. AB-V wrote the nanomaterial part of the article. IT wrote the “aggregates” part of the article.

## FUNDING

This work is supported by Agence nationale de sécurité sanitaire de l'alimentation, de l'environnement et du travail (ANSES) grant SILIMMUN.

- IL-1beta. *Proc Natl Acad Sci U S A* (2010) 107(45):19449–54. doi:10.1073/pnas.1008155107
31. Baron L, Gombault A, Fanny M, Villeret B, Savigny F, Guillou N, et al. The NLRP3 inflammasome is activated by nanoparticles through ATP, ADP and adenosine. *Cell Death Dis* (2015) 6:e1629. doi:10.1038/cddis.2014.576
  32. Nakanishi K, Tsukimoto M, Tanuma S, Takeda K, Kojima S. Silica nanoparticles activate purinergic signaling via P2X7 receptor in dendritic cells, leading to production of pro-inflammatory cytokines. *Toxicol In Vitro* (2016) 35:202–11. doi:10.1016/j.tiv.2016.06.003
  33. Ilinskaya AN, Dobrovolskaia MA. Understanding the immunogenicity and antigenicity of nanomaterials: past, present and future. *Toxicol Appl Pharmacol* (2016) 299:70–7. doi:10.1016/j.taap.2016.01.005
  34. Ratanji KD, Derrick JP, Dearman RJ, Kimber I. Immunogenicity of therapeutic proteins: influence of aggregation. *J Immunotoxicol* (2014) 11(2):99–109. doi:10.3109/1547691X.2013.821564
  35. Wang W, Singh SK, Li N, Toler MR, King KR, Nema S. Immunogenicity of protein aggregates—concerns and realities. *Int J Pharm* (2012) 431(1–2):1–11. doi:10.1016/j.ijpharm.2012.04.040
  36. den Engelsman J, Garidel P, Smulders R, Koll H, Smith B, Bassarab S, et al. Strategies for the assessment of protein aggregates in pharmaceutical biotech product development. *Pharm Res* (2011) 28(4):920–33. doi:10.1007/s11095-010-0297-1
  37. Mahler HC, Friess W, Grauschopf U, Kiese S. Protein aggregation: pathways, induction factors and analysis. *J Pharm Sci* (2009) 98(9):2909–34. doi:10.1002/jps.21566
  38. Gallais Y, Szely N, Legrand FX, Leroy A, Pallardy M, Turbica I. Effect of growth hormone and IgG aggregates on dendritic cells activation and T-cells polarization. *Immunol Cell Biol* (2016) 95(3):306–15. doi:10.1038/icb.2016.100
  39. Mahler HC, Muller R, Friess W, Delille A, Matheus S. Induction and analysis of aggregates in liquid IgG1 antibody formulation. *Eur J Pharm Biopharm* (2005) 59(3):407–17. doi:10.1016/j.ejpb.2004.12.004
  40. Rao G, Iyer V, Kosloski MP, Pisal DS, Shin E, Middaugh CR, et al. Use of a folding model and in situ spectroscopic techniques for rational formulation development and stability testing of monoclonal antibody therapeutics. *J Pharm Sci* (2010) 99(4):1697–706. doi:10.1002/jps.21938
  41. Fathallah AM, Chiang M, Mishra A, Kumar S, Xue L, Middaugh R, et al. The effect of small oligomeric protein aggregates on the immunogenicity of intravenous and subcutaneous administered antibodies. *J Pharm Sci* (2015) 104(11):3691–702. doi:10.1002/jps.24592
  42. Filipe V, Jiskoot W, Basmeleh AH, Halim A, Schellekens H, Brinks V. Immunogenicity of different stressed IgG monoclonal antibody formulations in immune tolerant transgenic mice. *MAbs* (2012) 4(6):740–52. doi:10.4161/mabs.22066
  43. Joubert MK, Luo Q, Nashed-Samuel Y, Wypych J, Narhi LO. Classification and characterization of therapeutic antibody aggregates. *J Biol Chem* (2011) 286(28):25118–33. doi:10.1074/jbc.M110.160457
  44. Fradkin AH, Carpenter JF, Randolph TW. Glass particles as an adjuvant: a model for adverse immunogenicity of therapeutic proteins. *J Pharm Sci* (2011) 100(11):4953–64. doi:10.1002/jps.22683
  45. Seidl A, Hainzl O, Richter M, Fischer R, Bohm S, Deutel B, et al. Tungsten-induced denaturation and aggregation of epoetin alfa during primary packaging as a cause of immunogenicity. *Pharm Res* (2012) 29(6):1454–67. doi:10.1007/s11095-011-0621-4
  46. Casadevall N, Nataf J, Viron B, Kolta A, Kiladjian JJ, Martin-Dupont P, et al. Pure red-cell aplasia and antierythropoietin antibodies in patients treated with recombinant erythropoietin. *N Engl J Med* (2002) 346(7):469–75. doi:10.1056/NEJMoa011931
  47. Bee JS, Chiu D, Sawicki S, Stevenson JL, Chatterjee K, Freund E, et al. Monoclonal antibody interactions with micro- and nanoparticles: adsorption, aggregation, and accelerated stress studies. *J Pharm Sci* (2009) 98(9):3218–38. doi:10.1002/jps.21768
  48. Liu L, Randolph TW, Carpenter JF. Particles shed from syringe filters and their effects on agitation-induced protein aggregation. *J Pharm Sci* (2012) 101(8):2952–9. doi:10.1002/jps.23225
  49. Krayukhina E, Tsumoto K, Uchiyama S, Fukui K. Effects of syringe material and silicone oil lubrication on the stability of pharmaceutical proteins. *J Pharm Sci* (2015) 104(2):527–35. doi:10.1002/jps.24184
  50. Hermeling S, Schellekens H, Maas C, Gebbink MF, Crommelin DJ, Jiskoot W. Antibody response to aggregated human interferon alpha2b in wild-type and transgenic immune tolerant mice depends on type and level of aggregation. *J Pharm Sci* (2006) 95(5):1084–96. doi:10.1002/jps.20599
  51. van Beers MM, Sauerborn M, Gilli F, Brinks V, Schellekens H, Jiskoot W. Aggregated recombinant human interferon beta induces antibodies but no memory in immune-tolerant transgenic mice. *Pharm Res* (2010) 27(9):1812–24. doi:10.1007/s11095-010-0172-0
  52. Abdolvahab MH, Fazeli A, Halim A, Sediq AS, Fazeli MR, Schellekens H. Immunogenicity of recombinant human interferon beta-1b in immune-tolerant transgenic mice corresponds with the biophysical characteristics of aggregates. *J Interferon Cytokine Res* (2016) 36(4):247–57. doi:10.1089/jir.2015.0108
  53. Joubert MK, Hokom M, Eakin C, Zhou L, Deshpande M, Baker MP, et al. Highly aggregated antibody therapeutics can enhance the in vitro innate and late-stage T-cell immune responses. *J Biol Chem* (2012) 287(30):25266–79. doi:10.1074/jbc.M111.330902
  54. Telikepalli S, Shinogle HE, Thapa PS, Kim JH, Deshpande M, Jawa V, et al. Physical characterization and in vitro biological impact of highly aggregated antibodies separated into size-enriched populations by fluorescence-activated cell sorting. *J Pharm Sci* (2015) 104(5):1575–91. doi:10.1002/jps.24379
  55. Moussa EM, Kotarek J, Blum JS, Marszał E, Topp EM. Physical characterization and innate immunogenicity of aggregated intravenous immunoglobulin (IGIV) in an in vitro cell-based model. *Pharm Res* (2016) 33(7):1736–51. doi:10.1007/s11095-016-1914-4
  56. Fathallah AM, Bankert RB, Balu-Iyer SV. Immunogenicity of subcutaneously administered therapeutic proteins—a mechanistic perspective. *AAPS J* (2013) 15(4):897–900. doi:10.1208/s12248-013-9510-6
  57. Rombach-Riegraf V, Karle AC, Wolf B, Sorde L, Koepke S, Gottlieb S, et al. Aggregation of human recombinant monoclonal antibodies influences the capacity of dendritic cells to stimulate adaptive T-cell responses in vitro. *PLoS One* (2014) 9(1):e86322. doi:10.1371/journal.pone.0086322
  58. Ahmadi M, Bryson CJ, Cloake EA, Welch K, Filipe V, Romeijn S, et al. Small amounts of sub-visible aggregates enhance the immunogenic potential of monoclonal antibody therapeutics. *Pharm Res* (2015) 32(4):1383–94. doi:10.1007/s11095-014-1541-x
  59. Shang L, Nienhaus K, Nienhaus GU. Engineered nanoparticles interacting with cells: size matters. *J Nanobiotechnology* (2014) 12:5. doi:10.1186/1477-3155-12-5
  60. Couceiro JR, Gallardo R, De Smet F, De Baets G, Baatsen P, Annaert W, et al. Sequence-dependent internalization of aggregating peptides. *J Biol Chem* (2015) 290(1):242–58. doi:10.1074/jbc.M114.586636
  61. Li N, Georas S, Alexis N, Fritz P, Xia T, Williams MA, et al. A work group report on ultrafine particles (American Academy of Allergy, Asthma & Immunology): why ambient ultrafine and engineered nanoparticles should receive special attention for possible adverse health outcomes in human subjects. *J Allergy Clin Immunol* (2016) 138(2):386–96. doi:10.1016/j.jaci.2016.02.023
  62. Li Y, Italiani P, Casals E, Valkenborg D, Mertens I, Baggerman G, et al. Assessing the immunosafety of engineered nanoparticles with a novel in vitro model based on human primary monocytes. *ACS Appl Mater Interfaces* (2016) 8(42):28437–47. doi:10.1021/acsmami.6b06278

**Conflict of Interest Statement:** The authors declare that the research was conducted in the absence of any commercial or financial relationships that could be construed as a potential conflict of interest.

Copyright © 2017 Pallardy, Turbica and Biola-Vidamment. This is an open-access article distributed under the terms of the Creative Commons Attribution License (CC BY). The use, distribution or reproduction in other forums is permitted, provided the original author(s) or licensor are credited and that the original publication in this journal is cited, in accordance with accepted academic practice. No use, distribution or reproduction is permitted which does not comply with these terms.



# Graphene and the Immune System: A Romance of Many Dimensions

Sourav P. Mukherjee<sup>1</sup>, Massimo Bottini<sup>2,3</sup> and Bengt Fadeel<sup>1\*</sup>

<sup>1</sup>Nanosafety and Nanomedicine Laboratory, Division of Molecular Toxicology, Institute of Environmental Medicine, Karolinska Institutet, Stockholm, Sweden, <sup>2</sup>Department of Experimental Medicine and Surgery, University of Rome 'Tor Vergata', Rome, Italy, <sup>3</sup>Sanford Burnham Prebys Medical Discovery Institute, La Jolla, CA, United States

Graphene-based materials (GBMs) are emerging as attractive materials for biomedical applications. Understanding how these materials are perceived by and interact with the immune system is of fundamental importance. Phagocytosis is a major mechanism deployed by the immune system to remove pathogens, particles, and cellular debris. Here, we discuss recent studies on the interactions of GBMs with different phagocytic cells, including macrophages, neutrophils, and dendritic cells. The importance of assessing GBMs for endotoxin contamination is discussed as this may skew results. We also explore the role of the bio-corona for interactions of GBMs with immune cells. Finally, we highlight recent evidence for direct plasma membrane interactions of GBMs.

## OPEN ACCESS

### Edited by:

Paola Italiani,  
Consiglio Nazionale Delle  
Ricerche (CNR), Italy

### Reviewed by:

Seyed Moein Moghimi,  
Durham University,  
United Kingdom  
Aldo Tagliabue,  
ALTA, Italy

### \*Correspondence:

Bengt Fadeel  
bengt.fadeel@ki.se

### Specialty section:

This article was submitted  
to Inflammation,  
a section of the journal  
*Frontiers in Immunology*

Received: 08 April 2017

Accepted: 24 May 2017

Published: 13 June 2017

### Citation:

Mukherjee SP, Bottini M and Fadeel B (2017) Graphene and the Immune System: A Romance of Many Dimensions. *Front. Immunol.* 8:673.  
doi: 10.3389/fimmu.2017.00673

**Keywords:** graphene, macrophage, endotoxin, inflammasome, pattern recognition receptors

O brave new worlds, that have such people in them!

Edwin A. Abbott, *Flatland. A Romance of Many Dimensions* (1884).

## INTRODUCTION

Graphene and its derivatives have attracted considerable attention for various applications in science and technology (1, 2). Graphene oxide (GO), in particular, is being intensively investigated for various biomedical applications including drug delivery and bioimaging, and as biosensors (3). GO offers interesting physicochemical properties including its large surface area, ease of surface functionalization, and superior colloidal stability in aqueous media (4). However, increasing production and use of graphene-based materials (GBMs) also necessitates careful scrutiny of the impact of such materials on cells and tissues (5). Understanding the interactions with the immune system is of particular importance (6). Once inside the body, a foreign material will encounter phagocytic cells of the innate immune system, such as neutrophils, macrophages, and dendritic cells (DCs). These cells represent the first line of defense against foreign intrusion (microorganisms, particles), and they also clear cell debris, thus playing an important role in tissue homeostasis. Macrophages are involved in the initiation, propagation, and resolution of inflammation (7), while DCs are antigen-presenting cells that act as a bridge between the innate and adaptive arms of the immune system. Neutrophils are specialized in killing bacteria and other microorganisms, although recent studies have suggested that these cells may also orchestrate adaptive immune responses (8). It is important to note that macrophages that reside in different tissues are not only important effectors of the innate immune response but may also contribute to acute or chronic tissue injury resulting from toxicant exposure through the release of a host of soluble mediators, e.g., reactive oxygen or reactive nitrogen species, proteolytic enzymes, and pro-inflammatory cytokines or chemokines (9). Thus, as emphasized before by Laskin et al. (9), macrophages are mediators of both "defense and destruction."

Recently, a classification system (**Figure 1**) was proposed by researchers in the EU-funded GRAPHENE Flagship Project as a starting point for the categorization of distinct graphene types (10). In brief, three physicochemical properties of GBMs were highlighted: (i) the number of graphene layers, (ii) the average lateral dimensions, and (iii) the carbon-to-oxygen (C/O) atomic ratio; the inclusion of the C/O ratio as a functional property can be justified by the fact that GBMs are both structurally and chemically heterogeneous. Indeed, as stated by Wick et al. (10) different members of the GBM family do not share the same “standard” surface. The surface of pristine graphene is hydrophobic while in the case of GO, surfaces consist of hydrophobic islands interspersed with hydrophilic regions. This could potentially influence the interactions of these materials with biological systems. Here, we discuss recent studies on the interaction of GBMs with cells of the innate immune system, including macrophages, neutrophils, and DCs. Notably, while these cells all share the propensity for phagocytosis, we also explore emerging evidence that GBMs may exert direct effects on the plasma membrane of immune cells in the absence of cellular uptake. The biodegradation of carbon-based materials by immune cells including neutrophils and macrophages has been highlighted in other recent review articles (3, 11, 12) and is not discussed here. We will mainly focus our discussion on studies using macrophages or macrophage-like

cell lines as there are few studies to date on GBM effects on neutrophils and DCs. Nevertheless, as more and more studies are emerging, we may begin to understand how the immune system responds to 2D objects—a journey into flatland.

## THE IMPORTANCE OF ENDOTOXIN ASSESSMENT

Endotoxins, also known as lipopolysaccharides (LPS), are large (200–1,000 kDa), hydrophobic, heat-stable molecules that form part of the outer membrane of gram negative bacteria (13). LPS is a potent inflammatory mediator which activates immune cells *via* pattern recognition receptors leading to the secretion of pro-inflammatory mediators, e.g., tumor necrosis factor (TNF)- $\alpha$ , and interleukin (IL)-1 $\beta$  (14). As many nanomaterial-enabled drug carriers or diagnostic devices are engineered to target the immune system (or to avoid interactions with it), it is increasingly important to understand immune response to these materials (15, 16). Of particular importance in this context is the fact that nano-biomaterials and pharmaceutical products alike are commonly contaminated with endotoxins which could lead to septic shock and organ failure if administered to patients (17). Endotoxin detection in pharmaceutical products is performed using two different methods. The rabbit pyrogen test (RPT) enables the detection

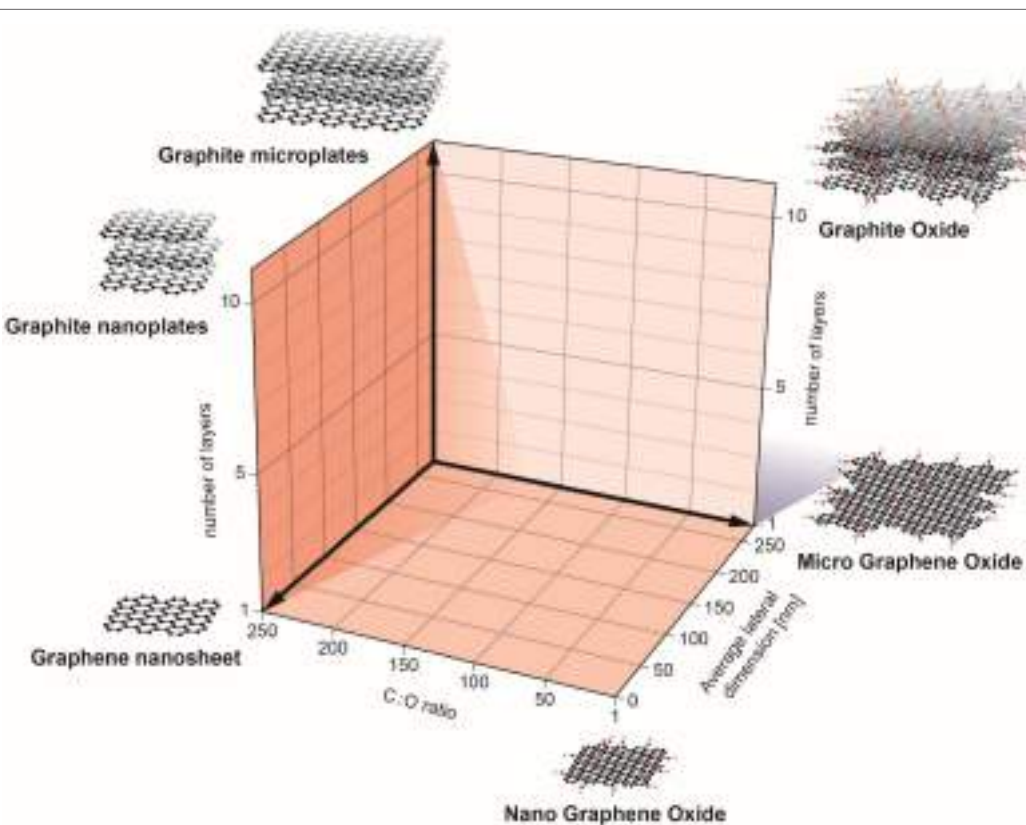


**FIGURE 1** | Classification of graphene-based materials (GBM). In the European Commission funded GRAPHENE Flagship project, three physicochemical descriptors were defined to enable the classification of GBMs: number of graphene layers, average lateral dimension, and atomic carbon/oxygen ratio. The proposed classification framework will help to determine the role of specific physicochemical properties on the health and safety profile of GBMs. Reproduced from: Wick et al. (10) with permission from John Wiley & Sons, Inc.

of pyrogens in general by measurement of fever development after injection of the test sample; it is expensive and requires the use of large numbers of animals (18). The second type of endotoxin detection method, the *Limulus* amebocyte lysate (LAL) assay, is based on the blood of wild horseshoe crab populations. While the RPT assay can only detect the presence of endotoxins indirectly, the LAL assay is more specific to endotoxins as it takes advantage of the LPS-sensitive serine protease Factor C. Upon activation, Factor C induces a coagulation cascade leading to the amplification of the LPS stimulus and the formation of a firm gel clot. All LAL assays are in principle based on this coagulation cascade, but they have been further modified to enable quantitative determination of endotoxins (18). Both of these tests have a long history of use for traditional pharmaceuticals and medical devices and are routinely used in drug development. More recently, the recombinant factor C (rFC) assay and the macrophage activation test (MAT) were recognized as alternatives to the LAL assay. The MAT, which mimics the human fever reaction, was established as an alternative test for pyrogen testing (19). Importantly, the European Directive 2010/63/EU on the protection of animals used for scientific purposes enforces the replacement of animal tests when validated alternatives exist. While the LAL assay is known to be very sensitive, several laboratories have reported problems of interference of various types of nanomaterials with one or more of the LAL assay formats (20–22). Indeed, carbon-based nanomaterials including GBMs were shown to interfere with the LAL assay, which may lead to erroneous results or mask the effects of the materials themselves (23, 24). In a recent study, the authors suggested that repeated cycles of autoclaving may reduce the endotoxin content of carbon-based nanomaterials including pristine graphene and that the native versus depyrogenated materials elicited distinct macrophage responses *in vitro* (25). However, the chromogenic LAL assay was employed to assess for endotoxin contamination, calling into question whether the proposed depyrogenation procedure worked (25). TLR4 reporter cells were suggested as an alternative assay to evaluate endotoxin contamination of metal/metal oxide nanoparticles (21). However, recent work has implied that GO could trigger cell death in macrophages *via* TLR4 (discussed below), meaning that the use of such reporter cells could also yield ambiguous results. Mukherjee et al. (23) developed a novel assay for endotoxin detection to circumvent problems with assay interferences of GBMs. The assay, designated the TNF- $\alpha$  expression test (TET), is based on the detection of TNF- $\alpha$  secretion in primary human monocyte-derived macrophages incubated in the presence or absence of a specific endotoxin inhibitor. It was shown that when non-cytotoxic doses of GBMs were applied, the TET enabled unequivocal detection of LPS with a sensitivity that was comparable to the LAL assay. Guidelines for the preparation of endotoxin-free GO were also presented (23).

## BIO-CORONA FORMATION: SHELTER FROM THE STORM

When a nanomaterial is introduced into a living system it interacts with biological molecules (proteins, lipids, etc.) leading to the formation of a so-called bio-corona on the surface (26), or, to put this in immunological terms, the nanomaterial is opsonized

(the process whereby pathogens or cells are rendered more susceptible to phagocytosis). Detailed studies of various types of nanoparticles have shown that bio-corona formation depends not only on the size or surface curvature of the particle but also on surface properties such as the degree of hydrophobicity (27–29). The bio-corona has been shown to modulate cellular uptake of nanomaterials (30), and a recent study suggested that proteins present in the original protein corona are retained on the nanoparticles until they reach the lysosomes (31). Moreover, the adsorption of proteins may mitigate the cytotoxic effects of nanomaterials. Indeed, *in vitro* studies have shown that the adsorption of serum proteins reduces the cytotoxicity of carbon nanotubes (CNTs) (32) as well as GO (33), and based on a combination of experimental and theoretical approaches, it was suggested that the bio-corona mitigates the cytotoxicity of GO by limiting its penetration into the cell membrane (34). Furthermore, modeling studies suggested that graphene, due to its hydrophobic nature, may interrupt hydrophobic protein–protein interactions (35). Indeed, it is important to recognize the differences in physicochemical properties between different members of the GBM family, not least with respect to the potential interaction with proteins. Graphene is essentially a single atomically thin sheet of sp<sup>2</sup>-bonded carbon atoms, whereas GO is an oxidized graphene sheet derivatized by carbonyl and carboxyl groups at the edges and displaying epoxide and hydroxyl groups on the basal plane (36). Moreover, graphene and GO have different surface energies—an important parameter affecting dispersibility. Thus, graphene is hydrophobic and dispersible in organic solvents whereas GO can be dispersed in water (37). The latter property derives mostly from the ionizable edge carboxyl groups, the basal plane being essentially a network of hydrophobic islands of unoxidized benzene rings surrounded by polar groups (38). Additionally, small GO sheets are more hydrophilic than larger ones because of greater charge density, which could impact on bio-interactions.

Intravenously injected nanomaterials can adsorb a wide range of proteins in the blood (39). The bio-corona of blood proteins is rapidly formed, and it has been shown to affect hemolysis and thrombocyte activation (40). Furthermore, complement activation on the surface of nanomaterials is of particular concern when it comes to clinical applications. In fact, complement proteins have been consistently identified in or on nanoparticle coronas (28, 30, 40, 41). The complement system is a critical component of the innate immunity in the blood; it is a proteolytic cascade typically triggered *via* three distinct pathways (classical, lectin, and alternative) that converge to generate the same set of effector molecules at the third component of complement (C3) (42). Complement proteins opsonize pathogens and cells for engulfment *via* complement receptors and could conceivably promote nanomaterial uptake as well. However, certain complement factors may instead confer “stealth” properties to nanomaterials by preventing further complement activation, as shown in a recent study on GO (43). Complement activation also liberates two potent effector molecules (C3a and C5a) that play important roles in the recruitment and activation of inflammatory cells as well as anaphylaxis, a serious allergic reaction that is rapid in onset and may cause death (44). Several reports have documented pathway-specific

complement activation by various types of nanomaterials including carbon-based nanomaterials such as CNTs (45, 46) and GO (47, 48). The question is: could particle surfaces be engineered to avoid protein adsorption and/or unscheduled complement activation? The attachment of polymers such as poly(ethylene glycol) (PEG) on particle surfaces is a common approach in nanomedicine, and the traditional view has held that PEGylation completely prevents protein adsorption, thereby preventing the clearance of particles by the reticuloendothelial system. However, if this were true, then how does one explain complement activation on PEGylated particles? In recent years, the view has emerged that PEGylation of nanomaterials only partially blocks protein adsorption and may even promote the formation of a bio-corona that is distinct in comparison to the corona formed on pristine nanomaterials (49, 50). Indeed, in a recent study using macrophage-like RAW264.7 cells, the adsorption of specific proteins was shown to be required to prevent uptake of PEG- or poly(ethyl ethylene phosphate) (PEEP)-coated polystyrene particles (51).

The choice of polymer coating matters. Luo et al. (52) reported that PEG-coating prevented uptake of GO by murine peritoneal macrophages while coating with cationic poly(ether imide) (PEI) favored uptake at low doses, but compromised cell viability at high doses. In another recent study, the authors provided evidence that PEGylated GO of approximately 200 nm in lateral size induced immune responses (cytokine release) in murine peritoneal macrophages; interestingly, comparable levels of activation were also observed following PEGylation of the non-carbon-based 2D material, molybdenum-disulfide ( $\text{MoS}_2$ ) (53). The authors speculated that integrin signaling could account for the enhanced cytokine responses in cells exposed to PEG-GO. Overall, the study suggested that PEGylation does not serve to passivate the surfaces of 2D materials. Xu et al. (54) prepared a series of GO derivatives including aminated GO (GO-NH<sub>2</sub>), poly(acrylamide)-functionalized GO (GO-PAM), poly(acrylic acid)-functionalized GO (GO-PAA), and PEG-functionalized

GO (GO-PEG), and compared their toxicity with pristine GO. The GO materials all displayed lateral dimensions in the range of 100–500 nm and the  $\zeta$ -potential was negative for all the materials in cell culture medium due to protein adsorption. Among these GO derivatives, GO-PEG and GO-PAA induced less toxicity toward murine J774A.1 macrophage-like cells than pristine GO, and GO-PAA proved to be the most biocompatible one, both *in vitro* and in mice (54). The differences in biocompatibility were suggested to be due to differences in the compositions of the bio-corona, especially whether or not immunoglobulin G (IgG) was present; GO-PAA and GO-PEG had less IgG content in their protein coronas (30–40%) than GO, GO-NH<sub>2</sub>, and GO-PAM (50–70%). IgG is a well-known opsonin that plays a key role in the clearance of pathogens. This study points toward strategies for safe design of GO for biomedical applications and underscores the importance of the bio-corona (54).

## EFFECTS ON MACROPHAGES: BREAKING AND ENTERING

Macrophages (“big eaters”) are professional phagocytes arising from the bone marrow; these cells are referred to as monocytes when they are present in the peripheral circulation and “macrophages” when they reside in tissues. Macrophage phagocytosis of pathogens is facilitated through opsonization by immunoglobulins and components of the complement system, but engulfment may also be non-specific. We have noted that primary human monocyte-derived macrophages efficiently engulfed GO without signs of acute (24 h) cell death (Figure 2). GO was found in membrane-enclosed vesicles in the cytoplasm, suggesting uptake *via* endocytosis. Other recent studies using macrophage-like THP1 cells suggested that phagocytosis influences the degree of cytotoxicity of GO to some extent (55). However, while inhibition of phagocytosis blunted the cytotoxicity of single-layer GO, the effects of multi-layered GO were shown to be similar regardless

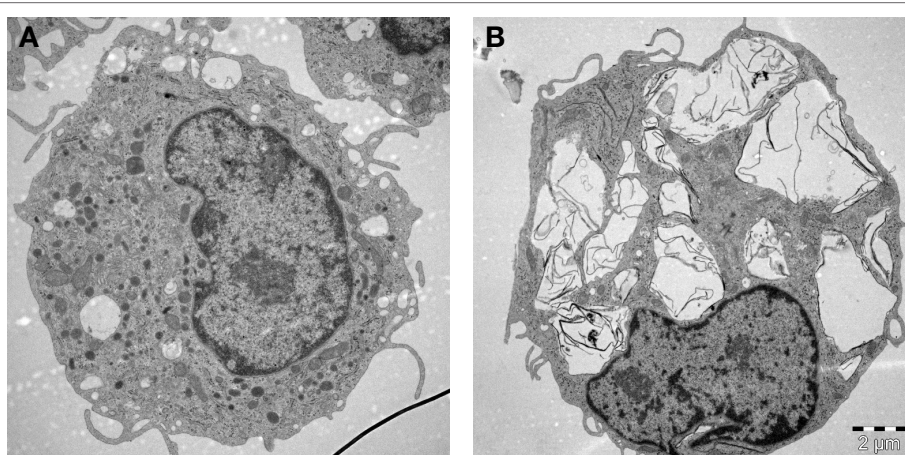


**FIGURE 2 |** Macrophages are professional phagocytic cells capable of ingesting micron-sized graphene oxide (GO). These TEM images show primary human monocyte-derived macrophages cultured for 24 h in cell medium alone (A) or with 10  $\mu\text{g}/\text{mL}$  GO (B). The cells readily internalized GO (present in cytoplasmic vesicles) without ultrastructural signs of cell death. Cells were maintained in RPMI-1640 medium supplemented with 10% fetal bovine serum. TEM: Kjell Hultenby, Electron Microscopy Core Facility, Karolinska Institutet.

of whether or not phagocytosis occurred. Furthermore, other recent studies have reported that GO sheets with large lateral dimensions could align with the plasma membrane of macrophages (so-called “masking” effect) and it was hypothesized that this parallel arrangement of GO sheets on the cell surface could either promote their internalization, or isolate the cells from their environment, thus compromising cell viability and/or cell function (56). Similarly, Ma et al. (57) reported that large GO sheets showed a stronger “adsorption” to the plasma membrane of murine macrophage-like J774.A1 cells with less phagocytosis, while small GO sheets were more readily taken up by cells. The authors also found that large GO promoted a pro-inflammatory polarization of macrophages both *in vitro* and *in vivo*. In contrast, other investigators have reported that small GO sheets elicited more profound effects on human immune cells (monocytes) when compared to large GO (58). Li et al. (59) suggested, on the basis of experimental and theoretical studies, that micron-sized graphene sheets entered cells through membrane piercing or slicing (“edge-first” uptake). In fact, several studies in recent years using different cell models have suggested that GO could exert direct effects on the plasma membrane of cells, with or without cell death. For instance, micron-sized GO sheets were found to induce the formation of vacuoles in the cytosolic compartment of cells leading to an increased cell membrane permeability for small molecules; this vacuolization was only observed in cells that overexpressed the water channel, aquaporin (AQP1) (60). GO was also shown to compromise plasma membrane and cytoskeletal function in various cell lines without significant signs of cell death, and interactions with integrins in the cell membrane were implicated in this process (61). The authors proposed that this could be exploited to sensitize cancer cells to chemotherapeutic agents, but it was not demonstrated whether these effects were specific for cancer cells. Furthermore, single-layer graphene was found to produce holes (pores) in the membranes of A549 lung carcinoma cells and macrophage-like RAW264.7 cells, leading to a substantial loss of cell viability (62). Pore formation occurred even in the presence of serum, and molecular dynamics simulations suggested that the pore formation was dependent on lipid extraction. Indeed, previous experimental and theoretical studies have suggested that the antibacterial behavior of graphene arises from the formation of pores in the bacterial cell wall (63), possibly due to lipid extraction from bacterial membranes (64). Finally, in another recent study, nano-sized GO sheets were shown to induce membrane ruffling in a variety of different cell lines with concomitant shedding of membrane fragments (65). The underlying mechanism was not disclosed, although changes in the levels of Ca<sup>2+</sup> in the cell are known to regulate the formation of such actin-driven membrane protrusions. Thus, it appears that GBMs are capable of interacting with cells in a variety of different ways including masking, piercing, ruffling/shedding, pore formation (possibly *via* membrane lipid extraction), and/or internalization into cells. How does one make sense of such disparate observations? First of all, there could be important differences in the test material itself, including the thickness and the lateral dimensions (and, of course, the dose of the material added to cell cultures). Moreover, differences in cell culture conditions (including whether or not the cell culture medium is supplemented with serum) may come

into play. Indeed, it has been noted that the composition of the cell culture medium itself could critically affect the way in which GO (and other nanomaterials) interact with cells (66). Finally, the fact that different cell models are used may account for the striking differences in cellular outcomes in the studies reported here. Thus, it is important to understand that transformed cell lines are only a model of normal cells, and that so-called macrophage-like cell lines do not fully recapitulate the behavior of primary macrophages (67). It is also important to realize that there are many different macrophage populations and that the phenotype or activation status of macrophages may affect how these cells respond to nanomaterials, as we and others have recently shown (68, 69). Notwithstanding, the view is emerging that GO could have direct effects on the cell membrane and further studies are needed to understand these interactions. This is obviously important if GBMs are to be used as “smart” carriers of a therapeutic payload to specific cell populations in the body.

## EFFECTS ON MACROPHAGES: INFLAMMASOME ACTIVATION

Inflammasomes are multiprotein complexes that activate caspase-1, which leads to maturation and secretion of the pro-inflammatory cytokines IL-1 $\beta$  and IL-18 (70). Inflammasome activation is important for host defense and pathogen clearance. In addition, inflammasome activation is implicated in the development of various chronic inflammatory diseases, and the NLRP3 inflammasome is activated by endogenous “danger” signals such as monosodium urate, the causative agent in gout (71), and by cholesterol crystals that are present in atherosclerotic lesions (72). Moreover, an emerging body of literature shows that carbon-based nanomaterials, including long and fiber-like multi-walled CNTs (73, 74) as well as small, spherical carbon nano-onions (75) and hollow carbon spheres (76), are able to activate the inflammasome complex in phagocytic cells (macrophages) with subsequent secretion of IL-1 $\beta$ . GO was recently shown to trigger IL-1 $\beta$  production in myeloid (THP1) and epithelial (BEAS-2B) cells, respectively (77). We have found that GO of varying lateral dimensions triggered the inflammasome in primary human monocyte-derived macrophages and we noted that cellular uptake of GO was required for IL-1 $\beta$  production (Mukherjee et al., unpublished observations). Similarly, Cho et al. (55) reported that phagocytosis inhibition abolished IL-1 $\beta$  secretion in THP1 cells exposed to single-layer GO, but not in cells exposed to multi-layered GO. Taken together, a range of carbon-based nanomaterials including not only fiber-like materials but also spherical particles and flat materials such as GO trigger inflammasome activation. Needless to say, it is important to exclude endotoxin contamination of the test material when conducting such experiments as LPS is known to act as a co-signal for inflammasome activation (78). Indeed, endotoxin is often used to stimulate cells *in vitro* when assessing NLRP3 inflammasome activation (73), and this is certainly relevant in the context of a microbial challenge. However, it is pertinent to ask how the inflammasome is activated in sterile (nanomaterial) induced inflammation. In a recent publication, Jessop et al. (79) provided evidence for a role of high-mobility group box 1 (HMGB1) for MWCNT-induced inflammasome

activation *in vitro* and *in vivo*. Cholesterol crystals are known to act as “danger” signals and a recent study demonstrated that cholesterol crystals triggered neutrophils to release neutrophil extracellular traps (NETs) (see below) which, in turn, primed macrophages for cytokine release (80). This finding suggests that a “danger” signal may drive sterile inflammation through its interaction with neutrophils. Further studies should address whether the release of HMGB1 or other “danger” signals plays a role in GO-induced inflammasome activation.

Toll-like receptors (TLRs) are so-called pattern recognition receptors that recognize structurally conserved molecules expressed by microbes, leading to the activation of immune responses (81). TLR4, the pattern recognition receptor for LPS (endotoxin), has been suggested to recognize a host of other endogenous factors, ranging from proteins to metal ions. However, direct activation of a single receptor by such a range of molecular signals is difficult to explain from a structural point of view, and care should be taken to exclude potential endotoxin contamination (82). On the other hand, it has been suggested that TLRs might sense the display of hydrophobic patches on a variety of molecules, which may explain the apparent promiscuity of this class of pattern recognition receptors (83). Interestingly, Qu et al. (84) reported that GO with a size of about 1–2  $\mu\text{m}$  induced TLR4-dependent cell death in bone marrow-derived macrophages from mice and presented evidence that this occurred, at least in part, through a paracrine TNF $\alpha$ -dependent mechanism. In previous work, Chen et al. (85) showed that GO induced autophagy and cytokine secretion in a TLR-dependent manner in the mouse macrophage cell line RAW264.7. In contrast, our recent studies have suggested that GO triggers inflammasome activation with secretion of IL-1 $\beta$  in primary human monocyte-derived macrophages without engaging the TLR signaling pathway (Mukherjee et al., unpublished results). Notably, no cell death was observed in macrophages exposed to GO, in marked contrast to the aforementioned studies. Care was taken to control for endotoxin contamination prior to cell exposures. We suggest that endotoxin testing should be mandatory when studying putative interactions of GO with TLRs.

In most of the examples provided here, the impact of GO on isolated macrophages or macrophage-like cells was investigated. While such studies may provide important insights regarding the mode of entry of GO into cells and on the signaling pathways affected following cellular interactions, studies in living organisms are needed to assess the overall response to GO and the interplay between both arms of the immune system. Shurin et al. (86) recently provided a detailed analysis of how exposure to GO modulates the allergic pulmonary response. To this end, the authors used a murine model of ovalbumin (OVA)-induced asthma, and found that GO, given at the sensitization stage, augmented airway hyperresponsiveness (AHR) and airway remodeling, while at the same time, the levels of the Th2 cytokines, IL-4, IL-5, and IL-13 were suppressed in bronchoalveolar lavage (BAL) fluid in exposed mice (86). Moreover, exposure to GO during sensitization with OVA decreased eosinophil accumulation and increased recruitment of macrophages in BAL fluid. Exposure to GO also increased the macrophage production of the mammalian chitinases, chitinase 3-like 1, and AMCase, whose expression is

associated with asthma (87), and molecular modeling suggested that GO may directly interact with chitinases, affecting their activity (Figure 3). Taken together, these results indicated that pulmonary exposure to GO initiates a novel mechanism of nanomaterial-induced airway remodeling and AHR in a mouse model of asthma that is independent from eosinophilic airway inflammation and Th2-mediated immune responses, with the possible involvement of mammalian chitinases (86).

## EFFECTS ON NEUTROPHILS: TANGLED UP IN BLUE

Neutrophils are the most abundant type of white blood cells and play a key role in the defense against invading pathogens. Neutrophils use a variety of strategies to eliminate invading microbes: (i) microbial uptake followed by intracellular destruction through an array of proteolytic and oxidative enzymes, (ii) degranulation and secretion of antimicrobial factors such as myeloperoxidase (MPO) leading to extracellular destruction of microbes, and (iii) release of NETs with entrapment and non-phagocytic killing of microbes (88, 89). NETs consist of a network of chromatin fibers decorated with antimicrobial proteins such as neutrophil elastase (NE) and MPO to enable the extracellular killing of bacteria or fungi. Interestingly, neutrophils are apparently able to sense the size of microbes and release NETs selectively in response to large pathogens, thereby minimizing the risk of tissue damage associated with the release of NETs (90). Moreover, increasing evidence suggests that the release of NETs might also occur in non-infectious, sterile inflammation, and may contribute to tissue damage (91). For instance, crystals of monosodium urate, the causative agent of gout, were shown to induce release of NETs (92). Cholesterol crystals can also trigger NET formation, leading to priming of macrophages for cytokine release (80). Furthermore, in a very recent study, exposure to high doses of polystyrene nanoparticles and nanodiamonds triggered a “self-limiting” (resolving) NETosis-driven inflammation in mice (93). No NET formation was seen in response to large (100–1,000 nm) particles. We recently observed size-dependent triggering of NETs in primary human neutrophils exposed to GO with a more pronounced effect seen for micrometer-sized GO sheets versus GO sheets with nano-sized lateral dimensions; we also observed a disruption of lipid rafts in neutrophils incubated with GO (Mukherjee et al., unpublished results). Care was taken to control for endotoxin contamination, as LPS is known to prime neutrophils for NET production. Effects of GBMs on neutrophils *in vivo* could impact adversely on the innate immune defense; this remains to be studied.

## EFFECTS ON DENDRITIC CELLS: AIDING AND ABETTING

DCs are professional antigen-presenting cells (94) and as such they are indispensable for the regulation of the balance between immunity (literally meaning “exemption,” the capability of an organism to resist microorganisms) and tolerance (i.e., indifference or non-reactivity toward substances that would

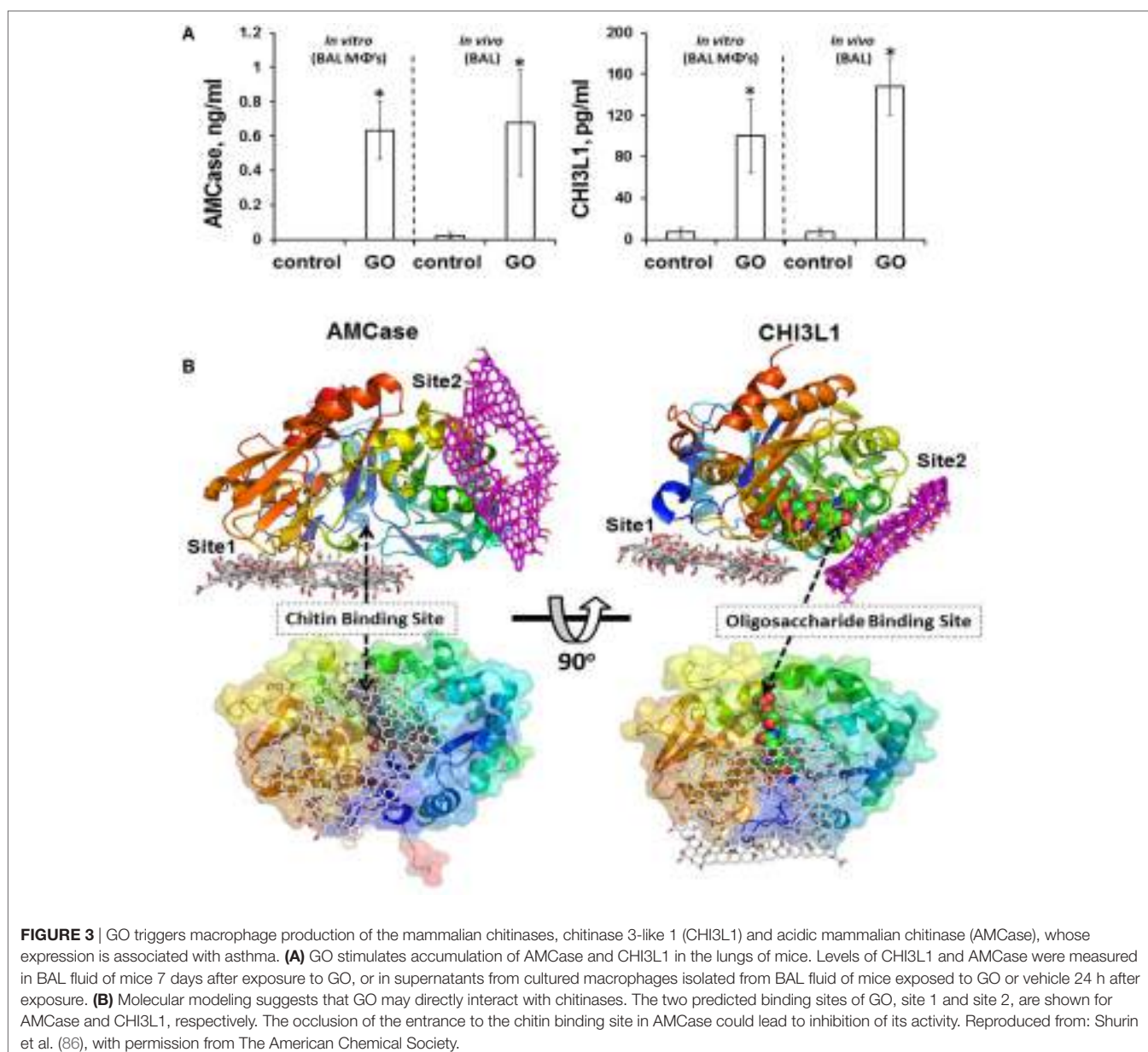


**FIGURE 3 |** GO triggers macrophage production of the mammalian chitinases, chitinase 3-like 1 (CHI3L1) and acidic mammalian chitinase (AMCase), whose expression is associated with asthma. **(A)** GO stimulates accumulation of AMCase and CHI3L1 in the lungs of mice. Levels of CHI3L1 and AMCase were measured in BAL fluid of mice 7 days after exposure to GO, or in supernatants from cultured macrophages isolated from BAL fluid of mice exposed to GO or vehicle 24 h after exposure. **(B)** Molecular modeling suggests that GO may directly interact with chitinases. The two predicted binding sites of GO, site 1 and site 2, are shown for AMCase and CHI3L1, respectively. The occlusion of the entrance to the chitin binding site in AMCase could lead to inhibition of its activity. Reproduced from: Shurin et al. (86), with permission from The American Chemical Society.

otherwise elicit an immune response; an active rather than a passive condition). DCs take up foreign molecules as well as host-derived proteins and process them intracellularly to antigens that are presented in the context of major histocompatibility (MHC) class I and II molecules on the cell surface. In a recent *in vitro* study, pristine GO was found to suppress antigen presentation to T cells using OVA as a model antigen (95). DCs were exposed to GO prior to OVA-loading and then mixed with B3Z86/90.14 (B3Z) CD8+ T cells specific for the H-2K<sup>b</sup>-restricted anti-mouse OVA257-264 (SIINFEKL) peptide. Production of IL-2 was monitored as a sign of T cell activation upon recognition of the OVA epitope 257–264 in the context of the H-2K<sup>b</sup> molecules (MHC class I). Interestingly, while GO also stimulated maturation of DCs, the immunosuppressive effect of GO was dominant (95). Further studies are needed to understand whether all GBMs

behave in this way. In fact, as discussed below, some varieties of GO have shown promise as antigen carriers.

Commonly used adjuvants (i.e., agents that are added to a vaccine to boost the immune response toward a specific antigen) include substances such as mineral oil and alum or other inorganic compounds. However, while these compounds have been in clinical use for many years, the precise mechanism of action remains poorly understood (96). Recent studies showed that the aluminum adjuvant, alum triggered the release of IL-1 $\beta$  in macrophages and DCs in an NLRP3-dependent manner (97), and mice deficient in Nalp3 failed to mount a significant antibody response to an antigen administered with aluminum adjuvants (98). In contrast, Freund's complete and incomplete adjuvant (i.e., mineral oil with or without inactivated mycobacteria) appeared to act in an inflammasome-independent manner.

Sun et al. (99) demonstrated that aluminum-based adjuvants can be engineered to optimize their immunostimulatory properties. Specifically, the authors synthesized a library of aluminum oxyhydroxide (AlOOH) nanorods and compared these to commercial alum and could show that shape, crystallinity, and hydroxyl content played an important role in NLRP3 inflammasome activation (99). Rettig et al. (100) provided evidence that particle size may also influence the immune response to “danger.” Using single-stranded RNA (a known “danger” signal) mixed with protamine to form particles of different sizes, the authors could show that particle size determined whether an anti-viral or anti-bacterial/anti-fungal immune response was triggered. This was suggested to be due at least in part to the selective phagocytosis of nano-sized particles by plasmacytoid DCs, which produced interferon- $\alpha$ . It will be of interest to study the potential effects of GBMs of differing lateral dimensions on DCs and whether these materials could also be exploited as adjuvants to stimulate immune responses. GBMs might also prove advantageous as antigen carriers. Li et al. (101) exploited the fact that GO can spontaneously adsorb proteins to explore the use of this material for intracellular vaccine delivery. Using an *in vitro* model, the authors could show that GO adsorbed proteins were efficiently internalized by DCs leading to antigen cross-presentation to CD8+ T cells. In a more recent *in vivo* study, polymer-modified GO (GO-PEG-PEI) with nano-scale lateral dimensions was shown to act as an antigen carrier to shuttle antigens into DCs (102). Furthermore, compared with free *Helicobacter pylori* Urease B antigen and the clinically approved aluminum adjuvant-based vaccine (Alum-Ure B), GO-PEG-PEI-Ure B was found to induce stronger cellular immunity upon intradermal administration (102). Pristine GO or GO-PEG did not show the same effect. The high surface area of GO allowing for high antigen loading capacity along with the positive charge afforded by the polymer coating could help to explain this effect. The possibility that GO *per se* could have adjuvant properties should also be explored, in light of the fact that small and large GO sheets trigger the NLRP3 inflammasome (discussed above). Finally, Meng et al. (103) recently reported that ultrasmall GO decorated with the antioxidant compound carnosine modulates innate immunity and improves adaptive immunity. The authors could show that GO covalently modified with carnosine, when mixed with the model antigen, OVA promoted robust and durable OVA-specific antibody responses, increased lymphocyte proliferation efficiency, and enhanced CD4+ T and CD8+ T cell activation. The authors proposed that GO-carnosine could be useful as an adjuvant to effectively enhance humoral and innate immune responses *in vivo*.

## CONCLUDING REMARKS

In the current essay, we have highlighted recent research on the interactions of GBMs, in particular GO, with the immune

system, focusing our discussion mainly on *in vitro* studies. While we are far from a comprehensive understanding of these interactions, one may ask whether there are any general conclusions at this point. One technical, yet non-trivial issue when performing studies of GBMs and immune-competent cells concerns the importance of knowing not only the test material (10), and whether there are traces of endotoxin as this may impact on subsequent immune responses, but also the test system, i.e., the cell model including the composition of the cell medium, and whether this is supplemented or not with serum. Furthermore, it is important to realize that the plasma membrane is not only an impassive barrier between the interior of a cell and the extracellular space but also serves as an important platform for cellular communication between cells, and between the exterior and interior of a cell (104). This is true not least for immune-competent cells that are specialized in sensing and sampling their environment. It follows from this argument that the effects of a biomaterial on the cell membrane could have ramifications for immune cell communication and function. It is of interest to note that the adjuvant, alum, was previously shown to trigger responses in DCs by altering membrane lipid structures, demonstrating that not all immune signaling is receptor mediated, and suggesting that the plasma membrane could behave as a “sensor” for solid structures (105). Thus, the impact of a biomaterial is not necessarily linked to whether or not the material is internalized as direct effects on the plasma membrane could also come into play. In the field of nanotoxicology, much time and effort has been devoted to the determination of the dose of nanoparticles delivered to and internalized by cells, but for atomically thin materials with large lateral dimensions, some toxicological outcomes may depend on direct effects on the plasma membrane, and not only on cellular uptake of the material. In other words, as we continue to probe immunological responses toward GBMs and other 2D materials, we should not forget that significant insights may come from studying seemingly superficial interactions. Or, as actress Ava Gardner once put it, “Deep down, I’m pretty superficial.”

## AUTHOR CONTRIBUTIONS

BF wrote the manuscript, with input from SPM and MB. The final version of the manuscript was discussed and approved by all participating authors.

## FUNDING

This work was supported by grants awarded to BF by the European Commission (Flagship Project GRAPHENE, grant no. 696656) and the Swedish Research Council (grant no. 2016-02040).

## REFERENCES

- Kostarelos K, Novoselov KS. Materials science. Exploring the interface of graphene and biology. *Science* (2014) 344:261–3. doi:10.1126/science.1246736
- Ferrari AC, Bonaccorso F, Fal’ko V, Novoselov KS, Roche S, Boggild P, et al. Science and technology roadmap for graphene, related two-dimensional crystals, and hybrid systems. *Nanoscale* (2015) 7(11):4598–810. doi:10.1039/c4nr01600a
- Bhattacharya K, Mukherjee SP, Gallud A, Burkert SC, Bistarelli S, Bellucci S, et al. Biological interactions of carbon-based nanomaterials: from coronation to degradation. *Nanomedicine* (2016) 12(2):333–51. doi:10.1016/j.nano.2015.11.011

4. Bitounis D, Ali-Boucetta H, Hong BH, Min DH, Kostarelos K. Prospects and challenges of graphene in biomedical applications. *Adv Mater* (2013) 25(16):2258–68. doi:10.1002/adma.201203700
5. Sanchez VC, Jachak A, Hurt RH, Kane AB. Biological interactions of graphene-family nanomaterials: an interdisciplinary review. *Chem Res Toxicol* (2012) 25(1):15–34. doi:10.1021/tx200339h
6. Farrera C, Fadeel B. It takes two to tango: understanding the interactions between engineered nanomaterials and the immune system. *Eur J Pharm Biopharm* (2015) 95(Pt A):3–12. doi:10.1016/j.ejpb.2015.03.007
7. Aderem A, Underhill DM. Mechanisms of phagocytosis in macrophages. *Annu Rev Immunol* (1999) 17:593–623. doi:10.1146/annurev.immunol.17.1.593
8. Nathan C. Neutrophils and immunity: challenges and opportunities. *Nat Rev Immunol* (2006) 6(3):173–82. doi:10.1038/nri1785
9. Laskin DL, Sunil VR, Gardner CR, Laskin JD. Macrophages and tissue injury: agents of defense or destruction? *Annu Rev Pharmacol Toxicol* (2011) 51:267–88. doi:10.1146/annurev.pharmtox.010909.105812
10. Wick P, Louw-Gaume AE, Kucki M, Krug HF, Kostarelos K, Fadeel B, et al. Classification framework for graphene-based materials. *Angew Chem Int Ed Engl* (2014) 53(30):7714–8. doi:10.1002/anie.201403335
11. Kotchey GP, Hasan SA, Kapralov AA, Ha SH, Kim K, Shvedova AA, et al. A natural vanishing act: the enzyme-catalyzed degradation of carbon nanomaterials. *Acc Chem Res* (2012) 45(10):1770–81. doi:10.1021/ar300106h
12. Chen M, Qin X, Zeng G. Biodegradation of carbon nanotubes, graphene, and their derivatives. *Trends Biotechnol* (2017). doi:10.1016/j.tibtech.2016.12.001
13. Rietschel ET, Kirikae T, Schade FU, Mamut U, Schmidt G, Loppnow H, et al. Bacterial endotoxin: molecular relationships of structure to activity and function. *FASEB J* (1994) 8:217–25.
14. Bishop RE. Fundamentals of endotoxin structure and function. *Contrib Microbiol* (2005) 12:1–27. doi:10.1159/000081687
15. Vallhov H, Qin J, Johansson SM, Ahlborg N, Muhammed MA, Scheinyus A, et al. The importance of an endotoxin-free environment during the production of nanoparticles used in medical applications. *Nano Lett* (2006) 6(8):1682–6. doi:10.1021/nl060860z
16. Delogu LG, Stanford SM, Santelli E, Magrini A, Bergamaschi A, Motamedchaboki K, et al. Carbon nanotube-based nanocarriers: the importance of keeping it clean. *J Nanosci Nanotechnol* (2010) 10(8):5293–301. doi:10.1166/jnn.2010.3083
17. Dobrovolskaia MA, Germolec DR, Weaver JL. Evaluation of nanoparticle immunotoxicity. *Nat Nanotechnol* (2009) 4(7):411–4. doi:10.1038/nnano.2009.175
18. Li Y, Boraschi D. Endotoxin contamination: a key element in the interpretation of nanosafety studies. *Nanomedicine (Lond)* (2016) 11(3):269–87. doi:10.2217/nmm.15.196
19. Hoffmann S, Peterbauer A, Schindler S, Fennrich S, Poole S, Mistry Y, et al. International validation of novel pyrogen tests based on human monocytoid cells. *J Immunol Methods* (2005) 298:161–73. doi:10.1016/j.jim.2005.01.010
20. Dobrovolskaia MA, Neun BW, Clogston JD, Ding H, Ljubimova J, McNeil SE. Ambiguities in applying traditional *Limulus* amebocyte lysate tests to quantify endotoxin in nanoparticle formulations. *Nanomedicine (Lond)* (2010) 5:555–62. doi:10.2217/nmm.10.29
21. Smulders S, Kaiser JP, Zuin S, Van Landuyt KL, Golanski L, Vanoirbeek J, et al. Contamination of nanoparticles by endotoxin: evaluation of different test methods. *Part Fibre Toxicol* (2012) 9:41. doi:10.1186/1743-8977-9-41
22. Kucki M, Cavelius C, Kraegeloh A. Interference of silica nanoparticles with the traditional *Limulus* amebocyte lysate gel clot assay. *Innate Immun* (2014) 20:327–36. doi:10.1177/1753425913492833
23. Mukherjee SP, Lozano N, Kucki M, Del Rio-Castillo AE, Newman L, Vázquez E, et al. Detection of endotoxin contamination of graphene based materials using the TNF- $\alpha$  expression test and guidelines for endotoxin-free graphene oxide production. *PLoS One* (2016) 11(11):e0166816. doi:10.1371/journal.pone.0166816
24. Yang M, Nie X, Meng J, Liu J, Sun Z, Xu H. Carbon nanotubes activate *Limulus* amebocyte lysate coagulation by interface adsorption. *ACS Appl Mater Interfaces* (2017) 9(10):8450–4. doi:10.1021/acsami.7b00543
25. Lahiani MH, Gokulan K, Williams K, Khodakovskaya MV, Khare S. Graphene and carbon nanotubes activate different cell surface receptors on macrophages before and after deactivation of endotoxins. *J Appl Toxicol* (2017). doi:10.1002/jat.3477
26. Monopoli MP, Åberg C, Salvati A, Dawson KA. Biomolecular coronas provide the biological identity of nanosized materials. *Nat Nanotechnol* (2012) 7(12):779–86. doi:10.1038/nnano.2012.207
27. Cedervall T, Lynch I, Lindman S, Berggård T, Thulin E, Nilsson H, et al. Understanding the nanoparticle-protein corona using methods to quantify exchange rates and affinities of proteins for nanoparticles. *Proc Natl Acad Sci U S A* (2007) 104(7):2050–5. doi:10.1073/pnas.0608582104
28. Lundqvist M, Stigler J, Elia G, Lynch I, Cedervall T, Dawson KA. Nanoparticle size and surface properties determine the protein corona with possible implications for biological impacts. *Proc Natl Acad Sci U S A* (2008) 105(38):14265–70. doi:10.1073/pnas.0805135105
29. Saha K, Rahimi M, Yazdani M, Kim ST, Moyano DF, Hou S, et al. Regulation of macrophage recognition through the interplay of nanoparticle surface functionality and protein corona. *ACS Nano* (2016) 10(4):4421–30. doi:10.1021/acsnano.6b00053
30. Walkey CD, Olsen JB, Song F, Liu R, Guo H, Olsen DW, et al. Protein corona fingerprinting predicts the cellular interaction of gold and silver nanoparticles. *ACS Nano* (2014) 8(3):2439–55. doi:10.1021/nn406018q
31. Bertoli F, Garry D, Monopoli MP, Salvati A, Dawson KA. The intracellular destiny of the protein corona: a study on its cellular internalization and evolution. *ACS Nano* (2016) 10(11):10471–9. doi:10.1021/acsnano.6b006411
32. Ge C, Du J, Zhao L, Wang L, Liu Y, Li D, et al. Binding of blood proteins to carbon nanotubes reduces cytotoxicity. *Proc Natl Acad Sci U S A* (2011) 108(41):16968–73. doi:10.1073/pnas.1105270108
33. Chong Y, Ge C, Yang Z, Garate JA, Gu Z, Weber JK, et al. Reduced cytotoxicity of graphene nanosheets mediated by blood-protein coating. *ACS Nano* (2015) 9(6):5713–24. doi:10.1021/nn5066606
34. Duan G, Kang SG, Tian X, Garate JA, Zhao L, Ge C, et al. Protein corona mitigates the cytotoxicity of graphene oxide by reducing its physical interaction with cell membrane. *Nanoscale* (2015) 7(37):15214–24. doi:10.1039/c5nr01839k
35. Luan B, Huynh T, Zhao L, Zhou R. Potential toxicity of graphene to cell functions via disrupting protein-protein interactions. *ACS Nano* (2015) 9(1):663–9. doi:10.1021/nn506011j
36. Dreyer DR, Park S, Bielawski CW, Ruoff RS. The chemistry of graphene oxide. *Chem Soc Rev* (2010) 39(1):228–40. doi:10.1039/b917103g
37. Wang S, Zhang Y, Abidi N, Cabrales L. Wettability and surface free energy of graphene films. *Langmuir* (2009) 25(18):11078–81. doi:10.1021/la901402f
38. Kim J, Cote LJ, Kim F, Yuan W, Shull KR, Huang J. Graphene oxide sheets at interfaces. *J Am Chem Soc* (2010) 132(23):8180–6. doi:10.1021/ja102777p
39. Moghimi SM, Hunter AC, Andrenes TL. Factors controlling nanoparticle pharmacokinetics: an integrated analysis and perspective. *Annu Rev Pharmacol Toxicol* (2012) 52:481–503. doi:10.1146/annurev-pharmtox-010611-134623
40. Tenzer S, Docter D, Kuharev J, Musyanovich A, Fetz V, Hecht R, et al. Rapid formation of plasma protein corona critically affects nanoparticle pathophysiology. *Nat Nanotechnol* (2013) 8(10):772–81. doi:10.1038/nnano.2013.181
41. Sacchetti C, Motamedchaboki K, Magrini A, Palmieri G, Mattei M, Bernardini S, et al. Surface polyethylene glycol conformation influences the protein corona of polyethylene glycol-modified single-walled carbon nanotubes: potential implications on biological performance. *ACS Nano* (2013) 7(3):1974–89. doi:10.1021/nn400409h
42. Ricklin D, Hajishengallis G, Yang K, Lambris JD. Complement: a key system for immune surveillance and homeostasis. *Nat Immunol* (2010) 11(9):785–97. doi:10.1038/ni.1923
43. Belling JN, Jackman JA, Yorulmaz Avsar S, Park JH, Wang Y, Potroz MG, et al. Stealth immune properties of graphene oxide enabled by surface-bound complement factor H. *ACS Nano* (2016) 10(11):10161–72. doi:10.1021/acsnano.6b05409
44. Moghimi SM, Andersen AJ, Hashemi SH, Lettieri B, Ahmadvand D, Hunter AC, et al. Complement activation cascade triggered by PEG-PL engineered nanomedicines and carbon nanotubes: the challenges ahead. *J Control Release* (2010) 146(2):175–81. doi:10.1016/j.jconrel.2010.04.003
45. Salvador-Morales C, Flahaut E, Sim E, Sloan J, Green ML, Sim RB. Complement activation and protein adsorption by carbon nanotubes. *Mol Immunol* (2006) 43(3):193–201. doi:10.1016/j.molimm.2005.02.006
46. Andersen AJ, Robinson JT, Dai H, Hunter AC, Andrenes TL, Moghimi SM. Single-walled carbon nanotube surface control of complement recognition and activation. *ACS Nano* (2013) 7(2):1108–19. doi:10.1021/nn3055175

47. Tan X, Feng L, Zhang J, Yang K, Zhang S, Liu Z, et al. Functionalization of graphene oxide generates a unique interface for selective serum protein interactions. *ACS Appl Mater Interfaces* (2013) 5(4):1370–7. doi:10.1021/am302706g
48. Wibroe PP, Petersen SV, Bovet N, Laursen BW, Moghimi SM. Soluble and immobilized graphene oxide activates complement system differently dependent on surface oxidation state. *Biomaterials* (2016) 78:20–6. doi:10.1016/j.biomaterials.2015.11.028
49. Mahon E, Salvati A, Baldelli Bombelli F, Lynch I, Dawson KA. Designing the nanoparticle-biomolecule interface for “targeting and therapeutic delivery”. *J Control Release* (2012) 161(2):164–74. doi:10.1016/j.jconrel.2012.04.009
50. Schöttler S, Landfester K, Mailänder V. Controlling the stealth effect of nanocarriers through understanding the protein corona. *Angew Chem Int Ed Engl* (2016) 55(31):8806–15. doi:10.1002/anie.201602233
51. Schöttler S, Becker G, Winzen S, Steinbach T, Mohr K, Landfester K, et al. Protein adsorption is required for stealth effect of poly(ethylene glycol)- and poly(phosphoester)-coated nanocarriers. *Nat Nanotechnol* (2016) 11(4):372–7. doi:10.1038/nnano.2015.330
52. Luo N, Ni D, Yue H, Wei W, Ma G. Surface-engineered graphene navigate divergent biological outcomes toward macrophages. *ACS Appl Mater Interfaces* (2015) 7(9):5239–47. doi:10.1021/am5084607
53. Luo N, Weber JK, Wang S, Luan B, Yue H, Xi X, et al. PEGylated graphene oxide elicits strong immunological responses despite surface passivation. *Nat Commun* (2017) 8:14537. doi:10.1038/ncomms14537
54. Xu M, Zhu J, Wang F, Xiong Y, Wu Y, Wang Q, et al. Improved in vitro and in vivo biocompatibility of graphene oxide through surface modification: poly(acrylic acid)-functionalization is superior to PEGylation. *ACS Nano* (2016) 10(3):3267–81. doi:10.1021/acsnano.6b00539
55. Cho YC, Pak PJ, Joo YH, Lee HS, Chung N. In vitro and in vivo comparison of the immunotoxicity of single- and multi-layered graphene oxides with or without pluronic F-127. *Sci Rep* (2016) 6:38884. doi:10.1038/srep38884
56. Russier J, Treossi E, Scarsi A, Perrozzi F, Dumortier H, Ottaviano L, et al. Evidencing the mask effect of graphene oxide: a comparative study on primary human and murine phagocytic cells. *Nanoscale* (2013) 5(22):11234–47. doi:10.1039/c3nr03543c
57. Ma J, Liu R, Wang X, Liu Q, Chen Y, Valle RP, et al. Crucial role of lateral size for graphene oxide in activating macrophages and stimulating pro-inflammatory responses in cells and animals. *ACS Nano* (2015) 9(10):10498–515. doi:10.1021/acsnano.5b04751
58. Orecchioni M, Jasim DA, Pescatori M, Manetti R, Fozza C, Sgarrella F, et al. Molecular and genomic impact of large and small lateral dimension graphene oxide sheets on human immune cells from healthy donors. *Adv Health Mater* (2016) 5(2):276–87. doi:10.1002/adhm.201500606
59. Li Y, Yuan H, von dem Bussche A, Creighton M, Hurt RH, Kane AB, et al. Graphene microsheets enter cells through spontaneous membrane penetration at edge asperities and corner sites. *Proc Natl Acad Sci U S A* (2013) 110(30):12295–300. doi:10.1073/pnas.1222276110
60. Wu C, Wang C, Zheng J, Luo C, Li Y, Guo S, et al. Vacuolization in cytoplasm and cell membrane permeability enhancement triggered by micrometer-sized graphene oxide. *ACS Nano* (2015) 9(8):7913–24. doi:10.1021/acsnano.5b01685
61. Zhu J, Xu M, Gao M, Zhang Z, Xu Y, Xia T, et al. Graphene oxide induced perturbation to plasma membrane and cytoskeletal meshwork sensitize cancer cells to chemotherapeutic agents. *ACS Nano* (2017) 11(3):2637–51. doi:10.1021/acsnano.6b07311
62. Duan G, Zhang Y, Luan B, Weber JK, Zhou RW, Yang Z, et al. Graphene-induced pore formation on cell membranes. *Sci Rep* (2017) 7:42767. doi:10.1038/srep42767
63. Pham VT, Truong VK, Quinn MD, Notley SM, Guo Y, Baulin VA, et al. Graphene induces formation of pores that kill spherical and rod-shaped bacteria. *ACS Nano* (2015) 9(8):8458–67. doi:10.1021/acsnano.5b03368
64. Tu Y, Lv M, Xiu P, Huynh T, Zhang M, Castelli M, et al. Destructive extraction of phospholipids from *Escherichia coli* membranes by graphene nanosheets. *Nat Nanotechnol* (2013) 8(8):594–601. doi:10.1038/nnano.2013.125
65. Sun C, Wakefield DL, Han Y, Muller DA, Holowka DA, Baird BA, et al. Graphene oxide nanosheets stimulate ruffling and shedding of mammalian cell plasma membranes. *Chem* (2016) 1(2):273–86. doi:10.1016/j.chempr.2016.06.019
66. Bussy C, Kostarelos K. Culture media critically influence graphene oxide effects on plasma membranes. *Chem* (2017) 2(3):322–3. doi:10.1016/j.chempr.2017.01.015
67. Lunov O, Syrovets T, Loos C, Beil J, Delacher M, Tron K, et al. Differential uptake of functionalized polystyrene nanoparticles by human macrophages and a monocytic cell line. *ACS Nano* (2011) 5(3):1657–69. doi:10.1021/nn2000756
68. Gallud A, Bondarenko O, Feliu N, Kupferschmidt N, Atluri R, Garcia-Bennett A, et al. Macrophage activation status determines the internalization of mesoporous silica particles of different sizes: exploring the role of different pattern recognition receptors. *Biomaterials* (2017) 121:28–40. doi:10.1016/j.biomaterials.2016.12.029
69. MacParland SA, Tsoi KM, Ouyang B, Ma XZ, Manuel J, Fawaz A, et al. Phenotype determines nanoparticle uptake by human macrophages from liver and blood. *ACS Nano* (2017) 11(3):2428–43. doi:10.1021/acsnano.6b06245
70. Broz P, Dixit VM. Inflammasomes: mechanism of assembly, regulation and signalling. *Nat Rev Immunol* (2016) 16:407–20. doi:10.1038/nri.2016.58
71. Martinon F, Pétrilli V, Mayor A, Tardivel A, Tschoopp J. Gout-associated uric acid crystals activate the NALP3 inflammasome. *Nature* (2006) 440(7081):237–41. doi:10.1038/nature04516
72. Duewell P, Kono H, Rayner KJ, Sirois CM, Vladimer G, Bauernfeind FG, et al. NLRP3 inflammasomes are required for atherosclerosis and activated by cholesterol crystals. *Nature* (2010) 464(7293):1357–61. doi:10.1038/nature08938
73. Palomäki J, Välimäki E, Sund J, Vippola M, Clausen PA, Jensen KA, et al. Long, needle-like carbon nanotubes and asbestos activate the NLRP3 inflammasome through a similar mechanism. *ACS Nano* (2011) 5(9):6861–70. doi:10.1021/nn200595c
74. Sun B, Wang X, Ji Z, Wang M, Liao YP, Chang CH, et al. NADPH oxidase-dependent NLRP3 inflammasome activation and its important role in lung fibrosis by multiwalled carbon nanotubes. *Small* (2015) 11(17):2087–97. doi:10.1002/smll.201402859
75. Yang M, Flavin K, Kopf I, Radics G, Hearnden CH, McManus GJ, et al. Functionalization of carbon nanoparticles modulates inflammatory cell recruitment and NLRP3 inflammasome activation. *Small* (2013) 9(24):4194–206. doi:10.1002/smll.201300481
76. Andón FT, Mukherjee SP, Gessner I, Wortmann L, Xiao L, Hultenby K, et al. Hollow carbon spheres trigger inflammasome-dependent IL-1 $\beta$  secretion in macrophages. *Carbon N Y* (2017) 113:243–51. doi:10.1016/j.carbon.2016.11.049
77. Wang X, Duch MC, Mansukhani N, Ji Z, Liao YP, Wang M, et al. Use of a pro-fibrogenic mechanism-based predictive toxicological approach for tiered testing and decision analysis of carbonaceous nanomaterials. *ACS Nano* (2015) 9(3):3032–43. doi:10.1021/nn507243w
78. Bhattacharya K, Andón FT, El-Sayed R, Fadeel B. Mechanisms of carbon nanotube-induced toxicity: focus on pulmonary inflammation. *Adv Drug Deliv Rev* (2013) 65(15):2087–97. doi:10.1016/j.addr.2013.05.012
79. Jessop F, Holian A. Extracellular HMGB1 regulates multi-walled carbon nanotube-induced inflammation in vivo. *Nanotoxicology* (2015) 9(3):365–72. doi:10.3109/17435390.2014.933904
80. Warnatsch A, Ioannou M, Wang Q, Papayannopoulos V. Neutrophil extracellular traps license macrophages for cytokine production in atherosclerosis. *Science* (2015) 349(6245):316–20. doi:10.1126/science.aaa8064
81. Gay NJ, Symmons MF, Gangloff M, Bryant CE. Assembly and localization of toll-like receptor signalling complexes. *Nat Rev Immunol* (2014) 14(8):546–58. doi:10.1038/nri3713
82. Manček-Keber M, Jerala R. Postulates for validating TLR4 agonists. *Eur J Immunol* (2015) 45(2):356–70. doi:10.1002/eji.201444462
83. Seong SY, Matzinger P. Hydrophobicity: an ancient damage-associated molecular pattern that initiates innate immune responses. *Nat Rev Immunol* (2004) 4(6):469–78. doi:10.1038/nri1372
84. Qu G, Liu S, Zhang S, Wang L, Wang X, Sun B, et al. Graphene oxide induces toll-like receptor 4 (TLR4)-dependent necrosis in macrophages. *ACS Nano* (2013) 7(7):5732–45. doi:10.1021/nn402330b
85. Chen GY, Yang HJ, Lu CH, Chao YC, Hwang SM, Chen CL, et al. Simultaneous induction of autophagy and toll-like receptor signaling pathways by graphene oxide. *Biomaterials* (2012) 33(27):6559–69. doi:10.1016/j.biomaterials.2012.05.064

86. Shurin MR, Yanamala N, Kisin ER, Tkach AV, Shurin GV, Murray AR, et al. Graphene oxide attenuates Th2-type immune responses, but augments airway remodeling and hyperresponsiveness in a murine model of asthma. *ACS Nano* (2014) 8(6):5585–99. doi:10.1021/nn406454u
87. Zhu Z, Zheng T, Homer RJ, Kim YK, Chen NY, Cohn L, et al. Acidic mammalian chitinase in asthmatic Th2 inflammation and IL-13 pathway activation. *Science* (2004) 304(5677):1678–82. doi:10.1126/science.1095336
88. Brinkmann V, Reichard U, Goosmann C, Fauler B, Uhlemann Y, Weiss DS, et al. Neutrophil extracellular traps kill bacteria. *Science* (2004) 303(5663):1532–5. doi:10.1126/science.1092385
89. Papayannopoulos V, Zychlinsky A. NETs: a new strategy for using old weapons. *Trends Immunol* (2009) 30(11):513–21. doi:10.1016/j.it.2009.07.011
90. Branzk N, Lubojemska A, Hardison SE, Wang Q, Gutierrez MG, Brown GD, et al. Neutrophils sense microbe size and selectively release neutrophil extracellular traps in response to large pathogens. *Nat Immunol* (2014) 15(11):1017–25. doi:10.1038/ni.2987
91. Jorch SK, Kubes P. An emerging role for neutrophil extracellular traps in noninfectious disease. *Nat Med* (2017) 23(3):279–87. doi:10.1038/nm.4294
92. Schauer C, Janko C, Munoz LE, Zhao Y, Kienhöfer D, Frey B, et al. Aggregated neutrophil extracellular traps limit inflammation by degrading cytokines and chemokines. *Nat Med* (2014) 20(5):511–7. doi:10.1038/nm.3547
93. Muñoz LE, Bilyy R, Biermann MH, Kienhöfer D, Maueröder C, Hahn J, et al. Nanoparticles size-dependently initiate self-limiting NETosis-driven inflammation. *Proc Natl Acad Sci USA* (2016) 113(40):E5856–65. doi:10.1073/pnas.1602230113
94. Steinman RM. Decisions about dendritic cells: past, present, and future. *Annu Rev Immunol* (2012) 30:1–22. doi:10.1146/annurev-immunol-100311-102839
95. Tkach AV, Yanamala N, Stanley S, Shurin MR, Shurin GV, Kisin ER, et al. Graphene oxide, but not fullerenes, targets immunoproteasomes and suppresses antigen presentation by dendritic cells. *Small* (2013) 9(9–10):1686–90. doi:10.1002/smll.201201546
96. De Gregorio E, Tritto E, Rappuoli R. Alum adjuvanticity: unraveling a century old mystery. *Eur J Immunol* (2008) 38(8):2068–71. doi:10.1002/eji.200838648
97. Kool M, Pétrilli V, De Smedt T, Rolaz A, Hammad H, van Nimwegen M, et al. Cutting edge: alum adjuvant stimulates inflammatory dendritic cells through activation of the NALP3 inflammasome. *J Immunol* (2008) 181(6):3755–9. doi:10.4049/jimmunol.181.6.3755
98. Eisenbarth SC, Colegio OR, O'Connor W, Sutterwala FS, Flavell RA. Crucial role for the Nalp3 inflammasome in the immunostimulatory properties of aluminum adjuvants. *Nature* (2008) 453(7198):1122–6. doi:10.1038/nature06939
99. Sun B, Ji Z, Liao YP, Wang M, Wang X, Dong J, et al. Engineering an effective immune adjuvant by designed control of shape and crystallinity of aluminum oxyhydroxide nanoparticles. *ACS Nano* (2013) 7(12):10834–49. doi:10.1021/nn404211j
100. Rettig L, Haen SP, Bittermann AG, von Boehmer L, Curioni A, Krämer SD, et al. Particle size and activation threshold: a new dimension of danger signaling. *Blood* (2010) 115(22):4533–41. doi:10.1182/blood-2009-11-247817
101. Li H, Fierens K, Zhang Z, Vanparijs N, Schuijs MJ, Van Steendam K, et al. Spontaneous protein adsorption on graphene oxide nanosheets allowing efficient intracellular vaccine protein delivery. *ACS Appl Mater Interfaces* (2016) 8(2):1147–55. doi:10.1021/acsmami.5b08963
102. Xu L, Xiang J, Liu Y, Xu J, Luo Y, Feng L, et al. Functionalized graphene oxide serves as a novel vaccine nano-adjuvant for robust stimulation of cellular immunity. *Nanoscale* (2016) 8(6):3785–95. doi:10.1039/c5nr09208f
103. Meng C, Zhi X, Li C, Li C, Chen Z, Qiu X, et al. Graphene oxides decorated with carnosine as an adjuvant to modulate innate immune and improve adaptive immunity in vivo. *ACS Nano* (2016) 10(2):2203–13. doi:10.1021/acsnano.5b06750
104. Lingwood D, Simons K. Lipid rafts as a membrane-organizing principle. *Science* (2010) 327(5961):46–50. doi:10.1126/science.1174621
105. Flach TL, Ng G, Hari A, Desrosiers MD, Zhang P, Ward SM, et al. Alum interaction with dendritic cell membrane lipids is essential for its adjuvanticity. *Nat Med* (2011) 17(4):479–87. doi:10.1038/nm.2306

**Conflict of Interest Statement:** The authors declare that the research was conducted in the absence of any commercial or financial relationships that could be construed as a potential conflict of interest.

Copyright © 2017 Mukherjee, Bottini and Fadeel. This is an open-access article distributed under the terms of the Creative Commons Attribution License (CC BY). The use, distribution or reproduction in other forums is permitted, provided the original author(s) or licensor are credited and that the original publication in this journal is cited, in accordance with accepted academic practice. No use, distribution or reproduction is permitted which does not comply with these terms.



# Intrinsic and Extrinsic Properties Affecting Innate Immune Responses to Nanoparticles: The Case of Cerium Oxide

**Eudald Casals<sup>1</sup>, Muriel F. Gusta<sup>1</sup>, Jordi Piella<sup>2</sup>, Gregori Casals<sup>3</sup>, Vladimiro Jiménez<sup>3,4</sup> and Victor Puntes<sup>1,2,5\*</sup>**

<sup>1</sup>Vall d'Hebron Institut of Research (VHIR), Barcelona, Spain, <sup>2</sup>Institut Català de Nanociència i Nanotecnologia (ICN2), CSIC and The Barcelona Institute of Science and Technology (BIST), Campus UAB, Barcelona, Spain, <sup>3</sup>Biochemistry and Molecular Genetics Service, Hospital Clínic Universitari, IDIBAPS, CIBERehd, Barcelona, Spain, <sup>4</sup>Department of Biomedicine, University of Barcelona, Barcelona, Spain, <sup>5</sup>Institució Catalana de Recerca i Estudis Avançats (ICREA), Barcelona, Spain

## OPEN ACCESS

### Edited by:

Lucio Roberto Cançado Castellano,  
Federal University of Paraíba,  
Brazil

### Reviewed by:

Martin J. D. Clift,  
Swansea University,  
United Kingdom  
Nicolas Riteau,  
National Institutes of Health,  
United States  
Wolfgang Parak,  
Philipps University of Marburg,  
Germany  
Liberato Manra,  
Fondazione Istituto Italiano  
di Tecnologia, Italy

### \*Correspondence:

Victor Puntes  
victor.puntes@vhir.org

### Specialty section:

This article was submitted  
to Inflammation,  
a section of the journal  
*Frontiers in Immunology*

**Received:** 28 February 2017

**Accepted:** 28 July 2017

**Published:** 14 August 2017

### Citation:

Casals E, Gusta MF, Piella J, Casals G, Jiménez W and Puntes V (2017) Intrinsic and Extrinsic Properties Affecting Innate Immune Responses to Nanoparticles: The Case of Cerium Oxide. *Front. Immunol.* 8:970.  
doi: 10.3389/fimmu.2017.00970

We review the apparent discrepancies between studies that report anti-inflammatory effects of cerium oxide nanoparticles ( $\text{CeO}_2$  NPs) through their reactive oxygen species-chelating properties and immunological studies highlighting their toxicity. We observe that several underappreciated parameters, such as aggregation size and degree of impurity, are critical determinants that need to be carefully addressed to better understand the NP biological effects in order to unleash their potential clinical benefits. This is because NPs can evolve toward different states, depending on the environment where they have been dispersed and how they have been dispersed. As a consequence, final characteristics of NPs can be very different from what was initially designed and produced in the laboratory. Thus, aggregation, corrosion, and interaction with extracellular matrix proteins critically modify NP features and fate. These modifications depend to a large extent on the characteristics of the biological media in which the NPs are dispersed. As a consequence, when reviewing the scientific literature, it seems that the aggregation state of NPs, which depends on the characteristics of the dispersing media, may be more significant than the composition or original size of the NPs. In this work, we focus on  $\text{CeO}_2$  NPs, which are reported sometimes to be protective and anti-inflammatory, and sometimes toxic and pro-inflammatory.

**Keywords:** nanoparticles, cerium oxide, nanoparticle evolution, nanoparticle agglomeration, ion leaching, antioxidant activity, inflammation, immune response

## INTRODUCTION

Nanotechnology has already qualified as the industrial revolution of the twenty-first century. Although its development is a logical continuation of the development of microelectronics and colloid chemistry, the beginning of the *nano era* corresponds, for most people, with Smalley's synthesis of fullerene ( $\text{C}_{60}$ ) (1). Since then, organic nanomaterials (e.g.,  $\text{C}_{60}$ , carbon nanotubes, graphene) have garnered much interest, but have also generated concerns regarding toxicity (2–4). Meanwhile, the development of inorganic nanomaterials has caused far less controversy, and it is only in the past few years that some of these materials (e.g.,  $\text{TiO}_2$ , Ag,  $\text{Fe}_3\text{O}_4$ ) have come under closer scrutiny to address human and environmental toxicity issues (5–7). It has also become increasingly common to examine the effects of a nanocomposite or nano-enabled products instead of the pristine nanoparticle (NP)

alone. Indeed, the effects of the “active ingredient” can be (and actually often are) deeply modified by the formulation of the final product and the properties of the media in which it is dispersed. This highlights the complexity of addressing the fate of a nanomaterial through its life cycle in a meaningful manner.

Cerium oxide nanoparticles ( $\text{CeO}_2$  NPs) have recently received much attention because of their excellent catalytic redox properties (8). In addition to being a rather chemically inert ceramic, a  $\text{CeO}_2$  nanocrystal has a fluorite-like structure where the unfilled 4f electronic orbital confers it a variety of relevant catalytic properties when it reaches the nanoscale. Consequently, nanoceria has been used in the petrochemical industry and in catalytic exhaust converters for decades.  $\text{CeO}_2$  NPs have high capacity to buffer electrons in redox environments due to the ease of oxidation and reduction from  $\text{Ce}^{3+}$  to  $\text{Ce}^{4+}$  and *vice versa* (9, 10), followed by the capture or release of oxygen. As a consequence, they act as *electron sponges* in the presence of free radicals degrading thus reactive oxygen species (ROS) (11). In detail, inflammation and oxidative stress are interconnected processes that contribute decisively to the pathogenesis of many diseases, including highly prevalent, age-related disorders, such as obesity, cardiovascular disease, diabetes mellitus, cancer, chronic respiratory diseases, and neurological diseases. Mutual stimulation between oxidative stress and inflammation contributes decisively to the chronic nature of these diseases. Oxidative stress involves elevated intracellular levels of ROS, such as peroxides, superoxides, hydroxyl radicals, and singlet oxygen, which have critical roles in physiological processes through the regulation of cell signaling cascades. Prolonged exposure to high ROS concentrations damages proteins, lipids, and nucleic acids, causing various metabolic complications.

Thus,  $\text{CeO}_2$  NPs in the size range of 3–50 nm have recently received increased attention for their participation in biochemical redox reactions, providing sites for free radical scavenging and reducing inflammation (12–14). Thus,  $\text{CeO}_2$  NPs have been reported to confer cellular protection, especially in the reduction of oxidative and nitrosative stress in living organisms, and are considered an alternative approach offering new opportunities for the treatment of physiopathological processes leading to chronic inflammation (15).

In this regard, most therapeutic  $\text{CeO}_2$  NPs applications are proposed based on their ability to reduce ROS levels and consequently, the levels of most inflammatory mediators, such as inducible nitric oxide synthase, nuclear factor  $\kappa\beta$ , tumor necrosis factor- $\alpha$ , and interleukins (16–19). Indeed,  $\text{CeO}_2$  NPs were recently found to have multi-enzyme mimetic properties, including those related to superoxide dismutase (SOD), catalase, and oxidase (8). In this context,  $\text{CeO}_2$  NPs have potential applications in many different medical fields. For example, in cardiology, intravenously administered  $\text{CeO}_2$  NPs in a transgenic murine model of cardiomyopathy were proved to reduce the myocardial oxidative stress, the endoplasmic reticulum stress, and suppress the inflammatory process, ensuring protection against progression of cardiac dysfunction (20). In oncology, antioxidant properties of  $\text{CeO}_2$  NPs were successfully tested to protect cells from radiation-induced damage (21). In another study, CRL8798 cells (immortalized normal human breast epithelial cell line) and MCF-7 (a breast carcinoma cell line), were exposed to radiation and  $\text{CeO}_2$  NPs were reported

to confer radioprotection to the normal human breast line but not to the tumoral one (22). In hepatology,  $\text{CeO}_2$  NPs were shown to display hepatoprotective effects against steatosis in rats with diet-induced non-alcoholic steatohepatitis (23) and to reduce steatosis, portal pressure, and ameliorate systemic inflammatory biomarkers, attenuating the intensity of the inflammatory response in a model of rats with induced liver fibrosis. In ophthalmology,  $\text{CeO}_2$  NPs are being tested to treat ocular diseases such as macular degeneration and glaucoma. The ability of  $\text{CeO}_2$  NPs to protect retinal neurons was shown for primary cell cultures of dissociated rat retinas injecting the suspension of  $\text{CeO}_2$  NPs into the vitreous of both eyes (9). Similarly, beneficial effects of the use of  $\text{CeO}_2$  NPs have been found in the case of neurodegenerative diseases (24). In this studies,  $\text{CeO}_2$  NPs are shown to display SOD mimetic activity (25, 26), catalase mimetic activity (11, 27), and/or nitric oxide (NO) scavenging abilities (17). Last,  $\text{CeO}_2$  NPs are also amenable to local targeting and delivery, as shown in the works of Li et al., (28) and Xu et al. (29).

## POSITIVE AND NEGATIVE EFFECTS OF NPs

Obviously, the safe and effective use of these promising therapeutic NPs requires the precise assessment of their potential risks and unwanted side effects. Despite the vast range of publications that address the toxicity and safety of nanomaterials, results are still controversial, with different observed effects for similar NPs ranging from severely toxic effects—as in the study of Kovriznykh et al. (30), which assess and compare the acute toxicity of 31 different nanomaterials to fish mature individuals of *Danio rerio*—to innocuous [e.g., Ref. (31)] or beneficial [e.g., Ref. (32, 33)].  $\text{CeO}_2$  NPs are no exception. While they have been reported many times to be safe and beneficial, protecting against oxidative stress (9, 13, 21, 22, 34), other studies, mainly related to the toxicity of  $\text{CeO}_2$  nanopowders employed in industry, reported *in vitro* and *in vivo* toxicity (35, 36). In addition, while some studies report  $\text{CeO}_2$  NP uptake by hepatocytes and anti-inflammatory effects in the liver (14, 37), others report macrophage (Kupffer cell) uptake and proinflammatory effects (38).

At the source of these discrepancies, one can observe the diversity of the materials actually employed in the different studies, which are presented under the same name. For instance, most research regarding  $\text{CeO}_2$  NP toxicity has been performed with commercially available NPs (often supplied in dry aggregated form) in order to assess the consequences of occupational and environmental exposure. These are different materials from those produced by wet chemistry routes in the laboratory, where the NPs are always kept isolated and well dispersed. In addition, for these types of studies, administered doses are usually higher than those proposed in nanomedicine (Figures 1A,B). In addition to their different initial characteristics, these materials are often prone to aggregation when dispersed into biological fluids, such as complete cell culture medium or serum (5, 39). For instance, He et al. (39) showed how intratracheally instilled  $\text{CeO}_2$  NPs into Wistar rats agglomerate and form sediments in the bronchoalveolar medium. Consequently, the actual objects that cells

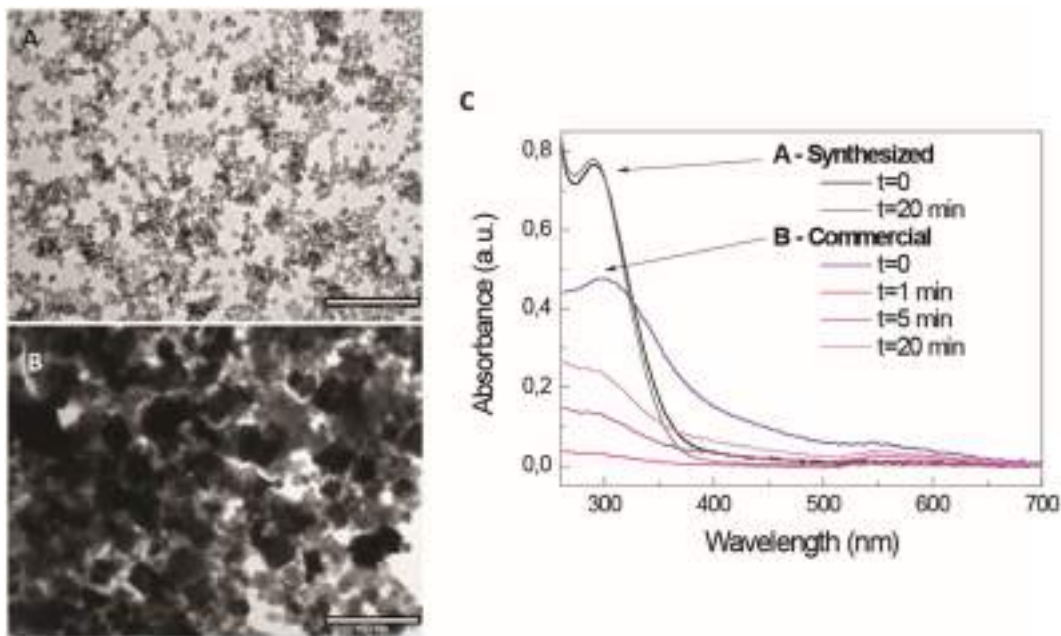


**FIGURE 1 |** Different aspect and stability of commercial and designed  $\text{CeO}_2$  nanoparticles (NPs). Different morphologies and sedimentation behavior of  $\text{CeO}_2$  nanopowders (commercial, nominal size <25 nm) and  $\text{CeO}_2$  NPs synthesized in the laboratory after dispersion in TMAOH 1 mM, a good stabilizer of metal oxide NPs. **(A,B)** Representative TEM images  $\text{CeO}_2$  NPs and  $\text{CeO}_2$  nanopowders, respectively (scale bar = 100 nm); **(C)** UV-VIS spectroscopy measurements over time of both samples after resuspension in TMAOH 1 mM and at the same NP concentration.

encounter may behave very differently from the initially designed and produced NPs (**Figure 1C**).

Comparing studies regarding nanomedicine and nanosafety, it seems that often the differently observed biological effects of NPs are related not only to its parental composition and purity but also to its final aggregation state (40), which is independent of the employed material and can be reproduced with other NPs. For instance, aggregates of  $\text{TiO}_2$  (41),  $\text{Al}_2\text{O}_3$  (42), and  $\text{Fe}_2\text{O}_3$  (43) NPs show similar toxicity to  $\text{CeO}_2$  aggregates (37, 44), as well as  $\text{CeO}_2$  (45) or Au NPs (46) carrying cationic amphiphatic molecules on their surfaces have been observed to be similarly toxic. Regarding aggregates, in the case of  $\text{CeO}_2$ , Rogers et al. (44) evaluate how exposure to different concentrations of aggregated  $\text{CeO}_2$  NPs affects indices of whole animal stress and survivability in *Caenorhabditis elegans*. Results showed that  $\text{CeO}_2$  aggregates promoted strain-dependent decreases in animal fertility, a decline in stress resistance as measured by thermotolerance and shortened worm length. Moreover, chronic exposure of  $\text{CeO}_2$  NP aggregates was found to be associated with increased levels of ROS and heat shock stress response (HSP-4). Regarding surface state, Dowding et al. (45) prepared different samples of  $\text{CeO}_2$  NPs using identical precursor (Cerium nitrate hexahydrate) through similar wet chemical process but using different oxidizer/reducer:  $\text{H}_2\text{O}_2$ ,  $\text{NH}_4\text{OH}$ , or hexamethylenetetramine (HMT). Results showed that unlike the other  $\text{CeO}_2$  NPs preparations, HMT- $\text{CeO}_2$  NPs were readily taken into endothelial cells and reduced cell viability at a 10-fold lower concentration than the others. This indicates that the biological effects of NPs depend not only on intrinsic but also extrinsic features, aspects related to the NP itself and

to its history and environment. Thus, colloidal stability, which determines the agglomeration and sedimentation, depends on the concentration and nature of ions and molecules present in the media at a certain temperature. This affects the hydrodynamic radius, which depends on temperature and viscosity; NP corrosion, which depends on the combined redox potential of the species present in the environment; and speciation of leached ions, which depends on the nature of the dispersing media (**Figure 2A**). The NP concentration will affect the kinetics of the previously coexisting phenomena.

In this context, interactions between NPs and the immune system are of particular interest for both their efficient use and their safety in biomedical applications. NPs are foreign objects, sized within the range of that detected and managed by the immune system, which has a responsibility for categorizing invasion and providing an appropriate response (**Figure 2B**). For example, NPs may exacerbate immune responses by ordering and repetition of ligands (47–49), as well as by altering redox status, both increasing (50) and decreasing ROS and inflammatory mediator levels (14).

## THE APPARENT CONTRADICTION

Lack of understanding NP characteristics and their evolution inside biological media is recognized as one of the key points underpinning the abovementioned controversies (40). Thus, as with many other inorganic NPs employed in nanomedical research,  $\text{CeO}_2$  NPs evolve when in contact with physiological media (5, 51). This evolution may entail the loss of intended catalytic activity, transforming beneficial NPs into deleterious ones.

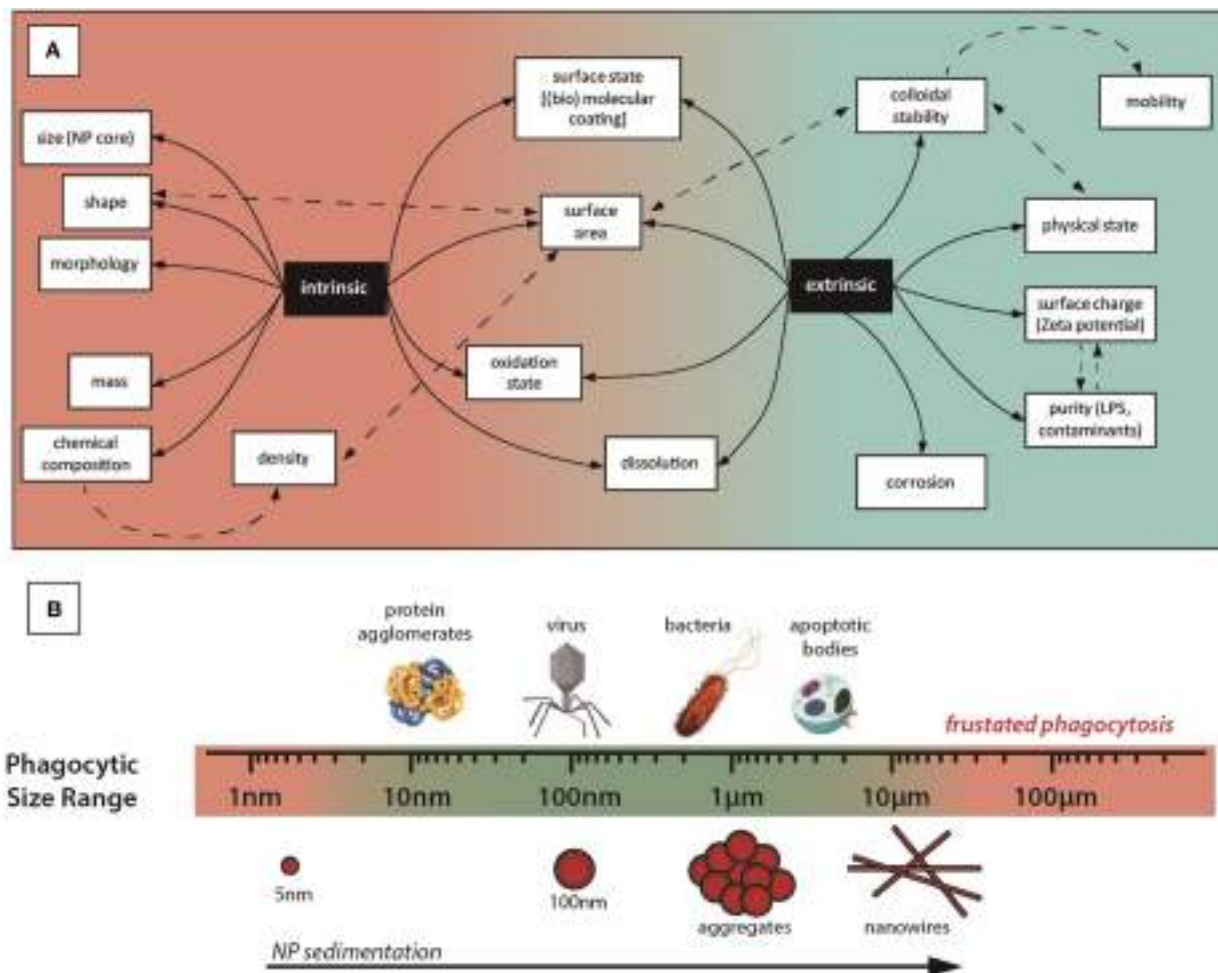


**FIGURE 2 | (A)** Intrinsic and extrinsic properties of nanoparticles (NPs). Different properties of the NP, related to the NP itself (intrinsic) or to the NP behavior in the exposure media (extrinsic). For instance, we can design CeO<sub>2</sub> NPs with specific sizes and shapes, but agglomeration in the exposure media leads to specific surfaces, concentrations, mobilities, etc., very different from the initially prepared NPs. As agglomerated NPs behave as a large particle, this makes the NP more immunogenic and affects the concentration of NPs in different parts of the body, where they are accumulated in organs of the MPS system. Importantly, for the (immuno)toxicity aspects, agglomerates of NPs are no longer on the nanometric regime of sizes and may have similar consequences as the incidental inorganic microparticles, extensively investigated during the last century: burning oil residues, silica from mining or asbestos have been found stacked in affected tissues, causing pathologies such as silicosis, asbestosis, and/or inflammatory reactions. Thus, in this example, even if CeO<sub>2</sub> NPs are not toxic (and therapeutically beneficial) by themselves, they may be risky because they could be a source of toxic aggregates. **(B)** Graphical representative sizes of key entities capable of generating immune response and different NP morphologies and NP aggregates.

The most significant alterations affecting the biological fate and effects of NPs when dispersed in biological media are: (i) agglomeration and aggregation of the NPs (5, 52, 53), (ii) formation of the NP protein corona as a result of the adsorption of proteins onto the inorganic surface (54, 55), and (iii) NP corrosion and/or dissolution into ionic species (56–59). Indeed, it has been proposed that the higher toxicity of unstable preparations of NPs may not be due to the material *per se* but to its rapid aggregation into final micro- or macrometric sizes (5, 51) and the leaching of toxic ionic species into the solution (57). For instance, in the work of Kirchner et al. (57), the release of toxic Cd<sup>2+</sup> ions from CdSe and CdSe/ZnS NPs and their stability toward aggregation were demonstrated to play an important role for the observed cytotoxic effects. Similarly, aggregation of NPs has been shown

to clearly determine the exposure of NPs to cells. Xia et al. (50), comparing the toxicity induced by different ambient and manufactured NPs, showed a dramatic change in their state of aggregation, dispersibility, and charge during transfer from a buffered aqueous solution to cell culture medium and how it affects the observed cellular responses. Cho et al. (60) studied how sedimentation affected the cellular uptake of gold NPs in *in vitro* experiments, dramatically altering their exposure and biological effects. Typically, *in vitro* experiments measure the uptake of NPs by exposing cells at the bottom of a culture plate to a suspension of NPs, and it is generally assumed that the suspension is well dispersed. But, if NPs sediment, their concentration on the cell surface may be higher than the initial bulk concentration, and this could lead to increased uptake by cells. Indeed, results

showed that cellular uptake of gold NPs mostly depended on the sedimentation and the diffusion velocities of the NPs.

Other NP transformations can also alter biological responses, leading to unexpected results. For example, Xue et al. (61) reported that CeO<sub>2</sub> NPs can protect DNA from damage in Tris-HCl and sulfate buffers, but not in phosphate-buffered saline. A mechanism of action was proposed: cerium phosphate is formed on the surface of the NPs, which interferes with redox cycling between Ce<sup>3+</sup> and Ce<sup>4+</sup>. As a result, the antioxidant activity of CeO<sub>2</sub> NPs is greatly affected by the external environment. Similarly, Perez et al. (62) observed that the antioxidant properties of CeO<sub>2</sub> NPs were pH-dependent. They suggested that a high concentration of H<sup>+</sup> interferes with the regeneration of Ce<sup>3+</sup>, resulting in a loss of antioxidant activity. However, disintegration of CeO<sub>2</sub> in acidic media could also account for the observed effects, similar to NP disintegration observed in different media (57, 63).

Given these effects, when conducting studies involving NPs for safety or medicine, it is essential to understand the changes that take place with their insertion into biological media, from complete cell culture media, to full blood, or lymph, to the intracellular cytoplasm. This includes NP colloidal stability, vicinity interactions, chemical transformations, association with plasma proteins, interaction with components of the immune system, and traditional absorption, distribution, metabolism, and excretion studies adapted to the unique specifications of NPs. Additionally, NPs can be complex and composed of different entities, all of which can have different fates. As an example, in the work of Feliu et al. (64), the authors review a vast collection of recent scientific literature indicating that NPs *in vivo* should no longer be considered as homogeneous entities. They conceptually divide a NP into the inorganic core, the engineered surface coating, comprising of the ligand shell and optionally also bioconjugates, and the corona of adsorbed biological molecules. The authors found empirical evidence showing that all of these three described components may degrade individually *in vivo*. Due to this, the life cycle and biodistribution of the whole heterostructure is drastically modified.

## CONCLUDING REMARKS

There is an increasing number of conflicting reports on the impact of CeO<sub>2</sub> NPs on oxidative stress and inflammation,

## REFERENCES

- Kroto HW, Heath JR, O'Brien SC, Curl RF, Smalley RE. C60: buckminsterfullerene. *Nature* (1985) 318(6042):162–3. doi:10.1038/318162a0
- Huczko A, Lange H, Calko E, Grubek-Jaworska H. Physiological testing of carbon nanotubes: are they asbestos-like? *Fullerene Sci Technol* (2001) 9:251–4. doi:10.1081/FST-100102973
- Hughes LS, Cass GR, Gone J, Ames M, Olmez I. Physical and chemical characterization of atmospheric ultrafine particles in the Los Angeles area. *Environ Sci Technol* (1998) 32:1153–61. doi:10.1021/es970280r
- Li X, Brown D, Smith S, MacNee W, Donaldson K. Short-term inflammatory responses following intratracheal instillation of fine and ultrafine carbon black in rats. *Inhal Toxicol* (1999) 11:709–31. doi:10.1080/089583799196826
- Casals E, Vázquez-Campos S, Bastús N, Puntes V. Distribution and potential toxicity of engineered inorganic nanoparticles and carbon nanostructures in biological systems. *Trends Anal Chem* (2008) 27(8):672–83. doi:10.1016/j.trac.2008.06.004
- Nel A, Xia T, Madler L, Li N. Toxic potential of materials at the nanolevel. *Science* (2006) 311(5761):622–7. doi:10.1126/science.1114397
- Oberdorster G, Oberdorster E, Oberdorster J. Nanotoxicology: an emerging discipline evolving from studies of ultrafine particles. *Environ Health Perspect* (2005) 113(7):723–39. doi:10.1289/ehp.7339
- Xu C, Qu X. Cerium oxide nanoparticle: a remarkably versatile rare earth nanomaterial for biological applications. *NPG Asia Mater* (2014) 6:e90. doi:10.1038/am.2013.88
- Chen JP, Patil S, Seal S, McGinnis JF. Rare earth nanoparticles prevent retinal degeneration induced by intracellular peroxides. *Nat Nanotechnol* (2006) 1(2):142–50. doi:10.1038/nnano.2006.91
- Esch F, Fabris S, Zhou L, Montini T, Africh C, Fornasiero P, et al. Electron localization determines defect formation on ceria substrates. *Science* (2005) 309(5735):752–5. doi:10.1126/science.1111568

with some studies reporting the promotion of oxidative stress induced by immune system activation, and others reporting protective effects against inflammatory processes. To overcome this apparent contradiction, understanding the physicochemical transformations and evolution of the NPs in biological systems is imperative. Understanding these mechanisms will enable the design of nanomaterials that work more precisely in medicine and safely in society.

The majority of negative immune effects reported in the scientific literature are related to NP aggregation and contamination, which cause biological effects independent of the composition, size, and shape of individual NPs. Generally, isolated, non-contaminated NPs show no toxicity, while contaminated and aggregated NPs are often described as immunotoxic (65, 66). This is especially dramatic in the case of CeO<sub>2</sub> NPs, which have been reported many times as anti-inflammatory or pro-inflammatory, often without a proper description of the material used or its purity (40).

## AUTHOR CONTRIBUTIONS

All authors listed have made substantial, direct, and intellectual contributions to the work and approved it for publication. VP suggested the topic and provided the concept and design of the work. EC and VP retrieved the relevant literature, compiled all information on the topic, and wrote the mini-review. MG contributed to the design of graphical information. JP contributed to the cerium oxide reactivity sections, retrieving the relevant literature, and participating in the discussion and writing. GC and WJ contributed to the oxidative stress, inflammatory processes, and antioxidant activity sections by retrieving the literature and participating in the discussion and writing.

## FUNDING

GC was supported by a grant from Ministerio de Economía y Competitividad, Instituto de Salud Carlos III PI15/00777. WJ was supported by grants from Ministerio de Economía y Competitividad (SAF2015-6412-R). Financial support from the FutureNanoNeeds Project (GA: 604602) financed by the European Community under the FP7 Programme (FP7-NMP-2013-LARGE-7) is gratefully acknowledged.

11. Cafun JD, Kvashnina KO, Casals E, Puntes VF, Glatzel P. Absence of Ce<sup>3+</sup> sites in chemically active colloidal ceria nanoparticles. *ACS Nano* (2013) 7(12):10726–32. doi:10.1021/nm403542p
12. DeCoteau W, Heckman K, Estevez A, Reed K, Costanzo W, Sandford D, et al. Cerium oxide nanoparticles with antioxidant properties ameliorate strength and prolong life in mouse model of amyotrophic lateral sclerosis. *Nanomedicine* (2016) 12(8):2311–20. doi:10.1016/j.nano.2016.06.009
13. Hirst S, Karakoti A, Tyler R, Sriranganathan N, Seal S, Reilly C. Anti-inflammatory properties of cerium oxide nanoparticles. *Small* (2009) 5(24):2848–56. doi:10.1002/smll.200901048
14. Oro D, Yudina T, Fernandez-Varo G, Casals E, Reichenbach V, Casals G, et al. Cerium oxide nanoparticles reduce steatosis, portal hypertension and display anti-inflammatory properties in rats with liver fibrosis. *J Hepatol* (2016) 64(3):691–8. doi:10.1016/j.jhep.2015.10.020
15. Karakoti AS, Monteiro-Riviere NA, Aggarwal R, Davis JP, Narayan RJ, Self WT, et al. Nanoceria as antioxidant: synthesis and biomedical applications. *JOM* (2008) 60(3):33–7. doi:10.1007/s11837-008-0029-8
16. Colon J, Hsieh N, Ferguson A, Kupelian P, Seal S, Jenkins DW, et al. Cerium oxide nanoparticles protect gastrointestinal epithelium from radiation-induced damage by reduction of reactive oxygen species and upregulation of superoxide dismutase 2. *Nanomedicine* (2010) 6(5):698–705. doi:10.1016/j.nano.2010.01.010
17. Dowding J, Dosani T, Kumar A, Seal S, Self W. Cerium oxide nanoparticles scavenge nitric oxide radical ((NO)-N-center dot). *Chem Commun* (2012) 48(40):4896–8. doi:10.1039/c2cc30485f
18. Estevez AY, Pritchard S, Harper K, Aston JW, Lynch A, Lucky JJ, et al. Neuroprotective mechanisms of cerium oxide nanoparticles in a mouse hippocampal brain slice model of ischemia. *Free Radic Biol Med* (2011) 51(6):1155–63. doi:10.1016/j.freeradbiomed.2011.06.006
19. Selvaraj V, Nepal N, Rogers S, Manne ND, Arvapalli R, Rice KM, et al. Inhibition of MAP kinase/NF- $\kappa$ B mediated signaling and attenuation of lipopolysaccharide induced severe sepsis by cerium oxide nanoparticles. *Biomaterials* (2015) 59:160–71. doi:10.1016/j.biomaterials.2015.04.025
20. Niu JL, Azfer A, Rogers LM, Wang XH, Kolattukudy PE. Cardioprotective effects of cerium oxide nanoparticles in a transgenic murine model of cardiomyopathy. *Cardiovasc Res* (2007) 73(3):549–59. doi:10.1016/j.cardiores.2006.11.031
21. Asati A, Santra S, Kaittanis C, Perez J. Surface-charge-dependent cell localization and cytotoxicity of cerium oxide nanoparticles. *ACS Nano* (2010) 4(9):5321–31. doi:10.1021/nn100816s
22. Tarnuzzer RW, Colon J, Patil S, Seal S. Vacancy engineered ceria nanostructures for protection from radiation-induced cellular damage. *Nano Lett* (2005) 5(12):2573–7. doi:10.1021/nl052024f
23. Carvajal S, Oró D, Fernández-Varo G, Yudina T, Perramón M, Oller L, et al. Therapeutic effect of cerium oxide nanoparticles (CeO<sub>2</sub>NPs) in rats with diet-induced non-alcoholic steatohepatitis. *J Hepatol* (2017) 66(1):S608. doi:10.1016/S0168-8278(17)31652-5
24. Schubert D, Dargusch R, Raitano J, Chan SW. Cerium and yttrium oxide nanoparticles are neuroprotective. *Biochem Biophys Res Commun* (2006) 342(1):86–91. doi:10.1016/j.bbrc.2006.01.129
25. Heckert E, Karakoti A, Seal S, Self W. The role of cerium redox state in the SOD mimetic activity of nanoceria. *Biomaterials* (2008) 29(18):2705–9. doi:10.1016/j.biomaterials.2008.03.014
26. Korsvik C, Patil S, Seal S, Self W. Superoxide dismutase mimetic properties exhibited by vacancy engineered ceria nanoparticles. *Chem Commun* (2007) 10:1056–8. doi:10.1039/b615134e
27. Pirmohamed T, Dowding J, Singh S, Wasserman B, Heckert E, Karakoti A, et al. Nanoceria exhibit redox state-dependent catalase mimetic activity. *Chem Commun* (2010) 46(16):2736–8. doi:10.1039/b922024k
28. Li M, Shi P, Xu C, Ren J, Qu X. Cerium oxide caged metal chelator: anti-aggregation and anti-oxidation integrated H<sub>2</sub>O<sub>2</sub>-responsive controlled drug release for potential Alzheimer's disease treatment. *Chem Sci* (2013) 4:2536–42. doi:10.1039/C3SC50697E
29. Xu C, Lin Y, Wang J, Wu L, Wei W, Ren J, et al. Nanoceria-triggered synergistic drug release based on CeO(2)-capped mesoporous silica host-guest interactions and switchable enzymatic activity and cellular effects of CeO(2). *Adv Health Mater* (2013) 2(12):1591–9. doi:10.1002/adhm.201200464
30. Kovriznych JA, Sotnikova R, Zelenkova D, Rollerova E, Szabova E, Wimmerova S. Acute toxicity of 31 different nanoparticles to zebrafish (*Danio rerio*) tested in adulthood and in early life stages – comparative study. *Interdiscip Toxicol* (2013) 6(2):67–73. doi:10.2478/intox-2013-0012
31. Connor E, Mwamuka J, Gole A, Murphy C, Wyatt M. Gold nanoparticles are taken up by human cells but do not cause acute cytotoxicity. *Small* (2005) 1(3):325–7. doi:10.1002/smll.200400093
32. Schwenk M. Ferumoxytol: a new intravenous iron preparation for the treatment of iron deficiency anemia in patients with chronic kidney disease. *Pharmacotherapy* (2010) 30(1):70–9. doi:10.1592/phco.30.1.70
33. Weissleder R, Stark D, Engelstad B, Bacon B, Compton C, White D, et al. Superparamagnetic iron-oxide – pharmacokinetics and toxicity. *Am J Roentgenol* (1989) 152(1):167–73. doi:10.2214/ajr.152.1.167
34. Minarchick VC, Stapleton PA, Sabolsky EM, Nurkiewicz TR. Cerium dioxide nanoparticle exposure improves microvascular dysfunction and reduces oxidative stress in spontaneously hypertensive rats. *Front Physiol* (2015) 6:339. doi:10.3389/fphys.2015.00339
35. Fisichella M, Berenguer F, Steinmetz G, Auffan M, Rose J, Prat O. Toxicity evaluation of manufactured CeO<sub>2</sub> nanoparticles before and after alteration: combined physicochemical and whole-genome expression analysis in Caco-2 cells. *BMC Genomics* (2014) 15:700. doi:10.1186/1471-2164-15-700
36. Mittal S, Pandey A. Cerium oxide nanoparticles induced toxicity in human lung cells: role of ROS mediated DNA damage and apoptosis. *Biomed Res Int* (2014) 891934. doi:10.1155/2014/891934
37. Oro D, Fernandez-Varo G, Reichenbach V, Yudina T, Casals E, Casals G, et al. Cerium oxide nanoparticles reduce portal hypertension and show anti-inflammatory properties in CCl<sub>4</sub>-treated rats. *Hepatology* (2014) 60:1175A. doi:10.1002/hep.27535
38. Nalabotu S, Kolli M, Triest W, Ma J, Manne N, Katta A, et al. Intratracheal instillation of cerium oxide nanoparticles induces hepatic toxicity in male Sprague-Dawley rats. *Int J Nanomedicine* (2011) 6:2327–35. doi:10.2147/IJN.S25119
39. He X, Zhang H, Ma Y, Bai W, Zhang Z, Lu K, et al. Lung deposition and extrapulmonary translocation of nano-ceria after intratracheal instillation. *Nanotechnology* (2010) 21(28):285103. doi:10.1088/0957-4484/21/28/285103
40. Krug H. Nanosafety research—are we on the right track? *Angewandte Chemie* (2014) 53(46):12304–19. doi:10.1002/anie.201403367
41. Noel A, Maghni K, Cloutier Y, Dion C, Wilkinson K, Halle S, et al. Effects of inhaled nano-TiO<sub>2</sub> aerosols showing two distinct agglomeration states on rat lungs. *Toxicol Lett* (2012) 214(2):109–19. doi:10.1016/j.toxlet.2012.08.019
42. Yoon D, Woo D, Kim J, Kim M, Kim T, Hwang E, et al. Agglomeration, sedimentation, and cellular toxicity of alumina nanoparticles in cell culture medium. *J Nanopart Res* (2011) 13(6):2543–51. doi:10.1007/s11051-010-0147-4
43. Zhu X, Tian S, Cai Z. Toxicity assessment of iron oxide nanoparticles in zebrafish (*Danio rerio*) early life stages. *PLoS One* (2012) 7(9):e46286. doi:10.1371/journal.pone.0046286
44. Rogers S, Rice KM, Manne ND, Shokuhfar T, He K, Selvaraj V, et al. Cerium oxide nanoparticle aggregates affect stress response and function in *Caenorhabditis elegans*. *SAGE Open Med* (2015) 3:2050312115575387. doi:10.1177/2050312115575387
45. Dowding J, Das S, Kumar A, Dosani T, McCormack R, Gupta A, et al. Cellular interaction and toxicity depend on physicochemical properties and surface modification of redox-active nanomaterials. *ACS Nano* (2013) 7(6):4855–68. doi:10.1021/nn305872d
46. Alkilany A, Nagaria P, Hexel C, Shaw T, Murphy C, Wyatt M. Cellular uptake and cytotoxicity of gold nanorods: molecular origin of cytotoxicity and surface effects. *Small* (2009) 5(6):701–8. doi:10.1002/smll.200801546
47. Bachmann MF, Rohrer UH, Kundig TM, Burki K, Hengartner H, Zinkernagel RM. The influence of antigen organization on B cell responsiveness. *Science* (1993) 262(5138):1448–51. doi:10.1126/science.8248784
48. Bastus N, Sanchez-Tillo E, Pujals S, Farrera C, Kogan M, Giralt E, et al. Peptides conjugated to gold nanoparticles induce macrophage activation. *Mol Immunol* (2009) 46(4):743–8. doi:10.1016/j.molimm.2008.08.277
49. Bastus N, Sanchez-Tillo E, Pujals S, Farrera C, Lopez C, Giralt E, et al. Homogeneous conjugation of peptides onto gold nanoparticles enhances macrophage response. *ACS Nano* (2009) 3(6):1335–44. doi:10.1021/nn8008273
50. Xia T, Kovochich M, Brant J, Hotze M, Sempf J, Oberley T, et al. Comparison of the abilities of ambient and manufactured nanoparticles to induce cellular toxicity according to an oxidative stress paradigm. *Nano Lett* (2006) 6(8):1794–807. doi:10.1021/nl061025k

51. Casals E, Gonzalez E, Puntes V. Reactivity of inorganic nanoparticles in biological environments: insights into nanotoxicity mechanisms. *J Phys D: Appl. Phys.* (2012) 45(44):443001. doi:10.1088/0022-3727/45/44/443001
52. Bastus N, Casals E, Vázquez-Campos S, Puntes V. Reactivity of engineered inorganic nanoparticles and carbon nanostructures in biological media. *Nanotoxicology* (2008) 2(3):99–112. doi:10.1080/17435390802217830
53. Moore TL, Rodriguez-Lorenzo L, Hirsch V, Balog S, Urban D, Jud C, et al. Nanoparticle colloidal stability in cell culture media and impact on cellular interactions. *Chem Soc Rev* (2015) 44(17):6287–305. doi:10.1039/c4cs00487f
54. Casals E, Pfaller T, Duschl A, Oostingh GJ, Puntes V. Time evolution of the nanoparticle protein corona. *ACS Nano* (2010) 4(7):3623–32. doi:10.1021/nn901372t
55. Casals E, Pfaller T, Duschl A, Oostingh GJ, Puntes VF. Hardening of the nanoparticle-protein corona in metal (Au, Ag) and oxide (Fe<sub>3</sub>O<sub>4</sub>, CoO, and CeO<sub>2</sub>) nanoparticles. *Small* (2011) 7(24):3479–86. doi:10.1002/smll.201101511
56. Chithrani B, Chan W. Elucidating the mechanism of cellular uptake and removal of protein-coated gold nanoparticles of different sizes and shapes. *Nano Lett* (2007) 7(6):1542–50. doi:10.1021/nl070363y
57. Kirchner C, Liedl T, Kudera S, Pellegrino T, Javier A, Gaub H, et al. Cytotoxicity of colloidal CdSe and CdSe/ZnS nanoparticles. *Nano Lett* (2005) 5(2):331–8. doi:10.1021/nl047996m
58. Muhammad F, Wang A, Qi W, Zhang S, Zhu G. Intracellular antioxidants dissolve man-made antioxidant nanoparticles: using redox vulnerability of nanoceria to develop a responsive drug delivery system. *ACS Appl Mater Interfaces* (2014) 6(21):19424–33. doi:10.1021/am5055367
59. Wang X, Ji Z, Chang C, Zhang H, Wang M, Liao Y, et al. Use of coated silver nanoparticles to understand the relationship of particle dissolution and bioavailability to cell and lung toxicological potential. *Small* (2014) 10(2):385–98. doi:10.1002/smll.201301597
60. Cho E, Zhang Q, Xia Y. The effect of sedimentation and diffusion on cellular uptake of gold nanoparticles. *Nat Nanotechnol* (2011) 6(6):385–91. doi:10.1038/nnano.2011.58
61. Xue Y, Zhai Y, Zhou K, Wang L, Tan H, Luan Q, et al. The vital role of buffer anions in the antioxidant activity of CeO<sub>2</sub> nanoparticles. *Chemistry* (2012) 18(35):11115–22. doi:10.1002/chem.201200983
62. Perez J, Asati A, Nath S, Kaittanis C. Synthesis of biocompatible dextran-coated nanoceria with pH-dependent antioxidant properties. *Small* (2008) 4(5):552–6. doi:10.1002/smll.200700824
63. Casals E, Barrena R, Garcia A, Gonzalez E, Delgado L, Busquets-Fite M, et al. Programmed iron oxide nanoparticles disintegration in anaerobic digesters boosts biogas production. *Small* (2014) 10(14):2801–8. doi:10.1002/smll.201303703
64. Feliu N, Docter D, Heine M, Del Pino P, Ashraf S, Kolosnjaj-Tabi J, et al. In vivo degeneration and the fate of inorganic nanoparticles. *Chem Soc Rev* (2016) 45(9):2440–57. doi:10.1039/c5cs00699f
65. Braydich-Stolle L, Hussain S, Schlager J, Hofmann M. In vitro cytotoxicity of nanoparticles in mammalian germline stem cells. *Toxicol Sci* (2005) 88(2):412–9. doi:10.1093/toxsci/kf256
66. Pfaller T, Colognato R, Nelissen I, Favilli F, Casals E, Ooms D, et al. The suitability of different cellular in vitro immunotoxicity and genotoxicity methods for the analysis of nanoparticle-induced events. *Nanotoxicology* (2010) 4(1):52–72. doi:10.3109/17435390903374001

**Conflict of Interest Statement:** The authors declare that the research was conducted in the absence of any commercial or financial relationships that could be construed as a potential conflict of interest.

Copyright © 2017 Casals, Gusta, Piella, Casals, Jiménez and Puntes. This is an open-access article distributed under the terms of the Creative Commons Attribution License (CC BY). The use, distribution or reproduction in other forums is permitted, provided the original author(s) or licensor are credited and that the original publication in this journal is cited, in accordance with accepted academic practice. No use, distribution or reproduction is permitted which does not comply with these terms.



# Endotoxin Contamination in Nanomaterials Leads to the Misinterpretation of Immunosafety Results

Yang Li<sup>1\*</sup>, Mayumi Fujita<sup>1</sup> and Diana Boraschi<sup>2</sup>

<sup>1</sup>Department of Dermatology, University of Colorado, Anschutz Medical Campus, Aurora, CO, USA,

<sup>2</sup>Institute of Protein Biochemistry, National Research Council (CNR), Napoli, Italy

## OPEN ACCESS

### Edited by:

Claudia Monaco,  
University of Oxford, UK

### Reviewed by:

Laleh Majlessi,  
Institut Pasteur, France  
Martin Himly,  
University of Salzburg, Austria

### \*Correspondence:

Yang Li  
yang.li.nano@gmail.com,  
yang.3.li@ucdenver.edu

### Specialty section:

This article was submitted  
to Inflammation,  
a section of the journal  
*Frontiers in Immunology*

Received: 28 December 2016

Accepted: 05 April 2017

Published: 08 May 2017

### Citation:

Li Y, Fujita M and Boraschi D (2017)  
Endotoxin Contamination in Nanomaterials Leads to the Misinterpretation of Immunosafety Results.  
*Front. Immunol.* 8:472.  
doi: 10.3389/fimmu.2017.00472

Given the presence of engineered nanomaterials in consumers' products and their application in nanomedicine, nanosafety assessment is becoming increasingly important. In particular, immunosafety aspects are being actively investigated. In nanomaterial immunosafety testing strategies, it is important to consider that nanomaterials and nanoparticles are very easy to become contaminated with endotoxin, which is a widespread contaminant coming from the Gram-negative bacterial cell membrane. Because of the potent inflammatory activity of endotoxin, contaminated nanomaterials can show inflammatory/toxic effects due to endotoxin, which may mask or misidentify the real biological effects (or lack thereof) of nanomaterials. Therefore, before running immunosafety assays, either *in vitro* or *in vivo*, the presence of endotoxin in nanomaterials must be evaluated. This calls for using appropriate assays with proper controls, because many nanomaterials interfere at various levels with the commercially available endotoxin detection methods. This also underlines the need to develop robust and bespoke strategies for endotoxin evaluation in nanomaterials.

**Keywords:** engineered nanomaterials, immunosafety assessment, endotoxin contamination, endotoxin evaluation, Limulus amebocyte lysate assay

## INTRODUCTION

Nanotechnology has undergone a rapid growth all over the world, with the production of a broad array of different nanomaterials in many consumers' products, to which the human population and the environment are therefore increasingly exposed. The health and environmental impacts of these new engineered nanomaterials (ENM) are a topic of considerable interest for nanotech industries and regulators as well as scientists, leading to the attempt of building safe-by-design ENM and the effort of establishing clear and relevant safety guidelines (1). Among nanotoxicity effects, induction of inflammation is considered a risk-predictive key effect (2). Several ENM were found to trigger inflammation in experimental models both *in vitro* and *in vivo*, suggesting a possible risk for human health (3–7). However, many experimental studies that show inflammatory effects triggered by ENM did not properly consider the possible presence of endotoxin. The Gram-negative endotoxin or lipopolysaccharide (LPS) is a ubiquitous contaminant in our environment and a potent inducer of inflammation and cell death. Hence, when evaluating the toxic and inflammatory effects of ENM to establish their safety, we must be aware that the presence of endotoxin in ENM can lead to inaccurate findings and consequently misleading conclusions (8).

Endotoxin/LPS is a molecule found in the outer membrane of Gram-negative bacteria and consists of a hydrophilic polysaccharide domain and a hydrophobic lipid domain. LPS plays an important role in bacterial virulence, because of its lipid part (lipid A) responsible for cytotoxicity. In mammalian tissues, LPS binds to a soluble LPS-binding protein, which transports LPS to the cell surface receptor, Toll-like receptor (TLR) 4. TLR4, together with MD2 and CD14, initiates signaling that leads to activation of inflammation pathways in different cell types (9). Because TLR4 is expressed by many cells, in particular innate immune cells such as monocytes and macrophages, these cells are very sensitive and responsive to LPS stimulation and raise a defensive inflammatory response against bacterial infections (10). LPS-activated cells produce and secrete a great number of inflammatory factors including interleukin (IL)-1 $\beta$ , IL-6, IL-8, and tumor necrosis factor- $\alpha$ . At high concentrations, LPS can also directly kill cells, although it depends on cell sensitivity. Given its potent inflammatory/toxic activity, exposure to endotoxin can induce serious and even life-threatening effects, including respiratory symptoms, asthma, and endotoxemia (11–14). Therefore, the acceptable endotoxin levels in medical products (such as surgical instruments or drugs) have been regulated by US FDA as early as 1985, updated thereafter, and accepted/adopted almost all over the world (15). Pharmaceutical companies must follow these regulations, and the presence of endotoxin in medical use products or intravenous (i.v.) drugs must be certified to be below a given limit before their release in the market. However, this regulation does not apply to ENM that are not intended for medical use, meaning that most industrially produced ENM are not screened for endotoxin contamination. While this may not be a health problem unless the ENM are administered i.v. into human beings, it still remains a relevant issue because the results from extremely sensitive nanosafety models used for assessing products' safety may be biased by the presence of contaminating endotoxin and reveal inflammatory/toxic effects that are not ENM specific but rather endotoxin dependent.

## ENDOTOXIN CONTAMINATION OF NANOMATERIALS

Endotoxin is a thermostable molecule that can persist in the environment in the absence of live Gram-negative bacteria. Its thermostability makes endotoxin resistant to the routine sterilization methods applied in biology laboratories (16). Thus, endotoxin is a ubiquitous environmental contaminant, present in all chemicals and glassware used in laboratories (17). Special attention or treatment is needed for avoiding/eliminating endotoxin contamination, which includes working in endotoxin-free conditions and depyrogenation of materials. A common and effective method for depyrogenation is incineration, which implies dry heating of tools and materials at high temperatures for given times, e.g., 180°C for 3 h or 250°C for 30 min (18). However, these extreme conditions are not suitable for depyrogenating most ENM, because the treatment may change the ENM physicochemical properties. França et al. used different methods (UV irradiation, gas-plasma treatment, ethylene oxide treatment, formaldehyde treatment, and autoclaving) for sterilizing/depyrogenizing two differently sized gold (Au) nanoparticles

(NPs). They found that the various methods caused changes in the Au NPs, the most common problem being NPs aggregation and consequent changes in UV-Vis spectra, morphology, and particle size distribution. They further tested the biological effects of these Au NPs and found that the different sterilization procedures could affect the NPs cytotoxic capacity and their ability to induce intracellular ROS (19). Hence, the best way to obtain endotoxin-free ENM is to take precautions and synthesize them in endotoxin-free conditions (20). As most chemical labs and manufactures do not apply particular precautions, the ENM undergoing nanosafety and preclinical nanomedicine efficacy studies are likely to get contaminated by endotoxin. Furthermore, ENM have a large reactive surface area, which tends to absorb molecules from the surrounding milieu to reduce its energy, thereby facilitating the adsorption of surface contaminants (21). The lipid domain allows endotoxin attachment to hydrophobic surfaces, while the negatively charged phosphate groups promote endotoxin interaction with cationic surfaces (22). In addition, coordinative binding can occur between the negatively charged LPS and loosely anionic surfaces (e.g., citrate-coated Au NPs), resulting in firm and stable binding (23).<sup>1</sup> Therefore, endotoxin can attach to virtually any surface, which makes endotoxin a common contaminant for many different kinds of ENM (8, 21). Darkow and coworkers have shown that functionalized NPs could bind endotoxin through Coulomb and van der Waals interactions (24). Bromberg et al. showed a strong interaction between lipid A (the toxic moiety of endotoxin) and functionalized paramagnetic ENM (25). The capacity of endotoxin to bind with NPs was also observed for polystyrene particles (26). Our recent study showed that endotoxin binds to the surface of Au NPs in a dose-dependent manner (23). Abadeer et al. studied the role of surface properties in the interaction of Au nanorods with endotoxin by using surface plasmon resonance sensing and found that endotoxin attaches more easily to a cationic surface compared to neutral or anionic surfaces (27). Our data with Au NPs indeed confirm that the ENM surface characteristics can affect the binding of endotoxin (23, see text footnote 1).

We have lab tested several commercial ENM or ENM received from collaborators and found variable degrees of endotoxin contamination (unpublished data; **Figure 1A**). In a study in which NPs synthesis was repeated in normal conditions or after glassware and tool depyrogenation, we could show that taking precautions could significantly dampen the endotoxin contamination in ENM (28). On the other hand, a heavy endotoxin contamination in polystyrene ENM after long-term storage (over 6 months) may have been due to the poor handling processes (29). Thus, we should be aware that endotoxin contamination in ENM is a common phenomenon.

## BIOLOGICAL EFFECTS OF ENDOTOXIN-CONTAMINATED NANOMATERIALS

The biological effects of endotoxin-contaminated ENM have been reviewed recently (8). Endotoxin-carrying ENM can initiate the

<sup>1</sup>Li Y, Shi Z, Radauer-Preiml I, Andosch A, Casals E, Luetz-Meindl U, et al. Bacterial Endotoxin (LPS) Binds to the Surface of Gold Nanoparticles, Interferes with Biocorona Formation and Induces Human Monocyte Inflammatory Activation.

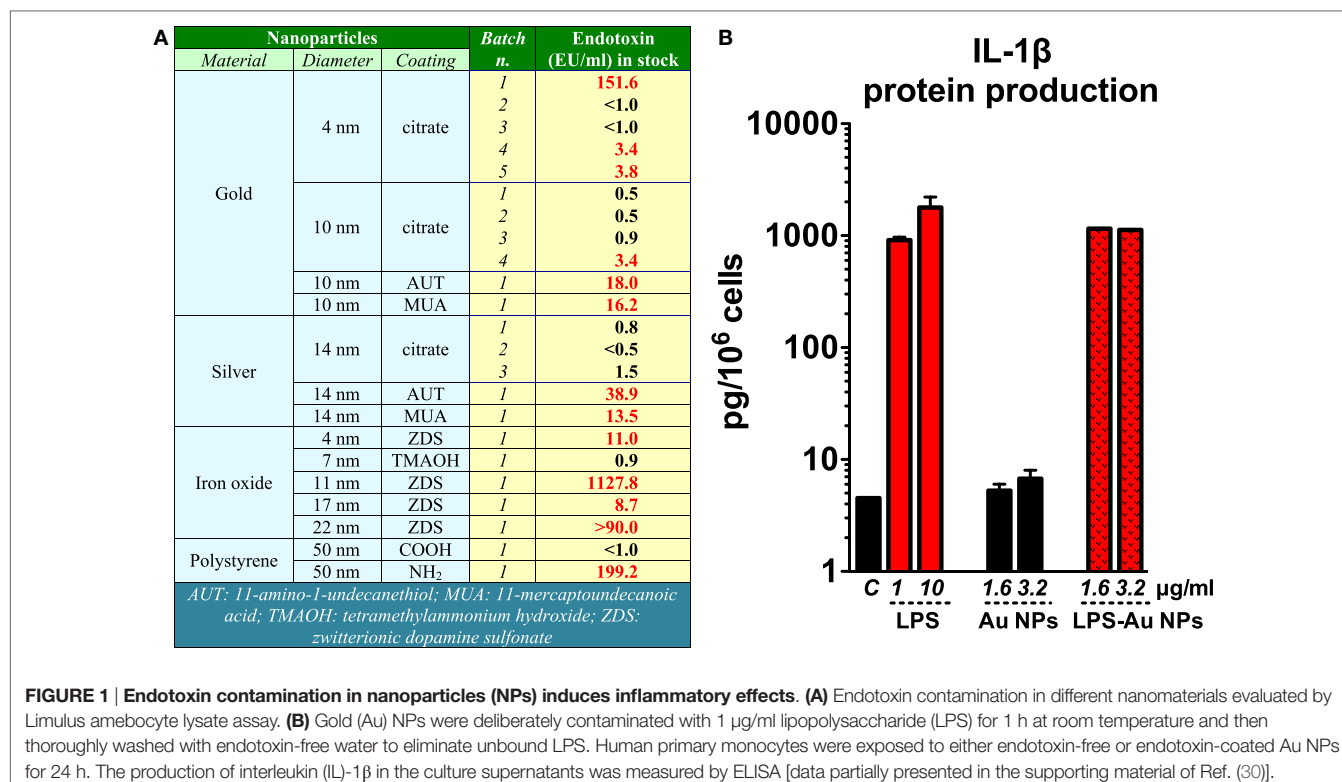


**FIGURE 1 | Endotoxin contamination in nanoparticles (NPs) induces inflammatory effects.** (A) Endotoxin contamination in different nanomaterials evaluated by Limulus amebocyte lysate assay. (B) Gold (Au) NPs were deliberately contaminated with 1  $\mu\text{g}/\text{ml}$  lipopolysaccharide (LPS) for 1 h at room temperature and then thoroughly washed with endotoxin-free water to eliminate unbound LPS. Human primary monocytes were exposed to either endotoxin-free or endotoxin-coated Au NPs for 24 h. The production of interleukin (IL)-1 $\beta$  in the culture supernatants was measured by ELISA [data partially presented in the supporting material of Ref. (30)].

TLR4 signaling pathway in innate immune cells, activate the inflammasome, and induce the secretion of IL-1 $\beta$ , a fundamental cytokine that plays an important role in physiological and pathological conditions (31), as well as many other inflammation-related factors. We have shown that the endotoxin bound on the surface of Au NPs turned those NPs from inactive to highly inflammatory and able to induce secretion of IL-1 $\beta$  in human primary monocytes (Figure 1B) (30). With this in mind, many reports that show inflammatory and toxic effects of ENM *in vitro* or *in vivo* on TLR4-expressing cells need to be taken with caution if the endotoxin level was not assessed. Studies have shown that ENM can activate a TLR4-dependent inflammatory response in the target cells. Some of these studies failed to assess or did not mention the potential contamination of the ENM under study with endotoxin (32, 33), which makes it impossible to assess the reliability of the results. On the other hand, other studies showed the ability of ENM to initiate TLR4-dependent activation in the absence of measurable endotoxin contamination or by excluding the effects of endotoxin [see, for instance, Ref. (34)], thereby suggesting a *bona fide* ENM effect. Qu et al. reported that graphene oxide can be sensed by TLR4 and induce macrophage necrosis through the caspase-3 pathway (35). Endotoxin was measured in this study with a Limulus amebocyte lysate (LAL) endpoint chromogenic kit from Lonza and declared to be about 0.1 EU/ml (1 ml containing 80  $\mu\text{g}$  of NPs). This brings us to another concern, i.e., the possible interference of graphene oxide with the LAL assay. Indeed, interference has been extensively reported for many ENM (36–39), which strongly suggests the need for testing the interference for each ENM under investigation. In addition, the Lonza QCL-1000 endpoint chromogenic LAL assay with readout at 405 nm has been shown to be unsatisfactory for measuring endotoxin in metal and

metal oxide (39) as well as graphene oxide ENM (40). With all this in mind, we conclude that not only should we measure endotoxin in ENM but also we must make sure that the endotoxin detection assay is reliable and relevant to the ENM under study. Without the formal proof of the absence of endotoxin contamination, the *bona fide* bioeffects of ENM cannot be accurately assessed.

## ENDOTOXIN EVALUATION METHODS IN NANOMATERIALS

The FDA-approved methods to detect endotoxin are the rabbit pyrogen test (RPT) as an *in vivo* test and the LAL assay as an *in vitro* test. Alternative and sensitive bioassays are also approved by the European Centre for the Validation of Alternative Methods (ECVAM) for assessing pyrogens, such as the human PBMC activation assay and the human monocytes activation test (MAT). However, the RPT *in vivo* assay and *in vitro* bioassays using PBMC and monocytes are not specific for endotoxin, because they measure inflammatory effects (induction of fever and induction of inflammatory cytokines) and thus detect responses from all types of inflammation-inducing agents (which may include ENM). Therefore, to specifically detect the endotoxin level in ENM, the LAL assay is recommended.

The LAL assay could provide fast, sensitive, and specific endotoxin assessment. The only other molecule that gives a positive result with the traditional LAL assay is  $\beta$ -glucan, which, however, can be inhibited by a specific buffer in the currently available commercial LAL kits. Because of its specificity, sensitivity, and reliability, the LAL assay has replaced the old *in vivo* RPT as the assay chosen by all regulatory agencies, such as FDA, European,

**TABLE 1 | Advantages and disadvantages of assays used to detect endotoxin.**

Limulus amoebocyte lysate (LAL) assay						Bioassay	
	Traditional	Turbidimetric	Chromogenic	Fluorogenic	Modified	Rabbit pyrogen test	In vitro activation assay
Pros	Short-term experiment and easy performance, specific for endotoxin, most used endotoxin measurement methods					Most relevant assays for pyrogen detection can be used to screen nanomedicine for preclinical usage	
Easy and cheap	Quantitative, high sensitivity	Quantitative, high sensitivity, two different detection wavelengths	High sensitivity, very specific (no recognition of $\beta$ -glucan)	Washing steps can eliminate interfering substances compared to other LAL assays, wide endotoxin detection range	NPs may interfere with lipopolysaccharide (LPS) antibody binding. Not clear if washing could detach LPS (bound to the wells) from particles, or remove LPS from wells together with particles, or leave LPS-coated particles in the wells. Residual particles in wells, if not washed off, may interfere with enzyme reaction or quench fluorescence	Non-specific for endotoxin, reactive to any inflammation-inducing agent (including some NPs). The interference of NPs with these assays still needs accurate evaluation	
Cons	Semiquantitative, low sensitivity, prone to subjective variations, not precise, proved to be interfered by nanoparticles (NPs)	Due to their turbidity, high optical density NPs or NPs at high concentration may interfere with this assay	Can be interfered by NPs with absorbance at or close the detection wavelength (405 or 540 nm)		Animal usage, high cost, low sensitivity	NPs may induce cytotoxicity and interfere with cell activation <i>in vitro</i> . NPs may also interfere with the ELISA procedures used for detecting inflammatory factors (e.g., antibody-antigen binding, color development, optical readouts)	
Use	NPs interference should be predetermined (e.g., turbidity, the optical interference), Appropriate procedures could be also applied to overcome interference, such as dilution or switching to another detection wavelength. Additional controls should be run to exclude interference with assay components (e.g., measuring endotoxin recovery rate)				Can be applied in combination with the LAL assay for analyzing the parenteral drugs (handdrug) during the earlier development phase. Generally used when different LAL assays show >25% variation. However, interference of NPs with bioassays may prevent from solving the problem		
	Final decision is usually made based on the gel clot assay in industry. This regulation is, however, unsuitable for NPs because of their significant interference with the assay	Applied to NPs that interfere with the chromogenic assay	Commonly used assay in biology labs. Can be used with NPs after appropriate controls	May be used for NPs that do not have autofluorescence and do not quench fluorescence	Use for NPs should be accurately validated (see Cons above)		

Chinese, and Japanese pharmacopeias (41–44). The use of the LAL assay for endotoxin detection in ENM is also regulated by ISO29701:2010 regulation “Nanotechnologies—Endotoxin test on nanomaterial samples for *in vitro* systems” (45).

In the LAL assay, factor C, an enzyme derived from the amebocytes of the horseshoe crab *Limulus polyphemus*, is activated by exposure to endotoxin and in turn induces activation of a clotting enzyme. Based on the types of detection of the clotting enzyme activity, three variants of the LAL assay are commercially available, including the gel clot, the turbidimetric, and the chromogenic assays. Recently, using recombinant factor C instead of the *Limulus* amebocyte lysate, new fluorescence-based assays have been developed. These assays have the advantage of being totally specific for endotoxin, because  $\beta$ -glucan activates factor G but not factor C. Although the LAL assay can reliably detect endotoxin in soluble reagents, the physicochemical characteristics of ENM pose a significant problem of interference with both the components and the detection readouts (fluorescence, optical density) of various assays (28, 36, 39). To overcome the interference problem, the available assays need to be validated for the lack of interference by ENM with the catalytic activity of the enzyme(s), substrate cleavage, and the final readout signals (8, 39). It has been shown that the gel clot LAL assay is not accurate for testing endotoxin contamination in particles, while the chromogenic LAL assay showed higher sensitivity and no interference (46). The unsuitability of the gel clot assay has also been shown for silica, silver (Ag), titanium dioxide, calcium carbonate, and other clinical-grade NPs (37, 38, 47), suggesting that the gel clot assay should not be used for testing endotoxin in ENM in general. However, despite these new evidences, the use of the gel clot assay is still recommended in a FDA guidance document to solve discrepancies between results from different LAL formats in industry (48). Furthermore, our results with the chromogenic LAL assay suggested that metal and metal oxide NPs may interfere with the final readout by absorbing the final dye (*p*-nitroaniline) and quenching the readout, leading to underestimating the endotoxin contamination (39). Therefore, Dobrovolskaia et al. have declared that none of the currently available LAL formats is optimal for endotoxin assessment in ENM and suggested that at least two LAL formats with different endpoints/readouts should be used. The results should also be confirmed by RPT when the LAL results show more than 25% difference (36, 38). This approach has been used at the Nanotechnology Characterization Laboratory of the National Cancer Institute (USA) for measuring the endotoxin contamination in ENM.

The bioassays, on the other hand, may be adequate to assess pyrogenic/inflammatory effects in general, in particular for the ENM for clinical use. These bioassays (RPT *in vivo* and PBMC and MAT *in vitro*) are not specific for endotoxin, since they are based on the development of an inflammatory response (e.g., fever, NF- $\kappa$ B activation, secretion of inflammatory cytokines), which can be induced by any kind of pyrogen, theoretically including ENM. Therefore, bioassays cannot distinguish between effects induced by endotoxin and other pyrogens and intrinsic effects of ENM. The use of the PBMC or the MAT tests in parallel to the LAL assay should allow us to detect, in addition to endotoxin, the possible presence of other pyrogenic agents, which may be present but cannot be detected with the LAL assays. Thus, Dobrovolskaia

et al. suggested to use such assays to confirm the LAL results (38). We have tested endotoxin contamination in Au, Ag, and iron oxide ( $Fe_3O_4$ ) NPs with the chromogenic LAL assay of Associates of Cape Cod (endpoint readout at 540 nm) and in parallel with the ECVAM-approved PBMC activation assay (IL-6 production) (39). The endotoxin contamination detected by the LAL assay was confirmed by the PBMC activation assay only for Au NPs, but not for Ag and  $Fe_3O_4$  NPs. This is probably due to the interference of NPs with some elements in the bioassay. Most likely, the NPs interfere with the ELISA-based IL-6 detection process by interfering with antigen/antibody interaction, adsorbing and subtracting IL-6, or quenching the optical signal that indicates the presence of IL-6. Thus, the biological assays also need an accurate characterization and validation before their results can be used to detect endotoxin in ENM. **Table 1** summarizes the pros and cons of different endotoxin evaluation methods for ENM.

## CONCLUSION AND FUTURE PERSPECTIVE

To reliably assess safety of ENM, either intended for medical use or included in commercial products, it is important to take into careful consideration the presence of unwanted bioactive contaminants, of which bacterial endotoxin is most common and abundant. This would eliminate misinterpretation of experimental results and erroneous attribution to ENM of toxic effects that may be entirely due to contaminants. Thus, nanosafety/nanomedicine researchers and regulators should be aware of the possible contamination of ENM with highly inflammatory contaminants such as endotoxin and design and adopt appropriately designed assays. Likewise, chemists/producers should design their synthesis processes to minimize endotoxin contamination. Furthermore, since the methods for endotoxin assessment in ENM are still challenging (Table 1) and the regulations on nanoproducts are still incomplete, robust strategies and bespoke assays need to be developed for endotoxin evaluation in ENM.

## AUTHOR CONTRIBUTIONS

YL wrote the paper, MF revised it, and DB contributed to writing and critically revised it.

## ACKNOWLEDGMENTS

The authors would like to thank Dr. Alessandro Ponti (CNR, Milano, Italy) for having provided several kinds of ENM. The authors are grateful to Prof. Victor F. Puntes (Institut Català de Nanociència i Nanotecnologia, Barcelona, Spain) for helpful discussion on LPS interaction with ENM.

## FUNDING

This work was supported by the EU Commission projects NANoREG (FP7 grant no. 310584) and PANDORA (H2020 grant no. 671881), the cluster project Medintech (CTN01\_00177\_96) of the Italian Ministry of Education, University and Research, and the Veterans Affairs Merit Review Award 5I01BX001228, NIH/NCI R01CA197919.

## REFERENCES

- Savolainen K, Backman U, Brouwer D, Fadeel B, Fernandes T, Kuhlbusch T, et al. *Nanosafety in Europe 2015-2025: Towards Safe and Sustainable Nanomaterials and Nanotechnology Innovations*. Helsinki: Finnish Institute of Occupational Health (2013).
- Nel A, Xia T, Mädler L, Li N. Toxic potential of materials at the nanolevel. *Science* (2006) 311(5761):622–7. doi:10.1126/science.1114397
- Johnston HJ, Hutchison G, Christensen FM, Peters S, Hankin S, Stone V. A review of the in vivo and in vitro toxicity of silver and gold particulates: particle attributes and biological mechanisms responsible for the observed toxicity. *Crit Rev Toxicol* (2010) 40(4):328–46. doi:10.3109/10408440903453074
- Li Y, Liu Y, Fu Y, Wei T, Le Guyader L, Gao G, et al. The triggering of apoptosis in macrophages by pristine graphene through the MAPK and TGF-beta signaling pathways. *Biomaterials* (2012) 33:402–11. doi:10.1016/j.biomaterials.2011.09.091
- Shannahan JH, Kodavanti UP, Brown JM. Manufactured and airborne nanoparticle cardiopulmonary interactions: a review of mechanisms and the possible contribution of mast cells. *Inhal Toxicol* (2012) 24(5):320–39. doi:10.3109/08958378.2012.668229
- Li Y, Monteiro-Riviere NA. Mechanisms of cell uptake, inflammatory potential and protein corona effects with gold nanoparticles. *Nanomedicine* (2016) 11(24):3185–203. doi:10.2217/nmm-2016-0303
- Rabolli V, Lison D, Huaux F. The complex cascade of cellular events governing inflammasome activation and IL-1 $\beta$  processing in response to inhaled particles. *Part Fibre Toxicol* (2016) 13(1):40. doi:10.1186/s12989-016-0150-8
- Li Y, Boraschi D. Endotoxin contamination: a key element in the interpretation of nanosafety studies. *Nanomedicine (Lond)* (2016) 11(3):269–87. doi:10.2217/nmm.15.196
- Lu YC, Yeh WC, Ohashi PS. LPS/TLR4 signal transduction pathway. *Cytokine* (2008) 42(2):145–51. doi:10.1016/j.cyto.2008.01.006
- Janeway CA Jr, Medzhitov R. Innate immune recognition. *Annu Rev Immunol* (2002) 20(1):197–216. doi:10.1146/annurev.immunol.20.083001.084359
- Danner RL, Elin R, Hosseini J, Wesley R, Reilly J, Parillo J. Endotoxemia in human septic shock. *Chest* (1991) 99(1):169–75. doi:10.1378/chest.99.1.169
- Braun-Fahrlander C, Riedler J, Herz W, Eder W, Waser M, Grize L, et al. Environmental exposure to endotoxin and its relation to asthma in school-age children. *N Engl J Med* (2002) 347(12):869–77. doi:10.1056/NEJMoa020057
- Liu AH. Endotoxin exposure in allergy and asthma: reconciling a paradox. *J Allergy Clin Immunol* (2002) 109(3):379–92. doi:10.1067/mai.2002.122157
- Rylander R. Review: endotoxin in the environment – exposure and effects. *J Endotoxin Res* (2002) 8(4):241–52. doi:10.1179/096805102125000452
- Malyala P, Singh M. Endotoxin limits in formulations for preclinical research. *J Pharm Sci* (2008) 97(6):2041–4. doi:10.1002/jps.21152
- Sandle T. A comparative study of different methods for endotoxin destruction. *Am Pharm Rev* (2013) 16(6):15–7.
- Gorbet MB, Sefton MV. Endotoxin: the uninvited guest. *Biomaterials* (2005) 26(34):6811–7. doi:10.1016/j.biomaterials.2005.04.063
- Williams KL. *Endotoxins: Pyrogens, LAL Testing and Depyrogenation*. New York, NY: Informa Healthcare (2007).
- França Á, Pelaz B, Moros M, Sánchez-Espinel C, Hernández A, Fernández-López C, et al. Sterilization matters: consequences of different sterilization techniques on gold nanoparticles. *Small* (2010) 6(1):89–95. doi:10.1002/smll.200901006
- Vallhov H, Qin J, Johansson SM, Ahlborg N, Muhammed MA, Scheynius A, et al. The importance of an endotoxin-free environment during the production of nanoparticles used in medical applications. *Nano Lett* (2006) 6(8):1682–6. doi:10.1021/nl060860z
- Jones CF, Grainger DW. In vitro assessments of nanomaterial toxicity. *Adv Drug Deliv Rev* (2009) 61(6):438–56. doi:10.1016/j.addr.2009.03.005
- Hirayama C, Sakata M. Chromatographic removal of endotoxin from protein solutions by polymer particles. *J Chromatogr B Analyt Technol Biomed Life Sci* (2002) 781:419–32. doi:10.1016/S1570-0232(02)00430-0
- Li Y, Tran N, Puntes VF, Boraschi D. Bacterial endotoxin binds to the surface of gold nanoparticles and triggers inflammation. *7th International Nanotoxicology Congress – Nanotox 2014*; Antalya, Turkey (2014).
- Darkow R, Groth T, Albrecht W, Lützow K, Paul D. Functionalized nanoparticles for endotoxin binding in aqueous solutions. *Biomaterials* (1999) 20(14):1277–83. doi:10.1016/S0142-9612(99)00022-8
- Bromberg L, Chang EP, Alvarez-Lorenzo C, Magarinos B, Concheiro A, Hatton TA. Binding of functionalized paramagnetic nanoparticles to bacterial lipopolysaccharides and DNA. *Langmuir* (2010) 26(11):8829–35. doi:10.1021/la904589p
- Peula-García J, Molina-Bolívar J, Velasco J, Rojas A, Galisteo-González F. Interaction of bacterial endotoxine (lipopolysaccharide) with latex particles: application to latex agglutination immunoassays. *J Colloid Interface Sci* (2002) 245(2):230–6. doi:10.1006/jcis.2001.7958
- Abadeer NS, Fulop G, Chen S, Kall M, Murphy CJ. Interactions of bacterial lipopolysaccharides with gold nanorod surfaces investigated by refractometric sensing. *ACS Appl Mater Interfaces* (2015) 7(44):24915–25. doi:10.1021/acsami.5b08440
- Oostingh GJ, Casals E, Italiani P, Colognato R, Stritzinger R, Ponti J, et al. Problems and challenges in the development and validation of human cell-based assays to determine nanoparticle-induced immunomodulatory effects. *Part Fibre Toxicol* (2011) 8(1):8. doi:10.1186/1743-8977-8-8
- Murali K, Kenesei K, Li Y, Demeter K, Környei Z, Madarász E. Uptake and bio-reactivity of polystyrene nanoparticles is affected by surface modifications, ageing and LPS adsorption: in vitro studies on neural tissue cells. *Nanoscale* (2015) 7(9):4199–210. doi:10.1039/c4nr06849a
- Li Y, Italiani P, Casals E, Valkenborg D, Mertens I, Baggerman G, et al. Assessing the immunosafety of engineered nanoparticles with a novel in vitro model based on human primary monocytes. *ACS Appl Mater Interfaces* (2016) 8(42):28437–47. doi:10.1021/acsami.6b06278
- Afonina IS, Müller C, Martin SJ, Beyaert R. Proteolytic processing of interleukin-1 family cytokines: variations on a common theme. *Immunity* (2015) 42(6):991–1004. doi:10.1016/j.immuni.2015.06.003
- Chen G-Y, Yang H-J, Lu C-H, Chao Y-C, Hwang S-M, Chen C-L, et al. Simultaneous induction of autophagy and toll-like receptor signaling pathways by graphene oxide. *Biomaterials* (2012) 33(27):6559–69. doi:10.1016/j.biomaterials.2012.05.064
- Chen Z, Liu Y, Sun B, Li H, Dong J, Zhang L, et al. Polyhydroxylated metallofullerenes stimulate IL-1 $\beta$  secretion of macrophage through TLRs/MyD88/NF- $\kappa$ B pathway and NLRP3 inflammasome activation. *Small* (2014) 10(12):2362–72. doi:10.1002/smll.201470069
- Bastús NG, Sánchez-Tilló E, Pujals S, Farrera C, Kogan MJ, Giralt E, et al. Peptides conjugated to gold nanoparticles induce macrophage activation. *Mol Immunol* (2009) 46(4):743–8. doi:10.1016/j.molimm.2008.08.277
- Qu G, Liu S, Zhang S, Wang L, Wang X, Sun B, et al. Graphene oxide induces toll-like receptor 4 (TLR4)-dependent necrosis in macrophages. *ACS Nano* (2013) 7(7):5732–45. doi:10.1021/nn402330b
- Dobrovolskaia MA, Neun BW, Clogston JD, Ding H, Ljubimova J, McNeil SE. Ambiguities in applying traditional Limulus amebocyte lysate tests to quantify endotoxin in nanoparticle formulations. *Nanomedicine* (2010) 5(4):555–62. doi:10.2217/nmm.10.29
- Smulders S, Kaiser JP, Zuin S, Van Landuyt KL, Golanski L, Vanoorbeek J, et al. Contamination of nanoparticles by endotoxin: evaluation of different test methods. *Part Fibre Toxicol* (2012) 9(1):41. doi:10.1186/1743-8977-9-41
- Dobrovolskaia MA, Neun BW, Clogston JD, Grossman JH, McNeil SE. Choice of method for endotoxin detection depends on nanoformulation. *Nanomedicine (Lond)* (2014) 9(12):1847–56. doi:10.2217/nmm.13.157
- Li Y, Italiani P, Casals E, Tran N, Puntes VF, Boraschi D. Optimising the use of commercial LAL assays for the analysis of endotoxin contamination in metal colloids and metal oxide nanoparticles. *Nanotoxicology* (2015) 9(4):462–73. doi:10.3109/17435390.2014.948090
- Mukherjee SP, Lozano N, Kucki M, Del Rio-Castillo AE, Newman L, Vázquez E, et al. Detection of endotoxin contamination of graphene based materials using the TNF- $\alpha$  expression test and guidelines for endotoxin-free graphene oxide production. *PLoS One* (2016) 11(11):e0166816. doi:10.1371/journal.pone.0166816
- FDA. *Guideline on Validation of the Limulus Amebocyte Lysate Test as an End-Product Endotoxin Test for Human and Animal Parenteral Drugs, Biological Products, and Medical Devices*. U.S. Department of Health and Human Services, Public Health Service, Food and Drug Administration (1987).

42. ChP. Bacterial endotoxins test. *Chinese Pharmacopoeia*. (2005).
43. EP. Bacterial endotoxins. *European Pharmacopoeia 5.0*. (2005). p. 161–8.
44. USP. Chapter 85: bacterial endotoxins test. *United States Pharmacopeia*. Rockville: United States Pharmacopeial Convention (2005).
45. ISO. *ISO/FDIS 29701: Nanotechnologies – Endotoxin Test on Nanomaterial Samples for In Vitro Systems – Limulus Amebocyte Lysate (LAL) Test*. (2010). Available from: [http://www.iso.org/iso/iso\\_catalogue/catalogue\\_tc/catalogue\\_detail.htm?csnumber=45640](http://www.iso.org/iso/iso_catalogue/catalogue_tc/catalogue_detail.htm?csnumber=45640)
46. Brooks R, Wimhurst J, Rushton N. Endotoxin contamination of particles produces misleading inflammatory cytokine responses from macrophages in vitro. *J Bone Joint Surg Br* (2002) 84(2):295–9. doi:10.1302/0301-620X.84B2.12061
47. Kucki M, Cavelius C, Kraegeloh A. Interference of silica nanoparticles with the traditional Limulus amebocyte lysate gel clot assay. *Innate Immun* (2014) 20(3):327–36. doi:10.1177/1753425913492833
48. FDA, CBER, CMV, CDRH, ORA. *Guidance for Industry. Pyrogen and Endotoxins Testing: Questions and Answers*. (2012).

**Conflict of Interest Statement:** The authors declare that the research was conducted in the absence of any commercial or financial relationships that could be construed as a potential conflict of interest.

Copyright © 2017 Li, Fujita and Boraschi. This is an open-access article distributed under the terms of the Creative Commons Attribution License (CC BY). The use, distribution or reproduction in other forums is permitted, provided the original author(s) or licensor are credited and that the original publication in this journal is cited, in accordance with accepted academic practice. No use, distribution or reproduction is permitted which does not comply with these terms.



# Lipopolysaccharide Adsorbed to the Bio-Corona of TiO<sub>2</sub> Nanoparticles Powerfully Activates Selected Pro-inflammatory Transduction Pathways

Massimiliano G. Bianchi<sup>1\*</sup>, Manfredi Allegri<sup>1</sup>, Martina Chiu<sup>1</sup>, Anna L. Costa<sup>2</sup>, Magda Blosi<sup>2</sup>, Simona Ortelli<sup>2</sup>, Ovidio Bussolati<sup>1\*</sup> and Enrico Bergamaschi<sup>3</sup>

<sup>1</sup> Department of Medicine and Surgery, University of Parma, Parma, Italy, <sup>2</sup> Institute of Science and Technology for Ceramics (CNR-ISTEC), National Research Council of Italy, Faenza, Ravenna, Italy, <sup>3</sup> Department of Public Health Science and Pediatrics, University of Turin, Turin, Italy

## OPEN ACCESS

### Edited by:

Paola Italiani,  
Consiglio Nazionale Delle Ricerche  
(CNR), Italy

### Reviewed by:

Francesco Maione,  
University of Naples Federico II, Italy  
Yang Li,  
University of Colorado Denver,  
United States

### \*Correspondence:

Massimiliano G. Bianchi  
massimiliano.bianchi@unipr.it;  
Ovidio Bussolati  
ovidio.bussolati@unipr.it

### Specialty section:

This article was submitted  
to Inflammation,  
a section of the journal  
*Frontiers in Immunology*

Received: 31 January 2017

Accepted: 07 July 2017

Published: 03 August 2017

### Citation:

Bianchi MG, Allegri M, Chiu M, Costa AL, Blosi M, Ortelli S, Bussolati O and Bergamaschi E (2017) Lipopolysaccharide Adsorbed to the Bio-Corona of TiO<sub>2</sub> Nanoparticles Powerfully Activates Selected Pro-inflammatory Transduction Pathways. *Front. Immunol.* 8:866.  
doi: 10.3389/fimmu.2017.00866

It is known that the adsorption of bioactive molecules provides engineered nanoparticles (NPs) with novel biological activities. However, the biological effects of the adsorbed molecules may also be modified by the interaction with NP. Bacterial lipopolysaccharide (LPS), a powerful pro-inflammatory compound, is a common environmental contaminant and is present in several body compartments such as the gut. We recently observed that the co-incubation of LPS with TiO<sub>2</sub> NPs markedly potentiates its pro-inflammatory effects on murine macrophages, suggesting that, when included in a NP bio-corona, LPS activity is enhanced. To distinguish the effects of adsorbed LPS from those of the free endotoxin, a pellet fraction, denominated P25/LPS, was isolated by centrifugation from a mixture of P25 TiO<sub>2</sub> NP (128 µg/ml) and LPS (10 ng/ml) in the presence of fetal bovine serum. Western blot analysis of the pellet eluate indicated that the P25/LPS fraction contained, besides proteins, also LPS, pointing to the presence of LPS-doped NP. The effects of adsorbed or free LPS were then compared in Raw264.7 murine macrophages. RT-PCR was used to evaluate the induction of cytokine genes, whereas active, phosphorylated isoforms of proteins involved in signaling pathways were assessed with western blot. At a nominal LPS concentration of 40 pg/ml, P25/LPS induced the expression of both NF-κB and IRF3-dependent cytokines at levels comparable with those observed with free LPS (10 ng/ml), although with different time courses. Moreover, compared to free LPS, P25/LPS caused a more sustained phosphorylation of p38 MAPK and a more prolonged induction of STAT1-dependent genes. Cytochalasin B partially inhibited the induction of *Tnfa* by P25/LPS, but not by free LPS, and suppressed the induction of IRF3-dependent genes by either P25/LPS or free LPS. These data suggest that, when included in the bio-corona of TiO<sub>2</sub> NP, LPS exhibits enhanced and time-shifted pro-inflammatory effects. Thus, in assessing the hazard of NP in real life, the enhanced effects of adsorbed bioactive molecules should be taken into account.

**Keywords:** lipopolysaccharide, endotoxin, titanium dioxide nanoparticles, bio-corona, macrophages, inflammation

## INTRODUCTION

When introduced in organic fluids, engineered nanoparticles (NP), due to their high ratio surface/volume, adsorb proteins, lipids, and other bioactive molecules present in the medium, forming a corona that is of fundamental relevance for the interactions with cells and tissues (1–3). The biological effects of nanomaterials are markedly influenced by the bio-corona and, therefore, are expected

to change in media or organic fluids of different composition (4). Conversely, the interaction with the nanomaterial may also change the conformation and/or the bioavailability of the adsorbed molecules (5), leading to enhancement or inhibition of their effects.

Although the formation and biological effects of protein corona have been extensively studied, other, non-protein bioactive molecules are expected to be adsorbed by nanomaterials. Bacterial lipopolysaccharide (LPS, endotoxin) is one of the most abundant bioactive molecules present in the environment as well as in several body compartments, such as the gut lumen. Although several mechanisms exist to limit the mucosal penetration of LPS, low endotoxin levels are also present in normal human plasma (6) and increase in several conditions (7, 8). LPS is an heat-stable component of the outer membrane of Gram-negative bacteria and works as a pathogen-associated molecular pattern, activating macrophages and promoting the production of a variety of pro-inflammatory proteins, such as tumor necrosis factor- $\alpha$  and other cytokines, or non-protein mediators, such as nitric oxide (NO) (9). In mammals, LPS mostly acts through transcriptional mechanisms, mediated by several, partially cross-linked transduction pathways, the most studied of which are those dependent by NF- $\kappa$ B and TRIF, elicited by LPS binding to the toll-like receptor 4 (TLR4). Signal transduction starts at the plasma membrane and later involves an endosomal compartment after the internalization of the complex LPS-TLR4 (10–12).

$\text{TiO}_2$  NPs are considered relatively safe materials and are widely used in a variety of applications. Similar to several other types of nanomaterials (13–17), also  $\text{TiO}_2$  NPs have been described to adsorb LPS (18), although the amount of endotoxin adsorbed was not easily quantifiable due to interference of the nanomaterial with the assay method. Interestingly, LPS adsorption to NP has been considered one of the possible factors that interfere with cell-based immunological tests employing NP (19), because either contamination may be easily overlooked or adsorption may modulate the effects of LPS on innate immune cells (19). Investigating this latter possibility, we have recently demonstrated that the co-exposure of murine macrophages to  $\text{TiO}_2$  NP and LPS in protein-rich medium powerfully synergizes the pro-inflammatory effects of the endotoxin (20). The synergy was hindered by the cytoskeletal drug cytochalasin B, which inhibits endocytosis and NP internalization, and blocked by the TLR4 inhibitors polymyxin B and CLI-095. On the basis of those results, we proposed that  $\text{TiO}_2$  NPs adsorb LPS and enhance macrophage activation by the endotoxin *via* a TLR4-dependent mechanism that is mainly triggered from an intracellular site (20).

However, the simultaneous cell treatment with NP and LPS does not allow to understand if the fraction of LPS adsorbed to NP has different biological effects compared with free LPS, since both forms of the endotoxin are actually co-administered to the test system. In particular, it would be important to determine if free and adsorbed LPS trigger different pathways, exhibit different potencies, or change the time-course of the activation process. In order to address these questions, we have adopted here an approach based on the separation of the two fractions through centrifugation. The results indicate that the adsorption to  $\text{TiO}_2$

NP strongly potentiates the effects of LPS on selected transduction pathways and changes the time-course of the macrophage activation process.

## MATERIALS AND METHODS

### Reagents

Fetal bovine serum (FBS) and culture media were purchased from Euro-Close SpA (Pero, Milan, Italy). LPS from *E. coli* O55:B5 serotype and cytochalasin B were from Sigma-Aldrich (Milan, Italy) as well as all of other chemicals used in this study, whenever not specified otherwise.

### $\text{TiO}_2$ NP Description, Dispersion, and Characterization

The NPs used were the  $\text{TiO}_2$  NP Aeroxide® P25 (anatase/rutile 83/17, Evonik Industries, Degussa GmbH, Germany), produced through the flame hydrolysis Aerosil® process. The physicochemical characterization of P25 under dry conditions is provided elsewhere (20). In particular, P25 have a specific surface area of 60 m<sup>2</sup>/g and an average crystallite size of 24 nm. TEM images of the same batch of Aeroxide® P25 used in this contribution have been recently published (21).

$\text{TiO}_2$  NP powder, previously heated at 230°C for 3 h for LPS decontamination, was suspended in culture medium without FBS to obtain 100× stock suspensions (12.8 mg/ml). For cell treatments, after vortexing for 30 s and a further incubation of 10 min in a Branson bath sonicator, the  $\text{TiO}_2$  NP stock suspension was 100-fold diluted in complete culture medium supplemented with 10% FBS so as to reach the working concentration of 128 µg/ml of NP.

The determination of NP size was performed, with minor modifications, as described in Bianchi et al. (20) at the same concentrations used for the cellular tests. Particle size distribution was evaluated by dynamic light scattering (DLS) technique assessing the hydrodynamic diameter of the dispersed NPs, using ZetasizerNano ZS (Malvern Instruments, UK) with standard polystyrene cuvettes. For the evaluation of particle size, data were recorded at 25 ± 1°C, in a backscattering detection mode (scattering angle of 173°). Each result corresponds to the average of three consecutive measurements, and each measurement is the average of 15 analyses. DLS analysis provides also a polydispersity index (PDI), which is a number ranging from 0 to 1 useful to quantify the colloidal dispersion degree: samples with PDI close to 0 are considered monodispersed. The results are presented in Figure 1 and indicate that, as expected, P25 NP aggregate when suspended.

### Formation of a LPS Corona on $\text{TiO}_2$ NP

Lipopolysaccharide corona formation on  $\text{TiO}_2$  NP (see Figure 2A) was obtained as described previously for silica NP (17) with some modifications. An aliquot of the suspension of  $\text{TiO}_2$  NP (128 µg/ml) was supplemented with 10 ng/ml of LPS (from a 100× stock solution in FBS-free medium) and incubated in an hybridizing oven for 1 h at 37°C under continuous rotation. The suspension was then centrifuged for 30 min at 1,900 × g, and the supernatant,

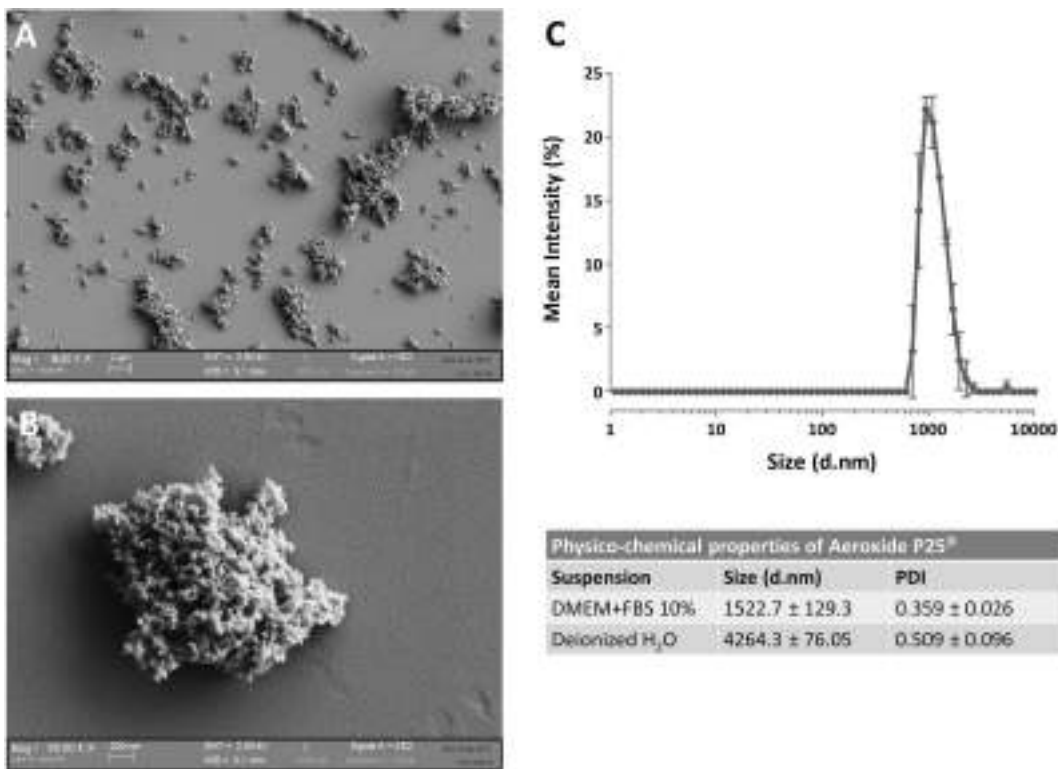


**FIGURE 1 |** Characterization of Aerioxide® P25 TiO<sub>2</sub> nanoparticles (NP). **(A,B)** SEM images of TiO<sub>2</sub> P25 NP dispersed in complete growth medium [Dulbecco's modified Eagle's medium (DMEM) + 10% fetal bovine serum (FBS)]. **(C)** Mean size distribution by intensity for P25 TiO<sub>2</sub> NP (128 µg/ml) dispersed in deionized water or complete culture medium.

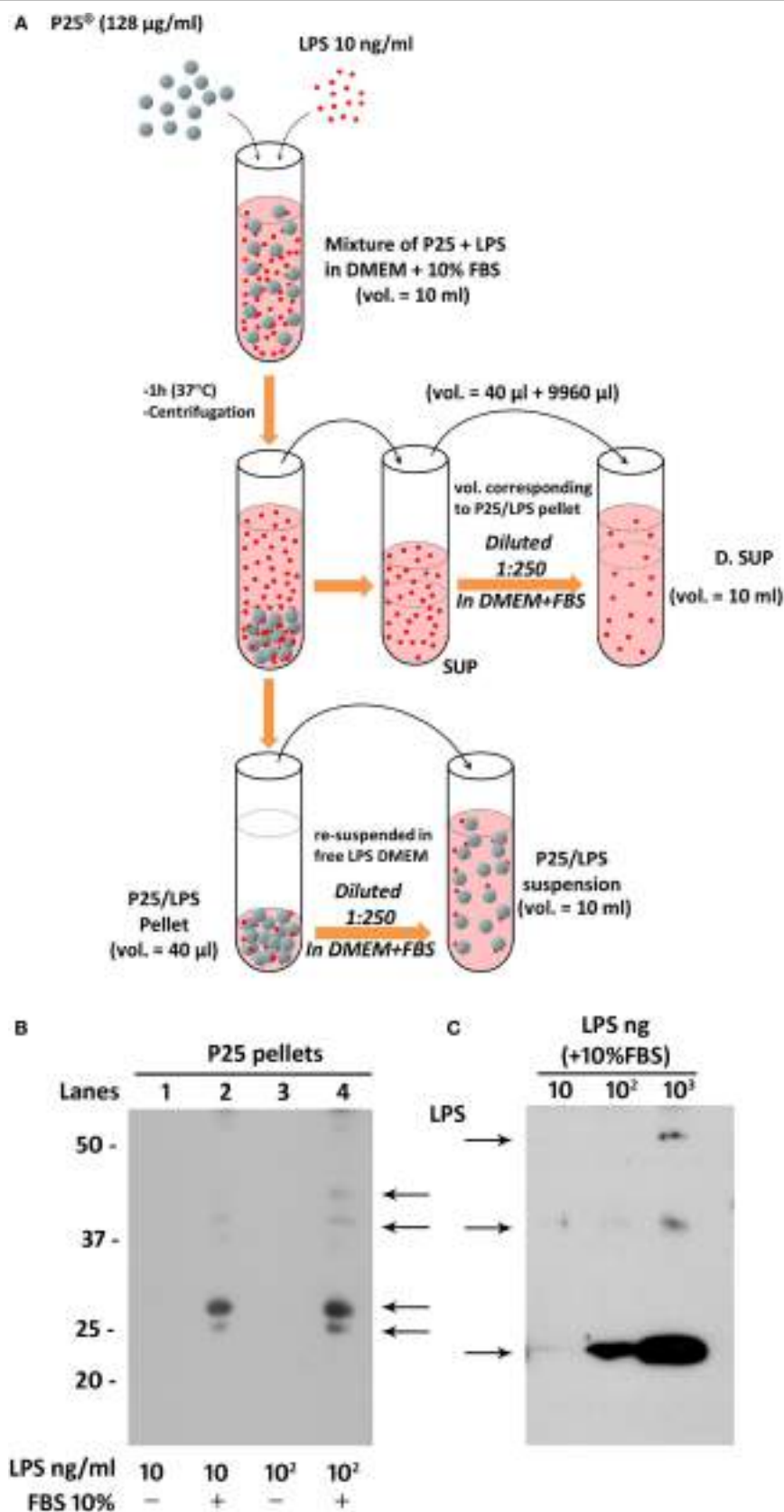
corresponding roughly to 996/1,000 of the original volume, was transferred in a new tube and named “SUP” (for supernatant). The pellet of P25 NP (4/1,000 of the original volume) was re-suspended in complete medium at a 1:250 dilution, to attain the original working concentration of 128 µg/ml, transferred into a new tube, vortexed for 1 min, and used in the experiments as “P25/LPS” suspension. To obtain the diluted SUP (D.SUP) fraction, 40 µl of the SUP fraction was diluted 1:250 with complete medium, so as to restore the original nominal LPS concentration. Another aliquot of the suspension of TiO<sub>2</sub> NP (128 µg/ml) underwent the same treatment (incubation, centrifugation, resuspension) without LPS supplementation and was used as P25 in the biological experiments.

### Western Blot of LPS in Pellet Eluates

To assess if LPS was adsorbed to P25 NP, we performed a western blot analysis against the endotoxin on the bio-corona obtained by incubating the NP with LPS. Moreover, to investigate the effect of serum proteins on LPS adsorption to NP, NP suspension and incubation with LPS was performed in the presence or in the absence of FBS 10%. Briefly, 10-ml suspensions of P25 in Dulbecco's modified Eagle's medium (DMEM) or in DMEM + 10% FBS were supplemented with 10 or 100 ng/ml of LPS. After centrifugation at 1,900 × g for 30 min, pellets were eluted in 40 µl of Laemmli buffer 1× (62.5 mM Tris-HCl, pH

6.8, 2% SDS, 10% glycerol, and 0.1 M DTT) and transferred in a clean Eppendorf tube. After heating at 95°C for 10 min, tubes were centrifuged at 12,000 rpm for 5 min. The combined elutes of two pellets (approximately 80 µl) were loaded on a 12% gel for SDS-PAGE. After the run, separated components were transferred to PVDF membranes (Immobilon-P, Millipore, Millipore Merck Corporation, MA, USA). Non-specific binding sites were blocked with an incubation of 1 h at room temperature in blocking solution (Western Blocking Reagent, Roche) diluted in Tris buffered saline (TBS, pH 7.5). The blots were then exposed at 4°C overnight to goat anti-LPS polyclonal antibody (Abcam, Cambridge, UK) diluted in the blocking solution at 1:500. After washing, the blots were exposed for 1 h at room temperature to HRP-conjugated anti-goat antibody (Cell Signaling), diluted 1:20,000 in blocking solution. Immunoreactivity was visualized with Westar HRP Substrate (Cyanagen srl, Bologna, Italy).

The results, reported in **Figure 2B**, showed an increase of LPS-positive bands for the samples with 10 (lane 2) and 100 ng/ml LPS (lane 4) at several apparent molecular weights. No bands were instead detectable for the eluates from NP incubated with the same doses of LPS but in the absence of FBS 10% (lanes 1 and 3). In parallel, the specificity of the antibody was validated in **Figure 2C**, through the western blot of different doses of LPS dissolved in Laemmli buffer 4×, supplemented with 10% FBS.

**FIGURE 2 |** Continued

**FIGURE 2 |** Continued

Preparation of P25/lipopolysaccharide (LPS) and free LPS fractions from a mixture of P25 TiO<sub>2</sub> NP and LPS. **(A)** The cartoon provides a schematic overview of the experimental approach adopted to obtain LPS-doped P25 nanoparticle (NP). The three fractions (SUP, D. SUP, and P25/LPS suspension) result from the centrifugation of the mixture of LPS (10 ng/ml) + P25 NP (128 µg/ml) in Dulbecco's modified Eagle's medium (DMEM) + 10% fetal bovine serum (FBS). The P25/LPS suspension is obtained re-suspending 1:250 the P25/LPS pellet in DMEM + 10% FBS so as to obtain the same nominal dose of P25 NP present in the original mixture. For comparison, also the D.SUP has been diluted 1:250. **(B)** Detection of LPS in extracts from pellets of P25 NP (128 µg/ml) and LPS mixtures. Lanes represent the run of eluates of the following pellets (see Materials and Methods): P25 in DMEM + LPS (10 ng/ml); P25 in DMEM (+10% FBS) + LPS (10 ng/ml); P25 in DMEM + LPS (100 ng/ml); and P25 in DMEM (+10% FBS) + LPS (100 ng/ml). The blot has been performed twice with comparable results. **(C)** Detection of LPS in western blot. The indicated amounts of LPS, dissolved in Laemmli buffer 4x supplemented with 10% FBS, were treated as described under "Materials and Methods."

## Cell Cultures and Experimental Treatments

Murine peritoneal macrophages Raw264.7 from the Istituto Zooprofilattico della Lombardia e dell'Emilia Romagna (Brescia, Italy) were cultured in DMEM completed with FBS 10%, streptomycin (100 µg/ml) and penicillin (100 U/ml) and 4 mM of glutamine. Cells were routinely cultured in 10-cm dishes under humidified atmosphere in the presence of 5% CO<sub>2</sub> in air. For the experiments, cells were seeded in 24-well plates at a density of  $75 \times 10^3/\text{cm}^2$  (20). After 24 h in culture, Raw264.7 cells were exposed to 128 µg/ml (corresponding to 80 µg/cm<sup>2</sup> of culture surface) of P25 NP, in the presence or in the absence of 10 ng/ml of LPS, to LPS (10 ng/ml), or to 128 µg/ml of P25/LPS NP for the times indicated in each experiments. Under these conditions, cell viability was not significantly affected by the experimental treatments (20).

## Nitrite Determination

The determination of nitrite concentration in culture medium was performed following the method described in Ref. (22). After 24 h of exposure of Raw264.7 to the experimental treatment, 100 µl of culture medium was transferred to black 96-well plates with a clear bottom (Corning, Cambridge, MA, USA). 20 µl of a solution of 0.025 mg/ml in 0.31 M HCl of 2,3-diaminonaphthalene (Invitrogen, Life Technologies, Monza, Italy) were then added and, after 10 min at room temperature, the reaction was stopped with 20 µl of 0.7 M NaOH. Standards were performed in the same medium from a solution of 1 mM sodium nitrite. Fluorescence was determined with a multimode plate reader Perkin Elmer Enspire.

## Western Blot of Proteins Involved in Transduction Pathways

Total protein extracts were obtained as previously described (20). Briefly, macrophages were homogenized in 70 µl of lysis buffer (20 mM Tris-HCl, pH 7.5, 150 mM NaCl, 1 mM EDTA, 1 mM EGTA, 1% Triton, 2.5 mM sodium pyrophosphate, 1 mM β-glycerophosphate, 1 mM Na<sub>3</sub>VO<sub>4</sub>, 1 mM NaF, 2 mM imidazole) supplemented with a protease inhibitors cocktail (Complete, Mini, EDTA-free, Roche, Monza, Italy). Lysates were transferred in Eppendorf tubes and mixed with 23 µl (1/3 of the lysate total volume) of Laemmli buffer 4x (250 mM Tris-HCl, pH 6.8, 8% SDS, 40% glycerol, and 0.4 M DTT). After heating at 95°C for 10 min, 30 µl of each samples was loaded on a 10% gel for SDS-PAGE. Separated proteins were transferred to PVDF membranes (Immobilon-P, Millipore, Millipore Merck Corporation, MA, USA). Non-specific binding sites were blocked with an

incubation of 1 h at room temperature in blocking solution (Western Blocking Reagent, Roche) diluted in TBS (pH 7.5). The blots were then exposed at 4°C overnight to the following antibodies diluted in 5% BSA in TBST (Tween 20 0.1% in TBS): anti-Nos2 (rabbit polyclonal, 1:400, Santa Cruz Biotechnology, Santa Cruz, CA, USA); anti-p-p38 (rabbit polyclonal, 1:500, R&D Systems, Minneapolis, MN, USA); anti-p38 (rabbit polyclonal, 1:500, R&D Systems); anti-p-ERK (rabbit polyclonal, 1:500, R&D Systems); anti-ERK (rabbit polyclonal, 1:500, R&D Systems); anti-p-IRF3 (rabbit polyclonal, 1:500, Biorbyt, Cowley Road, Cambridge, UK); anti-IRF3 (rabbit polyclonal, 1:1,000, Cell Signaling Technology, Danvers, MA, USA); anti-p-STAT1 (rabbit polyclonal, 1:1,000, Cell Signaling); anti-STAT1 (rabbit polyclonal, 1:1,000, Cell Signaling); anti-p-c-JUN (rabbit polyclonal, 1:1,000, Millipore Merck); anti-c-JUN (rabbit antiserum, 1:1,000, Millipore Merck); and anti-beta actin (mouse monoclonal, 1:2000, Santa Cruz Biotechnology). After washing, the blots were exposed for 1 h at room temperature to HRP-conjugated anti-rabbit or anti-mouse antibodies (Cell Signaling), diluted 1:20,000 in blocking solution. Immunoreactivity was visualized with Immobilon Western Chemiluminescent HRP Substrate (Millipore, Merck).

## RT-PCR

Total RNA was isolated with GenElute Mammalian Total RNA Miniprep Kit (Sigma-Aldrich) as described in Ref. (20). After reverse transcription, aliquots of cDNA from each sample were amplified in a total volume of 25 µl with the Go Taq PCR Master Mix (Promega Italia, Milan, Italy), along with the forward and reverse primers (5 pmol each) reported in Table 1. Real-time PCR was performed in a 36-well RotorGeneTM3000, version 5.0.60 (Corbett Research, Mortlake, VIC, Australia). For all the messengers to be quantified, each cycle consisted of a denaturation step at 95°C for 20 s, followed by separate annealing (30 s) and extension (30 s) steps at a temperature characteristic for each pair of primers (Table 1). Fluorescence was monitored at the end of each extension step. Melting curve analysis was added at the end of each amplification cycle. Data analysis was made according to the relative standard curve method. Expression data were reported as the ratio between each investigated mRNA and Gapdh mRNA.

## Confocal Microscopy of Live Cells

Raw264.7 cells were seeded on four-well chambered coverglasses at a density of  $75 \times 10^3/\text{cm}^2$ . The day after, cells were incubated in the presence or in the absence of cytochalasin B (20 µM, Sigma-Aldrich) for 1 h and then stained with LysoTracker™

**TABLE 1 |** Primers and temperatures of annealing adopted for RT-PCR experiments.

Gene	Forward	Reverse	T (°C)	Amplicon size (bp)
Tumor necrosis factor alpha ( <i>Tnfa</i> )	5'-CCCTCACACTC AGATCATCTTCT-3'	5'-GCTACGAGC TGGGCTACAG-3'	55°C	61
Interferon beta 1 ( <i>Ifnb</i> )	5'-CAGCTCCAAG AAAGGACGAAC-3'	5'-GGCAGTGAA CTCTTCTGCAT-3'	56°C	138
Interferon-induced protein with tetratricopeptide repeats 2 ( <i>Ifit2</i> )	5'-AGAACCAAAAC GAGAGAGTGAAG-3'	5'-TCCAGACGGT AGTCGCAATG-3'	57°C	106
Glyceraldehyde 3-phosphate dehydrogenase ( <i>Gapdh</i> )	5'-TGT TCC TAC CCC CAA TGT GT-3'	5'-GGT CCT CAG TGT AGC CCA AG-3'	57°C	137

Red DND-99 (70 nM, Molecular Probes, Life Technologies) and calcein-AM (1 μM, Millipore Merck) for 2 h. Stained cells were then treated with 5 μg/cm<sup>2</sup> of P25 NP or P25/LPS and imaged by an inverted LSM 510 Meta (Carl Zeiss, Jena, Germany) while maintained at 37°C, 5% CO<sub>2</sub> in a Kit Cell Observer (Carl Zeiss, Jena, Germany) (23–25). Single-plane confocal images were taken at 24 h of treatment using a 40× (1.3 NA) oil objective. Excitation at 633 nm and reflectance were used to visualize P25 TiO<sub>2</sub> NPs; excitation at 543 nm and emission recorded through a 580- to 630-nm band pass barrier filter were used for Lysotracker™ to visualize lysosomes; excitation at 488 nm and emission through a 515- to 540-nm band pass filter were used for calcein to visualize cytoplasm.

## Statistical Analysis

Data are expressed as means ± SD. For nitrite determination experiments, the statistical analysis was performed through one-way ANOVA for multiple comparisons, applying the Bonferroni correction. In all the other experiments, a two-tail Student's *t*-test for unpaired data was adopted. Graph Pad Prism™ software version 6.00 (Graph Pad Software Inc., San Diego, CA, USA) was used. Results were considered significant with *p* < 0.05.

## RESULTS

### P25/LPS Strongly Potentiates the LPS-Dependent NO Production and Nos2 Protein Expression in Murine Macrophages

We have previously demonstrated that the simultaneous exposure to TiO<sub>2</sub> NP and LPS synergized the pro-inflammatory effects of the two compounds (20). To assess if we could reproduce this effect with the P25/LPS fraction, nitrite medium concentration (as a proxy of NO production) and Nos2 expression were evaluated after 24 h of exposure of Raw264.7 cells to TiO<sub>2</sub> NP, LPS, the

mixture of NP, and LPS, and the two fractions resulting from the centrifugation of the mixture (the re-suspended pellet and the supernatant, see **Figure 2A** for details). The results, presented in **Figure 3A**, indicate that, while P25 NP alone did not significantly affect NO production, the P25/LPS fraction (nominal concentration of LPS 40 pg/ml) caused a huge increase in nitrite concentration in culture medium. The TLR4-dependence of the effect was confirmed by its suppression in cells treated with polymyxin B (50 μg/ml, results not shown). The magnitude of the effect was not significantly different to that caused by LPS alone, while it was smaller than that observed upon a simultaneous incubation with LPS and P25 NP. Free LPS in the undiluted supernatant fraction (nominal concentration of 10 ng/ml) also caused a comparable increase in nitrites. On the contrary, when diluted at the same ratio used for P25/LPS (1:250, nominal concentration of LPS 40 pg/ml), the supernatant fraction did not stimulate macrophages to produce NO. Consistently, results presented in **Figure 3C** indicate that free LPS at 40 pg/ml did not increase NO production that required a dose of LPS of at least 1 ng/ml.

Functional data were consistent with the results obtained by western blot. Indeed, Nos2 protein expression was markedly increased in cells exposed to P25/LPS, at levels comparable with those observed with LPS alone and only slightly lower than those observed after exposure to the mixture LPS plus NP (**Figure 3B**). As expected, the diluted supernatant (free LPS) did not affect the expression of Nos2.

### P25/LPS Promotes the Activation of both NF-κB/AP1 and IRF3-Dependent Genes

The induction of pro-inflammatory genes is the final result of a cascade of intracellular signals that involves different transduction pathways. To assess the effect of P25/LPS on the induction of pro-inflammatory genes dependent on different pathways, the expression of *Tnfa* and *Ifnb* was evaluated after 6 and 24 h of treatment by RT-PCR. While *Tnfa* expression is controlled by the MyD88-NF-κB-AP1-dependent pathway (26), *Ifnb* gene is mainly dependent on the TRIF pathway through the activation of IRF transcription factors (27). As reported in **Figure 4A**, the mixture of P25 and LPS markedly potentiated the LPS-dependent *Tnfa* induction after 6 h of exposure. While P25 NP alone did not affect significantly gene expression, the P25/LPS fraction induced *Tnfa* at levels comparable to those stimulated by free LPS. A comparable induction of *Tnfa* was also produced by the undiluted supernatant fraction, while the diluted supernatant was without effect. At 24 h *Tnfa* expression was further increased in cells treated with free LPS and undiluted supernatant, while it decreased in cells treated with the mixture and remained fairly stable with the P25/LPS fraction. The induction of *Ifnb* (**Figure 4B**) was clearly detectable after 6 h of exposure to free LPS, the mixture of LPS and NP, or the undiluted supernatant, while it was much lower, although significant, in cells treated with the P25/LPS fraction. When studied after 24 h of exposure, *Ifnb* mRNA levels markedly decreased in cells treated with free LPS, the mixture of LPS and NP, or the undiluted supernatant but, conversely, increased in cells incubated with the P25/LPS

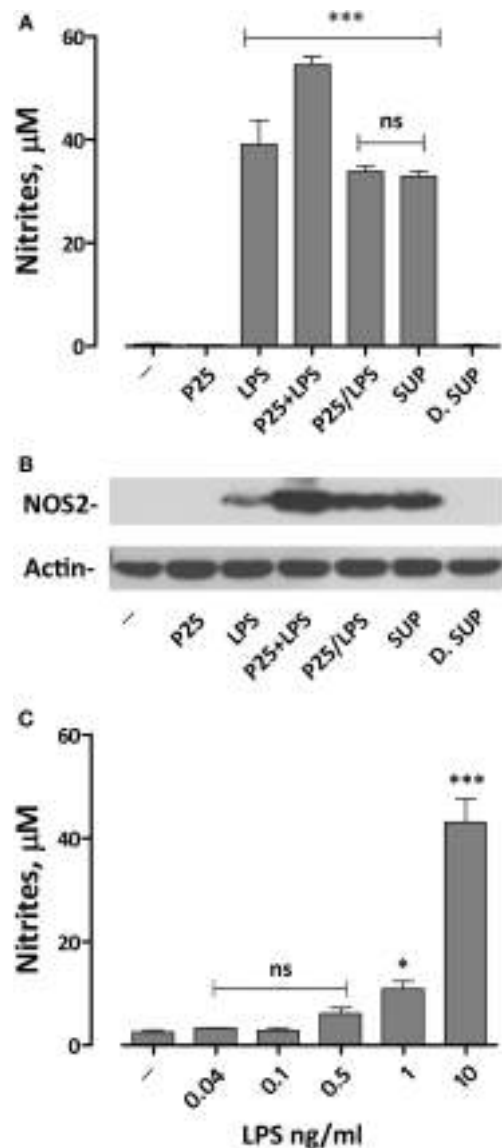


**FIGURE 3 |** Effects of the exposure to P25/lipopolysaccharide (LPS) on nitric oxide production and Nos2 expression in macrophages. Raw264.7 cells were incubated for 24 h in Dulbecco's modified Eagle's medium (DMEM) + 10% fetal bovine serum (FBS) in the presence of P25 (128  $\mu\text{g}/\text{ml}$ ), LPS (10 ng/ml), the mixture of P25 and LPS (128  $\mu\text{g}/\text{ml}$  + 10 ng/ml, respectively), P25/LPS (the pellet of the spun mixture, re-suspended at the original volume, with nominal doses of 128  $\mu\text{g}/\text{ml}$ , for TiO<sub>2</sub> NP, and 40 pg/ml for LPS), the undiluted (SUP, nominal LPS dose 10 ng/ml), or diluted (D.SUP, nominal LPS dose of 40 pg/ml) supernatant of the spun mixture. **(A)** At the end of the incubation, the culture medium was harvested to determine nitrite concentration. **(B)** The same cell monolayers were lysed to evaluate Nos2 expression through WB analysis. The experiment has been performed twice with comparable results. **(C)** Raw264.7 cells were incubated for 24 h in the presence of the indicated doses of LPS in DMEM + 10% FBS. At the end of the incubation, the culture medium was harvested to determine nitrite concentration. For **(A,C)**, data are means of four independent determinations  $\pm$  SD. For **(A)**, \*\*\*,  $p < 0.001$  vs. cells treated with P25; ns, not significant vs. LPS alone, as evaluated by one-way ANOVA for multiple comparisons with Bonferroni correction. For **(C)**, \*, \*\*,  $p < 0.05$ ,  $p < 0.001$  vs. LPS-untreated cells; ns, not significant vs. LPS-untreated cells, as evaluated by one-way ANOVA for multiple comparisons with Bonferroni correction.

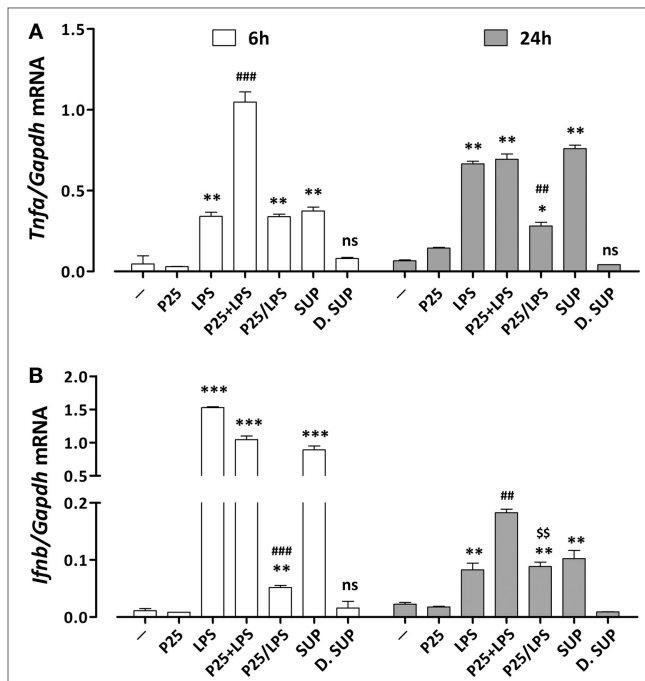
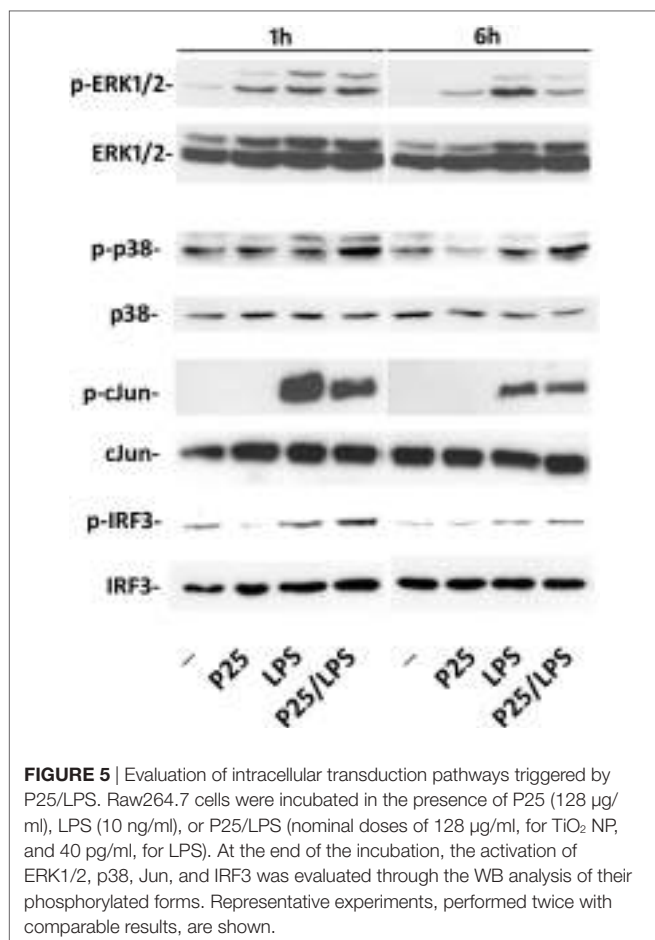


**FIGURE 4 |** Assessment of the pro-inflammatory gene response elicited by P25/lipopolysaccharide (LPS) in macrophages. mRNA expression levels of *Tnfa* **(A)** and *Ifnb* **(B)** were assessed in Raw264.7 cells after 6 and 24 h of exposure to the indicated experimental conditions (see legend to **Figure 2** for details). Control cells (–) were incubated in plain serum-supplemented medium. Data are means of two (for *Tnfa*) or three (for *Ifnb*) independent experiments each performed in duplicate with SD shown. \*, \*\*, \*\*\*  $p < 0.05$ ,  $p < 0.01$ ,  $p < 0.001$  vs. cells treated with P25 at the same experimental time; ##, ###,  $p < 0.01$ ,  $p < 0.001$  vs. cells treated with LPS at the same experimental time; \$\$,  $p < 0.01$  vs. cells treated with P25/LPS at 6 h, as evaluated by two-tailed *t*-test for unpaired data.

fraction. Also for this gene the diluted supernatant had no stimulatory effects.

### P25/LPS and Free LPS Differentially Activate Intracellular Transduction Pathways

The representative experiment shown in **Figure 5** reports the effect of P25/LPS and free LPS on several components of the transduction pathways activated by LPS. MAPK cascade is an integral part of the MyD88-dependent transduction pathway that ends in the phosphorylation of Jun and the subsequent activation of the transcription factor AP1. One hour after medium replacement, the ERK1/2 branch of the MAPK pathway was activated in cells incubated with P25, LPS, and P25/LPS, as revealed by the high abundance of the phosphorylated forms. ERK1/2 activation persisted at 6 h in cells incubated with LPS while decreased in cultures exposed to either P25 or P25/LPS. In contrast, P25/LPS produced a clearly larger activation of p38 than LPS at both experimental times. The JNK substrate Jun was strongly activated by LPS at 1 h of treatment and, at a lesser degree, by P25/LPS. In both conditions, Jun phosphorylated form decreased at 6 h. As expected by *Ifnb* induction, a clear-cut phosphorylation of



IRF3 was detected after 1 h of treatment in cells incubated with either free LPS or P25/LPS. In both conditions, activation of IRF3 decreased at 6 h, but it was still more evident in cells exposed to P25/LPS compared to LPS-treated cells extracted at the same time.

### P25/LPS Shifts the Kinetics of LPS-Dependent *Ifit2* Induction

To verify if adsorption to P25 NP effectively changes the time-course of *Ifnb* induction, we investigated the expression of *Ifit2*, an IFNβ-induced gene that encodes a member of a group of proteins responsible for the inhibition of viral replication (28). As many other IFN-dependent genes, *Ifit2* induction is activated by the phosphorylation of STAT transcription factors. STAT1 phosphorylation was already detectable after 1 h of incubation in cells treated with free LPS but not with P25/LPS. In contrast, after 6 h, a massive STAT1 activation was evident in cells treated with either LPS or P25/LPS (Figure 6A). Consistently, also *Ifit2* induction followed a different time-course in the two experimental conditions (Figure 6B). In cells incubated with free LPS, a huge increase of *Ifit2* mRNA was evident after 6 h of incubation while P25/LPS was completely ineffective at this time point. In contrast, at 24 h of treatment, P25/LPS caused a larger *Ifit2* induction than free LPS.

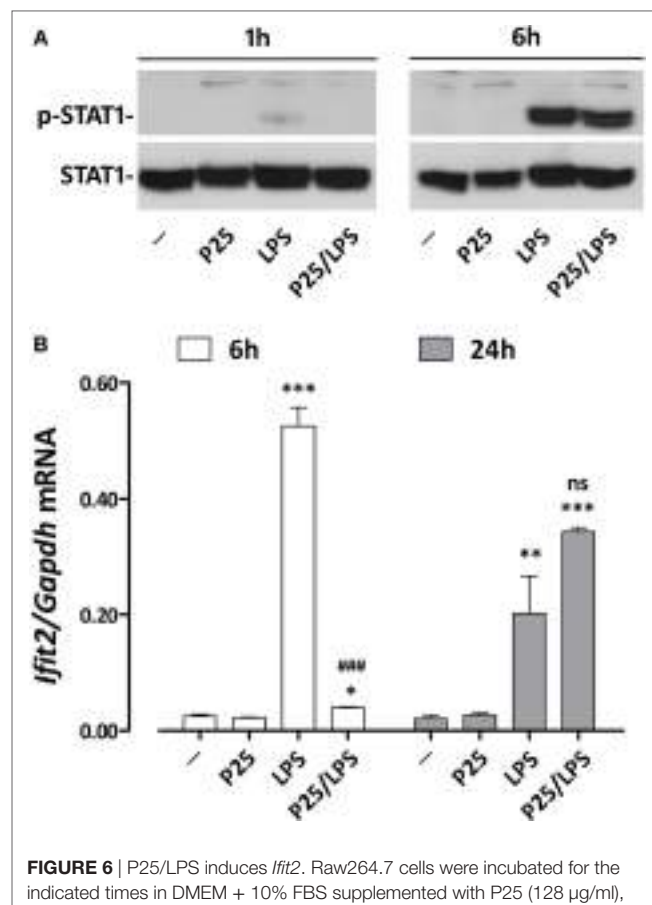


**FIGURE 6 |** P25/LPS induces *Ifit2*. Raw264.7 cells were incubated for the indicated times in DMEM + 10% FBS supplemented with P25 (128 µg/ml), LPS (10 ng/ml), or P25/LPS (nominal doses of 128 µg/ml, for TiO<sub>2</sub> NP, and 40 pg/ml, for LPS). Control cells (–) were incubated in plain DMEM + 10% FBS. (A) After 1 or 6 h, the activation of STAT1 was evaluated through WB analysis. A representative experiment, performed twice with comparable results, is shown. (B) After 6 or 24 h *Ifit2* expression was assessed by RT-PCR. Data are means of two independent experiments, each performed in duplicate, with SD shown. \*, \*\*, \*\*\*, p < 0.05, p < 0.01, or p < 0.001 vs. cells treated with P25 at the same experimental time; \*\*\*, p < 0.001 vs. cells treated with LPS at the same experimental time, as evaluated by two-tailed t-test for unpaired data.

### Cytoskeleton Disruption and Internalization Inhibition Differentially Affect the Induction of TRIF-Dependent and -Independent Genes

The confocal images (Figure 7) show the effects of LPS adsorption on TiO<sub>2</sub> NP internalization. Under our experimental conditions, most of the P25 NP formed aggregates that are well evident from the reflected light (Figures 7A–D, white). P25, which were preheated at 230°C so as to eliminate LPS before the experiment, were scarcely internalized by Raw264.7 macrophages, as indicated by their prevalent visualization in the extracellular compartment (Figure 7A, arrowheads). Consistently, in the same field, lysosomes were red or yellow (indicating a partial co-localization with calcein). On the contrary, P25/LPS were massively taken up by cells and internalized in discrete compartments (Figure 7C,

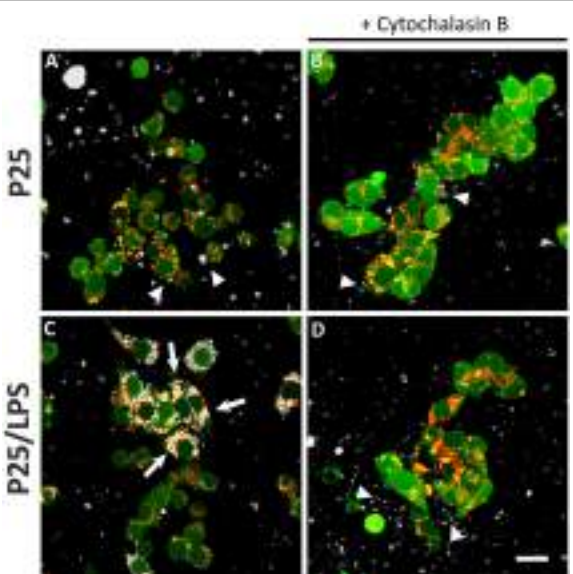


**FIGURE 7 |** Internalization of  $\text{TiO}_2$  P25 and P25/LPS. Raw264.7 cells were preincubated for 1 h in the absence (**A,C**) or in the presence of cytochalasin B [20  $\mu\text{M}$ ] (**B,D**) and then exposed to P25 [16  $\mu\text{g/ml}$ ] (**A,B**) or P25/LPS [nominal dose 16  $\mu\text{g/ml}$ ] (**C,D**) for further 24 h. At the end of the incubation, cell monolayers were stained with calcein-AM, for cytoplasm and nucleus, and LysoTracker<sup>®</sup>, for lysosomes, as reported in “Materials and Methods.” For each condition, a single horizontal confocal section of a representative field is shown. P25 or P25/LPS, white; cells, green; lysosomes, red. The experiment has been performed twice with similar results. Arrows, internalized NP aggregates. Arrowheads, extracellular NP aggregates in contact with the cell membrane. Bar = 20  $\mu\text{m}$ .

arrows), in some of which a co-localization with the lysosomal marker was evident. Under this condition, most of the NP in the field were intracellular. As expected, cytochalasin B blocked the internalization, although P25 NP aggregates were detected in close contact with the cells (**Figure 7D**, arrowheads).

To assess if the signal triggered by LPS or P25/LPS depends on internalization, p38 activity was investigated in cells exposed to free LPS or P25/LPS with or without a 1 h-pretreatment with cytochalasin B. The results (**Figure 8A**) indicate that inhibition of internalization did not impair the activation of p38 by free LPS, which was even increased, but markedly hindered the P25/LPS effect on the kinase. LPS-dependent stimulation of *Tnfa* expression, assessed at 6 h of exposure (**Figure 8B**), was not affected at all by cytoskeletal disruption, while a small, but significant inhibition was observed in P25/LPS-treated cells. On the contrary, cytochalasin B completely prevented the induction of both *Infb* (**Figure 8C**) and *Ifit2* (**Figure 8D**) by either LPS or P25/LPS.

## DISCUSSION

Once introduced into the body, engineered nanomaterials adsorb biomolecules from the biological fluids. Thus, the biological effects observed *in vivo* could be due not only to the synthetic identity of the materials but also to the bioactive agents adsorbed

on their surface (29). As far as LPS is concerned, experimental evidence describing LPS adsorption by different types of NP has been already reported, although the biological consequences of the interaction are controversial, with enhancing or mitigating effects reported in different contributions (13–17). These conflicting observations may be related to particular physico-chemical features of the NP tested. In particular, NP endowed with a low PDI tend to float in culture medium and may act as LPS quenchers in cultures of adherent cells. On the contrary, NP endowed with a high PDI in biological media, would work as LPS deliverers, given their tendency to aggregate and precipitate on adherent cells. Under the experimental conditions adopted here, P25 NP markedly aggregate and, as visualized with the confocal images, come in close contact with the cell monolayer. Thus, the bioavailability of adsorbed LPS would be enhanced.

In agreement with these arguments, we had observed that  $\text{TiO}_2$  P25 NP, co-administered with LPS, strongly enhanced the pro-inflammatory response triggered in murine macrophages by the endotoxin, a result that could be attributed to the presence of LPS adsorbed to NP (20). In order to discriminate the roles played by free LPS or LPS adsorbed on P25 NP in macrophage activation, we treated Raw264.7 cells with spun P25 NP obtained from a NP suspension preincubated in complete serum-supplemented medium in the presence of LPS. The pellet of P25/LPS has been re-suspended in the original volume of LPS-free medium, and its effects on macrophages were compared with those observed after exposure to free LPS. We avoided the washing of the pellet, so as to closely mimic the situation *in vivo*, in which cells are exposed to nanomaterials suspended in high-protein media endowed with both hard and soft corona (30, 31). In the biological matrix adopted here (DMEM supplemented with 10% FBS), LPS may be adsorbed to the NP bio-corona through its binding to proteins, thus interacting only indirectly with the NP. The western blot analysis shown in **Figure 2B** indicates that LPS can be indeed eluted from the spun  $\text{TiO}_2$  NP (the P25/LPS fraction). Interestingly, the endotoxin was detectable only if the incubation of the NP and LPS had been performed in the presence of serum, suggesting that proteins actually promote the adsorption of the endotoxin to the NP bio-corona. This means that the material that interacts with the cells does not consist of a binary complex aggregated NP-LPS but, most likely, of a ternary complex aggregated NP-serum proteins-LPS. Further investigations are needed to ascertain if the presence of LPS changes the quality or quantity of the serum proteins adsorbed and how the adsorbed proteins modulate the biological effects of the endotoxin.

In the previous paper, we limited our analysis to pro-inflammatory genes the induction of which relies on the activation of MyD88-dependent transduction pathways and AP1/NF- $\kappa$ B-dependent transcription, such as *Tnfa* and *Nos2* (20). In this contribution, besides confirming those effects (**Figures 3, 4** and **8**), we have studied pro-inflammatory genes, such as *Infb* and *Ifit2*, mainly dependent upon the activation of the TRIF pathway and IRF transcription factors. Also for these genes, P25/LPS was highly effective (**Figures 4, 6** and **8**), leading to a level of gene induction comparable with that caused by 10 ng/ml of free LPS, at least at later times of incubation. We have not extended our

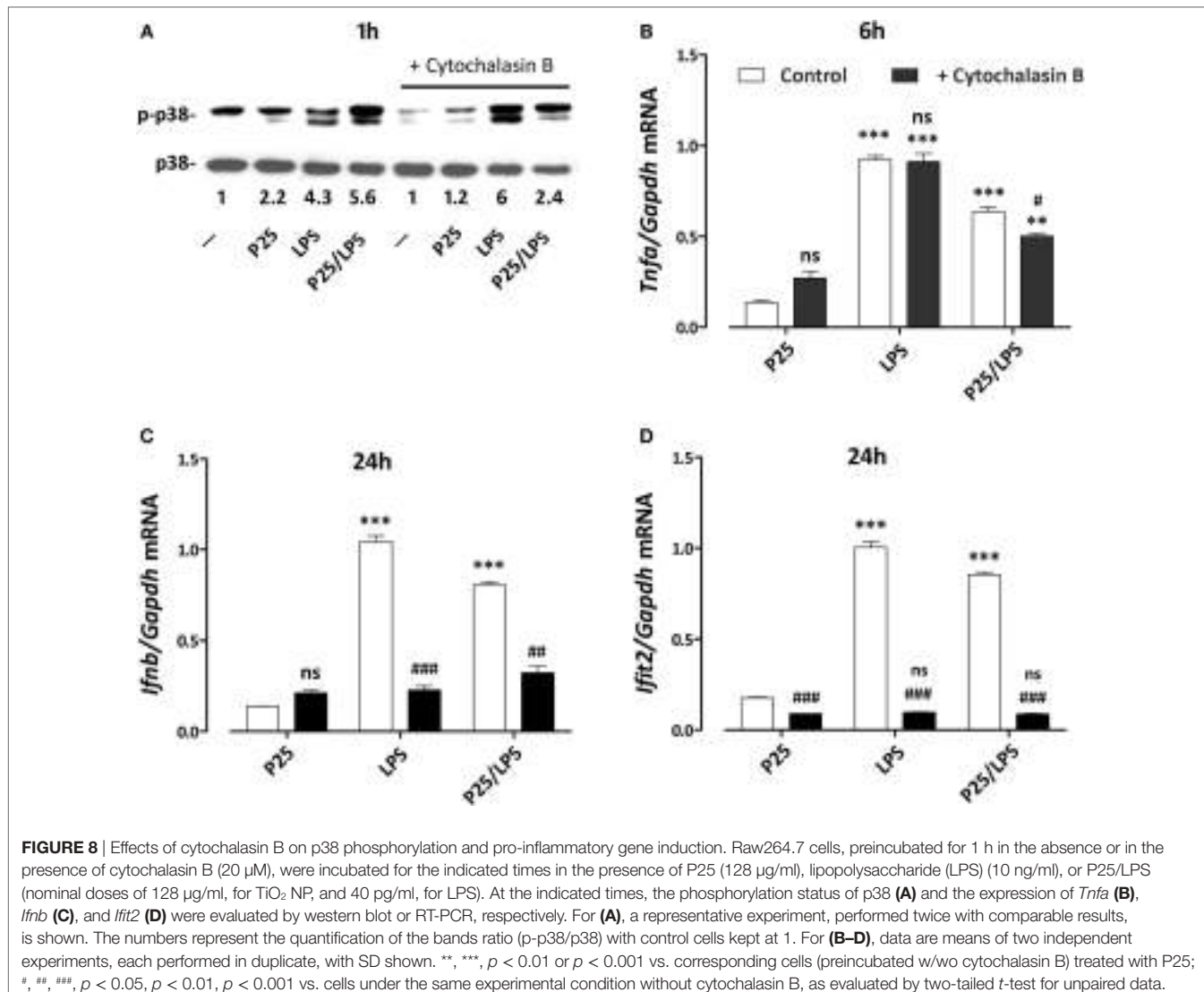


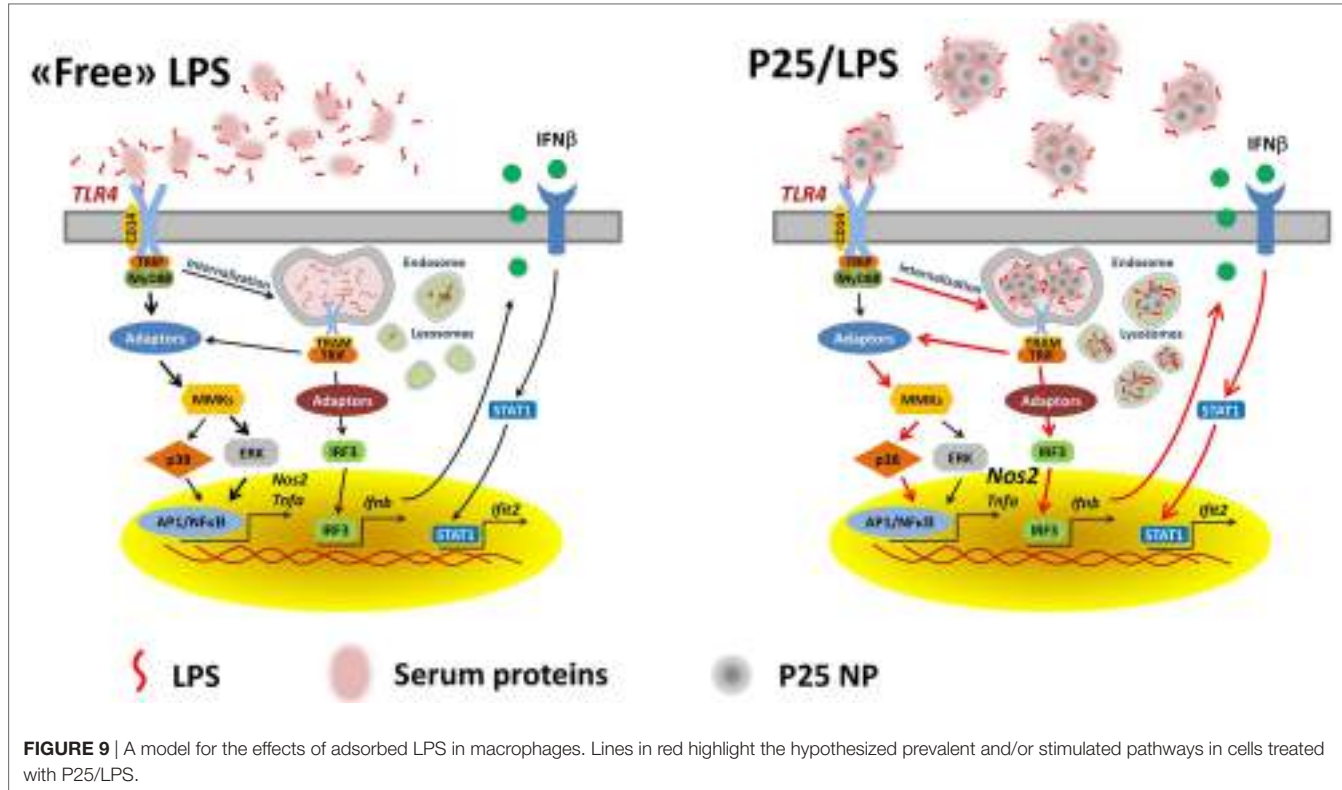
**FIGURE 8 |** Effects of cytochalasin B on p38 phosphorylation and pro-inflammatory gene induction. Raw264.7 cells, preincubated for 1 h in the absence or in the presence of cytochalasin B (20  $\mu$ M), were incubated for the indicated times in the presence of P25 (128  $\mu$ g/ml), lipopolysaccharide (LPS) (10 ng/ml), or P25/LPS (nominal doses of 128  $\mu$ g/ml, for TiO<sub>2</sub> NP, and 40 pg/ml, for LPS). At the indicated times, the phosphorylation status of p38 (**A**) and the expression of *Tnfa* (**B**), *Ifnb* (**C**), and *Ifit2* (**D**) were evaluated by western blot or RT-PCR, respectively. For (**A**), a representative experiment, performed twice with comparable results, is shown. The numbers represent the quantification of the bands ratio (p-p38/p38) with control cells kept at 1. For (**B–D**), data are means of two independent experiments, each performed in duplicate, with SD shown. \*\*, \*\*\*,  $p < 0.01$  or  $p < 0.001$  vs. corresponding cells (preincubated w/o cytochalasin B) treated with P25; #, ##, ###,  $p < 0.05$ ,  $p < 0.01$ ,  $p < 0.001$  vs. cells under the same experimental condition without cytochalasin B, as evaluated by two-tailed *t*-test for unpaired data.

analysis to protein products, since, being interested in mechanisms and time-course of signal transduction, changes in gene expression at mRNA levels is the earliest output while protein levels could be influenced by other regulatory mechanisms.

The activation of IRF3 and STAT1 was also quantitatively comparable in cells treated with free LPS and P25/LPS at 6 h of treatment (Figures 5 and 6). Given the very high dilution of the P25/LPS fraction before exposure (see Figure 2A), the clear-cut effects observed cannot be attributed to the residual free LPS (the nominal concentration of which would be 40 pg/ml), since free LPS at that concentration was without effect (Figure 3C). However, these results are consistent with the presence of LPS in the NP bio-corona, provided that adsorption increases the quantity of LPS present in the P25/LPS fraction or enhances its biological effects. We were not able to quantify this fraction either with silver staining or with Limulus test (not shown), possibly for the interference of the NP with the test. However, it is likely that this aliquot is low, as suggested by the substantially

comparable effects (Figures 3 and 4) of free LPS (at a concentration of 10 ng/ml) and the SUP fraction, which is the supernatant resulting from the centrifugation of the mixture NP + LPS (see Figure 4A).

Once included in the NP bio-corona, LPS caused a prolonged activation of p38 MAPK, while free LPS promoted a more evident activation, also at later times, of the ERK1/2 branch of MAPK (Figure 5). These data, consistent with the results reported by others with gold NPs (32), suggest that a differential activation of the two MAPK branches occurs if LPS is free or adsorbed to NP. Moreover, when compared to free endotoxin, P25/LPS had delayed effects on STAT1 activation and *Ifit2* induction (Figure 6), two typical IFN $\beta$ -dependent effects (33). Indeed, *Ifnb* induction was slower, but more stable, in cells treated with P25/LPS compared to free LPS (Figure 4). Conversely, as far as *Tnfa* is concerned, free LPS triggered a more prolonged gene induction. Taken together, these results highlight a different time-course of effects of P25/LPS and free LPS.



We proposed a model in which mixing LPS with P25 leads to higher and more prolonged biological activity of the endotoxin and attributed the enhanced effects to the capability of triggering different transduction pathways and, in particular, of recruiting intracellular sites for signal transduction (20). As far as this issue is concerned, the results presented here substantially confirm that model. Indeed, the activation of p38 by P25/LPS, but not by free LPS, was sensitive to cytochalasin B and, consistently, cytochalasin B partially inhibited *Tnfα* induction by P25/LPS, but not by free LPS. On the other hand, the confocal images presented in **Figure 7** indicate that the internalization of NP is much more evident for P25/LPS than for LPS-free NP, demonstrating that LPS adsorption enhances NP uptake, provides a facilitated access to endosomal sites of signal transduction and, likely, interferes with the processing of the LPS-TLR4 complex, thus ensuring a greater bio-persistence of the stimulus. However, cytochalasin B completely suppressed *Ifnb* and *Ifit2* induction by either free LPS or P25/LPS. This result is easily explained, if one considers that these genes are mainly TRIF-dependent and, hence, the relevant signals start from the endosomal compartment even in the case of free LPS, as demonstrated by the pivotal contribution by Kagan et al. (34). The evolution of the model on the basis of the data presented in this contribution is shown in **Figure 9**. In this model, we hypothesize that adsorbed LPS has enhanced and/or delayed effects due to an increased activity of internalization-dependent pathways.

The adsorption of LPS to TiO<sub>2</sub> NP may account for the inflammatory changes observed *in vivo* after exposure to the nanomaterials under non-sterile conditions, such as those encountered

in some working scenarios in which the exposure to TiO<sub>2</sub> NP is associated with lung inflammation (35). On the other hand, unpublished results from our laboratory indicate that a substantial enhancement of biological effects upon interaction with NP is observed not only for LPS but also for other TLR agonists, such as polyI:C and zymosan. Thus, the acquisition by NP of a novel, more active biological identity after contact with biological fluids containing proteins and bioactive molecules may significantly enhance the inflammatory risks for individuals with conditions associated with increased levels of endogenous or exogenous TLR agonists.

In conclusion, these data suggest that, when included in the bio-corona of TiO<sub>2</sub> NP, LPS exhibits enhanced and time-shifted pro-inflammatory effects. Thus, in assessing the hazard of NP in real life, the enhanced effects of adsorbed bioactive molecules should be taken into account.

## AUTHOR CONTRIBUTIONS

MGB, MA, and MC performed the experiments; AC, MB, and SO provided reagents and performed the characterization of TiO<sub>2</sub> NP; MGB and OB analyzed the data and wrote the manuscript; AC and EB critically read the manuscript. All the authors have approved the manuscript.

## FUNDING

This work was supported by EU FP7 SANOWORK (grant no. 280716) to EB.

## REFERENCES

- Fadeel B. Clear and present danger? Engineered nanoparticles and the immune system. *Swiss Med Wkly* (2012) 142:w13609. doi:10.4414/smw.2012.13609
- Neagu M, Piperigkou Z, Karamanou K, Engin AB, Docea AO, Constantin C, et al. Protein bio-corona: critical issue in immune nanotoxicology. *Arch Toxicol* (2016) 91:1031–48. doi:10.1007/s00204-016-1797-5
- Cai K, Wang AZ, Yin L, Cheng J. Bio-nano interface: the impact of biological environment on nanomaterials and their delivery properties. *J Control Release* (2017). doi:10.1016/j.jconrel.2016.11.034
- Monopoli MP, Aberg C, Salvati A, Dawson KA. Biomolecular coronas provide the biological identity of nanosized materials. *Nat Nanotechnol* (2012) 7:779–86. doi:10.1038/nnano.2012.207
- Parveen R, Shamsi TN, Fatima S. Nanoparticles-protein interaction: role in protein aggregation and clinical implications. *Int J Biol Macromol* (2017) 94:386–95. doi:10.1016/j.ijbiomac.2016.10.024
- Guerville M, Boudry G. Gastrointestinal and hepatic mechanisms limiting entry and dissemination of lipopolysaccharide into the systemic circulation. *Am J Physiol Gastrointest Liver Physiol* (2016) 311:G1–15. doi:10.1152/ajpgi.00098.2016
- Kallio KA, Hatonen KA, Lehto M, Salomaa V, Mannisto S, Pussinen PJ. Endotoxemia, nutrition, and cardiometabolic disorders. *Acta Diabetol* (2015) 52:395–404. doi:10.1007/s00592-014-0662-3
- Boutagy NE, McMillan RP, Frisard MI, Hulver MW. Metabolic endotoxemia with obesity: is it real and is it relevant? *Biochimie* (2016) 124:11–20. doi:10.1016/j.biochi.2015.06.020
- Tan Y, Kagan JC. A cross-disciplinary perspective on the innate immune responses to bacterial lipopolysaccharide. *Mol Cell* (2014) 54:212–23. doi:10.1016/j.molcel.2014.03.012
- Gangloff M. Different dimerisation mode for TLR4 upon endosomal acidification? *Trends Biochem Sci* (2012) 37:92–8. doi:10.1016/j.tibs.2011.11.003
- Wang Y, Yang Y, Liu X, Wang N, Cao H, Lu Y, et al. Inhibition of clathrin/dynamin-dependent internalization interferes with LPS-mediated TRAM-TRIF-dependent signaling pathway. *Cell Immunol* (2012) 274:121–9. doi:10.1016/j.cellimm.2011.12.007
- Watanabe S, Kumazawa Y, Inoue J. Liposomal lipopolysaccharide initiates TRIF-dependent signaling pathway independent of CD14. *PLoS One* (2013) 8:e60078. doi:10.1371/journal.pone.0060078
- Dutta D, Sundaram SK, Teeguarden JG, Riley BJ, Fifield LS, Jacobs JM, et al. Adsorbed proteins influence the biological activity and molecular targeting of nanomaterials. *Toxicol Sci* (2007) 100:303–15. doi:10.1093/toxsci/kfm217
- Shen L, Higuchi T, Tubbe I, Voltz N, Krummen M, Pektor S, et al. A trifunctional dextran-based nanovaccine targets and activates murine dendritic cells, and induces potent cellular and humoral immune responses in vivo. *PLoS One* (2013) 8:e80904. doi:10.1371/journal.pone.0080904
- Murali K, Kenesei K, Li Y, Demeter K, Kornyei Z, Madarasz E. Uptake and bio-reactivity of polystyrene nanoparticles is affected by surface modifications, ageing and LPS adsorption: in vitro studies on neural tissue cells. *Nanoscale* (2015) 7:4199–210. doi:10.1039/c4nr06849a
- Grosse S, Stenvik J, Nilsen AM. Iron oxide nanoparticles modulate lipopolysaccharide-induced inflammatory responses in primary human monocytes. *Int J Nanomedicine* (2016) 11:4625–42. doi:10.2147/IJN.S113425
- Di Cristo L, Movia D, Bianchi MG, Allegri M, Mohamed BM, Bell AP, et al. Proinflammatory effects of pyrogenic and precipitated amorphous silica nanoparticles in innate immunity cells. *Toxicol Sci* (2016) 150:40–53. doi:10.1093/toxsci/kfv258
- Smulders S, Kaiser JP, Zuin S, Van Landuyt KL, Golanski L, Vanoirbeek J, et al. Contamination of nanoparticles by endotoxin: evaluation of different test methods. *Part Fibre Toxicol* (2012) 9:41. doi:10.1186/1743-8977-9-41
- Oostingh GJ, Casals E, Italiani P, Colognato R, Stritzinger R, Ponti J, et al. Problems and challenges in the development and validation of human cell-based assays to determine nanoparticle-induced immunomodulatory effects. *Part Fibre Toxicol* (2011) 8:8. doi:10.1186/1743-8977-8-8
- Bianchi MG, Allegri M, Costa AL, Blosi M, Gardini D, Del Pivo C, et al. Titanium dioxide nanoparticles enhance macrophage activation by LPS through a TLR4-dependent intracellular pathway. *Toxicol Res* (2015) 4:385–98. doi:10.1039/c4tx00193a
- Stoccoro A, Di Buccianico S, Coppede F, Ponti J, Ubaldi C, Blosi M, et al. Multiple endpoints to evaluate pristine and remediated titanium dioxide nanoparticles genotoxicity in lung epithelial A549 cells. *Toxicol Lett* (2017) 276:48–61. doi:10.1016/j.toxlet.2017.05.016
- Misko TP, Schilling RJ, Salvemini D, Moore WM, Currie MG. A fluorometric assay for the measurement of nitrite in biological samples. *Anal Biochem* (1993) 214:11–6. doi:10.1006/abio.1993.1449
- Dall'Asta V, Gatti R, Orlandini G, Rossi PA, Rotoli BM, Sala R, et al. Membrane potential changes visualized in complete growth media through confocal laser scanning microscopy of bis-oxonol-loaded cells. *Exp Cell Res* (1997) 231:260–8. doi:10.1006/excr.1996.3469
- Gatti R, Belletti S, Orlandini G, Bussolati O, Dall'Asta V, Gazzola GC. Comparison of annexin V and calcein-AM as early vital markers of apoptosis in adherent cells by confocal laser microscopy. *J Histochem Cytochem* (1998) 46:895–900. doi:10.1177/002215549804600804
- Zimetti F, Adorni MP, Ronda N, Gatti R, Bernini F, Favari E. The natural compound berberine positively affects macrophage functions involved in atherosclerosis. *Nutr Metab Cardiovasc Dis* (2015) 25:195–201. doi:10.1016/j.numecd.2014.08.004
- Ahn CB, Jung WK, Park SJ, Kim YT, Kim WS, Je JY. Gallic acid-g-chitosan modulates inflammatory responses in LPS-stimulated RAW264.7 cells via NF-kappaB, AP-1, and MAPK pathways. *Inflammation* (2016) 39:366–74. doi:10.1007/s10753-015-0258-2
- Kenny EF, O'Neill LA. Signalling adaptors used by toll-like receptors: an update. *Cytokine* (2008) 43:342–9. doi:10.1016/j.cyto.2008.07.010
- Fensterl V, Sen GC. Interferon-induced Ifit proteins: their role in viral pathogenesis. *J Virol* (2015) 89:2462–8. doi:10.1128/JVI.02744-14
- Wang Z, Wang C, Liu S, He W, Wang L, Gan J, et al. Specifically formed corona on silica nanoparticles enhances transforming growth factor beta1 activity in triggering lung fibrosis. *ACS Nano* (2017) 11:1659–72. doi:10.1021/acsnano.6b07461
- Winzen S, Schoettler S, Baier G, Rosenauer C, Mailaender V, Landfester K, et al. Complementary analysis of the hard and soft protein corona: sample preparation critically effects corona composition. *Nanoscale* (2015) 7: 2992–3001. doi:10.1039/c4nr05982d
- Maiolo D, Bergese P, Mahon E, Dawson KA, Monopoli MP. Surfactant titration of nanoparticle-protein corona. *Anal Chem* (2014) 86:12055–63. doi:10.1021/ac5027176
- Liu Z, Li W, Wang F, Sun C, Wang L, Wang J, et al. Enhancement of lipopolysaccharide-induced nitric oxide and interleukin-6 production by PEGylated gold nanoparticles in RAW264.7 cells. *Nanoscale* (2012) 4:7135–42. doi:10.1039/c2nr31355c
- Siegfried A, Berchtold S, Manncke B, Deuschle E, Reber J, Ott T, et al. IFIT2 is an effector protein of type I IFN-mediated amplification of lipopolysaccharide (LPS)-induced TNF-alpha secretion and LPS-induced endotoxin shock. *J Immunol* (2013) 191:3913–21. doi:10.4049/jimmunol.1203305
- Kagan JC, Su T, Horng T, Chow A, Akira S, Medzhitov R. TRAM couples endocytosis of toll-like receptor 4 to the induction of interferon-beta. *Nat Immunol* (2008) 9:361–8. doi:10.1038/ni1569
- Pelclova D, Zdimal V, Kacer P, Fenclova Z, Vlckova S, Komarc M, et al. Leukotrienes in exhaled breath condensate and fractional exhaled nitric oxide in workers exposed to TiO<sub>2</sub> nanoparticles. *J Breath Res* (2016) 10:036004. doi:10.1088/1752-7155/10/3/036004

**Conflict of Interest Statement:** The authors declare that the research was conducted in the absence of any commercial or financial relationships that could be construed as a potential conflict of interest.

Copyright © 2017 Bianchi, Allegri, Chiu, Costa, Blosi, Ortelli, Bussolati and Bergamaschi. This is an open-access article distributed under the terms of the Creative Commons Attribution License (CC BY). The use, distribution or reproduction in other forums is permitted, provided the original author(s) or licensor are credited and that the original publication in this journal is cited, in accordance with accepted academic practice. No use, distribution or reproduction is permitted which does not comply with these terms.



# In Vitro and In Vivo Differences in Murine Third Complement Component (C3) Opsonization and Macrophage/Leukocyte Responses to Antibody-Functionalized Iron Oxide Nanoworms

## OPEN ACCESS

### Edited by:

Diana Boraschi,  
National Research Council, Italy

### Reviewed by:

Janos Szebeni,  
University of Miskolc, Hungary

Yang Li,  
University of Colorado Denver, USA

### \*Correspondence:

Dmitri Simberg  
dmitri.simberg@ucdenver.edu

### †Present address:

Swetha Inturi,  
Noven Pharmaceuticals,  
Miami, FL, USA

### Specialty section:

This article was submitted to  
Inflammation,  
a section of the journal  
Frontiers in Immunology

Received: 22 November 2016

Accepted: 30 January 2017

Published: 15 February 2017

### Citation:

Wang G, Griffin JI, Inturi S, Brenneman B, Banda NK, Holers VM, Moghimi SM and Simberg D (2017)  
*In Vitro and In Vivo Differences in Murine Third Complement Component (C3) Opsonization and Macrophage/Leukocyte Responses to Antibody-Functionalized Iron Oxide Nanoworms.*  
Front. Immunol. 8:151.  
doi: 10.3389/fimmu.2017.00151

Guankui Wang<sup>1</sup>, James I. Griffin<sup>1</sup>, Swetha Inturi<sup>1†</sup>, Barbara Brenneman<sup>1</sup>, Nirmal K. Banda<sup>2</sup>, V. Michael Holers<sup>2</sup>, Seyed Moein Moghimi<sup>3</sup> and Dmitri Simberg<sup>1\*</sup>

<sup>1</sup>The Skaggs School of Pharmacy and Pharmaceutical Sciences, University of Colorado Denver, Anschutz Medical Campus, Aurora, CO, USA, <sup>2</sup>Division of Rheumatology, School of Medicine, University of Colorado Denver, Anschutz Medical Campus, Aurora, CO, USA, <sup>3</sup>School of Medicine, Pharmacy and Health, Durham University, Queen's Campus, Stockton-on-Tees, UK

Balancing surface functionalization and low immune recognition of nanomedicines is a major challenge. Opsonization with the third component of the complement protein (C3) plays a major role in immune cell recognition of nanomedicines. We used dextran-coated superparamagnetic iron oxide nanoworms (SPIO NWs) to study the effect of surface functionalization on C3 opsonization in mouse serum and subsequent macrophage/leukocyte recognition *in vitro* as well as on intravenous injection into mice. Previously, we found that in mouse serum, SPIO NWs became opsonized with C3 via complement lectin pathway. Crosslinking the dextran shell with epichlorohydrin significantly decreased C3 opsonization and uptake by mouse peritoneal macrophages. Crosslinked nanoworms (NWs) further functionalized with polyethylene glycol (PEG) or with PEG-antibody (Ab) (~160 IgG molecules/particle) did not show an increase in C3 opsonization and peritoneal macrophage uptake *in vitro*. Following tail vein injection into mice, plain crosslinked NWs and PEGylated crosslinked NWs showed very low C3 opsonization and mouse leukocyte uptake. However, Ab-decorated crosslinked NWs showed significant C3 opsonization and high level of complement-dependent uptake by leukocytes in mice. Decreasing the number of conjugated Abs to 46 IgG molecules/particle significantly reduced C3 opsonization and leukocyte uptake. Using fresh mouse lepirudin plasma rather than serum showed better correlation with C3 opsonization *in vivo*. The reason for this difference could be related to the known instability of complement classical pathway in mouse sera. Our data illustrate that fine-tuning in nanoparticle surface functionalization with Abs is required to avoid excessive complement activation and complement-mediated immune uptake in mice, and raise issues with *in vitro* immunological assays of nanomedicines intended to mimic *in vivo* conditions.

**Keywords:** iron oxide, leukocyte, complement, antibody, PEG

## INTRODUCTION

The success of systemically and locally administered nanomaterials largely depends on the ability of nanosized carriers to efficiently evade the immune system (1). Several pathways of the innate immune system mediate clearance of nanoparticles by phagocytic cells. Complement system is an effector arm of the innate immune system composed of more than 30 blood proteins that accounts for about 5% of globulins in serum and is responsible for recognizing, eliminating, and destroying pathogens (2). The activation of complement system on foreign surface *via* lectin, classical, or alternative pathways [LP, classical pathway (CP), or AP, respectively] converges to cleave native C3 and generate a highly reactive thioester on C3b, which covalently attaches to reactive functional groups (e.g., hydroxyl and amines) on target surface (3–5). Opsonization by C3b and its cleavage products (iC3b, C3d) triggers particle recognition by leukocytes through complement receptors (6, 7), whereas soluble cleavage byproducts C3a and C5a are among the most potent anaphylatoxins and proinflammatory molecules with low nanomolar affinity (8). Numerous nanomaterials activate the complement system and become opsonized with C3 *in vitro* and *in vivo* (9–13).

Superparamagnetic iron oxide (SPIO) nanoparticles have been used as magnetic resonance imaging (MRI) contrast agents and also as carriers for drug delivery (14). SPIO nanoparticles consist of 5–8 nm magnetite–maghemite ( $\text{Fe}_3\text{O}_4$  and  $\gamma\text{-Fe}_2\text{O}_3$ ) crystalline cores coated with a polymer (15). Recently, we reported the synthesis of 20 kDa dextran-coated superparamagnetic iron oxide nanoworms (SPIO NWs) with high transverse relaxivity  $r_2$ , which makes them promising MRI contrast agents (16). Unfortunately, SPIO NWs potently activate complement in

both mice and humans (17). Previously, we demonstrated that mouse complement activation is *via* LP (17), whereas human complement activation is predominantly *via* the AP (18). As shown in Figure 1, initiation of the LP starts with the binding of mannose-binding lectin (MBL)-A/C, ficolins, or collectin-11 to the carbohydrates on the pathogen surfaces. The binding leads to activation of MBL-associated serine proteases (MASPs), leading to formation of the complement convertase C4b2a, cleavage of C3, deposition of initial C3b, and possible amplification *via* the alternative pathway convertase C3bBb. MASP-2 plays a direct role in formation of the complement convertase C4b2a (19) whereas MASP-1 and MASP-2 indirectly activate MASP-2 (20) and factor D (21, 22), respectively.

Interestingly, modifying the surface dextran coating with epichlorohydrin (ECH) [resulting in poly-(2-hydroxypropyl ether) hydrogel] blocked mouse complement C3 opsonization and leukocyte uptake (16). At the same time, it is not clear how further surface functionalization of ECH-crosslinked NWs (hereafter CL-NWs) affects complement activation and immune uptake. In view of the remarkable redundancy of pathways responsible for immune recognition (7) maintaining the delicate balance between surface functionalization and stealth properties could be a challenging task. In particular, the effect of addition of targeting ligands on “stealth” nanoparticles on complement activation and immune uptake has not been investigated in depth. In order to understand the impact of surface functionalization of CL-NWs with targeting antibodies (Abs) on complement activation and immune recognition, we modified CL-NWs with a polyethylene glycol (PEG) linker followed by a model anticancer Ab (trastuzumab). Here, we demonstrate that surface modification of CL-NWs that have low complement activation with trastuzumab can increase complement activation dependent on Ab surface

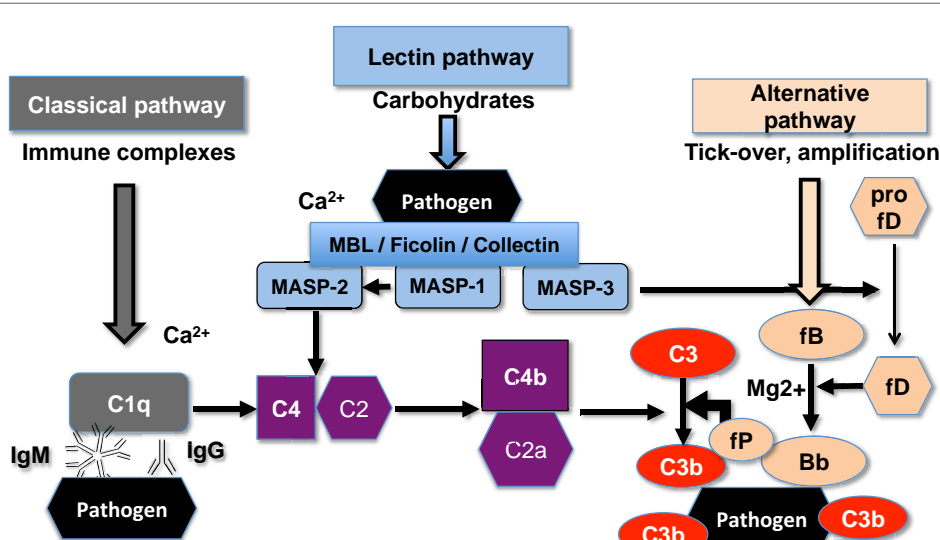


**FIGURE 1 |** The scheme of the upstream mouse complement pathways. C5a convertase and the terminal membrane attack complex pathway are not shown. There are three initiating complement pathways: classical, lectin, and alternative. All the pathways generate activated central complement protein component C3, liberating C3b, and its fixation on the pathogen (or nanoparticle) surface.

density, and further raise an issue of *in vitro* versus *in vivo* correlation assays of immune recognition of nanoparticles.

## RESULTS AND DISCUSSION

### Effect of Nanoworm (NW) Modification and Functionalization on C3 Opsonization and Immune Uptake in Mouse Sera

#### In Vitro

Dextran-coated SPIO NWs were prepared from 20 kDa dextran,  $\text{FeCl}_2$ , and  $\text{FeCl}_3$  by a modified Molday and MacKenzie precipitation protocol (23). According to transmitted electron microscopy (**Figure 2A**), nanoparticle cores contained worm-like aggregates of iron oxide crystals. On the outside, the cores are covered with a shell of dextran chains (**Figure 2B**). Dextran shell was crosslinked with ECH in the presence of NaOH to yield hydrogel-coated CL-NWs (**Figure 2B**). The residual epoxides on CL-NWs were treated with ammonia to generate primary amines that were further functionalized with heterobifunctional maleimide (MAL)-PEG<sub>3400</sub>-succinimidyl valerate (SVA) to yield CL-NWs-PEG-MAL (hereafter CL-NWs-PEG; **Figure 2B**). PEG-MAL-functionalized particles were modified with thiolated Ab trastuzumab (Herceptin<sup>®</sup>) to yield CL-NWs-PEG-Ab (**Figure 2B**). According to size measurements (see Materials and Methods) showed that on average there were ~160 IgG molecules per each CL-NWs-PEG-Ab nanoparticle.

In order to confirm the role of the LP as the inciting pathway of complement activation in mouse serum, SPIO NWs were

incubated in validated sera obtained from mice deficient for various complement pathways (**Figure 1**), washed, and analyzed for mouse C3 in Western blotting (the same amount of particles were used in the assay and loaded on the gel). According to **Figure 3**, SPIO NWs showed strong C3 (C3b/iC3b) opsonization in wild type (WT) mouse serum, whereas the opsonization was blocked in sera deficient for MBL-A/C (LP) and MBL-A/C/factor D (LP and AP). In addition, C3 opsonization was blocked in sera deficient for factor D and factor B (AP). These data confirm that complement is triggered by MBL/MASP-2-dependent LP activation, whereas the AP provides the amplification loop.

Next, we compared the efficiency of C3 opsonization of CL-NWs, CL-NWs-PEG, and CL-NWs-PEG-Ab with SPIO NWs. Particles were incubated in normal mouse serum or in sera deficient for the LP factors MBL-A/C and MASP-2, washed, loaded in the same amount on a gel, and analyzed by Western blotting. All CL-NWs formulations showed 80–85% decrease in C3 opsonization in normal serum compared with SPIO NWs (**Figures 4A,B**). Moreover, CL-NWs formulations incubated in MBL-A/C-deficient and MASP-2-deficient sera (**Figures 4A,B**) showed further reduction of C3 opsonization. These data demonstrate that crosslinking predominantly blocks complement activation and functionalization of CL-NWs with PEG or PEG-Ab does not enhance complement activation in mouse serum.

C3 is the critical opsonin mediating the uptake of foreign pathogens by macrophages and leukocytes (2). We tested whether functionalization of CL-NWs affected the uptake by non-activated mouse peritoneal macrophages in mouse serum. As shown in Figure S1 in Supplementary Material, over 70% of freshly isolated cells showed expression of CD11b (receptor for iC3b) and F4/80 (a macrophage marker). SPIO NWs, CL-NWs, CL-NWs-PEG, and CL-NWs-PEG-Ab were preincubated in normal (WT) mouse serum for 15 min, and then added to the

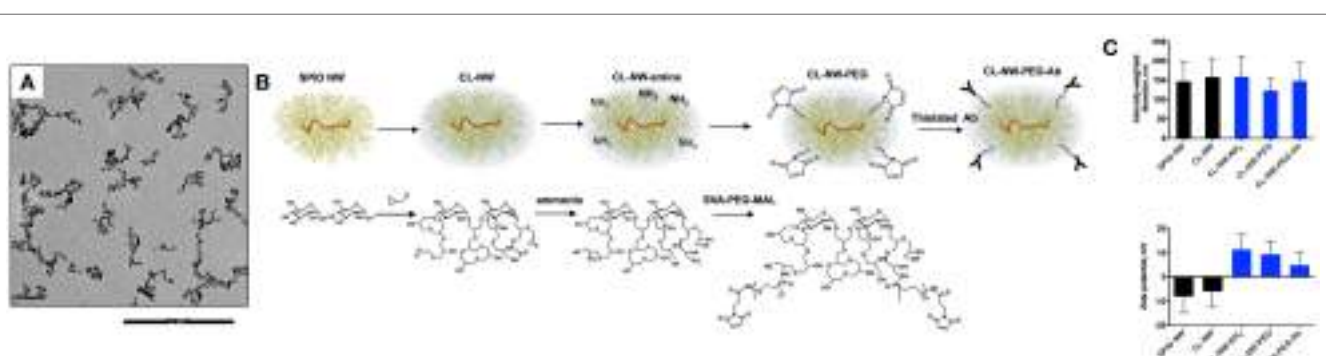


**FIGURE 2 |** Surface modification of superparamagnetic iron oxide nanoworms (SPIO NWs). **(A)** Representative transmission electron microscopy (TEM) image of SPIO NWs shows electron dense worm-like aggregates of magnetite crystals. Only the cores are visible in TEM. The scale bar is 200 nm; **(B)** graphic (top) and chemical (bottom) description of modifications of SPIO NWs. Dextran layer (yellow) was crosslinked with epichlorohydrin to form crosslinked hydrogel nanoworms (CL-NWs). The CL-NWs were then aminated using different concentrations of ammonium hydroxide to form CL-NWs-amine. CL-NWs-amine were further modified with succinimidyl valerate (SVA)-polyethylene glycol (PEG) maleimide and conjugated to thiolated antibodies (Abs); **(C)** the upper graph shows hydrodynamic size of nanoworms (NPs) measured by dynamic light scattering. The surface modifications did not significantly affect the hydrodynamic size of NPs. The lower graph represents the zeta potential values of NPs. The overall electric charge of CL-NWs switched from negative to positive after amination and for the corresponding functionalized particles.

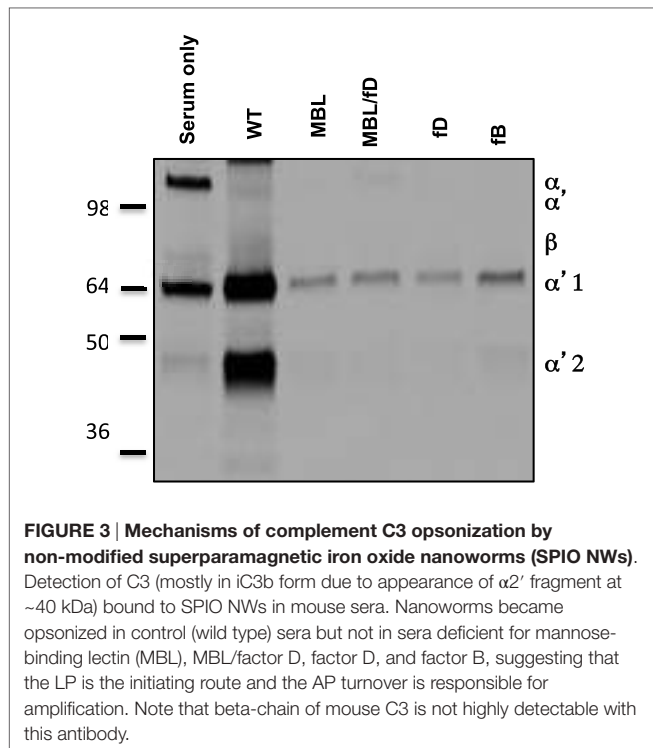


**FIGURE 3 | Mechanisms of complement C3 opsonization by non-modified superparamagnetic iron oxide nanoworms (SPIO NWs).**

Detection of C3 (mostly in iC3b form due to appearance of α<sup>1</sup> fragment at ~40 kDa) bound to SPIO NWs in mouse sera. Nanoworms became opsonized in control (wild type) sera but not in sera deficient for mannose-binding lectin (MBL), MBL/factor D, factor D, and factor B, suggesting that the LP is the initiating route and the AP turnover is responsible for amplification. Note that beta-chain of mouse C3 is not highly detectable with this antibody.

cells at 0.1 mg/mL Fe for 6 h. According to Prussian blue staining and quantification (Figures 5A,B, see Materials and Methods for details), SPIO NWs showed highly intense cytoplasmic accumulation of iron. CL-NWs showed 80% less uptake than SPIO NWs. The functionalized CL-NWs had the same level of residual uptake as non-functionalized CL-NWs, suggesting that PEG and Ab modifications do not trigger the uptake in mouse serum. Incubation of SPIO NWs and all CL-NWs formulations in C3-deficient mouse serum resulted in a complete blockade of the residual uptake of CL-NWs formulations (Figures 5A,B), suggesting that the uptake of SPIO NWs and the residual uptake of CL-NW formulations are mediated through C3 opsonization.

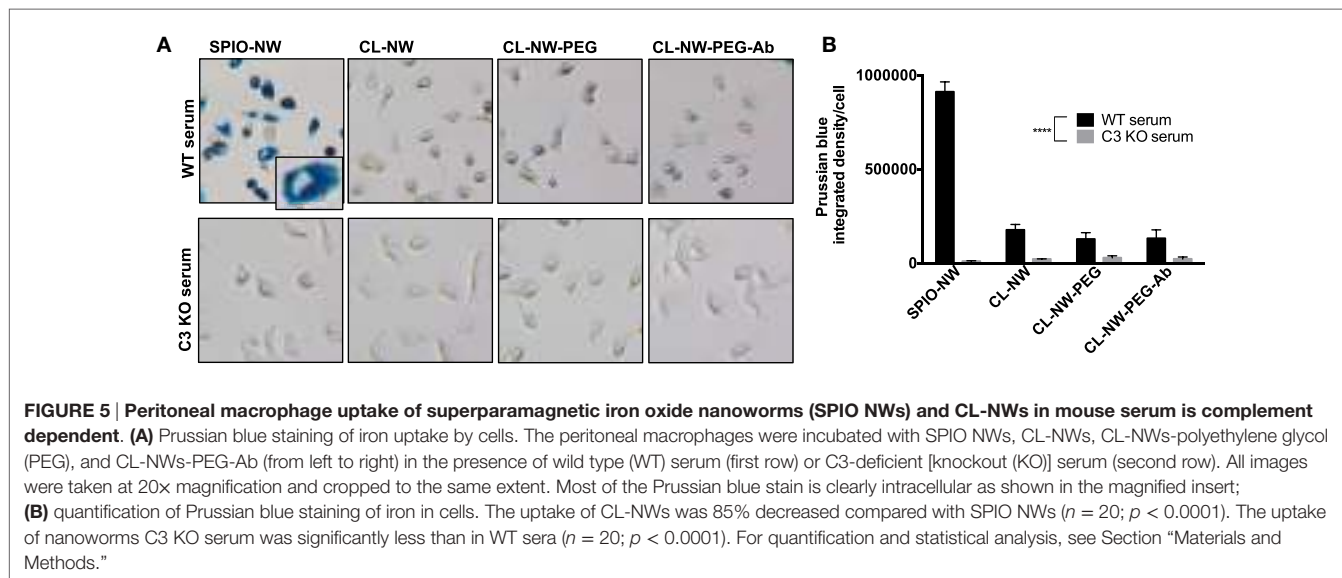
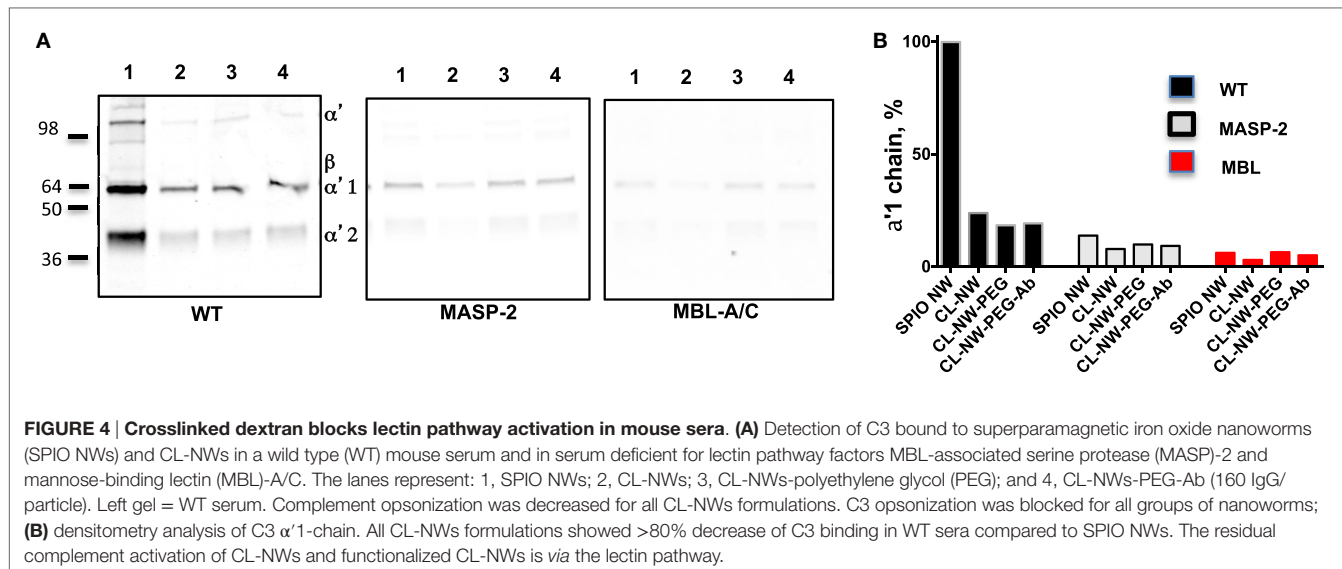
## Effect of Cl-NWs Functionalization on C3 Opsonization and Immune Uptake *In Vivo*

Previously, we demonstrated that complement C3 mediates the uptake of SPIO NWs by blood leukocytes in mice (10). SPIO NWs, CL-NWs-PEG, and CL-NWs-PEG-Ab were injected intravenously into mice at 5 mg Fe per kg body weight, recovered from blood 5 min post-injection using a magnetic column [in this process, both free particles and magnetically labeled leukocytes were enriched (10)], and analyzed for C3 opsonization and leukocyte uptake as shown in Figure 6A. We used a previously established (10, 16–18) dot-blot procedure to compare the levels of C3 opsonization on NWs. According to Figure S2 in Supplementary Material, C3 dot-blot assay correlates with C3 Western blot for determining the levels of C3 on particles. According to Figures 6B,C, SPIO NWs showed high level of C3 opsonization *in vivo* and leukocyte uptake. Similar to *in vitro* serum results, CL-NWs-PEG showed less than 10% of

C3 compared to SPIO NWs, and low level of leukocyte uptake. Non-modified CL-NWs also showed low level of *in vivo* C3 opsonization and leukocyte uptake (Figure S3 in Supplementary Material), confirming our previous findings (10). However, in contrast to *in vitro* measurements, CL-NWs-PEG-Ab decorated with ~160 IgG/particle showed 66% of C3 opsonization of SPIO NWs and high leukocyte uptake *in vivo* (Figures 6B,C). Injection of CL-NWs-PEG-Ab into C3 knockout (KO) mice that completely lacks C3 abolished the leukocyte uptake (Figure 6C). These data suggest that conjugation of IgG on the particles triggered complement activation and complement-dependent immune uptake that was not detected using *in vitro* assays in mouse serum.

Surface immobilized Abs and immune complexes, however, are known to trigger complement *via* the CP (24). It is likely that *in vivo* Ab-functionalized NWs trigger the CP. At least two surface-bound IgG molecules must be bridged by a C1q molecule before activation of the CP can proceed. In order to test whether the number of IgG per particle can control complement activation *in vivo*, we synthesized CL-NWs-PEG-Ab bearing different Ab densities and tested their C3 opsonization and leukocyte uptake *in vivo*. According to Figures 7A,B, CL-NWs-PEG-Ab with 1 IgG/particle, 8 IgG/particle, and 46 IgG/particle showed significantly lower levels of *in vivo* C3 opsonization (17, 3, and 22% of SPIO NWs, respectively) and leukocyte uptake than CL-NWs-PEG-Ab with 160 IgG/particle. However, the observation of higher C3 opsonization with CL-NW-PEG-Ab bearing a single Ab molecule compared with CL-NW-PEG-Ab with 8 IgG/particle is intriguing. The reason for this is unclear, but this suggests the involvement of other *in vivo* factors regulating complement activation and fixation and therefore requires further investigation. Nevertheless, these experiments suggest that decreasing surface density of Ab molecules can suppress complement activation and immune cell recognition *in vivo*. CL-NWs-PEG-Ab with 8 trastuzumab/particle showed specific uptake by HER2/neu + human breast cancer cell line SKBR-3 (Figure S4 in Supplementary Material), suggesting that the immobilized Ab is functional on the nanoparticles and therefore may bind to its designated target *in vivo*.

Next, we sought an explanation to the observed lack of complement activation by CL-NWs-PEG-Ab (160 IgG/particle) in serum (Figure 4) versus *in vivo*. Previous evidence suggested that the CP of the complement system is unstable in mouse sera (25–27) and, furthermore, starts losing its activity at room temperature (RT) and even during –70°C storage (26). Accordingly, blood clotting procedures and serum isolation steps could trigger loss of CP activity and explain poor C3 opsonization in mouse serum through this pathway. To address this, we repeated the experiments with fresh mouse plasma using recombinant hirudin (lepirudin) as anticoagulant. Lepirudin is the only known anticoagulant that does not interfere with complement activation. The results shown in Figure 7C demonstrate that SPIO NWs potently activate complement in fresh lepirudin plasma. CL-NWs-PEG showed only 26% of C3 opsonization of SPIO NWs in plasma. At the same time, CL-NWs-PEG-Ab (1 IgG/particle), CL-NWs-PEG-Ab (46 IgG/particle), and CL-NWs-PEG-Ab (160 IgG/particle) showed high C3 opsonization



compared to SPIO NWs [46, 88, and 110% of C3 opsonization to SPIO NWs, respectively (Figure 7C)]. Therefore, the results in plasma are better correlated with C3 opsonization *in vivo* than in serum. At the same time, the relative levels of C3 opsonization were much higher in plasma than *in vivo*. Thus, plasma C3 opsonization of CL-NWs-PEG-Ab (46 IgG/particle) was 88% of SPIO NWs (Figure 7C), whereas *in vivo* C3 opsonization level of the same particle was 22% of SPIO NWs (Figure 7A). These discrepancies may be related to the dynamic differences in NW protein corona *in vitro* versus *in vivo* conditions in regulating complement activation (28). In summary, these data suggest that C3 assay in plasma is a better predictor of *in vivo* complement activation for Ab-modified particles than in serum, but at the same time the opsonization efficiency *in vitro* does not fully correlate with the efficiency *in vivo*, likely due to differences in

dynamics of protein interaction, corona formation, and complement activation.

Our studies demonstrate that surface modifications of nanoparticles have profound effect on complement C3 opsonization and the resultant immune uptake. Previous studies using PEGylated liposomes and nanoparticles showed loss of stealth properties after tethering of Abs and ligands (29–31) and that surface functionalization affects the cellular uptake (32–34). Nevertheless, the mechanistic studies explaining the effect of surface functionalizations were lacking and our study demonstrates for the first time the balance between surface functionalization, complement activation, and immune cell uptake. Immune system, including the complement system, is generally redundant, meaning that multiple pathways are utilized to recognize foreign epitopes. While the exact pathway by which surface Ab

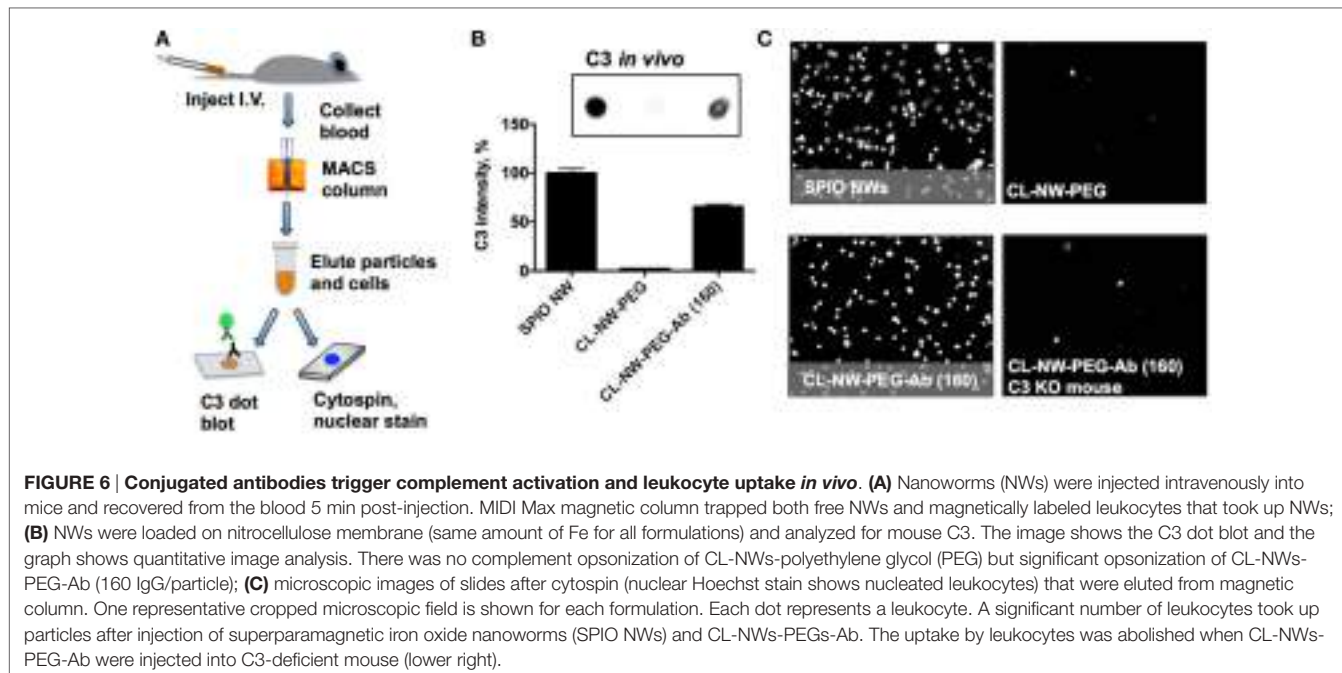


**FIGURE 6 | Conjugated antibodies trigger complement activation and leukocyte uptake in vivo.** **(A)** Nanoworms (NWs) were injected intravenously into mice and recovered from the blood 5 min post-injection. MIDI Max magnetic column trapped both free NWs and magnetically labeled leukocytes that took up NWs; **(B)** NWs were loaded on nitrocellulose membrane (same amount of Fe for all formulations) and analyzed for mouse C3. The image shows the C3 dot blot and the graph shows quantitative image analysis. There was no complement opsonization of CL-NWs-polyethylene glycol (PEG) but significant opsonization of CL-NWs-PEG-Ab (160 IgG/particle); **(C)** microscopic images of slides after cytopsin (nuclear Hoechst stain shows nucleated leukocytes) that were eluted from magnetic column. One representative cropped microscopic field is shown for each formulation. Each dot represents a leukocyte. A significant number of leukocytes took up particles after injection of superparamagnetic iron oxide nanoworms (SPIO NWs) and CL-NWs-PEGs-Ab. The uptake by leukocytes was abolished when CL-NWs-PEG-Ab were injected into C3-deficient mouse (lower right).

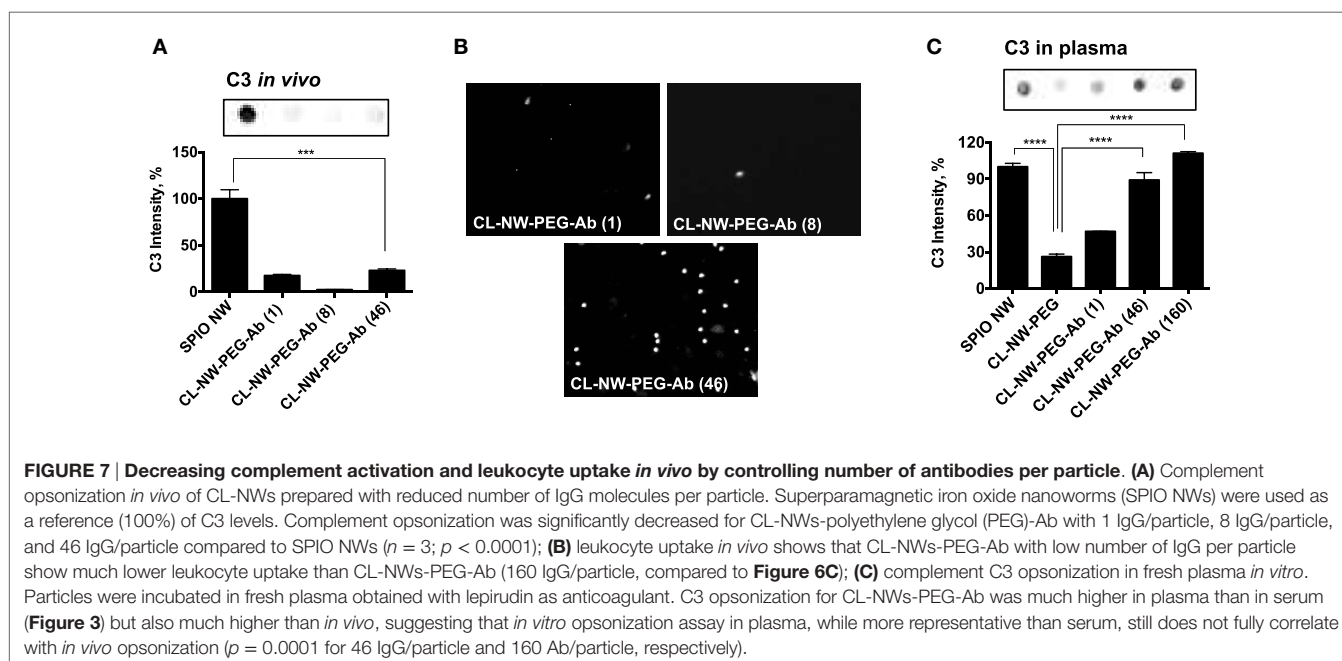


**FIGURE 7 | Decreasing complement activation and leukocyte uptake in vivo by controlling number of antibodies per particle.** **(A)** Complement opsonization in vivo of CL-NWs prepared with reduced number of IgG molecules per particle. Superparamagnetic iron oxide nanoworms (SPIO NWs) were used as a reference (100%) of C3 levels. Complement opsonization was significantly decreased for CL-NWs-polyethylene glycol (PEG)-Ab with 1 IgG/particle, 8 IgG/particle, and 46 IgG/particle compared to SPIO NWs ( $n = 3$ ;  $p < 0.0001$ ); **(B)** leukocyte uptake in vivo shows that CL-NWs-PEG-Ab with low number of IgG per particle show much lower leukocyte uptake than CL-NWs-PEG-Ab (160 IgG/particle, compared to Figure 6C); **(C)** complement C3 opsonization in fresh plasma in vitro. Particles were incubated in fresh plasma obtained with lepirudin as anticoagulant. C3 opsonization for CL-NWs-PEG-Ab was much higher in plasma than in serum (Figure 3) but also much higher than in vivo, suggesting that in vitro opsonization assay in plasma, while more representative than serum, still does not fully correlate with in vivo opsonization ( $p = 0.0001$  for 46 IgG/particle and 160 Ab/particle, respectively).

triggers complement activation needs to be elucidated further, the need to control complement activation *via* the number of conjugated Abs is an important aspect in the design of targetable nanomedicines.

Importantly, our study suggests that complement activation *via* surface immobilized Ab could be missed using *in vitro* assays in murine sera. Therefore, valid complement assays of nanoparticles should be used, at the very least using lepirudin plasma *in vitro*, but preferably in the animal *in vivo*. The lack

of correlation between *in vitro* and *in vivo* assays adds to the lack of correlation in pathways of complement activation in mice and humans (10, 17). Mouse models are widely used in preclinical studies of biodistribution and toxicity of drug delivery systems. In addition, complement-mediated mechanisms of immune uptake are likely similar in mice and humans (10). Despite these, any extrapolation of mouse data on the immune recognition of nanocarriers to humans should be interpreted with caution.

## MATERIALS AND METHODS

### Materials

All reagents used for NW synthesis including Fe salts and 20 kDa (range 15–25 kDa) dextran were purchased from Sigma-Aldrich (St. Louis, MO, USA). Cell culture media were purchased from Corning Life Sciences (Corning, NY, USA). Copper grids (300 mesh) were purchased from Electron Microscopy Sciences (Hatfield, PA, USA). Anti-HER2 Ab Herceptin® was generously donated by the Pharmacy of the University of Colorado Cancer Center, Anschutz Medical Campus. Anti-mouse anti-C3 Ab was purchased from MP Biomedicals (Solon, OH, USA). IRDye 800CW-labeled secondary Abs were purchased from Li-COR Biosciences (Lincoln, NE, USA). Purified anti-mouse/human CD11b Ab was purchased from BioLegend (San Diego, CA, USA). Anti-mouse F4/80 Ab was purchased from Caltag Medsystems Ltd. (Buckingham, UK). Hoechst 33342 for nuclei staining was purchased from Thermo Fisher Scientific (Waltham, MA, USA). The Abs for each experiment were diluted according to the recommendations from manufacturers. Mouse sera deficient for C3, MBL-A/C, MBL-A/C/factor D, and factor B were collected from mice that were bred in an animal vivarium at the University of Colorado Anschutz Medical Campus according to the Institutional Animal Care and Use Committee (IACUC) approved breeding protocol. Recombinant human hirudin (lepirudin, catalog No. ACM154) was obtained from Aniara Diagnostica, LLC (West Chester, OH, USA), reconstituted in water to 1 µg/µL (160 antithrombin units/µL), and stored aliquoted at -80°C. Lepirudin anticoagulated plasma (hereafter plasma) was obtained by collecting blood through the cardiac puncture (final lepirudin concentration 3–4 µg/mL) and centrifuging the tube at 2,000 g for 15 min.

### Synthesis of SPIO and Crosslinked Nanoworms (CL-NWs)

Nanoworms were synthesized by a modified one-pot Molday and MacKenzie (23) precipitation method as described earlier (16). Nanopure water (30 mL) was de-oxygenated with nitrogen gas and used to dissolve 6 g dextran (molecular weight 20 kDa, Sigma-Aldrich), 1.26 g Fe(III) chloride, and 0.498 g Fe(II) chloride in a round bottom flask. Next, 2.4 mL of cold 25% (v/v) ammonium hydroxide (NH<sub>4</sub>OH) was slowly added to the mixture of dextran and iron salts under nitrogen atmosphere with rapid stirring on ice. After formation of NWs, the mixture was heated at 80°C with stirring. After cooling, SPIO NWs were purified overnight using a 20 kDa dialysis cassette (Thermo Fisher Scientific, Waltham, MA, USA) against double distilled water to remove free dextran. The particles were chemically crosslinked using 1-chloro-2, 3-epoxy-propane (ECH) with sodium hydroxide as described before (16). SPIO NWs and CL-NWs were filtered through a 0.45 µm-pore filter (Millipore, Billerica, MA, USA) prior to use.

### Surface Modifications of CL-NWs

CL-NWs were aminated by adding different concentrations of ammonium hydroxide at 4°C overnight to form CL-NWs-NH<sub>2</sub> and dialyzed for 24 h to remove free NH<sub>4</sub>OH. For the Ab

conjugation, MAL-PEG-SVA (MAL-PEG-SVA, Laysan Bio) was reacted at excess with CL-NWs-NH<sub>2</sub> at RT for 30 min to form CL-NWs-PEG-MAL or CL-NWs-PEG. Anti-HER2 Ab Herceptin® was reacted in the last step with MAL-PEG to form CL-NWs-PEG-Ab. NWs were purified by ultracentrifugation at 55,000 rpm, filtered through a 0.45 µm pore filter, and finally, stored in Dulbecco's phosphate-buffered saline (DPBS) at pH 7.4 before use.

### Characterization of NWs

Transmission electron microscopy imaging was conducted to visualize the NWs using FEI Tecnai Spirit BioTwin electron microscope (Electron Microscopy Facility at the University of Colorado Boulder) at a 100 kV working voltage. Size measurements were done in DPBS and zeta potential measurements were done in 0.1× DPBS at RT using a Zetasizer Nano ZS (Malvern Instruments Ltd., Malvern, UK). The intensity-weighted size distribution peak value was used to report hydrodynamic diameters of the NWs. To quantify the Ab on the NWs, known amount of CL-NWs-PEG-Ab (0.2 µg Fe) was applied in triplicates onto a 0.2 µm pore nitrocellulose membrane (Bio-Rad). Standard dilutions of free trastuzumab were also applied onto the membrane to generate a standard curve. The membrane was blocked with 5% (w/w) non-fat dry milk in PBS-T (DPBS with 0.1% Tween® 20) for 1 h at RT and probed with IRDye 800CW-labeled antihuman Ab. The membrane was scanned with Odyssey infrared imager (Li-COR Biosciences, Lincoln, NE, USA). The integrated dot intensity in the scanned images was determined from 16-bit grayscale images using ImageJ software and plotted using Prism 6 software (GraphPad Software, Inc., La Jolla, CA, USA) to determine the number of Ab molecules per spot using the calibration curve. Concentration of particles per milligram Fe was determined with NanoSight (Malvern Instruments) and Fe concentration was determined with ferrozine iron assay as described before (16). The number of Abs per NW was determined after dividing the number of Abs per spot by the number of NWs per spot.

### Protein Binding Assay

Superparamagnetic iron oxide and CL-NWs (10 µL of 1 mg/mL) were incubated with 30 µL of mouse serum or lepirudin plasma for 15 min at RT. At the end of incubation, particles were washed three times with 1× PBS by centrifugation at 100,000 g at 4°C using Beckman Optima TLX ultracentrifuge. The pellets were resuspended in 20 µL DPBS, and the concentration of Fe in each sample was normalized with ferrozine iron assay as described before (16). For complement C3 western blot, 10 µL aliquots were used for gel electrophoresis. The samples were mixed with loading buffer [denaturing buffer containing 100 mM Tris, 20% glycerol, 4% SDS, 5% (v/v) 2-mercaptoethanol, 0.02% bromophenol blue] and then boiled at 95°C for 5 min. After cooling for 5 min, the samples and marker proteins (Precision Plus Proteins Dual Color Standards from Bio-Rad) were loaded onto Mini-PROTEAN TGX Gels (Bio-Rad, Hercules, CA, USA) and separated at 50 V for 5 min and then 100 V for 90 min. Gels were then transferred to nitrocellulose membranes using the Mini Trans-Blot cell system overnight at 50 V at 4°C. For C3 dot blot, 2 µL aliquots were applied in triplicates onto a nitrocellulose membrane.

The membranes were blocked using 5% non-fat dry milk in DPBS-T (DPBS with 0.1% Tween® 20) at RT for 1 h, probed with corresponding primary Abs at RT for 1 h, followed by washing the membranes 3× with DPBS-T, and finally, 1 h incubation with the corresponding IRDye 800CW-labeled secondary Abs against the primary Ab species (see Materials). The membranes after immunoblotting were visualized using an Odyssey infrared imager. The integrated dot intensity in the scanned images was quantitatively analyzed using ImageJ software and plotted with Prism 6 software as described above.

## Uptake of NWs *In Vitro*, Prussian Blue Staining, and Quantification

Human breast cancer cell line SKBR-3 cells were maintained in McCoy's 5A medium (ATCC) supplemented with 10% fetal bovine serum. Mouse peritoneal macrophages were obtained by peritoneal lavage with 5 mL ice cold PBS, post-mortem. For experiment, cells were plated into 96-well plate. For uptake experiments, NWs were preincubated for 15 m with WT mouse sera or C3 KO sera and added at 0.1 mg/mL Fe concentration to cells for 6 h. After the incubation, cells were washed using DPBS for three times, fixed in 4% paraformaldehyde at 4°C overnight, and then stained using Prussian blue for 1 h. Prussian blue staining is the standard method for detecting iron in cells and tissues, and has been extensively used for detecting uptake of iron oxide nanoparticles by our group and others (35, 36). The method is based on formation of insoluble, blue colored coordination complexes between Fe<sup>3+</sup> and potassium ferrocyanide. Maghemite crystals of SPIO contain both Fe<sup>3+</sup> and Fe<sup>2+</sup>, and the surface of crystals is always oxidized to Fe<sup>3+</sup>, so the complete degradation of nanoparticles is not required for the staining to work. In order to quantify the blue color of the complexes inside the cells, TIFF RGB images of stained cells were acquired with a Nikon Eclipse E600 microscope using same exposure and magnification. The images were combined into a gallery with Adobe Photoshop and color balance was adjusted with a Level tool to make the cell-free area white. The gallery image was exported into ImageJ, converted into YUV color space, and thresholded for blue and green components using a Threshold Color plugin. Then, the image was converted into a 16-bit gray scale and inverted. The background was completely subtracted with a Math Subtraction tool. A ROI was drawn around each cell and integrated pixel density was measured. The data were plotted as means and SD using Prism software. An average of at least 20 cells was used.

## Nanoparticle Uptake *In Vivo*

Wild type and C3<sup>-/-</sup> mice (Jax Laboratories: B6.129S4-C3<sup>tm1Crr/J</sup>) were bred in house according to the approval by University of Colorado Animal Protocol Committee. NWs were injected as a 5 mg/kg bolus *via* tail vein into WT and C3 KO mice (8 weeks

of age, females). Following the injection (5 min), mice were sacrificed and the blood was drawn *via* cardiac puncture using heparin as anticoagulant. Blood was applied on Miltenyi Mini MACS magnetic column (Miltenyi Biotech) and the trapped cells and particles were washed extensively with PBS. The particles and magnetic leukocytes were then eluted from the column. The cells were pelleted with tabletop Eppendorf centrifuge and the particles in the supernatant were further concentrated with ultracentrifuge for C3 dot-blot assay. The cell pellet was resuspended in 200 µL PBS and the cells were concentrated on slides using Shandon Cytospin 4 centrifuge (Thermo Fischer), fixed with 10% (v/v) formalin in PBS, and stained with Hoechst dye (Thermo Fischer) to enable leukocyte nuclei visualization. The images were taken with Nikon Eclipse E600 fluorescent microscope using DAPI filter at low (40×) magnification.

## Statistical Analysis

The statistical analysis was performed using Prism 6 software. The differences between means of experimental groups were analyzed using a two-tailed parametric *t*-test assuming 95% confidence interval. Data shown as means ± SD. Differences in all data are shown as \**p* < 0.05; \*\**p* < 0.001; \*\*\**p* < 0.0001.

## ETHICS STATEMENT

This study was carried out in accordance with the guidelines of the University of Colorado Office of Animal Care. The protocol was approved by the University of Colorado IACUC.

## AUTHOR CONTRIBUTIONS

GW designed and performed experiments, and analyzed data. JG performed experiments. SI performed experiments. BB performed experiments. NB analyzed data and provided reagents. VH analyzed data and provided reagents. SM designed experiments, analyzed data, and edited the paper. DS designed experiments, analyzed data, and wrote the paper.

## FUNDING

The study was funded by the University of Colorado Denver startup and NIH grants EB022040 and CA194058-01A1 to DS, and the Danish Agency for Science, Technology and Innovation (Det Strategiske Forskningsråd), reference 09-065746 as well as RiboBio Co. Ltd. (Guangzhou, China) to SM.

## SUPPLEMENTARY MATERIAL

The Supplementary Material for this article can be found online at <http://journal.frontiersin.org/article/10.3389/fimmu.2017.00151/full#supplementary-material>.

## REFERENCES

- Moghimi SM, Hunter AC, Murray JC. Long-circulating and target-specific nanoparticles: theory to practice. *Pharmacol Rev* (2001) 53(2): 283–318.
- Ricklin D, Hajishengallis G, Yang K, Lambris JD. Complement: a key system for immune surveillance and homeostasis. *Nat Immunol* (2010) 11(9):785–97. doi:10.1038/ni.1923
- Janssen BJC, Huizinga EG, Raaijmakers HCA, Roos A, Daha MR, Nilsson-Ekdahl K, et al. Structures of complement component C3 provide insights into

- the function and evolution of immunity. *Nature* (2005) 437(7058):505–11. doi:10.1038/nature04005
4. Arima Y, Kawagoe M, Toda M, Iwata H. Complement activation by polymers carrying hydroxyl groups. *ACS Appl Mater Interfaces* (2009) 1(10):2400–7. doi:10.1021/am9005463
  5. Lemarchand C, Gref R, Passirani C, Garcion E, Petri B, Muller R, et al. Influence of polysaccharide coating on the interactions of nanoparticles with biological systems. *Biomaterials* (2006) 27(1):108–18. doi:10.1016/j.biomaterials.2005.04.041
  6. Helmy KY, Katschke KJ Jr, Gorgani NN, Kljavin NM, Elliott JM, Diehl L, et al. CRIG: a macrophage complement receptor required for phagocytosis of circulating pathogens. *Cell* (2006) 124(5):915–27. doi:10.1016/j.cell.2005.12.039
  7. Taylor PR, Martinez-Pomares L, Stacey M, Lin HH, Brown GD, Gordon S. Macrophage receptors and immune recognition. *Annu Rev Immunol* (2005) 23:901–44. doi:10.1146/annurev.immunol.23.021704.115816
  8. Peng Q, Li K, Sacks SH, Zhou W. The role of anaphylatoxins C3a and C5a in regulating innate and adaptive immune responses. *Inflamm Allergy Drug Targets* (2009) 8(3):236–46. doi:10.2174/18715280978681038
  9. Dobrovolskaia MA, McNeil SE. Immunological properties of engineered nanomaterials. *Nat Nanotechnol* (2007) 2(8):469–78. doi:10.1038/nnano.2007.223
  10. Inturi S, Wang G, Banda NK, Holers VM, Wu L, et al. Modulatory role of surface coating of superparamagnetic iron oxide nanoworms in complement opsonization and leukocyte uptake. *ACS Nano* (2015) 9(11):10758–68. doi:10.1021/acsnano.5b05061
  11. Moghimi SM. Cancer nanomedicine and the complement system activation paradigm: anaphylaxis and tumour growth. *J Control Release* (2014) 190:556–62. doi:10.1016/j.jconrel.2014.03.051
  12. Hamad I, Al-Hanbali O, Hunter AC, Rutt KJ, Andresen TL, Moghimi SM. Distinct polymer architecture mediates switching of complement activation pathways at the nanosphere-serum interface: implications for stealth nanoparticle engineering. *ACS Nano* (2010) 4(11):6629–38. doi:10.1021/nn101990a
  13. Pham CT, Mitchell LM, Huang JL, Lubniewski CM, Schall OF, Killgore JK, et al. Variable antibody-dependent activation of complement by functionalized phospholipid nanoparticle surfaces. *J Biol Chem* (2011) 286(1):123–30. doi:10.1074/jbc.M110.180760
  14. Figueiro A, Di Corato R, Manna L, Pellegrino T. From iron oxide nanoparticles towards advanced iron-based inorganic materials designed for biomedical applications. *Pharmacol Res* (2010) 62(2):126–43. doi:10.1016/j.phrs.2009.12.012
  15. Gupta AK, Gupta M. Synthesis and surface engineering of iron oxide nanoparticles for biomedical applications. *Biomaterials* (2005) 26(18):3995–4021. doi:10.1016/j.biomaterials.2004.10.012
  16. Wang G, Inturi S, Serkova NJ, Merkulov S, McCrae K, Russek SE, et al. High-relaxivity superparamagnetic iron oxide nanoworms with decreased immune recognition and long-circulating properties. *ACS Nano* (2014) 8(12):12437–49. doi:10.1021/nn505126b
  17. Banda NK, Mehta G, Chao Y, Wang G, Inturi S, Fossati-Jimack L, et al. Mechanisms of complement activation by dextran-coated superparamagnetic iron oxide (SPIO) nanoworms in mouse versus human serum. *Part Fibre Toxicol* (2014) 11(1):64. doi:10.1186/s12989-014-0064-2
  18. Wang G, Chen F, Banda NK, Holers VM, Wu L, Moghimi SM, et al. Activation of human complement system by dextran-coated iron oxide nanoparticles is not affected by dextran/Fe ratio, hydroxyl modifications, and crosslinking. *Front Immunol* (2016) 7:418. doi:10.3389/fimmu.2016.00418
  19. Iwaki D, Kanno K, Takahashi M, Endo Y, Lynch NJ, Schwaeble WJ, et al. Small mannose-binding lectin-associated protein plays a regulatory role in the lectin complement pathway. *J Immunol* (2006) 177(12):8626–32. doi:10.4049/jimmunol.177.12.8626
  20. Takahashi M, Iwaki D, Kanno K, Ishida Y, Xiong J, Matsushita M, et al. Mannose-binding lectin (MBL)-associated serine protease (MASP)-1 contributes to activation of the lectin complement pathway. *J Immunol* (2008) 180(9):6132–8. doi:10.4049/jimmunol.180.9.6132
  21. Iwaki D, Kanno K, Takahashi M, Endo Y, Matsushita M, Fujita T. The role of mannose-binding lectin-associated serine protease-3 in activation of the alternative complement pathway. *J Immunol* (2011) 187(7):3751–8. doi:10.4049/jimmunol.1100280
  22. Takahashi M, Ishida Y, Iwaki D, Kanno K, Suzuki T, Endo Y, et al. Essential role of mannose-binding lectin-associated serine protease-1 in activation of the complement factor D. *J Exp Med* (2010) 207(1):29–37. doi:10.1084/jem.20090633
  23. Molday RS, MacKenzie D. Immunospecific ferromagnetic iron-dextran reagents for the labeling and magnetic separation of cells. *J Immunol Methods* (1982) 52(3):353–67. doi:10.1016/0022-1759(82)90007-2
  24. Dunkelberger JR, Song WC. Complement and its role in innate and adaptive immune responses. *Cell Res* (2010) 20(1):34–50. doi:10.1038/cr.2009.139
  25. Lachmann PJ. Preparing serum for functional complement assays. *J Immunol Methods* (2010) 352(1–2):195–7. doi:10.1016/j.jim.2009.11.003
  26. van Dijk H, Rademaker PM, Willers JM. Estimation of classical pathway of mouse complement activity by use of sensitized rabbit erythrocytes. *J Immunol Methods* (1980) 39(3):257–68. doi:10.1016/0022-1759(80)90060-5
  27. Ratelade J, Verkman AS. Inhibitor(s) of the classical complement pathway in mouse serum limit the utility of mice as experimental models of neuromyelitis optica. *Mol Immunol* (2014) 62(1):104–13. doi:10.1016/j.molimm.2014.06.003
  28. Chen F, Wang G, Griffin JI, Brenneman B, Banda NK, Holers VM, et al. Complement proteins bind to nanoparticle protein corona and undergo dynamic exchange in vivo. *Nat Nanotechnol* (2016). doi:10.1038/nnano.2016.269
  29. Cheng WW, Allen TM. Targeted delivery of anti-CD19 liposomal doxorubicin in B-cell lymphoma: a comparison of whole monoclonal antibody, Fab' fragments and single chain Fv. *J Control Release* (2008) 126(1):50–8. doi:10.1016/j.jconrel.2007.11.005
  30. Iden DL, Allen TM. In vitro and in vivo comparison of immunoliposomes made by conventional coupling techniques with those made by a new post-insertion approach. *Biochim Biophys Acta* (2001) 1513(2):207–16. doi:10.1016/S0005-2736(01)00357-1
  31. McNeely KM, Annapragada A, Bellamkonda RV. Decreased circulation time offsets increased efficacy of PEGylated nanocarriers targeting folate receptors of glioma. *Nanotechnology* (2007) 18(38):Art. 385101. doi:10.1088/0957-4484/18/38/385101
  32. Jiang XE, Dausend J, Hafner M, Musyanovych A, Rocker C, Landfester K, et al. Specific effects of surface amines on polystyrene nanoparticles in their interactions with mesenchymal stem cells. *Biomacromolecules* (2010) 11(3):748–53. doi:10.1021/bm901348z
  33. Ekkapongpisit M, Giovia A, Follo C, Caputo G, Isidoro C. Biocompatibility, endocytosis, and intracellular trafficking of mesoporous silica and polystyrene nanoparticles in ovarian cancer cells: effects of size and surface charge groups. *Int J Nanomedicine* (2012) 7:4147–58. doi:10.2147/IJN.S33803
  34. Villanueva A, Canete M, Roca AG, Calero M, Veintemillas-Verdaguer S, Serna CJ, et al. The influence of surface functionalization on the enhanced internalization of magnetic nanoparticles in cancer cells. *Nanotechnology* (2009) 20(11):115103. doi:10.1088/0957-4484/20/11/115103
  35. Raynal I, Prigent P, Peyramaure S, Najid A, Rebuzzi C, Corot C. Macrophage endocytosis of superparamagnetic iron oxide nanoparticles: mechanisms and comparison of ferumoxides and ferumoxtran-10. *Invest Radiol* (2004) 39(1):56–63. doi:10.1097/01.rli.0000101027.57021.28
  36. Chao Y, Karmali PP, Mukthavaram R, Kesari S, Kouzenetsova VL, Tsigelny IF, et al. Direct recognition of superparamagnetic nanocrystals by macrophage scavenger receptor SR-AI. *ACS Nano* (2013) 7(5):4289–98. doi:10.1021/nn400769e

**Conflict of Interest Statement:** The authors declare that the research was conducted in the absence of any commercial or financial relationships that could be construed as a potential conflict of interest.

The reviewer YL declared a shared affiliation, though no other collaboration, with several of the authors to the handling Editor, who ensured that the process nevertheless met the standards of a fair and objective review.

Copyright © 2017 Wang, Griffin, Inturi, Brenneman, Banda, Holers, Moghimi and Simberg. This is an open-access article distributed under the terms of the Creative Commons Attribution License (CC BY). The use, distribution or reproduction in other forums is permitted, provided the original author(s) or licensor are credited and that the original publication in this journal is cited, in accordance with accepted academic practice. No use, distribution or reproduction is permitted which does not comply with these terms.



# Activation of Human Complement System by Dextran-Coated Iron Oxide Nanoparticles Is Not Affected by Dextran/Fe Ratio, Hydroxyl Modifications, and Crosslinking

**Guankui Wang<sup>1†</sup>, Fangfang Chen<sup>1,2†</sup>, Nirmal K. Banda<sup>3</sup>, V. Michael Hokers<sup>3</sup>, LinPing Wu<sup>4</sup>, S. Moein Moghimi<sup>5</sup> and Dmitri Simberg<sup>1\*</sup>**

<sup>1</sup> Department of Pharmaceutical Sciences, Skaggs School of Pharmacy and Pharmaceutical Sciences, University of Colorado Anschutz Medical Campus, Aurora, CO, USA, <sup>2</sup> Department of Gastrointestinal Surgery, China-Japan Union Hospital, Jilin University, Changchun, China, <sup>3</sup> Division of Rheumatology, School of Medicine, University of Colorado Denver, Aurora, CO, USA, <sup>4</sup> Nanomedicine Laboratory, Department of Pharmacy, Centre for Pharmaceutical Nanotechnology and Nanotoxicology, University of Copenhagen, Copenhagen, Denmark, <sup>5</sup> School of Medicine, Pharmacy and Health, Durham University, Durham, UK

## OPEN ACCESS

### Edited by:

Paola Italiani,  
National Research Council, Italy

### Reviewed by:

Lucia Cottone,  
University College London, UK  
Shi Yue,  
University of Southern California, USA

### \*Correspondence:

Dmitri Simberg  
dmitri.simberg@ucdenver.edu

<sup>†</sup>Guankui Wang and Fangfang Chen contributed equally.

### Specialty section:

This article was submitted to Inflammation, a section of the journal *Frontiers in Immunology*

**Received:** 28 July 2016

**Accepted:** 27 September 2016

**Published:** 10 October 2016

### Citation:

Wang G, Chen F, Banda NK, Hokers VM, Wu L, Moghimi SM and Simberg D (2016) Activation of Human Complement System by Dextran-Coated Iron Oxide Nanoparticles Is Not Affected by Dextran/Fe Ratio, Hydroxyl Modifications, and Crosslinking. *Front. Immunol.* 7:418.  
doi: 10.3389/fimmu.2016.00418

While having tremendous potential as therapeutic and imaging tools, the clinical use of engineered nanoparticles has been associated with serious safety concerns. Activation of the complement cascade and the release of proinflammatory factors C3a and C5a may contribute to infusion-related reactions, whereas opsonization with C3 fragments promotes rapid recognition and clearance of nanomaterials by mononuclear phagocytes. We used dextran-coated superparamagnetic iron oxide nanoparticles (SPIO), which are potent activators of the complement system, to study the role of nanoparticle surface chemistry in inciting complement in human serum. Using complement inhibitors and measuring levels of fluid phase markers (sC5b-9, C5a, and Bb), we found that the majority of human complement activation by SPIO is through the alternative pathways (AP). SPIO prepared with high dextran/iron ratio showed some complement activation via calcium-sensitive pathways, but the AP was responsible for the bulk of complement activation and amplification. Activation via the AP required properdin, the positive regulator of the alternative C3bBb convertase. Modification of sugar alcohols of dextran with alkylating, acylating, or crosslinking agents did not overcome complement activation and C3 opsonization. These data demonstrate that human complement activation is independent of dextran modification of SPIO and suggest a crucial role of the AP in immune recognition of nano-assemblies in human serum.

**Keywords:** iron oxide nanoparticles, complement C3, complement system proteins, properdin, dextran, lectin pathway, alternative pathway of complement

## INTRODUCTION

Complement system is a critical component of the innate immunity that comprises ~5% of globulins and is responsible for eliminating and destroying pathogens (1). Complement activation via classical, lectin, and alternative pathways (AP) converge to form highly reactive thioester C3b that covalently binds to hydroxyls and amines on foreign surfaces (2, 3) resulting in the formation of membrane

pore complex C5b-9 and extremely potent anaphylatoxins C3a and C5a (4). Opsonization by C3b and its cleaved products (e.g., iC3b, C3d) triggers immune recognition by neutrophils, eosinophils, lymphocytes, monocytes, red blood cells, and macrophages (5, 6). Complement activation is also believed to contribute toward infusion-related reactions with clinically approved nanopharmaceuticals, such as Doxil (liposomal doxorubicin), Taxol (Cremophor-paclitaxel), and Sandimmune (Cremophor-cyclosporine A).

Despite the fact that numerous reports demonstrated complement activation by nanoparticles, liposomes, and micelles (7–22), the pathways of complement activation as function of surface properties are still poorly understood. One of the examples is superparamagnetic iron oxide (SPIO) nanoparticle, which is widely used not only as a contrast agent in magnetic resonance imaging (MRI) but also in the development of theranostic nanomedicines and experimental hyperthermia treatments (23). Previously, others and we described the preparation of high contrast SPIO nanoworms (SPIO NWs) (24–28) that consist of multiple  $\text{Fe}_3\text{O}_4$  crystals embedded in 20 kDa linear dextran. We further reported that dextran-coated SPIO NWs activate complement in mouse serum *via* the lectin pathway, but in human serum complement activation is *via* lectin and APs (24–28). Furthermore, others (3, 29–31) have pointed out that dextran-coated particles consume complement, where the projected surface polymer in brush conformation is less efficient in complement consumption than a side-on conformation. In addition, it has been reported that crosslinked dextran (Sephadex) enhances complement activation, and substitution of alcohol groups can partially prevent this effect (32–34). Despite these advances, the effect of carbohydrate modifications of dextran-coated SPIO on the efficiency of complement activation has not been investigated. This knowledge is not only very critical for SPIO nanoparticles, which are clinically useful nanomaterials, but also for surface engineering of other carbohydrate-coated materials. Indeed, several iron oxide-based clinical contrast agents, such as Feridex and Combidex, have induced adverse reactions in a large number of patients, presumably as a result of complement activation.

Here, we prepared SPIO using different dextran/Fe ratios and studied the pathway of complement activation by measuring generation of fluid phase markers. Our results point to the critical role of the AP in complement activation by SPIO regardless of the dextran/Fe ratio and the nanoparticle size. We then used SPIO NWs prepared with low dextran/Fe ratio to further understand the effect of modification of sugar hydroxyls with alkylating and crosslinking agents on C3 opsonization. The results suggest that modifications of dextran coat are not an effective strategy to mitigate AP activation by these nanoparticles in humans.

## RESULTS

### Alternative Pathway Is the Main Activation Pathway by SPIO Regardless of Dextran/Fe Ratio and Particle Size

We synthesized SPIO nanoparticles by mixing 20 kDa dextran with  $\text{FeCl}_2$  and  $\text{FeCl}_3$  and precipitating nanoparticles with

ammonia (35). For the precipitation reaction, we used different dextran/Fe ratios (low ratio: 3.0 g/133.4 mg; intermediate ratio: 6.0 g/133.4 mg; high ratio: 9.0 g/133.4 mg). Hydrodynamic size measurements (**Figure 1**) showed that particles prepared at intermediate and high dextran/Fe ratios (6 and 9 g dextran, respectively) were much smaller than particles prepared at low dextran/Fe ratio (3 g dextran), apparently due to a more efficient coating of individual crystals with dextran and prevention of intercrystal aggregation. Transmission electron microscopy (TEM) images (**Figure 1**) showed that SPIO particles prepared with higher dextran/Fe ratio were rounded with few crystalline  $\text{Fe}_3\text{O}_4$  cores (Figure 1, bottom schematic), whereas SPIO prepared with low dextran/Fe ratio (3 g) were predominantly polycrystalline worm-like structures (we term them SPIO nanoworms or SPIO NWs).

The human complement (**Figure 2**) is triggered by foreign surfaces *via* the formation of activated C3( $\text{H}_2\text{O}$ ) (AP turnover) or *via* calcium-sensitive pathways (classical or lectin). This activation leads to the initially deposited C3b that associates with factor B to form the AP convertase C3bBb, which cleaves additional C3 molecules. In order to study the pathway of complement activation, nanoparticles were added to human serum at Fe concentration of 0.2 mg/mL. Measurement of the soluble terminal complex marker sC5b-9 showed that all formulations triggered complement to the same extent, regardless of the size and dextran/Fe ratio (**Figure 3A**). Addition of calcium chelator 10 mM EGTA/2.5 mM  $\text{Mg}^{2+}$  [to inhibit operation of calcium-sensitive pathways (36)] dramatically decreased (by 40%) complement activation by NWs prepared with high and intermediate dextran/Fe ratios, but not by NWs prepared with low dextran/Fe ratio (**Figure 3A**). These data suggest that at higher dextran/Fe ratios, both calcium-sensitive and the APs contribute to complement activation, whereas at low dextran/Fe ratio, the activation proceeds exclusively *via* the AP. In order to investigate the contribution of calcium-sensitive pathways in formation of the AP convertase (**Figure 2**), we measured generation of Bb in sera deficient in C2, which is the critical

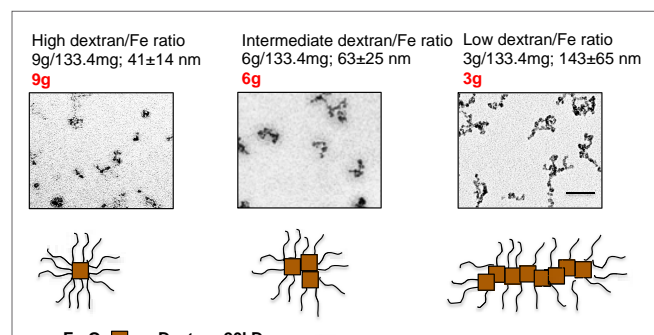


**FIGURE 1 | Preparation of SPIO NWs with different dextran/Fe ratios: the particles were prepared with different ratios of dextran to Fe salt.** The size of the SPIO aggregates increases as the ratio used in the precipitation reaction decreases, from single crystal (9 g) to smaller aggregates of several crystals (6 g) to polycrystalline (5–20 crystals) nanoworms (3 g).

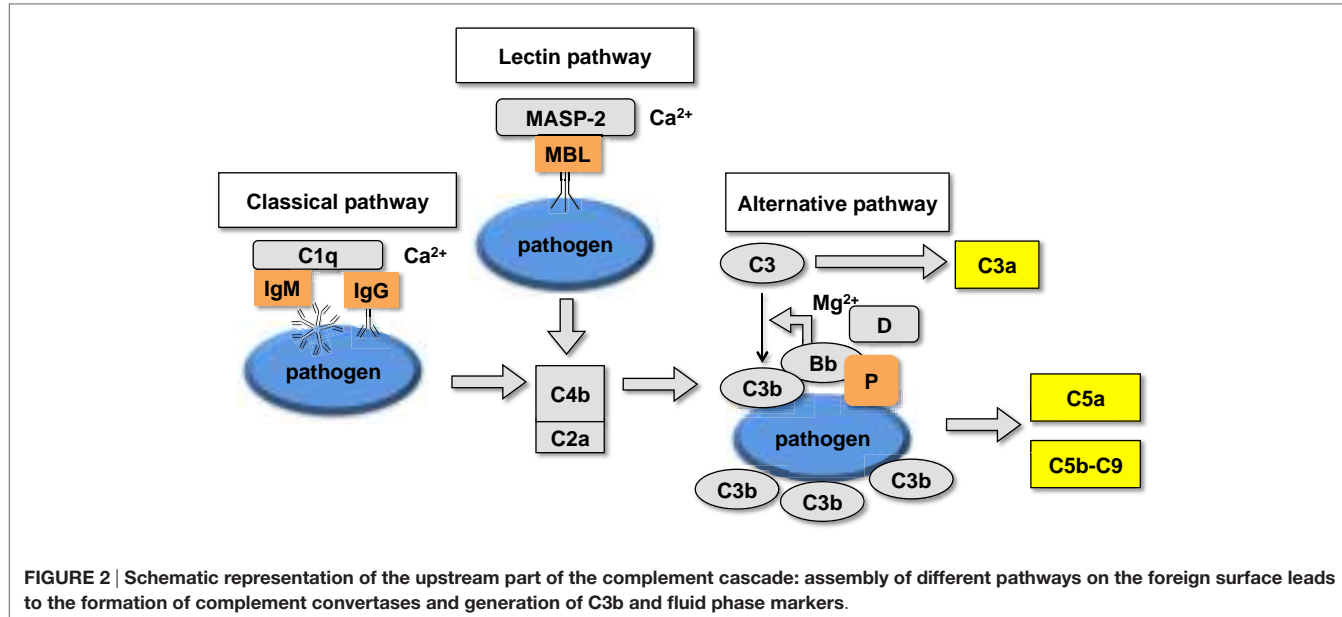


**FIGURE 2 |** Schematic representation of the upstream part of the complement cascade: assembly of different pathways on the foreign surface leads to the formation of complement convertases and generation of C3b and fluid phase markers.

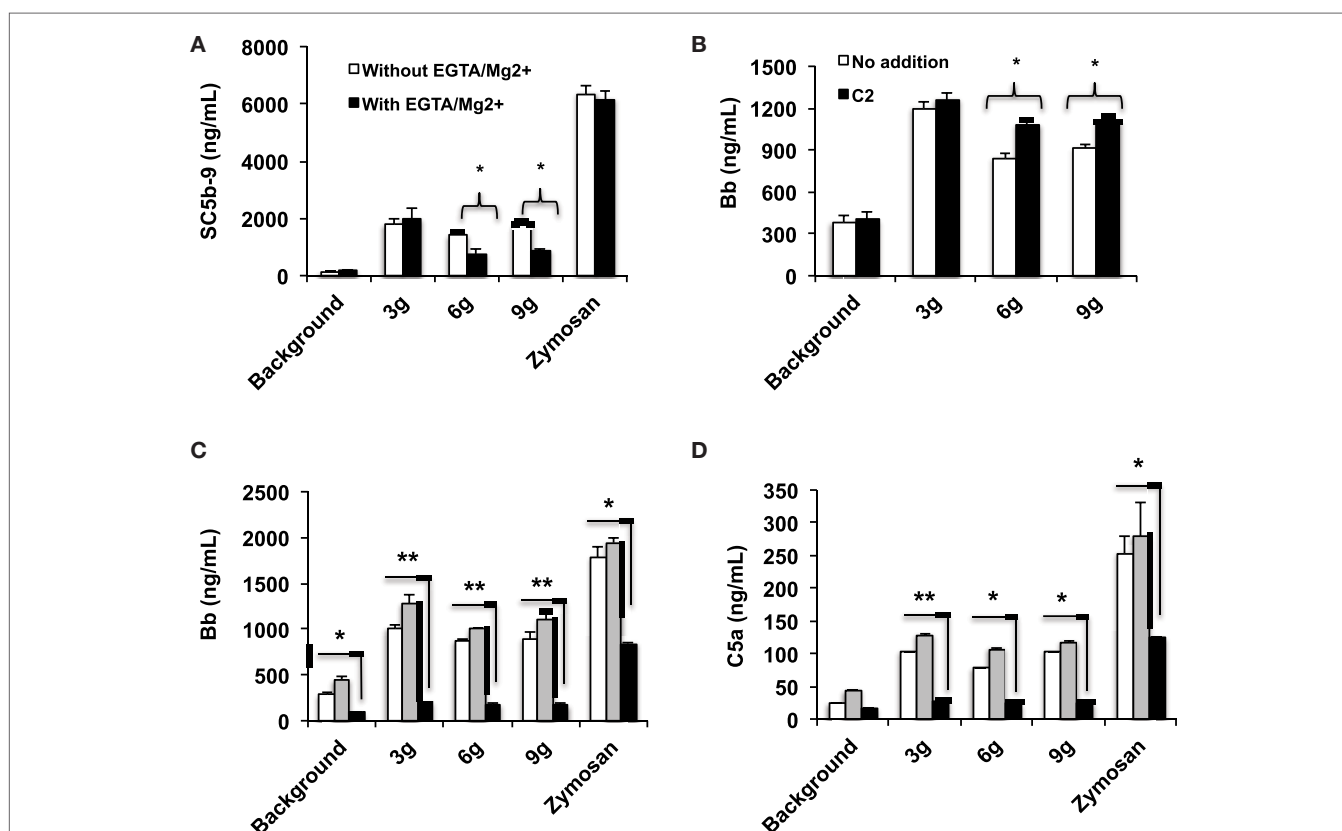


**FIGURE 3 |** Mechanisms of complement activation studied with fluid phase markers: formulations of SPIO NWs are described in Figure 1 (dextran/Fe ratios abbreviated as 3, 6, and 9 g) were incubated in human sera at 0.2 mg Fe/mL as described in Section “Materials and Methods”. Zymosan (positive control) was at 0.2 mg/mL; **(A)** generation of soluble terminal membrane attack complex sC5b-9 in a healthy human serum; **(B)** generation of Bb as a marker of the AP activation in C2-depleted serum [the same serum source as in **(A)**, where C2 was depleted immunochemically] and after addition of recombinant C2 (650 µg/mL) to C2-depleted serum; **(C,D)** effect of properdin antibody on AP activation and C5a generation, respectively. White bars: no inhibitor, gray bars: control isotype matched antibody, black bars: anti-P antibody. Non-parametric two sided *t*-test, *n* = 3 (two different human sera were used, and the results of a typical experiment are presented); \**p* < 0.05; \*\**p* < 0.01. None of the SPIO NWs generated sC5b and Bb in the presence of 10 mM EDTA (not shown).

factor for calcium-sensitive pathways. According to **Figure 3B**, SPIO NWs showed no decrease in Bb in the absence of C2, whereas 6 and 9 g SPIO showed a 25% decrease in Bb in the absence of C2. Bb levels were restored to normal levels when C2, at a physiological concentration (650 µg/mL), was added to the depleted serum. Collectively, these experiments confirm that calcium-sensitive pathways contribute to the complement activation by NWs with more polysaccharide content. In order to understand to what extent complement activation can proceed in the absence of the AP, we tested Bb and C5a formation in presence of anti-properdin (P) antibodies. The AP convertase is stabilized by P, being present in blood at ~20 µg/mL. For all formulations regardless of the dextran/Fe ratio, anti-P blocking antibody [a potent blocker of the AP (37)] inhibited AP convertase generation by over 80% (**Figure 3C**) and prevented C5a release by over 70% (**Figure 3D**). Collectively, these data suggest that despite contribution of the calcium-sensitive pathways to the initiation of complement and formation of the AP convertase by particles prepared at high dextran/Fe ratio, the AP still plays a predominant role on the propagation of complement and generation of fluid phase markers for all tested formulations.

## Surface Modifications of SPIO NWs Do Not Decrease Complement Activation and C3 Opsonization

Because 3 g SPIO NWs show only a single pathway of complement activation, as opposed to 6 and 9 g SPIO that exhibit also calcium-dependent activation, in the subsequent studies, we studied the effect of surface modifications of SPIO NWs on complement activation. SPIO NWs are highly efficient MRI contrast agents (35), and their opsonization by C3 leads to immune cell uptake (38), therefore, strategies to block complement activation would have a great value in the translation of these particles. Previously, we reported that crosslinking dextran coat of SPIO NWs with epichlorohydrin (resulting in CL-NWs, **Figure 4A**) blocked lectin pathway activation and C3 opsonization in mouse serum, but this procedure did not block C3 opsonization in sera from human subjects (35). In order to determine the pathway responsible for complement activation of CL-NWs in human serum, we measured the fluid markers sC5b-9 and Bb (**Figures 4B,C**). SPIO NWs and CL-NWs caused comparable AP activation that was not inhibited by 10 mM EGTA/2.5 mM Mg<sup>2+</sup>. At the same time, anti-P antibody, but not control antibody, blocked over 90% of sC5b-9 and Bb release for both SPIO NWs and CL-NWs. These

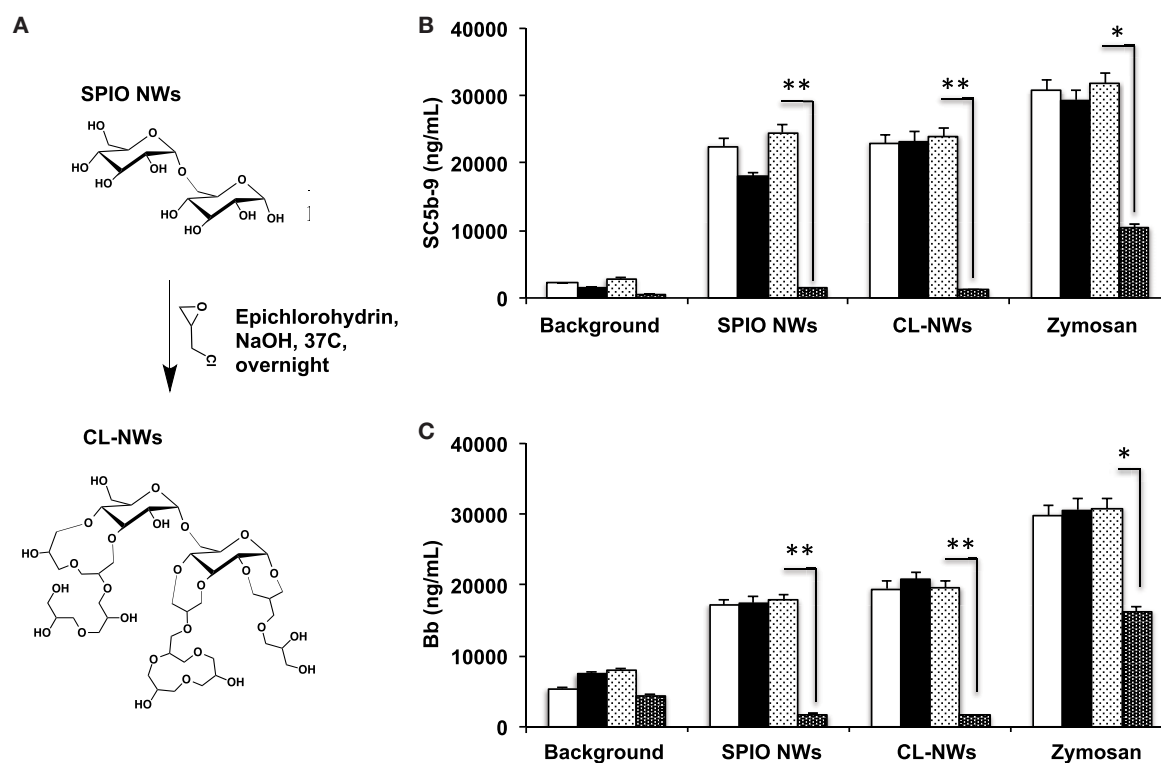
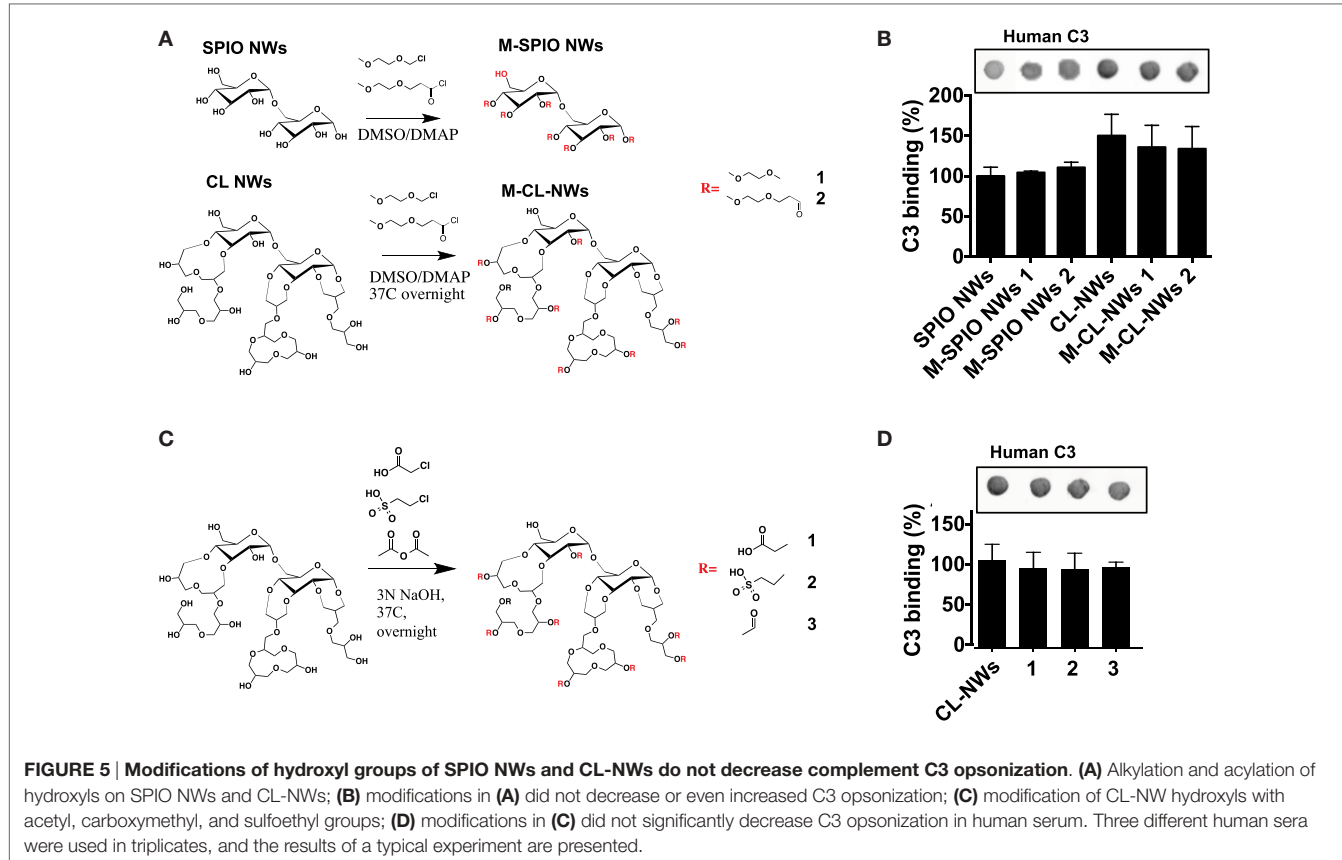


**FIGURE 4 | Effect of crosslinking of SPIO NWs on the complement activation as measured with fluid phase markers.** (A) Scheme of crosslinking as described previously (35) leads to the formation of 3D crosslinked hydrogel on the particle surface; (B,C) generation of membrane attack complex and Bb, respectively, in human serum. Particle concentration was 0.4 mg/mL, zymosan concentration was 0.2 mg/mL. White bars: no inhibitor; black bars: EGTA/Mg<sup>2+</sup>; light dotted bars: control isotype matched antibody; dark dotted bars: anti-P antibody. The crosslinking of dextran did not block complement activation and did not change the pathway of activation (AP). Non-parametric two-sided t-test,  $n = 3$ ; \* $p < 0.05$ ; \*\* $p < 0.01$  (two different human sera were used, and the results of a typical experiment are presented).



results confirm that complement activation by CL-NWs proceeds almost exclusively *via* the AP.

The AP is triggered by the initial deposition of C3b on a foreign surface *via* highly reactive thioester group that covalently attaches to amines and hydroxyls (39). Both dextran and crosslinked dextran contain hydroxyls available for nucleophilic attack of the thioester bond and subsequent deposition of C3b (**Figure 4A**). Previous report suggested that substituting hydroxyl groups could reduce complement consumption by Sephadex (crosslinked dextran beads) (32). In order to test the hypothesis whether substitution of dextran hydroxyls by alkylating and acylating agents could block complement activation, we modified hydroxyl groups of SPIO NWs and CL-NWs with an esterifying agent 2-(2-methoxyethoxy) acetyl chloride or etherifying agent 2-methoxyethoxymethyl chloride (**Figure 5A**) and measured C3 opsonization in human serum. According to **Figure 5B**, while there was a significant deposition of C3 on SPIO NWs, modification of hydroxyl groups did not diminish C3 opsonization. Moreover, there was no decrease in C3 opsonization after crosslinking and after modification of CL-NW hydroxyls (**Figures 5A,B**). There is evidence in the literature that the presence of anionic groups on the polysaccharide surface can promote binding of serum factor H, which is a negative regulator of the AP (3, 34). However, modification of hydroxyl groups of CL-NWs with carboxymethyl, acyl, or ethyl sulfonic groups (**Figure 5C**) did

not decrease the level of C3 opsonization in human serum (**Figure 5D**).

## DISCUSSION

Previous work has confirmed complement activation on a variety of carbohydrate-coated surfaces (29–31) as well as by crosslinked dextran beads [Sephadex (32)]. In this work, we determined the role of surface modification of dextran-coated iron oxides on the efficiency of complement activation in human sera. The fluid phase assays we employed are designed to dissect the role of the AP and calcium-sensitive pathways in the complement activation (7, 10, 40). Using these assays, we found that regardless of the ratio of dextran/Fe used in the preparation of nanoparticles, the complement activation predominantly proceeds *via* the AP, and with some minor contribution of the calcium-sensitive pathways for formulations prepared with a higher ratio of dextran/Fe. LP is likely the predominant calcium-sensitive pathway activated by these formulations due to the presence of polysaccharide coating, but this would need to be determined in a separate study. In addition, we found that particles prepared with low dextran/Fe ratio incite complement *via* only the AP.

Complement activity toward nanosurfaces is generally much higher in human sera than in sera from other species (41). The main reason for such activity is the continuous, but slow

activation of the AP due to tick-over, or formation of fluid phase AP convertase C3(H<sub>2</sub>O)Bb, the initial deposition of C3b on the foreign surface (42). Albeit activation of the AP could happen in the fluid phase, a foreign surface provides the scaffold for C3b and properdin binding, which enhances the assembly of the C3bBb convertase and complement amplification (43). Another mechanism of the AP convertase formation could be the direct binding of C3 to the surface (44). Therefore, we reasoned that the modification of nanoparticle hydroxyl groups could block the initial seeding of C3b and hence the AP activation. Previously, Labarre and colleagues showed that the blocking of alcohol groups (main groups that reacts with thioester of C3b) on Sephadex by carboxymethyl residues (32) prevented complement activation. In addition, the same group demonstrated that the presence of sulfate groups on a surface can mitigate complement activation by attracting factor H, the inhibitor of the AP convertase (33). Unlike these findings, we demonstrate that blocking hydroxyl groups for SPIO NWs and crosslinked CL-NWs with alkylating, crosslinking, and negatively charged groups did not decrease C3 opsonization of SPIO NWs in human sera. Based on the inability of dextran hydroxyl substitutions to block C3 opsonization of SPIO NWs and CL-NWs, it is possible that other surface entities could promote the binding of C3, including non-specifically absorbed proteins, and we are currently investigating this possibility. The differences between the above mentioned results and our particles could be related to the differences in the surface nano-architecture, which promote different binding of complement activators and inhibitors, and needs to be investigated further.

In conclusion, our data establish the AP as the critical pathway for many SPIO formulations. In recent years, the AP has shown to be the essential pathway of complement activation in health and disease (45). Due to its key role, the AP represents a unique therapeutic target in many pathological conditions (46–48). For many drug delivery nanoplatforms, the AP has shown to be a critical pathway for complement activation (20, 21, 49), and it is likely that this list will only grow. The future research will focus on specific approaches to block the AP activation, for example, by using properdin-blocking antibodies (50) or natural serum complement inhibitors (51).

## MATERIALS AND METHODS

### Materials

Iron salts (ferrous and ferric chloride) and 20 kDa dextran (range 15–25 kDa) were from Sigma-Aldrich (St. Louis, MO, USA). Epichlorohydrin, anhydrous DMSO, 2-chloroethanesulfonic acid, chloroacetic acid, and acetic anhydride were from Sigma, 2-(2-methoxyethoxy)acetyl chloride and 2-methoxyethoxymethyl chloride were from Alfa Aesar. Goat anti-human complement C3 polyclonal antibody (catalog No. 0855444) was purchased from MP Biomedicals (Solon, OH, USA). Anti-goat, IRDye 800CW-labeled, secondary antibodies were from LI-COR Biosciences (Lincoln, NE, USA). Copper grids (300 mesh) were purchased from Electron Microscopy Sciences (Hatfield, PA, USA). Sera from normal female subjects were collected by

Equitech-Bio (Kerrville, TX, USA) according to the company's Institutional Review Board Protocol. All blood products and complement proteins were kept aliquoted at -80°C.

### Synthesis and Modification of SPIO Nanoworms

Nanoworms were synthesized using a one-pot Molday and MacKenzie (52) precipitation method as described by us previously (35). The main variation of the protocol was the ratio of dextran and iron salts in the reaction as described in Figure 1. The molar ratio between Fe<sup>2+</sup> and Fe<sup>3+</sup> was kept the same. After the synthesis, particles were dialyzed in double distilled water, filtered through a 0.45-μm filter (Millipore), and stored at 4°C. TEM imaging was conducted to visualize the iron oxide core using FEI Tecnai Spirit BioTwin electron microscope (Electron Microscopy Facility at the University of Colorado Boulder). Size and zeta potential measurements of NPs were determined using a Zetasizer Nano ZS (Malvern Instruments Ltd., Malvern, UK). The intensity weighted size distribution peak value was used to report hydrodynamic diameters of NWs.

For dextran shell crosslinking with epichlorohydrin, a two-step procedure was used as described before (35). For modification of dextran hydroxyls, SPIO NWs prepared at low dextran/Fe ratio (3 g dextran per 133.4 mg Fe salts), or the corresponding crosslinked CL-NWs were washed by ultracentrifugation in anhydrous DMSO two times and resuspended in anhydrous DMSO at 5.0 mg/mL (Fe concentration) in a borosilicate glass vial in the presence of 1 mg/mL of 4-dimethylaminopyridine (DMAP). Then, 2 mg/mL of 2-(2-methoxyethoxy)acetyl chloride or 2 mg/mL of 2-methoxyethoxymethyl chloride were added to the nanoparticles under stirring. Nanoparticles were incubated under nitrogen atmosphere with stirring at 37°C overnight, washed 3× in DMSO, 2× in DDW by ultracentrifugation, and resuspended in PBS for complement measurement. For modification with acetic anhydride, chloroacetic acid, or chloroethanesulfonic acid, CL-NWs were resuspended in DDW at 5 mg/mL (Fe concentration), stirred for 30 min in 2N NaOH solution, and then reacted with acetic anhydride (5% v/v), chloroacetic acid (5 mg/mL), or chloroethanesulfonic acid (5 mg/mL) at 37°C overnight with stirring. The particles were washed by ultracentrifugation and resuspended in PBS.

### Complement Activation Studies

Details of human serum preparation, characterization, and functional assessment of complement pathways were described in detail elsewhere (7, 10, 20). Briefly, serum was prepared from freshly collected blood of two healthy volunteers according to procedure by Lachmann (53). C2 was immunochemically depleted from human serum, and the depleted serum was characterized as described elsewhere (7, 10). To measure complement activation *in vitro*, we determined NW-induced rise of serum complement activation products C4d, Bb, C5a, and sC5b-9 using respective Quidel (Quidel, San Diego, CA, USA) ELISA kits according to the manufacturer's protocols. In all measurements, the volume of NW to normal or C2-depleted sera volume was 1:4. NW-mediated complement activation was further monitored after restoration

of C2 (650 µg/mL) in C2-depleted serum. Zymosan (0.2 mg/mL) was used as a positive control for complement activation throughout. Each experiment was repeated three times with sera from two healthy individuals.

## Analysis of Binding of Proteins to Particles

For binding assay of complement C3 and properdin, 1 mg/mL (Fe) SPIO NWs were incubated with fresh serum at 1:3 volume ratio. At the end of incubation, particles were washed three times with 1× PBS by centrifugation at 100,000× g at 4°C in 2 mM Ca<sup>2+</sup>/Mg<sup>2+</sup> supplemented PBS using Beckman Optima TLX ultracentrifuge. The pellets were resuspended in 20 µL PBS, and 2 µL aliquots were applied in triplicate onto a nitrocellulose membrane (Bio-Rad). The membranes were blocked using 5% (w/w) non-fat dry milk in PBS-T (1× PBS with 0.1% v/v Tween® 20) for 1 h at room temperature, probed with corresponding primary antibodies for 1 h at room temperature, followed by washing the membranes three times with PBS-T, and finally 1 h incubation with the corresponding IRDye 800CW-labeled secondary antibodies against the primary antibody species. The signal was visualized using an Odyssey infrared imager (Li-COR Biosciences, Lincoln, NE, USA). The integrated dot intensity in the scanned images was determined from 16-bit grayscale images using ImageJ software and plotted using Prism 6 software

## REFERENCES

- Ricklin D, Hajishengallis G, Yang K, Lambris JD. Complement: a key system for immune surveillance and homeostasis. *Nat Immunol* (2010) 11:785–97. doi:10.1038/ni.1923
- Arima Y, Kawagoe M, Toda M, Iwata H. Complement activation by polymers carrying hydroxyl groups. *ACS Appl Mater Interfaces* (2009) 1:2400–7. doi:10.1021/am9005463
- Lemarchand C, Gref R, Passirani C, Garcion E, Petri B, Muller R, et al. Influence of polysaccharide coating on the interactions of nanoparticles with biological systems. *Biomaterials* (2006) 27:108–18. doi:10.1016/j.biomaterials.2005.04.041
- Peng Q, Li K, Sacks SH, Zhou W. The role of anaphylatoxins C3a and C5a in regulating innate and adaptive immune responses. *Inflamm Allergy Drug Targets* (2009) 8:236–46. doi:10.2174/187152809788681038
- Helmy KY, Katschke KJ Jr, Gorgani NN, Kljavin NM, Elliott JM, Diehl L, et al. CR1g: a macrophage complement receptor required for phagocytosis of circulating pathogens. *Cell* (2006) 124:915–27. doi:10.1016/j.cell.2005.12.039
- Taylor PR, Martinez-Pomares L, Stacey M, Lin HH, Brown GD, Gordon S. Macrophage receptors and immune recognition. *Annu Rev Immunol* (2005) 23:901–44. doi:10.1146/annurev.immunol.23.021704.115816
- Andersen AJ, Robinson JT, Dai H, Hunter AC, Andresen TL, Moghimi SM. Single-walled carbon nanotube surface control of complement recognition and activation. *ACS Nano* (2013) 7:1108–19. doi:10.1021/nn3055175
- Wang X, Ishida T, Kiwada H. Anti-PEG IgM elicited by injection of liposomes is involved in the enhanced blood clearance of a subsequent dose of PEGylated liposomes. *J Control Release* (2007) 119:236–44. doi:10.1016/j.jconrel.2007.02.010
- Auguste DT, Prud'homme RK, Ahl PL, Meers P, Kohn J. Association of hydrophobically-modified poly(ethylene glycol) with fusogenic liposomes. *Biochim Biophys Acta* (2003) 1616:184–95. doi:10.1016/j.bbapm.2003.08.007
- Hamad I, Hunter AC, Moghimi SM. Complement monitoring of Pluronic 127 gel and micelles: suppression of copolymer-mediated complement activation by elevated serum levels of HDL, LDL, and apolipoproteins AI and B-100. *J Control Release* (2013) 170:167–74. doi:10.1016/j.jconrel.2013.05.030
- Devine DV, Wong K, Serrano K, Chonn A, Cullis PR. Liposome-complement interactions in rat serum: implications for liposome survival studies. *Biochim Biophys Acta* (1994) 1191:43–51. doi:10.1016/0005-2736(94)90231-3
- (GraphPad Software, Inc., La Jolla, CA, USA). Each experiment was repeated two times using sera from two individuals.

## ETHICS STATEMENT

The study used de-identified human sera previously collected by commercial body for research purposes and as such was exempt from institutional review board protocol.

## AUTHOR CONTRIBUTIONS

GW, FC, and LW performed the experiments; NKB, VMH, and SMM provided reagents; SMM and DS analyzed the data and wrote the manuscript.

## FUNDING

The study was funded by the University of Colorado Denver startup funding and NIH 1R01EB022040 to DS. FC was supported by the International Postdoctoral Exchange Fellowship Program (2013) from China Postdoctoral Council. SMM acknowledges financial support by the Danish Agency for Science, Technology and Innovation (Det Strategiske Forskningsråd), reference 09-065746.

- Borchard G, Kreuter J. The role of serum complement on the organ distribution of intravenously administered poly (methyl methacrylate) nanoparticles: effects of pre-coating with plasma and with serum complement. *Pharm Res* (1996) 13:1055–8. doi:10.1023/A:1016010808522
- Dobrovolskaia MA, Patri AK, Zheng J, Clogston JD, Ayub N, Aggarwal P, et al. Interaction of colloidal gold nanoparticles with human blood: effects on particle size and analysis of plasma protein binding profiles. *Nanomedicine* (2009) 5(2):106–17. doi:10.1016/j.nano.2008.08.001
- Szebeni J. Complement activation-related pseudoallergy: a new class of drug-induced acute immune toxicity. *Toxicology* (2005) 216:106–21. doi:10.1016/j.tox.2005.07.023
- Andersen AJ, Hashemi SH, Andresen TL, Hunter AC, Moghimi SM. Complement: alive and kicking nanomedicines. *J Biomed Nanotechnol* (2009) 5:364–72. doi:10.1166/jbn.2009.1045
- Pedersen MB, Zhou X, Larsen EK, Sorensen US, Kjems J, Nygaard JV, et al. Curvature of synthetic and natural surfaces is an important target feature in classical pathway complement activation. *J Immunol* (2010) 184:1931–45. doi:10.4049/jimmunol.0902214
- Peracchia MT, Vauthier C, Passirani C, Couvreur P, Labarre D. Complement consumption by poly(ethylene glycol) in different conformations chemically coupled to poly(isobutyl 2-cyanoacrylate) nanoparticles. *Life Sci* (1997) 61:749–61. doi:10.1016/S0024-3205(97)00539-0
- Pham CT, Mitchell LM, Huang JL, Lubniewski CM, Schall OF, Killgore JK, et al. Variable antibody-dependent activation of complement by functionalized phospholipid nanoparticle surfaces. *J Biol Chem* (2011) 286:123–30. doi:10.1074/jbc.M110.180760
- Al-Hanbali O, Rutt KJ, Sarker DK, Hunter AC, Moghimi SM. Concentration dependent structural ordering of poloxamine 908 on polystyrene nanoparticles and their modulatory role on complement consumption. *J Nanosci Nanotechnol* (2006) 6:3126–33. doi:10.1166/jnn.2006.406
- Moghimi SM, Hamad I, Andresen TL, Jorgensen K, Szebeni J. Methylation of the phosphate oxygen moiety of phospholipid-methoxy(polyethylene glycol) conjugate prevents PEGylated liposome-mediated complement activation and anaphylatoxin production. *FASEB J* (2006) 20:2591–3. doi:10.1096/fj.06-6186fje
- Salvador-Morales C, Zhang L, Langer R, Farokhzad OC. Immunocompatibility properties of lipid-polymer hybrid nanoparticles with heterogeneous

- surface functional groups. *Biomaterials* (2009) 30:2231–40. doi:10.1016/j.biomaterials.2009.01.005
22. Moore A, Weissleder R, Bogdanov A Jr. Uptake of dextran-coated monocrystalline iron oxides in tumor cells and macrophages. *J Magn Reson Imaging* (1997) 7:1140–5. doi:10.1002/jmri.1880070629
  23. Gupta AK, Gupta M. Synthesis and surface engineering of iron oxide nanoparticles for biomedical applications. *Biomaterials* (2005) 26:3995–4021. doi:10.1016/j.biomaterials.2004.10.012
  24. Karmali PP, Chao Y, Park JH, Sailor MJ, Ruoslahti E, Esener SC, et al. Different effect of hydrogelation on antifouling and circulation properties of dextran-iron oxide nanoparticles. *Mol Pharm* (2012) 9:539–45. doi:10.1021/mp200375x
  25. Park JH, von Maltzahn G, Zhang L, Derfus AM, Simberg D, Harris TJ, et al. Systematic surface engineering of magnetic nanoworms for in vivo tumor targeting. *Small* (2009) 5:694–700. doi:10.1002/smll.200801789
  26. Park JH, Gu L, von Maltzahn G, Ruoslahti E, Bhatia SN, Sailor MJ. Biodegradable luminescent porous silicon nanoparticles for in vivo applications. *Nat Mater* (2009) 8:331–6. doi:10.1038/nmat2398
  27. Simberg D, Park JH, Karmali PP, Zhang WM, Merkulov S, McCrae K, et al. Differential proteomics analysis of the surface heterogeneity of dextran iron oxide nanoparticles and the implications for their in vivo clearance. *Biomaterials* (2009) 30:3926–33. doi:10.1016/j.biomaterials.2009.03.056
  28. Park JH, von Maltzahn G, Zhang L, Schwartz MP, Ruoslahti E, Bhatia S, et al. Magnetic iron oxide nanoworms for tumor targeting and imaging. *Adv Mater* (2008) 20:1630–5. doi:10.1002/adma.200800004
  29. Bertholon I, Vauthier C, Labarre D. Complement activation by core-shell poly(isobutylcyanoacrylate)-polysaccharide nanoparticles: influences of surface morphology, length, and type of polysaccharide. *Pharm Res* (2006) 23:1313–23. doi:10.1007/s11095-006-0069-0
  30. Labarre D, Vauthier C, Chauvierre C, Petri B, Muller R, Chehimi MM. Interactions of blood proteins with poly(isobutylcyanoacrylate) nanoparticles decorated with a polysaccharidic brush. *Biomaterials* (2005) 26:5075–84. doi:10.1016/j.biomaterials.2005.01.019
  31. Passirani C, Barratt G, Devissaguet JP, Labarre D. Interactions of nanoparticles bearing heparin or dextran covalently bound to poly(methyl methacrylate) with the complement system. *Life Sci* (1998) 62:775–85. doi:10.1016/S0024-3205(97)01175-2
  32. Carreno MP, Labarre D, Jozefowicz M, Kazatchkine MD. The ability of Sephadex to activate human complement is suppressed in specifically substituted functional Sephadex derivatives. *Mol Immunol* (1988) 25:165–71. doi:10.1016/0161-5890(88)90064-8
  33. Montdargent B, Maillet F, Carreno MP, Jozefowicz M, Kazatchkine M, Labarre D. Regulation by sulphonate groups of complement activation induced by hydroxymethyl groups on polystyrene surfaces. *Biomaterials* (1993) 14:203–8. doi:10.1016/0142-9612(93)90024-V
  34. Carreno MP, Labarre D, Maillet F, Jozefowicz M, Kazatchkine MD. Regulation of the human alternative complement pathway: formation of a ternary complex between factor H, surface-bound C3b and chemical groups on nonactivating surfaces. *Eur J Immunol* (1989) 19:2145–50. doi:10.1002/eji.1830191126
  35. Wang G, Inturi S, Serkova NJ, Merkulov S, McCrae K, Russek SE, et al. High-relaxivity superparamagnetic iron oxide nanoworms with decreased immune recognition and long-circulating properties. *ACS Nano* (2014) 8:12437–49. doi:10.1021/nn505126b
  36. Kirschfink M, Mollnes TE. Modern complement analysis. *Clin Diagn Lab Immunol* (2003) 10(6):982–9. doi:10.1128/CDLI.10.6.982-9.2003
  37. Gupta-Bansal R, Parent JB, Brunden KR. Inhibition of complement alternative pathway function with anti-properdin monoclonal antibodies. *Mol Immunol* (2000) 37:191–201. doi:10.1016/S0161-5890(00)00047-X
  38. Inturi S, Wang G, Chen F, Banda NK, Holers VM, Wu L, et al. Modulatory role of surface coating of superparamagnetic iron oxide nanoworms in complement opsonization and leukocyte uptake. *ACS Nano* (2015) 9:10758–68. doi:10.1021/acsnano.5b05061
  39. Kwan JJ, Borden MA. Lipid monolayer collapse and microbubble stability. *Adv Colloid Interface Sci* (2012) 18(3–184):82–99. doi:10.1016/j.cis.2012.08.005
  40. Hamada I, Hunter AC, Szelenyi J, Moghimi SM. Poly(ethylene glycol)s generate complement activation products in human serum through increased alternative pathway turnover and a MASp-2-dependent process. *Mol Immunol* (2008) 46:225–32. doi:10.1016/j.molimm.2008.08.276
  41. Neun BW, Dobrovolskaia MA. Qualitative analysis of total complement activation by nanoparticles. *Methods Mol Biol* (2011) 697:237–45. doi:10.1007/978-1-60327-198-1\_25
  42. Bexborn F, Andersson PO, Chen H, Nilsson B, Ekdahl KN. The tick-over theory revisited: formation and regulation of the soluble alternative complement C3 convertase (C3(H<sub>2</sub>O)Bb). *Mol Immunol* (2008) 45:2370–9. doi:10.1016/j.molimm.2007.11.003
  43. Spitzer D, Mitchell LM, Atkinson JP, Hourcade DE. Properdin can initiate complement activation by binding specific target surfaces and providing a platform for de novo convertase assembly. *J Immunol* (2007) 179:2600–8. doi:10.4049/jimmunol.179.4.2600
  44. Andersson J, Ekdahl KN, Larsson R, Nilsson UR, Nilsson B. C3 adsorbed to a polymer surface can form an initiating alternative pathway convertase. *J Immunol* (2002) 168:5786–91. doi:10.4049/jimmunol.168.11.5786
  45. Holers VM. Complement and its receptors: new insights into human disease. *Annu Rev Immunol* (2014) 32:433–59. doi:10.1146/annurev-immunol-032713-120154
  46. Holers VM, Thurman JM. The alternative pathway of complement in disease: opportunities for therapeutic targeting. *Mol Immunol* (2004) 41:147–52. doi:10.1016/j.molimm.2004.03.012
  47. Ricklin D. Manipulating the mediator: modulation of the alternative complement pathway C3 convertase in health, disease and therapy. *Immunobiology* (2012) 217:1057–66. doi:10.1016/j.imbio.2012.07.016
  48. Risitano AM, Notaro R, Pascaresso C, Sica M, del Vecchio L, Horvath CJ, et al. The complement receptor 2/factor H fusion protein TT30 protects paroxysmal nocturnal hemoglobinuria erythrocytes from complement-mediated hemolysis and C3 fragment. *Blood* (2012) 119:6307–16. doi:10.1182/blood-2011-12-398792
  49. Cunningham CM, Kingzette M, Richards RL, Alving CR, Lint TF, Gewurz H. Activation of human complement by liposomes: a model for membrane activation of the alternative pathway. *J Immunol* (1979) 122:1237–42.
  50. Pauly D, Nagel BM, Reinders J, Killian T, Wulf M, Ackermann S, et al. A novel antibody against human properdin inhibits the alternative complement system and specifically detects properdin from blood samples. *PLoS One* (2014) 9:e96371. doi:10.1371/journal.pone.0096371
  51. Wu YQ, Qu H, Sfyroera G, Tzekou A, Kay BK, Nilsson B, et al. Protection of nonself surfaces from complement attack by factor H-binding peptides: implications for therapeutic medicine. *J Immunol* (2011) 186:4269–77. doi:10.4049/jimmunol.1003802
  52. Molday RS, MacKenzie D. Immunospecific ferromagnetic iron-dextran reagents for the labeling and magnetic separation of cells. *J Immunol Methods* (1982) 52:353–67. doi:10.1016/0022-1759(82)90007-2
  53. Lachmann PJ. Preparing serum for functional complement assays. *J Immunol Methods* (2010) 352:195–7. doi:10.1016/j.jim.2009.11.003

**Conflict of Interest Statement:** The authors declare that the research was conducted in the absence of any commercial or financial relationships that could be construed as a potential conflict of interest.

Copyright © 2016 Wang, Chen, Banda, Holers, Wu, Moghimi and Simberg. This is an open-access article distributed under the terms of the Creative Commons Attribution License (CC BY). The use, distribution or reproduction in other forums is permitted, provided the original author(s) or licensor are credited and that the original publication in this journal is cited, in accordance with accepted academic practice. No use, distribution or reproduction is permitted which does not comply with these terms.



# Allergic Responses Induced by the Immunomodulatory Effects of Nanomaterials upon Skin Exposure

**Yasuo Yoshioka<sup>1,2,3,4\*</sup>, Etsushi Kuroda<sup>5</sup>, Toshiro Hirai<sup>6</sup>, Yasuo Tsutsumi<sup>4,7</sup> and Ken J. Ishii<sup>5,8</sup>**

<sup>1</sup>Vaccine Creation Project, BIKEN Innovative Vaccine Research Alliance Laboratories, Research Institute for Microbial Diseases, Osaka University, Suita, Osaka, Japan, <sup>2</sup>BIKEN Center for Innovative Vaccine Research and Development, The Research Foundation for Microbial Diseases of Osaka University, Suita, Osaka, Japan, <sup>3</sup>Laboratory of Nano-Design for Innovative Drug Development, Graduate School of Pharmaceutical Sciences, Osaka University, Suita, Osaka, Japan,

<sup>4</sup>The Center for Advanced Medical Engineering and Informatics, Osaka University, Suita, Osaka, Japan, <sup>5</sup>Laboratory of Vaccine Science, Immunology Frontier Research Center, World Premier International Research Center, Osaka University, Suita, Osaka, Japan, <sup>6</sup>Department of Dermatology and Immunology, University of Pittsburgh, Pittsburgh, PA, USA,

<sup>7</sup>Laboratory of Toxicology and Safety Science, Graduate School of Pharmaceutical Sciences, Osaka University, Suita, Osaka, Japan, <sup>8</sup>Laboratory of Adjuvant Innovation, National Institutes of Biomedical Innovation, Health and Nutrition, Ibaraki, Osaka, Japan

## OPEN ACCESS

### Edited by:

Diana Boraschi,  
National Research Council, Italy

### Reviewed by:

Albert Duschl,  
University of Salzburg, Austria  
Detlef Neumann,  
Hannover Medical School, Germany

### \*Correspondence:

Yasuo Yoshioka  
y-yoshioka@biken.osaka-u.ac.jp

### Specialty section:

This article was submitted to  
Inflammation,  
a section of the journal  
*Frontiers in Immunology*

**Received:** 28 December 2016

**Accepted:** 02 February 2017

**Published:** 16 February 2017

### Citation:

Yoshioka Y, Kuroda E, Hirai T, Tsutsumi Y and Ishii KJ (2017) Allergic Responses Induced by the Immunomodulatory Effects of Nanomaterials upon Skin Exposure. *Front. Immunol.* 8:169.  
doi: 10.3389/fimmu.2017.00169

Over the past decade, a vast array of nanomaterials has been created through the development of nanotechnology. With the increasing application of these nanomaterials in various fields, such as foods, cosmetics, and medicines, there has been concern about their safety, that is, nanotoxicity. Therefore, there is an urgent need to collect information about the biological effects of nanomaterials so that we can exploit their potential benefits and design safer nanomaterials, while avoiding nanotoxicity as a result of inhalation or skin exposure. In particular, the immunomodulating effect of nanomaterials is one of most interesting aspects of nanotoxicity. However, the immunomodulating effects of nanomaterials through skin exposure have not been adequately discussed compared with the effects of inhalation exposure, because skin penetration by nanomaterials is thought to be extremely low under normal conditions. On the other hand, the immunomodulatory effects of nanomaterials via skin may cause severe problems for people with impaired skin barrier function, because some nanomaterials could penetrate the deep layers of their allergic or damaged skin. In addition, some studies, including ours, have shown that nanomaterials could exhibit significant immunomodulating effects even if they do not penetrate the skin. In this review, we summarize our current knowledge of the allergic responses induced by nanomaterials upon skin exposure. First, we discuss nanomaterial penetration of the intact or impaired skin barrier. Next, we describe the immunomodulating effects of nanomaterials, focusing on the sensitization potential of nanomaterials and the effects of co-exposure of nanomaterials with substances such as chemical sensitizers or allergens, on the onset of allergy, following skin exposure. Finally, we discuss the potential mechanisms underlying the immunomodulating effects of nanomaterials by describing the involvement of the protein corona in the interaction of nanomaterials with biological components and by presenting recent data about the adjuvant effects of well-characterized particle adjuvant, aluminum salt, as an example of immunomodulatory particulate.

**Keywords:** adjuvant, allergy, aluminum salts, biodistribution, metal allergy, nanomaterial, sensitization, skin

## INTRODUCTION

Recently, advances in nanotechnology have made possible the design and production of many engineered nanomaterials—nanoparticles, nanofibers, and nanosheets—which are defined as materials with structures having at least one dimension less than 100 nm (1, 2). These products have become indispensable in various fields, such as electronics, foods, cosmetics, and medicines, because nanomaterials have unique physicochemical properties and exert innovative functions compared with conventional larger particles; these properties and functions include enhanced electrical conductivity, tensile strength, and chemical reactivity, and stem from an increase in the surface area per unit weight compared with a larger amount ( $>100$  nm) of the same material (3, 4). However, with the increasing use of nanomaterials, concerns about their safety, termed nanotoxicity, have been raised, specifically that the innovative functions of nanomaterials, such as high chemical reactivity and high tissue penetration, due to their small size might make them hazardous in some situations (5, 6). For example, our group has shown that intravenous injection of a large amount of silica ( $\text{SiO}_2$ ) nanoparticles induced pregnancy complications in mice, although it should be noted that the level of exposure used in the study is not representative of real-world human exposure (7). The health risks of engineered nanomaterials to humans have also been considered (8–10). Among the nanotoxic effects, those on host immunity are of particular interest, because the immune cells recognize foreign substances as part of the body's defenses, when those substances enter the body. Therefore, there have been many reports about the immunomodulating effects, both immune-activating and -suppressing effects, of nanomaterials *in vitro* and *in vivo* (11–13). To fully utilize the potential benefits of nanomaterials and design safer nanomaterials, it is essential for us to collect more information about nanotoxicity, because intentional and unintentional exposure to nanomaterials is unavoidable in our everyday life.

Our skin is exposed to nanomaterials in many situations, because nanomaterials are contained in cosmetics and other skincare products. For example, some nanoparticles, especially Zinc oxide ( $\text{ZnO}$ ) and titanium dioxide ( $\text{TiO}_2$ ) nanoparticles, have been used in sunscreens since the 1980s, because they have better ultraviolet (UV) protective properties than larger particles (14).  $\text{SiO}_2$  nanoparticles are used in a wide variety of cosmetics as an anti-setting agent (15). We are also exposed to silver ( $\text{Ag}$ ) nanoparticles through our everyday lives because  $\text{Ag}$  nanoparticles have been widely applied to consumer products such as clothing, antibacterial sprays, detergent, socks, and shoes for antimicrobial purposes (16). Therefore, an understanding of the absorption rate of nanomaterials after exposure *via* the skin has attracted increasing attention over the past few years, because it is important to consider the immunomodulatory effects of nanomaterials on the skin. In addition, because nanomaterials can interact with other substances easily (17), we must not forget that exposure to nanomaterials *via* skin often occurs simultaneously with exposure to other chemical compounds and allergens, such as foods and pollen and that this interaction might modulate the antigenicity of these compounds. Many recent reports have shown that skin is an important site for the onset of allergy (18, 19). For

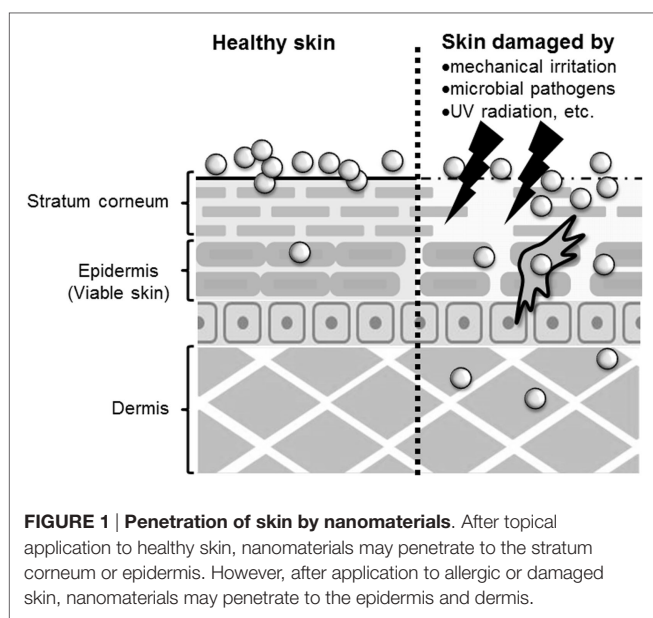
example, several reports have shown that transdermal exposure to food allergens can induce Th2-type immune responses and be sufficient to sensitize mice (20–22). Furthermore, individuals who used a facial soap containing hydrolyzed wheat protein were presumed to be sensitized to this protein (23, 24). Given these findings, there is an urgent need to understand the immunomodulatory effects of nanomaterials upon skin exposure, particularly effects that may lead to the onset or aggravation of allergy. However, while there have been many studies examining the nanotoxicity of nanomaterials to the respiratory system, there is a lack of knowledge about nanotoxicity following skin exposure to nanomaterials, especially the immunomodulating effects.

In this review, we summarize our current understanding of the skin penetration of nanomaterials and the immunomodulating effects of nanomaterials, focusing on the skin penetration of nanomaterials, the sensitization potential of nanomaterials, and the effects of co-exposure of nanomaterials with allergens on the onset of allergy upon skin exposure. In addition, we discuss potential mechanisms underlying the immunomodulating effects of nanomaterials by describing the involvement of the protein corona in the interaction of nanomaterials with complement proteins and by presenting recent study about the adjuvant effects of aluminum salts, which are well characterized in basic immunology.

## SKIN STRUCTURE AND PENETRATION OF SKIN BY NANOMATERIALS

The skin is composed of several barriers that prevent foreign substances from penetrating the body (25, 26). Healthy skin is divided into the epidermis and the dermis. In addition, there are two physical barriers in the epidermis: the stratum corneum, the outmost layer of the epidermis, and tight junctions, which are intercellular junctions that seal adjacent keratinocytes in the stratum granulosum below the stratum corneum (25, 26). It is generally believed that molecules, other than small lipophilic molecules ( $<500$  Da), are unable to penetrate healthy skin due to these barrier functions (27). The skin also contains hair follicles and sebaceous glands (28). Hair follicles extend into the dermis and might provide a means for penetration and absorption of compounds into the skin. Therefore, hair follicles may play an important role as a potential reservoir and penetration route for topically applied substances. It is also suggested that hair follicles have important functions in immune responses such as those regulating the trafficking of antigen presenting cells (29). In addition, many immune cells such as antigen presenting cells [e.g., Langerhans cells (LCs) in the epidermis and dermal dendritic cells in the dermis] and leukocytes are present in the skin to protect the body from external substances (30). Recently, tape stripping of murine skin showed that activated LCs could elongate their dendrites above the tight junctions of keratinocytes and take up antigens on the surface of the skin (31, 32).

Whether nanomaterials can penetrate the skin barrier *in vivo* remains controversial, although there have been several reports assessing the skin penetration of nanomaterials after topical application using both *in vitro* and *in vivo* models (Figure 1).



Because  $\text{TiO}_2$  and  $\text{ZnO}$  nanoparticles are essential components in sunscreens, many studies have examined the penetration rate of these nanoparticles, although it should be noted that these nanoparticles are typically present in sunscreens as 30- to 150-nm aggregates. Cross et al. and Larese et al. have shown that  $\text{ZnO}$  nanoparticles with diameters of 15–40 nm, and  $\text{Ag}$  nanoparticles with a diameter of 25 nm, can penetrate the upper layers of the stratum corneum but cannot reach the deeper layers of the viable epidermis and dermis by using an *in vitro* model of human skin (33, 34). Lin et al. also showed that  $\text{ZnO}$  nanoparticles with a diameter of 10–50 nm could not penetrate healthy skin or tape-stripped skin of human volunteers (35). These reports suggest that the stratum corneum and tight junctions of skin provide an effective barrier to prevent nanomaterial penetration of healthy skin. In contrast, Gulson et al. have shown that small amounts of  $\text{ZnO}$  nanoparticles with a diameter of 19 nm can penetrate the skin after repeated application to healthy humans (36, 37). These results suggest that nanomaterials may penetrate the skin after repeated application to even healthy skin (Figure 1). However, these different results might be due to differences in the analytical methods used, in the detection sensitivity of the analytical methods, in the sample volume or skin model used, or in the type of nanomaterials and their aggregation state. For example, although Gulson et al. used  $\text{ZnO}$  particles containing the stable isotope  $^{68}\text{Zn}$  and were able to detect the concentration of  $^{68}\text{Zn}$  in the body at high sensitivity (36, 37), other groups used conventional nanomaterials and transmission electron microscopy and inductively coupled plasma mass spectrometry techniques in their studies (33–35). In addition, although transmission electron microscopy and mass spectrometry techniques are useful for evaluating the penetration of skin by nanomaterials, transmission electron microscopy is a qualitative method that cannot be used to determine the amount of nanomaterials in the skin, and inductively coupled plasma mass spectrometry is a quantitative method that cannot distinguish between nanomaterials and their dissociated

ions. Therefore, the development of more sensitive qualitative and quantitative analysis methods is an important step in elucidating the penetration of nanomaterials through the skin.

The skin barrier is not always intact because skin is under constant assault every day by mechanical irritation, mechanical damage (cuts or scrapes), UV exposure, microbial pathogens, and the use of harsh soaps or cosmetic products that may contain chemical irritants (25). In addition, people with healthy skin and those with impaired skin barrier function apply sunscreens containing nanomaterials. In this regard, some studies have examined whether nanomaterials can penetrate deeply into allergic or damaged skin because nanomaterials may be able to penetrate skin with impaired barrier function. Ilves et al. showed that  $\text{ZnO}$  nanoparticles with a diameter of 20 nm could be observed in the epidermis and to a lesser extent also in the dermis of allergic skin of mice after topical application, but  $\text{ZnO}$  particles with a diameter of 240 nm were not detected (38). Similar to their observations, other studies using human skin explants with partially disrupted stratum corneum have shown that 40-nm polystyrene nanoparticles, but not 750- or 1500, and 40-nm  $\text{SiO}_2$  nanoparticles can translocate to the viable epidermis (39, 40). In addition, Mortensen et al. showed that quantum dot nanoparticles with a diameter of 45 nm could penetrate deep into the epidermis and dermis in sub-erythema dose UV radiation-exposed mice (41). These reports suggest that nanomaterials generally can penetrate the deep layers of the skin, such as the epidermis and the dermis of allergic or damaged skin (Figure 1). Although the precise number of penetrated nanoparticles needs to be quantified, these findings emphasize the importance of investigating the immunomodulatory effects of nanomaterials after topical application.

Recently, hair follicles have been considered an excellent target route for drug delivery *via* skin (42). Many researchers have tried to deliver drug compounds *via* hair follicles by using particles such as liposomes (42, 43). Hair follicles have the potential to be efficient, long-term reservoirs suited for accumulation of nanomaterials. Therefore, the hair follicular pathway may be one of the penetration pathways of nanomaterials, although it remains largely unknown whether nanomaterials can indeed penetrate the skin *via* hair follicles (44, 45).

## SENSITIZATION POTENTIAL OF NANOMATERIALS ON SKIN

Allergic contact dermatitis induced by chemicals is the most frequent manifestation of skin sensitization in humans (46). It is estimated that about 4,000 chemicals have the potential to be skin sensitizers (47). Because sensitization to chemicals is sometimes induced at relatively low levels of exposure to that substance *via* skin exposure, the sensitization potential of nanomaterials might be an important potential nanotoxicity.

Park et al. showed that neither amine-modified polystyrene nanoparticles with a diameter of 50 nm nor  $\text{TiO}_2$  nanoparticles (primary size <25 nm) induced skin sensitization after topical skin treatment, as assessed using a local lymph node assay (LLNA), which is a useful method for evaluating the sensitization potential of chemicals (48). Lee et al. evaluated the sensitization potential

of two types of  $\text{SiO}_2$  nanoparticles, mesoporous  $\text{SiO}_2$ , and colloidal  $\text{SiO}_2$ , with diameters of about 100 nm (49). Changes in ear skin thickness after painting the skin with each nanoparticle for three consecutive days were small. In addition, these authors also found that neither nanoparticle induced skin sensitization, as assessed using a LLNA. These results suggest that the sensitization potential of many nanomaterials after topical application to healthy skin might be low. Skin painting is a typical method used to analyze the sensitization potential of chemical compounds, but nanomaterials do not easily penetrate healthy skin. Therefore, subcutaneous or intradermal administration might be useful as alternative routes for examining the sensitization potential of nanomaterials, assuming that the particles are able to penetrate allergic or damaged skin.

Epidemiological studies have suggested that sensitizer metals contained in airborne particulates may also contribute to the onset of metal allergy (50–52). Since metal nanoparticles can release metal ions, we must pay attention to the sensitization potential of not only nanoparticles but also metal ions released from metal nanoparticles. Metal allergy, which is a major cause of allergic contact dermatitis, is prevalent in the general population, and up to 17% of women are reported to suffer from it (53, 54). Nickel is the most frequent cause of metal allergy, but gold, palladium, cobalt, mercury, beryllium, chromium, and silver also have sensitization potential (54). It is suggested that metal ions from jewelry and clothes (buttons, zippers, and belt buckles) cause metal allergy *via* the activation of innate and adaptive immunity. Although it is believed that metal allergy is caused by metal-ion-induced T cells, which are generally reactive to metal ions in the major histocompatibility complex, many attempts to sensitize mice by means of simple metal-ion treatment have failed (55, 56). Moreover, while some reports have shown that metal allergy in mice can be induced by concomitant application of inflammatory stimuli, such as lipopolysaccharide (LPS) (57, 58), the skin reactions in these models could be induced by irritant inflammation rather than allergic responses (59). Nevertheless, these studies raised the possibility that other unknown factors may contribute to the onset of metal allergy.

Recently, it was revealed that metal nanoparticles are generated in the environment and in our bodies naturally during our daily lives (60). For example, Glover et al. showed that metal nanoparticles were generated spontaneously from manmade objects such as earrings or metal wire, suggesting that macroscale metal objects might be a potential source of naturally occurring nanoparticles in the environment (61). In addition, naturally occurring metal nanoparticles are thought to be formed from ions *via* chemical and/or photochemical reduction of released metal ions from metal objects (61, 62). Therefore, we could be extemporaneously exposed to metal ions from metal objects when we wear metal accessories and then these ions could generate naturally occurring metal nanoparticles when we are sensitized to metal. In this regard, our group examined the contribution of metal nanoparticles to the onset of metal allergy by using Ag nanoparticles or nickel (Ni) nanoparticles with several kinds of diameters (63) (Figure 2). We showed that mice sensitized with Ag nanoparticles or nickel nanoparticles plus LPS exposure, but not with metal ions, experienced allergic inflammation in response to

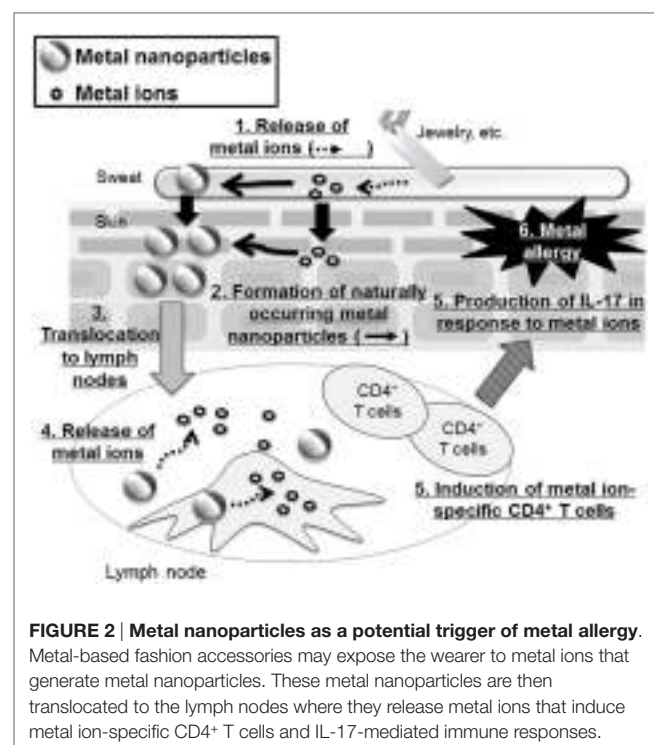


**FIGURE 2 |** Metal nanoparticles as a potential trigger of metal allergy.

Metal-based fashion accessories may expose the wearer to metal ions that generate metal nanoparticles. These metal nanoparticles are then translocated to the lymph nodes where they release metal ions that induce metal ion-specific CD4<sup>+</sup> T cells and IL-17-mediated immune responses.

both metal ions and metal nanoparticles in the elicitation phase. We also showed that LPS was necessary for sensitization to metal nanoparticles. However, gold and  $\text{SiO}_2$  nanoparticles, which are minimally ionizable, did not induce allergic inflammation, even when co-administered with LPS. In addition, smaller metal nanoparticles had stronger sensitization potential than larger ones. We observed that CD4<sup>+</sup> T cells were required for immune responses induced by metal nanoparticles and IL-17A-mediated inflammation was responsible for the allergic responses. On the basis of this study, we suggested that metal nanoparticles might play a role as a carrier, conveying metal ions to the lymph nodes for metal sensitization, because we found that smaller metal nanoparticles were transferred to the draining lymph nodes more readily than larger metal nanoparticles and metal ions. This study identifies metal nanoparticles as a new potential trigger of metal allergy and highlights the need to pay close attention to the indirect sensitization potential of metal nanoparticles when evaluating their safety.

## COMBINED EXPOSURE TO NANOMATERIALS AND OTHER SUBSTANCES

Our skin is often exposed to nanomaterials simultaneously with other chemical compounds and allergens, such as foods and pollen. Therefore, it is important to examine the possibility that skin exposure to nanomaterials contributes to allergen-induced onset of allergy.

Allergic contact dermatitis is generally induced by a chemical sensitizer. Hussain et al. showed the effect of  $\text{TiO}_2$  nanoparticles

with a diameter of 22 nm on the sensitization potential of dinitrochlorobenzene (DNCB), a well-known skin sensitizer (64). They showed that subcutaneous injection of TiO<sub>2</sub> nanoparticles before DNCB treatment increased DNCB-mediated lymph node proliferation in an LLNA and enhanced Th2-type cytokine production, whereas TiO<sub>2</sub> nanoparticles alone showed no dermal sensitization. This study suggests that some nanomaterials can enhance the sensitization potential of chemical sensitizers when they penetrate the skin. Moreover, several reports have shown that topical application of nanomaterials also has an effect on skin sensitization caused by chemicals. Lee et al. showed that 3 days of consecutive skin painting with mesoporous SiO<sub>2</sub> nanoparticles with a diameter of about 100 nm and 2,4-dinitroflourobenzene (DNFB) exacerbated DNFB-induced ear skin thickness and lymphocyte proliferation (49). Smulders et al. compared the effect of different topically applied nanoparticles (TiO<sub>2</sub>, Ag, and SiO<sub>2</sub> nanoparticles) on DNCB-induced dermal sensitization by an LLNA (65). They showed that only TiO<sub>2</sub> nanoparticles enhanced sensitization to DNCB by augmenting a Th2 response. Together, these reports demonstrate that some nanomaterials can enhance the potential of chemical sensitizers after either topical application or intradermal/subcutaneous injection, although the physiochemical properties of the nanomaterials (e.g., size, shape, composition, charge, and surface energy) might influence the effects. Further studies are needed to reveal the mechanisms behind these nanomaterial effects and to identify the threshold amounts that are hazardous.

It is estimated that 15–30% of children and 2–10% of adults suffer from atopic dermatitis (66). Atopic dermatitis is believed to progress to allergic rhinitis and asthma over time, which is referred to as the atopic march. Of note, the incidence of atopic dermatitis has increased gradually in industrialized countries (67, 68). Some reports have shown that co-exposure to nanomaterials and protein allergens affect atopic allergy. Yanagisawa et al. showed that intradermal injection of TiO<sub>2</sub> nanoparticles of different sizes (15, 50, or 100 nm) together with mite allergen, which is a major cause of atopic dermatitis, enhanced atopic dermatitis-like skin lesions and Th2-type cytokine production, as well as total IgE and histamine levels in serum (69). They observed that the size of the TiO<sub>2</sub> nanoparticles did not influence these effects. They also observed similar effects in NC/Nga mice treated with polystyrene nanoparticles (70). In this case, enhancement of allergic responses was totally depended on the size of particle, that is, the smaller polystyrene nanoparticles induced greater symptoms. We also investigated the co-exposure effects of SiO<sub>2</sub> particles of different sizes (30, 70, 100, 300, or 1000 nm) and mite antigen on atopic dermatitis in NC/Nga mice (71), and found that intradermal exposure of SiO<sub>2</sub> particles and mite antigen aggravated atopic dermatitis. This effect was correlated with excessive induction of total IgE and stronger systemic Th2 responses. Of note, the aggravating effects were more pronounced in the smaller SiO<sub>2</sub> nanoparticle-injected mice than in the mice exposed to the larger particles.

Other reports have shown the effects of nanomaterials on atopic dermatitis after topical skin painting. Ilves et al. used a mouse model of atopic dermatitis and showed that ZnO nanoparticles with a diameter of 20 nm cause an increase in IgE production

after repeated topical application. However, these nanoparticles decreased local skin inflammatory responses, such as cytokine induction, in this mouse model (38). Our group showed that topical skin painting with a mixture of SiO<sub>2</sub> nanoparticles and mite allergen suppressed allergen-specific IgG production without any changes in the IgE and Th1/Th2 immune responses (72). In addition, the suppression of IgG caused severe IgE-mediated hypersensitivity in an anaphylaxis model. Interestingly, low-level IgG production was induced when the mice were exposed to allergen-SiO<sub>2</sub> nanoparticle agglomerates, but not when the mice were exposed to nanoparticles applied separately from the allergen, to well-dispersed nanoparticles, or to nanoparticle agglomerates *via* routes other than the skin. Thus, agglomeration of the allergen and SiO<sub>2</sub> nanoparticles may have created a “depot” effect that could control the concentration of the exposed allergen and prolong allergen exposure. Thereby, we suggest that allergen-SiO<sub>2</sub> nanoparticle agglomerates facilitated IgE-biased allergic sensitization.

These reports suggest that any nanomaterials could control the immune responses induced by a chemical sensitizer or allergen on the skin of humans. However, the mechanism responsible for these effects remains unclear. In the study described above, Smulders et al. observed that titanium levels were increased in lymph node cells after topical application of TiO<sub>2</sub> nanoparticles, indicating that TiO<sub>2</sub> nanoparticles penetrated the skin and translocated to the lymph nodes (65). We know that nanomaterials (<100 nm) can move to the draining lymph nodes *via* lymphatic vessels, but larger particles become trapped in the tissue and tend to depot near the site of injection (73). Winter et al. showed that TiO<sub>2</sub> and SiO<sub>2</sub> nanoparticles induce the activation of murine dendritic cells *in vitro* by upregulating co-stimulatory molecules (74). Therefore, one of the immunomodulating mechanisms of nanomaterials might be that they move to the draining lymph nodes after topical application and activate dendritic cells in the lymph nodes. However, little is understood about how nanomaterials affect the function of immune cells such as LCs and γδ T cells in the skin. In addition, as mentioned earlier, hair follicles have recently been revealed to have important functions in regulating the trafficking of LCs and skin-resident memory T cells (29, 75), and nanomaterials are prone to accumulate in hair follicles. Future studies should include detailed investigations into the relationship between the qualitative and quantitative distribution of nanomaterials in the skin and the effects of nanomaterials on skin immune cells, keratinocytes, and hair follicles.

We also must pay attention to the interaction of nanomaterials with antigens. Nanomaterials can bind more antigen per mass unit than larger particles, because nanomaterials have a larger per unit surface area per mass than larger particles. This leads to an enhancement of antigen persistence and prolonged release, an effect referred to as the “depot effect.” It has been suggested that smaller TiO<sub>2</sub> nanoparticles bind more protein antigen per mass unit than larger ones and that the depot effect on the antigen due to this binding may lead to increased antigenicity (76). Furthermore, as described below, one of the immune-activating mechanisms of aluminum salts, which are a well-known vaccine adjuvant, is believed to involve the depot effect. Therefore, the depot effect might also be one of the immune-enhancing

mechanisms of nanomaterials, particularly when co-exposed with antigens.

As noted earlier, our study showed that the depot effect by allergen– $\text{SiO}_2$  nanoparticle agglomerates might modulate the exposure level of allergens on the skin and could change the immune responses, even though these allergen– $\text{SiO}_2$  nanoparticle agglomerates could not penetrate the skin (72). In fact, our group found that differences in the cutaneous exposure level of allergens modulates the level of allergen-specific IgG and affects susceptibility to the IgE-mediated allergic response observed in other report (77). Therefore, allergen–nanomaterial aggregates and agglomerates might modulate immune responses *via* persistent release of allergen, even though the complexes are not able to penetrate the stratum corneum or tight junctions of the epidermis. These results suggest that we must examine several types of depot effects of complexes between nanomaterials and allergens.

## THE PROTEIN CORONA, NANOMATERIALS, AND COMPLEMENT

As described above, it is important to pay attention to the binding of compounds with nanomaterials. It is generally understood that nanomaterials could interact with proteins and other biomolecules contained in a biological fluid, when nanomaterials enter a biological fluid such as blood. For example, proteins bind to nanomaterials to form a coating around the surface known as the protein corona; when nanomaterials are mixed with plasma, the protein corona forms rapidly (within 30 seconds) (78). The protein composition of the corona does not seem to change markedly over time, although the concentration of a specific protein in the corona may change (78). Therefore, we must consider the possibility that the protein corona is involved in one or more of the mechanisms underlying the immunomodulating effects of nanomaterials.

The formation of the protein corona is an important factor that determines the interactions of nanomaterials with cells. Lesniak et al. reported that the protein corona surrounding nanomaterials inhibits the adhesion of nanomaterials to the cell membrane, resulting in a low internalization efficiency (79). In addition, they showed that the protein corona modulates not only the amount of nanomaterial taken up into cells but also the intracellular localization of nanomaterials within cells. Furthermore, detailed examination of the proteins within the corona has suggested that not all proteins in the protein corona modulate the cellular uptake of nanomaterials. For example, Deng et al. showed in *in vitro* studies that negatively charged gold nanoparticles bind to fibrinogen (80), and that the interaction of gold nanoparticles with fibrinogen induces fibrinogen unfolding, which promotes an interaction with the integrin receptor, Mac-1, which is expressed on macrophages. The binding and activation of Mac-1 induces inflammatory responses in macrophages. Therefore, the protein corona might contribute to the immunomodulatory effects of some nanomaterials. Indeed, if the protein corona of nanoparticles contains complement and coagulation factors, it can induce complement activation and blood clotting followed by unwanted inflammatory responses (81–84). The complement system not

only works as an innate immune sensor but also plays an essential role as a trigger for inducing adaptive immunity. Although few studies have examined whether the protein corona containing complement proteins could contribute to the immunomodulatory effects of nanomaterials, some studies have suggested strategies involving the use of complement activation by nanomaterials as an adjuvant for vaccines (85, 86). Reddy et al. designed pluronic-stabilized polypropylene sulfide nanoparticles with a diameter of 25 nm that could strongly activate complement (85). They showed that the nanoparticle-conjugated antigen could induce antigen-specific immune responses. In the future, the effects of complement activation by nanomaterials on the onset of allergic responses should be investigated. In addition, few studies have systematically examined the relationship between the activation of complement and the surface properties of particles, because protein binding, including complement binding to nanomaterials, is known to depend on the physicality of nanomaterials, such as their size and surface properties (87). Elucidation of the fundamental rules that govern complement recognition of nanomaterials could help us to better predict the immunomodulatory effects of nanomaterials in the future.

## IMMUNOMODULATING MECHANISMS OF THE ADJUVANT EFFECTS OF PARTICLES

As described above, many nanomaterials have been reported to have the potential to enhance adaptive immunity, that is, they have adjuvant effects. However, the molecular mechanisms of the adjuvanticity of nanomaterials remain largely unknown. Many particles besides nanomaterials have been reported to have adjuvant effects, such as hemozoin, which is a heme metabolite during malaria infection, chitin particles from fungal cell walls, and monosodium urate crystals released from damaged cells (88–90). Aluminum salt is a well-known particle adjuvant that is widely used throughout the world as an adjuvant for human vaccines (91). Since aluminum salts are the most studied particle with adjuvant effects, we will introduce aluminum salts as a typical example to summarize the mechanism of adjuvant effects in the context of the immunomodulatory effects of nanomaterials.

About one century ago, the usefulness of aluminum, in its potassium salt form, as a vaccine adjuvant was described for the first time (92). Since this report, several reports have shown the adjuvant effects of aluminum salts, especially aluminum oxyhydroxide, because aluminum salts induce strong antigen-specific Th2 immune responses such as the production of IL-4 and IL-5 and the induction of IgE and IgG1. Nowadays, many vaccines formulated with aluminum salts, such as the diphtheria-tetanus-pertussis vaccine, the pneumococcal conjugate vaccine, and hepatitis B vaccine, are approved by the US Food and Drug Administration (93). Recently, progress was made in revealing the mode of action of aluminum salts, although a large part of the adjuvant mechanism remains unclear.

The surface charge of aluminum salts is positive at physiological pH and aluminum salts can bind to negatively charged compounds, including protein antigens (94, 95). Therefore, the depot effect is thought to play a part in the adjuvanticity of aluminum salts. However, some studies have questioned the importance of

depot effects in the adjuvanticity of aluminum salts (96–98). For example, Hutchison et al. showed that surgical removal of the injection site 2 hours after co-administration of antigen and aluminum salts had no effect on antigen-specific immune responses in mice (96). Thus, it may be that aluminum salts have additional effects that contribute to their adjuvanticity, with the depot effect being just one of the underlying mechanisms.

The NLRP3 inflammasome is gaining attention for its role in the initial stages of inflammation, such as the production of IL-1 $\beta$  and IL-18, which are generated in response to a number of diverse particles, including monosodium urate crystal, silica, asbestos, and aluminum salts (99–101). Some reports have shown that aluminum salts induce antigen-specific IgG1 responses that are dependent on the NLRP3 inflammasome (101, 102), although other reports suggest that the NLRP3 inflammasome is not required for the adjuvanticity of aluminum salts (103, 104). This discrepancy might stem from differences in the aluminum salts (Imject alum (101, 102) or aluminum hydroxide (103, 104)) or mice (C57BL/6 (101, 102, 104) or mixed C57BL/6–129 (103)) used in the studies, and the importance of the NLRP3 inflammasome for the adjuvanticity of aluminum salts remains controversial. Recently, it was revealed that several types of nanomaterials induce NLRP3 activation (105). For example, Simard et al. showed *in vitro* that Ag nanoparticles activate the NLRP3 inflammasome by inducing the degradation of the ER stress sensor ATF-6 (106). In addition, Sun et al. showed that NADPH oxidase-dependent NLRP3 inflammasome activation is crucial for the lung fibrosis induced by multiwalled carbon nanotubes (107). However, few studies have investigated the link between the activation of the NLRP3 inflammasome by nanomaterials and the induction of adaptive immunity. Detailed studies to test this hypothesis are expected.

Recently, Kuroda et al. explained the role of prostaglandin E2 (PGE<sub>2</sub>), a well-characterized proinflammatory lipid mediator, in the adjuvanticity of aluminum salts (108). Specifically, they clarified the importance of aluminum salt-induced PGE<sub>2</sub> for antigen-specific IgE production, rather than IgG1 production. This information will be useful to elucidate the mechanistic basis of the aggravation effects of nanomaterials on IgE-related allergies upon co-exposure with allergens.

Recently, aluminum salt-induced cell death was reported to be an important function of adjuvanticity. Marichal et al. showed that DNA molecules released from dying host cells as a function of aluminum salt-induced innate immune responses act as damage-associated molecular patterns (DAMPs) to effectively induce adaptive immunity (109). In addition, Miki et al. showed that the interaction of apoptotic host cells, induced by aluminum salts, with CD300a, an immunoreceptor for phosphatidylserine, was important for the adjuvant effects of aluminum salts (110). Although many reports have examined the cytotoxicity of nanomaterials, few have shown the effects on the immune system of DAMPs and dead cells induced by nanomaterials. In this regard, Rabollil et al. showed that IL-1 $\alpha$  from necrotic alveolar macrophages was important for SiO<sub>2</sub> nanoparticle-induced lung inflammation (111), although the importance of this IL-1 $\alpha$  production for the induction of adaptive immunity was not clear. Recently, Kuroda et al. also indicated that IL-1 $\alpha$

release from alveolar macrophage death induced by aluminum salts contribute to adjuvant activity in the lungs (112). Since LPS stimulation induce alveolar macrophage death and IL-1 $\alpha$  release (113), IL-1 $\alpha$  release in the lungs seems an important event for immune responses in the lung. In addition, Natsuaki et al. showed that IL-1 $\alpha$ -induced leukocyte clusters is important for efficient activation of T cells in skin (114), suggesting the essential immunological role of IL-1 $\alpha$  in skin. Cell death might be required for allergic responses in the skin, the precise mechanisms involved in cell death in skin after exposure to nanomaterials should be investigated.

Many reports have shown the seemingly linear relationship between the biological effects of nanomaterials and their size. However, several *in vitro* studies have shown that nanomaterials with a diameter of 50 nm induce more cellular uptake or cytotoxicity compared with their larger and smaller counterparts (115, 116), suggesting the existence of size-specific nanotoxicity. Yet, few reports have shown such size-specific effects of nanomaterials *in vivo*. Therefore, further studies are needed to elucidate the size-specific immunomodulating mechanisms of nanomaterials, which might be different from those of aluminum salts.

## FUTURE PROSPECTS AND CONCLUSION

It is difficult to judge whether topical application of nanomaterials to healthy skin poses a risk for disruption of immune homeostasis, because most nanomaterials cannot penetrate healthy skin. On the other hand, there is an urgent need to identify the potential of nanomaterials to cause sensitization either directly or *via* co-exposure with substances in people with allergic diseases and damaged skin. In this regard, there are many unresolved problems.

Recently, new information surfaced regarding the relationship between commensal bacteria and the host's immune system: the commensal bacteria on the skin may in fact influence the host's immune system (117, 118). For example, microbial diversity on skin is known to be markedly reduced in patients with atopic dermatitis, and treatment could restore this diversity (119). Therefore, we may need to consider both the direct effects of nanomaterials on the microbiota on skin and the indirect effects of nanomaterials on host immune systems *via* changes in the diversity and composition of the microbiota on skin. In addition, most bacteria have pathogen-associated molecular patterns (PAMPs), which are ligands of pattern recognition receptors, such as Toll-like receptors, Nod-like receptors, RIG-I-like receptors, and C-type lectin receptors (120). PAMPs could induce innate immunity, mediated by macrophages and dendritic cells, and activate innate immunity, such as the production of cytokines and chemokines, to induce effective adaptive immunity. Therefore, we need in-depth studies of the co-exposure effects of PAMPs and nanomaterials, in addition to the effects of DAMPs.

A range of toxicological studies have been conducted assessing various physicochemical characteristics of nanomaterials, such as particle size, surface charge, surface hydrophobicity, particle shape, and states of agglomeration and aggregation. However, the results have been inconsistent to date and definitive rules cannot yet be established. Systematic information about the relationships

among the physicochemical properties and biological effects of nanomaterials is still lacking.

Recent studies have revealed that particle-induced immune responses are involved in pathological processes of chronic inflammation such as allergy. It is not too much to say that the skin is the immune sentinel of our tissues. However, the underlying mechanisms of the effects of nanomaterials are not fully understood. To establish rules governing the contributions of nanomaterials to allergic responses, we need more information,

including an understanding of the molecular mechanisms of action of nanomaterials. These future studies could promote ways for us to live in harmony with nanomaterials. Furthermore, such studies would provide useful information to improve the safety and efficacy of nanomaterials used in skincare.

## AUTHOR CONTRIBUTIONS

YY, EK, TH, YT, and KI wrote the article and prepared the figures.

## REFERENCES

1. Auffan M, Rose J, Bottero JY, Lowry GV, Jolivet JP, Wiesner MR. Towards a definition of inorganic nanoparticles from an environmental, health and safety perspective. *Nat Nanotechnol* (2009) 4(10):634–41. doi:10.1038/nano.2009.242
2. Cheng Z, Al Zaki A, Hui JZ, Muzykantov VR, Tsurkcas A. Multifunctional nanoparticles: cost versus benefit of adding targeting and imaging capabilities. *Science* (2012) 338(6109):903–10. doi:10.1126/science.1226338
3. Bowman DM, van Calster G, Friedrichs S. Nanomaterials and regulation of cosmetics. *Nat Nanotechnol* (2010) 5(2):92. doi:10.1038/nano.2010.12
4. Fruijtier-Polloth C. The safety of nanostructured synthetic amorphous silica (SAS) as a food additive (E 551). *Arch Toxicol* (2016) 90(12):2885–916. doi:10.1007/s00204-016-1850-4
5. Xia T, Li N, Nel AE. Potential health impact of nanoparticles. *Annu Rev Public Health* (2009) 30:137–50. doi:10.1146/annurev.publhealth.031308.100155
6. Kunzmann A, Andersson B, Thurnherr T, Krug H, Scheynius A, Fadeel B. Toxicology of engineered nanomaterials: focus on biocompatibility, biodistribution and biodegradation. *Biochim Biophys Acta* (2011) 1810(3):361–73. doi:10.1016/j.bbagen.2010.04.007
7. Yamashita K, Yoshioka Y, Higashisaka K, Mimura K, Morishita Y, Nozaki M, et al. Silica and titanium dioxide nanoparticles cause pregnancy complications in mice. *Nat Nanotechnol* (2011) 6(5):321–8. doi:10.1038/nano.2011.41
8. Song Y, Li X, Du X. Exposure to nanoparticles is related to pleural effusion, pulmonary fibrosis and granuloma. *Eur Respir J* (2009) 34(3):559–67. doi:10.1183/09031936.00178308
9. Liao HY, Chung YT, Lai CH, Lin MH, Liou SH. Sneezing and allergic dermatitis were increased in engineered nanomaterial handling workers. *Ind Health* (2014) 52(3):199–215. doi:10.2486/indhealth.2013-0100
10. Wu WT, Liao HY, Chung YT, Li WF, Tsou TC, Li LA, et al. Effect of nanoparticles exposure on fractional exhaled nitric oxide (FENO) in workers exposed to nanomaterials. *Int J Mol Sci* (2014) 15(1):878–94. doi:10.3390/ijms15010878
11. Dobrovolskaia MA, McNeil SE. Immunological properties of engineered nanomaterials. *Nat Nanotechnol* (2007) 2(8):469–78. doi:10.1038/nano.2007.223
12. Shannahan JH, Brown JM. Engineered nanomaterial exposure and the risk of allergic disease. *Curr Opin Allergy Clin Immunol* (2014) 14(2):95–9. doi:10.1097/ACI.0000000000000031
13. Farrera C, Fadeel B. It takes two to tango: understanding the interactions between engineered nanomaterials and the immune system. *Eur J Pharm Biopharm* (2015) 95(Pt A):3–12. doi:10.1016/j.ejpb.2015.03.007
14. Wang SQ, Tooley IR. Photoprotection in the era of nanotechnology. *Semin Cutan Med Surg* (2011) 30(4):210–3. doi:10.1016/j.sder.2011.07.006
15. Nafsi S, Schafer-Korting M, Maibach HI. Perspectives on percutaneous penetration: silica nanoparticles. *Nanotoxicology* (2015) 9(5):643–57. doi:10.3109/17435390.2014.958115
16. Schluesener JK, Schluesener HJ. Nanosilver: application and novel aspects of toxicology. *Arch Toxicol* (2013) 87(4):569–76. doi:10.1007/s00204-012-1007-z
17. Krpetic Z, Anguissola S, Garry D, Kelly PM, Dawson KA. Nanomaterials: impact on cells and cell organelles. *Adv Exp Med Biol* (2014) 811:135–56. doi:10.1007/978-94-017-8739-0\_8
18. Valenta R, Hochwallner H, Linhart B, Pahr S. Food allergies: the basics. *Gastroenterology* (2015) 148(6):1120e–31e. doi:10.1053/j.gastro.2015.02.006
19. Yu W, Freeland DM, Nadeau KC. Food allergy: immune mechanisms, diagnosis and immunotherapy. *Nat Rev Immunol* (2016) 16(12):751–65. doi:10.1038/nri.2016.111
20. Tordesillas L, Goswami R, Benede S, Grishina G, Dunkin D, Jarvinen KM, et al. Skin exposure promotes a Th2-dependent sensitization to peanut allergens. *J Clin Invest* (2014) 124(11):4965–75. doi:10.1172/JCI75660
21. Noti M, Kim BS, Siracusa MC, Rak GD, Kubo M, Moghaddam AE, et al. Exposure to food allergens through inflamed skin promotes intestinal food allergy through the thymic stromal lymphopoietin-basophil axis. *J Allergy Clin Immunol* (2014) 133(5):e1–6. doi:10.1016/j.jaci.2014.01.021
22. Oyoshi MK, Oettgen HC, Chatila TA, Geha RS, Bryce PJ. Food allergy: insights into etiology, prevention, and treatment provided by murine models. *J Allergy Clin Immunol* (2014) 133(2):309–17. doi:10.1016/j.jaci.2013.12.1045
23. Lauriere M, Pecquet C, Bouchez-Mahiout I, Snegaroff J, Bayrou O, Raison-Peyron N, et al. Hydrolysed wheat proteins present in cosmetics can induce immediate hypersensitivities. *Contact Dermatitis* (2006) 54(5):283–9. doi:10.1111/j.0105-1873.2006.00830.x
24. Nakamura M, Yagami A, Hara K, Sano-Nagai A, Kobayashi T, Matsunaga K. Evaluation of the cross-reactivity of antigens in Glupearl 19S and other hydrolysed wheat proteins in cosmetics. *Contact Dermatitis* (2016) 74(6):346–52. doi:10.1111/cod.12551
25. Jatana S, DeLouise LA. Understanding engineered nanomaterial skin interactions and the modulatory effects of ultraviolet radiation skin exposure. *Wiley Interdiscip Rev Nanomed Nanobiotechnol* (2014) 6(1):61–79. doi:10.1002/wnnan.1244
26. Brandner JM, Zorn-Kruppa M, Yoshida T, Moll I, Beck LA, De Benedetto A. Epidermal tight junctions in health and disease. *Tissue Barriers* (2015) 3(1–2):e974451. doi:10.4161/21688370.2014.974451
27. Bos JD, Meinardi MM. The 500 Dalton rule for the skin penetration of chemical compounds and drugs. *Exp Dermatol* (2000) 9(3):165–9. doi:10.1034/j.1600-0625.2000.009003165.x
28. Chourasia R, Jain SK. Drug targeting through pilosebaceous route. *Curr Drug Targets* (2009) 10(10):950–67. doi:10.2174/138945009789577918
29. Nagao K, Kobayashi T, Moro K, Ohyama M, Adachi T, Kitashima DY, et al. Stress-induced production of chemokines by hair follicles regulates the trafficking of dendritic cells in skin. *Nat Immunol* (2012) 13(8):744–52. doi:10.1038/ni.2353
30. Honda T, Egawa G, Grabbe S, Kabashima K. Update of immune events in the murine contact hypersensitivity model: toward the understanding of allergic contact dermatitis. *J Invest Dermatol* (2013) 133(2):303–15. doi:10.1038/jid.2012.284
31. Kubo A, Nagao K, Yokouchi M, Sasaki H, Amagai M. External antigen uptake by Langerhans cells with reorganization of epidermal tight junction barriers. *J Exp Med* (2009) 206(13):2937–46. doi:10.1084/jem.20091527
32. Yoshida K, Kubo A, Fujita H, Yokouchi M, Ishii K, Kawasaki H, et al. Distinct behavior of human langerhans cells and inflammatory dendritic epidermal cells at tight junctions in patients with atopic dermatitis. *J Allergy Clin Immunol* (2014) 134(4):856–64. doi:10.1016/j.jaci.2014.08.001
33. Cross SE, Innes B, Roberts MS, Tsuzuki T, Robertson TA, McCormick P. Human skin penetration of sunscreen nanoparticles: in-vitro assessment of a novel micronized zinc oxide formulation. *Skin Pharmacol Physiol* (2007) 20(3):148–54. doi:10.1159/000098701

34. Larese FF, D'Agostin F, Crosera M, Adami G, Renzi N, Bovenzi M, et al. Human skin penetration of silver nanoparticles through intact and damaged skin. *Toxicology* (2009) 255(1–2):33–7. doi:10.1016/j.tox.2008.09.025
35. Lin LL, Grice JE, Butler MK, Zvyagin AV, Becker W, Robertson TA, et al. Time-correlated single photon counting for simultaneous monitoring of zinc oxide nanoparticles and NAD(P)H in intact and barrier-disrupted volunteer skin. *Pharm Res* (2011) 28(11):2920–30. doi:10.1007/s11095-011-0515-5
36. Gulson B, McCall M, Korsch M, Gomez L, Casey P, Oytam Y, et al. Small amounts of zinc from zinc oxide particles in sunscreens applied outdoors are absorbed through human skin. *Toxicol Sci* (2010) 118(1):140–9. doi:10.1093/toxsci/kfq243
37. Gulson B, Wong H, Korsch M, Gomez L, Casey P, McCall M, et al. Comparison of dermal absorption of zinc from different sunscreen formulations and differing UV exposure based on stable isotope tracing. *Sci Total Environ* (2012) 420:313–8. doi:10.1016/j.scitotenv.2011.12.046
38. Ilves M, Palomaki J, Vippola M, Lehto M, Savolainen K, Savinko T, et al. Topically applied ZnO nanoparticles suppress allergen induced skin inflammation but induce vigorous IgE production in the atopic dermatitis mouse model. *Part Fibre Toxicol* (2014) 11:38. doi:10.1186/s12989-014-0038-4
39. Vogt A, Combadiere B, Hadam S, Stieler KM, Lademann J, Schaefer H, et al. 40 nm, but not 750 or 1,500 nm, nanoparticles enter epidermal CD1a+ cells after transcutaneous application on human skin. *J Invest Dermatol* (2006) 126(6):1316–22. doi:10.1038/sj.jid.5700226
40. Rancan F, Gao Q, Graf C, Troppens S, Hadam S, Hackbart S, et al. Skin penetration and cellular uptake of amorphous silica nanoparticles with variable size, surface functionalization, and colloidal stability. *ACS Nano* (2012) 6(8):6829–42. doi:10.1021/nn301622h
41. Mortensen LJ, Oberdorster G, Pentland AP, Delouise LA. In vivo skin penetration of quantum dot nanoparticles in the murine model: the effect of UVR. *Nano Lett* (2008) 8(9):2779–87. doi:10.1021/nl801323y
42. Patzelt A, Lademann J. Drug delivery to hair follicles. *Expert Opin Drug Deliv* (2013) 10(6):787–97. doi:10.1517/17425247.2013.776038
43. Papakostas D, Rancan F, Sterry W, Blume-Peytavi U, Vogt A. Nanoparticles in dermatology. *Arch Dermatol Res* (2011) 303(8):533–50. doi:10.1007/s00403-011-1163-7
44. Alvarez-Roman R, Naik A, Kalia YN, Guy RH, Fessi H. Skin penetration and distribution of polymeric nanoparticles. *J Control Release* (2004) 99(1):53–62. doi:10.1016/j.jconrel.2004.06.015
45. Patzelt A, Richter H, Knorr F, Schafer U, Lehr CM, Dahne L, et al. Selective follicular targeting by modification of the particle sizes. *J Control Release* (2011) 150(1):45–8. doi:10.1016/j.jconrel.2010.11.015
46. Lalko JF, Kimber I, Dearman RJ, Gerberick GF, Sarlo K, Api AM. Chemical reactivity measurements: potential for characterization of respiratory chemical allergens. *Toxicol In Vitro* (2011) 25(2):433–45. doi:10.1016/j.tiv.2010.11.007
47. van Loveren H, Cockshott A, Gebel T, Gundert-Remy U, de Jong WH, Matheson J, et al. Skin sensitization in chemical risk assessment: report of a WHO/IPCS international workshop focusing on dose-response assessment. *Regul Toxicol Pharmacol* (2008) 50(2):155–99. doi:10.1016/j.yrtph.2007.11.008
48. Park YH, Jeong SH, Yi SM, Choi BH, Kim YR, Kim IK, et al. Analysis for the potential of polystyrene and TiO<sub>2</sub> nanoparticles to induce skin irritation, phototoxicity, and sensitization. *Toxicol In Vitro* (2011) 25(8):1863–9. doi:10.1016/j.tiv.2011.05.022
49. Lee S, Yun HS, Kim SH. The comparative effects of mesoporous silica nanoparticles and colloidal silica on inflammation and apoptosis. *Biomaterials* (2011) 32(35):9434–43. doi:10.1016/j.biomaterials.2011.08.042
50. Mann E, Ranft U, Eberwein G, Gladtko D, Sugiri D, Behrendt H, et al. Does airborne nickel exposure induce nickel sensitization? *Contact Dermatitis* (2010) 62(6):355–62. doi:10.1111/j.1600-0536.2010.01725.x
51. Otani S, Onishi K, Mu H, Yokoyama Y, Hosoda T, Okamoto M, et al. The relationship between skin symptoms and allergic reactions to Asian dust. *Int J Environ Res Public Health* (2012) 9(12):4606–14. doi:10.3390/ijerph9124606
52. Swinnen I, Goossens A. An update on airborne contact dermatitis: 2007–2011. *Contact Dermatitis* (2013) 68(4):232–8. doi:10.1111/cod.12022
53. Thyssen JP, Linneberg A, Menne T, Johansen JD. The epidemiology of contact allergy in the general population – prevalence and main findings. *Contact Dermatitis* (2007) 57(5):287–99. doi:10.1111/j.1600-0536.2007.01220.x
54. Thyssen JP, Menne T. Metal allergy – a review on exposures, penetration, genetics, prevalence, and clinical implications. *Chem Res Toxicol* (2010) 23(2):309–18. doi:10.1021/tx9002726
55. Kimber I, Bentley AN, Hilton J. Contact sensitization of mice to nickel sulphate and potassium dichromate. *Contact Dermatitis* (1990) 23(5):325–30.
56. Vreeburg KJ, de Groot K, van Hoogstraten IM, von Blomberg BM, Scheper RJ. Successful induction of allergic contact dermatitis to mercury and chromium in mice. *Int Arch Allergy Appl Immunol* (1991) 96(2):179–83.
57. Artik S, von VulTEE C, Gleichmann E, Schwarz T, Griem P. Nickel allergy in mice: enhanced sensitization capacity of nickel at higher oxidation states. *J Immunol* (1999) 163(3):1143–52.
58. Sato N, Kinbara M, Kuroishi T, Kimura K, Iwakura Y, Ohtsu H, et al. Lipopolysaccharide promotes and augments metal allergies in mice, dependent on innate immunity and histidine decarboxylase. *Clin Exp Allergy* (2007) 37(5):743–51. doi:10.1111/j.1365-2222.2007.02705.x
59. Johansen P, Wackerle-Men Y, Senti G, Kundig TM. Nickel sensitisation in mice: a critical appraisal. *J Dermatol Sci* (2010) 58(3):186–92. doi:10.1016/j.jdermsci.2010.03.011
60. Wiesner MR, Lowry GV, Casman E, Bertsch PM, Matson CW, Di Giulio RT, et al. Meditations on the ubiquity and mutability of nano-sized materials in the environment. *ACS Nano* (2011) 5(11):8466–70. doi:10.1021/nn204118p
61. Glover RD, Miller JM, Hutchison JE. Generation of metal nanoparticles from silver and copper objects: nanoparticle dynamics on surfaces and potential sources of nanoparticles in the environment. *ACS Nano* (2011) 5(11):8950–7. doi:10.1021/nn2031319
62. Yin Y, Liu J, Jiang G. Sunlight-induced reduction of ionic Ag and Au to metallic nanoparticles by dissolved organic matter. *ACS Nano* (2012) 6(9):7910–9. doi:10.1021/nn302293r
63. Hirai T, Yoshioka Y, Izumi N, Ichihashi K, Handa T, Nishijima N, et al. Metal nanoparticles in the presence of lipopolysaccharides trigger the onset of metal allergy in mice. *Nat Nanotechnol* (2016) 11(9):808–16. doi:10.1038/nano.2016.88
64. Hussain S, Smulders S, De Vooght V, Ectors B, Boland S, Marano F, et al. Nano-titanium dioxide modulates the dermal sensitization potency of DNCB. *Part Fibre Toxicol* (2012) 9:15. doi:10.1186/1743-8977-9-15
65. Smulders S, Golanski L, Smulders E, Vanhoirbeek J, Hoet PH. Nano-TiO<sub>2</sub> modulates the dermal sensitization potency of dinitrochlorobenzene after topical exposure. *Br J Dermatol* (2015) 172(2):392–9. doi:10.1111/bjd.13295
66. Williams H, Flohr C. How epidemiology has challenged 3 prevailing concepts about atopic dermatitis. *J Allergy Clin Immunol* (2006) 118(1):209–13. doi:10.1016/j.jaci.2006.04.043
67. Bieber T. Atopic dermatitis. *Ann Dermatol* (2010) 22(2):125–37. doi:10.5021/ad.2010.22.2.125
68. Plotz SG, Ring J. What's new in atopic eczema? *Expert Opin Emerg Drugs* (2010) 15(2):249–67. doi:10.1517/14728211003792518
69. Yanagisawa R, Takano H, Inoue K, Koike E, Kamachi T, Sadakane K, et al. Titanium dioxide nanoparticles aggravate atopic dermatitis-like skin lesions in NC/Nga mice. *Exp Biol Med (Maywood)* (2009) 234(3):314–22. doi:10.3181/0810-RM-304
70. Yanagisawa R, Takano H, Inoue KI, Koike E, Sadakane K, Ichinose T. Size effects of polystyrene nanoparticles on atopic dermatitis like skin lesions in NC/NGA mice. *Int J Immunopathol Pharmacol* (2010) 23(1):131–41. doi:10.1177/039463201002300112
71. Hirai T, Yoshikawa T, Nabeshi H, Yoshida T, Tochigi S, Ichihashi K, et al. Amorphous silica nanoparticles size-dependently aggravate atopic dermatitis-like skin lesions following an intradermal injection. *Part Fibre Toxicol* (2012) 9:3. doi:10.1186/1743-8977-9-3
72. Hirai T, Yoshioka Y, Takahashi H, Ichihashi K, Ueda A, Mori T, et al. Cutaneous exposure to agglomerates of silica nanoparticles and allergen results in IgE-biased immune response and increased sensitivity to anaphylaxis in mice. *Part Fibre Toxicol* (2015) 12:16. doi:10.1186/s12989-015-0095-3
73. Moyer TJ, Zmolek AC, Irvine DJ. Beyond antigens and adjuvants: formulating future vaccines. *J Clin Invest* (2016) 126(3):799–808. doi:10.1172/JCI81083

74. Winter M, Beer HD, Hornung V, Kramer U, Schins RP, Forster I. Activation of the inflammasome by amorphous silica and TiO<sub>2</sub> nanoparticles in murine dendritic cells. *Nanotoxicology* (2011) 5(3):326–40. doi:10.3109/17435390.2010.506957
75. Adachi T, Kobayashi T, Sugihara E, Yamada T, Ikuta K, Pittaluga S, et al. Hair follicle-derived IL-7 and IL-15 mediate skin-resident memory T cell homeostasis and lymphoma. *Nat Med* (2015) 21(11):1272–9. doi:10.1038/nm.3962
76. Larsen ST, Roursgaard M, Jensen KA, Nielsen GD. Nano titanium dioxide particles promote allergic sensitization and lung inflammation in mice. *Basic Clin Pharmacol Toxicol* (2010) 106(2):114–7. doi:10.1111/j.1742-7843.2009.00473.x
77. Hirai T, Yoshioka Y, Takahashi H, Handa T, Izumi N, Mori T, et al. High-dose cutaneous exposure to mite allergen induces IgG-mediated protection against anaphylaxis. *Clin Exp Allergy* (2016) 46(7):992–1003. doi:10.1111/cea.12722
78. Tenzer S, Docter D, Kuharev J, Musyanovich A, Fetz V, Hecht R, et al. Rapid formation of plasma protein corona critically affects nanoparticle pathophysiology. *Nat Nanotechnol* (2013) 8(10):772–81. doi:10.1038/nnano.2013.181
79. Lesniak A, Fenaroli F, Monopoli MP, Aberg C, Dawson KA, Salvati A. Effects of the presence or absence of a protein corona on silica nanoparticle uptake and impact on cells. *ACS Nano* (2012) 6(7):5845–57. doi:10.1021/nn300223w
80. Deng ZJ, Liang M, Monteiro M, Toth I, Minchin RF. Nanoparticle-induced unfolding of fibrinogen promotes Mac-1 receptor activation and inflammation. *Nat Nanotechnol* (2011) 6(1):39–44. doi:10.1038/nnano.2010.250
81. Vonarbourg A, Passirani C, Saulnier P, Simard P, Leroux JC, Benoit JP. Evaluation of pegylated lipid nanocapsules versus complement system activation and macrophage uptake. *J Biomed Mater Res A* (2006) 78(3):620–8. doi:10.1002/jbm.a.30711
82. Vonarbourg A, Passirani C, Saulnier P, Benoit JP. Parameters influencing the stealthiness of colloidal drug delivery systems. *Biomaterials* (2006) 27(24):4356–73. doi:10.1016/j.biomaterials.2006.03.039
83. Yoshida T, Yoshioka Y, Tochigi S, Hirai T, Uji M, Ichihashi K, et al. Intranasal exposure to amorphous nanosilica particles could activate intrinsic coagulation cascade and platelets in mice. *Part Fibre Toxicol* (2013) 10:41. doi:10.1186/1743-8977-10-41
84. Yoshida T, Yoshioka Y, Morishita Y, Aoyama M, Tochigi S, Hirai T, et al. Protein corona changes mediated by surface modification of amorphous silica nanoparticles suppress acute toxicity and activation of intrinsic coagulation cascade in mice. *Nanotechnology* (2015) 26(24):245101. doi:10.1088/0957-4484/26/24/245101
85. Reddy ST, van der Vlies AJ, Simeoni E, Angeli V, Randolph GJ, O’Neil CP, et al. Exploiting lymphatic transport and complement activation in nanoparticle vaccines. *Nat Biotechnol* (2007) 25(10):1159–64. doi:10.1038/nbt1332
86. Thomas SN, van der Vlies AJ, O’Neil CP, Reddy ST, Yu SS, Giorgio TD, et al. Engineering complement activation on polypropylene sulfide vaccine nanoparticles. *Biomaterials* (2011) 32(8):2194–203. doi:10.1016/j.biomaterials.2010.11.037
87. Tenzer S, Docter D, Rosfa S, Włodarski A, Kuharev J, Rekik A, et al. Nanoparticle size is a critical physicochemical determinant of the human blood plasma corona: a comprehensive quantitative proteomic analysis. *ACS Nano* (2011) 5(9):7155–67. doi:10.1021/nn201950e
88. Heyman SN, Brezis M, Epstein FH, Spokes K, Silva P, Rosen S. Early renal medullary hypoxic injury from radiocontrast and indomethacin. *Kidney Int* (1991) 40(4):632–42.
89. Coban C, Igari Y, Yagi M, Reimer T, Koyama S, Aoshi T, et al. Immunogenicity of whole-parasite vaccines against *Plasmodium falciparum* involves malarial hemozoin and host TLR9. *Cell Host Microbe* (2010) 7(1):50–61. doi:10.1016/j.chom.2009.12.003
90. Kool M, Willart MA, van Nimwegen M, Bergen I, Pouliot P, Virchow JC, et al. An unexpected role for uric acid as an inducer of T helper 2 cell immunity to inhaled antigens and inflammatory mediator of allergic asthma. *Immunity* (2011) 34(4):527–40. doi:10.1016/j.jimmuni.2011.03.015
91. Kuroda E, Coban C, Ishii KJ. Particulate adjuvant and innate immunity: past achievements, present findings, and future prospects. *Int Rev Immunol* (2013) 32(2):209–20. doi:10.3109/08830185.2013.773326
92. Glenny AT, Pope CG, Waddington H, Wallace U. Immunological notes XVII.–XXIV. *J Pathol Bacteriol* (1926) 29:31–40.
93. Baylor NW, Egan W, Richman P. Aluminum salts in vaccines – US perspective. *Vaccine* (2002) 20(Suppl 3):S18–23. doi:10.1016/S0264-410X(02)00166-4
94. al-Shakhshir R, Regnier F, White JL, Hem SL. Effect of protein adsorption on the surface charge characteristics of aluminium-containing adjuvants. *Vaccine* (1994) 12(5):472–4.
95. Matheis W, Zott A, Schwanig M. The role of the adsorption process for production and control combined adsorbed vaccines. *Vaccine* (2001) 20(1–2):67–73. doi:10.1016/S0264-410X(01)00317-6
96. Hutchison S, Benson RA, Gibson VB, Pollock AH, Garside P, Brewer JM. Antigen depot is not required for alum adjuvanticity. *FASEB J* (2012) 26(3):1272–9. doi:10.1096/fj.11-184556
97. Shi Y, HogenEsch H, Hem SL. Change in the degree of adsorption of proteins by aluminum-containing adjuvants following exposure to interstitial fluid: freshly prepared and aged model vaccines. *Vaccine* (2001) 20(1–2):80–5. doi:10.1016/S0264-410X(01)00313-9
98. Weissburg RP, Berman PW, Cleland JL, Eastman D, Farina F, Frie S, et al. Characterization of the MN gp120 HIV-1 vaccine: antigen binding to alum. *Pharm Res* (1995) 12(10):1439–46.
99. Martinon F, Petrilli V, Mayor A, Tardivel A, Tschopp J. Gout-associated uric acid crystals activate the NALP3 inflammasome. *Nature* (2006) 440(7081):237–41. doi:10.1038/nature04516
100. Hornung V, Bauernfeind F, Halle A, Samstad EO, Kono H, Rock KL, et al. Silica crystals and aluminum salts activate the NALP3 inflammasome through phagosomal destabilization. *Nat Immunol* (2008) 9(8):847–56. doi:10.1038/ni.1631
101. Eisenbarth SC, Colegio OR, O’Connor W, Sutterwala FS, Flavell RA. Crucial role for the Nalp3 inflammasome in the immunostimulatory properties of aluminium adjuvants. *Nature* (2008) 453(7198):1122–6. doi:10.1038/nature06939
102. Li H, Willingham SB, Ting JP, Re F. Cutting edge: inflammasome activation by alum and alum’s adjuvant effect are mediated by NLRP3. *J Immunol* (2008) 181(1):17–21. doi:10.4049/jimmunol.181.1.17
103. Franchi L, Nunez G. The Nlrp3 inflammasome is critical for aluminium hydroxide-mediated IL-1beta secretion but dispensable for adjuvant activity. *Eur J Immunol* (2008) 38(8):2085–9. doi:10.1002/eji.200838549
104. McKee AS, Munks MW, MacLeod MK, Fleenor CJ, Van Rooijen N, Kappler JW, et al. Alum induces innate immune responses through macrophage and mast cell sensors, but these sensors are not required for alum to act as an adjuvant for specific immunity. *J Immunol* (2009) 183(7):4403–14. doi:10.4049/jimmunol.0900164
105. Rabolli V, Lison D, Huaux F. The complex cascade of cellular events governing inflammasome activation and IL-1beta processing in response to inhaled particles. *Part Fibre Toxicol* (2016) 13(1):40. doi:10.1186/s12989-016-0150-8
106. Simard JC, Vallieres F, de Liz R, Lavastre V, Girard D. Silver nanoparticles induce degradation of the endoplasmic reticulum stress sensor activating transcription factor-6 leading to activation of the NLRP-3 inflammasome. *J Biol Chem* (2015) 290(9):5926–39. doi:10.1074/jbc.M114.610899
107. Sun B, Wang X, Ji Z, Wang M, Liao YP, Chang CH, et al. NADPH oxidase-dependent NLRP3 inflammasome activation and its important role in lung fibrosis by multiwalled carbon nanotubes. *Small* (2015) 11(17):2087–97. doi:10.1002/smll.201402859
108. Kuroda E, Ishii KJ, Uematsu S, Ohata K, Coban C, Akira S, et al. Silica crystals and aluminum salts regulate the production of prostaglandin in macrophages via NALP3 inflammasome-independent mechanisms. *Immunity* (2011) 34(4):514–26. doi:10.1016/j.immuni.2011.03.019
109. Marichal T, Ohata K, Bedoret D, Mesnil C, Sabaté C, Kobiyama K, et al. DNA released from dying host cells mediates aluminum adjuvant activity. *Nat Med* (2011) 17(8):996–1002. doi:10.1038/nm.2403
110. Miki H, Nakashashi-Oda C, Sumida T, Shibuya A. Involvement of CD300a phosphatidylserine immunoreceptor in aluminum salt adjuvant-induced

- Th2 responses. *J Immunol* (2015) 194(11):5069–76. doi:10.4049/jimmunol.1402915
111. Rabolli V, Badissi AA, Devosse R, Uwambayinema F, Yakoub Y, Palmai-Pallag M, et al. The alarmin IL-1 $\alpha$  is a master cytokine in acute lung inflammation induced by silica micro- and nanoparticles. *Part Fibre Toxicol* (2014) 11:69. doi:10.1186/s12989-014-0069-x
112. Kuroda E, Ozasa K, Temizoz B, Ohata K, Koo CX, Kanuma T, et al. Inhaled fine particles induce alveolar macrophage death and interleukin-1 $\alpha$  release to promote inducible bronchus-associated lymphoid tissue formation. *Immunity* (2016) 45(6):1299–310. doi:10.1016/j.jimmuni.2016.11.010
113. Dagvadorj J, Shimada K, Chen S, Jones HD, Tumurkhui G, Zhang W, et al. Lipopolysaccharide induces alveolar macrophage necrosis via CD14 and the P2X7 receptor leading to interleukin-1 $\alpha$  release. *Immunity* (2015) 42(4):640–53. doi:10.1016/j.jimmuni.2015.03.007
114. Natsuaki Y, Egawa G, Nakamizo S, Ono S, Hanakawa S, Okada T, et al. Perivascular leukocyte clusters are essential for efficient activation of effector T cells in the skin. *Nat Immunol* (2014) 15(11):1064–9. doi:10.1038/ni.2992
115. Jiang W, Kim BY, Rutka JT, Chan WC. Nanoparticle-mediated cellular response is size-dependent. *Nat Nanotechnol* (2008) 3(3):145–50. doi:10.1038/nnano.2008.30
116. Lu F, Wu SH, Hung Y, Mou CY. Size effect on cell uptake in well-suspended, uniform mesoporous silica nanoparticles. *Small* (2009) 5(12):1408–13. doi:10.1002/smll.200900005
117. Wesemann DR, Nagler CR. The Microbiome, Timing, and Barrier Function in the Context of Allergic Disease. *Immunity* (2016) 44(4):728–38. doi:10.1016/j.jimmuni.2016.02.002
118. Nakamizo S, Egawa G, Honda T, Nakajima S, Belkaid Y, Kabashima K. Commensal bacteria and cutaneous immunity. *Semin Immunopathol* (2015) 37(1):73–80. doi:10.1007/s00281-014-0452-6
119. Kong HH, Oh J, Deming C, Conlan S, Grice EA, Beatson MA, et al. Temporal shifts in the skin microbiome associated with disease flares and treatment in children with atopic dermatitis. *Genome Res* (2012) 22(5):850–9. doi:10.1101/gr.131029.111
120. Kumar H, Kawai T, Akira S. Pathogen recognition by the innate immune system. *Int Rev Immunol* (2011) 30(1):16–34. doi:10.3109/08830185.2010.529976

**Conflict of Interest Statement:** YY is employed by The Research Foundation for Microbial Diseases of Osaka University. The other authors declare that the research was conducted in the absence of any commercial or financial relationships that could be construed as a potential conflict of interest.

Copyright © 2017 Yoshioka, Kuroda, Hirai, Tsutsumi and Ishii. This is an open-access article distributed under the terms of the Creative Commons Attribution License (CC BY). The use, distribution or reproduction in other forums is permitted, provided the original author(s) or licensor are credited and that the original publication in this journal is cited, in accordance with accepted academic practice. No use, distribution or reproduction is permitted which does not comply with these terms.



# Nanomaterials in the Context of Type 2 Immune Responses—Fears and Potentials

Martin Himly, Robert Mills-Goodlet, Mark Geppert and Albert Duschl\*

Division of Allergy and Immunology, Department of Molecular Biology, University of Salzburg, Salzburg, Austria

## OPEN ACCESS

### Edited by:

Lucio Roberto Cançado Castellano,  
Federal University of Paraíba,  
Brazil

### Reviewed by:

Krzysztof Guzik,  
Jagiellonian University, Poland  
Pasquale Maffia,  
University of Glasgow, UK  
Ilaria Puxeddu,  
University of Pisa, Italy  
Joelma Rodrigues Souza,  
Federal University of Paraíba, Brazil

### \*Correspondence:

Albert Duschl  
albert.duschl@sbg.ac.at

### Specialty section:

This article was submitted  
to Inflammation,  
a section of the journal  
*Frontiers in Immunology*

Received: 28 December 2016

Accepted: 05 April 2017

Published: 25 April 2017

### Citation:

Himly M, Mills-Goodlet R, Geppert M and Duschl A (2017) Nanomaterials in the Context of Type 2 Immune Responses—Fears and Potentials. *Front. Immunol.* 8:471.  
doi: 10.3389/fimmu.2017.00471

The type 2 immune response is an adaptive immune program involved in defense against parasites, detoxification, and wound healing, but is predominantly known for its pathophysiological effects, manifesting as allergic disease. Engineered nanoparticles (NPs) are non-self entities that, to our knowledge, do not stimulate detrimental type 2 responses directly, but have the potential to modulate ongoing reactions in various ways, including the delivery of substances aiming at providing a therapeutic benefit. We review, here, the state of knowledge concerning the interaction of NPs with type 2 immune responses and highlight their potential as a multifunctional platform for therapeutic intervention.

**Keywords:** allergy, immunomodulation, immunotherapy, nanomedicine, nanoparticles, parasite infection, vaccine, wound healing

## NANOMATERIALS AND TYPE 2 IMMUNE RESPONSES

Upon contact with non-self entities, the adaptive immune system decides between one of three response programs. The tolerance program, orchestrated by regulatory T cells ( $T_{reg}$ ), ensures that no defense is initiated against harmless agents. If pathogens are identified, the adaptive immunity chooses between two main types of defensive responses (1). The first branch, a type 1 response, is characterized by the rapid removal of pathogens by macrophages and neutrophils, mediated by T helper 1 ( $T_{H1}$ ) and  $T_{H17}$  cells, which release pro-inflammatory cytokines, such as interferon (IFN)- $\gamma$  and interleukin (IL)-12. Type 1 responses are integrated seamlessly with inflammatory reactions. The role of inflammation and type 1 responses in the context of exposure to nanoparticles (NPs) is discussed elsewhere in this volume.

The second defensive branch, type 2 immunity, involves the key cytokines IL-4, IL-5, IL-13, and different types of immune cells, such as basophils, eosinophils, mast cells, anti-inflammatory (M2) macrophages, and  $T_{H2}$  cells (1). This type of response is often connected to parasitic infections, later stages of the wound healing process, and to chronic inflammatory conditions, such as asthma and allergy (2). Of note, some NPs are known to modulate type 2 immune responses (3). This review covers applications of NPs in the context of type 2 immune responses, such as parasitic infections, wound healing, and allergy, with a special focus on therapeutic approaches.

## PARASITIC INFECTIONS

Ancestral populations can be assumed to have been constantly subjected to parasite infections. Hence, macroparasites have played a large role in the evolution of type 2 immune responses. One particular purpose of type 2 responses is to limit the parasite load and is done so, via immunoglobulin (Ig)E type antibodies and effector cells (4). Parasitic diseases continue to be a serious health problem in

large areas of the world (5). Unfortunately, there are currently no studies regarding coexposure to parasites and nanomaterials. However, nanomedical approaches have been investigated for vaccination, diagnosis, and therapy of parasitic diseases (6–8). Some studies have looked specifically at a shift between type 1 and type 2 responses, as indicated by characteristic cytokines and antibody isotypes. In particular, numerous nanomedical studies concerning malaria have been performed, including studies about the response type (7). For example, self-assembled protein NPs were used to vaccinate mice with *Plasmodium* sp. antigens, resulting in the development of protective type 2 responses (9).

In contrast, chondroitin nanocapsules upregulate T<sub>H</sub>1 cytokines and downregulate T<sub>H</sub>2 cytokines in hamsters, leading to enhanced doxorubicin-induced apoptosis that eradicates infection with *Leishmania donovani* (10). Similarly, the host response of mice against *L. donovani* was supported by artemisinin-loaded NPs that shifted the cytokine profile from type 2 to type 1 (11). This corresponds to the conventional view that *Leishmania*, like other microparasites, is promoted by type 2 responses and controlled by type 1 responses. However, it should be borne in mind that careful analysis of this mouse model has revealed that the prototypic T<sub>H</sub>2 cytokines IL-4 and IL-13 can contribute to either the control or the exacerbation of disease (12). It is, thus, not always clear which role type 2 responses play in relation to specific parasites. NP adjuvants contribute to effective vaccination of mice against *Angiostrongylus costaricensis* and of pigs against *Trichinella spiralis*, but they do this by supporting a type 1 response in the first case and a type 2 response in the second (13, 14). Altogether, it is clear that NPs can influence the type of immune response toward a challenge, with either detrimental or protective effects for the host.

## WOUND HEALING

Wound healing is a natural process that repairs and regenerates damaged tissues, for example, in the skin (15), lung (16), or intestine (17). Numerous therapies have been developed to accelerate this process, involving, for example, pharmaceutics, stem cells, electrical stimulation, negative pressure, light, or radiation (15, 18–21). Furthermore, NPs, especially those with antimicrobial properties, are considered as valuable tools in accelerating the wound-healing process (22). Silver (Ag) was used for its antibacterial properties since the Roman empire, and nowadays, numerous therapeutic products containing ionic Ag or Ag NPs are on the market (22, 23). Several publications review the beneficial effects of ionic nanoparticulate Ag in wound healing (22, 24, 25). An earlier animal study by Tian et al. (26) showed that Ag NPs accelerate healing and improve cosmetic appearance of wounds in a dose-dependent manner. By analyzing bacterial growth and cytokine profiles in wound sections, the authors demonstrated the antimicrobial and anti-inflammatory potential of Ag NPs. Microbially synthesized Ag NPs enhanced wound-healing efficacy in rats (11, 27, 28). Using a transforming growth factor (TGF)- $\beta$  receptor inhibitor, Li and coworkers proposed the activation of the TGF- $\beta$ 1/Smad signaling pathway as a mechanism of wound-healing enhancement by polyvinylalcohol/chitosan oligosaccharide Ag nanofibers (29).

Gold (Au) NPs were successful in acceleration of wound healing in combination with photobiomodulation therapy in rats (15) or in combination with the antioxidants epigallocatechin gallate (EGCG) and  $\alpha$ -lipoic acid (ALA) in mice (30). The observed decrease of CD68 expression and increase of SOD1 expression around the wound area suggest that anti-inflammatory as well as antioxidative effects of the Au NP/EGCG/ALA mixture play a role in increased wound-healing efficiency (30). The inflammatory reaction in wounded skin of rats was investigated in a recent report. Phytochemically stabilized Au NPs accelerate wound healing in a process that involves alteration of the amounts of TGF- $\beta$ 1, vascular endothelial growth factor (VEGF), and the number of mast cells in the wounded skin sections compared to vehicle controls (31, 32). These observations indicate an involvement of the particles in type 2 immune functions during the healing process. A different approach for wound healing with Au NPs in diabetic mice, showed that spherical nucleic acid–Au NP conjugates efficiently to downregulate target genes in diabetic mice. Thus, resulting in full wound closure occurring within 12 days, compared to control wounds which were only 50% closed (33).

Aside from Ag and Au, other types of NPs, such as selenium (34), zinc oxide (35), copper oxide (36, 37), iron oxide (38), or polymeric NPs (39), were shown to be beneficial for wound healing (**Table 1**). Thereby, the beneficial effect is either a result of the NPs properties alone (i.e., antibacterial effects) or a combined result of the NPs with other substances. For example, TiO<sub>2</sub> NPs have been shown to enhance the wound-healing potential of chitosan (40), which is used as wound dressing material (41) and is currently commercially available (42). Some caution may be necessary when using very high concentrations of chitosan leading to a highly positively charged NP surface, as recently demonstrated in a study involving Au NPs (43). Increased uptake by phagocytic cells and an enhanced pro-inflammatory response were determined, rendering chitosan coating exceeding an optimal range counteractive for wound healing. Chitosan-based copper nanocomposites accelerate wound healing in rats by modulation of different cytokines and growth factors. The upregulation of VEGF, TGF- $\beta$ 1, and IL-10 as well as the downregulation of tumor necrosis factor  $\alpha$  (TNF- $\alpha$ ) indicate a shift toward type 2 immunity. An interesting approach using biodegradable NPs was published by Galili (44), who demonstrated that  $\alpha$ -Gal NPs can accelerate the process of wound healing. The mechanism involves binding of natural anti- $\alpha$ -Gal antibodies to the multiple  $\alpha$ -Gal epitopes, which are present on the NPs resulting in complement activation, recruitment, and activation of macrophages, which leads to tissue regeneration (44, 45). A summary of current therapeutic approaches for NPs is given in **Table 1**.

## ALLERGY

Allergy and asthma represent a global public health concern in developed countries, with a steady increase also occurring in emerging countries. According to the World Health Organization, approximately 300 million people worldwide are currently suffering from asthma, with a rising trend to increase up to 400 million by 2025 (85). Allergic diseases include the various forms

**TABLE 1 | Selected therapeutic nanoparticle (NP)-based approaches in the context of type 2 immune responses at different stages of development.**

Nanomaterial type	Therapeutic benefits	Reference
<b>In clinical practice</b>		
<b>Inorganic NPs</b>		
Silver	Most widely used NPs in wound healing due to their antimicrobial and anti-inflammatory properties. Several products already on the market	(22–24, 26)
<b>Organic/biodegradable NPs</b>		
Glatiramer acetate	Prolonged onset and reduced transition from relapsing remitting to progressive multiple sclerosis	(46, 47)
Lipids	T cell inhibition and immunosuppression by encapsulating sirolimus into nanostructured lipid carriers	(48)
<b>In clinical studies</b>		
<b>Organic/biodegradable NPs</b>		
L-leucin-L-glutamate copolymers	Enhanced depot effect for insulin upon subcutaneous injection	(49)
Polyethylene glycol (PEG)	Anti-tumor necrosis factor $\alpha$ antibody fragment against rheumatoid arthritis and Crohn's disease	(50)
Calcium phosphate	Enhanced depot effects for various drugs	(51)
Poly-L-lysine dendrimer	Antimicrobial protection from genital herpes and HIV infection	(52)
Virus-like particles (VLPs)	VLPs derived from Qbeta bacteriophages filled with CpG-DNA and filled with house dust mite extract, respectively, conjugated with Der p 1 peptide	(53, 54)
<b>In development/basic research studies</b>		
<b>Inorganic NPs</b>		
Gold	Successful acceleration of wound healing in combination with photobiomodulation therapy, antioxidants, or nucleic acids	(15, 30–33, 55, 56)
	Phytochemically stabilized Au NPs accelerate wound healing altering the amounts of transforming growth factor $\beta$ , <i>Plasmodium falciparum</i> antigen Pf525 or <i>Yersinia pestis</i> F1	
Cerium oxide	Acceleration of the wound-healing process by enhancement of the proliferation and migration of fibroblasts, keratinocytes, and vascular endothelial cells	(57)
Selenium	Shortening of healing duration of artificial wounds in Wistar rats	(34)
Zinc oxide	Castor oil/chitosan-modified ZnO NPs increase wound-healing efficacy in rats	(35)
Copper oxide	Enhanced wound-healing activity of CuO NPs by inhibiting pathogenic bacteria surviving in the wound sites	(36, 37)
	Acceleration of wound healing by chitosan-based copper nanocomposites involves a type 2 shift of immune response	
Iron oxide	Thrombin-conjugated magnetic $\gamma$ -Fe <sub>2</sub> O <sub>3</sub> NPs enhance wound healing in rats	(38, 58)
	Reeducation of TAMs from M2 toward M1 phenotype by FDA-approved ferumoxytol	
Titanium dioxide	TiO <sub>2</sub> NPs enhance wound-healing potential of chitosan	(40)
Fullerene	Induction of dendritic cells (DCs) maturation and activation of T <sub>H</sub> 1 immune response using [Gd@C <sub>62</sub> (OH) <sub>22</sub> ] <sub>n</sub> fullerene NPs	(59)
Silica	Boost of vaccine immune response against influenza virus	(60, 61)
	Lysozyme-loaded mesoporous silica NPs (nanopollens) with long-term antibacterial effects tested in ex vivo small intestine models	
Carbon nanotubes (CNTs)	<i>Plasmodium vivax</i> AMA-1 N-terminus peptide–CNT conjugate delayed parasitemia in infected <i>Plasmodium berghei</i> mouse model	(62)
<b>Organic/biodegradable NPs</b>		
Chondroitin	Doxorubicin-loaded chondroitin nanocapsules eradicate infection with <i>Leishmania donovani</i> in hamsters	(10)
Polyglutamic acid (PGA)	Timothy grass pollen extract-loaded PGA NPs as delivery vehicle to DCs	(63)
Poly-D,L-lactic-co-glycolic acid (PLGA)	Inhibition of T <sub>H</sub> 2 immune response and airway inflammation in mice	(11, 64–71, 72)
	Treatment for autoimmune disease by induction of antigen-specific tolerance using myelin bound to NPs	
	Reprogramming of TAMs by rabies virus glycoprotein peptide-loaded paclitaxel-carrying NPs in a mouse glioma model	
	CpG/peanut extract-PLGA enhance peanut-specific immunotherapy	
	Bet v 1-loaded PLGA NPs improve efficacy of allergen-specific immunotherapy (AIT) by downregulating ongoing T <sub>H</sub> 2 response in mouse models	
	Ole e 1-loaded PLGA (<2 $\mu$ m) microparticles as vehicle for AIT	
	Oral administration of major <i>Chenopodium album</i> pollen allergen Che a 3-PLGA downregulates T <sub>H</sub> 2 response in mouse model	
	Artemisinin-loaded PLGA NPs showed superior antileishmanial efficacy compared to free artemisinin in a mouse model and shifted cytokine profile from type 2 to type 1	
	Successful M cell targeting with birch pollen allergen-loaded PLGA NPs specifically functionalized with <i>Aleuria aurantia</i> lectin	
Polymethylvinyl ether-co-maleic anhydride (PVM-MA)	Ryegrass pollen extract-loaded PVM-MA NPs as adjuvant for AIT	(73)

(Continued)

**TABLE 1 | Continued**

Nanomaterial type	Therapeutic benefits	Reference
PEG	Self-assembled PEG-dendrimer efficiently delivered and increase anti-inflammatory effect of dexamethasone in allergic airways inflammation	(74, 75)
Chitosan	pH-sensitive PEG nanocarriers for grass pollen and house dust mite allergen encapsulation and controlled release from DCs Local nasal AIT with house dust mite-chitosan vaccine in mouse asthma model Intranasal AIT with immunodominant Der p 1 epitope reduced allergen-specific T cell reactivity and interleukin (IL)4 and IL5 levels in bronchoalveolar fluid of sensitized mice Oral DNA vaccine of house dust mite allergen Der p 1 formulated with chitosan NPs Induction of $T_{H}1$ immune response by DNA vaccine of Der p 2 with chitosan NPs Oral gene delivery of chitosan-formulated NPs in peanut-allergic mouse model with additional induction of mucosal dimeric allergen-specific immunoglobulin A	(76–80)
Polyanhydride NPs	Intradermal immunization of mice with polyanhydride NPs loaded with peanut proteins induced strong mixed $T_{H}1/T_{H}2$ immune response (immunostimulant)	(81)
Polyacrylic acid	Antibacterial activity of poly-phosphoester-based Ag-loaded NPs in lung infections	(82)
Protamine NPs	Liposome-protamine-DNA NPs induced strong $T_{H}1$ response upon subcutaneous AIT in <i>Chenopodium album</i> -sensitized mouse model	(83, 84)
Self-assembled protein NPs (SAPN)	Protamine-based NPs (proticles) with CpG complexed with Ara h 2 extracted from raw peanuts induced strong $T_{H}1$ response upon subcutaneous AIT in mice	(9)
Immunostimulatory complexes (ISCOMs)	Effective intranasal immunization of mice against <i>Angiostrongylus costaricensis</i> with ISCOM formed by a synthetic ppf 1 peptide linked to cholera toxin adjuvanted with saponin/phospholipids/cholesterol NPs	(14)
$\alpha$ -Gal NPs	Tissue regeneration induced by macrophages activated through binding of natural anti- $\alpha$ -Gal antibodies to multiple $\alpha$ -Gal epitopes present on the NPs	(44, 45)

of asthma, rhinitis, conjunctivitis, angioedema, urticaria, eczema, eosinophilic disorders, such as esophagitis and life-threatening anaphylaxis, as in the case of food, insect venom, or drug allergies. Patients with allergic diseases have a significantly reduced quality of life, and even milder forms such as allergic rhinitis have a significant economic impact (86). Globally, allergic diseases affect 20–30% of the population, and in the developed countries sensitization rates of up to 50% have been reported (87).

Allergy is defined by IgE reacting specifically with non-pathogenic environmental proteins, thus, being defined as allergens (88). Presence of allergen-specific IgE in the blood of affected individuals resulting from an overshooting  $T_{H}2$ -driven immune response, is hence the hallmark of being sensitized (89). The sensitization process is initiated upon first contact where a variety of potential functions of allergens may be involved (90–98); however, the overall mechanism of allergic sensitization still remains to be fully established. As potential risk factors, nutrition, and hygiene have been described (99). Upon second contact with the allergen, specific IgE-loaded allergic effector cells, i.e., tissue-resident mast cells and peripheral blood basophils, degranulate due to IgE receptor cross-linking and release vasoactive mediators (histamine, tryptase, etc.). During this process, being termed the effector function, the typical allergic symptoms emerge, including vasodilation and permeation resulting in swelling, itching, and redness, characteristic of the *wheel and flare reaction* in rhinoconjunctivitis. Furthermore, effector cells initiate the secretion of lipid mediators (leukotrienes) and cyto-/chemokines leading to bronchoconstriction, mucus production, intestinal hypermotility, as in the case of more severe forms, such as anaphylaxis (88). Furthermore, eosinophil infiltration,

chronicity, and amplification of the allergic response can lead to tissue remodeling, a characteristic of asthma (100).

Presently, few studies investigating the potential sensitization-aggravating effects of particulate matter itself or NP-associated allergens exist (101–103). Historically, research was conducted on combustion-derived particles as reviewed recently (104, 105). The interaction of allergens with engineered NPs, such as Au, Ag, ZnO, TiO<sub>2</sub>, SiO<sub>2</sub>, may arise at sites where such materials are handled, so risk of disease-aggravating conditions can be expected in occupational settings. Studies in mice have addressed the pro-allergic potential of Au, TiO<sub>2</sub>, and SiO<sub>2</sub> NPs in contact hypersensitivity. Such reactions are characterized by a T cell-mediated delayed-type adverse response without the presence of allergen-specific IgE or airway hyperresponsiveness with eosinophil infiltration, mucous cell metaplasia, and elevated type 2 cytokine secretion (106–108). Graphene nanosheets and multiwalled carbon nanotubes (MWCNTs) have been shown to induce a  $T_{H}2$  immune response in mouse models when administered intravenously (109). While in human *in vitro* studies including fullerene or MWCNTs contrasting results were reported (110, 111). Human skin-derived mast cells and peripheral blood basophils exhibited a significant inhibition of IgE-dependent mediator release by fullerene. Furthermore, MWCNTs were shown to inhibit allergen-induced type 2 cytokine secretion by peripheral blood mononuclear cells from house dust mite-allergic individuals, emphasizing the pro-inflammatory potential of MWCNTs which has recently been reviewed (112). In line with these reports, MWCNTs have been shown to suppress humoral immune effects in mice by a mechanism involving the activation of cyclooxygenases in the spleen in response to signals from

lung (113). Accordingly, iron oxide NPs were shown to attenuate serum levels of OVA-specific IgG<sub>1</sub> and IgG<sub>2a</sub> in mice (114). Protein corona formation represents a paradigm when studying the biological effects of NPs and it is well accepted that protein–NP interactions may alter the proteins' 3D structure and hence epitope integrity (115). In the context of type 2 immune effects, IgE epitope integrity is essential. Following this rationale, allergic disease-modulating effects were investigated upon interaction of three major inhalant allergens with Au NPs (116). This study showed that increased, decreased, or similar allergenic responses may be observed, presumably depending on the orientation and accessibility of the IgE epitopes of the allergens bound to the NPs.

Not only material composition has an influence on the type of immune response but the particle size of the same material can also be decisive upon inducing either a type 1 or a type 2 immune response. Bigger particles (>100 nm) are more prone to induce a type 2 response, in comparison to smaller particles (~50 nm) that rather induce a type 1 response (117, 118). Wen et al. showed that NPs were also able to induce both a T<sub>H</sub>1 and a T<sub>H</sub>2 response equally when using chitosan NPs in combination with ovalbumin in mice (119). The immune responses elicited by different NPs can be diverse and are highly dependent on material and size of the particles.

During the past two decades much progress has been made in the field of molecule-based diagnostics, also termed component-resolved diagnostics (CRD), with the development of two types of serological tests involving purified natural or recombinantly produced allergen molecules, coated to particles (ImmunoCAP™) or a glass surface (ISAC™) (120–122). The higher predictive value of CRD compared to extract-based methods has been appreciated by clinicians (123, 124). These two large studies advocate that CRD improves the decision-making process during the prescription of allergen-specific immunotherapy (AIT) due to its high specificity. AIT has been described >100 years ago and still remains the only effective treatment against allergy resulting in a shift from a type 2 immune response toward a tolerogenic state, which is characterized by the key cytokines IFN-γ, IL-10, and TGF-β and production of allergen-specific IgG<sub>4</sub> blocking antibodies (125–127). The potential of NPs being used for allergen therapeutics emerged from adjuvants which will be discussed next.

## ADJUVANTS

The idea to use adjuvants to aid in vaccination was established due to the finding that a higher specific antibody titer can be induced by an abscess at the site of inoculation (128, 129). Adjuvants comprise different classes of compounds, including microbial substances, mineral salts, emulsions, or microparticles, displaying potentiating and/or modulating effects on the human immune system, and they have even been quoted as “*dirty little secrets of immunologists*” (130, 131). The main desired effects of adjuvants in therapy or vaccination can be broken down into two groups. On the one hand they function as delivery vehicles of the active pharmaceutical ingredient (API) to antigen-presenting cells (APCs), like dendritic cells (DCs) and macrophages. On the other hand, they induce an immune potentiation effect that

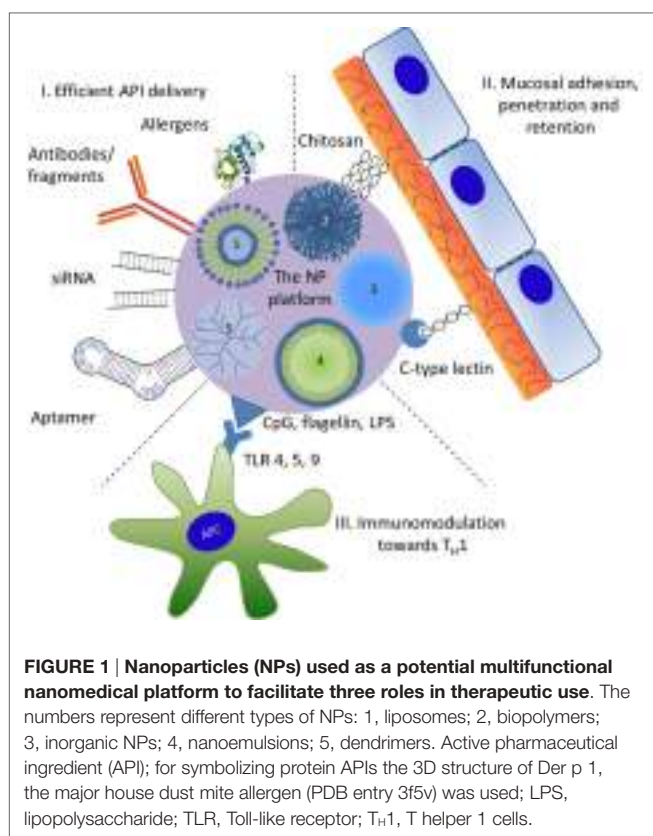
is achieved by activation of the APCs through specific receptors, thus creating an inflammatory context (132). Adjuvants have to be safe in formulation, stable during storage, easily expelled from the body, either by being biodegradable or by efficient excretion, and furthermore, the costs of their production should be low (133).

Aluminum hydroxide or alum has been in use as an adjuvant from as early as 1926 (134), widely used in vaccination ever since (135). Its clinical function also involves innate mechanisms established for recognition of crystals based on NLRP3 inflammasome activation (136). In the last two decades, the research into new adjuvants has increased, but many new adjuvants fall prey to local or systemic toxicity and are not suitable for the use in humans (137). A possible new approach is the use of nanosized inorganic or organic particles as an efficient antigen delivery vehicle (138, 139). Additional advantages of using NPs as adjuvants are that they can incorporate several desired effects of an adjuvant in one substance. They may (i) confer a depot function with enhanced abundance in the tissue/circulation, (ii) function as a delivery vehicle by binding the APIs and delivering them to the APCs, and (iii) be able to induce immunostimulatory effects (140). It has been demonstrated that different kinds of NPs ranging from inorganic NPs, like silica (60, 141) and gold (142), over lipids (143) to biodegradable polymeric particles (144, 145) show adjuvant potential. For some NPs the adjuvant effect is greater than that of alum (138, 141, 146).

Due to their unique properties, NPs readily bind substances like proteins, peptides, and nucleic acid vaccines (147). Those conjugates have been shown to be taken up by APCs (146, 148), and thus NPs are able to deliver the APIs to the APCs. The immune stimulatory effect of NPs has been shown, for example, using poly-γ-glutamic acid NPs and DCs (148), which facilitates the second major requirement for adjuvants—to provide a costimulatory signal for initiation of an immune response. Keeping all that in mind, several types of NPs bear the potential to act as efficient adjuvants in formulation.

## NPs—A POTENTIAL MULTIFUNCTIONAL PLATFORM FOR INTERACTIONS WITH THE IMMUNE SYSTEM

In addition to spontaneous interactions of proteins (or other biological substances) with NPs, engineered nanomaterials may form a platform where various functions of different chemical entities may be combined intentionally (**Figure 1**). It should be stated here that in particular for nanomedical approaches the strict nano definition by “ISO/TS27687:2008 Nanotechnologies—Terminology and definitions for nanoobjects—NP, nanofibre and nanoplate” confining NPs for a size range up to 100 nm is often relaxed. Therefore, nanomedicines usually list substances of particulate matter in the submicro size range. The surface of NPs can be functionalized covalently with specific ligands including antibodies and fragments thereof or other immunologically active proteins, such as allergens. Other ligands may include peptides, nucleic acids such as immunostimulatory CpG-DNA, small inhibitory (si-)RNAs, aptamers, carbohydrates, and other



biomolecules [vitamin D<sub>3</sub> or toll-like receptor (TLR) ligands]. Such NP conjugates may mediate (i) efficient delivery, i.e., cellular targeting and uptake, (ii) mucosal adhesion, penetration, and retention, or (iii) immunostimulatory or modulatory effects. Applied in a well-controlled manner, these ligands modify and can thus be used to optimize the safety profile, specificity, and efficacy of a vaccine candidate.

## NPs Mediate Efficient Delivery

Anticytokine therapy has been recognized since the early 2000s (149, 150), and a number of approaches are in the clinic or the pipeline. Examples include antibodies to counteract the effects of TNF-α or IL-1β in inflammatory bowel disease, rheumatoid arthritis, psoriatic arthritis, ankylosing spondylitis, and atherosclerosis. Such antibodies work *via* shifting the immune response from TH1 or TH17 toward TH2 (151, 152). Polyethylene glycol has been regarded as a nanomedical proponent which due to its non-degradable properties under physiological conditions confers a prolonged circulation time of the co-delivered API (153, 154). During AIT, clinical efficacy of a vaccine has to be counterbalanced by a well-defined safety profile of the whole formulation, i.e., API and adjuvant (155). Therefore, the “*hypoallergen concept*” emerged where substances with reduced IgE-binding capacities were used. By genetic engineering or chemical modification (allergoids) the IgE-binding epitopes were disrupted, and hence, higher amounts could be administered at lower risk of side-reactions (156–162).

## NPs Enable Mucosal Adhesion, Tissue Retention, and Penetration

Among the aforementioned ligands, carbohydrates may establish specific as well as non-specific interactions with the human immune system. Therefore, these hydrophilic moieties represent attractive functionalizations for enhanced mucosal delivery *via* the oral, nasal, or dermal routes of application. Upon adhesion with the mucosal or intradermal tissue, prolonged retention may result in a more effective presentation to immunocompetent cells in the dedicated lymphoid tissues (163, 164). Using NPs as a platform for additionally introducing mucoadhesive ligands can improve sublingual AIT, which have been shown effective in ovalbumin-sensitized mouse models (165–169). **Table 1** provides a list of potential candidate approaches based on specific (upon binding to lectins) and non-specific (upon hydrophilic interactions of chitosan with mucins) carbohydrate recognition aiming at enhanced efficacy of AIT.

## NPs for Immunostimulation and Modulation toward TH1

The response of the immune system against internal or external stimuli can be categorized into two reactions, stimulation or suppression (170). It is possible to push the response either to stimulation or suppression, and this regulation can be used in therapeutic treatment (171, 172). An immune stimulation may be desired for increasing vaccination or cancer treatment efficacy. On the contrary, undesired effects of immune stimulation can result from interactions of leukocytes with NPs (173–175). These may include IFN response, lymphocyte activation, and cytokine storm, leading to severe off-target effects limiting the therapeutic efficacy. Immunosuppression, as observed for inhaled MWCNTs in a mouse model (113), is desired for treatment of hypersensitivities like allergies or autoimmune diseases or in the context of organ transplantation for preventing organ rejection (172, 176, 177). The downside of suppression is that it may lead to an attenuated defense state of the body facilitating infections and cancerous diseases.

The interactions with NPs do not only lead to stimulation or suppression of the immune response but also influence the type of immune response. Both the ability to deviate an immune response from a type 2 to a type 1 response as well as a bias for different types of responses have been described for NPs. Reeducation of tumor-associated macrophages from M2 toward M1 phenotype by NP-mediated induction of pro-inflammatory responses was found effective using the FDA-approved iron oxide NP compound ferumoxytol (58). Similar effects were observed with rabies virus glycoprotein peptide-loaded paclitaxel-carrying biodegradable poly-D,L-lactic-co-glycolic acid (PLGA) NPs in a mouse glioma model, and notably, even crossing of the blood-brain barrier was achieved (66, 178). These polarizing effects may be due to an uptake preference reported for type 2 compared to type 1 macrophages (179). A modulation in immune response was observed using PLGA NPs which were able to downregulate an ongoing TH2 response in an allergic BALB/c mouse model (68). Additionally, PLGA NPs have been used to induce a TH1 response when delivering the TH2-biased peptide hepatitis B

surface antigen (180). A potential therapeutic use for PLGA NPs coated with CpG-DNA (TLR9 ligand) and peanut extract was demonstrated when peanut-allergic mice treated with the NPs were protected from anaphylaxis upon challenge and lower levels of T<sub>H</sub>2 cytokines were measured compared to untreated mice (67). Other possible candidate ligands acting as danger signals providing immunodeviation into type 1 include lipopolysaccharide, monophosphoryl lipid-A, cholera or *E. coli* toxins, or flagellin (181–187). **Table 1** gives an overview on nanomedical immunomodulatory approaches in particular in respect to AIT, which have recently been reviewed elsewhere (188).

## CONCLUDING REMARKS

As for other mechanisms of the immune system (inflammation, type 1 response, tolerance), NPs can modulate type 2 responses in different ways. It is a task for the community, working at the border between immunology and nanotechnology, to understand the parameters leading to NP induced up- or downregulation of

type 2 responses. Understanding of such concepts could enable the prediction of the outcomes of human exposure to NPs.

## AUTHOR CONTRIBUTIONS

All four authors were involved in concept drafting, literature screening, design of display items, writing, and editing of the paper.

## FUNDING

The authors gratefully acknowledge financial support by the International PhD Program “Immunity in Cancer and Allergy” of the Austrian Science Fund (FWF, grant No: W1213), the European Community’s Seventh Framework Program (FP7/2007-2013) under grant agreement No: 263147 (NanoValid—Development of reference methods for hazard identification, risk assessment, and LCA of engineered nanomaterials), and the PLUS Allergy-Cancer-BioNano (ACBN) Research Center.

## REFERENCES

- Gause WC, Wynn TA, Allen JE. Type 2 immunity and wound healing: evolutionary refinement of adaptive immunity by helminths. *Nat Rev Immunol* (2013) 13(8):607–14. doi:10.1038/nri3476
- Oliphant CJ, Barlow JL, McKenzie ANJ. Insights into the initiation of type 2 immune responses. *Immunology* (2011) 134(4):378–85. doi:10.1111/j.1365-2567.2011.03499.x
- Dobrovolskaia MA, Shurin M, Shvedova AA. Current understanding of interactions between nanoparticles and the immune system. *Toxicol Appl Pharmacol* (2016) 299:78–89. doi:10.1016/j.taap.2015.12.022
- Fitzsimmons CM, Falcone FH, Dunne DW. Helminth allergens, parasite-specific IgE, and its protective role in human immunity. *Front Immunol* (2014) 5:61. doi:10.3389/fimmu.2014.00061
- Hotez PJ, Alvarado M, Basanez MG, Bolliger I, Bourne R, Boussinesq M, et al. The global burden of disease study 2010: interpretation and implications for the neglected tropical diseases. *PLoS Negl Trop Dis* (2014) 8(7):e2865. doi:10.1371/journal.pntd.0002865
- Romero EL, Morilla MJ. Nanotechnological approaches against Chagas disease. *Adv Drug Deliv Rev* (2010) 62(4–5):576–88. doi:10.1016/j.addr.2009.11.025
- Aditya NP, Vathsala PG, Vieira V, Murthy RSR, Souto EB. Advances in nanomedicines for malaria treatment. *Adv Colloid Interface Sci* (2013) 201:1–17. doi:10.1016/j.cis.2013.10.014
- Torres-Sangiao E, Holban AM, Gestal MC. Advanced nanobiomaterials: vaccines, diagnosis and treatment of infectious diseases. *Molecules* (2016) 21(7):E867. doi:10.3390/molecules21070867
- McCoy ME, Golden HE, Doll TA, Yang Y, Kaba SA, Zou X, et al. Mechanisms of protective immune responses induced by the *Plasmodium falciparum* circumsporozoite protein-based, self-assembling protein nanoparticle vaccine. *Malar J* (2013) 12:136. doi:10.1186/1475-2875-12-136
- Chaurasia M, Pawar VK, Jaiswal AK, Dube A, Paliwal SK, Chourasia MK. Chondroitin nanocapsules enhanced doxorubicin induced apoptosis against leishmaniasis via Th1 immune response. *Int J Biol Macromol* (2015) 79:27–36. doi:10.1016/j.ijbiomac.2015.04.043
- Want MY, Islamuddin M, Chouhan G, Ozbak HA, Hemeg HA, Dasgupta AK, et al. Therapeutic efficacy of artemisinin-loaded nanoparticles in experimental visceral leishmaniasis. *Colloids Surf B Biointerfaces* (2015) 130:215–21. doi:10.1016/j.colsurfb.2015.04.013
- Hurdayal R, Brombacher F. The role of IL-4 and IL-13 in cutaneous leishmaniasis. *Immunol Lett* (2014) 161(2):179–83. doi:10.1016/j.imlet.2013.12.022
- Deville S, Pootier A, Aucourturier J, Laine-Prade V, Cote M, Boireau P, et al. Influence of adjuvant formulation on the induced protection of mice immunized with total soluble antigen of *Trichinella spiralis*. *Vet Parasitol* (2005) 132(1–2):75–80. doi:10.1016/j.vetpar.2005.05.029
- Solano-Parada J, Gonzalez-Gonzalez G, Torro LM, dos Santos MF, Espino AM, Burgos M, et al. Effectiveness of intranasal vaccination against *Angiostrongylus costaricensis* using a serine/threonine phosphatase 2A synthetic peptide and recombinant antigens. *Vaccine* (2010) 28(32):5185–96. doi:10.1016/j.vaccine.2010.05.072
- Lau P, Bidin N, Islam S, Shukri WN, Zakaria N, Musa N, et al. Influence of gold nanoparticles on wound healing treatment in rat model: photobiomodulation therapy. *Lasers Surg Med* (2016). doi:10.1002/lsm.22614
- Gardner A, Borthwick LA, Fisher AJ. Lung epithelial wound healing in health and disease. *Expert Rev Respir Med* (2010) 4(5):647–60. doi:10.1586/ers.10.62
- Iizuka M, Konno S. Wound healing of intestinal epithelial cells. *World J Gastroenterol* (2011) 17(17):2161–71. doi:10.3748/wjg.v17.i17.2161
- Haubner F, Ohmann E, Pohl F, Strutz J, Gassner HG. Wound healing after radiation therapy: review of the literature. *Radiat Oncol* (2012) 7:162. doi:10.1186/1748-717X-7-162
- Jackson WM, Nesti LJ, Tuan RS. Mesenchymal stem cell therapy for attenuation of scar formation during wound healing. *Stem Cell Res Ther* (2012) 3(3):20. doi:10.1186/scrt111
- Thakral G, Lafontaine J, Najafi B, Talal TK, Kim P, Lavery LA. Electrical stimulation to accelerate wound healing. *Diabet Foot Ankle* (2013) 4. doi:10.3402/dfa.v4i0.22081
- Huang C, Leavitt T, Bayer LR, Orgill DP. Effect of negative pressure wound therapy on wound healing. *Curr Probl Surg* (2014) 51(7):301–31. doi:10.1067/j.cpsurg.2014.04.001
- Das S, Baker AB. Biomaterials and nanotherapeutics for enhancing skin wound healing. *Front Bioeng Biotechnol* (2016) 4:82. doi:10.3389/fbioe.2016.00082
- Konop M, Damps T, Misicka A, Rudnicka L. Certain aspects of silver and silver nanoparticles in wound care: a minireview. *J Nanomat* (2016). doi:10.1155/2016/7614753
- Wilkinson LJ, White RJ, Chipman JK. Silver and nanoparticles of silver in wound dressings: a review of efficacy and safety. *J Wound Care* (2011) 20(11):543–9. doi:10.12968/jowc.2011.20.11.543
- Oyarzun-Ampuero F, Vidal A, Concha M, Morales J, Orellana S, Moreno-Villalada I. Nanoparticles for the treatment of wounds. *Curr Pharm Des* (2015) 21(29):4329–41. doi:10.2174/1381612821666150901104601
- Tian J, Wong KK, Ho CM, Lok CN, Yu WY, Che CM, et al. Topical delivery of silver nanoparticles promotes wound healing. *ChemMedChem* (2007) 2(1):129–36. doi:10.1002/cmdc.200600171
- Pourali P, Razavian Zadeh N, Yahyaei B. Silver nanoparticles production by two soil isolated bacteria, *Bacillus thuringiensis* and *Enterobacter cloacae*, and

- assessment of their cytotoxicity and wound healing effect in rats. *Wound Repair Regen* (2016) 24(5):860–9. doi:10.1111/wrr.12465
28. Pourali P, Yahyaei B. Biological production of silver nanoparticles by soil isolated bacteria and preliminary study of their cytotoxicity and cutaneous wound healing efficiency in rat. *J Trace Elem Med Biol* (2016) 34:22–31. doi:10.1016/j.jtemb.2015.11.004
  29. Li CW, Wang Q, Li J, Hu M, Shi SJ, Li ZW, et al. Silver nanoparticles/chitosan oligosaccharide/poly(vinyl alcohol) nanofiber promotes wound healing by activating TGFbeta1/Smad signaling pathway. *Int J Nanomedicine* (2016) 11:373–86. doi:10.2147/IJN.S91975
  30. Leu JG, Chen SA, Chen HM, Wu WM, Hung CF, Yao YD, et al. The effects of gold nanoparticles in wound healing with antioxidant epigallocatechin gallate and alpha-lipoic acid. *Nanomedicine* (2012) 8(5):767–75. doi:10.1016/j.nano.2011.08.013
  31. Kim JE, Lee J, Jang M, Kwak MH, Go J, Kho EK, et al. Accelerated healing of cutaneous wounds using phytochemically stabilized gold nanoparticle deposited hydrocolloid membranes. *Biomater Sci* (2015) 3(3):509–19. doi:10.1039/c4bm00390j
  32. Lee J, Kim J, Go J, Lee JH, Han DW, Hwang D. Transdermal treatment of the surgical and burned wound skin via phytochemical-capped gold nanoparticles. *Colloids Surf B Biointerfaces* (2015) 135:166–74. doi:10.1016/j.colsurfb.2015.07.058
  33. Randeria PS, Seeger MA, Wang XQ, Wilson H, Shipp D, Mirkin CA, et al. siRNA-based spherical nucleic acids reverse impaired wound healing in diabetic mice by ganglioside GM3 synthase knockdown. *Proc Natl Acad Sci U S A* (2015) 112(18):5573–8. doi:10.1073/pnas.1505951112
  34. Ramya S, Shanmugasundaram T, Balagurunathan R. Biomedical potential of actinobacterially synthesized selenium nanoparticles with special reference to anti-biofilm, anti-oxidant, wound healing, cytotoxic and anti-viral activities. *J Trace Elem Med Biol* (2015) 32:30–9. doi:10.1016/j.jtemb.2015.05.005
  35. Diez-Pascual AM, Diez-Vicente AL. Wound healing bionanocomposites based on castor oil polymeric films reinforced with chitosan-modified ZnO nanoparticles. *Biomacromolecules* (2015) 16(9):2631–44. doi:10.1021/acs.biomac.5b00447
  36. Gopal A, Kant V, Gopalakrishnan A, Tandan SK, Kumar D. Chitosan-based copper nanocomposite accelerates healing in excision wound model in rats. *Eur J Pharmacol* (2014) 731:8–19. doi:10.1016/j.ejphar.2014.02.033
  37. Sankar R, Baskaran A, Shivashangari KS, Ravikumar V. Inhibition of pathogenic bacterial growth on excision wound by green synthesized copper oxide nanoparticles leads to accelerated wound healing activity in Wistar Albino rats. *J Mater Sci Mater Med* (2015) 26(7):214. doi:10.1007/s10856-015-5543-y
  38. Ziv-Polat O, Topaz M, Brosh T, Margel S. Enhancement of incisional wound healing by thrombin conjugated iron oxide nanoparticles. *Biomaterials* (2010) 31(4):741–7. doi:10.1016/j.biomaterials.2009.09.093
  39. Nurhasni H, Cao J, Choi M, Kim I, Lee BL, Jung Y, et al. Nitric oxide-releasing poly(lactic-co-glycolic acid)-polyethylenimine nanoparticles for prolonged nitric oxide release, antibacterial efficacy, and in vivo wound healing activity. *Int J Nanomedicine* (2015) 10:3065–80. doi:10.2147/IJN.S82199
  40. Archana D, Dutta J, Dutta PK. Evaluation of chitosan nano dressing for wound healing: characterization, in vitro and in vivo studies. *Int J Biol Macromol* (2013) 57:193–203. doi:10.1016/j.ijbiomac.2013.03.002
  41. Jayakumar R, Prabaharan M, Kumar PTS, Nair SV, Tamura H. Biomaterials based on chitin and chitosan in wound dressing applications. *Biotechnol Adv* (2011) 29(3):322–37. doi:10.1016/j.biotechadv.2011.01.005
  42. Brown MA, Daya MR, Worley JA. Experience with Chitosan dressings in a Civilian Ems System. *J Emerg Med* (2009) 37(1):1–7. doi:10.1016/j.jemermed.2007.05.043
  43. Boyles MS, Kristl T, Andosch A, Zimmermann M, Tran N, Casals E, et al. Chitosan functionalisation of gold nanoparticles encourages particle uptake and induces cytotoxicity and pro-inflammatory conditions in phagocytic cells, as well as enhancing particle interactions with serum components. *J Nanobiotechnology* (2015) 13:84. doi:10.1186/s12951-015-0146-9
  44. Galili U. Acceleration of wound healing by alpha-gal nanoparticles interacting with the natural anti-Gal antibody. *J Immunol Res* (2015) 2015:589648. doi:10.1155/2015/589648
  45. Galili U. Anti-Gal: an abundant human natural antibody of multiple pathogenes and clinical benefits. *Immunology* (2013) 140(1):1–11. doi:10.1111/imm.12110
  46. Duda PW, Schmied MC, Cook SL, Krieger JI, Hafler DA. Glatiramer acetate (Copaxone®) induces degenerate, Th2-polarized immune responses in patients with multiple sclerosis. *J Clin Invest* (2000) 105(7):967–76. doi:10.1172/JCI8970
  47. Comi G, Martinelli V, Rodegher M, Moiola L, Bajenaru O, Carra A, et al. Effect of glatiramer acetate on conversion to clinically definite multiple sclerosis in patients with clinically isolated syndrome (PreCISE study): a randomised, double-blind, placebo-controlled trial. *Lancet* (2009) 374(9700):1503–11. doi:10.1016/S0140-6736(09)61259-9
  48. Yu Q, Hu X, Ma Y, Xie Y, Lu Y, Qi J, et al. Lipids-based nanostructured lipid carriers (NLCs) for improved oral bioavailability of sirolimus. *Drug Deliv* (2016) 23(4):1469–75. doi:10.3109/10717544.2016.1153744
  49. Chan Y-P, Meyrueix R, Kravtzoff R, Soula O, Soula G, Basulin, a long-acting formulation of human insulin based on medusa nanoparticles. *Nanobiotechnology* (2005) 1(3):317–8. doi:10.1007/s12030-005-0061-5
  50. Fleischmann R, Vencovsky J, van Vollenhoven RF, Borenstein D, Box J, Coteur G, et al. Efficacy and safety of certolizumab pegol monotherapy every 4 weeks in patients with rheumatoid arthritis failing previous disease-modifying antirheumatic therapy: the FAST4WARD study. *Ann Rheum Dis* (2009) 68(6):805–11. doi:10.1136/ard.2008.099291
  51. Masson JD, Thibaudon M, Belec L, Crepeaux G. Calcium phosphate: a substitute for aluminum adjuvants? *Expert Rev Vaccines* (2016) 16:289–99. doi:10.1080/14760584.2017.1244484
  52. Moscicki AB, Kaul R, Ma Y, Scott ME, Daud II, Bukusi EA, et al. Measurement of mucosal biomarkers in a phase 1 trial of intravaginal 3% StarPharma LTD 7013 gel (VivaGel) to assess expanded safety. *J Acquir Immune Defic Syndr* (2012) 59(2):134–40. doi:10.1097/QAI.0b013e31823f2aeb
  53. Kundig TM, Senti G, Schnetzler G, Wolf C, Prinz Vavricka BM, Fulurija A, et al. Der p 1 peptide on virus-like particles is safe and highly immunogenic in healthy adults. *J Allergy Clin Immunol* (2006) 117(6):1470–6. doi:10.1016/j.jaci.2006.01.040
  54. Senti G, Johansen P, Haug S, Bull C, Gottschaller C, Muller P, et al. Use of A-type CpG oligodeoxynucleotides as an adjuvant in allergen-specific immunotherapy in humans: a phase I/IIa clinical trial. *Clin Exp Allergy* (2009) 39(4):562–70. doi:10.1111/j.1365-2222.2008.03191.x
  55. Gregory AE, Williamson ED, Prior JL, Butcher WA, Thompson IJ, Shaw AM, et al. Conjugation of Y. pestis F1-antigen to gold nanoparticles improves immunogenicity. *Vaccine* (2012) 30(48):6777–82. doi:10.1016/j.vaccine.2012.09.021
  56. Kumar R, Ray PC, Datta D, Bansal GP, Angov E, Kumar N. Nanovaccines for malaria using *Plasmodium falciparum* antigen Pf525 attached gold nanoparticles. *Vaccine* (2015) 33(39):5064–71. doi:10.1016/j.vaccine.2015.08.025
  57. Chigurupati S, Mughal MR, Okun E, Das S, Kumar A, McCaffery M, et al. Effects of cerium oxide nanoparticles on the growth of keratinocytes, fibroblasts and vascular endothelial cells in cutaneous wound healing. *Biomaterials* (2013) 34(9):2194–201. doi:10.1016/j.biomaterials.2012.11.061
  58. Zanganeh S, Hutter G, Spitler R, Lenkov O, Mahmoudi M, Shaw A, et al. Iron oxide nanoparticles inhibit tumour growth by inducing pro-inflammatory macrophage polarization in tumour tissues. *Nat Nanotechnol* (2016) 11(11):986–94. doi:10.1038/nnano.2016.168
  59. Yang D, Zhao Y, Guo H, Li Y, Tewary P, Xing G, et al. [Gd@C82(OH)22]n nanoparticles induce dendritic cell maturation and activate Th1 immune responses. *ACS Nano* (2010) 4(2):1178–86. doi:10.1021/nn901478z
  60. Russell RF, McDonald JU, Lambert L, Tregoning JS. Use of the microparticle nanoscale silicon dioxide as an adjuvant to boost vaccine immune responses against influenza virus in neonatal mice. *J Virol* (2016) 90(9):4735–44. doi:10.1128/JVI.03159-15
  61. Song H, Ahmad Nor Y, Yu M, Yang Y, Zhang J, Zhang H, et al. Silica nanoparticles enhance adhesion for long-term bacterial inhibition. *J Am Chem Soc* (2016) 138(20):6455–62. doi:10.1021/jacs.6b00243
  62. Yandar N, Pastorini G, Prato M, Bianco A, Patarroyo ME, Lozano JM. Immunological profile of a *Plasmodium vivax* AMA-1 N-terminus peptide-carbon nanotube conjugate in an infected *Plasmodium berghei* mouse model. *Vaccine* (2008) 26(46):5864–73. doi:10.1016/j.vaccine.2008.08.014
  63. Broos S, Lundberg K, Akagi T, Kadowaki K, Akashi M, Greiff L, et al. Immunomodulatory nanoparticles as adjuvants and allergen-delivery system to human dendritic cells: implications for specific immunotherapy. *Vaccine* (2010) 28(31):5075–85. doi:10.1016/j.vaccine.2010.05.004

64. Smarr CB, Yap WT, Neef TP, Pearson RM, Hunter ZN, Ifergan I, et al. Biodegradable antigen-associated PLG nanoparticles tolerize Th2-mediated allergic airway inflammation pre- and postsensitization. *Proc Natl Acad Sci U S A* (2016) 113(18):5059–64. doi:10.1073/pnas.1505782113
65. Hunter Z, McCarthy DP, Yap WT, Harp CT, Getts DR, Shea LD, et al. A biodegradable nanoparticle platform for the induction of antigen-specific immune tolerance for treatment of autoimmune disease. *ACS Nano* (2014) 8(3):2148–60. doi:10.1021/nn405033r
66. Zou L, Tao Y, Payne G, Do L, Thomas T, Rodriguez J, et al. Targeted delivery of nano-PTX to the brain tumor-associated macrophages. *Oncotarget* (2017) 8(4):6564–78. doi:10.18632/oncotarget.14169
67. Srivastava KD, Siefert A, Fahmy TM, Caplan MJ, Li X-M, Sampson HA. Investigation of peanut oral immunotherapy with CpG/peanut nanoparticles in a murine model of peanut allergy. *J Allergy Clin Immunol* (2016) 138(2):536–43.e4. doi:10.1016/j.jaci.2016.01.047
68. Schöll I, Weissenböck A, Förster-Waldl E, Untersmayr E, Walter F, Willheim M, et al. Allergen-loaded biodegradable poly(D,L-lactic-co-glycolic) acid nanoparticles down-regulate an ongoing Th2 response in the BALB/c mouse model. *Clin Exp Allergy* (2004) 34(2):315–21. doi:10.1111/j.1365-2222.2004.01884.x
69. Scholl I, Kopp T, Bohle B, Jensen-Jarolim E. Biodegradable PLGA particles for improved systemic and mucosal treatment of Type I allergy. *Immunol Allergy Clin North Am* (2006) 26(2):349–364.ix. doi:10.1016/j.iac.2006.02.007
70. Batanero E, Barral P, Villalba M, Rodriguez R. Biodegradable poly (DL-lactide glycolide) microparticles as a vehicle for allergen-specific vaccines: a study performed with Ole e 1, the main allergen of olive pollen. *J Immunol Methods* (2002) 259(1–2):87–94. doi:10.1016/S0022-1759(01)00497-5
71. Salari F, Varasteh AR, Vahedi F, Hashemi M, Sankian M. Down-regulation of Th2 immune responses by sublingual administration of poly (lactic-co-glycolic) acid (PLGA)-encapsulated allergen in BALB/c mice. *Int Immunopharmacol* (2015) 29(2):672–8. doi:10.1016/j.intimp.2015.09.011
72. Roth-Walter F, Scholl I, Untersmayr E, Fuchs R, Boltz-Nitulescu G, Weissenböck A, et al. M cell targeting with *Aleuria aurantia* lectin as a novel approach for oral allergen immunotherapy. *J Allergy Clin Immunol* (2004) 114(6):1362–8. doi:10.1016/j.jaci.2004.08.010
73. Gomez S, Gamazo C, San Roman B, Grau A, Espuelas S, Ferrer M, et al. A novel nanoparticulate adjuvant for immunotherapy with *Lolium perenne*. *J Immunol Methods* (2009) 348(1–2):1–8. doi:10.1016/j.jim.2009.06.005
74. Kenyon NJ, Bratt JM, Lee J, Luo J, Franz LM, Zeki AA, et al. Self-assembling nanoparticles containing dexamethasone as a novel therapy in allergic airways inflammation. *PLoS One* (2013) 8(10):e77730. doi:10.1371/journal.pone.0077730
75. Pohlitz H, Bellinghausen I, Schomer M, Heydenreich B, Saloga J, Frey H. Biodegradable pH-sensitive poly(ethylene glycol) nanocarriers for allergen encapsulation and controlled release. *Biomacromolecules* (2015) 16(10):3103–11. doi:10.1021/acs.biomac.5b00458
76. Liu Z, Guo H, Wu Y, Yu H, Yang H, Li J. Local nasal immunotherapy: efficacy of Dermatophagoides farinae-chitosan vaccine in murine asthma. *Int Arch Allergy Immunol* (2009) 150(3):221–8. doi:10.1159/000222674
77. Hall G, Lund L, Lamb JR, Jarman ER. Kinetics and mode of peptide delivery via the respiratory mucosa determine the outcome of activation versus TH2 immunity in allergic inflammation of the airways. *J Allergy Clin Immunol* (2002) 110(6):883–90. doi:10.1067/mai.2002.129800
78. Chew JL, Wolfowicz CB, Mao HQ, Leong KW, Chua KY. Chitosan nanoparticles containing plasmid DNA encoding house dust mite allergen, Der p 1 for oral vaccination in mice. *Vaccine* (2003) 21(21–22):2720–9. doi:10.1016/S0264-410X(03)00228-7
79. Li GP, Liu ZG, Liao B, Zhong NS. Induction of Th1-type immune response by chitosan nanoparticles containing plasmid DNA encoding house dust mite allergen Der p 2 for oral vaccination in mice. *Cell Mol Immunol* (2009) 6(1):45–50. doi:10.1038/cmi.2009.6
80. Roy K, Mao HQ, Huang SK, Leong KW. Oral gene delivery with chitosan – DNA nanoparticles generates immunologic protection in a murine model of peanut allergy. *Nat Med* (1999) 5(4):387–91. doi:10.1038/7385
81. Reboucas Jde S, Irache JM, Camacho AI, Esparza I, Del Pozo V, Sanz ML, et al. Development of poly(anhydride) nanoparticles loaded with peanut proteins: the influence of preparation method on the immunogenic properties. *Eur J Pharm Biopharm* (2012) 82(2):241–9. doi:10.1016/j.ejpb.2012.06.014
82. Zhang F, Smolen JA, Zhang S, Li R, Shah PN, Cho S, et al. Degradable polyphosphoester-based silver-loaded nanoparticles as therapeutics for bacterial lung infections. *Nanoscale* (2015) 7(6):2265–70. doi:10.1039/C4NR07103D
83. Nouri HR, Varasteh A, Jaafari MR, Davies JM, Sankian M. Induction of a Th1 immune response and suppression of IgE via immunotherapy with a recombinant hybrid molecule encapsulated in liposome-protamine-DNA nanoparticles in a model of experimental allergy. *Immunol Res* (2015) 62(3):280–91. doi:10.1007/s12026-015-8659-8
84. Pali-Scholl I, Szollosi H, Starkl P, Scheicher B, Stremnitzer C, Hofmeister A, et al. Protamine nanoparticles with CpG-oligodeoxynucleotide prevent an allergen-induced Th2-response in BALB/c mice. *Eur J Pharm Biopharm* (2013) 85(3 Pt A):656–64. doi:10.1016/j.ejpb.2013.03.003
85. Pawankar R. Allergic diseases and asthma: a global public health concern and a call to action. *World Allergy Organ J* (2014) 7(1):12. doi:10.1186/1939-4551-7-12
86. Braido F, Arcadipane F, Marugo F, Hayashi M, Pawankar R. Allergic rhinitis: current options and future perspectives. *Curr Opin Allergy Clin Immunol* (2014) 14(2):168–76. doi:10.1097/ACI.0000000000000043
87. Stemmeseder T, Klinglmayr E, Moser S, Luettenegger L, Lang R, Himly M, et al. Cross-sectional study on allergic sensitization of Austrian adolescents using molecule-based IgE profiling. *Allergy* (2016) 72:754–63. doi:10.1111/all.13071
88. Abbas AK, Lichtman AH, Pillai S. *Cellular and Molecular Immunology*. Philadelphia, PA: Elsevier Saunders (2012).
89. Demoly P, Tanno LK, Akdis CA, Lau S, Calderon MA, Santos AF, et al. Global classification and coding of hypersensitivity diseases – an EAACI – WAO survey, strategic paper and review. *Allergy* (2014) 69(5):559–70. doi:10.1111/all.12386
90. Schulz O, Laing P, Sewell HF, Shakib F. Der p 1, a major allergen of the house dust mite, proteolytically cleaves the low-affinity receptor for human IgE (CD23). *Eur J Immunol* (1995) 25(11):3191–4. doi:10.1002/eji.1830251131
91. Schulz O, Sewell HF, Shakib F. Proteolytic cleavage of CD25, the alpha subunit of the human T cell interleukin 2 receptor, by Der p 1, a major mite allergen with cysteine protease activity. *J Exp Med* (1998) 187(2):271–5. doi:10.1084/jem.187.2.271
92. Shakib F, Schulz O, Sewell H. A mite subversive: cleavage of CD23 and CD25 by Der p 1 enhances allergenicity. *Immunol Today* (1998) 19(7):313–6. doi:10.1016/S0167-5699(98)01284-5
93. Wan H, Winton HL, Soeller C, Tovey ER, Gruenert DC, Thompson PJ, et al. Der p 1 facilitates transepithelial allergen delivery by disruption of tight junctions. *J Clin Invest* (1999) 104(1):123–33. doi:10.1172/JCI5844
94. Shreffler WG, Castro RR, Kucuk ZY, Charlop-Powers Z, Grishina G, Yoo S, et al. The major glycoprotein allergen from *Arachis hypogaea*, Ara h 1, is a ligand of dendritic cell-specific ICAM-grabbing non-integrin and acts as a Th2 adjuvant in vitro. *J Immunol* (2006) 177(6):3677–85. doi:10.4049/jimmunol.177.6.3677
95. Trompette A, Divanovic S, Visintin A, Blanchard C, Hegde RS, Madan R, et al. Allergenicity resulting from functional mimicry of a toll-like receptor complex protein. *Nature* (2009) 457(7229):585–8. doi:10.1038/nature07548
96. Hsu SC, Chen CH, Tsai SH, Kawasaki H, Hung CH, Chu YT, et al. Functional interaction of common allergens and a C-type lectin receptor, dendritic cell-specific ICAM3-grabbing non-integrin (DC-SIGN), on human dendritic cells. *J Biol Chem* (2010) 285(11):7903–10. doi:10.1074/jbc.M109.058370
97. Ziegler SF, Artis D. Sensing the outside world: TSLP regulates barrier immunity. *Nat Immunol* (2010) 11(4):289–93. doi:10.1038/ni.1852
98. Machado Y, Freier R, Scheiblhofer S, Thalhamer T, Mayr M, Briza P, et al. Fold stability during endolysosomal acidification is a key factor for allergenicity and immunogenicity of the major birch pollen allergen. *J Allergy Clin Immunol* (2016) 137(5):1525–34. doi:10.1016/j.jaci.2015.09.026
99. Vercelli D. Mechanisms of the hygiene hypothesis – molecular and otherwise. *Curr Opin Immunol* (2006) 18(6):733–7. doi:10.1016/j.coi.2006.09.002
100. Puxeddu I, Ribatti D, Crivellato E, Levi-Schaffer F. Mast cells and eosinophils: a novel link between inflammation and angiogenesis in allergic diseases. *J Allergy Clin Immunol* (2005) 116(3):531–6. doi:10.1016/j.jaci.2005.06.007
101. Diaz-Sanchez D, Tsien A, Fleming J, Saxon A. Combined diesel exhaust particulate and ragweed allergen markedly enhances human in vivo

- nasal ragweed-specific IgE and skews cytokine production to a T helper cell 2-type pattern. *J Immunol* (1997) 158(5):2406–13.
102. Knox RB, Suphioglu C, Taylor P, Desai R, Watson HC, Peng JL, et al. Major grass pollen allergen Lol p 1 binds to diesel exhaust particles: implications for asthma and air pollution. *Clin Exp Allergy* (1997) 27(3):246–51. doi:10.1046/j.1365-2222.1997.d01-508.x
  103. Brandt EB, Biagini Myers JM, Acciani TH, Ryan PH, Sivaprasad U, Ruff B, et al. Exposure to allergen and diesel exhaust particles potentiates secondary allergen-specific memory responses, promoting asthma susceptibility. *J Allergy Clin Immunol* (2015) 136(2):295–303.e7. doi:10.1016/j.jaci.2014.11.043
  104. Miller RL, Peden DB. Environmental effects on immune responses in patients with atopy and asthma. *J Allergy Clin Immunol* (2014) 134(5):1001–8. doi:10.1016/j.jaci.2014.07.064
  105. Brandt EB, Myers JM, Ryan PH, Hershey GK. Air pollution and allergic diseases. *Curr Opin Pediatr* (2015) 27(6):724–35. doi:10.1097/MOP.0000000000000286
  106. Hussain S, Vanoirbeek JA, Luyts K, De Vooght V, Verbeken E, Thomassen LC, et al. Lung exposure to nanoparticles modulates an asthmatic response in a mouse model. *Eur Respir J* (2011) 37(2):299–309. doi:10.1183/09031936.00168509
  107. Brandenberger C, Rowley NL, Jackson-Humbles DN, Zhang Q, Bramble LA, Lewandowski RP, et al. Engineered silica nanoparticles act as adjuvants to enhance allergic airway disease in mice. *Part Fibre Toxicol* (2013) 10:26. doi:10.1186/1743-8977-10-26
  108. Smulders S, Golanski I, Smolders E, Vanoirbeek J, Hoet PH. Nano-TiO<sub>2</sub> modulates the dermal sensitization potency of dinitrochlorobenzene after topical exposure. *Br J Dermatol* (2015) 172(2):392–9. doi:10.1111/bjd.13295
  109. Wang X, Podila R, Shannahan JH, Rao AM, Brown JM. Intravenously delivered graphene nanosheets and multiwalled carbon nanotubes induce site-specific Th2 inflammatory responses via the IL-33/ST2 axis. *Int J Nanomedicine* (2013) 8:1733–48. doi:10.2147/IJN.S44211
  110. Ryan JJ, Bateman HR, Stover A, Gomez G, Norton SK, Zhao W, et al. Fullerene nanomaterials inhibit the allergic response. *J Immunol* (2007) 179(1):665–72. doi:10.4049/jimmunol.179.1.665
  111. Laverny G, Casset A, Purohit A, Schaeffer E, Spiegelhalter C, de Blay F, et al. Immunomodulatory properties of multi-walled carbon nanotubes in peripheral blood mononuclear cells from healthy subjects and allergic patients. *Toxicol Lett* (2013) 217(2):91–101. doi:10.1016/j.toxlet.2012.12.008
  112. Boyles M, Stoehr L, Schlinkert P, Himly M, Duschl A. The significance and insignificance of carbon nanotube-induced inflammation. *Fibers* (2014) 2(1):45–74. doi:10.3390/fib2010045
  113. Mitchell LA, Lauer FT, Burchiel SW, McDonald JD. Mechanisms for how inhaled multiwalled carbon nanotubes suppress systemic immune function in mice. *Nat Nanotechnol* (2009) 4(7):451–6. doi:10.1038/nnano.2009.151
  114. Shen CC, Wang CC, Liao MH, Jan TR. A single exposure to iron oxide nanoparticles attenuates antigen-specific antibody production and T-cell reactivity in ovalbumin-sensitized BALB/c mice. *Int J Nanomedicine* (2011) 6:1229–35. doi:10.2147/IJN.S21019
  115. Monopoli MP, Aberg C, Salvati A, Dawson KA. Biomolecular coronas provide the biological identity of nanosized materials. *Nat Nanotechnol* (2012) 7(12):779–86. doi:10.1038/nnano.2012.207
  116. Radauer-Preiml I, Andosch A, Hawranek T, Luetz-Meindl U, Wiederstein M, Horejs-Hoeck J, et al. Nanoparticle-allergen interactions mediate human allergic responses: protein corona characterization and cellular responses. *Part Fibre Toxicol* (2016) 13(1):3. doi:10.1186/s12989-016-0113-0
  117. Mottram PL, Leong D, Crimeen-Irwin B, Gloster S, Xiang SD, Meanger J, et al. Type 1 and 2 immunity following vaccination is influenced by nanoparticle size: formulation of a model vaccine for respiratory syncytial virus. *Mol Pharm* (2007) 4(1):73–84. doi:10.1021/mp060096p
  118. Hardy CL, Lemusurier JS, Mohamud R, Yao J, Xiang SD, Rolland JM, et al. Differential uptake of nanoparticles and microparticles by pulmonary APC subsets induces discrete immunological imprints. *J Immunol* (2013) 191(10):5278–90. doi:10.4049/jimmunol.1203131
  119. Wen Z-S, Xu Y-L, Zou X-T, Xu Z-R. Chitosan nanoparticles act as an adjuvant to promote both Th1 and Th2 immune responses induced by ovalbumin in mice. *Mar Drugs* (2011) 9(6):1038. doi:10.3390/md9061038
  120. Ferrer M, Sanz ML, Sastre J, Bartra J, del Cuivillo A, Montoro J, et al. Molecular diagnosis in allergology: application of the microarray technique. *J Investig Allergol Clin Immunol* (2009) 19(Suppl 1):19–24.
  121. Martinez-Aranguren R, Lizaso MT, Goikoetxea MJ, Garcia BE, Cabrer-Freitag P, Trellez O, et al. Is the determination of specific IgE against components using ISAC 112 a reproducible technique? *PLoS One* (2014) 9(2):e88394. doi:10.1371/journal.pone.0088394
  122. Matricardi PM, Kleine-Tebbe J, Hoffmann HJ, Valenta R, Hilger C, Hofmaier S, et al. EAACI molecular allergology user's guide. *Pediatr Allergy Immunol* (2016) 27(Suppl 23):1–250. doi:10.1111/pai.12563
  123. Stringari G, Tripodi S, Caffarelli C, Dondi A, Asero R, Di Renzo Businco A, et al. The effect of component-resolved diagnosis on specific immunotherapy prescription in children with hay fever. *J Allergy Clin Immunol* (2014) 134(1):75–81. doi:10.1016/j.jaci.2014.01.042
  124. Asarnoj A, Hamsten C, Waden K, Lupinek C, Andersson N, Kull I, et al. Sensitization to cat and dog allergen molecules in childhood and prediction of symptoms of cat and dog allergy in adolescence: a BAMSE/MeDALL study. *J Allergy Clin Immunol* (2016) 137(3): 813–21.e7. doi:10.1016/j.jaci.2015.09.052
  125. Noon L. Prophylactic inoculation against hay fever. *Lancet* (1911) 1:1572–3. doi:10.1016/S0140-6736(00)78276-6
  126. Larche M, Akdis CA, Valenta R. Immunological mechanisms of allergen-specific immunotherapy. *Nat Rev Immunol* (2006) 6(10):761–71. doi:10.1038/nri1934
  127. Akdis CA, Akdis M. Mechanisms of allergen-specific immunotherapy. *J Allergy Clin Immunol* (2011) 127(1):18–27; quiz 28–19. doi:10.1016/j.jaci.2010.11.030
  128. Ramon G. Sur l'augmentation anormale de l'antitoxine chez les chevaux producteurs de serum antidiptérique. *Bull Soc Centr Med Vet* (1925) 101:227–34.
  129. Ramon G. Procédés pour accroître la production des antitoxines. *Ann Inst Pasteur* (1926) 40(1).
  130. Janeway CA Jr. Approaching the asymptote? Evolution and revolution in immunology. *Cold Spring Harb Symp Quant Biol* (1989) 54(Pt 1):1–13. doi:10.1101/SQB.1989.054.01.003
  131. Brewer JM, Alexander J. Cytokines and the mechanisms of action of vaccine adjuvants. *Cytokines Cell Mol Ther* (1997) 3(4):233–46.
  132. O'Hagan DT, Valiante NM. Recent advances in the discovery and delivery of vaccine adjuvants. *Nat Rev Drug Discov* (2003) 2(9):727. doi:10.1038/nrd1176
  133. Reed SG, Bertholet S, Coler RN, Friede M. New horizons in adjuvants for vaccine development. *Trends Immunol* (2009) 30(1):23–32. doi:10.1016/j.it.2008.09.006
  134. Glenny A, Pope C, Waddington H, Wallace U. The antigenic value of toxoid precipitated by potassium alum. *J Pathol Bacteriol* (1926) 29(29):31–40. doi:10.1002/path.1700290106
  135. Schöll I, Boltz-Nitulescu G, Jensen-Jarolim E. Review of novel particulate antigen delivery systems with special focus on treatment of type I allergy. *J Control Release* (2005) 104(1):1–27. doi:10.1016/j.jconrel.2004.12.020
  136. Lambrecht BN, Kool M, Willart MA, Hammad H. Mechanism of action of clinically approved adjuvants. *Curr Opin Immunol* (2009) 21(1):23–9. doi:10.1016/j.co.2009.01.004
  137. Aguilar JC, Rodriguez EG. Vaccine adjuvants revisited. *Vaccine* (2007) 25(19):3752–62. doi:10.1016/j.vaccine.2007.01.111
  138. Fifis T, Gamvrellis A, Crimeen-Irwin B, Pietersz GA, Li J, Mottram PL, et al. Size-dependent immunogenicity: therapeutic and protective properties of nano-vaccines against tumors. *J Immunol* (2004) 173(5):3148–54. doi:10.4049/jimmunol.173.5.3148
  139. Akagi T, Baba M, Akashi M. Biodegradable nanoparticles as vaccine adjuvants and delivery systems: regulation of immune responses by nanoparticle-based vaccine. *Adv Polym Sci* (2012) 247:31–64. doi:10.1007/12\_2011\_150
  140. Kalkanidis M, Pietersz GA, Xiang SD, Mottram PL, Crimeen-Irwin B, Ardiipradja K, et al. Methods for nano-particle based vaccine formulation and evaluation of their immunogenicity. *Methods* (2006) 40(1):20–9. doi:10.1016/j.ymeth.2006.05.018
  141. Mercuri LP, Carvalho LV, Lima FA, Quayle C, Fantini MCA, Tanaka GS, et al. Ordered mesoporous silica SBA-15: a new effective adjuvant to induce antibody response. *Small* (2006) 2(2):254–6. doi:10.1002/smll.200500274
  142. Xu L, Liu Y, Chen Z, Li W, Liu Y, Wang L, et al. Surface-engineered gold nanorods: promising DNA vaccine adjuvant for HIV-1 treatment. *Nano Lett* (2012) 12(4):2003–12. doi:10.1021/nl300027p

143. Olbrich C, Kayser O, Müller R, Grubhofer N. Solid lipid nanoparticles (SLN) as vaccine adjuvant – study in sheep with a mycoplasma bovis antigen and stability testing. *Intern Symp Control Rel Bioact Mater* (2000) 27:8110.
144. Wheeler AW, Woroniecki SR. Immunological adjuvants in allergy vaccines: past, present future. *Allergol Int* (2001) 50(4):295–301. doi:10.1046/j.1440-1592.2001.00230.x
145. Francis JN, Durham SR. Adjuvants for allergen immunotherapy: experimental results and clinical perspectives. *Curr Opin Allergy Clin Immunol* (2004) 4(6):543–8. doi:10.1097/00130832-200412000-00012
146. Uto T, Akagi T, Toyama M, Nishi Y, Shima F, Akashi M, et al. Comparative activity of biodegradable nanoparticles with aluminum adjuvants: antigen uptake by dendritic cells and induction of immune response in mice. *Immunol Lett* (2011) 140(1–2):36–43. doi:10.1016/j.imlet.2011.06.002
147. Csaba N, Garcia-Fuentes M, Alonso MJ. Nanoparticles for nasal vaccination. *Adv Drug Deliv Rev* (2009) 61(2):140–57. doi:10.1016/j.addr.2008.09.005
148. Uto T, Wang X, Sato K, Haraguchi M, Akagi T, Akashi M, et al. Targeting of antigen to dendritic cells with poly( $\gamma$ -glutamic acid) nanoparticles induces antigen-specific humoral and cellular immunity. *J Immunol* (2007) 178(5):2979–86. doi:10.4049/jimmunol.178.5.2979
149. Maini RN, Taylor PC. Anti-cytokine therapy for rheumatoid arthritis. *Annu Rev Med* (2000) 51:207–29. doi:10.1146/annurev.med.51.1.207
150. van den Berg WB. Anti-cytokine therapy in chronic destructive arthritis. *Arthritis Res* (2001) 3(1):18–26. doi:10.1186/ar136
151. Guo J, Jiang X, Gui S. RNA interference-based nanosystems for inflammatory bowel disease therapy. *Int J Nanomedicine* (2016) 11:5287–310. doi:10.2147/IJN.S116902
152. Thompson C, Davies R, Choy E. Anti cytokine therapy in chronic inflammatory arthritis. *Cytokine* (2016) 86:92–9. doi:10.1016/j.cyto.2016.07.015
153. Owens DE III, Peppas NA. Opsonization, biodistribution, and pharmacokinetics of polymeric nanoparticles. *Int J Pharm* (2006) 307(1):93–102. doi:10.1016/j.ijpharm.2005.10.010
154. Duncan R. Polymer therapeutics as nanomedicines: new perspectives. *Curr Opin Biotechnol* (2011) 22(4):492–501. doi:10.1016/j.copbio.2011.05.507
155. Bousquet J, Lockey R, Malling HJ, Alvarez-Cuesta E, Canonica GW, Chapman MD, et al. Allergen immunotherapy: therapeutic vaccines for allergic diseases. World Health Organization. American Academy of Allergy, Asthma and Immunology. *Ann Allergy Asthma Immunol* (1998) 81(5):401–5. doi:10.1016/S1081-1206(10)63136-5
156. Marsh DG, Norman PS, Roebber M, Lichtenstein LM. Studies on allergoids from naturally occurring allergens. III. Preparation of ragweed pollen allergoids by aldehyde modification in two steps. *J Allergy Clin Immunol* (1981) 68(6):449–59. doi:10.1016/0091-6749(81)90199-8
157. Grammer LC, Shaughnessy MA, Patterson R. Modified forms of allergen immunotherapy. *J Allergy Clin Immunol* (1985) 76(2 Pt 2):397–401. doi:10.1016/0091-6749(85)90661-X
158. Maasch HJ, Marsh DG. Standardized extracts modified allergens – allergoids. *Clin Rev Allergy* (1987) 5(1):89–106. doi:10.1007/BF02802259
159. Ferreira F, Ebner C, Kramer B, Casari G, Briza P, Kungl AJ, et al. Modulation of IgE reactivity of allergens by site-directed mutagenesis: potential use of hypoallergenic variants for immunotherapy. *FASEB J* (1998) 12(2):231–42.
160. Casanovas M, Fernandez-Caldas E, Alamar R, Basomba A. Comparative study of tolerance between unmodified and high doses of chemically modified allergen vaccines of Dermatophagooides pteronyssinus. *Int Arch Allergy Immunol* (2005) 137(3):211–8. doi:10.1159/000086333
161. Lund L, Henmar H, Wurtzen PA, Lund G, Hjortskov N, Larsen JN. Comparison of allergenicity and immunogenicity of an intact allergen vaccine and commercially available allergoid products for birch pollen immunotherapy. *Clin Exp Allergy* (2007) 37(4):564–71. doi:10.1111/j.1365-2222.2007.02687.x
162. Henmar H, Lund G, Lund L, Petersen A, Wurtzen PA. Allergenicity, immunogenicity and dose-relationship of three intact allergen vaccines and four allergoid vaccines for subcutaneous grass pollen immunotherapy. *Clin Exp Immunol* (2008) 153(3):316–23. doi:10.1111/j.1365-2249.2008.03710.x
163. Novak N, Bieber T, Allam JP. Immunological mechanisms of sublingual allergen-specific immunotherapy. *Allergy* (2011) 66(6):733–9. doi:10.1111/j.1398-9995.2010.02535.x
164. Scheiblhofer S, Machado Y, Feinle A, Thalhamer J, Husing N, Weiss R. Potential of nanoparticles for allergen-specific immunotherapy – use of silica nanoparticles as vaccination platform. *Expert Opin Drug Deliv* (2016) 13(12):1777–88. doi:10.1080/17425247.2016.1203898
165. Gomez S, Gamazo C, San Roman B, Vauthier C, Ferrer M, Irachet JM. Development of a novel vaccine delivery system based on Gantrez nanoparticles. *J Nanosci Nanotechnol* (2006) 6(9–10):3283–9. doi:10.1166/jnn.2006.471
166. Roman BS, Espuelas S, Gomez S, Gamazo C, Sanz ML, Ferrer M, et al. Intradermal immunization with ovalbumin-loaded poly-epsilon-caprolactone microparticles conferred protection in ovalbumin-sensitized allergic mice. *Clin Exp Allergy* (2007) 37(2):287–95. doi:10.1111/j.1365-2222.2007.02654.x
167. Pandey RS, Sahu S, Sudheesh MS, Madan J, Kumar M, Dixit VK. Carbohydrate modified ultrafine ceramic nanoparticles for allergen immunotherapy. *Int Immunopharmacol* (2011) 11(8):925–31. doi:10.1016/j.intimp.2011.02.004
168. Kawakita A, Shirasaki H, Yasutomi M, Tokuriki S, Mayumi M, Naiki H, et al. Immunotherapy with oligomannose-coated liposomes ameliorates allergic symptoms in a murine food allergy model. *Allergy* (2012) 67(3):371–9. doi:10.1111/j.1398-9995.2011.02777.x
169. Weinberger EE, Himly M, Myschik J, Hauser M, Altmann F, Isakovic A, et al. Generation of hypoallergenic neoglycoconjugates for dendritic cell targeted vaccination: a novel tool for specific immunotherapy. *J Control Release* (2013) 165(2):101–9. doi:10.1016/j.jconrel.2012.11.002
170. Landesman-Milo D, Peer D. Altering the immune response with lipid-based nanoparticles. *J Control Release* (2012) 161(2):600–8. doi:10.1016/j.jconrel.2011.12.034
171. De Temmerman M-L, Rejman J, Demeester J, Irvine DJ, Gander B, De Smedt SC. Particulate vaccines: on the quest for optimal delivery and immune response. *Drug Discov Today* (2011) 16(13–14):569–82. doi:10.1016/j.drudis.2011.04.006
172. Goldsmith M, Mizrahy S, Peer D. Grand challenges in modulating the immune response with RNAi nanomedicines. *Nanomedicine* (2011) 6(10):1771–85. doi:10.2217/nmm.11.162
173. Peer D, Park EJ, Morishita Y, Carman CV, Shimaoka M. Systemic leukocyte-directed siRNA delivery revealing cyclin D1 as an anti-inflammatory target. *Science* (2008) 319(5863):627–30. doi:10.1126/science.1149859
174. Kedmi R, Ben-Arie N, Peer D. The systemic toxicity of positively charged lipid nanoparticles and the role of toll-like receptor 4 in immune activation. *Biomaterials* (2010) 31(26):6867–75. doi:10.1016/j.biomaterials.2010.05.027
175. Yazdi AS, Guarda G, Riteau N, Drexler SK, Tardivel A, Couillin I, et al. Nanoparticles activate the NLR pyrin domain containing 3 (Nlrp3) inflammasome and cause pulmonary inflammation through release of IL-1 $\alpha$  and IL-1 $\beta$ . *Proc Natl Acad Sci U S A* (2010) 107(45):19449–54. doi:10.1073/pnas.1008155107
176. Dobrovolskaia MA, McNeil SE. Immunological properties of engineered nanomaterials. *Nat Nanotechnol* (2007) 2(8):469–78. doi:10.1038/nnano.2007.223
177. Zolnik BS, González-Fernández Á, Sadrieh N, Dobrovolskaia MA. Minireview: nanoparticles and the immune system. *Endocrinology* (2010) 151(2):458–65. doi:10.1210/en.2009-1082
178. Blanco E, Shen H, Ferrari M. Principles of nanoparticle design for overcoming biological barriers to drug delivery. *Nat Biotechnol* (2015) 33(9):941–51. doi:10.1038/nbt.3330
179. MacParland SA, Tsoi KM, Ouyang B, Ma XZ, Manuel J, Fawaz A, et al. Phenotype determines nanoparticle uptake by human macrophages from liver and blood. *ACS Nano* (2017) 11(3):2428–43. doi:10.1021/acsnano.6b06245
180. Lutsiak MEC, Kwon GS, Samuel J. Biodegradable nanoparticle delivery of a Th2-biased peptide for induction of Th1 immune responses. *J Pharm Pharmacol* (2006) 58(6):739–47. doi:10.1211/jpp.58.6.0004
181. Mowat AM, Maloy KJ, Donachie AM. Immune-stimulating complexes as adjuvants for inducing local and systemic immunity after oral immunization with protein antigens. *Immunology* (1993) 80(4):527–34.
182. Tighe H, Takabayashi K, Schwartz D, Van Nest G, Tuck S, Eiden JJ, et al. Conjugation of immunostimulatory DNA to the short ragweed allergen amb a 1 enhances its immunogenicity and reduces its allergenicity. *J Allergy Clin Immunol* (2000) 106(1 Pt 1):124–34. doi:10.1067/mai.2000.107927
183. Simons FE, Shikishima Y, Van Nest G, Eiden JJ, HayGlass KT. Selective immune redirection in humans with ragweed allergy by injecting Amb a 1 linked to immunostimulatory DNA. *J Allergy Clin Immunol* (2004) 113(6):1144–51. doi:10.1016/j.jaci.2004.03.003
184. Tulic MK, Fiset PO, Manoukian JJ, Frenkel S, Lavigne F, Eidelman DH, et al. Role of toll-like receptor 4 in protection by bacterial lipopolysaccharide in the nasal mucosa of atopic children but not adults. *Lancet* (2004) 363(9422):1689–97. doi:10.1016/S0140-6736(04)16253-3

185. Creticos PS, Schroeder JT, Hamilton RG, Balcer-Whaley SL, Khattignavong AP, Lindblad R, et al. Immunotherapy with a ragweed-toll-like receptor 9 agonist vaccine for allergic rhinitis. *N Engl J Med* (2006) 355(14):1445–55. doi:10.1056/NEJMoa052916
186. Pfaar O, Barth C, Jaschke C, Hormann K, Klimek L. Sublingual allergen-specific immunotherapy adjuvanted with monophosphoryl lipid A: a phase I/IIa study. *Int Arch Allergy Immunol* (2011) 154(4):336–44. doi:10.1159/000321826
187. Marciani DJ. New Th2 adjuvants for preventive and active immunotherapy of neurodegenerative proteinopathies. *Drug Discov Today* (2014) 19(7):912–20. doi:10.1016/j.drudis.2014.02.015
188. Himly M, Grotz B, Sageder M, Geppert M, Duschl A. Immune frailty and nanomaterials: the case of allergies. *Curr Bionanotechnol* (2016) 2(1):20–8. doi:10.2174/2213529402666160601124654

**Conflict of Interest Statement:** The authors declare that the research was conducted in the absence of any commercial or financial relationships that could be construed as a potential conflict of interest.

The reviewer, JS, and handling Editor declared their shared affiliation, and the handling editor states that the process nevertheless met the standards of a fair and objective review.

Copyright © 2017 Himly, Mills-Goodlet, Geppert and Duschl. This is an open-access article distributed under the terms of the Creative Commons Attribution License (CC BY). The use, distribution or reproduction in other forums is permitted, provided the original author(s) or licensor are credited and that the original publication in this journal is cited, in accordance with accepted academic practice. No use, distribution or reproduction is permitted which does not comply with these terms.



# Nanoparticle Interactions with the Immune System: Clinical Implications for Liposome-Based Cancer Chemotherapy

Ninh M. La-Beck<sup>1\*†</sup> and Alberto A. Gabizon<sup>2\*†</sup>

<sup>1</sup>Department of Immunotherapy and Biotechnology, Texas Tech University Health Sciences Center School of Pharmacy, Abilene, TX, USA, <sup>2</sup>Oncology Institute, Shaare Zedek Medical Center, Hebrew University-School of Medicine, Jerusalem, Israel

## OPEN ACCESS

### Edited by:

Diana Boraschi,  
Consiglio Nazionale Delle  
Ricerche (CNR), Italy

### Reviewed by:

Yang Li,  
University of Colorado Denver, USA  
Jack Rivers-Auty,  
University of Manchester, UK

### \*Correspondence:

Ninh M. La-Beck  
irene.la-beck@ttuhsc.edu;  
Alberto A. Gabizon  
alberto.gabizon@gmail.com

<sup>†</sup>These authors are the sole contributors to this manuscript, with equal contributions.

### Specialty section:

This article was submitted  
to Inflammation,  
a section of the journal  
*Frontiers in Immunology*

Received: 03 February 2017

Accepted: 23 March 2017

Published: 06 April 2017

### Citation:

La-Beck NM and Gabizon AA (2017)  
*Nanoparticle Interactions with the  
Immune System: Clinical  
Implications for Liposome-Based  
Cancer Chemotherapy.*  
*Front. Immunol.* 8:416.  
doi: 10.3389/fimmu.2017.00416

The development of stable and long-circulating liposomes provides protection of the drug cargo from degradation and increases tumor drug delivery, leading to the design of liposome formulations with great potential in cancer therapy. However, despite the sound pharmacologic basis, many liposomal as well as other nanoparticle-based drug formulations have failed to meet regulatory criteria for approval. The question that arises is whether we have missed key liposome–host interactions that can account for the gap between the major pharmacologic advantages in preclinical studies and the modest impact of the clinical effects in humans. We will discuss here the nanoparticle–immune system interactions that may undermine the antitumor effect of the nanodrug formulations and contribute to this gap. To overcome this challenge and increase clinical translation, new preclinical models need to be adopted along with comprehensive immunopharmacologic studies and strategies for patient selection in the clinical phase.

**Keywords:** liposome, immunosuppression, oncology, doxorubicin, alendronate, immune modulation

## INTRODUCTION

In the field of nanomedicine, liposomes are the most common nanocarrier platforms among the approved agents and those under clinical investigation. The development of stable and long-circulating liposomes provides protection of the drug cargo from degradation (1) and increases tumor drug delivery by exploiting the enhanced permeability and retention (EPR) effect (2). This has led to the design of liposome formulations with great potential in cancer therapy. However, despite the sound pharmacologic basis, many of the liposomal drugs as well as other nanoparticle-based drug formulations have failed to meet regulatory criteria for approval or have shown modest effects in phase 3 clinical studies (3–8). In fact, some of the approvals have been based on reduced toxicity rather than increased efficacy. A recent meta-analysis of 14 randomized clinical trials that directly compared the anticancer efficacy of liposomal cytotoxic chemotherapy to their conventional “free” drug formulation found that liposome encapsulation of drugs did not improve objective response rates, progression-free survival, or overall survival in cancer patients (6). This highlights a major roadblock: despite the pharmacological advantages of improved drug delivery, liposome-mediated therapies have largely failed to increase anticancer efficacy over conventional formulations. Yet, they remain attractive delivery platforms due to their ability to considerably improve drug tolerability and decrease toxicity in cancer patients. The question that arises is whether we have missed some

liposome–host interactions that can account for the gap between the major pharmacologic advantages in preclinical studies, on the one hand, and the modest impact of the clinical effects in humans, on the other hand. We will discuss here the possibility that some nanoparticle–immune system interactions may undermine the antitumor effect of the nanodrug formulations and contribute to this gap (Figure 1).

## CLINICAL EVIDENCE OF NANOPARTICLE–IMMUNE INTERACTIONS

Nanoparticles are known to interact with the innate immune system, including the complement system and the mononuclear phagocyte system (MPS) to varying extents, and these interactions with the immune system have significant clinical consequences. They can activate circulating complement proteins (9, 10), leading sometimes to an infusion reaction known as complement activation-related pseudoallergy (CARPA). Blood complement activation by pegylated liposomal doxorubicin (PLD) has been implicated as the cause of acute infusion reactions in cancer patients (11). Importantly, it has been reported that polymer nanoparticles that activate the complement system can promote tumor growth through generation of C5a (12), a complement anaphylatoxin that has been shown to induce tumor growth *via* recruitment of myeloid-derived suppressor cells (MDSCs) (13). Nonetheless, the clinical relevance of this is unclear since the nanoparticles in these studies were engineered to activate complement, whereas all clinically relevant nanoparticles have been designed to limit complement activation. Furthermore, while

most nanoparticles still activate blood complement proteins to some extent, it is not known whether and how much they activate complement in the tumor microenvironment.

In addition to the complement system, the MPS is known to interact extensively with nanoparticles. The MPS is comprised primarily of monocytes and macrophages in the blood, spleen, and liver. These cells, especially when activated, have high phagocytic capacity and normally function to scavenge and clear cellular debris, damaged/apoptotic cells, and foreign materials including bacteria, viruses, and nanoparticles. In cancer patients, peripheral blood monocyte count was found to correlate with PLD clearance rates: a decrease in monocyte count was associated with a decrease in clearance rate (14), suggesting a direct relationship between functionality of the MPS and nanoparticle drug pharmacokinetics (PK). This was further supported by a subsequent clinical study showing that phagocytic capacity of the MPS, as measured by *in vivo* technetium sulfur colloid uptake, correlated with liposome clearance rates in patients (15).

In addition to clearance of debris and foreign particles, the MPS also regulates the adaptive immune response through the antigen-presentation functions of dendritic cells and can stimulate or inhibit T cell proliferation and cytokine responses (16). Hence, it is in theory possible for nanoparticle interactions with the innate immune system to impact adaptive immunity. For example, PLD has been reported to suppress patient sensitization and allergic reactions to carboplatin in patients receiving a combination of both the drugs (17), suggesting that PLD liposomes may have direct or indirect suppressive effects on lymphocytes. However, overall, the interactions between nanoparticles and

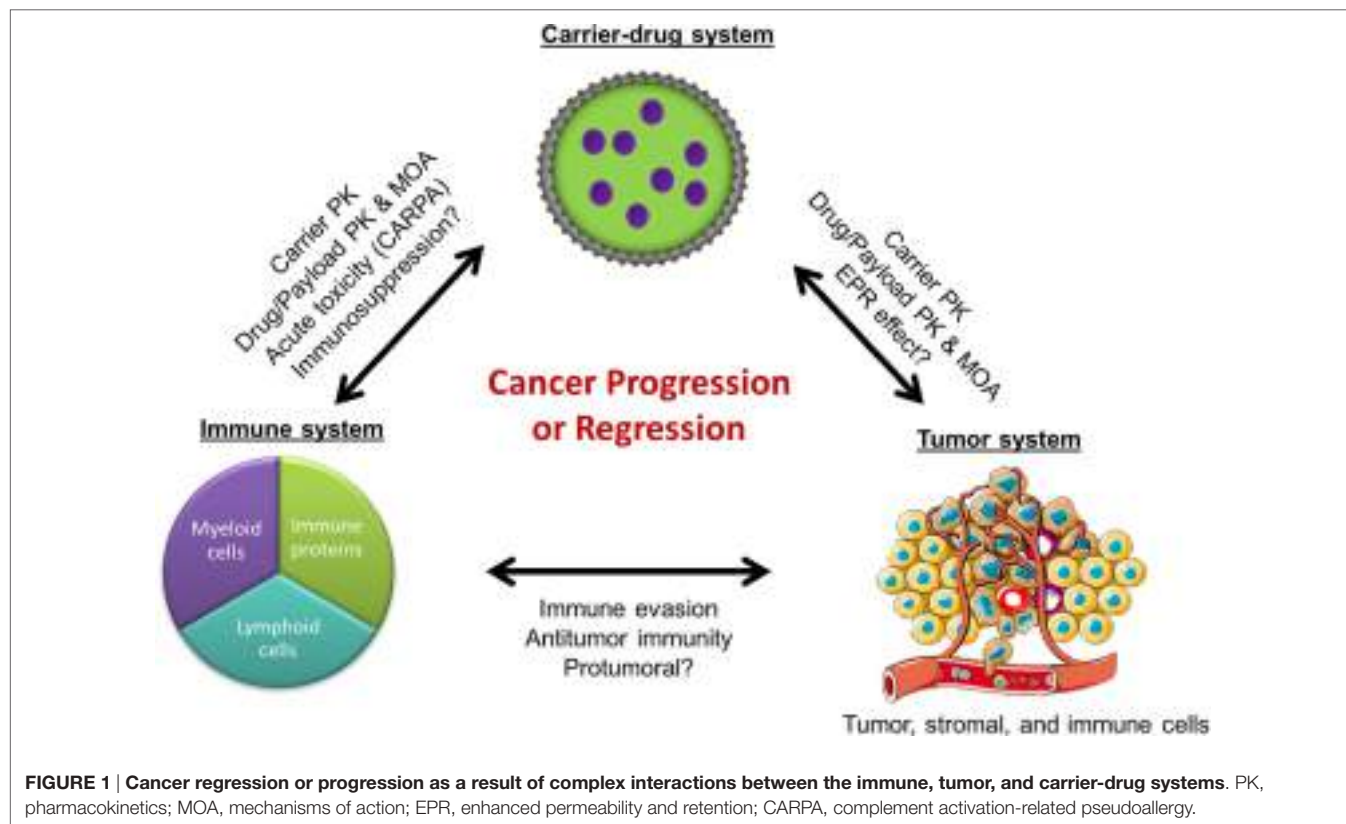


**FIGURE 1 |** Cancer regression or progression as a result of complex interactions between the immune, tumor, and carrier-drug systems. PK, pharmacokinetics; MOA, mechanisms of action; EPR, enhanced permeability and retention; CARPA, complement activation-related pseudoallergy.

the adaptive immune system have received comparatively little attention in clinical trials of carrier-mediated anticancer drugs. One application of nanomedicine that is focused on the adaptive immune system is the use of nanoparticles as vehicles to deliver antigens and boost their immunogenicity as vaccines. The particles used in this context are designed to exploit uptake by antigen-presenting cells, mostly dendritic cells, and thereby enabling induction of antigen-specific adaptive immunity (18). While it is difficult to generalize findings from this field to the cancer drug delivery field, it is clear that nanoparticles have the potential to modulate immune status at the interface between the innate and adaptive immune system.

When considering immunomodulatory carrier-mediated effects, one liposome component that stands out is the polyethylene glycol (PEG) polymer coating used in many liposomal formulations (19). PEG is well known for reducing immunogenicity (20) and for its immunocamouflage properties (21). PEG-modification (pegylation) is generally believed to diminish complement activation responses and evade clearance by the immune system, thereby enabling long circulation of nanoparticles (22). However, PEG has also been found to induce complement activation in this scenario as well (23). In preclinical models, accelerated blood clearance (ABC) of subsequent doses of pegylated liposomes was observed in animals, and this has been associated with the production of anti-PEG antibodies (24). However others have attributed the ABC phenomenon to non-specific binding of PEG to complement proteins, leading to complement activation and subsequent clearance of the particles (25). The clinical relevance of these findings is unclear. Preexisting anti-PEG antibodies may be present in 56–72% of the general population (26), yet the ABC phenomenon has not been reported in humans. Interestingly, the opposite effect, decreased clearance of subsequent doses of doxorubicin-loaded pegylated liposomes, was seen in cancer patients (27). Nonetheless, these reports strongly support a role for PEG in the immunopharmacology of liposome-mediated drugs and highlight critical gaps in current understanding of the mechanisms of PEG–immune interactions in the setting of cancer drug delivery.

## POTENTIAL IMPACT ON CANCER PROGRESSION AND REGRESSION

It is evident that nanoparticle interactions with the immune system affect drug tolerability, immunogenicity, and PK. However, their impact on anticancer efficacy remains to be elucidated. The tumor microenvironment is complex, and tumors are often infiltrated by immune cells such as monocytes, macrophages, and MDSCs, which are believed to have protumoral functions through their inhibition of T cell antitumor responses and enhancement of tumor angiogenesis (28, 29). Interestingly, it was recently reported that a pegylated liposomal drug carrier, similar to that used in patients, significantly enhanced tumor growth in a mouse model of HPV-induced cancer (30). This was associated with suppression of antitumor immunity as indicated by decreased interferon- $\gamma$  production by tumor-associated macrophages and cytotoxic T cells, diminished tumor infiltration of tumor antigen-specific T cells, and decreased number of dendritic

cells in tumor-draining lymph nodes. It is important to point out that these preclinical studies used an immunogenic tumor model and liposomes that did not contain any drug cargo. Therefore, the clinical relevance of these findings is uncertain since human cancers are not always immunogenic, and liposomes always have a drug payload that may affect the immune interactions as well. Yet, these data suggest that the tumor-promoting potential of the carrier may mitigate the benefits of carrier-mediated drug delivery and could partially explain why there is often an insufficient improvement in the clinical efficacy of liposomal drugs over free drugs (4, 5, 7, 31). Clearly, more preclinical and clinical research efforts are needed to elucidate the precise mechanisms by which nanoparticles interact with immune cells, the consequences of this interaction on cancer progression, and the impact of the drug cargo as well as the tumor immunologic milieu on these carrier–immune interactions.

Importantly, recent studies combining liposomal doxorubicin with immune modulatory drugs in mouse models of cancer suggest that this strategy can overcome carrier-associated immunosuppression and even result in synergistic anticancer effects. Co-encapsulation of doxorubicin with alendronate, an amino-bisphosphonate with immune stimulatory effects, in a pegylated liposome showed greater anticancer efficacy than PLD in immunocompetent mouse tumor models (32). Likewise, combining PLD with immune checkpoint inhibitors targeting the PD-1 and CTLA-4 pathways also resulted in enhanced anticancer efficacy as compared to PLD in immunocompetent mice (33). Notably, these combination treatment approaches failed to show improved efficacy over PLD in immunocompromised mice, supporting the pivotal role of the immune system in determining the efficacy of the nanomedicine-based anticancer treatments (33). This host effect was much less important in the case of some low molecular weight drugs such as doxorubicin and gemcitabine. Moreover, all but one mouse with complete tumor response following PLD treatment rejected a rechallenge with the same tumor cells, indicating that they had become immunized (33). Since these observations were done with a cargo of doxorubicin, a drug that is well known for often leading to immunogenic tumor cell death (34), we cannot make extrapolations to other nanomedicines. Nonetheless, clinical trials examining the anticancer efficacy of combined liposomal chemotherapy with immune checkpoint inhibitor antibodies are clearly warranted.

## ARE WE USING THE RIGHT PRECLINICAL MODELS?

If indeed the liposome carriers and/or their drug payload have immunomodulatory effects, then the use of immunocompetent mice is critical for observing the full pharmacologic effect. This entails the use of mouse syngeneic tumor models, since allogeneic xenografts such as human tumors would not grow in immunocompetent mice. In the last two decades, there has been a shift to models based on human tumor xenografts implanted in immunocompromised mice whether athymic mice (lacking T cells), SCID mice (lacking T and B cells), or Beige mice (lacking natural killer lymphocytes), the reasoning being that human tumors will be more predictive of the activity of new drugs in the clinic. This

is probably the case for low molecular weight drugs, but, when more complex systems are used such as nanomedicines, the risk of overlooking an important interaction with the immune system may override any advantage that a human tumor model may offer over a syngeneic tumor, as mentioned above (32, 33).

Among the various immunocompetent mouse models, there are important distinctions in global immune status (e.g., balance of Th1–Th2 cytokines or M1–M2 macrophages) that may affect nanoparticle disposition. The Th1-dominant mouse strains such as C57BL/6 and B10D2 have been reported to have slower rates of clearance of pegylated 300-nm cylindrical hydrogel nanoparticles than the Th2-dominant strains such as BALB/c and DBA/2 (35). These differences in clearance were correlated with increased M1 macrophage polarization and lower particle uptake in Th1-dominant strains, and increased M2 macrophage polarization and higher particle uptake in the Th2-dominant strains. Likewise, when silica nanoparticles were tested *in vitro* with THP1 cells, an immortalized human monocytic cell line, alternatively activated (M2-like) THP1 cells demonstrated higher nanoparticle uptake than classically activated (M1-like) THP1 cells (36). In contrast, another study found that the uptake of pegylated or non-pegylated spherical polystyrene nanoparticles by murine bone marrow-derived macrophages is highest in classically activated M1 macrophages, followed by alternatively activated M2 macrophages, and lowest in unactivated M0 cells (37). There is likely no single ideal mouse model, and selection should take into consideration the clinical immune characteristics of the host, type of cancer, and type of nanoparticle that are being modeled.

To counter the shortfalls of immunocompromised mice as hosts of human tumor xenografts, humanized mouse models, in which the immune system of SCID mice is reconstituted with human bone marrow, have been developed and are being increasingly used particularly in cancer studies that involve immunotherapeutic approaches (38). One step further is the use of patient-derived tumor xenografts (39), instead of the commonly used human tumor cell lines. The testing of nanomedicines in humanized mice is still lagging behind but, conceivably, may provide an important insight on the interplay of nanomedicines with the human immune system.

Another major tumor model factor affecting the testing of nanomedicines is the choice between primary tumor implants and metastatic tumors. Given that the EPR effect is the main mechanism for selective accumulation of nanomedicines in tumors (2), tumor sites with high or poor EPR will respond differently to nanomedicines. This is because the degree of EPR appears to be dependent on the tumor type and on the site of tumor growth (40). Primary tumor implants, particularly those inoculated subcutaneously, recruit new blood vessels for growth and usually demonstrate high EPR. Less well known is the degree of EPR of orthotopically implanted tumors. However, when hematogenous metastases occur either by detachment from primary tumors or by intravenous injection, tumor cells form multiple and separate colonies in lungs and other organs. These tumor colonies grow around well-developed and mature blood vessels of the host organ and often derive their blood supply by a process known as co-option of normal blood vessels, which results in blood vessels

less permeable and less responsive to antiangiogenic treatments and, consequently, less likely to display the EPR effect (41, 42). Clearly, given that the clinical challenge is to treat patients with metastases, an effort should be made to include metastatic tumor models in the testing of nanomedicines to achieve a better prediction of their potential performance in human cancer (43).

## ARE WE USING THE RIGHT CLINICAL TRIAL DESIGNS AND ASSESSMENTS?

Most, if not all, clinical studies with liposome-based chemotherapy and other nanomedicines have been performed without any attempt to select for those cancer patients with tumors that display high liposome uptake. This may have contributed to some disappointing clinical results. For example, in the phase 3 study of PLD against doxorubicin single agent in metastatic breast cancer, no survival advantage was observed (4) despite the clear superiority of PLD in animal tumor models. Recent studies in mouse models using radionuclide SPECT imaging with In<sup>111</sup>-labeled liposomes and PET imaging with Zr<sup>89</sup>-labeled liposomes admixed with PLD have observed that higher tumor uptake of liposomes correlates with greater antitumor activity at the individual level (44, 45). These studies also show a correlation between tumor uptake and tumor microvessel density and reveal remarkable heterogeneity in liposomal tumor accumulation. Based on the preclinical data, one would predict that the efficacy results of clinical studies with stable nanomedicines such as PLD could have been much improved by selection of a patient population with high EPR tumors. By imaging the fate of the nanoparticles, the EPR-dependent tumor uptake of the drug payload can be predicted in each specific case and correlated with the clinical response. This would provide direct clinical data to determine whether or not selecting patients based on the EPR characteristics of their tumor could lead to improved therapeutic benefit of PLD or any other nanoparticle-based therapy (46, 47).

Another aspect of nanomedicines that has not been addressed in clinical studies is the interaction with the immune system. Future clinical studies should incorporate immunopharmacologic tests to gain an insight on these interactions. With liposomes, immunomodulation can occur at least at two different levels:

1. The CARPA reaction has been described in the preceding section of this article. While nanoparticle-induced blood complement activation may be common in patients, CARPA seldom manifests clinically in patients treated with PLD when infusion protocols are carefully followed (11). Nonetheless, we do not know the incidence of subclinical complement activation and whether it may affect the immune system in the local tumor environment.
2. Macrophage function is a major factor in liposome clearance. Liver and spleen macrophages determine systemic clearance, and local tissue macrophages in tumors and other tissues are also important scavengers of extravasated liposomes. Based on this, peripheral blood monocytes have been proposed as a surrogate marker that can predict macrophage-mediated liposome clearance (14). Importantly, nanomedicines that

suppress or activate macrophages either due to carrier-related effects or drug-specific effects may have direct and/or indirect consequences blunting or boosting the ultimate antitumor effect observed.

## FUTURE OUTLOOK

A key roadblock in the development of efficacious cancer therapies is the systemic toxicity of the majority of these agents. Drug delivery using nanoparticle carriers has been an important and valuable strategy in overcoming this challenge by dramatically improving the tolerability of anticancer drugs in patients (48). However, this approach has not yet achieved a sound improvement in clinical efficacy as predicted from its pharmacologic

advantages. We propose that the immune system is a key player in the pharmacology of nanoparticle-based therapy, probably more so than for conventional low molecular weight drugs, and that new understanding of the mechanisms of immune modulation by nanoparticles and their associated drug cargo can lay the foundation for future work that will realize the full clinical potential of cancer nanomedicines.

## FUNDING

NL-B received research funding from the National Institutes of Health (grant #R15CA192097) and the Development Corporation of Abilene. AG received research funding from the Israel Cancer Association and from Lipomedix Pharmaceuticals.

## REFERENCES

- Allen TM, Cullis PR. Liposomal drug delivery systems: from concept to clinical applications. *Adv Drug Deliv Rev* (2013) 65:36–48. doi:10.1016/j.addr.2012.09.037
- Maeda H, Fang J, Inutsuka T, Kitamoto Y. Vascular permeability enhancement in solid tumor: various factors, mechanisms involved and its implications. *Int Immunopharmacol* (2003) 3:319–28. doi:10.1016/S1567-5769(02)00271-0
- Gordon AN, Fleagle JT, Guthrie D, Parkin DE, Gore ME, Lacave AJ. Recurrent epithelial ovarian carcinoma: a randomized phase III study of pegylated liposomal doxorubicin versus topotecan. *J Clin Oncol* (2001) 19:3312–22. doi:10.1200/JCO.2001.19.14.3312
- O'Brien ME, Wigler N, Inbar M, Rosso R, Grischke E, Santoro A, et al. Reduced cardiotoxicity and comparable efficacy in a phase III trial of pegylated liposomal doxorubicin HCl (CAELYX/Doxil) versus conventional doxorubicin for first-line treatment of metastatic breast cancer. *Ann Oncol* (2004) 15:440–9. doi:10.1093/annonc/mdh097
- Gibson JM, Alzghari S, Ahn C, Trantham H, La-Beck NM. The role of pegylated liposomal doxorubicin in ovarian cancer: a meta-analysis of randomized clinical trials. *Oncologist* (2013) 18:1022–31. doi:10.1634/theoncologist.2013-0126
- Petersen GH, Alzghari SK, Chee W, Sankari SS, La-Beck NM. Meta-analysis of clinical and preclinical studies comparing the anticancer efficacy of liposomal versus conventional non-liposomal doxorubicin. *J Control Release* (2016) 232:255–64. doi:10.1016/j.jconrel.2016.04.028
- Lammers T, Kiessling F, Hennink WE, Storm G. Drug targeting to tumors: principles, pitfalls and (pre-) clinical progress. *J Control Release* (2012) 161:175–87. doi:10.1016/j.jconrel.2011.09.063
- Anchordoquy TJ, Barenholz Y, Boraschi D, Chorny M, Decuzzi P, Dobrovolskaia MA, et al. Mechanisms and barriers in cancer nanomedicine: addressing challenges, looking for solutions. *ACS Nano* (2017) 11:12–8. doi:10.1021/acsnano.6b08244
- Dobrovolskaia MA, Aggarwal P, Hall JB, McNeil SE. Preclinical studies to understand nanoparticle interaction with the immune system and its potential effects on nanoparticle biodistribution. *Mol Pharm* (2008) 5:487–95. doi:10.1021/mp800032f
- Szebeni J, Baranyi L, Savay S, Milosevits J, Bunger R, Laverman P, et al. Role of complement activation in hypersensitivity reactions to doxil and hynic PEG liposomes: experimental and clinical studies. *J Liposome Res* (2002) 12:165–72. doi:10.1081/LPR-120004790
- Chanan-Khan A, Szebeni J, Savay S, Liebes L, Rafique NM, Alving CR, et al. Complement activation following first exposure to pegylated liposomal doxorubicin (Doxil): possible role in hypersensitivity reactions. *Ann Oncol* (2003) 14:1430–7. doi:10.1093/annonc/mdg374
- Moghimi SM. Cancer nanomedicine and the complement system activation paradigm: anaphylaxis and tumour growth. *J Control Release* (2014) 190:556–62. doi:10.1016/j.jconrel.2014.03.051
- Markiewski MM, DeAngelis RA, Benencia F, Ricklin-Lichtsteiner SK, Koutoulaki A, Gerard C, et al. Modulation of the antitumor immune response by complement. *Nat Immunol* (2008) 9:1225–35. doi:10.1038/ni.1655
- La-Beck NM, Zamboni BA, Gabizon A, Schmeeda H, Amantea M, Gehrig PA, et al. Factors affecting the pharmacokinetics of pegylated liposomal doxorubicin in patients. *Cancer Chemother Pharmacol* (2012) 69:43–50. doi:10.1007/s00280-011-1664-2
- Caron WP, Lay JC, Fong AM, La-Beck NM, Kumar P, Newman SE, et al. Translational studies of phenotypic probes for the mononuclear phagocyte system and liposomal pharmacology. *J Pharmacol Exp Ther* (2013) 347: 599–606. doi:10.1124/jpet.113.208801
- Sukari A, Nagasaki M, Al-Hadidi A, Lum LG. Cancer immunology and immunotherapy. *Anticancer Res* (2016) 36:5593–606. doi:10.21873/anticancres.11144
- Markman M, Moon J, Wilczynski S, Lopez AM, Rowland KM Jr, Michelin DP, et al. Single agent carboplatin versus carboplatin plus pegylated liposomal doxorubicin in recurrent ovarian cancer: final survival results of a SWOG (S0200) phase 3 randomized trial. *Gynecol Oncol* (2010) 116:323–5. doi:10.1016/j.ygyno.2009.11.026
- Gregory AE, Titball R, Williamson D. Vaccine delivery using nanoparticles. *Front Cell Infect Microbiol* (2013) 3:13. doi:10.3389/fcimb.2013.00013
- Milla P, Dosio F, Cattell L. PEGylation of proteins and liposomes: a powerful and flexible strategy to improve the drug delivery. *Curr Drug Metab* (2012) 13:105–19. doi:10.2174/138920012798356934
- Veronese FM, Mero A. The impact of PEGylation on biological therapies. *BioDrugs* (2008) 22:315–29. doi:10.2165/00063030-200822050-00004
- Chen AM, Scott MD. Current and future applications of immunological attenuation via pegylation of cells and tissue. *BioDrugs* (2001) 15:833–47. doi:10.2165/00063030-200115120-00005
- Gref R, Luck M, Quellec P, Marchand M, Dellacherie E, Harnisch S, et al. ‘Stealth’ corona-core nanoparticles surface modified by polyethylene glycol (PEG): influences of the corona (PEG chain length and surface density) and of the core composition on phagocytic uptake and plasma protein adsorption. *Colloids Surf B Biointerfaces* (2000) 18:301–13. doi:10.1016/S0927-7765(99)00156-3
- Verhoef JJ, Anchordoquy TJ. Questioning the use of PEGylation for drug delivery. *Drug Deliv Transl Res* (2013) 3:499–503. doi:10.1007/s13346-013-0176-5
- Ichihara M, Shimizu T, Imoto A, Hashiguchi Y, Uehara Y, Ishida T, et al. Anti-PEG IgM response against PEGylated liposomes in mice and rats. *Pharmaceutics* (2010) 3:1–11. doi:10.3390/pharmaceutics3010001
- Schellekens H, Hennink WE, Brinks V. The immunogenicity of polyethylene glycol: facts and fiction. *Pharm Res* (2013) 30:1729–34. doi:10.1007/s11095-013-1067-7
- Yang Q, Jacobs TM, McCallen JD, Moore DT, Huckaby JT, Edelstein JN, et al. Analysis of pre-existing IgG and IgM antibodies against polyethylene glycol (PEG) in the general population. *Anal Chem* (2016) 88:11804–12. doi:10.1021/acs.analchem.6b03437
- Gabizon A, Isacson R, Rosengarten O, Tzemach D, Shmeeda H, Sapir R. An open-label study to evaluate dose and cycle dependence of the pharmacokinetics of pegylated liposomal doxorubicin. *Cancer Chemother Pharmacol* (2008) 61:695–702. doi:10.1007/s00280-007-0525-5
- Mantovani A, Sozzani S, Locati M, Allavena P, Sica A. Macrophage polarization: tumor-associated macrophages as a paradigm for polarized M2

- mononuclear phagocytes. *Trends Immunol* (2002) 23:549–55. doi:10.1016/S1471-4906(02)02302-5
29. Gabrilovich DI, Nagaraj S. Myeloid-derived suppressor cells as regulators of the immune system. *Nat Rev Immunol* (2009) 9:162–74. doi:10.1038/nri2506
30. Sabnani MK, Rajan R, Rowland B, Mavinkurve V, Wood LM, Gabizon AA, et al. Liposome promotion of tumor growth is associated with angiogenesis and inhibition of antitumor immune responses. *Nanomedicine* (2015) 11:259–62. doi:10.1016/j.nano.2014.08.010
31. Markman M, Gordon AN, McGuire WP, Muggia FM. Liposomal anthracycline treatment for ovarian cancer. *Semin Oncol* (2004) 31:91–105. doi:10.1053/j.seminoncol.2004.08.004
32. Shmeeda H, Amitay Y, Gorin J, Tzemach D, Mak L, Stern ST, et al. Coencapsulation of aleandronate and doxorubicin in pegylated liposomes: a novel formulation for chemoimmunotherapy of cancer. *J Drug Target* (2016) 24(9):878–89. doi:10.1080/1061186X.2016.1191081
33. Rios-Doria J, Durham N, Wetzel L, Rothstein R, Chesebrough J, Holowecyk N, et al. Doxil synergizes with cancer immunotherapies to enhance antitumor responses in syngeneic mouse models. *Neoplasia* (2015) 17:661–70. doi:10.1016/j.neo.2015.08.004
34. Zitvogel L, Apetoh L, Ghiringhelli F, Kroemer G. Immunological aspects of cancer chemotherapy. *Nat Rev Immunol* (2008) 8:59–73. doi:10.1038/nri2216
35. Jones SW, Roberts RA, Robbins GR, Perry JL, Kai MP, Chen K, et al. Nanoparticle clearance is governed by Th1/Th2 immunity and strain background. *J Clin Invest* (2013) 123:3061–73. doi:10.1172/JCI66895
36. Hoppstadter J, Seif M, Dembek A, Cavelius C, Huwer H, Kraegeloh A, et al. M2 polarization enhances silica nanoparticle uptake by macrophages. *Front Pharmacol* (2015) 6:55. doi:10.3389/fphar.2015.00055
37. Qie Y, Yuan H, von Roemeling CA, Chen Y, Liu X, Shih KD, et al. Surface modification of nanoparticles enables selective evasion of phagocytic clearance by distinct macrophage phenotypes. *Sci Rep* (2016) 6:26269. doi:10.1038/srep26269
38. Morton JJ, Bird G, Refaeli Y, Jimeno A. Humanized mouse xenograft models: narrowing the tumor-microenvironment gap. *Cancer Res* (2016) 76:6153–8. doi:10.1158/0008-5472.CAN-16-1260
39. Izumchenko E, Meir J, Bedi A, Wysocki PT, Hoque MO, Sidransky D. Patient-derived xenografts as tools in pharmaceutical development. *Clin Pharmacol Ther* (2016) 99:612–21. doi:10.1002/cpt.354
40. Prabhakar U, Maeda H, Jain RK, Sevick-Muraca EM, Zamboni W, Farokhzad OC, et al. Challenges and key considerations of the enhanced permeability and retention effect for nanomedicine drug delivery in oncology. *Cancer Res* (2013) 73:2412–7. doi:10.1158/0008-5472.CAN-12-4561
41. Nagy JA, Dvorak HF. Heterogeneity of the tumor vasculature: the need for new tumor blood vessel type-specific targets. *Clin Exp Metastasis* (2012) 29:657–62. doi:10.1007/s10585-012-9500-6
42. Donnem T, Hu J, Ferguson M, Adighibe O, Snell C, Harris AL, et al. Vessel co-option in primary human tumors and metastases: an obstacle to effective anti-angiogenic treatment? *Cancer Med* (2013) 2:427–36. doi:10.1002/cam4.105
43. Kerbel RS. A decade of experience in developing preclinical models of advanced- or early-stage spontaneous metastasis to study antiangiogenic drugs, metronomic chemotherapy, and the tumor microenvironment. *Cancer J* (2015) 21:274–83. doi:10.1097/PPO.0000000000000134
44. Ito K, Hamamichi S, Asano M, Hori Y, Matsui J, Iwata M, et al. Radiolabeled liposome imaging determines an indication for liposomal anticancer agent in ovarian cancer mouse xenograft models. *Cancer Sci* (2016) 107:60–7. doi:10.1111/cas.12841
45. Perez-Medina C, Abdel-Atti D, Tang J, Zhao Y, Fayad ZA, Lewis JS, et al. Nanoreporter PET predicts the efficacy of anti-cancer nanotherapy. *Nat Commun* (2016) 7:11838. doi:10.1038/ncomms11838
46. Petersen AL, Hansen AE, Gabizon A, Andresen TL. Liposome imaging agents in personalized medicine. *Adv Drug Deliv Rev* (2012) 64:1417–35. doi:10.1016/j.addr.2012.09.003
47. Gabizon A, Bradbury M, Prabhakar U, Zamboni W, Libutti S, Grodzinski P. Cancer nanomedicines: closing the translational gap. *Lancet* (2014) 384:2175–6. doi:10.1016/S0140-6736(14)61457-4
48. Gabizon AA, Patil Y, La-Beck NM. New insights and evolving role of pegylated liposomal doxorubicin in cancer therapy. *Drug Resist Updat* (2016) 29:90–106. doi:10.1016/j.drup.2016.10.003

**Conflict of Interest Statement:** The authors declare that the research was conducted in the absence of any commercial or financial relationships that could be construed as a potential conflict of interest.

The handling editor declared a past coauthorship with the authors and states that the process nevertheless met the standards of a fair and objective review.

Copyright © 2017 La-Beck and Gabizon. This is an open-access article distributed under the terms of the Creative Commons Attribution License (CC BY). The use, distribution or reproduction in other forums is permitted, provided the original author(s) or licensor are credited and that the original publication in this journal is cited, in accordance with accepted academic practice. No use, distribution or reproduction is permitted which does not comply with these terms.



# Advanced Strategies in Immune Modulation of Cancer Using Lipid-Based Nanoparticles

**Shoshy Mizrahy**<sup>1,2,3,4</sup>, **Inbal Hazan-Halevy**<sup>1,2,3,4</sup>, **Dalit Landesman-Milo**<sup>1,2,3</sup>, **Brandon D. Ng**<sup>1,2,3,4</sup> and **Dan Peer**<sup>1,2,3,4\*</sup>

<sup>1</sup>Laboratory of Precision NanoMedicine, Department of Cell Research and Immunology, George S. Wise Faculty of Life Sciences, Tel Aviv University, Tel Aviv, Israel, <sup>2</sup>Department of Materials Sciences and Engineering, Iby and Aladar Fleischman Faculty of Engineering, Tel Aviv University, Tel Aviv, Israel, <sup>3</sup>Center for Nanoscience and Nanotechnology, Tel Aviv University, Tel Aviv, Israel, <sup>4</sup>Cancer Biology Research Center, Tel Aviv University, Tel Aviv, Israel

Immunotherapy has a great potential in advancing cancer treatment, especially in light of recent discoveries and therapeutic interventions that lead to complete response in specific subgroups of melanoma patients. By using the body's own immune system, it is possible not only to specifically target and eliminate cancer cells while leaving healthy cells unharmed but also to elicit long-term protective response. Despite the promise, current immunotherapy is limited and fails in addressing all tumor types. This is probably due to the fact that a single treatment strategy is not sufficient in overcoming the complex antitumor immunity. The use of nanoparticle-based system for immunotherapy is a promising strategy that can simultaneously target multiple pathways with the same kinetics to enhance antitumor response. Here, we will highlight the recent advances in the field of cancer immunotherapy that utilize lipid-based nanoparticles as delivery vehicles and address the ongoing challenges and potential opportunities.

## OPEN ACCESS

### Edited by:

Diana Boraschi,  
National Research Council, Italy

### Reviewed by:

Yang Li,  
University of Colorado Denver, USA  
Ji Ho Park,  
KAIST, South Korea

### \*Correspondence:

Dan Peer  
peer@tauex.tau.ac.il

### Specialty section:

This article was submitted to  
Inflammation,  
a section of the journal  
*Frontiers in Immunology*

**Received:** 26 November 2016

**Accepted:** 16 January 2017

**Published:** 06 February 2017

### Citation:

Mizrahy S, Hazan-Halevy I, Landesman-Milo D, Ng BD and Peer D (2017) Advanced Strategies in Immune Modulation of Cancer Using Lipid-Based Nanoparticles. *Front. Immunol.* 8:69.  
doi: 10.3389/fimmu.2017.00069

## INTRODUCTION

### Tumor Immunology

Hundred years after Paul Ehrlich coined the term "magic bullet," it is well established that the immune system can be utilized in the epic battle against cancer. Immune cells possess a unique ability to distinguish between cancer and normal cells with reliance on specific expression of cell-surface tumor-associated antigens (TAA) or self-antigens. Due to this ability, immune cells can act as "killing bullets" that are able to specifically eliminate tumors cells.

The development of a tumor is a dynamic process whereby the immune system not only protects against cancer development but also shapes the character of emerging tumors, a process named "Cancer Immunoediting." This complex process can be divided to three phases according to the nature of the interaction of tumor cells with the immune system: elimination, equilibrium, and escape (1).

In the elimination phase, both the innate and adaptive immune systems detect and destroy early tumors (2). Tumor cells express TAA-derived peptides in context of MHC molecules that are recognized by TAA-specific-cytotoxic CD8<sup>+</sup>T-lymphocytes (CTL). Activated CTL and natural killer (NK) cells directly induce tumor cell apoptosis and, in addition, release IFN-γ that mediates inhibition of tumor-cell proliferation and angiogenesis. Antigen-presenting cells (APCs),

such as tumor-associated macrophages (TAMs) and dendritic cells (DC), take up TAAs from tumor cells debris and present their peptides in the context of MHC to TAA-specific CD8<sup>+</sup> and CD4<sup>+</sup>T-lymphocytes. Activated CD4<sup>+</sup>T-lymphocytes produce inflammatory cytokines such as, IFN- $\gamma$  and TNF- $\alpha$ , that can both suppress tumor survival and upregulate the expression of MHC molecules on the surface of tumor cells. This upregulation facilitates the recognition of cancer cells by CTL, which mediates their killing mechanism (1, 3).

The equilibrium phase is a balance phase upon which tumor progression is still controlled by the immune system; however, sporadic tumor cells manage to survive immune destruction (1, 4).

In the escape phase, tumors manage to evade immune surveillance, begin to grow progressively and establish an immunosuppressive tumor microenvironment (TME) (1, 5, 6). In this phase, tumor cells acquire the ability to escape from host immune response through different strategies; first, tumor cells downregulate MHC expression, thus preventing recognition and attack by CTL (7). Second, tumor cells upregulate their expression of immune checkpoints proteins, such as PD-L1 and CD80/CD86, which ligate the negative co-stimulators PD1 and CTLA4 on the T-lymphocyte's membrane. This results in attenuation of T-lymphocytes activation (8, 9). Furthermore, tumor cells induce the infiltration of other cell types (fibroblasts, endothelial, and immune cells) and instruct them to establish TME that promotes tumor progression (10). For example, infiltration of regulatory T-cells (Tregs) into the TME inhibits CTL (11). Finally, tumor cells encourage cells in TME to release anti-inflammatory cytokines, such as IL-10 and TGF- $\beta$ . These cytokines suppress the ability of resident immune cells to act against tumor cells, prevent the recruitment of CTL and NK cells, and, therefore, promote tumor growth (12).

In the past few years, the rapidly advancing field of cancer immunotherapy has produced several new opportunities for treating cancer: either by stimulating the activities of specific components of the immune system or by counteracting immunosuppressive signals produced by tumor cells. Efficient anti-tumor immunotherapy can be achieved by combining delivery of TAAs to APC along with removing tumor-derived negative regulators of immune cell activation (13, 14). Therefore, delivery of immunomodulatory molecules to the appropriate cells is crucial for the successful development of cell-based antitumor immunotherapy.

## Nanotechnology-Based Therapies

Nanotechnology affords a unique opportunity to deliver therapeutic molecules to specific cells and simultaneously attack several biological avenues promoting tumor eradication (15). A variety of delivery platform vehicles are under development to target immune cells, such as antibodies (16), polymers (17), aptamers (18), and lipid nanoparticles (LNPs) (19, 20). In comparison to other NPs, LNPs have attractive biological properties, which include general biocompatibility, biodegradability, and the ability to entrap both hydrophilic and hydrophobic drugs (15, 21). Multiple properties of LNPs can be altered *via* different lipid composition and ratios or by surface

chemistry, including their size, charge, and surface functionality (22). LNPs serve as carriers for a variety of therapeutic molecules: from nucleic acid to proteins, small molecules and chemotherapy drugs, and combinations of the aforementioned agents (22–24). LNPs shelter their cargo from clearance in the surrounding biological milieu, increasing the half-life in circulation, minimizing systemic toxicity, and hence enabling a wide therapeutic window (15, 22, 25). In addition, LNPs can promote delivery of their cargo directly to specific immune cell, such as APC or T-lymphocytes (20, 26, 27). Here, we review the latest developments in nanoparticle-based cancer immunotherapy, centering on LNPs.

## THE EFFECTS OF THE PHYSICOCHEMICAL PROPERTIES OF LNPs ON IMMUNE MODULATION

The physicochemical characteristics of LNPs are crucial for their fate and performance following administration. Several parameters were examined including nanoparticle size, shape, surface charge, lipid composition, and aggregation. Size is one of the major causes for immune stimulation by LNPs. This can be related to the fact that these nanoparticles fall within the size range of pathogens, such as viruses and small bacteria (28). Size has a significant impact on blood circulation half-life as an optimal vesicle should be large enough to avoid renal clearance but small enough to avoid clearance *via* the mononuclear phagocytic system (15). The size of NPs should be also adjusted in accordance to the route of administration and delivery purposes. For example, it was shown that, following intravenous administration, 25 nm size NPs are significantly more efficient than 100 nm-sized NPs, as these smaller nanoparticles are better delivered to the lymph nodes (29). In addition, size of below 100 nm enables NPs to utilize the enhanced permeability and retention effect characteristic of solid tumors. Below 100 nm, NPs can reach solid tumors by extravasation *via* the leaky tumor vasculature and accumulate due to poor lymphatic drainage (15).

The shape and curvature of NPs can also affect immune activation as it was shown that oblate-shaped NPs have a lower macrophage uptake in comparison to spherical nanoparticles and, therefore, longer circulation time and altered biodistribution (30).

Surface features of LNPs have also been thoroughly investigated. Surface charge is another major contributor of immune activation, as positively charged LNPs can better interact with the negatively charged mucosal surface. This results in better uptake of positively charged LNPs by cells in comparison to their negatively charged or neutral counterparts (31). However, positively charged LNPs have toxic effects including induction of pro-inflammatory response (32). Surface charge (both negative and positive) and high membrane cholesterol content are also related to complement activation by liposomes (28). Contrarily, the presence of phosphatidylserine (PS) has an anti-inflammatory effect probably due to specific recognition by PS receptors (33, 34).

Surface functionalization has been widely used to improve LNPs performance. One of the main causes for the immune recognition of LNPs is the absence of self-discriminating molecules (such as complement control proteins) on the bilayer membrane, which protect “self” cells from attack by the complement system (28). Among the most common of these are hydrophilic moieties, such as polyethylene glycol (PEG), which enables prolonged blood circulation time and improved biodistribution by protecting NPs from opsonization (15). Despite the multiple advantages, functionalization with PEG can induce complement activation (5, 35, 36). In addition, subsequent injections of PEGylated liposomes can result in their accelerated blood clearance, probably due to transient IgM production (37). Another option for hydrophilic surface coating is polysaccharides. These naturally occurring molecules are a great alternative as they are characterized by low toxicity, low immunogenicity, biocompatibility, stability, low cost, cryoprotection, and availability of reactive sites for chemical modification (38). A specific example is hyaluronan (HA), which is also characterized by bioadhesive properties as part of the extracellular matrix. In addition, HA is the major ligand for CD44 and CD168 receptors and, therefore, suitable for specific targeting to cells, such as those in tumors that overexpress these receptors (39–42).

Additional surface functionalization includes ligands that enable specific cell targeting, such as antibodies, peptides, and aptamers (15). However, despite the advantage, LNPs decorated with proteins or peptides can elicit an unwanted immune

response, cross link receptors, and generate an outside-in signaling cascade (43–45).

There are additional factors that induce immune activation of LNPs; among these are inhomogeneity of size or shape, multilamellar structure, endotoxin contamination, aggregation, and the presence of non-encapsulated drugs that can bind and aggregate lipids. Ultimately, it seems that the longest circulation time is obtained using LNPs that better mimic natural membranes. Therefore, there are increasing efforts to create LNPs using natural materials and even natural membrane-derived LNPs. Recently, Rodriguez et al. have shown that surface modification of LNPs with a “self” peptide segment of CD47 resulted in reduced blood clearance by macrophages and, therefore, longer circulation time (46, 47).

The vast progress in the field of drug delivery enables tailoring specific NPs for a particular location (TME, lymph nodes) and cell type while avoiding unwanted non-specific immune responses and toxicities as detailed below.

## LNP-BASED IMMUNOTHERAPIES

### Immunomodulation of APCs

Therapeutic anticancer vaccination is a strategy that attempts to improve host immunity to cancer by upregulating host immune response against TAAs. Tumor vaccines deliver the antigen and/or adjuvant to APCs for the activation of both humoral and cellular immunity as presented in **Figure 1**.

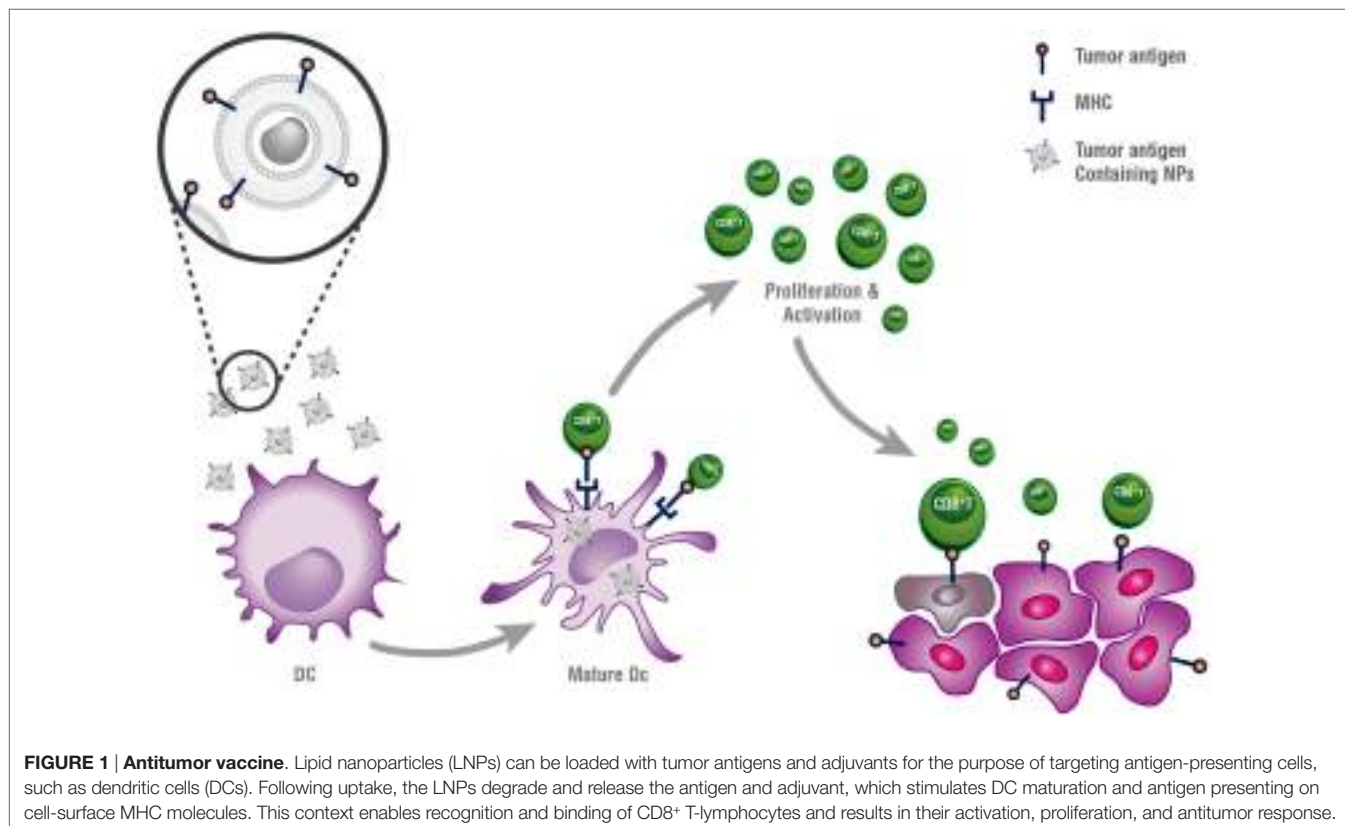


**FIGURE 1 | Antitumor vaccine.** Lipid nanoparticles (LNPs) can be loaded with tumor antigens and adjuvants for the purpose of targeting antigen-presenting cells, such as dendritic cells (DCs). Following uptake, the LNPs degrade and release the antigen and adjuvant, which stimulates DC maturation and antigen presenting on cell-surface MHC molecules. This context enables recognition and binding of CD8<sup>+</sup> T-lymphocytes and results in their activation, proliferation, and antitumor response.

NP delivery can significantly boost immunogenicity of tumor antigens by co-delivery of antigens and adjuvants to the same location (48). One such platform is interbilayer-crosslinked multilamellar vesicles (ICMVs), which entrap high amounts of protein antigens in the vesicle core and lipid-based adjuvant in the vesicle walls (49). The authors found that ICMVs elicited robust antibody titers greater than simple liposomes or multi-lamellar vesicles of identical lipid compositions. These synthetic vesicles triggered steadily increasing antibody production and CTL responses following repeated administrations.

Several NP-based vaccine formulations have been developed to deliver antigens specifically to APCs, especially to DCs and TAMs. Recently, Kranz et al. (50) used RNA-lipoplexes (RNA-LPX), which are LNPs encapsulated with an RNA-encoded antigen, for systemic targeting of DCs. Targeting the DCs by RNA-LPX is based on optimally adjusting the net charge of the LNPs without functionalization of particles. RNA-LPX encoding antigens induce strong effector and memory T-cell responses and mediate potent IFN $\alpha$ -dependent rejection of progressive tumors. Leuschner et al. developed LNPs platform encapsulated with siRNA for modulation of monocytes and macrophages (51). The authors used this platform to encapsulate siRNA against CCR2, an important monocyte homing factor, and tested it in a mouse lymphoma model. Systemic administration of these nanoparticles resulted in a lower numbers of TAMs and reduction of tumor size.

Others have shown targeting of DCs using NPs decorated by specific anti DC antibodies. For example, Macho-Fernandez et al. (52) used NPs generated from poly lactic-co-glycolic acid (PLGA), coated with lipid-PEG and decorated by Abs recognizing DEC205, a cell-surface receptor that is expressed on spleen and lymph node CD8 $^{+}$ DCs. Using these NPs, they have demonstrated that co-delivery of an agonist (a-GalCer) and a protein antigen (ovalbumin) to CD8 $^{+}$ DCs triggers optimal humoral and CTL responses. In addition, this platform promotes potent antitumor responses in a B16F10 murine melanoma tumor model.

## Immunomodulation of Tumor Cells and TME

Over time, cancer cells can develop phenotypes that are less immunogenic in order to escape immune surveillance. One strategy used by cancer cells is an elevated expression of self-markers to avoid immune recognition by professional phagocytes. An example of using this strategy is the over expression of CD47 on the cancer cell surface, which labels the cells with the “self” marker and correlates with poor clinical prognosis (53–55). Yang et al. developed a systemic delivery strategy based on CD47 siRNA encapsulated in HA-coated LNPs, which led to an efficient knockdown of CD47 in cancer cells. Decreased expression of CD47 eventually led to growth inhibition of melanoma tumors and suppressed lung metastasis in a B16F10 murine melanoma tumor model (56).

Additional strategy used by cancer cells to avoid immune recognition is secretion of anti-inflammatory cytokines. Anti-inflammatory cytokines prevent the recruitment of immune cells to the TME and suppress the ability of resident immune cells to

act against tumor cells. In order to block these complex interactions, immune modulation based on targeting both the tumor cells and DCs was developed by Xu et al. (57). They delivered a combination of NPs: liposome-protamine-HA NPs encapsulated with siRNA against the immune-suppressive cytokine TGF- $\beta$ , and mannose-modified lipid-calcium-phosphate NPs encapsulated with tumor antigen and adjuvant. TGF- $\beta$  downregulation boosted the vaccine efficacy and inhibited tumor growth, as a result of increased levels of tumor infiltrating CD8 $^{+}$  T-lymphocytes and decreased level of Tregs.

A liposomal polymeric gel system developed by Park et al., which combines the delivery of TGF- $\beta$  inhibitor and the pro-inflammatory cytokine IL-2, is another example for a complex approach of immunomodulation (Figure 2) (58). IL-2 was shown to enhance NK and CTL activity against several cancer types; however, this ability is hampered due to the secretion of anti-inflammatory agents, such as TGF- $\beta$  by tumor cells (59). The authors showed a significant reduction of tumor growth *in vivo* and an increased immune response.

Another example of combining several immunotherapy strategies was recently presented by Moynihan et al. (61). The authors used the amphiphilic vaccine platform containing a tumor antigen and adjuvant conjugated to albumin binding lipid. This enables utilizing the “albumin hitchhiking” strategy upon which binding with albumin directly targets molecules to lymphatics and draining LNs, thereby allowing them to accumulate in APCs. This platform was combined with systemic administration of tumor antigen-specific antibodies, IL-2, and anti-PD-1 antibodies. The authors showed recruitment of both innate and adaptive immune cells that led to elimination of large established tumor burdens in syngeneic and genetically engineered murine tumor models. The treatment also elicited long protective T cell memory response.

## SEQUENTIAL TREATMENT OF CHEMOTHERAPY FOLLOWED BY IMMUNOTHERAPY

A combined chemo-immunotherapeutic approach may be beneficial for the efficient elimination of cancer. Chemotherapy eliminates tumor cells, causing the cancer to shrink. As a result, tumor-derived antigens, such as peptides or proteins isolated from the tumor cells, can be efficiently internalized by APCs, thereby increasing the antitumor immunity of CTL. Lu et al. (62) developed cisplatin LNPs and CpG-encapsulated liposomes for treatment of melanoma. Such combination therapy established strong synergistic effects, both on the apoptotic level and subsequent abrogation of tumor growth. Heo et al. (63) sequentially subjected tumor-bearing mice to chemotherapy consisting of paclitaxel dissolved in HA in addition to immunotherapy using CpG ODNs and IL-10 siRNA incorporated into PLGA NPs. The sequential treatment with chemotherapeutic drugs followed by a combined immunostimulation strategy resulted in a synergistic effect against solid tumors.

A recent study by He et al. designed coordination polymer LNPs, which combines two therapeutic modalities,

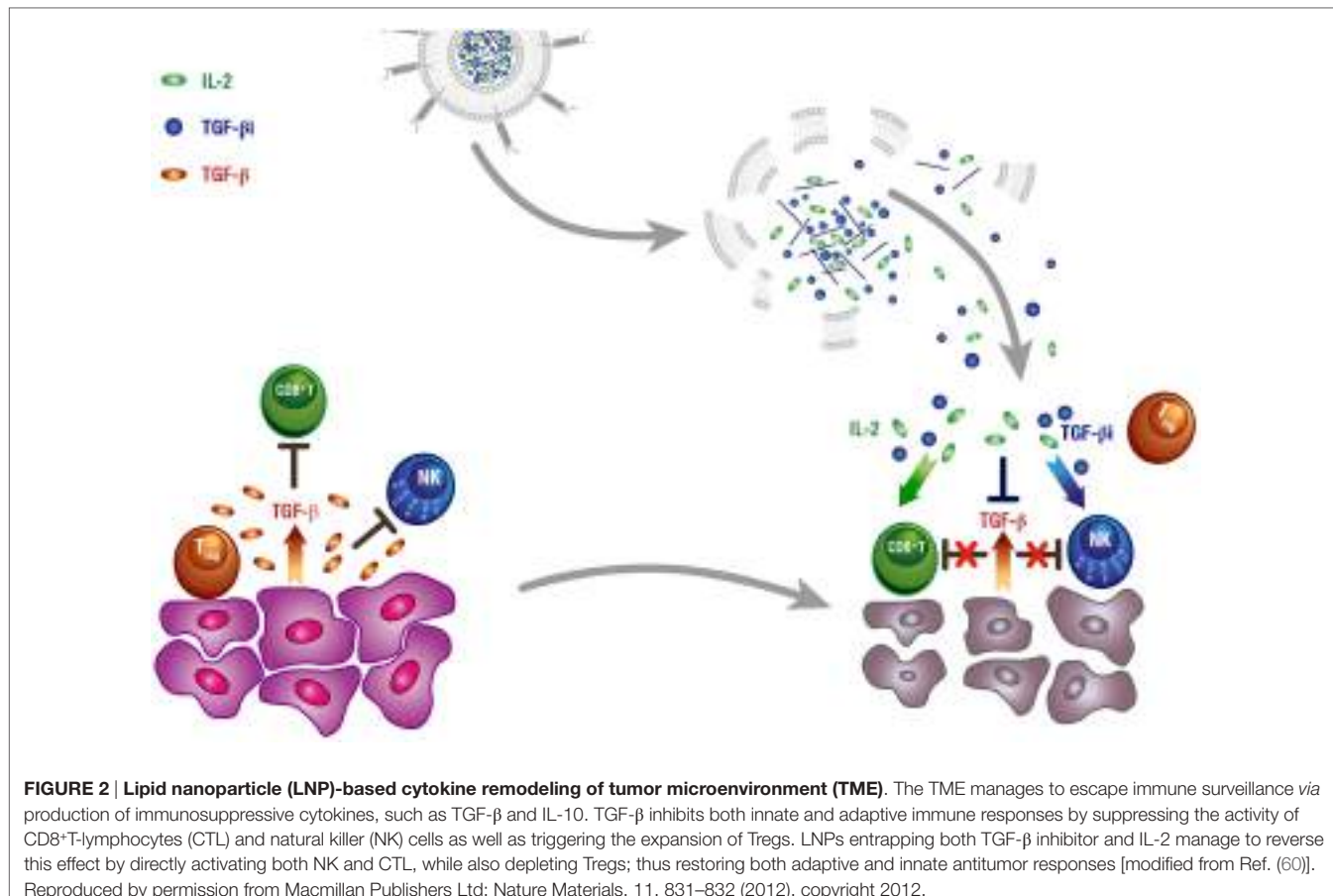


**FIGURE 2 | Lipid nanoparticle (LNP)-based cytokine remodeling of tumor microenvironment (TME).** The TME manages to escape immune surveillance via production of immunosuppressive cytokines, such as TGF- $\beta$  and IL-10. TGF- $\beta$  inhibits both innate and adaptive immune responses by suppressing the activity of CD8 $^{+}$ T-lymphocytes (CTL) and natural killer (NK) cells as well as triggering the expansion of Tregs. LNPs entrapping both TGF- $\beta$  inhibitor and IL-2 manage to reverse this effect by directly activating both NK and CTL, while also depleting Tregs; thus restoring both adaptive and innate antitumor responses [modified from Ref. (60)]. Reproduced by permission from Macmillan Publishers Ltd: Nature Materials, 11, 831–832 (2012), copyright 2012.

chemotherapy and photodynamic therapy, to elicit antitumor immunity (64). These LNPs kill cancer cells by inducing apoptosis and necrosis, stimulating host immune system, and causing an acute inflammation and leukocyte infiltration to the tumors; all of which increase the presentation of tumor-derived antigens to T cells. Combining polymer NPs treatment with PD-L1 checkpoint blockade therapy led to the regression of the primary tumors treated locally with irradiation, and also resulted in the regression of the distant tumors in bilateral syngeneic mouse tumor models of CT26 and MC38.

## CONCLUSION AND FUTURE OUTLOOK

Cancer immunotherapy has been getting a lot of attention in the past few years and for many good reasons. There are multiple benefits for immunotherapy in comparison to conventional medicine, as the former treatment modality enables utilization of the immune system to eliminate tumor cells, while leaving healthy cells untouched. As our understanding of the complex interplay between cancer cells and the immune system deepens, the potential for achieving efficient therapeutics grows. Advances in research in the past few years have provided a solid basis for the development of several therapeutic strategies on the basis of targeting specific pathways and checkpoints. Further understanding of the immunosuppressive TME and

antitumor immunity is the key for successful treatments and avoiding unfavorable outcome such as induction of autoimmunity.

NP-based immunotherapy provides multiple advantages upon administration of immune modulators since it enables targeted delivery both locally and temporally, therefore enhancing the effectiveness and reducing toxicity. It also enables transport of several compounds simultaneously and delivery of RNAi-based therapeutics, significantly increasing the therapeutic index.

A successful immunotherapy requires both innate and adoptive responses. Tumor cells utilize several mechanisms to escape immune recognition and induce immune-suppressive TME; thus, tackling only one pillar would not be sufficient. This may be responsible for the limited clinical achievements of current immunotherapy. Indeed, recent treatments combining several immune effectors were reported to be synergistic. The identification of the optimal combination of NPs and immune modulators for the appropriate TME is also crucial, and further development may be aided by the use of computerized biology. Improvement of currently used murine tumor models to appropriately reflect the complex TME is also required. Many reports are treating early-stage tumors in which the immune-suppressive TME is not completely developed. In addition, direct manipulation of tumor-residing lymphocytes has not yet been achieved and

the appropriate delivery system is still an unmet need. This is especially significant in light of the recently approved anti-T-lymphocyte treatments (anti-CTLA-4 and anti-PD-1 antibodies) that emphasize the potential of T-lymphocyte modulation for immunotherapy. Currently, lymphocyte manipulation can be achieved indirectly via specific modulators; and direct targeting of specific subsets of APCs has already been demonstrated. Some reports even show this simply by controlling lipid composition or charge, avoiding the use of targeting moieties altogether. The effectiveness of such untargeted systems in humans still has yet to be determined. To date, impressive therapeutic effects have been achieved upon using adoptive cell transfer therapy; however, this approach is not feasible for large-scale treatment. Therefore, the optimal NP-based system should include the appropriate immune mediator combination that would elicit highly effective and wholly endogenous response.

## REFERENCES

- Mittal D, Gubin MM, Schreiber RD, Smyth MJ. New insights into cancer immunoediting and its three component phases – elimination, equilibrium and escape. *Curr Opin Immunol* (2014) 27:16–25. doi:10.1016/j.co.2014.01.004
- Kapadia CH, Perry JL, Tian S, Luft JC, DeSimone JM. Nanoparticulate immunotherapy for cancer. *J Control Release* (2015) 219:167–80. doi:10.1016/j.jconrel.2015.09.062
- Gajewski TF, Schreiber H, Fu YX. Innate and adaptive immune cells in the tumor microenvironment. *Nat Immunol* (2013) 14:1014–22. doi:10.1038/ni.2703
- Dunn GP, Old LJ, Schreiber RD. The immunobiology of cancer immuno-surveillance and immunoediting. *Immunity* (2004) 21:137–48. doi:10.1016/j.immuni.2004.07.017
- Hanahan D, Weinberg RA. Hallmarks of cancer: the next generation. *Cell* (2011) 144:646–74. doi:10.1016/j.cell.2011.02.013
- Vinay DS, Ryan EP, Pawelec G, Talib WH, Stagg J, Elkord E, et al. Immune evasion in cancer: mechanistic basis and therapeutic strategies. *Semin Cancer Biol* (2015) 35:S185–98. doi:10.1016/j.semcaner.2015.03.004
- Wu JD, Higgins LM, Steinle A, Cosman D, Haugk K, Plymate SR. Prevalent expression of the immunostimulatory MHC class I chain-related molecule is counteracted by shedding in prostate cancer. *J Clin Invest* (2004) 114:560–8. doi:10.1172/JCI200422206
- Gribbin JG, Freeman GJ, Boussiottis VA, Rennert P, Jellis CL, Greenfield E, et al. CTLA4 mediates antigen-specific apoptosis of human T cells. *Proc Natl Acad Sci U S A* (1995) 92:811–5. doi:10.1073/pnas.92.3.811
- Iwai Y, Ishida M, Tanaka Y, Okazaki T, Honjo T, Minato N. Involvement of PD-L1 on tumor cells in the escape from host immune system and tumor immunotherapy by PD-L1 blockade. *Proc Natl Acad Sci U S A* (2002) 99:12293–7. doi:10.1073/pnas.192461099
- Goubran HA, Kotb RR, Stakiewicz J, Emara ME, Burnouf T. Regulation of tumor growth and metastasis: the role of tumor microenvironment. *Cancer Growth Metastasis* (2014) 7:9–18. doi:10.4137/CGM.S11285
- Khazaie K, von Boehmer H. The impact of CD4+CD25+ Treg on tumor specific CD8+ T cell cytotoxicity and cancer. *Semin Cancer Biol* (2006) 16:124–36. doi:10.1016/j.semcaner.2005.11.006
- Tang X, Mo C, Wang Y, Wei D, Xiao H. Anti-tumour strategies aiming to target tumour-associated macrophages. *Immunology* (2013) 138:93–104. doi:10.1111/imm.12023
- Vanneman M, Dranoff G. Combining immunotherapy and targeted therapies in cancer treatment. *Nat Rev Cancer* (2012) 12:237–51. doi:10.1038/nrc3237
- Pardoll DM. The blockade of immune checkpoints in cancer immunotherapy. *Nat Rev Cancer* (2012) 12:252–64. doi:10.1038/nrc3239
- Peer D, Karp JM, Hong S, Farokhzad OC, Margalit R, Langer R. Nanocarriers as an emerging platform for cancer therapy. *Nat Nanotechnol* (2007) 2:751–60. doi:10.1038/nnano.2007.387
- Song E, Zhu P, Lee SK, Chowdhury D, Kussman S, Dykxhoorn DM, et al. Antibody mediated in vivo delivery of small interfering RNAs via cell-surface receptors. *Nat Biotechnol* (2005) 23:709–17. doi:10.1038/nbt1101
- Chou ST, Mixson AJ. siRNA nanoparticles: the future of RNAi therapeutics for oncology? *Nanomedicine (Lond)* (2014) 9:2251–4. doi:10.2217/nmm.14.157
- Wheeler LA, Trifonova R, Vrbanac V, Basar E, McKernan S, Xu Z, et al. Inhibition of HIV transmission in human cervicovaginal explants and humanized mice using CD4 aptamer-siRNA chimeras. *J Clin Invest* (2011) 121:12401–12. doi:10.1172/JCI45876
- Peer D. A daunting task: manipulating leukocyte function with RNAi. *Immunol Rev* (2013) 253:185–97. doi:10.1111/imr.12044
- Ramishetti S, Kedmi R, Goldsmith M, Leonard F, Sprague AG, Godin B, et al. Systemic gene silencing in primary T lymphocytes using targeted lipid nanoparticles. *ACS Nano* (2015) 9:6706–16. doi:10.1021/acsnano.5b02796
- Bunjes H. Lipid nanoparticles for the delivery of poorly water-soluble drugs. *J Pharm Pharmacol* (2010) 62:1637–45. doi:10.1111/j.2042-7158.2010.01024.x
- Torchilin VP. Recent advances with liposomes as pharmaceutical carriers. *Nat Rev Drug Discov* (2005) 4:145–60. doi:10.1038/nrd1632
- Kanasty R, Dorkin JR, Vegas A, Anderson D. Delivery materials for siRNA therapeutics. *Nat Mater* (2013) 12:967–77. doi:10.1038/nmat3765
- Yin H, Kanasty RL, Eltoukhy AA, Vegas AJ, Dorkin JR, Anderson DG. Non-viral vectors for gene-based therapy. *Nat Rev Genet* (2014) 15:541–55. doi:10.1038/nrg3763
- Torchilin VP. Multifunctional, stimuli-sensitive nanoparticulate systems for drug delivery. *Nat Rev Drug Discov* (2014) 13:813–27. doi:10.1038/nrd4333
- Shao K, Singha S, Clemente-Casares X, Tsai S, Yang Y, Santamaría P. Nanoparticle-based immunotherapy for cancer. *ACS Nano* (2015) 9:16–30. doi:10.1021/nn506209
- Smith DM, Simon JK, Baker JR Jr. Applications of nanotechnology for immunology. *Nat Rev Immunol* (2013) 13:592–605. doi:10.1038/nri3517
- Szebeni J, Barenholz YC. Chapter 11: Complement activation, immunogenicity, and immune suppression as potential side effects of liposomes. In: Peer D, editor. *Handbook of Harnessing Biomaterials in Nanomedicine – Preparation, Toxicity and Applications*. Singapore: Pan Stanford (2012). p. 309–35.
- Reddy ST, van der Vlies AJ, Simeoni E, Angeli V, Randolph GJ, O’Neil CP, et al. Exploiting lymphatic transport and complement activation in nanoparticle vaccines. *Nat Biotechnol* (2007) 25:1159–64. doi:10.1038/nbt1332

## AUTHOR CONTRIBUTIONS

SM, IH-H, DL-M, and BN wrote the manuscript. DP wrote and edited the manuscript.

## FUNDING

This work was supported in part by grants from the Israel Science Foundation (1178/16); The Dotan Hematology Center at Tel Aviv University; The Lewis Family Trust; The William Cohen Trust for CLL; the I-CORE Program of the Planning and Budgeting Committee and The Israel Science Foundation (Grant 41/11); the FTA: Nanomedicines for Personalized Theranostics of the Israeli National Nanotechnology Initiative; and by The Leona M. and Harry B. Helmsley Nanotechnology Research Fund awarded to DP.

30. Toy R, Peiris PM, Ghaghada KB, Karathanasis E. Shaping cancer nanomedicine: the effect of particle shape on the in vivo journey of nanoparticles. *Nanomedicine (Lond)* (2014) 9:121–34. doi:10.2217/nnm.13.191
31. Verma A, Stellacci F. Effect of surface properties on nanoparticle-cell interactions. *Small* (2010) 6:12–21. doi:10.1002/smll.200901158
32. Kedmi R, Ben-Arie N, Peer D. The systemic toxicity of positively charged lipid nanoparticles and the role of toll-like receptor 4 in immune activation. *Biomaterials* (2010) 31:6867–75. doi:10.1016/j.biomaterials.2010.05.027
33. Fadok VA, Bratton DL, Rose DM, Pearson A, Ezekowitz RA, Henson PM. A receptor for phosphatidylserine-specific clearance of apoptotic cells. *Nature* (2000) 405:85–90. doi:10.1038/35011084
34. Ramos GC, Fernandes D, Charao CT, Souza DG, Teixeira MM, Assreuy J. Apoptotic mimicry: phosphatidylserine liposomes reduce inflammation through activation of peroxisome proliferator-activated receptors (PPARs) in vivo. *Br J Pharmacol* (2007) 151:844–50. doi:10.1038/sj.bjp.0707302
35. Moghimi SM, Hamad I, Andresen TL, Jorgensen K, Szebeni J. Methylation of the phosphate oxygen moiety of phospholipid-methoxy(polyethylene glycol) conjugate prevents PEGylated liposome-mediated complement activation and anaphylatoxin production. *FASEB J* (2006) 20:2591–3. doi:10.1096/fj.06-6186fje
36. Szebeni J, Baranyi L, Savay S, Milosevits J, Bunger R, Laverman P, et al. Role of complement activation in hypersensitivity reactions to doxil and hynic PEG liposomes: experimental and clinical studies. *J Liposome Res* (2002) 12:165–72. doi:10.1081/LPR-120004790
37. Dams ET, Laverman P, Oyen WJ, Storm G, Scherphof GL, van Der Meer JW, et al. Accelerated blood clearance and altered biodistribution of repeated injections of sterically stabilized liposomes. *J Pharmacol Exp Ther* (2000) 292:1071–9.
38. Mizrahy S, Peer D. Polysaccharides as building blocks for nanotherapeutics. *Chem Soc Rev* (2012) 41:2623–40. doi:10.1039/c1cs15239d
39. Cohen K, Emmanuel R, Kisin-Finifer E, Shabat D, Peer D. Modulation of drug resistance in ovarian adenocarcinoma using chemotherapy entrapped in hyaluronan-grafted nanoparticle clusters. *ACS Nano* (2014) 8:2183–95. doi:10.1021/nn500205b
40. Cohen ZR, Ramishetti S, Peshes-Yaloz N, Goldsmith M, Wohl A, Zibly Z, et al. Localized RNAi therapeutics of chemoresistant grade IV glioma using hyaluronan-grafted lipid-based nanoparticles. *ACS Nano* (2015) 9:1581–91. doi:10.1021/nn506248s
41. Mizrahy S, Goldsmith M, Levitan-Ben-Arye S, Kisin-Finifer E, Redy O, Srinivasan S, et al. Tumor targeting profiling of hyaluronan-coated lipid based-nanoparticles. *Nanoscale* (2014) 6:3742–52. doi:10.1039/c3nr06102g
42. Yerushalmi N, Arad A, Margalit R. Molecular and cellular studies of hyaluronic acid-modified liposomes as bioadhesive carriers for topical drug delivery in wound healing. *Arch Biochem Biophys* (1994) 313:267–73. doi:10.1006/abbi.1994.1387
43. Reissmann S. Cell penetration: scope and limitations by the application of cell-penetrating peptides. *J Pept Sci* (2014) 20:760–84. doi:10.1002/psc.2672
44. Peer D, Shimaoka M. Systemic siRNA delivery to leukocyte-implicated diseases. *Cell Cycle* (2009) 8:853–9. doi:10.4161/cc.8.6.7936
45. Imai Y, Park EJ, Peer D, Peixoto A, Cheng G, von Andrian UH, et al. Genetic perturbation of the putative cytoplasmic membrane-proximal salt bridge aberrantly activates alpha(4) integrins. *Blood* (2008) 112:5007–15. doi:10.1182/blood-2008-03-144543
46. Oldenborg PA, Zheleznyak A, Fang YF, Lagenaar CF, Gresham HD, Lindberg FP. Role of CD47 as a marker of self on red blood cells. *Science* (2000) 288:2051–4. doi:10.1126/science.288.5473.2051
47. Rodriguez PL, Harada T, Christian DA, Pantano DA, Tsai RK, Discher DE. Minimal “self” peptides that inhibit phagocytic clearance and enhance delivery of nanoparticles. *Science* (2013) 339:971–5. doi:10.1126/science.1229568
48. Goldberg MS. Immunoengineering: how nanotechnology can enhance cancer immunotherapy. *Cell* (2015) 161:201–4. doi:10.1016/j.cell.2015.03.037
49. Moon JJ, Suh H, Bershteyn A, Stephan MT, Liu H, Huang B, et al. Interbilayer-crosslinked multilamellar vesicles as synthetic vaccines for potent humoral and cellular immune responses. *Nat Mater* (2011) 10:243–51. doi:10.1038/nmat2960
50. Kranz LM, Diken M, Haas H, Kreiter S, Loquai C, Reuter KC, et al. Systemic RNA delivery to dendritic cells exploits antiviral defence for cancer immunotherapy. *Nature* (2016) 534:396–401. doi:10.1038/nature18300
51. Leuschner F, Dutta P, Gorbatov R, Novobrantseva TI, Donahoe JS, Courties G, et al. Therapeutic siRNA silencing in inflammatory monocytes in mice. *Nat Biotechnol* (2011) 29:1005–10. doi:10.1038/nbt.1989
52. Macho-Fernandez E, Cruz LJ, Ghinnagow R, Fontaine J, Bialecki E, Frisch B, et al. Targeted delivery of alpha-galactosylceramide to CD8alpha+ dendritic cells optimizes type I NKT cell-based antitumor responses. *J Immunol* (2014) 193:961–9. doi:10.4049/jimmunol.1303029
53. Chan KS, Espinosa I, Chao M, Wong D, Ailles L, Diehn M, et al. Identification, molecular characterization, clinical prognosis, and therapeutic targeting of human bladder tumor-initiating cells. *Proc Natl Acad Sci U S A* (2009) 106:14016–21. doi:10.1073/pnas.0906549106
54. Jaiswal S, Jamieson CH, Pang WW, Park CY, Chao MP, Majeti R, et al. CD47 is upregulated on circulating hematopoietic stem cells and leukemia cells to avoid phagocytosis. *Cell* (2009) 138:271–85. doi:10.1016/j.cell.2009.05.046
55. Majeti R, Chao MP, Alizadeh AA, Pang WW, Jaiswal S, Gibbs KD Jr, et al. CD47 is an adverse prognostic factor and therapeutic antibody target on human acute myeloid leukemia stem cells. *Cell* (2009) 138:286–99. doi:10.1016/j.cell.2009.05.045
56. Wang Y, Xu Z, Guo S, Zhang L, Sharma A, Robertson GP, et al. Intravenous delivery of siRNA targeting CD47 effectively inhibits melanoma tumor growth and lung metastasis. *Mol Ther* (2013) 21:1919–29. doi:10.1038/mtn.2013.135
57. Xu Z, Wang Y, Zhang L, Huang L. Nanoparticle-delivered transforming growth factor-beta siRNA enhances vaccination against advanced melanoma by modifying tumor microenvironment. *ACS Nano* (2014) 8:3636–45. doi:10.1021/nn500216y
58. Park J, Wrzesinski SH, Stern E, Look M, Criscione J, Ragheb R, et al. Combination delivery of TGF-beta inhibitor and IL-2 by nanoscale liposomal polymeric gels enhances tumour immunotherapy. *Nat Mater* (2012) 11:895–905. doi:10.1038/nmat3355
59. Wrzesinski SH, Wan YY, Flavell RA. Transforming growth factor-beta and the immune response: implications for anticancer therapy. *Clin Cancer Res* (2007) 13:5262–70. doi:10.1158/1078-0432.CCR-07-1157
60. Brinker CJ. Nanoparticle immunotherapy: combo combat. *Nat Mater* (2012) 11:831–2. doi:10.1038/nmat3434
61. Moynihan KD, Opel CF, Szeto GL, Tzeng A, Zhu EF, Engreitz JM, et al. Eradication of large established tumors in mice by combination immunotherapy that engages innate and adaptive immune responses. *Nat Med* (2016) 22:1402–10. doi:10.1038/nm.4200
62. Lu Y, Wang Y, Miao L, Haynes M, Xiang G, Huang L. Exploiting in situ antigen generation and immune modulation to enhance chemotherapy response in advanced melanoma: a combination nanomedicine approach. *Cancer Lett* (2016) 379:32–8. doi:10.1016/j.canlet.2016.05.025
63. Heo MB, Kim SY, Yun WS, Lim YT. Sequential delivery of an anticancer drug and combined immunomodulatory nanoparticles for efficient chemoimmunotherapy. *Int J Nanomedicine* (2015) 10:5981–92. doi:10.2147/IJN.S90104
64. He C, Duan X, Guo N, Chan C, Poon C, Weichselbaum RR, et al. Core-shell nanoscale coordination polymers combine chemotherapy and photodynamic therapy to potentiate checkpoint blockade cancer immunotherapy. *Nat Commun* (2016) 7:12499. doi:10.1038/ncomms12499

**Conflict of Interest Statement:** DP declares a financial interest in Quiet Therapeutics. The other authors declare no conflict of interest.

Copyright © 2017 Mizrahy, Hazan-Halevy, Landesman-Milo, Ng and Peer. This is an open-access article distributed under the terms of the Creative Commons Attribution License (CC BY). The use, distribution or reproduction in other forums is permitted, provided the original author(s) or licensor are credited and that the original publication in this journal is cited, in accordance with accepted academic practice. No use, distribution or reproduction is permitted which does not comply with these terms.



# Nanoparticle-Based Magnetic Resonance Imaging on Tumor-Associated Macrophages and Inflammation

Natalie J. Serkova<sup>1,2,3,4\*</sup>

<sup>1</sup>Department of Anesthesiology, Anschutz Medical Center, Aurora, CO, USA, <sup>2</sup>Department of Radiology, Anschutz Medical Center, Aurora, CO, USA, <sup>3</sup>Department of Radiation Oncology, Anschutz Medical Center, Aurora, CO, USA, <sup>4</sup>Animal Imaging Shared Resources, University of Colorado Cancer Center, Anschutz Medical Center, Aurora, CO, USA

## OPEN ACCESS

**Edited by:**

Diana Boraschi,  
Consiglio Nazionale Delle Ricerche  
(CNR), Italy

**Reviewed by:**

Luciana D'Apice,  
Consiglio Nazionale Delle Ricerche  
(CNR), Italy  
Aldo Tagliaabe,  
ALTA srl, Italy

**\*Correspondence:**

Natalie J. Serkova  
[natalie.serkova@ucdenver.edu](mailto:natalie.serkova@ucdenver.edu)

**Specialty section:**

This article was submitted to *Inflammation*, a section of the journal *Frontiers in Immunology*

**Received:** 11 April 2017

**Accepted:** 04 May 2017

**Published:** 22 May 2017

**Citation:**

Serkova NJ (2017) Nanoparticle-Based Magnetic Resonance Imaging on Tumor-Associated Macrophages and Inflammation. *Front. Immunol.* 8:590.  
doi: 10.3389/fimmu.2017.00590

The inflammatory response, mediated by tissue-resident or newly recruited macrophages, is an underlying pathophysiological condition for many diseases, including diabetes, obesity, neurodegeneration, atherosclerosis, and cancer. Paradoxically, inflammation is a double-edged sword in oncology. Macrophages are, generally speaking, the major drivers of inflammatory insult. For many solid tumors, high density of cells expressing macrophage-associated markers have generally been found in association with a poor clinical outcome, characterized by inflamed microenvironment, a high level of dissemination and resistance to conventional chemotherapies. On another hand, radiation treatment also triggers an inflammatory response in tumors (often referred to as pseudoprogression), which can be associated with a positive treatment response. As such, non-invasive imaging of cancer inflammation and tumor-associated macrophages (TAMs) provides a revolutionary diagnostic tool and monitoring strategy for anti-inflammatory, immuno- and radiotherapies. Recently, quantitative T2-weighted magnetic resonance imaging (qT2wMRI), using injection of superparamagnetic iron oxide nanoparticles (SPIONs), has been reported for the assessment of TAMs non-invasively in animal models and in human trials. The SPIONs are magnetic resonance imaging (MRI) contrast agents that significantly decrease T2 MR relaxation times in inflamed tissues due to the macrophage-specific uptake and retention. It has been shown that macrophage-populated tumors and metastases will accumulate iron oxide nanoparticles and decrease T2-relaxation time that will result in a negative (dark) contrast in qT2wMRI. Non-invasive imaging of TAMs using SPION holds a great promise for staging the inflammatory microenvironment of primary and metastatic tumors as well monitoring the treatment response of cancer patients treated with radiation and immunotherapy.

**Keywords:** magnetic resonance imaging, iron oxide nanoparticles, tumor-associated macrophages, inflammation, cancer

## INTRODUCTION

The tumor microenvironment subsidizes to tumor progression, invasion, metabolic reprogramming, and resistance to therapy. In the past decade, it has become increasingly clear that immune-competent cells, including macrophages, represent one of the main contributors to the aggressive tumor milieu (1, 2). Macrophages are phagocytizing cells that penetrate into and reside in the affected tissue; they

originate from circulating blood monocytes (3). Two distinct classes of macrophages have been described: classically activated M1 macrophages and alternatively activated M2 macrophages (4, 5). In most tumors, the inflamed microenvironment is driven by M2-type macrophages (6, 7).

Given the growing body of evidence of the tumor-associated macrophages (TAMs) playing a significant role in tumorigenesis, a non-invasive assessment of TAMs to detect the level of tumor inflammation becomes a critical and limiting factor. The gold standard for TAM assessment, as of now, is immunohistochemistry, histological examination, and, in rare case, flow cytometry on excised biopsies—all techniques can be applied *ex vivo* only (8). A biopsy comes at great costs to the patient, its invasiveness can have detrimental health consequences, and since it is very challenging, if not impossible, to perform sequential biopsies, these protocols are limited in the assessment of TAM infiltration over time. Unfortunately, the circulating levels of monocytes, which can be assessed by semi-invasive venipuncture (phlebotomy), do not bear any therapeutic values for correlating with the levels of TAMs. Molecular and cellular imaging is a fast growing area in translational and clinical research. Dozens of novel molecularly targeted imaging probes have been tested in animal models of cancer and some of them are successfully used in human imaging (9–11). Fortunately, macrophages are well known as “professional phagocytes” and are responsible for “cleaning” various exogenous microbes, toxins, and nanoparticles. Also, macrophages are responsible for endogenous and exogenous iron metabolism. Fortunately again, iron-based nanoparticles have been known as T2-weighted contrast for magnetic resonance imaging (MRI). The recent studies have shown that superparamagnetic iron oxide nanoparticles (SPIONs) have a potential for non-invasive T2-weighted MRI assessment on tissue residential macrophages, including TAMs (12). This approach has a high-translational potential, since several of the existing SPION agents are approved in Europe for MR imaging and commercially available for human use. Ferumoxytol is another ultrasmall SPION formulation (with an average particle size of 25–30 nm) that is approved by the US Food and Drug Administration as an iron supplement for intravenous treatment of iron deficiency in renal failure patients (13). Ferumoxytol has superb magnetic properties and has been safely used in animal and human trials as an off-label MRI contrast agent (12, 14–22).

## TAMs AND INFLAMMATION IN CANCER

The relationship between chronic inflammation and cancer development was recognized well before the molecular origins of both diseases had been deciphered—Rudolph Virchow postulated an association between these two diseases in the 1860s (23). Inflammation is triggered by a cellular response, mediated mostly by neutrophils and macrophages, in response to pathophysiological stimuli. In general, macrophages are large white blood cells that ingest pathogens, microbes, and other invading substances. While neutrophils represent the first immune defense during the acute inflammation stage, the macrophages are predominant in chronic inflammation. All macrophages, including TAMs, are recruited through the local

expression of chemoattractant stimuli such as macrophage chemoattractant protein 1 and colony-stimulating factor 1 (24–27). Overexpression of both these factors is correlated with poor prognosis in various tumors, including most aggressive breast cancer, pancreatic adenocarcinomas, lung cancer, and high-grade gliomas. In many solid tumor types, poor prognosis directly correlates with the abundance of TAMs. In breast cancer, for example, TAMs play a crucial role in epithelial/stromal cross talk, as shown for invasive ductal carcinoma and ductal carcinoma *in situ* (28). Macrophage depletion in animal models leads to the impaired lung tumor growth and the decreased metastatic spread to the lung from breast cancer (29–31). TAMs have been directly linked to matrix remodeling, angiogenesis, stimulation of tumor growth, and motility (27, 32, 33)—all these functions are also reported during wound healing; as such, tumors are often described as “wounds that never heal” (1, 7). Similar to Virchow, our contemporary scientists, Gonda et al. concluded that chronic inflammation results in a myriad of molecular event that produce a microenvironment that is favorable for the development of cancer (34). Agents that control the inflammatory cascade, such as ibuprofen and other non-steroidal anti-inflammatory drugs, are thought to reduce cancer risk or enhance other anticancer treatments.

In another scenario, TAMs can be recruited from circulating monocytes as a result of therapy-induced apoptosis resulting in tumor inflammation after, for example, radiation or chemotherapy. Radiation induces a genetic signature of chronic inflammation, which is enriched in genes regulating transendothelial migration, monocyte maturation, and leukocyte chemoattraction (35–37). In this case, surprisingly, the recruited macrophages can accelerate antitumoral effects of radiation treatment (38). As such, a non-invasive assessment of TAMs can serve a surrogate marker for a specific and early response to several anticancer therapies.

Recently, several phenotypes (or “states”) of macrophages/macrophage activation have been identified: two most extreme states are known as antitumor M1 and protumor M2 macrophages (39). M2-type TAMs promote tumor growth, angiogenesis, and metastases by promoting high-level expression of epidermal growth factor receptor and secretion of vascular endothelial growth factors. M1 phenotype, on the other hand, can directly or indirectly mediate tumor phagocytosis. Two classes have distinct molecular signatures—the antitumor M1 phenotype has relatively low IL-10 and high IL-12 expression, whereas protumor M2 macrophages express high IL-10 and low IL-12 levels. It has been hypothesized that the bad “protumor” M2 phenotype is responsible for intrinsically inflamed solid tumors promoting fast cell proliferation, angiogenesis, dissemination, and immunosuppression, while the good M1 macrophages mature in response to radiation and chemotherapy and, as such, can help other immunocompetent T-cells to recognize and fight cancer (40, 41). Nevertheless, clinically, most of the current IHC protocols are not capable to distinguish between two TAM phenotypes. Hence, it becomes increasingly imperative to non-invasively characterize patient’s tumor microenvironment for the presence of TAMs in order to stratify the patients to TAM-depleting and/or -directed therapies and to repeatedly monitor their treatment response.

## SPIONs AND IRON METABOLISM

The cytoplasm of a macrophage contains granules (also called packets) consisting of several enzymes and chemicals that are wrapped in a membrane; its membrane has an arsenal of highly effective scavenger receptors. They allow the macrophage to engulf a broad spectrum of invading microorganisms, pathogens, and nanoparticles as well as endogenous cell debris and apoptotic bodies. In fact, macrophages are known as “professional phagocytes” (42), and their phagocytizing and pro-inflammatory abilities are directly linked to each other. There are some differences in terminology, which are related to the size of the digested material—some nanoscientists have introduced the term of “pinocytosis” for the uptake of soluble material or a nanoparticle, in contrast to the uptake of large material (“phagocytosis”) (43). But the fact remains undisputable—the macrophages take their responsibility of engulfing large and small nanoparticles very seriously; their macrophage scavenger receptors represent a very efficient system for recognizing a broad spectrum of surface modification and coating.

Fortunately for the MRI scientific community, iron-based nanoparticles represent even a higher level of attraction for the hard-working macrophages. Indeed, the macrophages are trained to maintain endogenous iron homeostasis while recycling and storing iron from senescent erythrocytes and other damaged cells (44, 45). They are very capable to store excessive levels of iron and, in response to systemic iron requirements, they can also release iron from their intracellular compartment into plasma. Therefore, after digesting (pinocytizing) an iron-containing nanoparticle (SPION), a macrophage will dutifully retain iron as long as the circulating iron load remains within its physiological range. This macrophage-retained iron load can be easily detected by T2-weighted MRI.

## T2 CONTRAST IN MRI

Modern oncologic imaging offers a variety of different modalities for the non-invasive detection and characterization of cancerous lesions (46–50). The common modalities include MRI, computed tomography, ultrasound, positron emission tomography (PET), single-photon emission computerized tomography, and optical imaging. Each modality has its advantages and disadvantages (46) and offers various non-invasive imaging endpoints related to tumor dimensions, tissue cellularity, angiogenesis, cancer metabolism, proliferation, and metastatic spread, just to mention a few. MRI is a non-invasive radiological technique with no ionizing radiation and high-spatial resolution, which is widely clinically used to detect, follow, and characterize solid tumors and metastases. MRI has complex physics and is based on physical properties of protons (mostly hydrogens) in a strong external magnetic field. Since water ( $H_2O$ ) is the main metabolite in all mammalian tissues, MRI detects small but distinct changes in spin frequencies of water hydrogens based on their surroundings when exposed to a high-magnetic field and radiofrequency excitation. The typical magnetic strength of human MRI scanner is 1.5 and 3 T, and for small animal imaging 4.7 and 7 T—however, the scanners tuned to even higher field, such as 9.4 T, 14 even 20 T, can be found in dedicated research facilities. One of the main strength of MRI is its ability to detect small changes (intrinsic contrast) within soft

tissues and cell populations, which can be further enhanced by the use of intravenous contrast agents.

It is important to understand the relationship between superparamagnetic nanoparticles and their effect on MR relaxation of the surrounding tissue water. Contrast agents can be principally divided into T1- and T2-relaxing contrast agents (Figure 1A). Paramagnetic contrast agents, such as gadolinium chelates also known as gadolinium-based contrast agents (GBCA), which are broadly used in the clinic, they predominantly shorten the spin-lattice T1 relaxation time (51). The shortening in T1 relaxation produces an increased signal intensity on a T1-weighted MRI images (Figures 1A–C). Clinically used GBCA (Magnevist, Omniscan, Mutihance, etc.) are intravascular contrast agents, not tailored to any specific cell type, and their specific accumulation in tumorous tissues is strictly based on liking vasculature of cancer. Figure 1C demonstrates an appearance of a small brain metastasis in GBCA-enhanced T1-weighted MRI (bright yellow arrow) in a melanoma patient.

On the other hand, all T2-shortening contrast agents consist of iron oxide nanoparticles, which are known as superparamagnetic (hence, the SPION abbreviation). By reducing the spin-spin T2-relaxation time of surrounding tissue water, the SPION (Feridex, Resovist, Ferumoxytol, etc.) produce darker contrast on T2-weighted MRI (Figures 1A,D,E) (52). Most importantly, unlike gadolinium, iron is a naturally occurring element in human bodies with low toxicity; and, the SPION are highly attractive to all phagocytizing cells including macrophages (as well as Kupffer cells and the reticuloendothelial system, RES). The precise changes in T2-relaxation times (calculated from quantitative T2-weighted magnetic resonance imaging) can be used as a semi-quantitative assessment of TAM presence in a cancerous lesion. The Figure 1E shows a pronounced darkening in the inflamed mammary gland of a mouse by T2-weighted MRI (dark yellow arrows).

## NON-INVASIVE IMAGING OF TAMs USING SPIONs

Gadolinium-based contrast agents are, without any doubt, the major class of MRI contrast agents used in the clinic. Over the past 25 years, more than 100 million patients have undergone GBCA-enhanced T1-MRI. However, increased concerns about gadolinium deposition and toxicity of free gadolinium have impacted how GBCA are currently used. A severe side effect, known as nephrogenic systemic fibrosis, is associated with decreased renal clearance of GBCA in renally impaired patients (53), since acute toxicity of free gadolinium has been known for several decades. It can significantly limit the GBCA use for MRI in cancer patients with chemotherapy-induced low glomerulofiltration rate. Most recently, a very concerning study was published in *Radiology* on residual gadolinium deposition in the brain of patients after multiple GBCA injections for MRI (54). Alternative contrast agents to gadolinium chelates are being discussed, and the SPIONs are being increasingly used for various clinical scenarios in the recent years (20, 55).

Initially, all SPIONs were used for diagnostic liver imaging (mostly in hepatocellular carcinoma or liver metastases) and

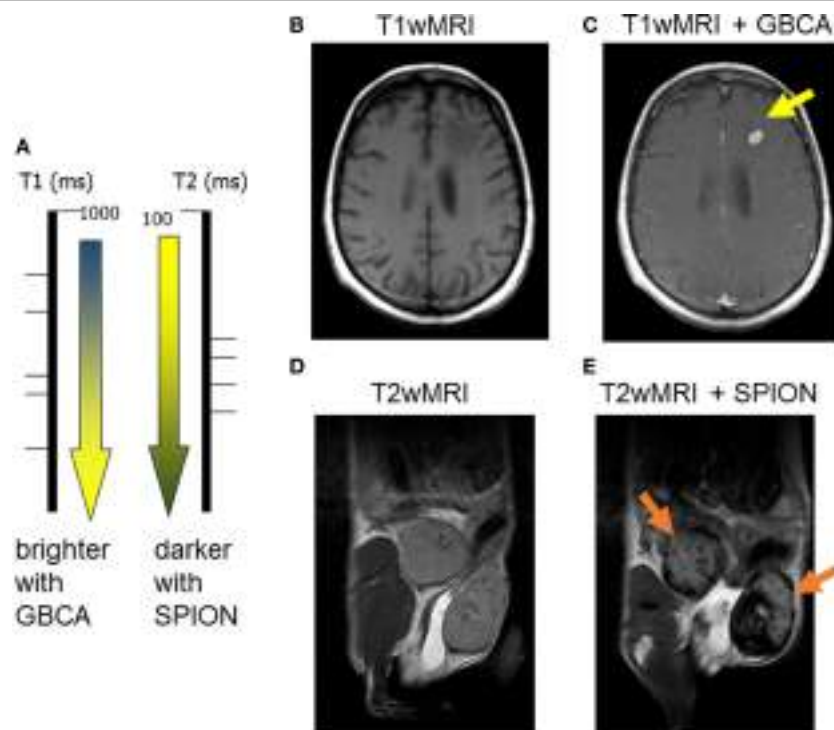


**FIGURE 1 |** Two major classes of magnetic resonance imaging (MRI) contrast agents: (A) paramagnetic gadolinium-based contrast agents (GBCA) are considered T1-positive contrast agents, by decreasing the spin-lattice T1 relaxation time, they produce bright T1 images; superparamagnetic iron oxide (SPION) is negative T2 contrast, iron oxide decreases the spin-spin T2-relaxation time producing darkening of T2-weighted images; (B) pre- and (C) post-GBCA T1-weighted MRI on a brain metastasis in a melanoma patient (15 min postinjection); (D) pre- and (E) post-SPION T2-weighted MRI on inflamed mouse mammary gland tumors (24 h postinjection).

considered as safe MRI contrast (56). Their use was based on the high uptake of the SPION by the Kupffer cells: a drop of T2 signal was seen in normal hepatic parenchyma due to the Kupffer cell uptake, with no signal changes in liver lesions. There were also attempts to stage lymph node metastases due to SPION retention and phagocytosis in the RES and lymph nodes (57, 58). As all nanoparticles, SPIONs have enhanced permeability and retention (EPR) in solid tumors (52). However, the previous generation of SPION with larger particle sizes (around and above 50 nm) had been mostly captured by the RES, decreasing their half-life times and, as such, their penetration into tumors.

Ferumoxytol is a colloid-based ultrasmall SPION, which consists of an iron oxide core with a size of ca. 6 nm and a carboxymethylxanthate coat, resulting in a hydrodynamic diameter of 30 nm. Unlike larger SPIONs (e.g., Resovist), ferumoxytol has a prolonged circulating half-life time (>14 h in humans and 2 h in rodents), mostly because of it partially escaping phagocytosis by the RES (spleen, liver, and bone marrow). As such, ferumoxytol has a favorable EPR profile and a potential for higher tumoral biodistribution. It slowly leaks across highly permeable tumor vasculature into the tumor interstitial space; after that, ferumoxytol nanoparticles are attacked by the TAMs and slowly phagocytized—a process that takes hours. Our studies and those from others have shown that the peak of iron accumulation in a tumor ( $T_{max}$ ) lies between 16

and 24 h after intravenous injection of ferumoxytol (12, 15, 59). **Figure 2A** shows representative quantitative T2-MRI maps of a high-grade inflamed glioma allograft (a mouse flank model) before (top) and 24 h after ferumoxytol infusion (bottom). The T2 histograms on **Figure 2B** show a clear decrease in tumoral T2-rerelaxation times after 24 h of SPION injection (from 58 to 44 ms), with all iron being completely localized intracellularly in TAMs. The same effect can be seen in humans; a residual reduction in T2-relaxation times in inflamed cancerous lesions can sometimes be observed a week after ferumoxytol administration (15, 19, 60).

## CONCLUSION AND FUTURE DIRECTIONS

Nanotechnology and nanomedicine have been increasingly utilized in translational and clinical practice in the past decade. This development has been supported by both federal and pharmaceutical funds, ever since, in 2004, the National Cancer Institute announced the Alliance for Nanotechnology in Cancer (61). The majority of nanoparticle research in cancer is focused on the targeted drug delivery of chemotherapeutic drugs, mostly for increasing tumor accumulation and decreasing systemic toxicity (62). Recently, an exciting area of nanomedicine has evolved, known as theranostics, based on the idea that the same drug carriers can be designed as potent

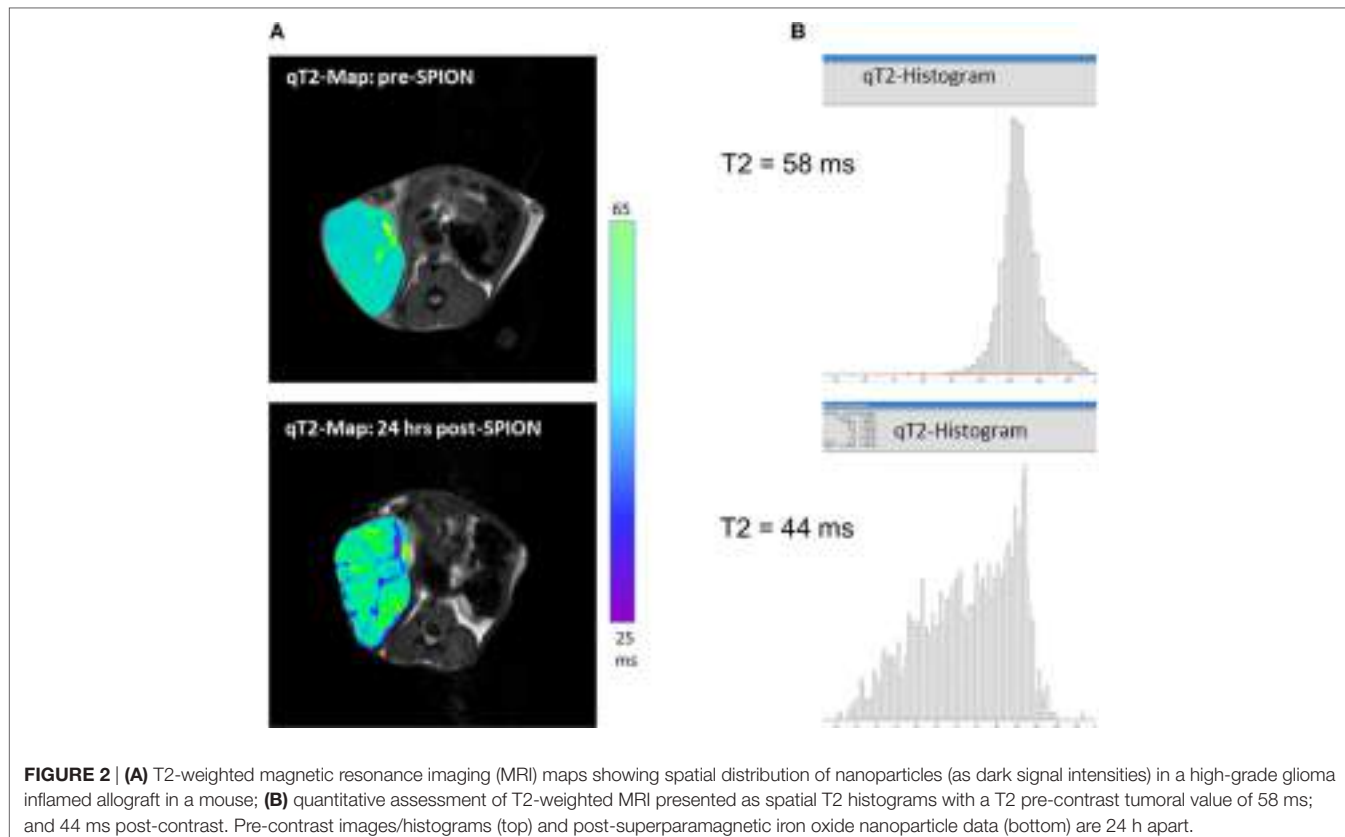


**FIGURE 2 | (A)** T2-weighted magnetic resonance imaging (MRI) maps showing spatial distribution of nanoparticles (as dark signal intensities) in a high-grade glioma inflamed allograft in a mouse; **(B)** quantitative assessment of T2-weighted MRI presented as spatial T2 histograms with a T2 pre-contrast tumoral value of 58 ms; and 44 ms post-contrast. Pre-contrast images/histograms (top) and post-superparamagnetic iron oxide nanoparticle data (bottom) are 24 h apart.

imaging agents (63–65). SPIONs are increasingly used for T2wMRI in oncology, including fast-evolving macrophage imaging. Macrophage-driven uptake of iron allows for the non-invasive assessment of the tissue inflammation status in cancer, diabetes, and ischemia/reperfusion injury. In the future, the same SPIONs can be loaded with an anti-inflammatory or chemotherapeutic agent to selectively deliver a therapy to the inflamed lesion.

An alternative to the use of SPION agents is the use of perfluorocarbons that can be visualized for fluorine (<sup>19</sup>F) magnetic resonance spectroscopy (MRS) for cell tracking of inflammatory cells (66). Some limitations to the <sup>19</sup>F-MRS application include low sensitivity to the target (usually, in the millimolars range). Another alternative might arise from the use of hyperpolarized <sup>13</sup>C-arginine by <sup>13</sup>C-MRS (67), since upregulated expression of arginase has been found in M2-like macrophages. However, the hyperpolarized <sup>13</sup>C-MRS approach is technically and clinically challenging and available only at the very limited number of academic hospitals. For PET, the uptake of radioactive glucose analog (18F-fluoro-deoxyglucose) by inflamed tissue is well known, but unfortunately, is rather non-specific since the tumor cells also have elevated glucose uptake (68, 69). Most recent studies try to use a specific <sup>18</sup>F-tracer for the translocator protein to image activated microglial cells and, possibly, TAMs in inflamed gliomas (70). But, as of today, the SPION-based T2-MRI approach appears to be clinically the most feasible path to image TAMs and to follow the response to anti-inflammatory treatment non-invasively. In the future, the combined PET/

MRI might be the best available option for human imaging, since the first multimodality scanners have recently became available (71). Ideally, the future imaging studies should be designed to non-invasively discriminate the protumour M2 versus antitumor M1 macrophages, since this phenotyping might play a crucial role in assessing tumor response to novel checkpoint inhibitors and other immunotherapies (72). A non-invasive TAM imaging will enable to characterize the inflamed tumor microenvironment, selectively deliver novel anti-inflammatory and anticancer drugs, and monitor their efficacy non-invasively and in the real time, providing new horizons for oncological imaging well above the limitations of conventional “volumetric” criteria.

## AUTHOR NOTES

The original data provided in Figures 1 and 2 were acquired in NS group.

## AUTHOR CONTRIBUTIONS

NS was solely responsible for literature search and composing this manuscript.

## FUNDING

This work was supported by the NIH P30 CA046934, UL1 TR001082, R21 CA194477, and 1S10 OD023485 grants.

## REFERENCES

- Pollard JW. Tumour-educated macrophages promote tumour progression and metastasis. *Nat Rev Cancer* (2004) 4(1):71–8. doi:10.1038/nrc1256
- Bingle L, Brown NJ, Lewis CE. The role of tumour-associated macrophages in tumour progression: implications for new anticancer therapies. *J Pathol* (2002) 196(3):254–65. doi:10.1002/path.1027
- Gouon-Evans V, Lin EY, Pollard JW. Requirement of macrophages and eosinophils and their cytokines/chemokines for mammary gland development. *Breast Cancer Res* (2002) 4(4):155–64. doi:10.1186/bcr441
- Gordon S. Alternative activation of macrophages. *Nat Rev Immunol* (2003) 3(1):23–35. doi:10.1038/nri978
- Mosser DM, Edwards JP. Exploring the full spectrum of macrophage activation. *Nat Rev Immunol* (2008) 8(12):958–69. doi:10.1038/nri2448
- DeNardo DG, Johansson M, Coussens LM. Immune cells as mediators of solid tumor metastasis. *Cancer Metastasis Rev* (2008) 27(1):11–8. doi:10.1007/s10555-007-9100-0
- Hanahan D, Coussens LM. Accessories to the crime: functions of cells recruited to the tumor microenvironment. *Cancer Cell* (2012) 21(3):309–22. doi:10.1016/j.ccr.2012.02.022
- Bates SE. Molecular diagnostics: are we there yet? *Clin Cancer Res* (2012) 18(6):1514. doi:10.1158/1078-0432.CCR-11-2207
- Blasberg R, Piwnica-Worms D. Imaging: strategies, controversies, and opportunities. *Clin Cancer Res* (2012) 18(3):631–7. doi:10.1158/1078-0432.CCR-11-2020
- El-Deiry WS, Sigman CC, Kelloff GJ. Imaging and oncologic drug development. *J Clin Oncol* (2006) 24(20):3261–73. doi:10.1200/JCO.2006.06.5623
- Linden HM, Dehdashti F. Novel methods and tracers for breast cancer imaging. *Semin Nucl Med* (2013) 43(4):324–9. doi:10.1053/j.semnuclmed.2013.02.003
- Daldrup-Link HE, Golovko D, Ruffell B, Denardo DG, Castaneda R, Ansari C, et al. MRI of tumor-associated macrophages with clinically applicable iron oxide nanoparticles. *Clin Cancer Res* (2011) 17(17):5695–704. doi:10.1158/1078-0432.CCR-10-3420
- Coyne DW. Ferumoxytol for treatment of iron deficiency anemia in patients with chronic kidney disease. *Expert Opin Pharmacother* (2009) 10(15):2563–8. doi:10.1517/14656560903224998
- Muehe AM, Feng D, von Eyben R, Luna-Fineman S, Link MP, Muthig T, et al. Safety report of ferumoxytol for magnetic resonance imaging in children and young adults. *Invest Radiol* (2016) 51(4):221–7. doi:10.1097/RLI.0000000000000230
- Fredrickson J, Serkova NJ, Wyatt SK, Carano RA, Pirzkall A, Rhee I, et al. Clinical translation of ferumoxytol-based vessel size imaging (VSI): feasibility in a phase I oncology clinical trial population. *Magn Reson Med* (2016) 77(2):814–25. doi:10.1002/mrm.26167
- Khurana A, Nejadnik H, Gawande R, Lin G, Lee S, Messing S, et al. Intravenous ferumoxytol allows noninvasive MR imaging monitoring of macrophage migration into stem cell transplants. *Radiology* (2012) 264(3):803–11. doi:10.1148/radiol.12112393
- Nayak AB, Luhar A, Hanudel M, Gales B, Hall TR, Finn JP, et al. High-resolution, whole-body vascular imaging with ferumoxytol as an alternative to gadolinium agents in a pediatric chronic kidney disease cohort. *Pediatr Nephrol* (2015) 30(3):515–21. doi:10.1007/s00467-014-2953-x
- McCullough BJ, Kolokythas O, Maki JH, Green DE. Ferumoxytol in clinical practice: implications for MRI. *J Magn Reson Imaging* (2013) 37(6):1476–9. doi:10.1002/jmri.23879
- Bashir MR, Bhatti L, Marin D, Nelson RC. Emerging applications for ferumoxytol as a contrast agent in MRI. *J Magn Reson Imaging* (2015) 41(4):884–98. doi:10.1002/jmri.24691
- Hope MD, Hope TA, Zhu C, Faraji F, Haraldsson H, Ordovas KG, et al. Vascular imaging with ferumoxytol as a contrast agent. *AJR Am J Roentgenol* (2015) 205(3):W366–73. doi:10.2214/AJR.15.14534
- Walker JP, Nosova E, Sigovan M, Rapp J, Grenon MS, Owens CD, et al. Ferumoxytol-enhanced magnetic resonance angiography is a feasible method for the clinical evaluation of lower extremity arterial disease. *Ann Vasc Surg* (2015) 29(1):63–8. doi:10.1016/j.avsg.2014.09.003
- Ramanathan RK, Korn R, Raghunand N, Sachdev JC, Newbold RG, Jameson G, et al. Correlation between ferumoxytol uptake in tumor lesions by MRI and response to nanoliposomal irinotecan in patients with advanced solid tumors: a pilot study. *Clin Cancer Res* (2017). doi:10.1158/1078-0432.CCR-16-1990
- Multhoff G, Molls M, Radons J. Chronic inflammation in cancer development. *Front Immunol* (2011) 2:98. doi:10.3389/fimmu.2011.00098
- Lin EY, Gouon-Evans V, Nguyen AV, Pollard JW. The macrophage growth factor CSF-1 in mammary gland development and tumor progression. *J Mammary Gland Biol Neoplasia* (2002) 7(2):147–62. doi:10.1023/A:1020399802795
- Pyontek SM, Gadea BB, Wang HW, Gocheva V, Hunter KE, Tang LH, et al. Deficiency of the macrophage growth factor CSF-1 disrupts pancreatic neuroendocrine tumor development. *Oncogene* (2012) 31(11):1459–67. doi:10.1038/onc.2011.337
- Pyontek SM, Akkari L, Schuhmacher AJ, Bowman RL, Sevenich L, Quail DF, et al. CSF-1R inhibition alters macrophage polarization and blocks glioma progression. *Nat Med* (2013) 19(10):1264–72. doi:10.1038/nm.3337
- Coussens LM, Werb Z. Inflammatory cells and cancer: think different! *J Exp Med* (2001) 193(6):F23–6. doi:10.1084/jem.193.6.F23
- Borges VF, Schedin PJ. Pregnancy-associated breast cancer: an entity needing refinement of the definition. *Cancer* (2012) 118(13):3226–8. doi:10.1002/cncr.26643
- Fritz JM, Tennis MA, Orlicky DJ, Lin H, Ju C, Redente EF, et al. Depletion of tumor-associated macrophages slows the growth of chemically induced mouse lung adenocarcinomas. *Front Immunol* (2014) 5:587. doi:10.3389/fimmu.2014.00587
- Sica A, Rubino L, Mancino A, Larghi P, Porta C, Rimoldi M, et al. Targeting tumour-associated macrophages. *Expert Opin Ther Targets* (2007) 11(9):1219–29. doi:10.1517/1472822.11.9.1219
- Jinushi M, Chiba S, Yoshiyama H, Masutomi K, Kinoshita I, Dosaka-Akita H, et al. Tumor-associated macrophages regulate tumorigenicity and anticancer drug responses of cancer stem/initiating cells. *Proc Natl Acad Sci U S A* (2011) 108(30):12425–30. doi:10.1073/pnas.1106645108
- Allavena P, Sica A, Solinas G, Porta C, Mantovani A. The inflammatory micro-environment in tumor progression: the role of tumor-associated macrophages. *Crit Rev Oncol Hematol* (2008) 66(1):1–9. doi:10.1016/j.critrevonc.2007.07.004
- Siveen KS, Kuttan G. Role of macrophages in tumour progression. *Immunol Lett* (2009) 123(2):97–102. doi:10.1016/j.imlet.2009.02.011
- Gonda TA, Tu S, Wang TC. Chronic inflammation, the tumor microenvironment and carcinogenesis. *Cell Cycle* (2009) 8(13):2005–13. doi:10.4161/cc.8.13.8985
- Schaeue D, Micewicz ED, Ratikan JA, Xie MW, Cheng G, McBride WH. Radiation and inflammation. *Semin Radiat Oncol* (2015) 25(1):4–10. doi:10.1016/j.semradonc.2014.07.007
- Nguyen DH, Oketch-Rabah HA, Illa-Bochaca I, Geyer FC, Reis-Filho JS, Mao JH, et al. Radiation acts on the microenvironment to affect breast carcinogenesis by distinct mechanisms that decrease cancer latency and affect tumor type. *Cancer Cell* (2011) 19(5):640–51. doi:10.1016/j.ccr.2011.03.011
- Bower JE, Ganz PA, Tao ML, Hu W, Belin TR, Sepah S, et al. Inflammatory biomarkers and fatigue during radiation therapy for breast and prostate cancer. *Clin Cancer Res* (2009) 15(17):5534–40. doi:10.1158/1078-0432.CCR-08-2584
- Russell JS, Brown JM. The irradiated tumor microenvironment: role of tumor-associated macrophages in vascular recovery. *Front Physiol* (2013) 4:157. doi:10.3389/fphys.2013.00157
- Mukhtar RA, Nseyo O, Campbell MJ, Esserman LJ. Tumor-associated macrophages in breast cancer as potential biomarkers for new treatments and diagnostics. *Expert Rev Mol Diagn* (2011) 11(1):91–100. doi:10.1586/erm.10.97
- Brown JM, Recht L, Strober S. The promise of targeting macrophages in cancer therapy. *Clin Cancer Res* (2017). doi:10.1158/1078-0432.CCR-16-3122
- Barbay V, Houssari M, Mekki M, Banquet S, Edwards-Levy F, Henry JP, et al. Role of M2-like macrophage recruitment during angiogenic growth factor therapy. *Angiogenesis* (2015) 18(2):191–200. doi:10.1007/s10456-014-9456-z
- Han CZ, Juncadella IJ, Kinchen JM, Buckley MW, Klibanov AL, Dryden K, et al. Macrophages redirect phagocytosis by non-professional phagocytes and influence inflammation. *Nature* (2016) 539(7630):570–4. doi:10.1038/nature20141
- Raynal I, Prigent P, Peyramaure S, Najid A, Rebuzzi C, Corot C. Macrophage endocytosis of superparamagnetic iron oxide nanoparticles: mechanisms and comparison of ferumoxides and ferumoxtran-10. *Invest Radiol* (2004) 39(1):56–63. doi:10.1097/01.rli.0000101027.57021.28

44. Ganz T. Macrophages and systemic iron homeostasis. *J Innate Immun* (2012) 4(5–6):446–53. doi:10.1159/000336423
45. Ganz T. Macrophages and iron metabolism. *Microbiol Spectr* (2016) 4(5). doi:10.1128/microbiolspec.MCHD-0037-2016
46. Serkova NJ, Garg K, Bradshaw-Pierce EL. Oncologic imaging end-points for the assessment of therapy response. *Recent Pat Anticancer Drug Discov* (2009) 4(1):36–53. doi:10.2174/157489209787002434
47. O'Connor JP, Jackson A, Parker GJ, Roberts C, Jayson GC. Dynamic contrast-enhanced MRI in clinical trials of antivascular therapies. *Nat Rev Clin Oncol* (2012) 9(3):167–77. doi:10.1038/nrclinonc.2012.2
48. Kircher MF, Willmann JK. Molecular body imaging: MR imaging, CT, and US. Part II. Applications. *Radiology* (2012) 264(2):349–68. doi:10.1148/radiol.12111703
49. Kircher MF, Willmann JK. Molecular body imaging: MR imaging, CT, and US. Part I. Principles. *Radiology* (2012) 263(3):633–43. doi:10.1148/radiol.12102394
50. Wahl RL, Jacene H, Kasamon Y, Lodge MA. From RECIST to PERCIST: evolving considerations for PET response criteria in solid tumors. *J Nucl Med* (2009) 50(Suppl 1):122S–50S. doi:10.2967/jnumed.108.057307
51. Zhou Z, Lu ZR. Gadolinium-based contrast agents for magnetic resonance cancer imaging. *Wiley Interdiscip Rev Nanomed Nanobiotechnol* (2013) 5(1):1–18. doi:10.1002/wnnan.1198
52. Anchordoquy TJ, Barenholz Y, Boraschi D, Chorny M, Decuzzi P, Dobrovolskaia MA, et al. Mechanisms and barriers in cancer nanomedicine: addressing challenges, looking for solutions. *ACS Nano* (2017) 11(1):12–8. doi:10.1021/acsnano.6b08244
53. Hasebroock KM, Serkova NJ. Toxicity of MRI and CT contrast agents. *Expert Opin Drug Metab Toxicol* (2009) 5(4):403–16. doi:10.1517/17425250902873796
54. Kanal E, Tweedle MF. Residual or retained gadolinium: practical implications for radiologists and our patients. *Radiology* (2015) 275(3):630–4. doi:10.1148/radiol.2015150805
55. Cantow K, Pohlmann A, Flemming B, Ferrara F, Waiczies S, Grosenick D, et al. Acute effects of ferumoxytol on regulation of renal hemodynamics and oxygenation. *Sci Rep* (2016) 6:29965. doi:10.1038/srep29965
56. Onishi H, Murakami T, Kim T, Hori M, Hirohashi S, Matsuki M, et al. Safety of ferucarbotran in MR imaging of the liver: a pre- and postexamination questionnaire-based multicenter investigation. *J Magn Reson Imaging* (2009) 29(1):106–11. doi:10.1002/jmri.21608
57. Mouli SK, Zhao LC, Omary RA, Thaxton CS. Lymphotropic nanoparticle enhanced MRI for the staging of genitourinary tumors. *Nat Rev Urol* (2010) 7(2):84–93. doi:10.1038/nrurol.2009.254
58. Oghabian MA, Gharehaghaji N, Amirmohseni S, Khoei S, Guiti M. Detection sensitivity of lymph nodes of various sizes using USPIO nanoparticles in magnetic resonance imaging. *Nanomedicine* (2010) 6(3):496–9. doi:10.1016/j.nano.2009.11.005
59. Serkova NJ, Renner B, Larsen BA, Stoldt CR, Hasebroock KM, Bradshaw-Pierce EL, et al. Renal inflammation: targeted iron oxide nanoparticles for molecular MR imaging in mice. *Radiology* (2010) 255(2):517–26. doi:10.1148/radiol.09091134
60. Harman A, Chang KJ, Dupuy D, Rintels P. The long-lasting effect of ferumoxytol on abdominal magnetic resonance imaging. *J Comput Assist Tomogr* (2014) 38(4):571–3. doi:10.1097/RCT.0000000000000086
61. Grodzinski P, Farrell D. Future opportunities in cancer nanotechnology – NCI strategic workshop report. *Cancer Res* (2014) 74(5):1307–10. doi:10.1158/0008-5472.CAN-13-2787
62. Monk BJ, Brady MF, Aghajanian C, Lankes HA, Rizack T, Leach J, et al. A phase 2, randomized, double-blind, placebo controlled study of chemo-immunotherapy combination using motolimod with pegylated liposomal doxorubicin in recurrent or persistent ovarian cancer: a Gynecologic Oncology Group partners study. *Ann Oncol* (2017) 28(5):996–1004. doi:10.1093/annonc/mdx049
63. Lee H, Shields AF, Siegel BA, Miller KD, Krop I, Ma CX, et al. 64Cu-MM-302 positron emission tomography quantifies variability of enhanced permeability and retention of nanoparticles in relation to treatment response in patients with metastatic breast cancer. *Clin Cancer Res* (2017). doi:10.1158/1078-0432.CCR-16-3193
64. Fan CH, Ting CY, Lin HJ, Wang CH, Liu HL, Yen TC, et al. SPIO-conjugated, doxorubicin-loaded microbubbles for concurrent MRI and focused-ultrasound enhanced brain-tumor drug delivery. *Biomaterials* (2013) 34(14):3706–15. doi:10.1016/j.biomaterials.2013.01.099
65. Hadjipanayis CG, Machaidze R, Kaluzova M, Wang L, Schuette AJ, Chen H, et al. EGFRvIII antibody-conjugated iron oxide nanoparticles for magnetic resonance imaging-guided convection-enhanced delivery and targeted therapy of glioblastoma. *Cancer Res* (2010) 70(15):6303–12. doi:10.1158/0008-5472.CAN-10-1022
66. Waiczies S, Lepore S, Sydow K, Drechsler S, Ku MC, Martin C, et al. Anchoring dipalmitoyl phosphoethanolamine to nanoparticles boosts cellular uptake and fluorine-19 magnetic resonance signal. *Sci Rep* (2015) 5:8427. doi:10.1038/srep08427
67. Najac C, Chaumeil MM, Kohanbash G, Guglielmetti C, Gordon JW, Okada H, et al. Detection of inflammatory cell function using (13)C magnetic resonance spectroscopy of hyperpolarized [6-(13)C]-arginine. *Sci Rep* (2016) 6:31397. doi:10.1038/srep31397
68. Shroff GS, Carter BW, Viswanathan C, Benveniste MF, Wu CC, Marom EM, et al. Challenges in interpretation of staging PET/CT in thoracic malignancies. *Curr Probl Diagn Radiol* (2016) S0363-0188(16):30107–4. doi:10.1067/j.cpradiol.2016.11.012
69. Lammers T, Aime S, Hennink WE, Storm G, Kiessling F. Theranostic nanomedicine. *Acc Chem Res* (2011) 44(10):1029–38. doi:10.1021/ar200019c
70. Zinnhardt B, Pigeon H, Theze B, Viel T, Wachsmuth L, Fricke IB, et al. Combined PET imaging of the inflammatory tumor microenvironment identifies margins of unique radiotracer uptake. *Cancer Res* (2017) 77(8):1831–41. doi:10.1158/0008-5472.CAN-16-2628
71. Rolle AM, Hasenberg M, Thornton CR, Solouk-Saran D, Mann L, Weski J, et al. ImmunoPET/MR imaging allows specific detection of *Aspergillus fumigatus* lung infection in vivo. *Proc Natl Acad Sci U S A* (2016) 113(8):E1026–33. doi:10.1073/pnas.1518836113
72. Petty AJ, Yang Y. Tumor-associated macrophages: implications in cancer immunotherapy. *Immunotherapy* (2017) 9(3):289–302. doi:10.2217/imt-2016-0135

**Conflict of Interest Statement:** The author declares that the research was conducted in the absence of any commercial or financial relationships that could be construed as a potential conflict of interest.

The reviewer, LD, and handling editor declared their shared affiliation, and the handling editor states that the process nevertheless met the standards of a fair and objective review.

Copyright © 2017 Serkova. This is an open-access article distributed under the terms of the Creative Commons Attribution License (CC BY). The use, distribution or reproduction in other forums is permitted, provided the original author(s) or licensor are credited and that the original publication in this journal is cited, in accordance with accepted academic practice. No use, distribution or reproduction is permitted which does not comply with these terms.



# Macrophage Polarization Contributes to the Anti-Tumoral Efficacy of Mesoporous Nanovectors Loaded with Albumin-Bound Paclitaxel

Fransisca Leonard<sup>1</sup>, Louis T. Curtis<sup>2</sup>, Matthew James Ware<sup>3</sup>, Taraz Nosrat<sup>1</sup>, Xuewu Liu<sup>1</sup>, Kenji Yokoi<sup>1</sup>, Hermann B. Frieboes<sup>2,4†</sup> and Biana Godin<sup>1\*†</sup>

<sup>1</sup>Department of Nanomedicine, Houston Methodist Research Institute, Houston, TX, United States, <sup>2</sup>Department of Bioengineering, University of Louisville, Louisville, KY, United States, <sup>3</sup>Department of Surgery, Baylor College of Medicine, Houston, TX, United States, <sup>4</sup>James Graham Brown Cancer Center, University of Louisville, Louisville, KY, United States

## OPEN ACCESS

### Edited by:

Diana Boraschi,

Consiglio Nazionale Delle Ricerche

(CNR), Italy

### Reviewed by:

Detlef Neumann,

Hannover Medical School, Germany

Chae-Heui Yun,

Seoul National University,

South Korea

### \*Correspondence:

Biana Godin

[bgodin@houstonmethodist.org](mailto:bgodin@houstonmethodist.org),

[bianagodinv@gmail.com](mailto:bianagodinv@gmail.com)

<sup>†</sup>Shared senior authorship.

### Specialty section:

This article was submitted to

Inflammation,

a section of the journal

Frontiers in Immunology

**Received:** 04 April 2017

**Accepted:** 29 May 2017

**Published:** 16 June 2017

### Citation:

Leonard F, Curtis LT, Ware MJ, Nosrat T, Liu X, Yokoi K, Frieboes HB and Godin B (2017) Macrophage Polarization Contributes to the Anti-Tumoral Efficacy of Mesoporous Nanovectors Loaded with Albumin-Bound Paclitaxel. *Front. Immunol.* 8:693.

doi: 10.3389/fimmu.2017.00693

Therapies targeted to the immune system, such as immunotherapy, are currently shaping a new, rapidly developing branch of promising cancer treatments, offering the potential to change the prognosis of previously non-responding patients. Macrophages comprise the most abundant population of immune cells in the tumor microenvironment (TME) and can undergo differentiation into functional phenotypes depending on the local tissue environment. Based on these functional phenotypes, tumor-associated macrophages (TAMs) can either aid tumor progression (M2 phenotype) or inhibit it (M1 phenotype). Presence of M2 macrophages and a high ratio of M2/M1 macrophages in the TME are clinically associated with poor prognosis in many types of cancers. Herein, we evaluate the effect of macrophage phenotype on the transport and anti-cancer efficacy of albumin-bound paclitaxel (nAb-PTX) loaded into porous silicon multistage nanovectors (MSV). Studies in a coculture of breast cancer cells (3D-spheroid) with macrophages and *in vivo* models were conducted to evaluate the therapeutic efficacy of MSV-nAb-PTX as a function of macrophage phenotype. Association with MSV increased drug accumulation within the macrophages and the tumor spheroids, shifting the inflammation state of the TME toward the pro-inflammatory, anti-tumorigenic milieu. Additionally, the treatment increased macrophage motility toward cancer cells, promoting the active transport of therapeutic nanovectors into the tumor lesion. Consequently, apoptosis of cancer cells was increased and proliferation decreased in the MSV-nAb-PTX-treated group as compared to controls. The results also confirmed that the tested system shifts the macrophage differentiation toward an M1 phenotype, possessing an anti-proliferative effect toward the breast cancer cells. These factors were further incorporated into a mathematical model to help analyze the synergistic effect of the macrophage polarization state on the efficacy of MSV-nAb-PTX in alleviating hypovascularized tumor lesions. In conclusion, the ability of MSV-nAb-PTX to polarize TAM to the M1 phenotype, causing (1) enhanced penetration of the drug-carrying macrophages to the center of the tumor lesion and (2) increased toxicity to tumor cells may explain the increased anti-cancer efficacy of the system in comparison to nAb-PTX and other controls.

**Keywords:** macrophage polarization, nanotherapy, breast cancer, computational modeling, tumor microenvironment

## INTRODUCTION

Tumor initiation, growth, and progression rely on the bidirectional interaction of the tumor cells with the cells in the tumor microenvironment (TME). Solid tumors comprise variable amounts of neoplastic and stromal cells. The tumor stroma includes endothelial cells, fibroblasts, and immune cells, mainly macrophages and lymphocytes. Macrophages are a plastic and heterogeneous immune cell population. In particular, tumor-associated macrophages (TAMs), derived from monocytic precursors, comprise the most abundant population of immune cells in the TME (1–3). Macrophages in the TME can undergo functional changes and be polarized from the resting M0 phenotype to the classically activated pro-inflammatory M1 or anti-inflammatory (alternatively activated) M2 general subsets, based on the stimuli in the residing milieu (4). M1 macrophages are characterized by their expression of inducible nitric oxide synthase, production of pro-inflammatory cytokines (e.g., TNF, IL-1, -6, and -12) and reactive oxygen species (ROS). This subpopulation of macrophages promotes strong immune responses and is anti-tumorigenic (5, 6). On the contrary, M2 macrophages antagonize the inflammation and are present in the advanced stages of the healing process. M2 macrophages enhance the formation of tumor stroma by recruiting fibroblasts and activating their differentiation to myofibroblasts, causing the release of pro-angiogenic factors that enable recruitment of endothelial progenitor cells and neovasculogenesis and suppression of inflammation through decreased production of ROS and pro-inflammatory cytokines (7, 8). While M2 macrophages possess a significant role in host defense and Th2-mediated activation of the humoral immune response, their presence in the TME promotes tumor development. Presence of M2 macrophages and a high ratio of M2/M1 macrophages in the TME are clinically associated with poor prognosis in many types of cancers (9–12).

It is noteworthy that the tight distinction between M1 and M2 macrophages does not fully describe the continuum of their functions and can be considered as a simplified classification of the two sides of the polarization spectrum (13). TAMs are usually considered M2-like macrophages (14–16), which abandon the M1-related innate and adaptive immune responses capable of destroying malignant cells. Changes in the stimuli of the TME can cause reprogramming of macrophages from an M1 phenotype to an M2-activated state and *vice versa* (17, 18). Macrophage reprogramming has been recently shown to inhibit cancer progression and metastasis (19, 20). Controlling the macrophage polarization state in the TME could provide a novel approach to treating related diseases. Reprogramming M2 macrophages toward the M1 subset is an important focus of recent research, with a number of recent publications demonstrating the ability of some nanomaterials to induce macrophages between polarization states (21–23).

Our previous studies have shown that TAMs play a significant role in therapeutic efficacy of albumin-bound paclitaxel (nAb-PTX) loaded into porous silicon multistage nanovectors (MSV) in liver metastasis of breast and lung tumors (24). Although tumor lesions in the liver have inefficient vascularization, we demonstrated an increased concentration of macrophages acting

as chemotherapeutic depots near these lesions. This significantly enhanced efficacy and extended survival in two tested animal models of liver metastases. Furthermore, we have mathematically modeled the efficacy of MSV-nAb-PTX nanovectors in 3D tumor models to project MSV-nAb-PTX efficacy in hypovascularized lesions and concluded that the proposed 3D coculture of macrophages and tumor cells serve as a good model for the *in vivo* condition (25). However, based on the integrated experimental and mathematical analysis of the data, it appears that the efficacy of MSV-nAb-PTX was more than expected solely from macrophages acting as a depot for the drug.

Herein, we aim to evaluate the effect of macrophage phenotype on the anti-cancer efficacy of MSV-nAb-PTX, as well as the effect of these nanovectors on macrophage polarization state. For this purpose, the experiments were performed *in vitro* using a validated coculture of breast cancer tumor cells (3D spheroids) with macrophages and *in vivo* in the breast cancer tumor metastasis mouse model. Our *in vitro* and *in vivo* findings show that treatment with MSV-nAb-PTX affected the macrophages to polarize from the M2-type to the anti-tumorigenic M1 phenotype. Additionally, the treatment increased macrophage motility toward cancer cells, promoting the penetration of therapeutic nanovectors into the tumor lesion. These findings were further incorporated into a mathematical model to help analyze the synergistic effect of macrophage polarization state on the efficacy of MSV-nAb-PTX in treating hypovascularized tumor lesions.

## RESULTS

### Efficacy of Macrophage-Associated MSV-nAb-PTX in 3D TME *In Vitro* Model of Hypovascularized Breast Tumor Lesions

In this study, we use a validated TME model of hypovascularized breast tumor lesions, which consist of macrophages surrounding 4T1 cell spheroids. Rapamycin was used as a factor shifting polarization of macrophages toward the M1 phenotype (26), a positive control of macrophage differentiation.

As shown in **Figure 1**, Ki67 staining indicated that the cells in the control spheres actively proliferated. All treatment groups including nAb-PTX, MSV-nAb-PTX, and rapamycin induced apoptosis in the spheres [terminal deoxynucleotidyl transferase dUTP nick end labeling (TUNEL) staining] and reduced tumor cell proliferation (**Figure 1A**). Similar to previously reported *in vivo* data (24), treatment with MSV-nAb-PTX and nAb-PTX both resulted in a high apoptosis rate, as shown by green signals from the cells in **Figure 1A**. Rapamycin induced apoptosis in a similar rate to MSV-nAb-PTX, and cell proliferation was only slightly inhibited by rapamycin. This inhibition was not as efficient as exhibited in the nAb-PTX and MSV-nAb-PTX treatment groups. Spheroids treated with nAb-PTX displayed low proliferation profiles, as observed by a weak Ki67 signal, mostly within the ~75 µm of the outer layer of the spheres. In the MSV-nAb-PTX-treated group, the effect was more pronounced and only cells within ~20 µm from the outer layer of the spheroids were still proliferating (**Figure 1A**). The ratio of the tumor cells

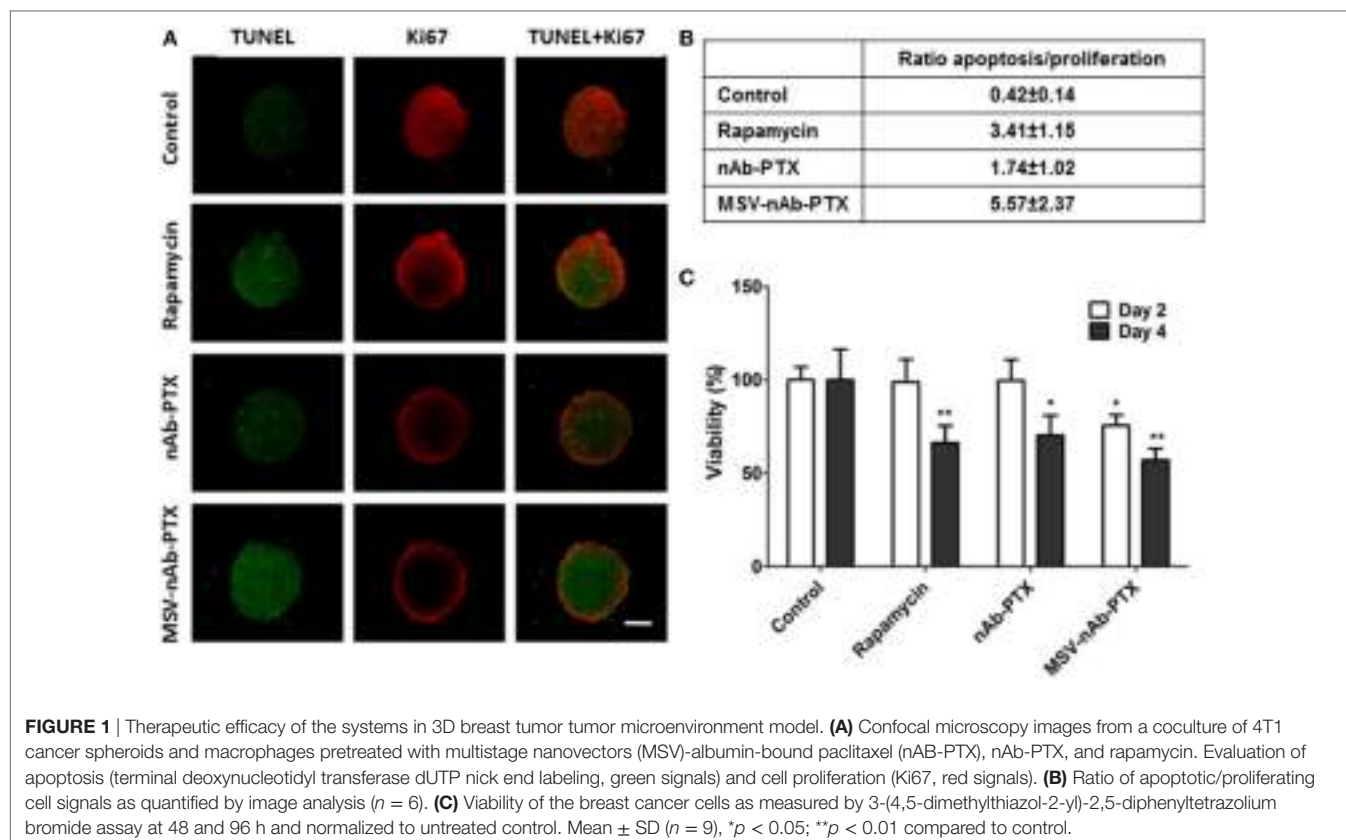


**FIGURE 1 |** Therapeutic efficacy of the systems in 3D breast tumor tumor microenvironment model. **(A)** Confocal microscopy images from a coculture of 4T1 cancer spheroids and macrophages pretreated with multistage nanovectors (MSV)-albumin-bound paclitaxel (nAb-PTX), nAb-PTX, and rapamycin. Evaluation of apoptosis (terminal deoxynucleotidyl transferase dUTP nick end labeling, green signals) and cell proliferation (Ki67, red signals). **(B)** Ratio of apoptotic/proliferating cell signals as quantified by image analysis ( $n = 6$ ). **(C)** Viability of the breast cancer cells as measured by 3-(4,5-dimethylthiazol-2-yl)-2,5-diphenyltetrazolium bromide assay at 48 and 96 h and normalized to untreated control. Mean  $\pm$  SD ( $n = 9$ ), \* $p < 0.05$ ; \*\* $p < 0.01$  compared to control.

undergoing apoptosis/proliferation is in the following order: MSV-nAb-PTX > rapamycin > nAb-PTX > untreated control (Figure 1B). Furthermore, 3-(4,5-dimethylthiazol-2-yl)-2,5-diphenyltetrazolium bromide (MTT) assay showed that at 2 days from treatment, tumor cell viability was reduced (by >30%) only in the cells treated with MSV-nAb-PTX. At 4 days, more than 30% of tumor cells were not viable following preincubation of macrophages with nAb-PTX and rapamycin, while MSV-nAb-PTX reduced viability by >60% (Figure 1C).

## Macrophage Pretreatment with MSV-nAb-PTX Shifts Their Phenotype toward M1

To investigate the effect of the systems on macrophage polarization state, macrophages pretreated with MSV-nAb-PTX, nAb-PTX, and rapamycin and incubated with breast tumor spheres were tested vs. untreated control for the expression of the cell surface markers CD80 and CD204 (markers for M1 and M2 general polarization states, respectively) (Figure 2). Untreated macrophages in coculture of tumor spheres displayed the M2-like phenotype, as indicated by >85% of the population positive to CD204 staining (Figures 2A,B). This finding is in line with the general polarization of TAM toward the M2 phenotype, as documented previously (5). More than 96% of macrophages in coculture shifted to an M1-like phenotype (CD80 expression) following the treatment with MSV-nAb-PTX. In nAb-PTX- and rapamycin-treated systems,  $44.0 \pm 9.6$  and  $65.6 \pm 10.1\%$  of cells expressed M1 membrane marker.

We have further confirmed these findings *in vivo* (Figure 2C) in the mouse model of liver metastasis of breast tumors. The predominant population of macrophages in the untreated control group was of M2-like polarization state. MSV-nAb-PTX significantly shifted the population of macrophages toward the M1 phenotype (by twofold), while nAb-PTX had no effect on the macrophage polarization state (Figure 2D). Interestingly, more macrophages were present in the breast cancer metastatic liver lesions treated with MSV-nAb-PTX, which prompted us to look for the effect of nanovectors on macrophage migration.

## Effect of MSV-nAb-PTX on Macrophage Migration toward and into 4T1 Cancer Cell Spheres

In order to evaluate the effect of MSV-nAb-PTX pretreatment on macrophage migration toward the tumor spheres and into the sphere core, experiments were performed in the 3D TME model we previously developed (25). Time-lapse videos of live-cell images of pretreated macrophages introduced to the tumor spheroids have shown specific directionality and enhanced speed of macrophages pretreated with MSV-nAb-PTX as compared to controls (Figure 3). NIS elements analysis of the videos revealed an increased speed of macrophages treated with MSV-nAb-PTX within the first 5 h (Figure 3B). The increased speed does correlate with a slight increase in path length of the distance traveled by MSV-nAb-PTX macrophages (Figure 3C). All other treatments did not alter the path length compared to the control. However,

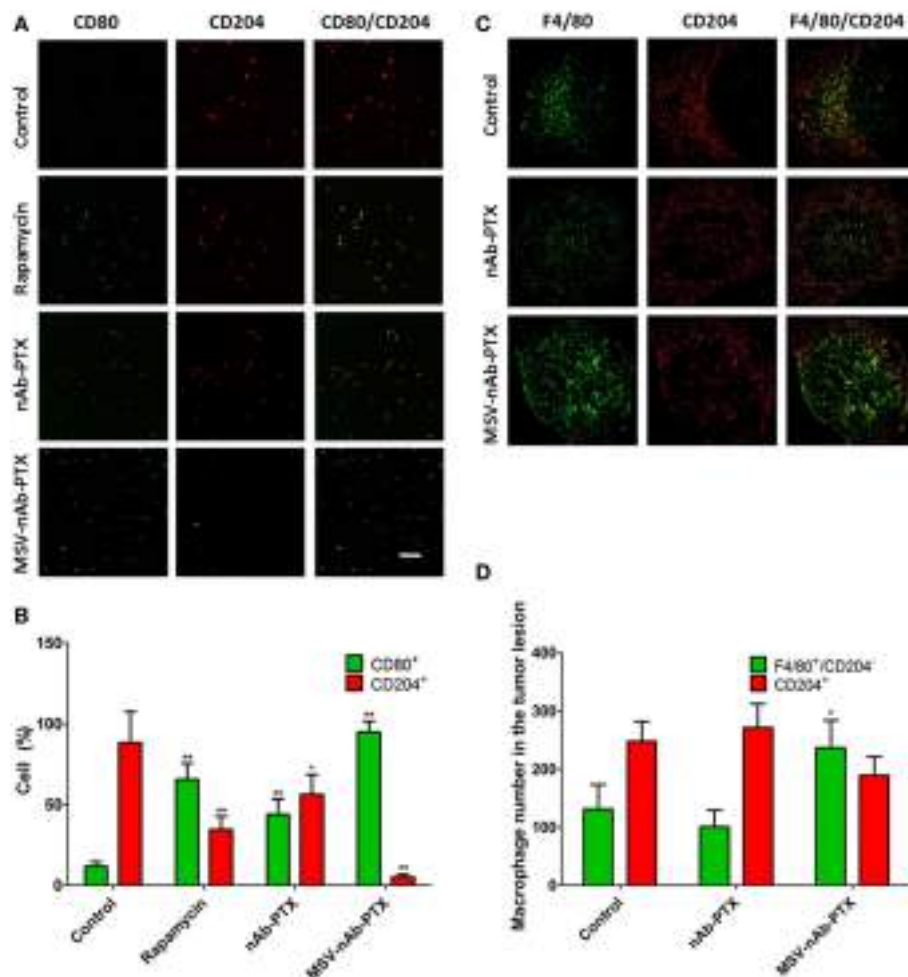


**FIGURE 2 |** Polarization of macrophages in response to treatment *in vitro* and *in vivo*. **(A)** Confocal microscopy images from a coculture of 4T1 cancer spheroids and macrophages pretreated with multistage nanovectors (MSV)-albumin-bound paclitaxel (nAb-PTX), nAb-PTX, and rapamycin. Macrophages are immunostained for either CD80 (green, M1 marker) or CD204 (red, M2 marker) membranal expression. **(B)** Quantification of CD80 and CD204 signals from the images presented in **(A)**; **(C)** confocal images of breast tumor lesions in the liver stained for F4/80 (green, total macrophages) and CD204 (red, M2 macrophages). **(D)** Quantification of M1 and M2 signals (M1 number obtained from F4/80<sup>+</sup>/CD204<sup>-</sup> cells). The results are presented as mean  $\pm$  SD ( $n = 6-9$ ), \* $p < 0.05$ ; \*\* $p < 0.01$  to control.

the most significant change was observed in the directionality of the macrophage migration. The analysis of macrophage displacement toward the tumor sphere within the 5 h time frame showed a significantly specific movement toward the tumor spheres by the macrophages treated with MSV-nAb-PTX. On the other hand, no specific directionality in the movement of macrophages was observed in the cells treated with MSV or nAb-PTX (Figure 3D).

Macrophages pretreated with various systems were tracked and counted in the different depths of the tumor sphere, in increments of 50  $\mu\text{m}$  (Figure 4), focusing on the central part of the spheroid (average diameter 450–500  $\mu\text{m}$ ). The density of macrophages in the deep layers of the tumor sphere significantly increased (>2-fold compared to control) after they were pretreated with MSV-nAb-PTX treatment. nAb-PTX only caused moderate increase in the macrophage number in the innermost layer of the spheres. Further analysis revealed that most of the macrophages found in the center of the spheres were M1-like phenotype. These data

correlate well with an *in vivo* analysis of macrophage localization in breast cancer liver metastatic lesions previously published (25).

We further tested various components of the MSV-nAb-PTX system to determine the factors crucial for macrophage motility toward the center of the sphere (Figure 4C). Various elements of MSV-nAb-PTX were tested for their effect on macrophage motility: fluorescently labeled albumin (Ab) as a major component of nAb-PTX; MSV; MSV-Ab; and nAb-PTX. MSV did not affect the number of macrophages in the center of the tumor spheroid as compared to untreated control, while Ab, MSV-Ab, and nAb-PTX, surprisingly, slightly increased it. MSV-nAb-PTX enabled an increased migration of the macrophages into the deep layers of the tumor sphere. The number of macrophages in the deep layers of the tumor sphere treated with MSV-nAb-PTX was more than the summary of the effects of all individual components of the system, pointing toward the potential synergy of the factors being involved.

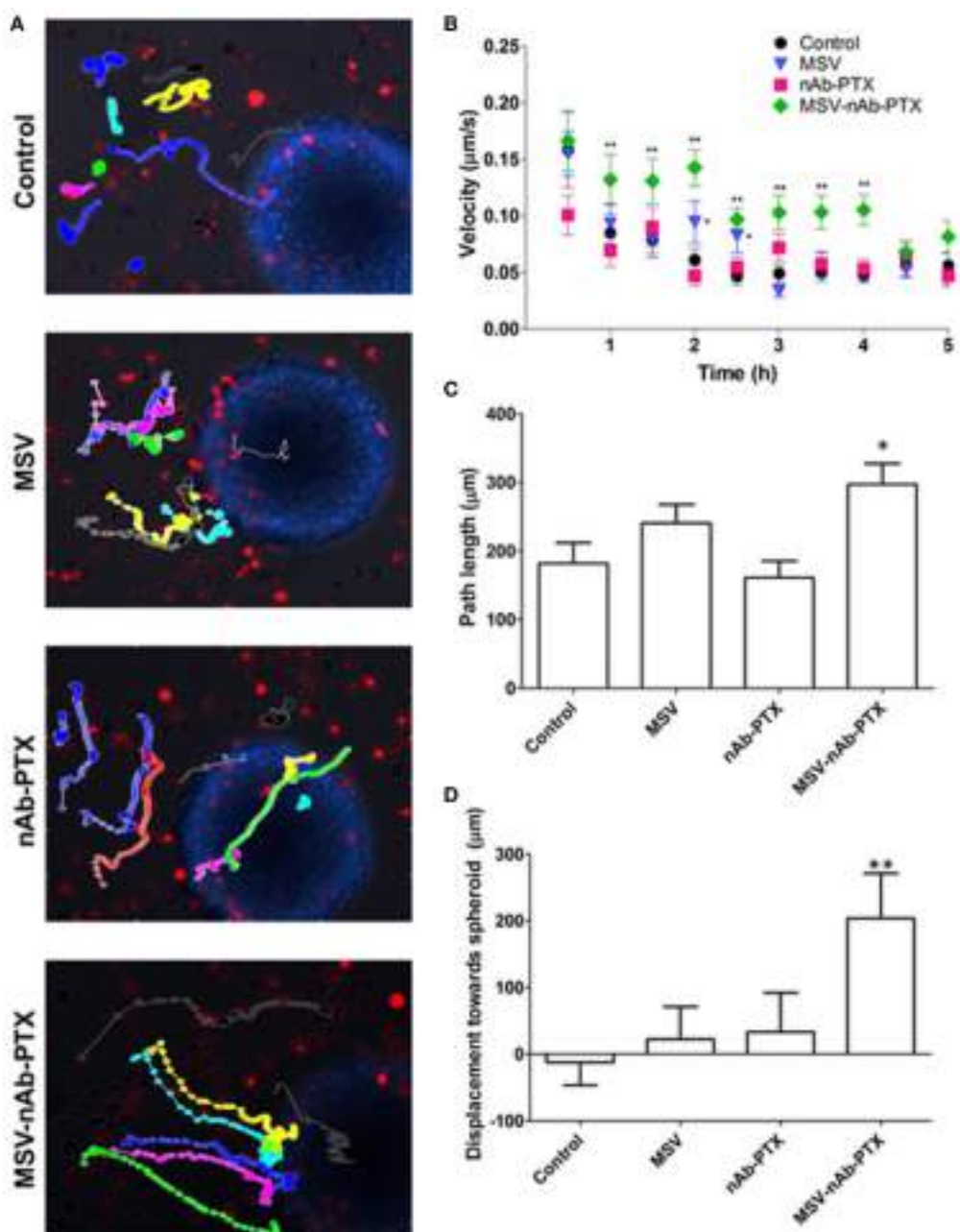
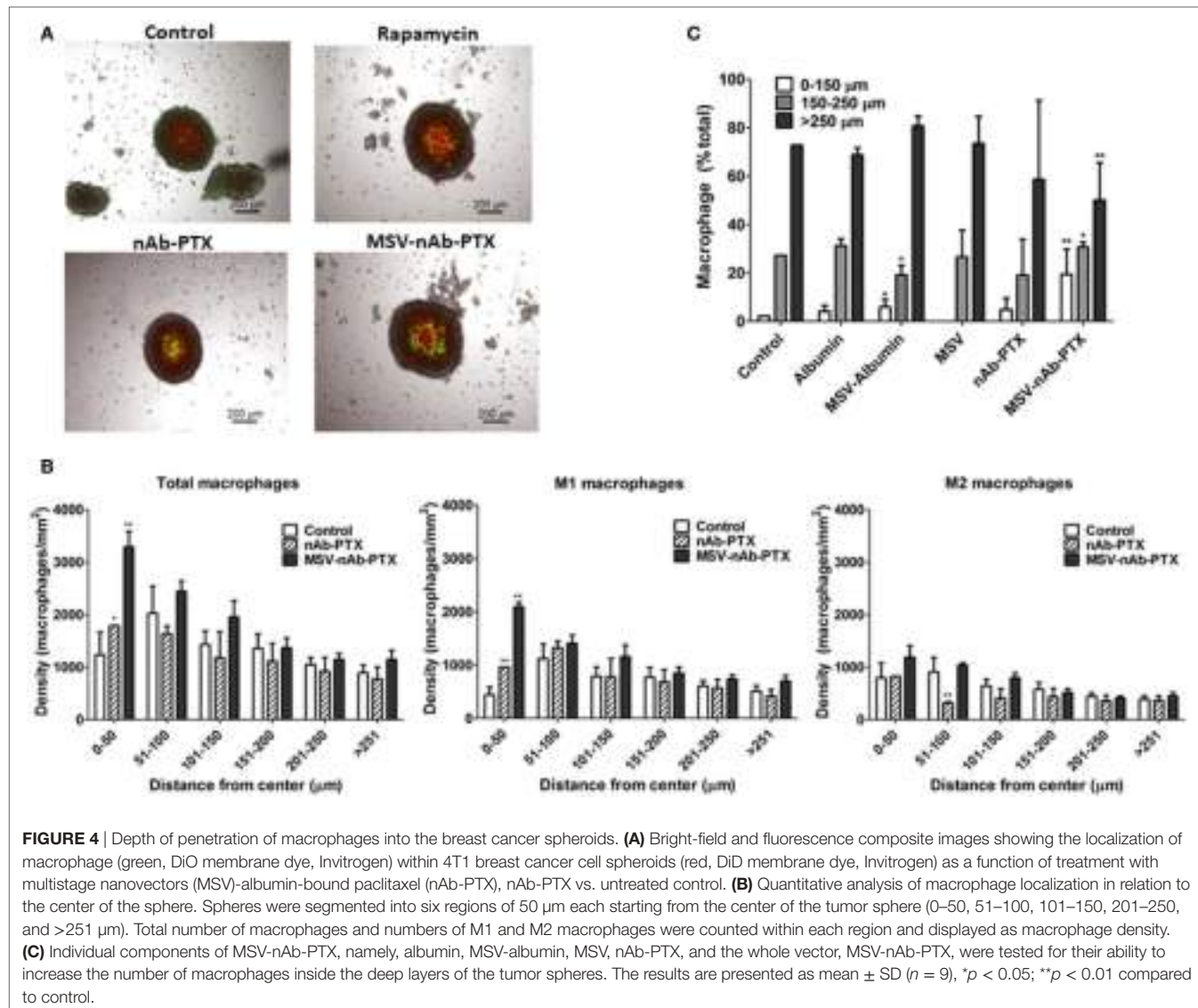


**FIGURE 3 |** Tracking of macrophage migration kinetics, directionality, and dynamics as a function of treatments. **(A)** Macrophage trajectories following the preincubation with multistage nanovectors (MSV)-albumin-bound paclitaxel (nAb-PTX), nAb-PTX, MSV, and no treatment control were tracked relative to the movement of the tumor spheres. Individual trajectories are presented in different colors. Red: macrophages stained DiD membrane dye. Blue: 4T1 breast tumor cells stained with Hoechst 33342 nucleus dye. The trajectories were tracked by live imaging for 5 h and analyzed for velocity **(B)**, path length **(C)**, and directionality **(D)** based on the displacement toward the breast tumor. The results are presented as mean  $\pm$  SEM ( $n = 20\text{--}25$ ), \* $p < 0.05$ ; \*\* $p < 0.01$  as compared to control.

## Effect of MSV-nAb-PTX Pretreatment of Macrophages on Cytokine Production by the Tumors *In Vitro* and *In Vivo*

The main function of the macrophages in the TME is tightly related to their interaction with cancer cells, resulting in the secretion of soluble factors that shape the tumor milieu. Therefore, we further

performed a thorough analysis of the cytokines and chemokines in the TME 3D model *in vitro* and in hepatic metastases of cancerous breast lesions *in vivo*. Interestingly, neither nAb-PTX nor MSV-nAb-PTX had an effect on the release of the cytokines from the macrophages following direct incubation with the systems (Figure S1 in Supplementary Material). The quantification of the factors released by the tumor cells as a response to the conditioned



media from macrophages pretreated with nAb-PTX and MSV-nAb-PTX *in vitro* and *in vivo* is summarized in Figure 5. Cytokine levels measured in tumor cells in response to conditioned media and *in vivo* follow very similar trends. The following factors were increased in both *in vitro* and *in vivo* settings in the TME for MSV-nAb-PTX: G- colony-stimulating factor (CSF), GM-CSF, IFN-gamma, IL-1beta, IL-6, IL-12, IP-10, CCL3, CCL4, CCL5, and TNF-alpha. These data point toward the significant effect of the whole MSV-nAb-PTX system on the macrophage polarization state *in vitro* and *in vivo*. Interestingly, only MCP-1 increased for nAb-PTX-treated macrophages both *in vitro* and *in vivo* settings.

## Mathematical Modeling to Simulate Effect of Macrophage Polarization on Tumor Response *In Vivo*

In order to further analyze the treatment efficacy of MSV-nAb-PTX, we mathematically modeled the effect of MSV-nAb-PTX on

hypovascularized liver lesions *in vivo* coupled with macrophage differentiation into M1 and M2 subtypes. As in our previous work (25), the lesion growth was simulated in parallel with the dynamic drug distribution.

Figure 6 illustrates the effects of therapy with the MSV-nAb-PTX-loaded macrophages. Undifferentiated macrophages extravasate from the vasculature and migrate toward the lesion based on the chemotactic gradient of attractants (such as pro-angiogenic factors released by tumor cells) in the surrounding microenvironment. During this process, the macrophages differentiate into M1 or M2 subtypes depending on the ratio of pro-M1 and pro-M2 macrophage factors being released by viable tumor cells in response to the MSV-nAb-PTX system. M1 macrophages are simulated to release nitric oxide, which inhibits cell viability, while M2 macrophages release tumor growth factors, which promote cellular proliferation (5). Each macrophage acts as a source of drug to simulate the release of PTX from the MSV-nAb-PTX formulation. With MSV-nAb-PTX at 24 h post single treatment,

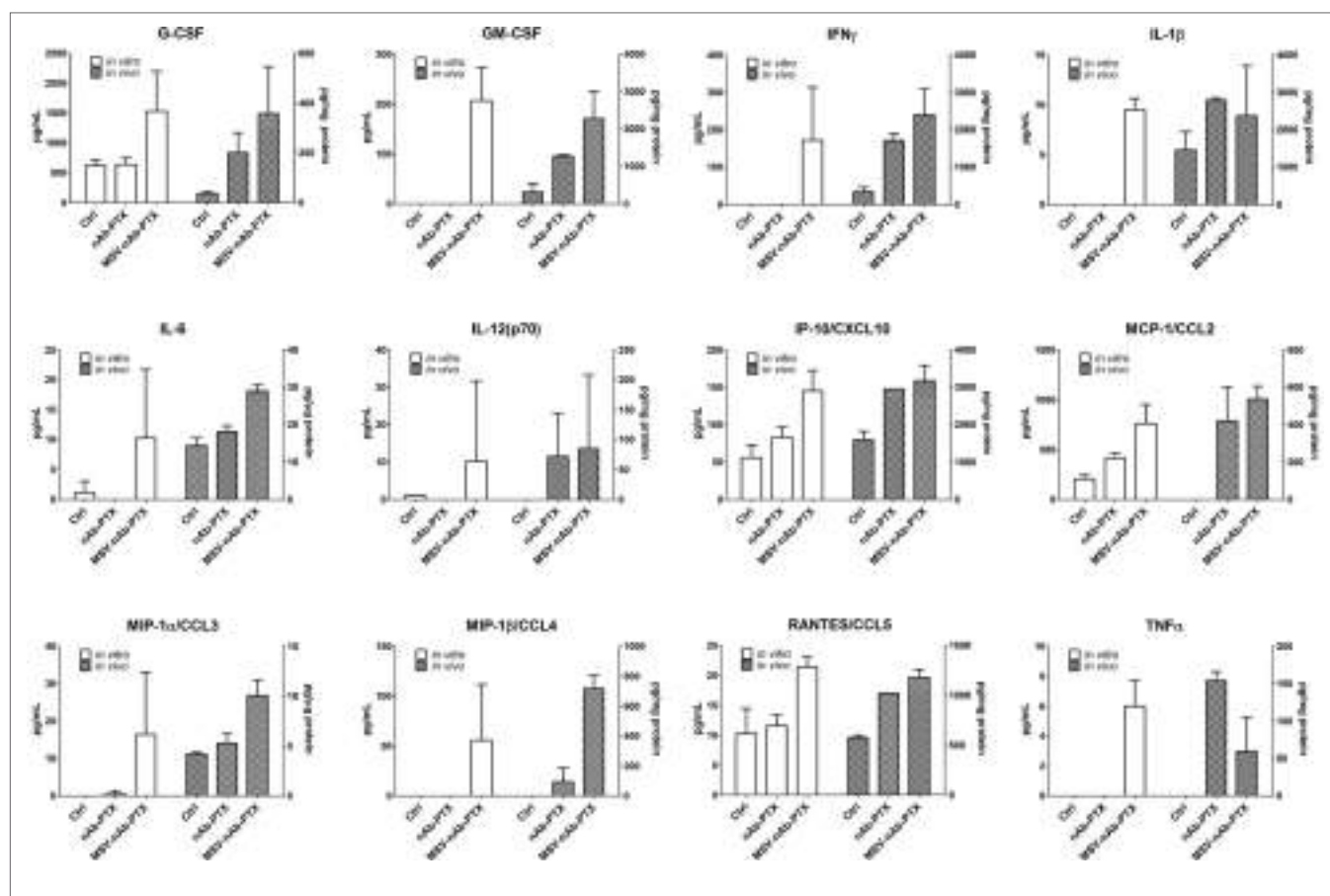


**FIGURE 5 |** Effect of pretreatment of macrophages with multistage nanovectors (MSV)-albumin-bound paclitaxel (nAb-PTX) vs. nAb-PTX and control of cytokine production by the tumors *in vitro* and *in vivo*. Cytokine release was analyzed using MILLIPLEX MAP Mouse Cytokine/Chemokine Immunology Multiplex Assay (EMD Millipore, Billerica, MA, USA) and measured by Luminex 200™ (Luminex, Austin, TX, USA). For *in vitro* evaluation, the systems were preincubated with macrophages and the conditioned media were introduced to the tumor spheres and incubated for 2 days. For the *in vivo* study, liver metastatic lesions as well as the surrounding area of the lesion (tumor microenvironment) were dissected and processed for analysis as described in Section “Materials and Methods.”

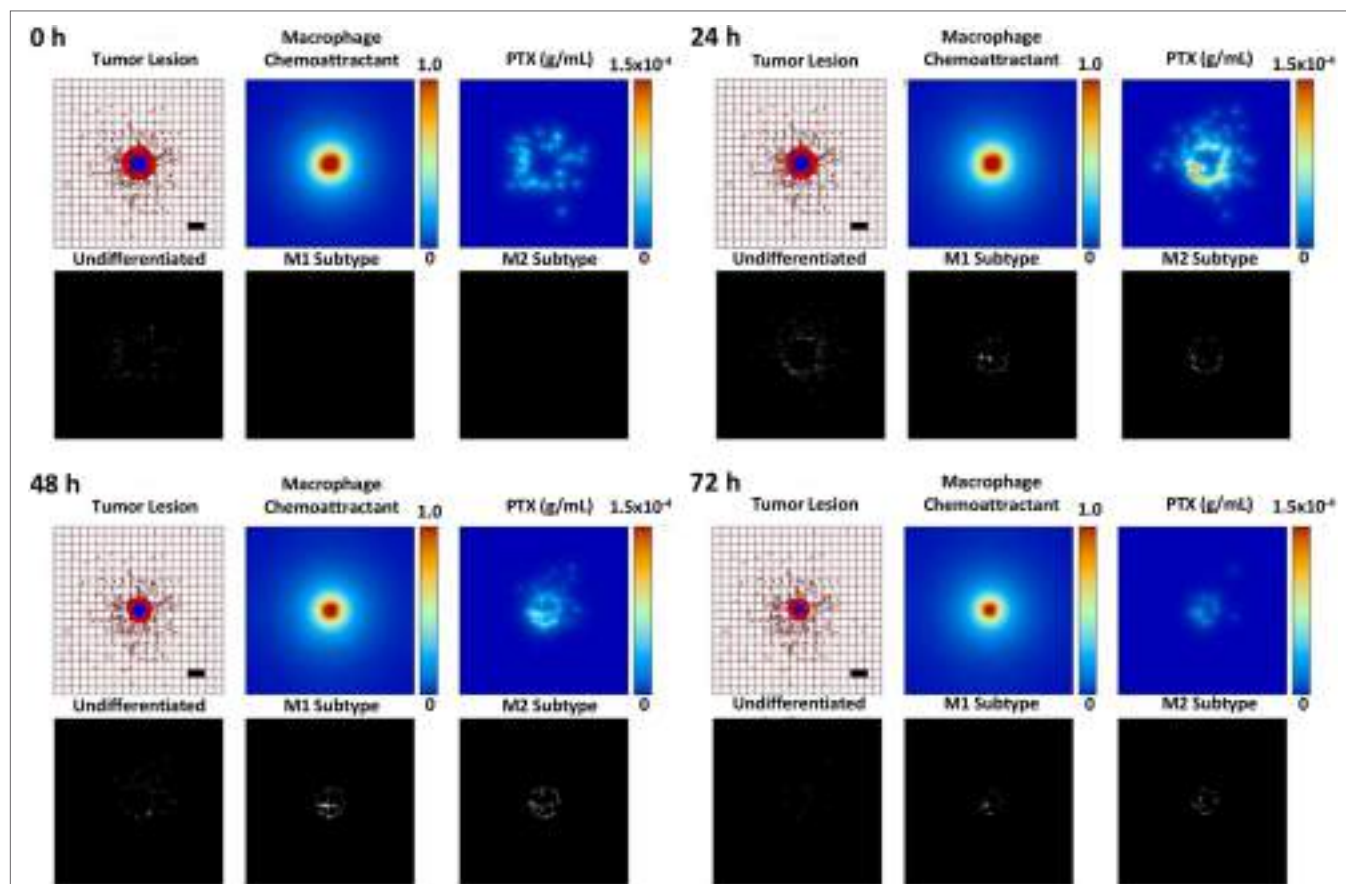
the tumor has slightly shrunk (top right) compared to the initial lesion (5% radius decrease), while the drug is being released by the macrophages. At 72 h, the lesion radius attains the highest regression (68% of its original size), by which time most of the drug has been released from the surrounding macrophages. These results are consistent with our previous modeling work (25).

Figure 7 compares the relative contribution of the macrophage polarization in conjunction with MSV-delivered drug to the tumor progression over the course of 5 days after a single treatment. As expected, the cases without treatment are projected to grow unbounded, with the M2-only and the M1/M2 cases attaining 157 and 156% of their original radius, respectively, while the case without M1/M2 or M1-only, respectively, reaches 143 or 138%. In contrast, all of the MSV-nAb-PTX-treated cases experience regression, which is modulated by the contribution of the macrophage differentiation. The most therapeutically effective scenario is the case with M1-only, reaching 83% of the original radius, followed by the case with both M1 and M2 present, attaining 94%. The cases with M2-only and without any macrophages are anticipated to reach 118 and 111% of their original radius, respectively. Interestingly, the model projects that the presence

of the M2 phenotype enhances drug cytotoxicity due to the M2 tumor growth-promoting effect enlarging the subset of the tumor population that is susceptible to the cell cycle-specific activity of PTX. However, over the long term, the cases with M2 macrophages recover faster than the cases without their presence, thus promoting tumor growth.

## DISCUSSION

It is currently well recognized that the fine interplay between deregulation of tumor cells and the cells of the TME is imperative for all stages of tumor development (27). Macrophages represent the major population of infiltrating immune cells in TME (28). Macrophage polarization is detrimental in the development and progression of cancer (28). TAMs generally belong to the subclass of alternatively differentiated, M2-like macrophages. They have been shown to modulate tissue remodeling and angiogenesis, suppress T cell proliferation, and play a significant role in tumor survival (5). High M2 macrophage density has been clinically correlated with poor prognosis in several epithelial cancers, including breast cancer (29) and hepatocellular carcinoma (30).



**FIGURE 6 |** Simulation of breast cancer liver metastasis therapy with multistage nanovectors (MSV)-albumin-bound paclitaxel (nAb-PTX) over the course of 72 h post treatment initiation. For each of the four sets of panels presented for post therapy initiation (0, 24, 48, and 72 h), the tumor lesion is shown (upper left panels) with viable tumor tissue (red) enclosing a hypoxic region (blue) without necrosis. The dense liver capillary network is modeled by the rectangular grid (brown), with irregular sprouts generated through angiogenesis during the lesion progression. Individual macrophages (white dots, lower left panels) are recruited to the vicinity of the lesion based on chemoattractants released by the tumor cells (upper middle panels) and as a response to MSV-nAb-PTX therapy. During this process, the macrophages differentiate into M1 (white dots, lower middle panels) or M2 subtypes (white dots, lower right panels), which, respectively, either hinder or aid the tumor progression. The MSV-nAb-PTX is retained near and within the lesion by the macrophage infiltration, while the drug is slowly released from them in the tumor proximity (upper right panels). The effect of the therapy on the overall lesion size is evident by 72 h. Bar = 200  $\mu$ m.

On the other hand, clinical studies have shown that an increased M1/M2 ratio in the TME is linked to extended survival in ovarian (31), gastric (10), colorectal (32), and lung (33) tumors. M2-like TAMs are characterized by a constitutive high expression of multiple tumor growth promoting factors, including VEGF, FGF1 and 2, PDGF, GM-CSF, insulin-like growth factor-1, and TGF- $\beta$  (34). For example, in a mouse model of breast cancer, expression of CSF-1 was highest at the invasive edge of the malignancy, which was consequently enriched with M2 macrophages. Epidermal growth factor released by these macrophages increased tumor cell migration and metastasis (35). Flexibility and plasticity represent the key characteristics of the cells of mononuclear phagocytic system and their activation states (5, 36). Polarization of the macrophages between the M1 and M2 general subtypes can be reversed, as was shown in *in vitro* and *in vivo* studies (37). Pathological changes in inflammatory states can sculpt this transition, with M1 macrophages present at initiation and during progression of the inflammatory process and M2 macrophages participating in its resolution. In cancer,

histidine-rich glycoprotein (a host-produced protein deposited in the stroma) was shown to induce TAM reprogramming from M2 to M1, resulting in vascular normalization and improved response to chemotherapy (38).

Our previous study also identified the enrichment of macrophages in the tumor periphery of breast cancer liver metastases in a mouse model (24). We have shown that by directing transport of an Ab-bound drug, nAb-PTX, toward the macrophages in the tumor periphery in the liver using MSV, we could increase the concentration of the drug in the lesions and, consequently, the tumor killing efficiency. However, the pronounced anti-tumor effect observed with MSV-nAb-PTX in this study could not be fully explained only by the shift of the concentration of the drug toward the tumor lesions; thus, in the present work we aimed to evaluate the effect of MSV-nAb-PTX on the inflammatory state of the TME, the migratory potential of the macrophages in the tumor lesion and on the interactions of macrophages with the tumor cells. The studies were performed *in vitro* in a previously

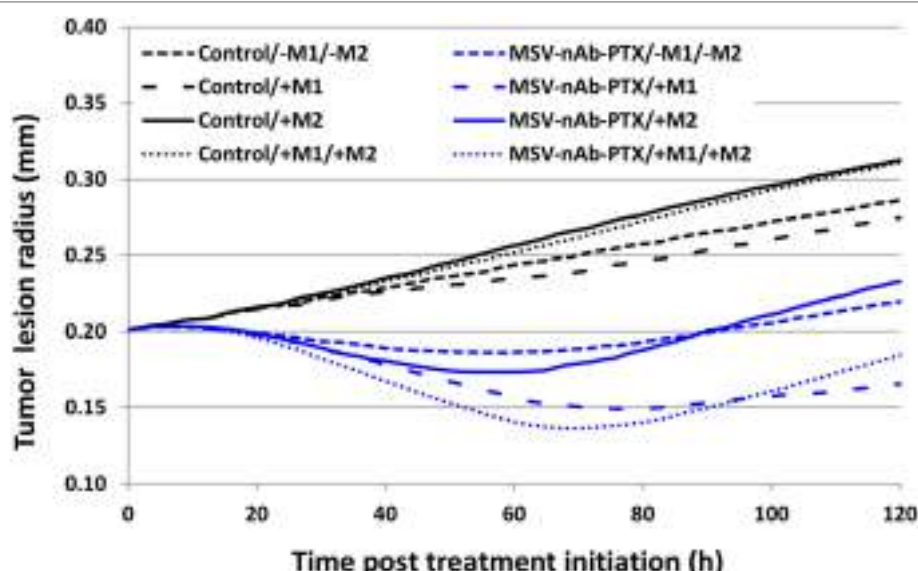


**FIGURE 7 |** Simulation of tumor progression for untreated and multistage nanovectors (MSV)-albumin-bound paclitaxel (nAb-PTX)-treated cases including various combinations of macrophage polarizations simulated over the course of 5 days post treatment initiation. Control: untreated tumors; MSV-nAb-PTX: tumors treated with the therapeutic system. M1 and M2 refer to the addition of the polarized macrophage populations to the model. The cytotoxic effect of the M1 subtypes is simulated to affect the tissue proportional to the concentration of nitrous oxide released in the immediate vicinity of the macrophage. M2 macrophages release diffusible growth factors which promote tumor proliferation. In addition, treated macrophages (M1 and M2) are simulated to release drug which only affects proliferating tissue due to the cell cycle-dependent effect of PTX.

validated 3D model of hypovascularized breast cancer lesions with macrophages on the lesion periphery (25, 39).

Tumor cell proliferation and apoptosis analysis (Figure 1) confirmed that MSV-nAb-PTX preincubated with macrophages had a pronounced therapeutic efficacy, in line with the *in vivo* data (24). It is important to note that in this experimental set we did not expose the tumor spheres to the drugs directly, but only to the macrophages preincubated with the systems, similar to the *in vivo* situation, where hypovascularized breast cancer lesions in the liver are surrounded by macrophages. Preincubation of macrophages with rapamycin, an mTOR inhibitor that is known to induce the polarization of macrophages toward the M1 phenotype (26), had a mild effect on tumor cell proliferation, but significantly increased the number of apoptotic cells in the lesions; thus showing that M1 polarization induced tumor cell apoptosis.

Furthermore, we have analyzed the number of M1 and M2 polarized macrophages in the tumor lesions and the localization of the macrophages within the tumor cores *in vitro* and *in vivo* (Figures 2–4). As expected, the control (untreated) tumors had increased population of alternatively activated M2-like macrophages. The M2 phenotype is characterized by an improved phagocytic activity (40), since this general subcategory of macrophages fights inflammation and participates in tissue remodeling. M2 macrophages uptake solid particles more efficiently, which helps to concentrate nAb-PTX delivered through MSV. *In vitro*, all treatments shifted this ratio to a new homeostasis, increasing the population of M1 macrophages and decreasing the fraction of M2 macrophages (Figure 2). With MSV-nAb-PTX, this effect was the most prominent, and the population of M1 activated macrophages increased 20-fold while M2 macrophages represented

less than 5% of the total number of macrophages. Treatment with nAb-PTX *in vitro* yielded equal populations of M1 and M2 macrophages. Although M1 macrophages predominated with rapamycin, the overall number of macrophages decreased due to a toxic effect of the drug related to inhibition of the mTOR pathway, which is in line with the reported mechanism of rapamycin to induce apoptotic cell death in M0/M2 but not M1 macrophages (26). Interestingly, only MSV-nAb-PTX, but not nAb-PTX caused the shift in the macrophage polarization state *in vivo*. This could be due to the longer retention of the MSV-nAb-PTX in the lesion and specific association of the carrier with the macrophages (24). PTX has been reported to possess a lipopolysaccharide (LPS)-like property, activating murine macrophages by mimicking bacterial LPS through binding to MD2, an extracellular protein of TLR4 (41). LPS-dependent TLR4 can be activated by PTX and internalized into endosomes, activating downstream signaling pathways via endocytic shuttling, and therefore promoting polarization of macrophages toward the M1 phenotype. A recent study demonstrated the ability of nAb-PTX to enhance the macrophage activation process due to macropinocytic uptake and the fusing of macropinosomes and endosomes (42). In our study, the increased concentration of PTX in the TME mediated by MSV-nAb-PTX induced the release of pro-inflammatory cytokines by the tumor cells, promoting the pro-inflammatory milieu in the TME and modulating the macrophages to undergo M2 to M1 polarization. Our results also suggest that the Ab component of the nAb-PTX may be involved in this process and slightly increased macrophage migration toward the center of the tumor spheroids (Figure 4), although further study is needed for deeper understanding. Ab has been previously reported to contribute to the intratumoral

concentration increase of nAb-PTX *via* binding to the 60 kDa glycoprotein receptor and thus increasing transcytosis (43).

We extended the computational model presented in our previous study by Leonard et al (25) to account for macrophage polarization into M1 and M2 subtypes. The simulations provide a platform to analyze the respective effects of different subsets of macrophages in the tumor in combination with MSV-nAb-PTX therapy with the ultimate goal to optimize treatment outcomes. The modeling results suggest that a single therapy may delay the tumor growth *in vivo* but not completely eradicate the lesion. One reason is that insufficient drug is released by the macrophages in the tumor vicinity to kill all of the tumor cells. Modulation of the macrophage population to increase its size and further drive its polarization toward tumorigenicity, e.g., with an immunotherapy, may achieve a stronger one-time response. However, as shown in our previous study, repeated treatments at regular intervals may still be necessary for complete remission to account for the time it takes for hypoxic (quiescent) cells to resume cycling and thus be sensitive to the chemotherapeutic. We further note that the simulations reflect the variability in experimental measurements regarding the effect of the macrophages. The untreated case with no macrophages and the untreated case with both subtypes could be more similar than shown in Section “Results” (Figure 7), while the effect of the M1 macrophages was calibrated to the low end of possible values. Adjusting for these factors, however, does not affect the overall response difference predicted between untreated and treated cases or the response-modulating effect projected for the M2 macrophages.

Various effects can contribute to the increased efficacy of MSV-nAb-PTX *via* inflammatory modulation. Overall, MSV-nAb-PTX increased the motility and directionality of the macrophages toward the tumor sphere (Figure 3). The increased macrophage recruitment may be a response to the increased chemokine release by tumor cells such as CXCL-10, CCL-2, CCL3, CCL4, and CCL5 (Figure 5). Furthermore, the treatment caused deeper macrophage penetration inside the spheroid/tumor lesions (Figure 4), which can correspond with the apoptotic feedback between the dying tumor cells (Figure 1) and the macrophages bearing MSV-nAb-PTX. It is interesting to note that in the therapeutic concentration tested, macrophage polarization (Figure S1 in Supplementary Material) and viability (24, 25) were not affected by the treatment with any of the tested systems.

In hypovascularized lesions in the liver, tumor cells are not directly exposed to the circulating drugs, while the macrophages present in the liver vasculature are exposed to the intravenously administered drug/particles. To mimic this situation, we further incubated the macrophages with nAb-PTX and MSV-nAb-PTX for 1 h [in clinic, 90% of nAb-PTX is cleared from the circulation in this time frame (44)] and further let the macrophages release soluble factors and the internalized drug, exposing the tumor cells to supernatants from the pretreated macrophages (conditioned media collected at 24 h past drug removal). Cytokine and chemokine profiles were also analyzed in the murine model of liver metastasis. In both the *in vitro* tumor spheres and the *in vivo* murine model, there was a significant increase in the factors associated with M1 macrophage polarization, such as CCR5-binding chemokines (CCL3, CCL4, and CCL5) (45), interleukins (IL-6 and IL-1 $\beta$ ), and TNF- $\alpha$  (46). A significant increase in GM-CSF

levels released by the tumors *in vitro* and *in vivo* in response to exposure to macrophages preincubated with MSV-nAb-PTX can impart an additional feedback on the M1 polarization state (47), as exposure to GM-CSF was previously shown to promote M1 polarization of the macrophages (47, 48).

These findings could explain the attraction of the macrophages toward the tumor spheres *in vitro* and into the tumor core *in vitro* and *in vivo*. In contrast to previous studies showing that cancer cell apoptosis shifted the phenotype of macrophages toward M2 (49, 50), we have observed that the effects of MSV-nAb-PTX enhanced apoptosis of tumor cells. This can be explained by the fact that there is a direct effect of the system on the macrophage polarization toward the M1 phenotype. Activated M1 macrophages have been recently reported to produce and excrete chitotriosidases (or family 18 chitinases), which can modulate proteases and cause damage to cancer cell membranes (51).

In conclusion, our data demonstrate that macrophages carried MSV-nAb-PTX while not being affected by the therapeutics. The phagocytosis of the solid particles by the macrophages enhanced the drug concentrations inside of these immune system cells (24), consequently enhancing concentrations of the drug released by macrophages in the TME. As a result, tumor cells were exposed to higher concentrations of drug, resulting in enhanced tumor-cell killing, while also inducing an LPS-like effect of PTX as described by Byrd-Leifer et al. (52). This prompted tumor cells to release higher levels of pro-inflammatory cytokines, causing further shift of macrophage polarization toward the anti-tumorigenic M1 phenotype. The data also suggest that polarization of the nanovectors contributes to the toxicity toward cancer cells. Altogether, these phenomena could be utilized to design improved nanovector-based cancer therapies.

## MATERIALS AND METHODS

### Fabrication of nAb-PTX-MSV

Albumin-bound paclitaxel-multistage nanovectors— or fluorescently labeled Ab loaded, Ab-MSV, were fabricated and characterized as previously described (24, 25). Briefly, MSV with  $1 \times 0.4 \mu\text{m}$  ( $d \times h$ ) dimensions were fabricated in a microelectronics facility *via* photolithography and electrochemical etching and further oxidized with 3-aminopropyl-triethoxysilane (APTES) (24, 53). APTES-MSV were lyophilized using the Freezone Freeze Dry System (Labconco, Kansas City, MO, USA). nAb-PTX (Abraxane®, Celgene, Summit, NJ, USA) or Ab (Ab-fluorescein isothiocyanate conjugate, Sigma-Aldrich, St. Louis, MO, USA) concentrated solution was loaded to dried MSV particles in aliquots. Loading was enhanced by a drying process *via* incubation of the particles under low pressure (25, 54). nAb-PTX-MSV was characterized for morphology, zeta potential, and the loading efficiency as described earlier (24, 25).

### Cell Culture

Breast cancer 4T1 cells (ATCC, Manassas, VA, USA) were cultured in Minimum Essential Medium (MEM) with 10% FBS, 1% antibiotic/antimycotic, 1% GlutaMAX, 1% NEAA, 1% MEM vitamin, and 1% sodium pyruvate supplements and maintained in humidified atmosphere at 37°C and 5% CO<sub>2</sub>. Mice macrophages

were obtained by isolation from fresh mice bone marrow. Monocytes were washed twice with PBS and erythrocytes were lysed by red cell lysis buffer (Sigma, USA), and cells were filtered with a 70  $\mu\text{m}$  filter (BD Lifesciences, USA). Differentiation of monocytes to resting macrophages was initiated by 7-day incubation with macrophage medium, containing 10% FBS and 1% penicillin/streptomycin in RPMI 1640 medium.

### 3D TME Model: Coculture of Breast Cancer Spheres and Macrophages

Tumor spheres were generated using the Bio-Assembler™ system based on protocols we recently reported (39, 55) and grown to ~450–500  $\mu\text{m}$  diameter before cytotoxicity and migration studies. Depending on the studies, macrophages were treated with rapamycin, Ab, MSV-Ab, nAb-PTX, MSV, or MSV-nAb-PTX for 4 h and stained with Vybrant Cell-Labeling Solutions (Molecular Probes, Eugene, OR, USA). After treatment, supernatants were removed and cells were washed with fresh medium to ensure that no 4T1 cancer cells are not in contact with drugs in the solution (similar to the clinically relevant situation in hypovascularized tumor lesions). Primary macrophages ( $1 \times 10^3$ ) were cultured together with 4T1 spheres in a 96-well plate and kept in an incubator. Images were taken by fluorescent microscopy after 24, 48, 72, and 96 h and analyzed with NIS-Elements software.

Transwell plates (Corning Inc., Corning, NY, USA) were utilized for coculture study to analyze macrophage differentiation. 4T1 cells ( $1.5 \times 10^4$ ) were seeded on the apical side while ( $1.5 \times 10^3$ ) macrophages were seeded on the basolateral side. After 96 h, macrophages were harvested and stained for CD80 and CD204.

### Cell Staining and Confocal Microscopy

Cocultures of macrophages and 4T1 spheres were fixed with 4% paraformaldehyde before staining. Spheres were stained for TUNEL with FITC for apoptosis detection with Promega TUNEL kit (Promega, Madison, WI, USA) according to the manufacturer's protocol. To assess proliferation the samples were incubated overnight with primary rabbit anti-mouse Ki67 antibody (1:500, Abcam, Cambridge, UK), washed twice with PBS and incubated with Alexa Fluor 647-labeled goat anti-rabbit secondary antibody for 4 h. Samples were washed twice with PBS before further analysis by confocal microscopy.

Rat anti-mouse CD80 (Thermo Scientific, Rockford, IL, USA) and Alexa Fluor 647-labeled CD204 (Abcam, Cambridge, UK) were utilized for surface marker staining of the macrophages in the coculture. After paraformaldehyde fixation, samples were washed twice with PBS and incubated with 1% BSA for 20 min. CD80 antibody (5  $\mu\text{g}/\text{ml}$ ) was added and incubated with the samples overnight at 4°C. After washing with PBS, goat anti-rat FITC-labeled antibody was added to the samples for 2 h at RT. Furthermore, samples were washed and stained with Alexa Fluor 647-labeled anti-CD204 (2 h, RT). Prior to confocal microscopy analysis, the samples were washed twice with PBS.

Tumor spheres and macrophages were visualized using a Nikon A1 confocal microscope (Nikon Inc., Melville, NY, USA) based on the fluorescence of the respective probes and analyzed

with NIS elements software (Nikon Inc.). Macrophage signal intensity, quantification of macrophages of various phenotypes, and macrophage penetration into the tumor lesion were assessed as below.

### Tracking of Macrophage Migration Kinetics, Directionality, and Dynamics As a Function of Treatments

For the tracking of macrophage migration toward the tumor spheres, the cells were stained with DiD membrane dye (Invitrogen, USA), pretreated with nAb-PTX, MSV, or MSV-nAb-PTX for 1 h and washed. Furthermore, the macrophages were cocultured with breast cancer spheres as described earlier. To differentiate between the two cell populations, 4T1 breast cancer cells were prestained with 1  $\mu\text{g}/\text{mL}$  Hoechst 33342 dye (Thermo Scientific). Tumor spheres and macrophage movements were tracked using a live-imaging system Nikon TiEclipse fluorescence microscope (Nikon Inc., USA) over the time course of 10 h and analyzed with NIS elements. The motility of 4T1 spheres was recorded over time and used as the reference for macrophage displacement calculation. Macrophages speed, path length, as well as coordinates were tracked using NIS elements and calculated for their directionality toward 4T1 spheres using the initial coordinates of the cell vs. the tumor sphere as a reference point.

### MTT Assay

3-(4,5-Dimethylthiazol-2-yl)-2,5-diphenyltetrazolium bromide (Sigma, USA) assay was performed to access cell viability. 4T1 spheres in coculture with macrophages were seeded on 96-well plates before treatment. After 48 or 96 h of incubation, the cells were washed twice with PBS and the MTT assay was run based on the manufacturer instructions. The absorbance was determined using a spectrophotometer (Biotek, Winooski, VT, USA) at 570 nm.

### In Vivo Model of Breast Cancer Liver Metastasis

Animal studies were performed in accordance with approved protocols by Houston Methodist Research Institute Institutional Animal Care and Use Committee (AUP-0514-0032). Balb/c mice were purchased from Charles Rivers Laboratories and mouse breast cancer liver metastases xenograft were generated by splenic injection of  $10^5$  4T1 tumor cells/100  $\mu\text{L}$  PBS as we previously described (24, 43). Splenectomy was conducted immediately after injection to prevent primary tumor growth in the spleen, and the xenografts were grown for at least 10 days before therapy.

### In Vivo Evaluation of Macrophage Quantity within the Microenvironment

For analysis of TME changes in response to therapy *in vivo*, mice with cancer liver metastasis were randomly divided into three groups ( $n = 4$ ): control, nAb-PTX, MSV-nAb-PTX·nAb-PTX, and MSV-nAb-PTX containing 75 mg/kg nAb-PTX (7.5 mg/kg PTX) were injected via the tail vein. The treatment was repeated every 3 days and the mice were sacrificed after three treatments.

The liver was dissected, embedded in OCT compound (Sakura® Finetek USA, Inc., Torrance, CA, USA), and cut in 4  $\mu$ m sections for histological and immunofluorescence analyses. The frozen sections were fixed with ice-cold acetone and stained with Alexa Fluor 488-tagged rat anti-mouse F4/80 antibody and TRITC anti-mouse CD204 antibody to detect total macrophages and the M2 subpopulation, respectively. We have used the CD204 marker to characterize alternatively polarized M2 macrophages (56, 57) and F4/80 as a marker for general population of macrophages. Cell nuclei were stained with 4,6-diamidino-2-phenylindole, dihydrochloride.

## Cytokines Analysis

For *in vitro* cytokine and chemokine analysis, macrophages were plated in a 96-well plate, with a density of 10,000 cells/well and treated with 150 ng nAb-PTX or MSV-nAb-PTX for 1 h. Drug treatment was removed, cells were washed twice with PBS, and fresh medium was added to the macrophages. This was performed to mimic the clinically relevant situation, as clinical studies with nAb-PTX revealed that more than 90% of the drug is cleared from circulation within 1 h following intravenous administration (44). Supernatants (conditioned media) were harvested from macrophages after 24 h and 50  $\mu$ L of this conditioned media were added to 50  $\mu$ L fresh media to culture preformed tumor spheres. Supernatants from 4T1 spheres were harvested after 2 days, and the cytokine and chemokine release was analyzed by MILLIPLEX MAP Mouse Cytokine/Chemokine Immunology Multiplex Assay (EMD Millipore, Billerica, MA, USA) and measured by Luminex 200™ (Luminex, Austin, TX, USA). Additionally, to determine the effect of treatments to the macrophages themselves, the treated macrophages were further cultured with 100  $\mu$ L fresh medium for 3 days. After incubation, the culture media were collected for a cyto-/chemokine release study.

From the *in vivo* studies, liver metastatic lesions as well as the surrounding area of the lesion (TME) were dissected. Tissues were weighed, 500  $\mu$ L PBS with 1× HALTTM protease inhibitor cocktail (Thermo Fisher Scientific, Waltham, MA, USA) was added to the samples, and the samples were homogenized using Polytron PT2100 homogenizer (Kinematica AG, Lucerne, Switzerland). Tissue lysates were incubated under constant agitation for 2 h and the supernatants were separated by centrifugation at 10,000  $\times g$  for 20 min at 4°C. Supernatants containing protein extracts were used for cyto-/chemokine measurements. Protein content of the supernatants was determined using Pierce™ BCA Protein Assay Kit (Thermo Fisher Scientific, Waltham, MA, USA) for normalization of further measurements. Cyto-/chemokines were analyzed by MILLIPLEX MAP Mouse Cytokine/Chemokine Immunology Multiplex Assay (EMD Millipore, Billerica, MA, USA) and measured by Luminex 200™ (Luminex, Austin, TX, USA).

## Mathematical Model

We applied mathematical modeling to computationally simulate the tumor response as a function of MSV-nAb-PTX-coupled

macrophages differentiating into M1- and M2 subtypes. As described in our previous work (25), the model (58–61) simulates viable and necrotic tissue in hepatic metastases, including the transport of macrophages and molecules through this tissue. The tumor growth is obtained through balance of cell proliferation and death. Proliferation depends on adequate oxygen and cell nutrients, while death is induced by levels of oxygen below a threshold of viability as well as drug above a certain level of cytotoxicity. Values for the model parameters were calibrated to our experimental data as in Ref. (25, 58–61). We simulated release of paclitaxel from nAb-PTX carried by nanovector-loaded macrophages infiltrating the tumor tissue and differentiating into M1- and M2 subtypes. The model and associated parameters are further described in the Supplementary Material.

## Statistical Analysis

All quantitative parameters are presented as mean values with SD. Statistical analysis was performed by *t*-test for unpaired samples using Graphpad Prism software, with *p*-value <0.05 accepted as indicative of significant difference, <0.01 as a statistically very significant difference.

## ETHICS STATEMENT

Animal studies were performed in accordance with approved protocols by Houston Methodist Research Institute Institutional Animal Care and Use Committee (IACUC) (AUP-0514-0032).

## AUTHOR CONTRIBUTIONS

BG, FL, and HF conceived the idea and designed the research. FL and TN performed *in vitro* experiments and analyzed the data. FL and MW analyzed the live-cell imaging data. FL and KY performed *in vivo* studies. LC and HF developed computational models and therapy simulations. XL fabricated MSV. FL, HF, and BG wrote the manuscript. All the authors reviewed and approved the manuscript.

## ACKNOWLEDGMENTS

We would like to thank Megumi Kai and Yan Ting Liu for providing mice bone marrow for monocyte isolation, and Carlotta Borsoi for her assistance with immunostaining of the histological slides from *in vivo* studies.

## FUNDING

BG acknowledges the support from R21HD08947. BG and XL acknowledge the support from 1R21CA190024-01A1.

## SUPPLEMENTARY MATERIAL

The Supplementary Material for this article can be found online at <http://journal.frontiersin.org/article/10.3389/fimmu.2017.00693/full#supplementary-material>.

## REFERENCES

- Balkwill F, Mantovani A. Inflammation and cancer: back to Virchow? *Lancet* (2001) 357:539–45. doi:10.1016/S0140-6736(00)04046-0
- Coussens LM, Werb Z. Inflammation and cancer. *Nature* (2002) 420:860–7. doi:10.1038/nature01322
- Balkwill F, Charles KA, Mantovani A. Smoldering and polarized inflammation in the initiation and promotion of malignant disease. *Cancer Cell* (2005) 7:211–7. doi:10.1016/j.ccr.2005.02.013
- Martinez FO. Regulators of macrophage activation. *Eur J Immunol* (2011) 41:1531–4. doi:10.1002/eji.201141670
- Mantovani A, Sozzani S, Locati M, Allavena P, Sica A. Macrophage polarization: tumor-associated macrophages as a paradigm for polarized M2 mononuclear phagocytes. *Trends Immunol* (2002) 23:549–55. doi:10.1016/S1471-4906(02)02302-5
- Jakubzick CV, Randolph GJ, Henson PM. Monocyte differentiation and antigen-presenting functions. *Nat Rev Immunol* (2017) 17(6):349–62. doi:10.1038/nri.2017.28
- Sica A, Schioppa T, Mantovani A, Allavena P. Tumour-associated macrophages are a distinct M2 polarised population promoting tumour progression: potential targets of anti-cancer therapy. *Eur J Cancer* (2006) 42:717–27. doi:10.1016/j.ejca.2006.01.003
- Mantovani A, Allavena P, Sica A. Tumour-associated macrophages as a prototypic type II polarised phagocyte population: role in tumour progression. *Eur J Cancer* (2004) 40:1660–7. doi:10.1016/j.ejca.2004.03.016
- Cao W, Peters JH, Nieman D, Sharma M, Watson T, Yu J. Macrophage subtype predicts lymph node metastasis in oesophageal adenocarcinoma and promotes cancer cell invasion in vitro. *Br J Cancer* (2015) 113:738–46. doi:10.1038/bjc.2015.292
- Pantano F, Berti P, Guida FM, Perrone G, Vincenzi B, Amato MMC, et al. The role of macrophages polarization in predicting prognosis of radically resected gastric cancer patients. *J Cell Mol Med* (2013) 17:1415–21. doi:10.1111/jcmm.12109
- Lan C, Huang X, Lin S, Huang H, Cai Q, Wan T, et al. Expression of M2-polarized macrophages is associated with poor prognosis for advanced epithelial ovarian cancer. *Technol Cancer Res Treat* (2013) 12:259–67. doi:10.7785/tctr.2012.500312
- Bronkhorst IHG, Ly LV, Jordanova ES, Vrolijk J, Versluis M, Luyten GPM, et al. Detection of M2-macrophages in uveal melanoma and relation with survival. *Invest Ophthalmol Vis Sci* (2011) 52:643–50. doi:10.1167/iovs.10-5979
- Chávez-Galán L, Olleros ML, Vesin D, García I. Much more than M1 and M2 macrophages, there are also CD169(+) and TCR(+) macrophages. *Front Immunol* (2015) 6:263. doi:10.3389/fimmu.2015.00263
- Goswami KK, Ghosh T, Ghosh S, Sarkar M, Bose A, Baral R. Tumor promoting role of anti-tumor macrophages in tumor microenvironment. *Cell Immunol* (2017) 316:1–10. doi:10.1016/j.cellimm.2017.04.005
- Mantovani A, Sica A, Allavena P, Garlanda C, Locati M. Tumor-associated macrophages and the related myeloid-derived suppressor cells as a paradigm of the diversity of macrophage activation. *Hum Immunol* (2009) 70:325–30. doi:10.1016/j.humimm.2009.02.008
- Takeya M, Komohara Y. Role of tumor-associated macrophages in human malignancies: friend or foe? *Pathol Int* (2016) 66:491–505. doi:10.1111/pin.12440
- Sica A, Mantovani A. Macrophage plasticity and polarization: in vivo veritas. *J Clin Invest* (2012) 122:787–95. doi:10.1172/JCI59643
- Stout RD, Jiang C, Matta B, Tietzel I, Watkins SK, Suttles J. Macrophages sequentially change their functional phenotype in response to changes in microenvironmental influences. *J Immunol* (2005) 175:342–9. doi:10.4049/jimmunol.175.1.342
- Georgoudaki A-M, Prokopek KE, Boura VF, Hellqvist E, Sohn S, Östling J, et al. Reprogramming tumor-associated macrophages by antibody targeting inhibits cancer progression and metastasis. *Cell Rep* (2016) 15:2000–11. doi:10.1016/j.celrep.2016.04.084
- Olsson A, Nakhlé J, Sundstedt A, Plas P, Bauchet A-L, Pierron V, et al. Tasquinimod triggers an early change in the polarization of tumor associated macrophages in the tumor microenvironment. *J Immunother Cancer* (2015) 3:53. doi:10.1186/s40425-015-0098-5
- Jain S, Tran T-H, Amiji M. Macrophage repolarization with targeted alginate nanoparticles containing IL-10 plasmid DNA for the treatment of experimental arthritis. *Biomaterials* (2015) 61:162–77. doi:10.1016/j.biomaterials.2015.05.028
- Tran T-H, Rastogi R, Shelke J, Amiji MM. Modulation of macrophage functional polarity towards anti-inflammatory phenotype with plasmid DNA delivery in CD44 targeting hyaluronic acid nanoparticles. *Sci Rep* (2015) 5:16632. doi:10.1038/srep16632
- Miao X, Leng X, Zhang Q. The current state of nanoparticle-induced macrophage polarization and reprogramming research. *Int J Mol Sci* (2017) 18:336. doi:10.3390/ijms18020336
- Tanei T, Leonard F, Liu X, Alexander JF, Saito Y, Ferrari M, et al. Redirecting transport of nanoparticle albumin-bound paclitaxel to macrophages enhances therapeutic efficacy against liver metastases. *Cancer Res* (2016) 76:429–39. doi:10.1158/0008-5472.CAN-15-1576
- Leonard F, Curtis LT, Yesantharao P, Tanei T, Alexander JF, Wu M, et al. Enhanced performance of macrophage-encapsulated nanoparticle albumin-bound paclitaxel in hypo-perfused cancer lesions. *Nanoscale* (2016) 8:12544–52. doi:10.1039/c5nr07796f
- Mercallì A, Calavita I, Dugnani E, Citro A, Cantarelli E, Nano R, et al. Rapamycin unbalances the polarization of human macrophages to M1. *Immunology* (2013) 140:179–90. doi:10.1111/imm.12126
- Quail DF, Joyce JA. Microenvironmental regulation of tumor progression and metastasis. *Nat Med* (2013) 19:1423–37. doi:10.1038/nm.3394
- Mantovani A, Marchesi F, Malesci A, Laghi L, Allavena P. Tumour-associated macrophages as treatment targets in oncology. *Nat Rev Clin Oncol* (2017). doi:10.1038/nrclinonc.2016.217
- Laoui D, Movahedi K, Van Overmeire E, Van den Bossche J, Schouppe E, Mommer C, et al. Tumor-associated macrophages in breast cancer: distinct subsets, distinct functions. *Int J Dev Biol* (2011) 55:861–7. doi:10.1387/ijdb.113371dl
- Zhang QW, Liu L, Gong CY, Shi HS, Zeng YH, Wang XZ, et al. Prognostic significance of tumor-associated macrophages in solid tumor: a meta-analysis of the literature. *PLoS One* (2012) 7:e50946. doi:10.1371/journal.pone.0050946
- Zhang M, He Y, Sun X, Li Q, Wang W, Zhao A, et al. A high M1/M2 ratio of tumor-associated macrophages is associated with extended survival in ovarian cancer patients. *J Ovarian Res* (2014) 7:19. doi:10.1186/1757-2215-7-19
- Edin S, Wikberg ML, Dahlin AM, Rutegård J, Öberg Å, Oldenborg P-A, et al. The distribution of macrophages with a M1 or M2 phenotype in relation to prognosis and the molecular characteristics of colorectal cancer. *PLoS One* (2012) 7:e47045. doi:10.1371/journal.pone.0047045
- Yuan A, Hsiao YJ, Chen HY, Chen HW, Ho CC, Chen YY, et al. Opposite effects of M1 and M2 macrophage subtypes on lung cancer progression. *Sci Rep* (2015) 5:14273. doi:10.1038/srep14273
- Hanahan D, Coussens L. Accessories to the crime: functions of cells recruited to the tumor microenvironment. *Cancer Cell* (2012) 21:309–22. doi:10.1016/j.ccr.2012.02.022
- Wyckoff J, Wang W, Lin EY, Wang Y, Pixley F, Stanley ER, et al. A paracrine loop between tumor cells and macrophages is required for tumor cell migration in mammary tumors. *Cancer Res* (2004) 64:7022–9. doi:10.1158/0008-5472.CAN-04-1449
- Biswas SK, Mantovani A. Macrophage plasticity and interaction with lymphocyte subsets: cancer as a paradigm. *Nat Immunol* (2010) 11:889–96. doi:10.1038/ni.1937
- Guiducci C, Vicari AP, Sangaletti S, Trinchieri G, Colombo MP. Redirecting in vivo elicited tumor infiltrating macrophages and dendritic cells towards tumor rejection. *Cancer Res* (2005) 65:3437–46. doi:10.1158/0008-5472.CAN-04-4262
- Rolny C, Mazzone M, Tugues S, Laoui D, Johansson I, Coulon C, et al. HRG inhibits tumor growth and metastasis by inducing macrophage polarization and vessel normalization through downregulation of PIGF. *Cancer Cell* (2011) 19:31–44. doi:10.1016/j.ccr.2010.11.009
- Leonard F, Godin B. 3D in vitro model for breast cancer research using magnetic levitation and bioprinting method. *Methods Mol Biol* (2016) 1406:239–51. doi:10.1007/978-1-4939-3444-7\_21
- Gordon S, Martinez FO. Alternative activation of macrophages: mechanism and functions. *Immunity* (2010) 32:593–604. doi:10.1016/j.immuni.2010.05.007
- Zimmer SM, Liu J, Clayton JL, Stephens DS, Snyder JP. Paclitaxel binding to human and murine MD-2. *J Biol Chem* (2008) 283:27916–26. doi:10.1074/jbc.M802826200
- Cullis J, Siolas D, Avanzi A, Barui S, Maitra A, Bar-Sagi D. Macropinocytosis of Nab-paclitaxel drives macrophage activation in pancreatic cancer. *Cancer Immunol Res* (2017) 5:182–90. doi:10.1158/2326-6066.CIR-16-0125

43. Desai N, Trieu V, Yao Z, Louie L, Ci S, Yang A, et al. Increased antitumor activity, intratumor paclitaxel concentrations, and endothelial cell transport of cremophor-free, albumin-bound paclitaxel, ABI-007, compared with cremophor-based paclitaxel. *Clin Cancer Res* (2006) 12:1317–24. doi:10.1158/1078-0432.CCR-05-1634
44. Sparreboom A, Scripture CD, Trieu V, Williams PJ, De T, Yang A, et al. Comparative preclinical and clinical pharmacokinetics of a cremophor-free, nanoparticle albumin-bound paclitaxel (abi-007) and paclitaxel formulated in cremophor (Taxol). *Clin Cancer Res* (2005) 11:4136–43. doi:10.1158/1078-0432.CCR-04-2291
45. Cassol E, Cassetta L, Rizzi C, Alfano M, Poli G. M1 and M2a polarization of human monocyte-derived macrophages inhibits HIV-1 replication by distinct mechanisms. *J Immunol* (2009) 182:6237–46. doi:10.4049/jimmunol.0803447
46. Luckett-Chastain L, Calhoun K, Schartz T, Gallucci RM. IL-6 influences the balance between M1 and M2 macrophages in a mouse model of irritant contact dermatitis. *J Immunol* (2016) 196 (1 Suppl):196.17.
47. Hamilton JA. Rheumatoid arthritis: opposing actions of haemopoietic growth factors and slow-acting anti-rheumatic drugs. *Lancet* (1993) 342:536–9. doi:10.1016/0140-6736(93)91653-4
48. Fleetwood AJ, Lawrence T, Hamilton JA, Cook AD. Granulocyte-macrophage colony-stimulating factor (CSF) and macrophage CSF-dependent macrophage phenotypes display differences in cytokine profiles and transcription factor activities: implications for CSF blockade in inflammation. *J Immunol* (2007) 178:5245–52. doi:10.4049/jimmunol.178.8.5245
49. Weigert A, Tzinelly N, von Knethen A, Johann AM, Schmidt H, Geisslinger G, et al. Tumor cell apoptosis polarizes macrophages role of sphingosine-1-phosphate. *Mol Biol Cell* (2007) 18:3810–9. doi:10.1091/mbc.E06-12-1096
50. Ferracini M, Rios FJO, Pecenin M, Jancar S. Clearance of apoptotic cells by macrophages induces regulatory phenotype and involves stimulation of CD36 and platelet-activating factor receptor. *Mediators Inflamm* (2013) 2013:8. doi:10.1155/2013/950273
51. Pan XQ. The mechanism of the anticancer function of M1 macrophages and their use in the clinic. *Chin J Cancer* (2012) 31:557–63. doi:10.5732/cjc.012.10046
52. Byrd-Leifer CA, Block EF, Takeda K, Akira S, Ding A. The role of MyD88 and TLR4 in the LPS-mimetic activity of Taxol. *Eur J Immunol* (2001) 31:2448–57. doi:10.1002/1521-4141(200108)31:8<2448::AID-IMMU2448>3.0.CO;2-N
53. Godin B, Chiappini C, Srinivasan S, Alexander JF, Yokoi K, Ferrari M, et al. Discoidal porous silicon particles: fabrication and biodistribution in breast cancer bearing mice. *Adv Funct Mater* (2012) 22:4225–35. doi:10.1002/adfm.201290121
54. Leonard F, Margulis-Goshen K, Liu X, Srinivasan S, Magdassi S, Godin B. Low pressure mediated enhancement of nanoparticle and macromolecule loading into porous silicon structures. *Mesoporous Biomater* (2014) 1. doi:10.2478/mesi-2014-0002
55. Jaganathan H, Gage J, Leonard F, Srinivasan S, Souza GR, Dave B, et al. Three-dimensional in vitro co-culture model of breast tumor using magnetic levitation. *Sci Rep* (2014) 4:6468. doi:10.1038/srep06468
56. Kawamura K, Komohara Y, Takaishi K, Katabuchi H, Takeya M. Detection of M2 macrophages and colony-stimulating factor 1 expression in serous and mucinous ovarian epithelial tumors. *Pathol Int* (2009) 59:300–5. doi:10.1111/j.1440-1827.2009.02369.x
57. Soldano S, Pizzorni C, Paolino S, Trombetta AC, Montagna P, Brizzolara R, et al. Alternatively activated (M2) macrophage phenotype is inducible by endothelin-1 in cultured human macrophages. *PLoS One* (2016) 11:e0166433. doi:10.1371/journal.pone.0166433
58. Wu M, Frieboes HB, McDougall SR, Chaplain MAJ, Cristini V, Lowengrub J. The effect of interstitial pressure on tumor growth: coupling with the blood and lymphatic vascular systems. *J Theor Biol* (2013) 320:131–51. doi:10.1016/j.jtbi.2012.11.031
59. van de Ven AL, Wu M, Lowengrub J, McDougall SR, Chaplain MAJ, Cristini V, et al. Integrated intravital microscopy and mathematical modeling to optimize nanotherapeutics delivery to tumors. *AIP Adv* (2012) 2:11208. doi:10.1063/1.3699060
60. Macklin P, McDougall S, Anderson ARA, Chaplain MAJ, Cristini V, Lowengrub J. Multiscale modelling and nonlinear simulation of vascular tumour growth. *J Math Biol* (2009) 58:765–98. doi:10.1007/s00285-008-0216-9
61. Wu M, Frieboes HB, Chaplain MAJ, McDougall SR, Cristini V, Lowengrub JS. The effect of interstitial pressure on therapeutic agent transport: coupling with the tumor blood and lymphatic vascular systems. *J Theor Biol* (2014) 355:194–207. doi:10.1016/j.jtbi.2014.04.012

**Conflict of Interest Statement:** The authors declare that the research was conducted in the absence of any commercial or financial relationships that could be construed as a potential conflict of interest.

Copyright © 2017 Leonard, Curtis, Ware, Nosrat, Liu, Yokoi, Frieboes and Godin. This is an open-access article distributed under the terms of the Creative Commons Attribution License (CC BY). The use, distribution or reproduction in other forums is permitted, provided the original author(s) or licensor are credited and that the original publication in this journal is cited, in accordance with accepted academic practice. No use, distribution or reproduction is permitted which does not comply with these terms.



# Ameliorating Amyloid- $\beta$ Fibrils Triggered Inflammation via Curcumin-Loaded Polymeric Nanoconstructs

**Andrea Ameruoso<sup>1</sup>, Roberto Palomba<sup>1</sup>, Anna Lisa Palange<sup>1</sup>, Antonio Cervadoro<sup>1</sup>, Aeju Lee<sup>2</sup>, Daniele Di Mascolo<sup>1†</sup> and Paolo Decuzzi<sup>1†\*</sup>**

<sup>1</sup>Laboratory of Nanotechnology for Precision Medicine, Fondazione Istituto Italiano di Tecnologia, Genoa, Italy,

<sup>2</sup>International Research Organization for Advanced Science and Technology (IROAST), Kumamoto University, Kumamoto, Kumamoto Prefecture, Japan

## OPEN ACCESS

### Edited by:

Paola Italiani,  
Consiglio Nazionale Delle  
Ricerche (CNR), Italy

### Reviewed by:

Attilio Iemolo,  
University of California,  
San Diego, United States  
Seyed Moein Moghimi,  
Durham University,  
United Kingdom

### \*Correspondence:

Paolo Decuzzi  
paolo.decuzzi@iit.it

<sup>†</sup>These author share  
the senior authorship.

### Specialty section:

This article was submitted  
to Inflammation,  
a section of the journal  
*Frontiers in Immunology*

**Received:** 31 January 2017

**Accepted:** 11 October 2017

**Published:** 31 October 2017

### Citation:

Ameruoso A, Palomba R, Palange AL, Cervadoro A, Lee A, Di Mascolo D and Decuzzi P (2017) Ameliorating Amyloid- $\beta$  Fibrils Triggered Inflammation via Curcumin-Loaded Polymeric Nanoconstructs. *Front. Immunol.* 8:1411. doi: 10.3389/fimmu.2017.01411

Inflammation is a common hallmark in several diseases, including atherosclerosis, cancer, obesity, and neurodegeneration. In Alzheimer's disease (AD), growing evidence directly correlates neuronal damage with inflammation of myeloid brain cells, such as microglia. Here, polymeric nanoparticles were engineered and characterized for the delivery of anti-inflammatory molecules to macrophages stimulated via direct incubation with amyloid- $\beta$  fibers. 200 nm spherical polymeric nanoconstructs (SPNs) and 1,000 nm discoidal polymeric nanoconstructs (DPNs) were synthesized using poly(lactic-co-glycolic acid) (PLGA), polyethylene glycol (PEG), and lipid chains as building blocks. First, the internalization propensity in macrophages of both nanoparticles was assessed via cytofluorimetric and confocal microscopy analyses, demonstrating that SPNs are by far more rapidly taken up as compared to DPNs ( $99.6 \pm 0.11$  vs  $14.4 \pm 0.06\%$ , within 24 h). Then, Curcumin-loaded SPNs (Curc-SPNs) were realized by encapsulating Curcumin, a natural anti-inflammatory molecule, within the PLGA core of SPNs. Finally, Curc-SPNs were shown to diminish up to 6.5-fold the production of pro-inflammatory cytokines—IL-1 $\beta$ ; IL-6, and TNF- $\alpha$ —in macrophages stimulated via amyloid- $\beta$  fibers. Although more sophisticated *in vitro* models and systematic analyses on the blood–brain barrier permeability are critically needed, these findings hold potential in the development of nanoparticles for modulating inflammation in AD.

**Keywords:** nanoparticle, inflammation, systemic delivery, neurodegenerative diseases, macrophage activation

## INTRODUCTION

Inflammation is a defense response to external pathogens and other insults which is precisely orchestrated by our immune system. However, under certain conditions, inflammatory processes could become detrimental and lead to severe pathological states (1). This is the case of atherosclerosis where monocyte infiltration into the vessel walls and maturation into macrophages are key events in the formation and progression of vascular plaques (2). Inflammation and immune cells play a role in cancer too where tumor-associated macrophages could protect and sustain the growth of malignant cells (3). Moreover, in obesity, macrophage infiltration in adipose tissue causes local and systemic inflammation eventually leading to insulin resistance (4). Similarly, in Alzheimer's

disease (AD), mounting evidence indicates that macrophages of the central nervous system—microglia—contribute to the onset of the disease and sustain neurotoxicity (5, 6). While under physiological conditions, microglia serve as immune surveilling cells, upon injury or immune stimuli activation, microglia secrete pro-inflammatory cytokines that are eventually responsible of neuronal death. Following the amyloid cascade hypothesis, microglia activation is triggered in Alzheimer's disease by amyloid- $\beta$  plaques (A $\beta$ s), resulting from the extracellular accumulation of amyloid- $\beta$  peptides, and neurofibrillary tangles, deriving from the clustering of the microtubule-associated protein tau. Over a sufficiently long time, this is responsible of chronic brain inflammation and production of pro-inflammatory cytokines, such as IL-1 $\beta$ , IL-6, TNF- $\alpha$ , and many others (7).

Nanomedicines are slowly but surely accessing clinical practice for the treatment of deadly diseases, so far primarily involving cancer and cardiovascular (8, 9). Over 40 liposomal and polymeric nanoparticles are currently undergoing clinical investigation and a few nano-based products are already routinely used by oncologists (liposomal doxorubicin and albumin-bound paclitaxel). Over single therapeutic agents, nanomedicines can carry and deliver multiple drug molecules to diseased sites following specific release profiles; protect the payload from enzymatic degradations and enhance bioavailability; provide useful information at the cellular and tissue scales for designing patient-specific therapeutic interventions. Furthermore, the size, shape, surface properties, and mechanical stiffness of nanomedicines can be often precisely tailored during the fabrication process to enhance accumulation at the biological target and mitigate adverse effects deriving by off-targeting (10–15). Importantly, properly designed nanoparticles can be rapidly taken up by activated macrophages residing in different vascular districts and tissues. This gives the opportunity of efficiently using nanoparticles to deliver directly into activated macrophages anti-inflammatory agents, possibly modulating both locally and systemically the inflammatory state. The authors and other groups have loaded nanoparticles with a variety of anti-inflammatory molecules, starting with the natural, broad-spectrum molecule Curcumin and moving to drugs with more specific sub-cellular targets as diclofenac (16–18). Note that both Curcumin and diclofenac are hydrophobic, exhibit a poor bioavailability and their specific, systemic administration can be largely improved *via* encapsulation into nanoparticles.

This work aims at selecting nanoparticles for the specific delivery of Curcumin to macrophages which have been activated by incubation with amyloid- $\beta$  fibrils. First, two different nanoparticle configurations were considered, namely spherical polymeric nanoconstruct (SPNs) with a characteristic size of about 200 nm and discoidal polymeric nanoconstructs (DPNs) with a diameter of 1,000 nm and height of 400 nm (15, 17). Both nanoparticles were realized with biodegradable and biocompatible polymers—poly(lactic-co-glycolic acid) (PLGA), polyethylene glycol (PEG)—mixed with lipid chains. Then, the most effective configuration was selected based on macrophage internalization assays involving cytofluorimetric and confocal microscopy analyses. Finally, the selected configuration was loaded with Curcumin and delivered to macrophages, in the

presence of amyloid- $\beta$  fibrils, for assessing IL-1 $\beta$ ; IL-6 and TNF- $\alpha$  production.

## MATERIALS AND METHODS

### Materials

Poly(lactic-co-glycolic acid) (50:50, Carboxy-terminated, MW 38,000–54,000 Da) was purchased from Sigma Aldrich (St. Louis, MO, USA). 1,2-dipalmitoyl-sn-glycero-3-phosphocholine (DPPC) and 1,2-distearoyl-sn-glycero-3-phosphoethanolamine-N-[Carboxy(Polyethylene Glycol)-2000] (DSPE-PEG) were obtained from Avanti Polar Lipids (Alabaster, Alabama). Curcumin (95% total curcuminoïd content) was purchased from Alfa Aesar. Chloroform, Acetonitrile and other solvents were obtained from Sigma Aldrich.

### Nanoparticle Synthesis and Characterization

Spherical polymeric nanoconstructs (SPNs) were synthesized by employing an emulsion/solvent evaporation technique (17). DSPE-PEG was dissolved in a 4% ethanol solution to a final volume of 3 ml to obtain the aqueous phase, whereas 1 mg of PLGA and an appropriate quantity of DPPC were dissolved in chloroform to create the oil phase. A v/v ratio of 6:1 between the aqueous and organic phase, a lipids/polymer w/w ratio of 20% and a DPPC/DSPE-PEG molar ratio of 7.5:2.5 were used. Then, the oil phase was added in a dropwise manner to the aqueous solution under ultrasonication at 60% amplitude (Q125 sonicator, Q-Sonica). The resulting emulsion was then gently stirred at room temperature and in a reduced pressure environment for 4 h to allow solvent evaporation. Finally, nanoparticles were washed with water by centrifugation using Amicon Ultra-4, Centrifugal Filter 10,000 Da (Millipore) at 3,500 rpm for 8 min for three times to remove any possible debris obtained in the synthesis process. SPN size and surface zeta potential were estimated by dynamic light scattering (DLS) (Malvern Zetasizer, ZEN 3600). To this end, nanoparticles solution was centrifuged at 12,000 rpm for 20 min and the pellet was resuspended in 1 ml of Milli-Q water; then, 20  $\mu$ l were diluted in 1 ml of Milli-Q water and the resulting solution was transferred into a folded capillary cell (Malvern). The Smoluchowski model was used to calculate zeta potential values. For scanning electron microscopy (SEM) analysis, the SPN solution was dropped directly onto a polished silicon wafer. After drying, samples were sputter-coated with platinum prior to imaging, to enhance polymer contrast. The stability of the nanoparticles was evaluated over a period of 9 days. Nanoparticles were suspended in 1 ml of Milli-Q water and kept at 37°C for the whole time span. At various time points (namely at days 1, 2, 3, 5, and 9), a DLS analysis on each sample was performed as described above. For each characterization study, the number of analyzed samples was 3.

Discoidal polymeric nanoconstructs were synthesized by employing a top-down fabrication process described in details in our previous works (14, 15). Briefly, this fabrication approach involves the use of electron beam lithography (EBL) to fabricate a silicon master template presenting an array of cylindrical holes

with a fixed diameter (1,000 nm) and height (400 nm). This pattern is then replicated into PDMS and subsequently PVA templates, by using soft lithography techniques. Once the holes of the sacrificial template (PVA) are filled with the polymeric mixture composed by PLGA and PEG, the PVA is dissolved in water to collect the resulting particles. To perform internalization experiments, lipid Rhodamine was added to the polymeric mixture composing DPNs. DPN physical chemical characterization was performed through Multisizer (Beckman Coulter) to calculate DPN concentration and size distribution profile, and DLS to estimate the zeta potential. The samples for transmission electron microscopy (TEM) were prepared by the drop casting method over copper grid. The samples were negatively stained for 10 min with 2% (w/v) uranyl acetate aqueous solution, and then washed twice with distilled water and dried before imaging. The stability of the DPNs was evaluated as described above for the SPNs ( $n = 3$ ).

## Cell Cultures

Raw 264.7 cells were purchased from the American Type Culture Collection (ATCC, Rockville, MD, USA) and maintained in Dulbecco's Modified Eagle's Medium high-glucose (DMEM) (Euroclone) supplemented with 10% fetal bovine serum (ATCC) and 1% penicillin/streptomycin. Cells were grown at 37°C in an 80% humidified atmosphere of 5% CO<sub>2</sub>.

## Internalization Experiments

$2 \times 10^5$  RAW 264.7 cells were seeded into a 12 well plate. Cells were treated with SPNs (1.5 µg/ml), Fluoresbrite® Carboxyl NYO Carboxylate Microspheres 0.20 µm (Polyscience) (30 Particles per cell), and DPNs (10 particles per cell). 24 h later cells were harvested in phenol red free DMEM (Lonza) and analyzed by flow cytometry using BD FACS Aria (Beckton Dickinson).  $2 \times 10^5$  events per sample were analyzed, and experiments were run in triplicate. For microscopy analyses,  $1 \times 10^4$  RAW 264.7 cells were seeded into a Lab-Tek II Chambered Coverglass (Thermo Fisher). Cells were treated following the same condition described above. Images were acquired using A1 + Nikon confocal microscope system (Nikon). Statistic was performed analyzing four images per each group and performed in triplicate.

## Drug Loading (DL) and Release

Curcumin-loaded SPNs (Curc-SPNs) were synthesized by employing the same emulsion/solvent evaporation technique described above. Simply, the 200 µg of Curcumin was dissolved in chloroform and added to the oil phase per each milligram of PLGA. To estimate loading and encapsulation efficiency (EE), SPNs were resuspended in 1 ml of water and freeze-dried. After lyophilization, a known amount of particles was dissolved in acetonitrile to free the entrapped drug. The absorbance of Curcumin at 430 nm, with a baseline wavelength of 650 nm, was measured and used to calculate the amount of molecule. Each sample was evaluated in triplicate. Loading efficiency was expressed as the weight percentage of drug mass with respect to the total mass of the nanoparticles, whereas EE was expressed as the weight percentage of entrapped drug mass as compared

to the initial drug input. The *in vitro* release of Curcumin was evaluated under physiological conditions in PBS at 37°C and pH 7.4 up to 72 h. 200 µl of nanoparticle solution at 10 µM Curcumin were transferred into Slide-A-Lyzer MINI dialysis cups with a molecular cutoff of 10 kDa (Thermo Scientific, Rockford, IL, USA) and dialyzed against 4 l of PBS. At each time point, three replicates were retrieved and analyzed. Quantification of the amount of drug released was obtained through a spectrophotometric measurement, using a method akin to the one employed in assessing the loading efficiency. The content of each cup was collected and centrifuged at 12,000 rpm for 20 min, and the resulting pellet of nanoparticles was dissolved in acetonitrile. Then, for each sample, the absorbance at 430 nm with a baseline wavelength of 650 nm was measured. Results for each time point are expressed as a percentage with respect to the initial time point.

## In Vitro Production of Amyloid-β Fibrils

Amyloid-β (Aβ) peptides (Aβ 1–42) (MW 4415.26, Sigma Aldrich) were dissolved by briefly vortexing in a 0.02% ammonia solution at a concentration of 1 mM at 4°C and stored at -80°C. Formation of Aβ fibrils was obtained through a polymerization reaction conducted as described by Ono and Hasegawa: Aβ peptides were dissolved in 50 mM phosphate buffer (pH 7.4, 100 mM NaCl) to a final concentration of 25 µM and to a final volume of 950 µl and incubated for 6 and 16 h at 37°C. The reaction was stopped by storing the samples at 4°C. Aβ fibrils were visualized via TEM. 4 µl of fibril solution were cast on a carbon-coated copper grid and positively stained for 10 min with a 2% (w/v) uranyl acetate aqueous solution. Samples were then washed with distilled water and dried before imaging.

## Cell Viability Assay

Dead Cell Apoptosis Kit with Annexin V FITC and PI (ThermoFisher) was used to initially detect any apoptotic effect of PLGA, as main constituent of our particles, both SPNs and DPNs. Cells ( $2 \times 10^5$ ) were seeded and, after reaching confluence, were treated with empty nanoparticles, at three different concentrations, namely 0.05, 1.5, and 15 µg/ml of PLGA. After 12 h, cells were detached from the plates and stained using the aforementioned kit. Then FACS analyses were performed. An MTT(3-(4,5-Dimethylthiazol-2-yl)-2,5-Diphenyltetrazolium Bromide) proliferation assay (Sigma Aldrich) was used to evaluate the cytotoxicity of free Curcumin, empty nanoparticles, and Curcumin-loaded nanoparticles. Cells were seeded at a density of  $5 \times 10^3$  cells per well in 96 well plates and cultured for 24 h. Free Curcumin was suspended in DMSO and diluted to various concentrations with complete cell media. DMSO was always kept at a final concentration below 0.1% v/v. Empty SPNs and Curcumin-SPNs were resuspended in complete media at various concentrations. These solutions were used to treat cells. After 24 h, the medium was removed and the MTT working solution was added according to the manufacturer's instructions. After 4 h, medium was removed and DMSO was added to each well to solubilize the purple precipitates. Upon complete solubilization, the absorbance at 570 nm was measured for each sample. In all groups, five replicates were analyzed per each of the used

concentration. Data are expressed as the percentage of viable cells with respect to controls.

## Real-time RT-PCR

Raw 264.7 macrophages were seeded at a density of  $2 \times 10^5$  cells/well in 6-well plates, containing 2 ml of culture media. Cells were pre-treated for 5 h with 10  $\mu\text{M}$  free Curcumin or Curc-SPNs and then exposed to 2  $\mu\text{M}$  A $\beta$  fibrils and 100 ng/ml LPS (Sigma Aldrich). Cells were also exposed to empty SPNs, A $\beta$  fibrils and LPS without previous treatment with Curc-SPNs. After 6 h, total RNA was extracted using RNeasy Plus Mini Kit (Qiagen) according to the manufacturer's instructions and quantified using Nanodrop 2000 UV-Vis Spectrophotometer (Thermo Scientific). Real Time RT-PCR were carried out using a Power SYBR Green RNA-to-Ct 1-Step Kit (Applied Biosystems). The reactions were performed in a final volume of 20  $\mu\text{l}$  of the following reaction mixture: 2X Power SYBR Green RT-PCR Mix, 200 nM respective primer pairs, 125X RT Enzyme Mix, 100 ng of RNA template for retrotranscription and amplification of TNF- $\alpha$ , IL-1 $\beta$ , or IL-6 gene product. GAPDH was used as housekeeping gene. Oligonucleotide primer pairs were as follows: for GAPDH, 5'-GAACATCATCCCTGCATCCA-3' and 5'-CCAGTGAGCTCCCGTTCA-3'; for TNF- $\alpha$ , 5'-GGTG CCTATGTCTCAGCCTCTT-3' and 5'-GCCATAGAACTGATG AGAGGGAG-3'; for IL-1 $\beta$ , 5'-TGGACCTTCAGGATGAGGA CA-3' and 5'-GTTCATCTCGGAGCCTGTAGTG-3'; for IL-6, 5'-TACCACTTCACAAGTCGGAGGC-3' and 5'-CTGCAAAGTG CATCATCGTTGTT-3'. The fold change in gene expression was evaluated by  $\Delta\Delta^{\text{Ct}}$  method, relative to the control. All experimental groups were tested in triplicate.

## Statistical Analysis

Statistical analysis of significance was performed using ANOVA, after that equal-variance assumption was confirmed, using the robust Brown–Forsythe Levene-type test for homogeneity of variance. Multiple comparisons were performed using, as *post hoc* test, the Tukey's honestly significant difference (HSD) test. Comparisons with a *p*-value lower or equal to 0.05 was considered statistically significant different with respect to control. Data are presented as mean  $\pm$  SD.

## RESULTS

### Synthesis and Physico-Chemical Characterization of Spherical and DPNs

Spherical Polymeric Nanoconstructs (SPNs) were synthetized *via* an emulsion/solvent evaporation technique, as detailed in the Section "Materials and Methods" and in previous reports by the authors and other scientists (16, 17, 19). As schematically depicted in Figure 1A, SPNs exhibit a hydrophobic polymeric core made out of PLGA which is stabilized externally by a lipid monolayer comprising a mixture of dipalmitoyl-sn-glycero-3-phosphocholine (DPPC) and 1,2-distearoyl-sn-glycero-3-phosphoethanolamine-N-[amino(polyethylene glycol)-2000] with a carboxylic termination (DSPE-PEG-COOH). Following synthesis, SPNs were characterized for their physico-chemical properties. Specifically, SPN geometry (size and shape) was

analyzed *via* DLS and SEM. The SPN hydrodynamic size in de-ionized (DI) water resulted of  $184.19 \pm 15.06$  nm, with a polydispersity index (PDI) of  $0.115 \pm 0.036$ , based on DLS measurements (Figure 1B). The monodisperse population of SPNs is confirmed by the moderate PDI and the SEM image in Figure 1C. The  $\zeta$ -potential of SPNs was of  $-43.18 \pm 9.23$  mV, documenting the presence of negative surface charges associated with the carboxylic termination of the DSPE-PEG-COOH chains. The colloidal stability of SPNs was also assessed by measuring longitudinally, over a period of 9 days, both the hydrodynamic size and PDI. The resulting data (Figure 1D) document a remarkable stability of SPNs with a negligible size and PDI variation over the whole period.

Discoidal polymeric nanoconstructs were synthetized *via* a top-down fabrication approach combining lithographic techniques, template replications and polymer mixture loading, as previously described by the authors (14, 15). As shown in Figure 1E, DPNs appear as circular disks resulting from cross linking PLGA and poly(ethylene glycol) diacrylate (PEG-DA) chains. Following synthesis, DPNs were characterized for their physico-chemical properties. Specifically, DPN geometry (size and shape) was analyzed *via* Multisizer characterization and TEM. Size assessment of DPNs, measured in DI water *via* Multisizer, returned an average size of  $787 \pm 27$  nm (Figure 1F). Given the non-sphericity of DPNs, their size spectrum cannot present a single, sharp peak as for SPNs in Figure 1B. The TEM image in Figure 1G confirms the discoidal shape with a diameter of  $\sim 1,000$  nm and a height of  $\sim 400$  nm. The  $\zeta$ -potential of DPNs was around  $-19.9 \pm 4.56$  mV, resulting from the balance between the neutral charge of the PEG chains and the negative surface charge associated with the carboxylic termination on the PLGA chains. The colloidal stability of DPNs was also assessed by measuring longitudinally, over a period of 9 days, the average size *via* Multisizer. The data reported in Figure 1H document a remarkable stability over time even for this second nanoplatform.

### Analysis of Macrophage Interaction with SPNs and DPNs

Cytofluorimetric analysis was performed in order to assess SPN and DPN internalization into professional phagocytic cells. The same volume ( $\sim 1 \times 10^6 \mu\text{m}^3$ ) of polymeric particles was used. Specifically, SPNs (1.5  $\mu\text{g}/\text{ml}$ ), DPNs (10 particles per cells), and 200 nm carboxylated polystyrene particles (P200) (30 particles per cells) were incubated with Raw 264.7 cells up to 24 h. At 24 h, the percentage of RAW 264.7 cells associated with particles was  $99.6 \pm 0.11\%$  for SPNs,  $84.9 \pm 0.40\%$  for P200, and  $14.4 \pm 0.06\%$  for DPNs (Figure 2A). This trend was also confirmed *via* confocal microscopy analyses. Figure 2B shows that 100% of RAW 264.7 cells within a region of interest resulted to be positive to SPNs and P200, while only  $25.3 \pm 6.63\%$  of macrophages turned to be associated with DPNs. The panel of Figure 2C shows representative microscopy images of RAW 264.7 cells 24-h post incubation with SPNs, P200 and DPNs. In Figure 2C, nuclei and actin filaments were stained in blue and green, respectively, whereas nanoparticles appeared as red dots.

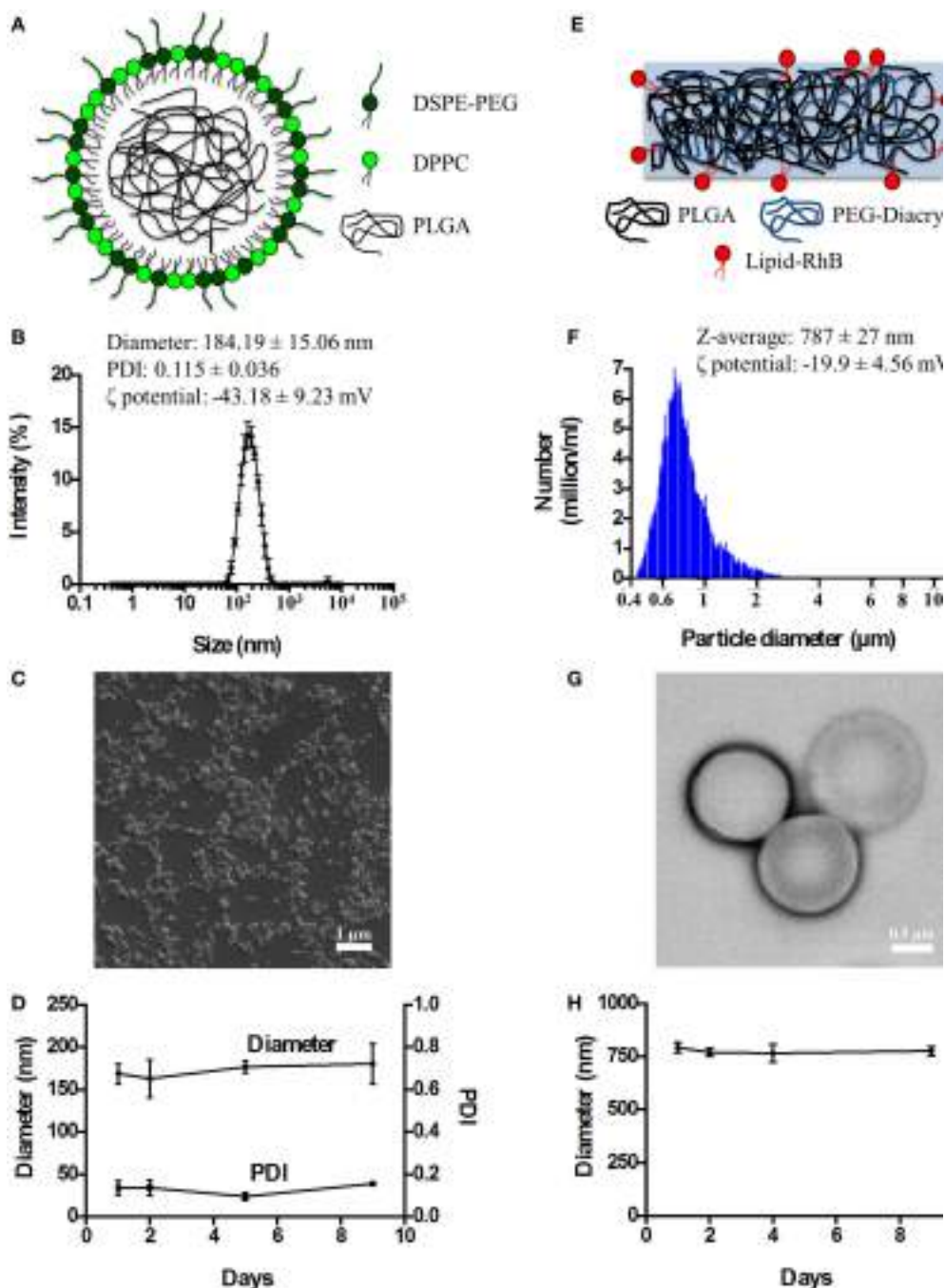


**FIGURE 1 |** The physico-chemical characterization of spherical and discoidal polymeric nanoconstructs. **(A)** Schematic representation of SPNs synthesized via emulsion/solvent evaporation method comprising a hydrophobic [poly(lactic-co-glycolic acid) (PLGA)] core stabilized by an external lipid monolayer (a mixture of DPPC and DSPE-PEG-COOH). **(B)** Size distribution of SPNs via dynamic light scattering analysis ( $n = 3$ ). **(C)** Scanning electron microscopy image of SPNs. **(D)** Colloidal stability of SPNs in de-ionized (DI) water ( $n = 3$ ). **(E)** Schematic representation of DPNs synthesized via a top-down approach and resulting by the crosslinking of PLGA and poly(ethylene glycol) diacrylate (PEG-DA) chains. **(F)** Size distribution of DPNs via Multisizer analysis ( $n = 3$ ). **(G)** Transmission electron microscopy image of DPNs. **(H)** Colloidal stability of DPNs in DI water ( $n = 3$ ).

It is clearly confirmed the large difference in cell uptake between the spherical nanoparticles, SPNs and P200, and the discoidal nanoconstructs DPNs. Also, multiple SPNs and P200 are associated with the same cell.

## Pharmacological and Cytotoxicity Properties of SPNs

Based on the cell internalization results, SPNs were selected to be loaded with the natural, anti-inflammatory compound

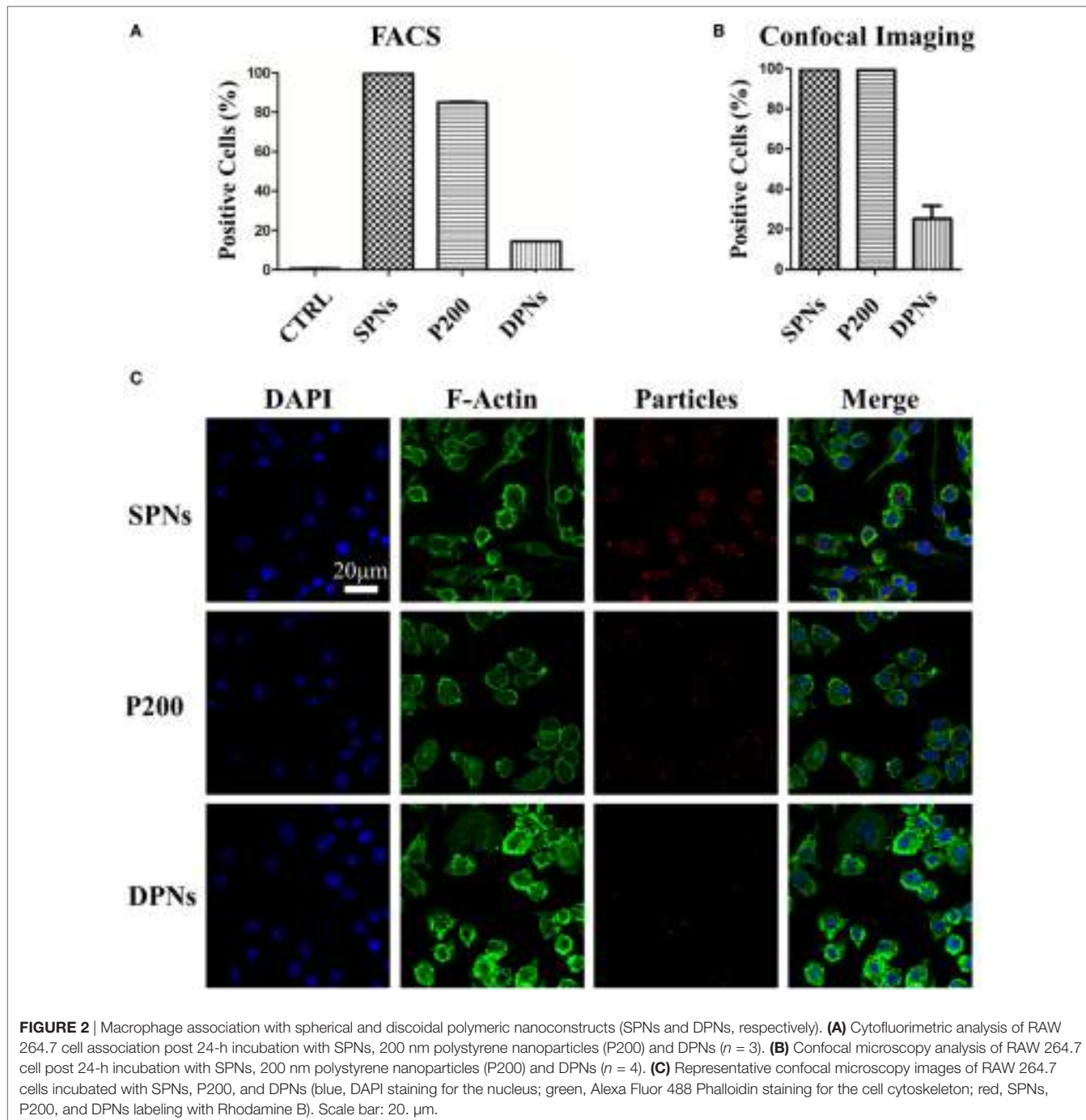


**FIGURE 2 |** Macrophage association with spherical and discoidal polymeric nanoconstructs (SPNs and DPNs, respectively). **(A)** Cytofluorimetric analysis of RAW 264.7 cell association post 24-h incubation with SPNs, 200 nm polystyrene nanoparticles (P200) and DPNs ( $n = 3$ ). **(B)** Confocal microscopy analysis of RAW 264.7 cell post 24-h incubation with SPNs, 200 nm polystyrene nanoparticles (P200) and DPNs ( $n = 4$ ). **(C)** Representative confocal microscopy images of RAW 264.7 cells incubated with SPNs, P200, and DPNs (blue, DAPI staining for the nucleus; green, Alexa Fluor 488 Phalloidin staining for the cell cytoskeleton; red, SPNs, P200, and DPNs labeling with Rhodamine B). Scale bar: 20.  $\mu$ m.

Curcumin. Given the hydrophobicity profile of this molecule, Curcumin was directly entrapped within the hydrophobic PLGA core of SPNs. Curc-SPNs present a hydrodynamic size of  $193.4 \pm 6.9$  nm and a zeta potential of  $-43.8 \pm 4.56$  mV. The pharmacological properties of Curc-SPNs were characterized by quantifying DL and release, and cytotoxicity on RAW 264.7 macrophages. To this end, Curcumin EE and loading were assessed *via* spectrophotometric analysis. DL was calculated as the percentage in weight of loaded Curcumin compared to the total nanoparticle mass; whereas the EE was determined

as the percentage of loaded Curcumin over the initial input amount of Curcumin. Data returned a DL of  $2.31\% \pm 0.84$  and an EE of  $13.23\% \pm 5.41$ , as graphically reported in **Figure 3A**. The release profile of Curcumin was determined over a period of 72 h, under physiological conditions ( $pH = 7.4$  and  $37^\circ\text{C}$ ). As documented by the plot of **Figure 3B**, 50% of Curcumin was released within the first 6 h (see inset of **Figure 3B**), whereas the remaining 50% of anti-inflammatory molecules was slowly released within the following 66 h. The effect of SPNs in generating apoptosis, if any, was tested. **Figure 3C** shows the FITC

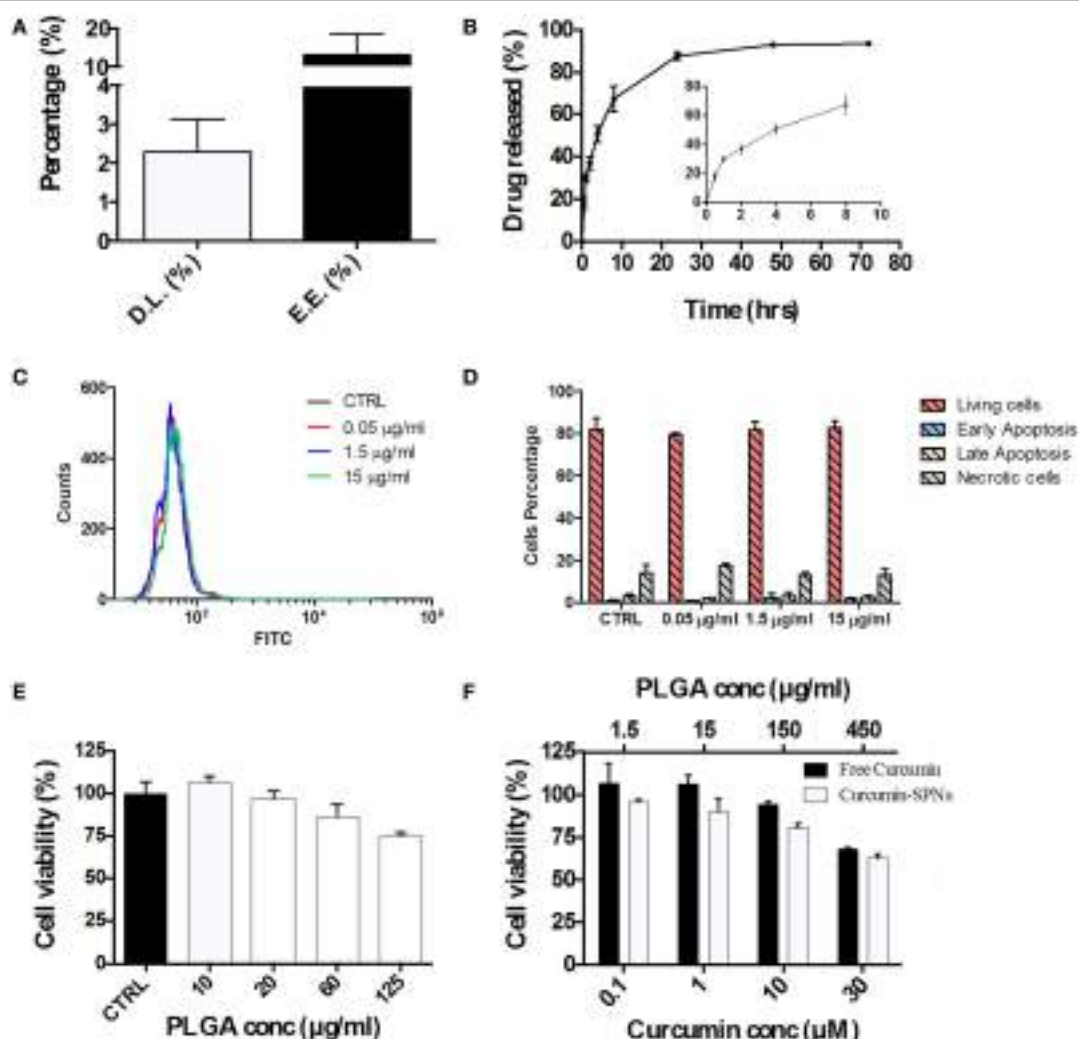


**FIGURE 3 |** Pharmacological and cytotoxicity properties of SPNs and curcumin-loaded SPNs (Curc-SPNs). **(A)** Drug loading (DL) and encapsulation efficiency (EE) for Curc-SPNs ( $n = 3$ ). **(B)** *In vitro* release profile of curcumin up to 72 h, under physiological conditions (pH 7.4 and 37°C). The inset shows the earlier time points of the curve ( $n = 3$ ). **(C)** FITC fluorescent profile associated with Annexin V presence on cells membrane, after empty SPNs treatment or in control group. **(D)** Cells population distribution analysis on cells treated or not with nanoparticles, showing the level of viable, apoptotic, or necrotic cells. **(E)** Raw 264.7 cell viability at 24 h post incubation with empty SPNs ( $n = 5$ ). **(F)** Raw 264.7 cell viability at 24 h post exposure to free Curcumin and Curc-SPNs ( $n = 5$ ). Data are expressed as mean  $\pm$  SD.

intensity profiles, indicating the level of apoptosis, for all the experimental conditions used. There is no difference among cells untreated or treated with different empty SPNs concentrations, not even at a concentration three times higher than the one used for internalization experiments. **Figure 3D** shows more insights on the cell populations analyzed, showing the level of living cells, necrotic cells, or cells in early or late apoptosis. Also in this case, cells distribution in these subgroups is similar, despite the treatment used. Taken together, these results prove that our SPNs do not induce apoptosis, at least in the time frame and in the conditions used for the subsequent Curc-SPNs efficacy experiments. Finally, the cytotoxicity on Raw 264.7 cells of empty SPNs, free Curcumin, and Curc-SPNs was quantified at 24 h, using a MTT cell proliferation assay.

**Figure 3E** shows the cell viability of Raw 264.7 incubated with empty SPNs. No significant toxicity of SPNs was detected up to more than 20  $\mu\text{g}/\text{ml}$  of polymer. For larger concentrations, cell viability slightly reduces reaching an average value above 75% for 125  $\mu\text{g}/\text{ml}$  of polymer, although without any significant difference with control. This is very important as this is the polymer concentration representing the amount of polymer of 10  $\mu\text{M}$  Curc-SPNs. **Figure 3F** directly compares the cytotoxicity potential of free Curcumin and Curc-SPNs. No significant toxicity was detected up to 10  $\mu\text{M}$  of Curcumin, whereas, for larger concentrations, cell viability reduced steadily in a concentration dependent fashion. Also, Curc-SPNs and free Curcumin returned comparable cytotoxicity activities on RAW 264.7.

## Anti-inflammatory Efficacy of Curc-SPNs

Inflammation was induced in RAW 264.7 cells by two different methods: incubation with A $\beta$  fibrils and incubation with LPS, as positive control. Fibrils were obtained through spontaneous polymerization by incubating A $\beta$  (1–42) peptides at 37°C for 6 or 16 h. Both procedures yielded fibrillar structures of 6–9 nm in diameter and more than 200 nm in length, as shown in Figures 4A,B. Since no dramatic differences were observed between the two polymerization protocols, the 6-h polymerization was selected for all subsequent experiments.

For assessing the anti-inflammatory potential of Curc-SPNs, Raw 264.7 macrophages were pre-incubated for 5 h with Curc-SPNs (10  $\mu$ M) and then exposed to an inflammatory stimulus

for 6 h (2  $\mu$ M of fibrillar A $\beta$  or 100 ng/ml of LPS, as a positive control) (Figure 4C). The inflammatory response was assessed by measuring the levels of relevant pro-inflammatory cytokines, namely IL-1 $\beta$ , IL-6, and TNF- $\alpha$ , via RT-PCR (Figures 4D–F). No changes in gene expression were observed when treating cells with an equivalent dose empty SPNs, this additional control prove the presence of negligible levels of endotoxins, if any. Figures 4D–F show the relative fold expression levels for the three cytokines in six different experimental groups: the control group (CTRL)—cells were neither treated with SPNs not exposed to pro-inflammatory stimuli; the empty-SPNs group—cells were exposed to empty SPNs to verify the possible pro-inflammatory potential of nanoparticles; the LPS group—cells were exposed

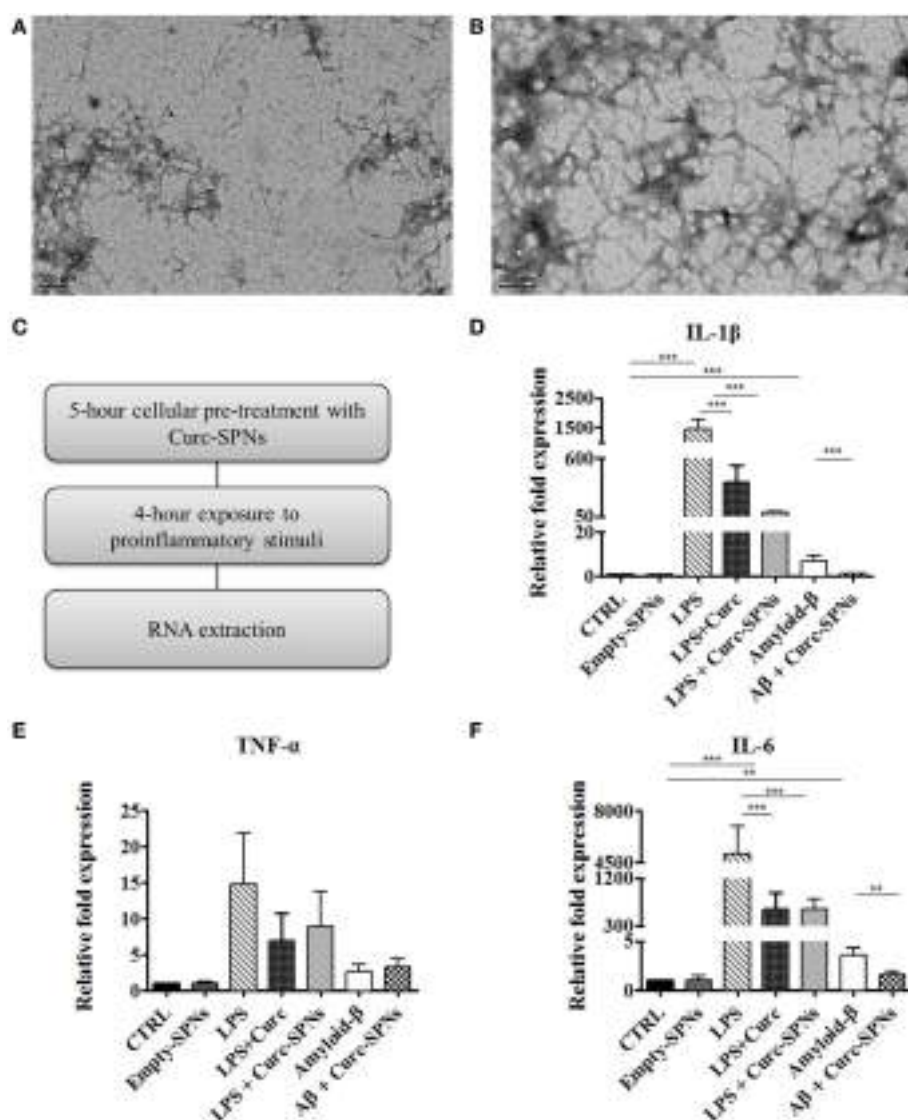


**FIGURE 4 |** Mitigating cytokine production by Raw 264.7 macrophages. Transmission electron microscopy images of amyloid- $\beta$  fibrils obtained by incubating A $\beta$  (1–42) peptides at 37°C in 50 mM phosphate buffer (100 mM NaCl) for 6 h (A) and 16 h (B). Following the experimental protocol showed in (C), total RNA was collected and the mRNA levels of IL-1 $\beta$  (D), TNF- $\alpha$  (E), and IL-6 (F) were semi-quantified against GAPDH via Real Time RT-PCR ( $n = 3$ ). Data are plotted as mean  $\pm$  SD (\*\* denotes statistically significant difference at  $p \leq 0.01$ . \*\*\* denotes statistically significant difference at  $p \leq 0.005$ ).

for 6 h to LPS without any SPN pre-treatment; the LPS + free Curcumin group—cells were pre-treated with 10  $\mu$ M Curcumin and then stimulated by LPS; the LPS + Curc-SPNs group—cells were prior incubated with Curc-SPNs for 5 h and subsequently exposed to LPS for 6 h; the Amyloid- $\beta$  group—cells were exposed for 6 h to fibrillar A $\beta$  without any SPN pre-treatment; the A $\beta$  + Curc-SPNs group—cells were prior incubated with Curc-SPNs for 5 h, and subsequently exposed to fibrillar A $\beta$  for 6 h. **Figure 4D** shows that the cellular production of IL-1 $\beta$  is dramatically inhibited by a 5-h pre-treatment with Curc-SPNs. The relative cytokine expression reduces by ~15 times with respect to the case of LPS (from  $1,439.67 \pm 340.77$  for LPS to  $96.47 \pm 4.33$  for LPS + Curc-SPNs) and by ~6.5 times compared to fibrillar A $\beta$  stimulation (from  $7.21 \pm 2.08$  for Amyloid- $\beta$  to  $1.1 \pm 0.17$  for A $\beta$  + Curc-SPNs). Free Curcumin treatment was also able to reduce IL-1 $\beta$ , although at a more modest level ( $369.28 \pm 164.33$ ) compared LPS stimulation. Similar observations can be drawn from **Figure 4E** for IL-6. The relative cytokine expression reduces by ~8 times when compared to the case of LPS stimulation (from  $5,053.44 \pm 1,928.49$  for LPS to  $618.19 \pm 189.49$  for LPS + Curc-SPNs) and by ~2.3 times to the case of fibrillar A $\beta$  stimulation (from  $3.61 \pm 0.78$  for Amyloid- $\beta$  to  $1.57 \pm 0.41$  for A $\beta$  + Curc-SPNs). In this respect, free curcumin showed a very similar behavior ( $620.123 \pm 302.51$ ). Although the same general trend can also be depicted in **Figure 4F**, no statistically significant variations in the expression of TNF- $\alpha$  was observed for LPS and fibrillar A $\beta$  stimulations, both in the case of free Curcumin and Curc-SPNs pre-treatment. This could be due to the specific phenotype of RAW 264.7 cells, stimulation times, and concentrations of pro-inflammatory stimuli.

## DISCUSSION

Inflammation is relevant in the onset and progression of several diseases, including cancer, cardiovascular, metabolic, and neurodegenerative. Until the harmful stimulus persists, the inflammatory machinery evolves into a chronic process, reinforcing and turning itself into a injurious course, worsening the condition at the damaged site. Macrophages, phagocytic cells of myeloid origin, are key players in this kind of chronic inflammation (20). They can be found in every body tissue, assuming different phenotypes and roles: they can be differentiated into several kinds of cells, including microglia, Kupffer cells, and more. In this chronic insult scenario, macrophages proceed in their accumulation resulting in their continuous activation largely responsible for inducing damage. AD pathology is also characterized by an inflammatory response, which is primarily driven by the brain-resident macrophages, i.e., microglia, most likely toward A $\beta$  plaques, exacerbating the pathology of the disease, escalating with its progression (5, 6). Microglia surrounds and is intimately associated with A $\beta$  plaques, which in turn leads to the production of inflammatory cytokines and chemokines *in vitro* (21–28). Furthermore, a panoply of typical inflammatory mediators can be detected both in *in vivo* models and in brains or CSF from AD patients, including TNF- $\alpha$ , IL-1 $\beta$ , IL-6, GM-CSF, IL-12, and IL-23 (29–32). Even though microglia have the capacity to phagocytose A $\beta$ , it is also true that the

inefficient clearance of amyloid plaques is a major pathogenic factor in AD (33). Based on this, it is of crucial importance to try to modulate macrophages phenotype, inducing a regression in their pro-inflammatory activity. In this work, two different nanoconstructs—SPNs and DPNs—were presented and characterized with the objective of selecting the best nanoplatform for tempering inflammation in AD. Recently, different studies are trying to better understand and evaluate the interaction of nanoparticles and immune system cells. Small spherical nanoparticles, below 200 nm in diameter, seem to be more easily internalized by dendritic cells (34). Nonetheless, also nanoparticles' softness and deformability plays a very important role in this process. In fact, both *in vitro* and *in vivo* data showed that harder particles are more prone to be phagocytized, as well as to be removed from blood circulation (e.g., through spleen filtration) (15, 35). Moreover, the comparison between SPNs and DPNs was not only instrumental to choose the best platform to be used, but also increased the knowledge of this special interaction, so useful for any nano-based drug delivery system. Cytofluorimetric analysis revealed that, at 24 h post incubation, 99.6% of RAW 264.7 cells were associated with SPNs as opposed to only 14.4% for DPNs. This behavior was also confirmed *via* confocal microscopy analysis. Notably, SPNs worked even better than polystyrene particles, chosen as a positive control since they are easily taken up by phagocytic cells, as well documented in the literature (36, 37). The ability of SPNs to be internalized and modulate macrophages activity was already demonstrated by the authors (38–40). Therefore, these new data provide additional information, unequivocally suggesting that spherical nanoparticles are far better candidates for delivering anti-inflammatory drugs directly into macrophages compared to discoidal nanoconstructs. Consequently, SPNs were selected as the delivery platform and were loaded with Curcumin, a natural anti-inflammatory molecule, in order to deliver their payload inside target cells. Curcumin (diferuloylmethane) is a polyphenol that represents the major curcuminoid extracted from the *Curcuma longa* plant, which is extensively used for its anti-inflammatory, antioxidant, analgesic, antiseptic, and anticancer activity (41). In particular, its anti-inflammatory effect, mostly due to the inhibition of NF- $\kappa$ B transcription factor, makes Curcumin a highly desirable candidate as a therapeutic agent in several inflammation-based pathologies (42). However, Curcumin has a poor bioavailability of its hydrophobicity. For instance, in pre-clinical studies on rats, an oral dose of 500 mg/kg resulted in a peak plasma concentration of only 1.8 ng/ml (43). In a phase II clinical trial, 25 patients with pancreatic cancer were administered daily with 8 g of Curcumin leading to a maximum plasma level concentration of only 41 ng/ml (44, 45). In this manuscript, RAW 264.7 cells were exposed to amyloid- $\beta$  fibrils and LPS, two potent pro-inflammatory stimuli, in order to replicate an inflamed environment and treated with free Curcumin and Curc-SPNs. Note that the stimulation of macrophages with A $\beta$  fibrils was considered as a preliminary model of neuro-inflammation in AD (46). Results demonstrated a significant efficacy of Curc-SPNs in modulating the production of pro-inflammatory cytokines, namely IL-1 $\beta$ , IL-6, and TNF- $\alpha$ . Importantly, no changes in

gene expression (in particular for IL-6 and TNF- $\alpha$ ) (47) was observed upon the incubation of macrophages with empty SPNs. This additional control indirectly confirm the absence of endotoxin or of any unintentional contamination with minute amount of LPS, which would have induced a powerful inflammatory response (48). Interestingly, at the considered concentrations, the pro-inflammatory effect of LPS was always stronger than that associated with fibrillar A $\beta$  incubation. Finally, no cytotoxic effect was observed after the incubation of the cells with the vehicle *per se*, as well as the ability of the system to preserve the structure and the function of Curcumin, after being loaded into the polymeric matrix. Altogether these findings demonstrate that spherical polymeric nanoconstructs can efficiently target macrophages and alleviate inflammation by the specific, intracellular delivery of Curcumin. This approach holds potential in the mitigation of inflammation in AD. However, future works should progress along two parallel paths. On the one hand, more sophisticated *in vitro* models will have to be considered where primary microglia and neurons are co-cultured and monitored over time during treatment for assessing cytokine production as well as neuronal activity. On the other hand, the role of tissue inflammation on the blood

brain barrier permeability to nanoparticles should be elucidated using imaging and different pre-clinical models of AD.

## AUTHOR CONTRIBUTIONS

AA: synthesis and chemico-physical and biological characterization of the spherical polymeric nanoconstructs (SPNs); RP: performed confocal microscopy and FACS analyses; AP: synthesis and chemico-physical and biological characterization of the discoidal polymeric nanoparticles (DPNs); AL and AC: helped with the synthesis and characterization of SPNs; DM: helped with the synthesis and characterization of SPNs and manuscript writing; PD: coordinated the work and manuscript writing. Results were analyzed and discussed by all authors.

## ACKNOWLEDGMENTS

This work was partially supported by the European Research Council, under the European Union's Seventh Framework Programme (FP7/2007-2013)/ERC grant agreement no. 616695 and the AIRC (Italian Association for Cancer Research) under the individual investigator grant no. 17664.

## REFERENCES

- Medzhitov R. Origin and physiological roles of inflammation. *Nature* (2008) 454:428–35. doi:10.1038/nature07201
- Rocha VZ, Libby P. Obesity, inflammation, and atherosclerosis. *Nat Rev Cardiol* (2009) 6:399–409. doi:10.1038/nrccardio.2009.55
- Gajewski TF, Schreiber H, Fu YX. Innate and adaptive immune cells in the tumor microenvironment. *Nat Immunol* (2013) 14:1014–22. doi:10.1038/ni.2703
- Hotamisligil GS. Inflammation and metabolic disorders. *Nature* (2006) 444:860–7. doi:10.1038/nature05485
- Heppner FL, Ransohoff RM, Becher B. Immune attack: the role of inflammation in Alzheimer disease. *Nat Rev Neurosci* (2015) 16:358–72. doi:10.1038/nrn3880
- Akiyama H, Barger S, Barnum S, Bradt B, Bauer J, Cole GM, et al. Inflammation and Alzheimer's disease. *Neurobiol Aging* (2000) 21:383–421. doi:10.1016/S0197-4580(00)00124-X
- Mandrekar-Colucci S, Landreth GE. Microglia and inflammation in Alzheimer's disease. *CNS Neurol Disord Drug Targets* (2010) 9:156–67. doi:10.2174/187152710791012071
- Peer D, Karp JM, Hong S, Farokhzad OC, Margalit R, Langer R. Nanocarriers as an emerging platform for cancer therapy. *Nat Nanotechnol* (2007) 2:751–60. doi:10.1038/nnano.2007.387
- Min Y, Caster JM, Eblan MJ, Wang AZ. Clinical translation of nanomedicine. *Chem Rev* (2015) 115:11147–90. doi:10.1021/acs.chemrev.5b00116
- Champion JA, Katare YK, Mitragotri S. Particle shape: a new design parameter for micro- and nanoscale drug delivery carriers. *J Control Release* (2007) 121:3–9. doi:10.1016/j.jconrel.2007.03.022
- Decuzzi P, Pasqualini R, Arap W, Ferrari M. Intravascular delivery of particulate systems: does geometry really matter? *Pharm Res* (2009) 26:235–43. doi:10.1007/s11095-008-9697-x
- Gratton SE, Ropp PA, Pohlhaus PD, Luft JC, Madden VJ, Napier ME, et al. The effect of particle design on cellular internalization pathways. *Proc Natl Acad Sci U S A* (2008) 105:11613–8. doi:10.1073/pnas.0801763105
- Merkel TJ, Chen K, Jones SW, Pandya AA, Tian S, Napier ME, et al. The effect of particle size on the biodistribution of low-modulus hydrogel PRINT particles. *J Control Release* (2012) 162:37–44. doi:10.1016/j.jconrel.2012.06.009
- Key J, Aryal S, Gentile F, Ananta JS, Zhong M, Landis MD, et al. Engineering discoidal polymeric nanoconstructs with enhanced magneto-optical properties for tumor imaging. *Biomaterials* (2013) 34:5402–10. doi:10.1016/j.biomaterials.2013.03.078
- Key J, Palange AL, Gentile F, Aryal S, Stigliano C, Di Mascolo D, et al. Soft discoidal polymeric nanoconstructs resist macrophage uptake and enhance vascular targeting in tumors. *ACS Nano* (2015) 9:11628–41. doi:10.1021/acsnano.5b04866
- Stigliano C, Key J, Ramirez M, Aryal S, Decuzzi P. Radiolabeled polymeric nanoconstructs loaded with docetaxel and curcumin for cancer combinatorial therapy and nuclear imaging. *Adv Funct Mater* (2015) 25:3371–9. doi:10.1002/adfm.201500627
- Lee A, Di Mascolo D, Francardi M, Piccardi F, Bandiera T, Decuzzi P. Spherical polymeric nanoconstructs for combined chemotherapeutic and anti-inflammatory therapies. *Nanomedicine* (2016) 12:2139–47. doi:10.1016/j.nano.2016.05.012
- Palange AL, Di Mascolo D, Carallo C, Gnasso A, Decuzzi P. Lipid-polymer nanoparticles encapsulating curcumin for modulating the vascular deposition of breast cancer cells. *Nanomedicine* (2014) 10:e991–1002. doi:10.1016/j.nano.2014.02.004
- Zhang L, Chan JM, Gu FX, Rhee JW, Wang AZ, Radovic-Moreno AF, et al. Self-assembled lipid-polymer hybrid nanoparticles: a robust drug delivery platform. *ACS Nano* (2008) 2:1696–702. doi:10.1021/nn800275r
- Murray PJ, Wynn TA. Protective and pathogenic functions of macrophage subsets. *Nat Rev Immunol* (2011) 11:723–37. doi:10.1038/nri3073
- El Khoury J, Hickman SE, Thomas CA, Cao L, Silverstein SC, Loike JD. Scavenger receptor-mediated adhesion of microglia to  $\beta$ -amyloid fibrils. *Nature* (1996) 382:716–9. doi:10.1038/382716a0
- Bamberger ME, Harris ME, McDonald DR, Husemann J, Landreth GE. A cell surface receptor complex for fibrillar  $\beta$ -amyloid mediates microglial activation. *J Neurosci* (2003) 23:2665–74.
- Paresce DM, Ghosh RN, Maxfield FR. Microglial cells internalize aggregates of the Alzheimer's disease amyloid  $\beta$ -protein via a scavenger receptor. *Neuron* (1996) 17:553–65. doi:10.1016/S0896-6273(00)80187-7
- Stewart CR, Stuart LM, Wilkinson K, van Gils JM, Deng J, Halle A, et al. CD36 ligands promote sterile inflammation through assembly of a toll-like receptor 4 and 6 heterodimer. *Nat Immunol* (2010) 11:155–61. doi:10.1038/ni.1836
- Sheedy FJ, Grebe A, Rayner KJ, Kalantari P, Ramkhelawon B, Carpenter SB, et al. CD36 coordinates NLRP3 inflammasome activation by facilitating intracellular nucleation of soluble ligands into particulate ligands in sterile inflammation. *Nat Immunol* (2013) 14:812–20. doi:10.1038/ni.2639

26. Koenigsknecht J, Landreth G. Microglial phagocytosis of fibrillar  $\beta$ -amyloid through a  $\beta 1$  integrin-dependent mechanism. *J Neurosci* (2004) 24:9838–46. doi:10.1523/JNEUROSCI.2557-04.2004
27. Fassbender K, Walter S, Kühl S, Landmann R, Ishii K, Bertsch T, et al. The LPS receptor (CD14) links innate immunity with Alzheimer's disease. *FASEB J* (2004) 18:203–5. doi:10.1096/fj.03-0364fje
28. El Khoury JB, Moore KJ, Means TK, Leung J, Terada K, Toft M, et al. CD36 mediates the innate host response to  $\beta$ -amyloid. *J Exp Med* (2003) 197:1657–66. doi:10.1084/jem.20021546
29. Griffin WS, Stanley LC, Ling C, White L, MacLeod V, Perrot LJ, et al. Brain interleukin 1 and S-100 immunoreactivity are elevated in Down syndrome and Alzheimer disease. *Proc Natl Acad Sci U S A* (1989) 86:7611–5. doi:10.1073/pnas.86.19.7611
30. Patel NS, Paris D, Mathura V, Quadros AN, Crawford FC, Mullan MJ. Inflammatory cytokine levels correlate with amyloid load in transgenic mouse models of Alzheimer's disease. *J Neuroinflammation* (2005) 2:1. doi:10.1186/1742-2094-2-9
31. Vom Berg J, Prokop S, Miller KR, Obst J, Kälin RE, Lopategui-Cabezas I, et al. Inhibition of IL-12/IL-23 signaling reduces Alzheimer's disease-like pathology and cognitive decline. *Nat Med* (2012) 18:1812–9. doi:10.1038/nm.2965
32. Fillit H, Ding WH, Buee L, Kalman J, Altstiel L, Lawlor B, et al. Elevated circulating tumor necrosis factor levels in Alzheimer's disease. *Neurosci Lett* (1991) 129:318–20. doi:10.1016/0304-3940(91)90490-K
33. Mawuenyega KG, Sigurdson W, Ovod V, Munsell L, Kasten T, Morris JC, et al. Decreased clearance of CNS  $\beta$ -amyloid in Alzheimer's disease. *Science* (2010) 330:1774–1774. doi:10.1126/science.1197623
34. Kumar S, Anselmo AC, Banerjee A, Zakrewsky M, Mitragotri S. Shape and size-dependent immune response to antigen-carrying nanoparticles. *J Control Release* (2015) 220:141–8. doi:10.1016/j.jconrel.2015.09.069
35. Anselmo AC, Zhang M, Kumar S, Vogus DR, Menegatti S, Helgeson ME, et al. Elasticity of nanoparticles influences their blood circulation, phagocytosis, endocytosis, and targeting. *ACS Nano* (2015) 9:3169–77. doi:10.1021/acsnano.5b00147
36. Lunov O, Syrovets T, Loos C, Beil J, Delacher M, Tron K, et al. Differential uptake of functionalized polystyrene nanoparticles by human macrophages and a monocytic cell line. *ACS Nano* (2011) 5:1657–69. doi:10.1021/nn2000756
37. Dos Santos T, Varela J, Lynch I, Salvati A, Dawson KA. Quantitative assessment of the comparative nanoparticle-uptake efficiency of a range of cell lines. *Small* (2011) 7:3341–9. doi:10.1002/smll.201101076
38. Di Mascolo D, J Lyon C, Aryal S, Ramirez MR, Wang J, Candeloro P, et al. Rosiglitazone-loaded nanospheres for modulating macrophage-specific inflammation in obesity. *J Control Release* (2013) 170:460–8. doi:10.1016/j.jconrel.2013.06.012
39. Stigliano C, Ramirez MR, Singh JV, Aryal S, Key J, Blanco E, et al. Methotrexate-loaded hybrid nanoconstructs target vascular lesions and inhibit atherosclerosis progression in ApoE $^{-/-}$  mice. *Adv Healthcare Mater* (2017) 6:1601286. doi:10.1002/adhm.201601286
40. Lee A, Mei CD, Ferreira M, Marotta R, Yoon HY, Kim K, et al. Dexamethasone-loaded polymeric nanoconstructs for monitoring and treating inflammatory bowel disease. *Theranostic* (2017) 7(15):3654. doi:10.7150/thno.18183
41. Wilken R, Veena MS, Wang MB, Srivatsan ES. Curcumin: a review of anti-cancer properties and therapeutic activity in head and neck squamous cell carcinoma. *Mol Cancer* (2011) 10:12. doi:10.1186/1476-4598-10-12
42. Shehzad A, Rehman G, Lee YS. Curcumin in inflammatory diseases. *Biofactors* (2013) 39:69–77. doi:10.1002/biof.1066
43. Ireson C, Orr S, Jones DJ, Verschoyle R, Lim CK, Luo JL, et al. Characterization of metabolites of the chemopreventive agent curcumin in human and rat hepatocytes and in the rat *in vivo*, and evaluation of their ability to inhibit phorbol ester-induced prostaglandin E2 production. *Cancer Res* (2001) 61:1058–64.
44. Sharma RA, McLellan HR, Hill KA, Ireson CR, Euden SA, Manson MM, et al. Pharmacodynamic and pharmacokinetic study of oral curcuma extract in patients with colorectal cancer. *Clin Cancer Res* (2001) 7:1894–900.
45. Dhillon N, Aggarwal BB, Newman RA, Wolff RA, Kunnumakkara AB, Abbruzzese JL, et al. Phase II trial of curcumin in patients with advanced pancreatic cancer. *Clin Cancer Res* (2008) 14:4491–9. doi:10.1158/1078-0432.CCR-08-0024
46. Smits HA, van Beelen AJ, de Vos NM, Rijmsma A, van der Bruggen T, Verhoef J, et al. Activation of human macrophages by amyloid- $\beta$  is attenuated by astrocytes. *J Immunol* (2001) 166:6869–76. doi:10.4049/jimmunol.166.11.6869
47. Schwarz H, Gornicic J, Neuper T, Parigiani MA, Wallner M, Duschl A, et al. Biological activity of masked endotoxin. *Sci Rep* (2017) 7:44750. doi:10.1038/srep44750
48. Boraschi D, Italiani P, Palomba R, Decuzzi P, Duschl A, Fadeel B, et al. Nanoparticles and innate immunity: new perspectives on host defence. *Semin Immunol* (2017). doi:10.1016/j.smim.2017.08.013

**Conflict of Interest Statement:** The authors declare that the research was conducted in the absence of any commercial or financial relationships that could be construed as a potential conflict of interest.

Copyright © 2017 Ameruoso, Palomba, Palange, Cervadoro, Lee, Di Mascolo and Decuzzi. This is an open-access article distributed under the terms of the Creative Commons Attribution License (CC BY). The use, distribution or reproduction in other forums is permitted, provided the original author(s) or licensor are credited and that the original publication in this journal is cited, in accordance with accepted academic practice. No use, distribution or reproduction is permitted which does not comply with these terms.



# Role of Metallic Nanoparticles in Vaccinology: Implications for Infectious Disease Vaccine Development

Lázaro Moreira Marques Neto, André Kipnis and Ana Paula Junqueira-Kipnis\*

Department of Microbiology, Immunology, Pathology and Parasitology, Institute of Tropical Pathology and Public Health, Federal University of Goiás, Goiânia, Goiás, Brazil

## OPEN ACCESS

**Edited by:**

Paola Italiani,  
Consiglio Nazionale Delle Ricerche  
(CNR), Italy

**Reviewed by:**

Nicolas Riteau,  
National Institutes of Health, USA  
Toshiyuki Murai,  
Osaka University, Japan

**\*Correspondence:**

Ana Paula Junqueira-Kipnis  
apkipnis@gmail.com

**Specialty section:**

This article was submitted to  
Inflammation,  
a section of the journal  
*Frontiers in Immunology*

**Received:** 28 December 2016

**Accepted:** 20 February 2017

**Published:** 08 March 2017

**Citation:**

Marques Neto LM, Kipnis A and Junqueira-Kipnis AP (2017) Role of Metallic Nanoparticles in Vaccinology: Implications for Infectious Disease Vaccine Development. *Front. Immunol.* 8:239.  
doi: 10.3389/fimmu.2017.00239

Subunit vaccines are safer but less immunogenic than live-attenuated vaccines or whole cell inactivated vaccines. Adjuvants are used to enhance and modulate antigen (Ag) immunogenicity, aiming to induce a protective and long-lasting immune response. Several molecules and formulations have been studied for their adjuvanticity, but only seven have been approved to formulate human vaccines. Metallic nanoparticles (MeNPs), particularly those containing gold and iron oxides, are widely used in medicine for diagnosis and therapy and have been used as carriers for drugs and vaccines. However, little is known about the immune response elicited by MeNPs or about their importance in the development of new vaccines. There is evidence that these particles display adjuvant characteristics, promoting cell recruitment, antigen-presenting cell activation, cytokine production, and inducing a humoral immune response. This review focuses on the characteristics of MeNPs that could facilitate the induction of a cellular immune response, particularly T-helper 1 and T-helper 17, and their potential functions as adjuvants for subunit vaccines.

**Keywords:** particulate vaccine, adjuvant, immune response, Th1, Th17

## INTRODUCTION

Adjuvant selection for subunit vaccines is a key to increasing immunogenicity and, therefore, guiding stimulation of innate immunity and the development of the appropriate protective response to combat the microorganism of interest. Adjuvants are classified as particulate formulations, immunomodulatory molecules, or a combination of both characteristics. In addition to acting on the diversity of the humoral and cellular immune response, they can act in several different ways: by decreasing the vaccine dose, accelerating the immune response, or prolonging the immune response (1, 2). Among the seven approved vaccine adjuvants for human use, aluminum salts (alum), emulsions (e.g., MF59), and virosomes are particulate formulations. While alum induces efficient antibody (Ab) production and a predominant T-helper 2 (Th2) response, the other two have the capacity to induce T-helper 1 (Th1) and Th2 as well as Ab. Adjuvant system (AS) 01 and 04 used the combination of an immunomodulatory molecule and a particulate formulation composed of a Toll-like receptor 4 (TLR4) agonist, monophosphoryl lipid A that also induces Ab. The incorporation of alum in AS04 improved the humoral response, while the association of saponin (QS-21) and liposome in AS01 favored Th1 responses (3, 4). Imidazoquinolines (TLR7 and TLR8 agonists) and lipid A analogs

(TLR4 agonists) are immunomodulatory molecules, capable of generating a Th1 response (5).

There is a demand for safe adjuvants capable of inducing efficient cellular immunity, especially Th1 and Th17, to be used against tuberculosis, leishmaniasis, malaria, and other diseases caused by intracellular microorganisms (1, 6). The majority of molecules with this type of adjuvanticity (Th1 driven) are related toward the response of danger receptors to trigger inflammation, thus safety and tolerance could be major barriers that prevent their use in human vaccines (7). However, comparing Alum and CpG/DNA adjuvants in human trials, only common adverse effects, including local site reaction, flu-like symptoms and headache were observed when CpG/DNA was used (8). Also, Verstraeten et al. (9), analyzing more than 30,000 individuals, who received vaccine-containing AS01, observed that only common side effects occurred.

Nanoparticles (NPs) are classically described as structures smaller than 100 nm and can be classified, based on their composition, as polymeric, inorganic, liposomes, immunostimulating complexes, virus-like particles, emulsions, or self-assembled proteins (10). They are made of different materials and differ in size, shape, and surface properties; interactions with biological systems, therefore, are varied, with several applications in modern medicine. In vaccinology, they are classically thought to have delivery and deposit properties. However, many NPs have been shown to stimulate immune responses, including cell recruitment, activation of antigen (Ag)-presenting cells (APCs), and induction of cytokine and chemokine release. The development of nanostructures and nanoadjuvants may therefore offer alternatives to currently used adjuvants once studies establish ways for them to elicit innate immune response and support the development of adaptive immune response in the context of vaccine formulations (10).

Metallic nanoparticles (MeNPs) are relatively non-biodegradable, have rigid structures, and possess simple synthesis methodology. Many have been studied for their immunological properties (11). However, there are still gaps in understanding the immune response generated by NPs, especially MeNPs. Few studies have compared NPs of different types and there is no standardization among published methodologies, which hampers comparisons of immunostimulatory characteristics. Several important characteristics, therefore, have not been well studied. For example, how chemical and physical properties (including material composition, size, shape, surface charge, and hydrophobicity) impact vaccine immune response (5). This review focuses on the use of MeNPs in formulations against infectious diseases, aiming to assess progress of their use in vaccinology and their possible applications as adjuvant.

## THE IMMUNE RESPONSE GENERATED BY MeNP-FORMULATED VACCINES

**Table 1** summarizes the articles that report the use of MeNPs as part of vaccine formulations against infectious diseases and the immune responses they elicited. A range of immune responses is required to fight a diverse group of microorganisms. The type of protective immune response can be simplistically divided based

on the type of microorganism: extracellular bacteria and toxin, intracellular bacteria, viruses, fungi, and protozoa. Among the vaccines targeting extracellular bacteria and toxin, two were formulated with lipopolysaccharide (LPS) in glycopeptide Ag. The use of glycoantigen and LPS can trigger an intense response through TLR4 and B cell receptor activation; the presence of gold NPs (AuNPs) may have minimal influence on this response. However, in the work of Gregory et al. (12) and Torres et al. (13), the use of AuNPs in the formulation generated a different response, improving anti-LPS immunoglobulin G (IgG) response, decreasing bacterial burden, generating a more efficient humoral response, and improving animal survival, showing that AuNPs may influence immune response and protection.

Using protein Ag, Barhate et al. (22) formulated a vaccine using AuNPs and toxoid Ag and demonstrated that their formulation could induce a mucosal and systemic IgG and IgA response. When co-administered with *Asparagus racemosus* extract, a botanically derived adjuvant, the response was further enhanced (22). Dakterzada et al. (24) developed a vaccine against *Pseudomonas aeruginosa* using the flagellin subunit and AuNPs that elicited an IgG response comparable to that induced by Freund Adjuvant. Flagellin is a TLR5 agonist but the recognition and signaling is structure dependent. This study, however, used only the 1–161aa from flagellin and its ability to activated TLR5 could not be maintained (24). Gregory et al. (12) used an F1 *Yersinia pestis* Ag conjugated to AuNPs that induced an Ab response with higher IgG2a associated with higher levels of interferon gamma (IFN $\gamma$ ), suggesting activation of Th1 cells.

Among the studies that used MeNPs in vaccine formulation, only one targeted intracellular bacteria (*Listeria monocytogenes*). The protective immune response against intracellular bacterial infections requires Th1 activation and, therefore, APCs activation and Ag presentation through major histocompatibility complex II (MHC II). To generate a Th1 response, an AuNP and Listeria Ag formulation were used in different strategies. Although the authors tested direct vaccination, when dendritic cells (DC), *in vitro* loaded with AuNP plus Listeria Ag, were adoptively transferred to a naïve animal, they induced Th1, CD8+, and natural killer (NK) cells that provided better protection against *L. monocytogenes* than the traditional vaccine approach (23).

In evaluating vaccines developed with MeNPs against viral infections, Niikura et al. (20) used West Nile virus (WNV); Tao et al. (21) used the extracellular portion of Matrix 2 protein (M2) of the influenza virus; Chen et al. (15) conjugated AuNPs with a 28 amino acid VP1-foot-and-mouth virus protein (pFMDV); and Staroverov et al. (17) co-administered AuNPs and partially purified enteropathogenic swine-transmissible gastroenteritis virus. All the above studies evaluated the Ab immune responses and all formulations demonstrated efficient humoral response induction. Tao et al. (21) also evaluated the addition of cytosine and guanine linked by phosphodiester unmethylated (CpG/DNA) and found that it improved Ab levels and animals' survival rates. Another important feature of studies by Niikura et al. (20) and Chen et al. (15) was the use of various NP sizes and the demonstration that all different NP shapes were capable of inducing a humoral response. The levels of Ab were size dependent, but the results were inconsistent: the first study found that a 40 nm sphere

**TABLE 1 | Studies describing immune responses to vaccination with metallic nanoparticles, listed by NPs material and year of publication (*n* = 18 studies).**

NP material	Complementary adjuvant	Animal model (route of vaccination)	Evaluation of immunogenicity	Reference
Gold		C57BL/6 (H-2b) and BALB/c (H-2d) mice used for protection experiments (intraperitoneal)	CD4+, IL-2+, and duration and avidity of total immunoglobulin G (IgG) (IgG1, IgG2a, IgG2b, and IgG2c)	Kaba et al. (14)
		BALB/c mice (intraperitoneal and subcutaneous)	IgG (total)	Chen et al. (15)
	Alum, CFA/IFA	BALB/c mice (subcutaneous)	IgG1, IgG2a, IgG2b, and IgG3	Parween et al. (16)
		Albino mice and rabbits (intraperitoneal)	IgG, circulant IFN- $\gamma$ , and ROS <i>in vivo</i> generation by peritoneal macrophages	Staroverov et al. (17)
	Alhydrogel	BALB/c mice (intramuscular)	IgG1 and IgG2a titer, CD4 and CD8 activation, and IFN- $\gamma$ release	Gregory et al. (12)
		C57BL/6 (H-2b) and BALB/c (H-2d) mice used for protection experiments (intramuscular/intraperitoneal)	Total IgG, IgM and IgA titer and avidity, and CD8+ memory population (effector, central, and long-term central)	Kaba et al. (18)
		C57BL/6 mice (intramuscular/intraperitoneal)	IgG1, IgG2c, IgG3, and IgE titers	Mccoy et al. (19)
		C3H/HeNJc1 mice (intraperitoneal)	IgG	Niikura et al. (20)
	CpG/DNA (TLR9 agonist)	BALB/c mice (intranasal)	IgG1 and IgG2a	Tao et al. (21)
	Asparagus racemosus extract	Swiss albino mice (oral)	Serum IgG, serum IgA, intestinal IgA, and fecal IgA	Barhate et al. (22)
Iron	LPS (TLR4 agonist)	BALB/c mice (intranasal)	IgG1 and IgG2a	Gregory et al. (12)
	LPS (TRL4 agonist)	Rhesus macaques (subcutaneous)	IgG	Torres et al. (13)
	Adavax™ adjuvant	BALB/c mice (intraperitoneal and intravenous)	T-helper 1, CD8+, and NK cells	Rodriguez-Del Rio et al. (23)
		BALB/c mice (subcutaneous)	IgG (total)	Dakterzada et al. (24)
		SW mice (intraperitoneal, intramuscular, and subcutaneous), <i>Aotus lemurinus trivirgatus</i> monkeys (intramuscular)	Total Ab response, IFN- $\gamma$ , and IL-4 (mice) and total Ab response (monkeys)	Pusic et al. (25)
Nickel		BALB/c mice (subcutaneous)	IgG response	Fischer et al. (26)
		BALB/c mice (subcutaneous)	IgG1 and IgG2a serum titer and IL-12/p40 and RANTES/CCL5 serum concentration	Wadhwa et al. (27)
		BALB/c mice (subcutaneous)	Specific serum IgG, IgG1 and IgG2a Ab titers and IFN- $\gamma$ (splenocytes)	Yan et al. (28)

Ab, antibody; Alum, aluminum salts; CFA, complete Freund adjuvant; IFA, incomplete Freund adjuvant; IFN, interferon; Ig, immunoglobulin; IL, interleukin; LPS, lipopolysaccharide; NK, natural killer; NP, nanoparticle; ROS, reactive oxygen species; SW, Swiss Webster mouse; Th, T-helper; TLR, Toll-like receptor.

was the most efficient Ab inducer and the second study found that the 8 nm and 12 nm spheres performed best.

A special case of the use of MeNPs was the use of nickel-functionalized nanolipoprotein particles (NiNLPs) by Yan et al. (28) and Wadhwa et al. (27) in combination with HIV Ag. NiNLPs are nanometer-sized nanolipoprotein particles with nickel incorporation into their surface in order to induce polyhistidine tagged proteins adsorption (29). They demonstrated that specific IgG (IgG1 and IgG2a) levels were greater than those obtained when alum was used in the formulation. Fischer et al. (26) used truncated WNV envelope protein Ag and found that a single dose vaccination induced a superior anti-WNV IgG response and improved protection against a WNV challenge (26). These responses were associated with nickel functionalization, described as a hapten, and triggered responses through activation of human TLR4 and intracellular transduction signals through myeloid differentiation primary response (MyD-88), nuclear factor- $\kappa$ B (NF- $\kappa$ B), and mitogen-activated protein kinase (MAPK), inducing pro-inflammatory responses [tumor necrosis factor (TNF)- $\alpha$  and interleukin (IL)-8] (30, 31).

For protozoan infections, Parween et al. (16), using *Plasmodium falciparum* merozoite surface protein subunit and AuNPs, evaluated the humoral immune response (IgG1, IgG2a, IgG2b, and IgG3) and found an intense IgG1 response compared with the alum formulation (16). Kaba et al. (14), using *P. berghei* circumsporozoite protein and AuNPs, generated long-lasting protective immunity with Th that produced IL-2 and mixed high avidity IgG1/IgG2a (Th2/Th1) (14). In other studies, these authors replaced Ag with *P. falciparum* circumsporozoite protein; vaccination was shown to induce protective cytotoxic (CD8+) cells, high avidity Ab titers, and specific effector memory, central memory, and long-term central memory CD8+ T cells in draining lymph nodes, spleen, and liver (18). This response was shown to be generated by DC cross-presentation, which had delayed fusion and interaction of endosomes with lysosomes caused by the AuNP formulation (19). Finally, PfMSP was used with dextran-coated iron oxide NPs (IONPs) and was capable of inducing a humoral response in two animal models (mouse and monkey). This response was also shown to inhibit parasite growth by 55–100% (25).

Most studies evaluated immunogenicity through measurement of the humoral immune response. According to their findings, the use of NPs was efficient in inducing an Ab-based response. Based on heavy chain structure, there are five types of Ab, each with a different role: IgG, IgM, IgA, IgD, and IgE. IgG and IgA can be subdivided as IgG1, IgG2, IgG3, IgG4, IgA1, and IgA2 based on additional small differences in their heavy chain. With regard to vaccination, humoral immunity is especially important in responding to infection by extracellular pathogens, toxins, protozoa, and viruses. Its importance is associated with the biological activities of immunoglobulins, including microorganism opsonization and phagocytosis; complement activation (32); toxins and microorganism neutralization (33); and mast cells and basophil activation (32, 34). In addition, immunoglobulins can help target cytotoxicity against infected cells (Ab-dependent cell cytotoxicity of CD8 T cells and NK). In some cases, however, the pathogens have the ability to evade the humoral system or can even use immunoglobulins as a way to facilitate cell invasion, as in the cases of *Mycobacterium tuberculosis* and *Leishmania* spp. (35, 36).

The studies described above clearly show that MeNPs (gold, iron, and nickel) can be used for vaccine development. Different MeNPs were used in conjunction with several Ag for distinct microorganisms and showed the ability to generate humoral and cytotoxic responses. Although the generation of IgG2a and IFN- $\gamma$  shown in some studies are indicators of Th1 responses using MeNPs as adjuvant, further research is needed to specifically assess the role of different MeNP vaccines in Th1 induction.

## IMPORTANT PHYSICOCHEMICAL CHARACTERISTICS OF MeNPs AS ACTIVATORS OF IMMUNE RESPONSES

To understand the possible uses of MeNPs as platforms for vaccines against infectious diseases, analysis is needed of the impact of different physicochemical characteristics of NPs on the innate immune response (Figure 1). Several strategies have included MeNPs as vaccine platforms, involving MeNPs of different materials (including gold, iron oxide, and nickel); shapes (including spheres, cubes, rods, and disks); sizes (from 2 nm to over 200 nm); and types of coating [e.g., citrate, chitosan, dextran, or cetyltrimethylammonium bromide/4-styrenesulfonic acid-co-maleic acid (CTAB/PSS-MA)].

The material from which an NP is made has a direct influence on the functions of APCs; gold NPs (AuNPs) have been most commonly used in vaccinology (Table 2). The most recent studies involving AuNPs demonstrate the effects of gold sodium thiomalate on macrophage function, showing lysosomal enzyme inhibition and reducing phagocytosis (37). Similar effects were seen in macrophages of several origins, which, when stimulated with AuNPs, showed diminished bactericidal activity against *Staphylococcus aureus* (38) and low or absent cytokine production IL-6, IL-10, and TNF- $\alpha$  (39, 40). Moreover, when splenocytes were stimulated with LPS, the addition of AuNP reduced IL-17 and TNF- $\alpha$  release (40). Some of these results raise the concern on the use of AuNPs as adjuvants, since these immunomodulatory properties can act inhibiting the generation of Th1. However, the response to AuNPs is also correlated with other physicochemical

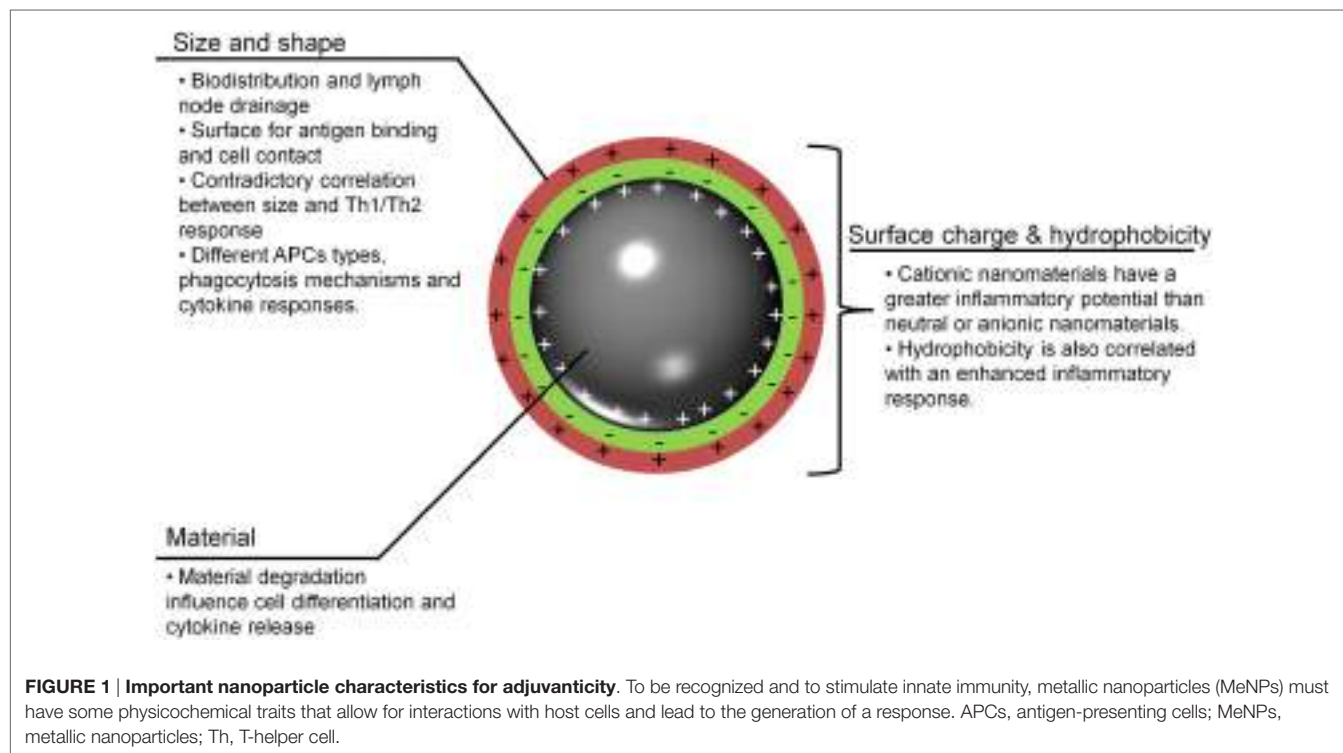


**TABLE 2 | Studies describing NPs and antigens used as vaccines against infectious diseases, listed by NPs material and year of publication (*n* = 18 studies).**

NP material	Size in nm (shape)	Functionalization	Antigen (microorganism)	Reference
Gold	25 (sphere)		<i>P. berghei</i> circumsporozoite protein ( <i>Plasmodium berghei</i> )	Kaba et al. (14)
	2, 5, 8, 12, 17, 27, 32, and 50 (sphere)	Citrate	pFMDV (foot-and-mouth virus)	Chen et al. (15)
	17 (sphere)	Citrate	PfMSP-1 <sub>19</sub> ( <i>P. falciparum</i> )	Parween et al. (16)
	15 (sphere)	Citrate	Partially purified enteropathogenic STG coronavirus	Staroverov et al. (17)
	15.6 (sphere)	Citrate	F1-antigen ( <i>Yersinia pestis</i> )	Gregory et al. (12)
	40 (sphere)		Pf CSP ( <i>P. falciparum</i> )	Kaba et al. (18)
	35–40 (sphere)	Citrate	Pf CSP ( <i>P. falciparum</i> )	Mccoy et al. (19)
	20 and 40 (sphere), 40 × 10 (rod), and 40 × 40 × 40 (cubic)	CTAB and PSS-MA	WNVE protein (WNV)	Niikura et al. (20)
	12 (sphere)	Citrate	Extracellular portion of M2 protein (influenza virus)	Tao et al. (21)
	40 (sphere)	Chitosan	Tetanus toxoid bulk from <i>Clostridium tetani</i>	Barhate et al. (22)
Iron	15 (sphere)	Citrate	TetHC and modified LPS from <i>Clostridium tetani</i>	Gregory et al. (12)
	15 (sphere)	Citrate	LPS conjugated to FlIC as glycoantigen ( <i>Burkholderia thailandensis</i> )	Torres et al. (13)
	1.5 (sphere)		T cell epitopes, LLO <sub>91–99</sub> , and LLO <sub>189–201</sub> ( <i>Listeria monocytogenes</i> )	Rodriguez-Del Rio et al. (23)
	15 (sphere)	Citrate	Flagellin <sub>1–161</sub> ( <i>Pseudomonas aeruginosa</i> )	Dakterzada et al. (24)
	20 (sphere)	Dextran	PfMSP-1 <sub>1–42</sub> ( <i>P. falciparum</i> )	Pusic et al. (25)
	23 (discoidal)		Truncated WNVE protein (WNV)	Fischer et al. (26)
Nickel	199, 214, and 270 (capsule)		Gag p41 (HIV)	Wadhwa et al. (27)
	100 (capsule)		Gag p41 or p24/his-Nef (HIV)	Yan et al. (28)

CTAB, cetyltrimethylammonium bromide; HIV, human immunodeficiency virus; LPS, lipopolysaccharide; NP, nanoparticle; Pf CSP, *P. falciparum* circumsporozoite protein; pFMDV; PfMSP, *P. falciparum* merozoite surface protein; PSS-MA, poly(4-styrenesulfonic acid- comaleic acid); STG, swine-transmissible gastroenteritis; TetHC, Hc fragment (TetHC) of tetanus toxin; WNV, West Nile virus; WNVE, WNV envelope.

characteristics that will be discussed below, which may be tailored to improve immunostimulatory or immunomodulatory capacity.

Iron oxide nanoparticles have also been used as adjuvants. Iron is an important ion in the homeostasis of all cells and in generating immune responses to several microorganisms. The effect of IONPs phagocytosis have been explored in several studies, for example, M2 macrophages after exposure to IONPs induced reactive oxygen species (ROS), but after 24 h induced IL-10 production (41). The use of IONPs in BALB/c mice demonstrated the immunomodulatory capacity of this NP by diminishing splenocyte cytokine production (IL-4 and IFN- $\gamma$ ) (42) as well as suppressing the response to pancreatic Ag in diabetic mice (43). Sindrilaru et al. (44), however, showed that macrophages, under iron overloaded conditions, became unrestrained M1 (with an incomplete switch to M2 macrophages) and produced more TNF- $\alpha$ , which impaired wound healing and had an important role in the immunopathology of chronic venous leg ulcers. Consequently, IONP response seems to have direct correlation with time and dose, once iron overload seems to be a requisite to developed pro-inflammatory response and this aspect must be evaluated to avoid the inhibition of the desired immune response.

Other critical characteristics are the shape and size of NPs, which have a direct impact on vaccine efficiency, Ag load capacity, and interaction with cells (phagocytes and APCs). These characteristics have been studied in different NPs; Shah et al. (45) published a review focusing on the impact of size for alum, oil-in-water, emulsion, polymeric particles, and liposome adjuvanticity, but did not evaluated MeNPs. In the studies reviewed here, NP sizes range from 2 nm nanospheres to 270 nm nanocapsules. Two authors

have evaluated the impact of size and shape for MeNPs (Table 2): Chen et al. (15) evaluated differences in immune response based on AuNP sizes (ranging from 2 to 50 nm nanospheres) and found that 8 and 12 nm were the most drained NP (15); Niikura et al. (20) went further and, using four different shapes of NP (20 nm sphere, 40 nm sphere, cube, and rod), showed that Ab responses and TNF- $\alpha$  were directly correlated with the specific NP surface area (the ratio of the total surface area per single NP volume). Furthermore, 40 nm spheres appear to be the most efficient in generating immune responses (IL-6 and IL-12) and granulocyte macrophage colony-stimulating factor production.

Surface charge and hydrophobicity are additional important NP characteristics for immune response induction and are directly influenced by NP functionalization (chemical modification of NPs surface by adding or replacing functional groups) and coating (Ag) (46). Most studies used citrate-coated NPs, but dextran and CTAB/PSS-MA have also been used; all three result in negatively charged (anionic) particles. Only one NP, revised here, used positive charged (cationic) functionalization [(22); Table 2]. The higher hydrophobicity of AuNP was shown to activate the innate immune system (TNF- $\alpha$  secretion) (47). Although the surface charge of other non-metallic NPs has been studied (48), to our knowledge the studies using MeNPs did not address the other characteristics associated with immune response induction. For non-metallic NPs, it appears that a positive charge signified a greater ability to induce immune responses than a negative charge. Interestingly, negatively charged non-metallic NPs were associated with Ag-specific tolerance (48). Further studies are needed to investigate whether or not the charge imputed by NP

coating influences the immune response. Though the size and shape of MeNPs had little to no impact on the innate response elicited, coating modifications may improve the capacity of these molecules to influence immune responses. Finally, it is important to note that the majority of adjuvant characteristics were evaluated using non-metallic NPs.

## NPs AS ADJUVANTS TO GENERATE Th1 and Th17 RESPONSES

T-helper 1 cells are associated with immunity against intracellular pathogens and the secretion of IFN- $\gamma$ , which, in turn, is essential for the activation of mononuclear phagocytes, including macrophages, resulting in enhanced phagocytic activity (49). Th17 cells (IL-17A and IL-17F producer cells) are associated mainly with stimulation and chemotaxis of neutrophils to the site of inflammation. However, their function goes beyond this and includes the targeting of various cell types, including non-lymphoid cells and the stimulation of cytokine, chemokine, and prostaglandin production. Another characteristic of these cells is their memory effector subset, which is maintained in mucosal tissues for extended periods. This subset has high plasticity and is able to transform into Th1 or Th2 phenotypes depending on the cytokine milieu at mucosal sites. This diversity of function and actuation make Th17 cells very important in defense against several microorganisms, mainly those acquired through mucosal routes (49, 50).

T-helper 1 and Th17 cells have their own distinct sets of functions and differentiation factors. Both cell types require T cell receptor downstream activation by Ag presentation cells through MHC II and co-stimulatory molecules (6). Consequently, cytokine release during Ag presentation is correlated with the type of adaptive immune response generated. While Th1 differentiation requires stimulation by IL-12, Th17 generation requires transforming growth factor- $\beta$  and IL-6. However, this generation is influenced by other factors and how MeNP are involved in the possible induction of Th1 or Th17 will be discussed below.

In this review, only one study investigated the development of the direct Th1 (type 1 T helper cell) and Th17 response. Using a Listeria Ag, Rodriguez-Del Rio et al. (23) showed that in contrast to Advax<sup>TM</sup> adjuvant alone, a combination of 25 nm AuNPs and Advax<sup>TM</sup> was capable of inducing the highest Th1 response. Pusic et al. (25) immunized mice with IONPs covered with rMSP1, a *P. falciparum* merozoite Ag, and showed that after immunization (intramuscular, subcutaneous, or intraperitoneal), production of IL-4 was greater than that of IFN- $\gamma$ , suggesting a predominant Th2 response (although the cellular immune response was not directly evaluated).

The first major determinant in generating Th1 and Th17 populations is the route of vaccine administration, which dictates the cell dynamic and initial response to the vaccine. For example, Mohanan et al. (51), in a cross-sectional study using a liposome plus Ag (OVA) vaccine formulation, compared intradermal (high IgG1; intermediate IgG2; and IFN- $\gamma$ ), intralymphatic (high IgG1, IgG2, and IFN- $\gamma$ ), intramuscular (high IgG1; intermediate IgG2 and IFN- $\gamma$ ), and subcutaneous (high IgG1; low IgG2 and IFN- $\gamma$ ) routes of administration (51). The predominant Th1 response to

administration through the intradermal route was most likely due to the cooperation between Langerhans cells, the primary innate immune response cells and keratinocytes that may also be stimulated by the formulation. These elicited the production of cytokines and chemokines that helped in the activation of other APCs (52).

The early phase of vaccination is characterized by recruitment of neutrophils and monocytes to the site of inoculation. Both cell types can also act as APCs, delivering Ag-specific and co-stimulatory signals to T cells. Their collaborative endeavors have been found to modulate (positively or negatively) the activity of different effector T cell subsets (53, 54). Neutrophils are the first cell lineage to migrate to inflammation sites and, when stimulated, they produce cytokines and chemokines that will attract and activate other cell types. For example, neutrophils were shown to be an important inducer of Th1 and Th17 cells (55), but their role in cytokine secretion is much broader (56). Moreover, signals may elicit different function in neutrophils and therefore, influence the quality of T cell responses. For example, AuNPs have been described as capable of inducing neutrophil extracellular traps, which act as damage-associated molecular patterns and stimulate immune system through DNA receptors such as TLR9 (57). Upon stimulation by NPs (TiO<sub>2</sub>—titanium dioxide—and alum), Duffin et al. (58) demonstrated neutrophil influx to the lungs and also induced production of IL-18. Silver NPs were also shown to be capable of interacting with neutrophils, inducing apoptosis of these cells, and inducing caspase-1\caspase-4 partially dependent IL-1 $\beta$  secretion (59). In another study, cobalt and nickel NPs were shown to induce higher nitric oxide, TNF- $\alpha$ , and CXCL2 chemokine production, by human peripheral blood neutrophils, than titanium NPs (TiO<sub>2</sub>NP) (60). Nonetheless, TiO<sub>2</sub>NPs also induced polymorphonuclear cell activation through phosphorylation of several proteins, including p38 MAPK and extracellular signal-regulated kinases-1/2 (Erk-1/2), which were associated with increased neutrophil life-span and production of several cytokines and chemokines (61).

Classically, APCs, macrophages, and DCs act at the site of vaccine inoculation by sensing foreign agents, through TLRs and other receptors, and triggering inflammation. APCs play a key role in the initiation, maintenance, and selectivity of inflammation, through their three major functions: endocytosis, Ag presentation, and production of various cytokines and growth factors (1). The main family of pattern recognition receptors in microbial recognition is the TLRs, part of the family of transmembrane proteins, which affect the transcription of genes involved in inflammatory and immune response-enhancing cellular activities such as phagocytosis, endocytosis, cytotoxic functions, and cytokine production (62, 63).

The adjuvants most frequently used for the induction of Th1 and Th17 responses are TLR agonists, such as AS04, CPG/DNA, and others. MeNPs seems to have capacity to induce the expression of Toll-like receptors, such as TiO<sub>2</sub>NPs and zirconium oxide NPs that have been described to enhance TLR3, TLR7, and TLR10 expression in macrophages (64) and TLR2 and TLR4 in mouse liver cells (65). Zinc oxide NPs (plus OVA) generated an inflammatory response in BALB/c mice and also improve TLR-2, -4 and -6 expression, followed by activation of Src family kinases (66). Consequently, TiO<sub>2</sub>NPs and IONPs were shown to induce

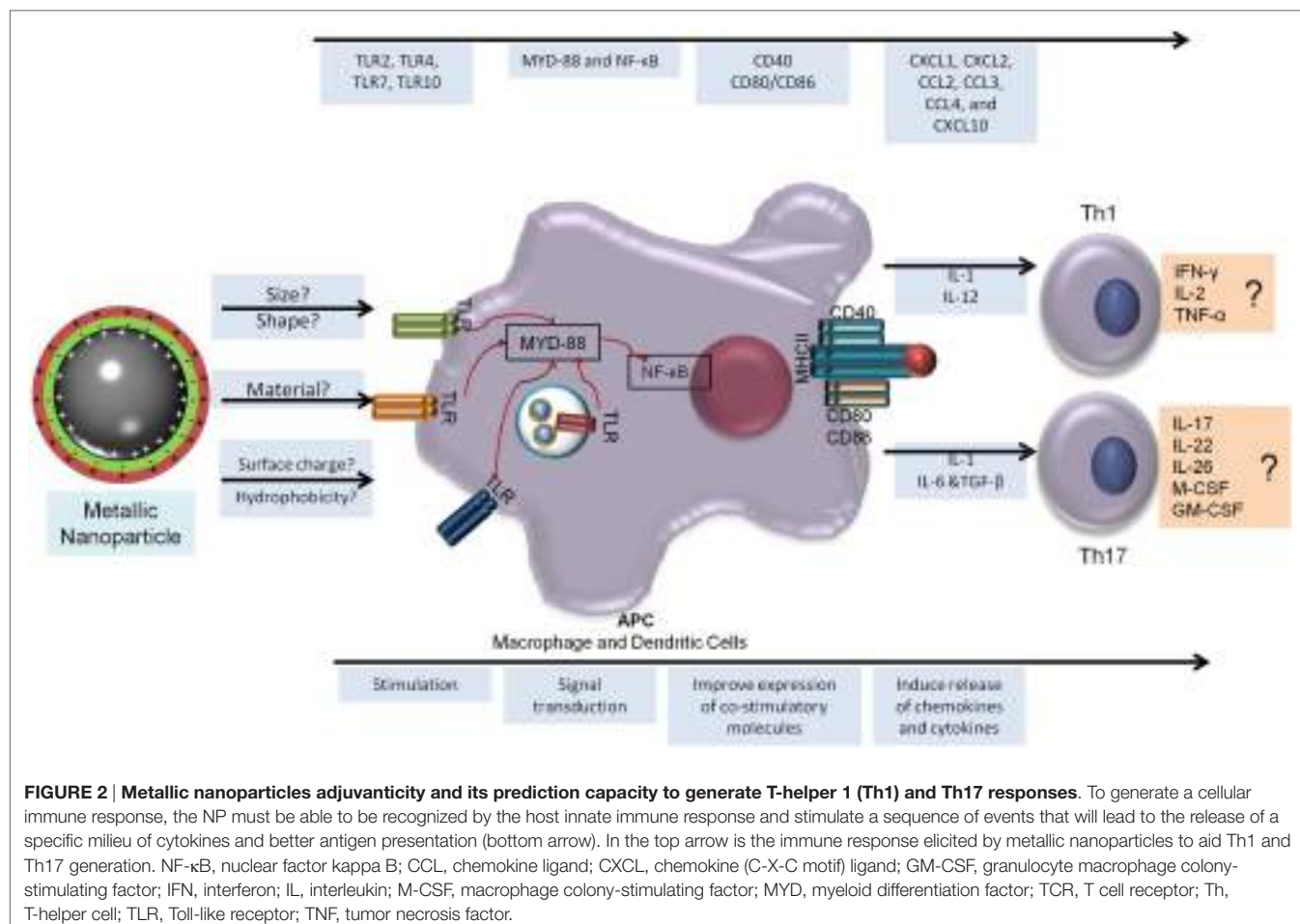


**FIGURE 2 | Metallic nanoparticles adjuvanticity and its prediction capacity to generate T-helper 1 (Th1) and Th17 responses.** To generate a cellular immune response, the NP must be able to be recognized by the host innate immune response and stimulate a sequence of events that will lead to the release of a specific milieu of cytokines and better antigen presentation (bottom arrow). In the top arrow is the immune response elicited by metallic nanoparticles to aid Th1 and Th17 generation. NF- $\kappa$ B, nuclear factor kappa B; CCL, chemokine ligand; CXCL, chemokine (C-X-C motif) ligand; GM-CSF, granulocyte macrophage colony-stimulating factor; IFN, interferon; IL, interleukin; M-CSF, macrophage colony-stimulating factor; MYD, myeloid differentiation factor; TCR, T cell receptor; Th, T-helper cell; TLR, Toll-like receptor; TNF, tumor necrosis factor.

DC upregulation of co-stimulatory molecules (MHC II, CD80) (25, 67, 68), which can also be related to TLR stimuli pathways. However, none of these works demonstrate the direct interaction of NPs with TLR (using Knock-out mice, agonists, or antagonist molecules) thus, this interaction must be further studied.

The next step in the generation of adaptive responses is the tailoring of cytokine secretion by APCs at immunological synapses, which will guide the development of the response. Several NPs have been reported to trigger cytokine and chemokine production, which may be used as biomarkers for immunotoxicity (69). Among those described, TiO<sub>2</sub>NPs were used in mimetic systems composed of blood vein endothelial component (including PBMC) and was reported to trigger pro-inflammatory cytokines (IL-6, IFN- $\gamma$ , and TNF $\alpha$ ) (67); Zinc oxide NPs were shown to be preferentially associated with monocytes and, when used in PBMC, induced IFN- $\gamma$ , TNF- $\alpha$ , and IL-12 cytokine production (70); AuNP-stimulated bone marrow-derived DC produced IL-6, TNF- $\alpha$ , and IFN- $\gamma$  (20); and IONPs were shown to induce the activation of APCs with an increase of IL-6, TNF- $\alpha$ , IFN- $\gamma$ , and IL-12, as well as chemokines. The response generated by IONPs, however, was weaker than that generated by the positive control LPS which may be beneficial in controlling possible side effects (25).

The generation of a cellular response associated with protection against intracellular pathogens is the ultimate goal of vaccination.

However, the direct effects of NPs on cellular responses have been evaluated in only a few studies. TiO<sub>2</sub>NPs were shown to activate and induce proliferation of naïve CD4+ T cells and to generate a pronounced Th1 response with IFN- $\gamma$  and TNF- $\alpha$  production, associated with pro-inflammatory cytokine production (IL-6, IL-1a, IL-1b) and DC maturation (CD86+ and CD83+ expressions increase). Schanen et al. (71) hypothesized that the oxidative capacity of an NP could impact the response and trigger pro-inflammatory (oxidant capacity) or anti-inflammatory (anti-oxidant capacity) responses. This oxidant effect could control ROS generation and thus control downstream pro-inflammatory effects while antioxidants prevent the initiation of the innate immunity in LPS-stimulated macrophages (71). This study was, however, conducted with mitogens (non-specific stimuli) and not with vaccine stimuli, but nevertheless serves as a warning about the direct action of NPs, not only on the innate immune system but specifically on T cells.

## CONCLUSION

There is enough evidence to suggest that MeNPs are not only particulate formulations but also immunostimulatory molecules with several studies demonstrating their capacity to generate humoral and cytotoxic responses. MeNPs clearly have

immunostimulatory capacity and can induce several reactions in all phases of vaccine development. These capabilities correlated with NP physicochemical characteristics such as size, charge, and hydrophobicity, but there are several gaps in our understanding of their mechanism of actions and how they may lead to adjuvanticity, immunomodulation, or tolerance to the Ag formulated with NPs. There are also evidence of MeNP being capable of help in the generation of Th1 and Th17; **Figure 2** presents an overview of the generation of these cells subsets and the possible role of MeNP in this induction.

## AUTHOR CONTRIBUTIONS

LN designed the review and wrote the first draft. AJ-K edited the first draft and critically reviewed the manuscript. AK edited

the first draft and critically reviewed the manuscript. All authors read and approved the final version of the manuscript and agreed to submission.

## ACKNOWLEDGMENTS

This work is part of LN PhD thesis at Biotechnology and Biodiversity Graduate Program from CAPES.

## FUNDING

This work was funded by FAPEG (grant number 20131026700-1143) and CNPq (grant number: 405198/2015-9). LN received a PhD fellow from CAPES, and APJK (#303675/2015-2) and AK (#307186-2013-0) received a productivity research fellow from CNPq.

## REFERENCES

- Reed SG, Orr MT, Fox CB. Key roles of adjuvants in modern vaccines. *Nat Med* (2013) 19:1597–608. doi:10.1038/nm.3409
- Agger EM. Novel adjuvant formulations for delivery of anti-tuberculosis vaccine candidates. *Adv Drug Deliv Rev* (2016) 102:73–82. doi:10.1016/j.addr.2015.11.012
- Morrison C. Landmark green light for Mosquirix malaria vaccine. *Nat Biotechnol* (2015) 33:1015–6. doi:10.1038/nbt1015-1015
- Didierlaurent AM, Laupeze B, Di Pasquale A, Hergl N, Collignon C, Garcon N. Adjuvant system AS01: helping to overcome the challenges of modern vaccines. *Expert Rev Vaccines* (2017) 16:55–63. doi:10.1080/14760584.2016.1213632
- Di Pasquale A, Preiss S, Tavares Da Silva F, Garcon N. Vaccine adjuvants: from 1920 to 2015 and beyond. *Vaccines (Basel)* (2015) 3:320–43. doi:10.3390/vaccines3020320
- Damsker JM, Hansen AM, Caspi RR. Th1 and Th17 cells: adversaries and collaborators. *Ann N Y Acad Sci* (2010) 1183:211–21. doi:10.1111/j.1749-6632.2009.05133.x
- Knudsen NP, Olsen A, Buonsanti C, Follmann F, Zhang Y, Coler RN, et al. Different human vaccine adjuvants promote distinct antigen-independent immunological signatures tailored to different pathogens. *Sci Rep* (2016) 6:19570. doi:10.1038/srep19570
- Cooper CL, Davis HL, Morris ML, Efeler SM, Adhami MA, Krieg AM, et al. CPG 7909, an immunostimulatory TLR9 agonist oligodeoxynucleotide, as adjuvant to Enerix-B HBV vaccine in healthy adults: a double-blind phase I/II study. *J Clin Immunol* (2004) 24:693–701. doi:10.1007/s10875-004-6244-3
- Verstraeten T, Descamps D, David MP, Zahaf T, Hardt K, Izurieta P, et al. Analysis of adverse events of potential autoimmune aetiology in a large integrated safety database of AS04 adjuvanted vaccines. *Vaccine* (2008) 28:6630–8. doi:10.1016/j.vaccine.2008.09.049
- Zhao L, Seth A, Wibowo N, Zhao CX, Mitter N, Yu C, et al. Nanoparticle vaccines. *Vaccine* (2014) 32:327–37. doi:10.1016/j.vaccine.2013.11.069
- Hofmann-Achtenbrink M, Grainger DW, Hofmann H. Nanoparticles in medicine: current challenges facing inorganic nanoparticle toxicity assessments and standardizations. *Nanomedicine* (2015) 11:1689–94. doi:10.1016/j.nano.2015.05.005
- Gregory AE, Judy BM, Qazi O, Blumentritt CA, Brown KA, Shaw AM, et al. A gold nanoparticle-linked glycoconjugate vaccine against *Burkholderia mallei*. *Nanomedicine* (2015) 11:447–56. doi:10.1016/j.nano.2014.08.005
- Torres AG, Gregory AE, Hatcher CL, Vinet-Oliphant H, Morici LA, Titball RW, et al. Protection of non-human primates against glanders with a gold nanoparticle glycoconjugate vaccine. *Vaccine* (2015) 33:686–92. doi:10.1016/j.vaccine.2014.11.057
- Kaba SA, Brando C, Guo Q, Mittelholzer C, Raman S, Tropel D, et al. A nonadjuvanted polypeptide nanoparticle vaccine confers long-lasting protection against rodent malaria. *J Immunol* (2009) 183:7268–77. doi:10.4049/jimmunol.0901957
- Chen YS, Hung YC, Lin WH, Huang GS. Assessment of gold nanoparticles as a size-dependent vaccine carrier for enhancing the antibody response against synthetic foot-and-mouth disease virus peptide. *Nanotechnology* (2010) 21:195101. doi:10.1088/0957-4484/21/19/195101
- Parween S, Gupta PK, Chauhan VS. Induction of humoral immune response against PfMSP-1(19) and PvMSP-1(19) using gold nanoparticles along with alum. *Vaccine* (2011) 29:2451–60. doi:10.1016/j.vaccine.2011.01.014
- Staroverov SA, Vidyasheva IV, Gabalov KP, Vasilenko OA, Laskavyi VN, Dykman LA. Immunostimulatory effect of gold nanoparticles conjugated with transmissible gastroenteritis virus. *Bull Exp Biol Med* (2011) 151:436–9. doi:10.1007/s10517-011-1350-8
- Kaba SA, McCoy ME, Doll TA, Brando C, Guo Q, Dasgupta D, et al. Protective antibody and CD8+ T-cell responses to the *Plasmodium falciparum* circumsporozoite protein induced by a nanoparticle vaccine. *PLoS One* (2012) 7:e48304. doi:10.1371/journal.pone.0048304
- McCoy ME, Golden HE, Doll TA, Yang Y, Kaba SA, Zou X, et al. Mechanisms of protective immune responses induced by the *Plasmodium falciparum* circumsporozoite protein-based, self-assembling protein nanoparticle vaccine. *Malar J* (2013) 12:136. doi:10.1186/1475-2875-12-136
- Niihura K, Matsunaga T, Suzuki T, Kobayashi S, Yamaguchi H, Orba Y, et al. Gold nanoparticles as a vaccine platform: influence of size and shape on immunological responses in vitro and in vivo. *ACS Nano* (2013) 7:3926–38. doi:10.1021/nn3057005
- Tao W, Ziemer KS, Gill HS. Gold nanoparticle-M2e conjugate coformulated with CpG induces protective immunity against influenza A virus. *Nanomedicine* (2014) 9(2):237–51. doi:10.2217/nnm.13.58
- Barhate G, Gautam M, Gairola S, Jadhav S, Pokharkar V. Enhanced mucosal immune responses against tetanus toxoid using novel delivery system comprised of chitosan-functionalized gold nanoparticles and botanical adjuvant: characterization, immunogenicity, and stability assessment. *J Pharm Sci* (2014) 103:3448–56. doi:10.1002/jps.24161
- Rodriguez-Del Rio E, Marradi M, Calderon-Gonzalez R, Frande-Cabanes E, Penades S, Petrovsky N, et al. A gold glyco-nanoparticle carrying a Listeriolysin O peptide and formulated with Advax delta inulin adjuvant induces robust T-cell protection against listeria infection. *Vaccine* (2015) 33:1465–73. doi:10.1016/j.vaccine.2015.01.062
- Dakterzada F, Mohabati Mobarez A, Habibi Roudkenar M, Mohsenifar A. Induction of humoral immune response against *Pseudomonas aeruginosa* flagellin(1–161) using gold nanoparticles as an adjuvant. *Vaccine* (2016) 34:1472–9. doi:10.1016/j.vaccine.2016.01.041
- Pusic K, Aguilar Z, McLoughlin J, Kobuch S, Xu H, Tsang M, et al. Iron oxide nanoparticles as a clinically acceptable delivery platform for a recombinant blood-stage human malaria vaccine. *FASEB J* (2013) 27:1153–66. doi:10.1096/fj.12-218362
- Fischer NO, Infante E, Ishikawa T, Blanchette CD, Bourne N, Hoeprich PD, et al. Conjugation to nickel-chelating nanolipoprotein particles increases the potency and efficacy of subunit vaccines to prevent West Nile encephalitis. *Bioconjug Chem* (2010) 21:1018–22. doi:10.1021/bc100083d
- Wadhwala S, Jain A, Woodward JG, Mumper RJ. Lipid nanocapsule as vaccine carriers for his-tagged proteins: evaluation of antigen-specific immune

- responses to HIV I His-Gag p41 and systemic inflammatory responses. *Eur J Pharm Biopharm* (2012) 80:315–22. doi:10.1016/j.ejpb.2011.10.016
28. Yan W, Jain A, O'Carra R, Woodward JG, Li W, Li G, et al. Lipid nanoparticles with accessible nickel as a vaccine delivery system for single and multiple His-tagged HIV antigens. *HIV AIDS (Auckl)* (2009) 2009:1–11. doi:10.2147/HIV.S5729
  29. Fischer NO, Blanchette CD, Chromy BA, Kuhn EA, Segelke BW, Corzett M, et al. Immobilization of His-tagged proteins on nickel-chelating nanolipoprotein particles. *Bioconjug Chem* (2009) 20:460–5. doi:10.1021/bc8003155
  30. Schmidt M, Raghavan B, Muller V, Vogl T, Fejer G, Tchaptchet S, et al. Crucial role for human Toll-like receptor 4 in the development of contact allergy to nickel. *Nat Immunol* (2010) 11:814–9. doi:10.1038/ni.1919
  31. Schmidt M, Goebeler M. Nickel allergies: paying the toll for innate immunity. *J Mol Med (Berl)* (2011) 89:961–70. doi:10.1007/s00109-011-0780-0
  32. Schroeder HW Jr, Cavacini L. Structure and function of immunoglobulins. *J Allergy Clin Immunol* (2010) 125:S41–52. doi:10.1016/j.jaci.2009.09.046
  33. Woof JM, Kerr MA. The function of immunoglobulin A in immunity. *J Pathol* (2006) 208:270–82. doi:10.1002/path.1877
  34. Kawakami T, Galli SJ. Regulation of mast-cell and basophil function and survival by IgE. *Nat Rev Immunol* (2002) 2:773–86. doi:10.1038/nri914
  35. Schorey JS, Carroll MC, Brown EJ. A macrophage invasion mechanism of pathogenic mycobacteria. *Science* (1997) 277:1091–3. doi:10.1126/science.277.5329.1091
  36. Dominguez M, Torano A. Immune adherence-mediated opsonophagocytosis: the mechanism of Leishmania infection. *J Exp Med* (1999) 189:25–35. doi:10.1084/jem.189.1.25
  37. Turkall RM, Warr GA, Tsan MF. Effect of in vivo administration of gold sodium thiomalate on rat macrophage function. *Agents Actions* (1982) 12:489–98. doi:10.1007/BF01965932
  38. Davis P, Johnston C. Effects of gold compounds on function of phagocytic cells. Comparative inhibition of activated polymorphonuclear leukocytes and monocytes from rheumatoid arthritis and control subjects. *Inflammation* (1986) 10:311–20. doi:10.1007/BF00916126
  39. Bancos S, Stevens DL, Tyner KM. Effect of silica and gold nanoparticles on macrophage proliferation, activation markers, cytokine production, and phagocytosis in vitro. *Int J Nanomedicine* (2015) 10:183–206. doi:10.2147/IJN.S72580
  40. Kingston M, Pfau JC, Gilmer J, Brey R. Selective inhibitory effects of 50-nm gold nanoparticles on mouse macrophage and spleen cells. *J Immunotoxicol* (2016) 13:198–208. doi:10.3109/1547691X.2015.1035819
  41. Rojas JM, Sanz-Ortega L, Mulens-Arias V, Gutierrez L, Perez-Yague S, Barber DF. Superparamagnetic iron oxide nanoparticle uptake alters M2 macrophage phenotype, iron metabolism, migration and invasion. *Nanomedicine* (2016) 12:1127–38. doi:10.1016/j.nano.2015.11.020
  42. Shen CC, Wang CC, Liao MH, Jan TR. A single exposure to iron oxide nanoparticles attenuates antigen-specific antibody production and T-cell reactivity in ovalbumin-sensitized BALB/c mice. *Int J Nanomedicine* (2011) 6:1229–35. doi:10.2147/IJN.S21019
  43. Tsai S, Shameli A, Yamanouchi J, Clemente-Casares X, Wang J, Serra P, et al. Reversal of autoimmunity by boosting memory-like autoregulatory T cells. *Immunity* (2010) 32:568–80. doi:10.1016/j.immuni.2010.03.015
  44. Sindrilaru A, Peters T, Wieschalka S, Baican C, Baican A, Peter H, et al. An unrestrained proinflammatory M1 macrophage population induced by iron impairs wound healing in humans and mice. *J Clin Invest* (2011) 121:985–97. doi:10.1172/JCI44490
  45. Shah RR, O'hagan DT, Amiji MM, Brito LA. The impact of size on particulate vaccine adjuvants. *Nanomedicine (Lond)* (2014) 9:2671–81. doi:10.2217/nnm.14.193
  46. Mout R, Moyano DF, Rana S, Rotello VM. Surface functionalization of nanoparticles for nanomedicine. *Chem Soc Rev* (2012) 41:2539–44. doi:10.1039/c2cs15294k
  47. Moyano DF, Goldsmith M, Solfield DJ, Landesman-Milo D, Miranda OR, Peer D, et al. Nanoparticle hydrophobicity dictates immune response. *J Am Chem Soc* (2012) 134:3965–7. doi:10.1021/ja2108905
  48. Fromen CA, Rahhal TB, Robbins GR, Kai MP, Shen TW, Luft JC, et al. Nanoparticle surface charge impacts distribution, uptake and lymph node trafficking by pulmonary antigen-presenting cells. *Nanomedicine* (2016) 12:677–87. doi:10.1016/j.nano.2015.11.002
  49. Golubovskaya V, Wu L. Different subsets of T cells, memory, effector functions, and CAR-T immunotherapy. *Cancers (Basel)* (2016) 8:E36. doi:10.3390/cancers8030036
  50. Zambrano-Zaragoza JF, Romo-Martinez EJ, Duran-Avelar Mde J, Garcia-Magallanes N, Vibanco-Perez N. Th17 cells in autoimmune and infectious diseases. *Int J Inflam* (2014) 2014:651503. doi:10.1155/2014/651503
  51. Mohanan D, Slutter B, Henriksen-Lacey M, Jiskoot W, Bouwstra JA, Perrie Y, et al. Administration routes affect the quality of immune responses: a cross-sectional evaluation of particulate antigen-delivery systems. *J Control Release* (2010) 147:342–9. doi:10.1016/j.jconrel.2010.08.012
  52. Kawase A, Isaji K, Yamaoka A, Kobayashi N, Nishikawa M, Takakura Y. Enhanced antigen-specific antibody production following polyplex-based DNA vaccination via the intradermal route in mice. *Vaccine* (2006) 24:5535–45. doi:10.1016/j.vaccine.2006.04.056
  53. Didierlaurent AM, Collignon C, Bourguignon P, Wouters S, Fierens K, Fochesato M, et al. Enhancement of adaptive immunity by the human vaccine adjuvant AS01 depends on activated dendritic cells. *J Immunol* (2014) 193:1920–30. doi:10.4049/jimmunol.1400948
  54. Iwasaki A, Medzhitov R. Control of adaptive immunity by the innate immune system. *Nat Immunol* (2015) 16:343–53. doi:10.1038/ni.3123
  55. Abi Abdallah DS, Egan CE, Butcher BA, Denkers EY. Mouse neutrophils are professional antigen-presenting cells programmed to instruct Th1 and Th17 T-cell differentiation. *Int Immunol* (2011) 23:317–26. doi:10.1093/intimm/dxr007
  56. Tecchio C, Micheletti A, Cassatella MA. Neutrophil-derived cytokines: facts beyond expression. *Front Immunol* (2014) 5:508. doi:10.3389/fimmu.2014.00508
  57. Schaefer L. Complexity of danger: the diverse nature of damage-associated molecular patterns. *J Biol Chem* (2014) 289:35237–45. doi:10.1074/jbc.R114.619304
  58. Duffin R, Tran L, Brown D, Stone V, Donaldson K. Proinflammogenic effects of low-toxicity and metal nanoparticles in vivo and in vitro: highlighting the role of particle surface area and surface reactivity. *Inhal Toxicol* (2007) 19:849–56. doi:10.1080/08958370701479323
  59. Liz R, Simard JC, Leonardi LB, Girard D. Silver nanoparticles rapidly induce atypical human neutrophil cell death by a process involving inflammatory caspases and reactive oxygen species and induce neutrophil extracellular traps release upon cell adhesion. *Int Immunopharmacol* (2015) 28:616–25. doi:10.1016/j.intimp.2015.06.030
  60. Mo Y, Mo Y, Zhu X, Mo Y, Zhu X, Hu X, et al. Cytokine and NO release from peripheral blood neutrophils after exposure to metal nanoparticles: in vitro and ex vivo studies. *Nanotoxicology* (2008) 2:79–87. doi:10.1080/17435390802112874
  61. Gonçalves DM, Chiasson S, Girard D. Activation of human neutrophils by titanium dioxide (TiO<sub>2</sub>) nanoparticles. *Toxicol In Vitro* (2010) 24:1002–8. doi:10.1016/j.tiv.2009.12.007
  62. Platt A, Wetzler L. Innate immunity and vaccines. *Curr Top Med Chem* (2013) 13:2597–608. doi:10.2174/15680266113136660185
  63. Junqueira-Kipnis AP, Marques Neto LM, Kipnis A. Role of fused *Mycobacterium tuberculosis* immunogens and adjuvants in modern tuberculosis vaccines. *Front Immunol* (2014) 5:188. doi:10.3389/fimmu.2014.00188
  64. Lucarelli M, Gatti AM, Savarino G, Quattroni P, Martinelli L, Monari E, et al. Innate defence functions of macrophages can be biased by nano-sized ceramic and metallic particles. *Eur Cytokine Netw* (2004) 15:339–46.
  65. Cui Y, Liu H, Zhou M, Duan Y, Li N, Gong X, et al. Signaling pathway of inflammatory responses in the mouse liver caused by TiO<sub>2</sub> nanoparticles. *J Biomed Mater Res A* (2011) 96:221–9. doi:10.1002/jbm.a.32976
  66. Roy R, Kumar D, Sharma A, Gupta P, Chaudhari BP, Tripathi A, et al. ZnO nanoparticles induced adjuvant effect via toll-like receptors and Src signaling in Balb/c mice. *Toxicol Lett* (2014) 230:421–33. doi:10.1016/j.toxlet.2014.08.008
  67. Schanen BC, Karakoti AS, Seal S, Drake DR III, Warren WL, Self WT. Exposure to titanium dioxide nanomaterials provokes inflammation of an in vitro human immune construct. *ACS Nano* (2009) 3:2523–32. doi:10.1021/nn900403h
  68. Winter M, Beer HD, Hornung V, Kramer U, Schins RP, Forster I. Activation of the inflammasome by amorphous silica and TiO<sub>2</sub> nanoparticles in murine dendritic cells. *Nanotoxicology* (2011) 5:326–40. doi:10.3109/17435390.2010.506957

69. Elsabahy M, Wooley KL. Cytokines as biomarkers of nanoparticle immunotoxicity. *Chem Soc Rev* (2013) 42:5552–76. doi:10.1039/c3cs60064e
70. Hanley C, Thurber A, Hanna C, Punnoose A, Zhang J, Wingett DG. The influences of cell type and ZnO nanoparticle size on immune cell cytotoxicity and cytokine induction. *Nanoscale Res Lett* (2009) 4:1409–20. doi:10.1007/s11671-009-9413-8
71. Schanen BC, Das S, Reilly CM, Warren WL, Self WT, Seal S, et al. Immunomodulation and T helper TH(1)/TH(2) response polarization by CeO<sub>2</sub> and TiO<sub>2</sub> nanoparticles. *PLoS One* (2013) 8:e62816. doi:10.1371/journal.pone.0062816

**Conflict of Interest Statement:** The authors declare that the research was conducted in the absence of any commercial or financial relationships that could be construed as a potential conflict of interest.

Copyright © 2017 Marques Neto, Kipnis and Junqueira-Kipnis. This is an open-access article distributed under the terms of the Creative Commons Attribution License (CC BY). The use, distribution or reproduction in other forums is permitted, provided the original author(s) or licensor are credited and that the original publication in this journal is cited, in accordance with accepted academic practice. No use, distribution or reproduction is permitted which does not comply with these terms.



# Co-delivery of Dual Toll-Like Receptor Agonists and Antigen in Poly(Lactic-Co-Glycolic) Acid/Polyethylenimine Cationic Hybrid Nanoparticles Promote Efficient *In Vivo* Immune Responses

Mahboubeh Ebrahimian<sup>1,2</sup>, Maryam Hashemi<sup>3</sup>, Mohsen Maleki<sup>4</sup>, Gholamreza Hashemitarbar<sup>4</sup>, Khalil Abnous<sup>5</sup>, Mohammad Ramezani<sup>5</sup> and Alireza Haghparast<sup>1,2\*</sup>

<sup>1</sup>Division of Biotechnology, Faculty of Veterinary Medicine, Ferdowsi University of Mashhad, Mashhad, Iran, <sup>2</sup>Immunology Section, Faculty of Veterinary Medicine, Ferdowsi University of Mashhad, Mashhad, Iran, <sup>3</sup>Nanotechnology Research Center, School of Pharmacy, Mashhad University of Medical Sciences, Mashhad, Iran, <sup>4</sup>Department of Pathobiology, Faculty of Veterinary Medicine, Ferdowsi University of Mashhad, Mashhad, Iran, <sup>5</sup>Pharmaceutical Research Center, Mashhad University of Medical Sciences, Mashhad, Iran

## OPEN ACCESS

### Edited by:

Diana Boraschi,  
Consiglio Nazionale Delle  
Ricerche (CNR), Italy

### Reviewed by:

Aldo Tagliafue,  
ALTA, Italy  
Luciana Leite,  
Instituto Butantan, Brazil

### \*Correspondence:

Alireza Haghparast  
haghparast@um.ac.ir,  
alireza.haghparast@gmail.com

### Specialty section:

This article was submitted  
to Inflammation,  
a section of the journal  
*Frontiers in Immunology*

Received: 08 April 2017

Accepted: 18 August 2017

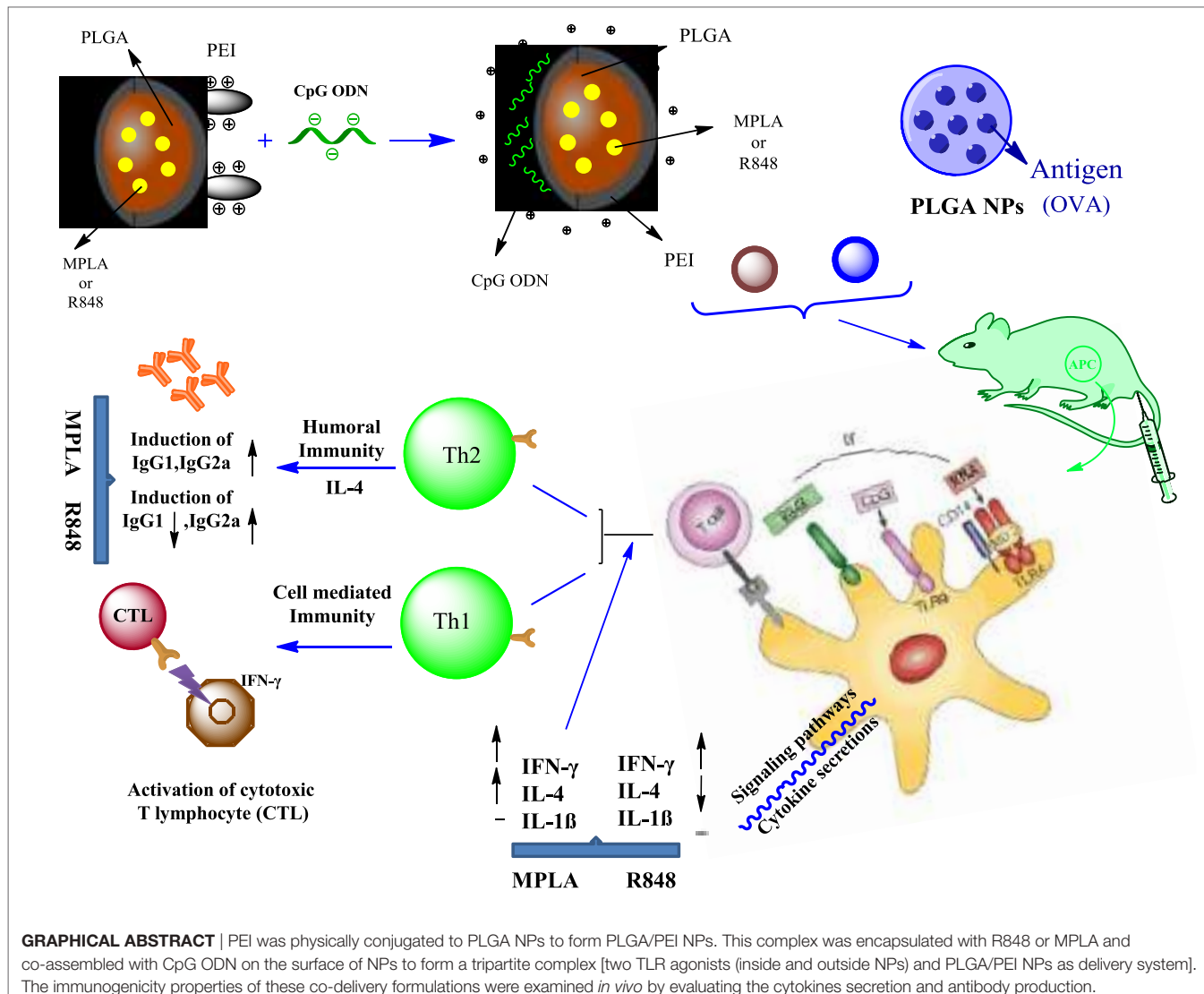
Published: 13 September 2017

### Citation:

Ebrahimian M, Hashemi M, Maleki M,  
Hashemitarbar G, Abnous K,  
Ramezani M and Haghparast A  
(2017) Co-delivery of Dual Toll-Like  
Receptor Agonists and Antigen in  
Poly(Lactic-Co-Glycolic) Acid/  
Polyethylenimine Cationic Hybrid  
Nanoparticles Promote Efficient  
*In Vivo* Immune Responses.  
*Front. Immunol.* 8:1077.  
doi: 10.3389/fimmu.2017.01077

Strategies to design delivery vehicles are critical in modern vaccine-adjuvant development. Nanoparticles (NPs) encapsulating antigen(s) and adjuvant(s) are promising vehicles to deliver antigen(s) and adjuvant(s) to antigen-presenting cells (APCs), allowing optimal immune responses against a specific pathogen. In this study, we developed a novel adjuvant delivery approach for induction of efficient *in vivo* immune responses. Polyethylenimine (PEI) was physically conjugated to poly(lactic-co-glycolic) acid (PLGA) to form PLGA/PEI NPs. This complex was encapsulated with resiquimod (R848) as toll-like receptor (TLR) 7/8 agonist, or monophosphoryl lipid A (MPLA) as TLR4 agonist and co-assembled with cytosine–phosphorothioate–guanine oligodeoxynucleotide (CpG ODN) as TLR9 agonist to form a tripartite formulation [two TLR agonists (inside and outside NPs) and PLGA/PEI NPs as delivery system]. The physicochemical characteristics, cytotoxicity and cellular uptake of these synthesized delivery vehicles were investigated. Cellular viability test revealed no pronounced cytotoxicity as well as increased cellular uptake compared to control groups in murine macrophage cells (J774 cell line). In the next step, PLGA (MPLA or R848)/PEI (CpG ODN) were co-delivered with ovalbumin (OVA) encapsulated into PLGA NPs to enhance the induction of immune responses. The immunogenicity properties of these co-delivery formulations were examined *in vivo* by evaluating the cytokine (IFN- $\gamma$ , IL-4, and IL-1 $\beta$ ) secretion and antibody (IgG1, IgG2a) production. Robust and efficient immune responses were achieved after *in vivo* administration of PLGA (MPLA or R848)/PEI (CpG ODN) co-delivered with OVA encapsulated in PLGA NPs in BALB/c mice. Our results demonstrate a rational design of using dual TLR agonists in a context-dependent manner for efficient nanoparticulate adjuvant-vaccine development.

**Keywords:** adjuvants, CpG ODN, monophosphoryl lipid A, poly(lactic-co-glycolic) acid nanoparticles, polyethylenimine, resiquimod, toll-like receptor agonist, vaccine



**GRAPHICAL ABSTRACT** | PEI was physically conjugated to PLGA NPs to form PLGA/PEI NPs. This complex was encapsulated with R848 or MPLA and co-assembled with CpG ODN on the surface of NPs to form a tripartite complex [two TLR agonists (inside and outside NPs) and PLGA/PEI NPs as delivery system]. The immunogenicity properties of these co-delivery formulations were examined *in vivo* by evaluating the cytokines secretion and antibody production.

## INTRODUCTION

The recent advances in vaccine development have moved the area from traditional vaccines using whole microorganisms to subunit vaccines containing only purified or modified antigenic proteins. Low immunogenic potential of such vaccines compared to live attenuated pathogens has motivated the research toward developing new adjuvants with biomimetic potentials to promote robust and effective innate and adaptive immune responses. Pattern recognition receptors (PRRs) are the main class of innate immunity sensors, recognizing diverse sets of pathogen-associated molecular patterns (PAMPs) and considered to be the target of novel molecular adjuvant developments. One of the major families of PRRs, Toll-like receptors (TLRs) are expressed by a variety of cells and capable of inducing innate immune responses and initiate the

pathways toward effective adaptive immune responses. During natural infection, most pathogens encounter with the immune system through multiple danger signals including PAMPs to stimulate multiple PRRs, resulting in a synergistic upregulation of pro-inflammatory cytokines and chemokines and subsequent activation of antigen-presenting cells (APCs). Therefore, the combination of multiple PRRs agonists and proper delivery systems may be a promising strategy in any artificial immunization approach to induce effective immune responses in the context of vaccine-adjuvant development (1–4).

There is strong evidence suggesting that engagement of TLRs with PAMPs results in the skewing of T helper (Th) immune responses toward either Th1 or Th2 cytokine profiles (5–7).

Optimal vaccine design requires antigen(s), adjuvant(s), and a vehicle, in which co-administration of antigen and adjuvant will

be delivered by a biocompatible vehicle to sentinel dendritic cells (DCs) in draining lymph nodes, promoting the development of effective immune responses (8). Recently, nanoparticles (NPs) have emerged as an attractive vehicle for synchronized targeted delivery of antigens and adjuvants to the immune system. NPs prepared from the biodegradable and biocompatible polymer, poly (lactic-co-glycolic acid) (PLGA), have extensively been used in clinical settings for drug delivery and are currently the subject of intensive investigation as antigen and adjuvant delivery system for vaccine purposes (9, 10). Synergistic activation of cytokine production in human and mouse DCs by combinations of TLRs ligands has been demonstrated *in vitro* (11). Such synergies may also be relevant for *in vivo* responses to vaccination. For instance, in non-human primates, combinations of TLR7/8 and TLR9 agonists enhanced the induction of neutralizing antibody titers against a human immunodeficiency virus envelope glycoprotein (12). When Rhesus macaques were immunized with PLGA NPs encapsulating TLR4 and TLR7/8 agonists mixed with two soluble recombinant antigens of simian immunodeficiency virus, vaccine containing PLGA NPs delivering dual TLRs agonists (TLR4 and TLR7/8) induced robust innate as well as antigen-specific antibody immune responses, which was greater in magnitude and persistence, and enhanced plasmablast responses compared to those achieved with aluminum hydroxide (alum)-adjuvanted vaccine (13). Encapsulating TLR4 and TLR7 agonists in PLGA NPs was found to induce a synergistically high antibody titers and increase the number of germinal centers in lymph nodes following vaccination in mice, while preventing the toxic side effects of the free adjuvant compounds (14). Further studies have shown that the delivery of TLRs agonists by PLGA NPs promotes the induction of protective and therapeutic immune responses against diseases such as leishmaniasis (15), hepatitis B (16), West Nile Encephalitis (17), avian influenza (18), and cancer (19–21). These studies highlight the potential of PLGA NP-encapsulated TLR ligands as vaccine adjuvants.

Therefore, in the present study we sought to construct and evaluate a PLGA NP-based adjuvant delivery platform using unmethylated cytosine-phosphorothioate-guanine oligodeoxynucleotide (CpG ODN) as TLR9 agonist, monophosphoryl lipid A (MPLA), a TLR4 agonist, and clinically approved Th1 polarizing adjuvant which is 100–10,000 times less toxic than lipopolysaccharide (LPS) (22) and resiquimod (R848) as TLR7/8 agonist. Additionally, we sought to enhance the co-delivery of MPLA or R848-encapsulated PLGA NPs along with CpG ODN in one platform using polyethylenimine (PEI), a cationic polymer which has previously been shown to increase the magnitude of the adaptive immune response with a shift toward Th1 response (23, 24).

Polyethylenimine was physically conjugated to PLGA NPs to form PLGA/PEI NPs. This complex was encapsulated with R848 or MPLA and co-assembled with CpG ODN on the surface of NPs to form a tripartite complex [two TLR agonists (inside and outside NPs) and PLGA/PEI NPs as delivery system]. Cellular toxicity assay was performed with murine macrophage cells (J774 cell line) for evaluating the cytotoxicity of cationic PLGA/PEI NPs. The uptake capacity of cationic NPs containing dual

adjuvant CpG ODN and either MPLA or R848 was evaluated using FITC-labeled PEIs. Ovalbumin (OVA)-encapsulated PLGA NPs as model antigen and alum as standard adjuvant were used as control immunization. The immunogenic potentials of these multiple NP adjuvant formulations were examined *in vivo* by evaluating the cytokine secretion (IFN- $\gamma$ , IL-4, and IL-1 $\beta$ ) and antibody production (IgG1 and IgG2a). The results demonstrated enhanced and robust Th1/Th2 immune responses elicited by co-delivery of dual TLRs agonist in PLGA/PEI NPs.

## MATERIALS AND METHODS

### Materials

Poly (lactic-co-glycolic acid) (50:50, Resomer® RG 502H), polyvinyl alcohol (PVA; MW 31,000–50,000), and albumin from chicken egg white (OVA) grade VI were purchased from Sigma-Aldrich (Munich, Germany). Type C CpG ODN 2395 as TLR9 agonist was purchased from Pioneer (Daejeon, Korea). Synthetic MPLA as TLR4 ligand and imidazoquinoline compound (R848) as TLR7/8 ligand were purchased from InvivoGen (San Diego, CA, USA). Branched PEI (average MW 10 kDa) was purchased from Polyscience, Inc. (Warrington, FL, USA). Ethidium bromide was obtained from Cinnagen (Tehran, Iran). Spectra/Por dialysis membranes were purchased from Spectrum Laboratories (Houston, TX, USA). Cell Titer 961 aqueous one solution cell proliferation assay (MTT) was obtained from Promega (Madison, WI, USA). All other reagents were of analytical grade and received from commercial sources.

### Cell Culture

J774 (murine macrophage) cell line was purchased from Pasteur Institute of Iran and cultured at 37°C, 95% humidity, and 5% CO<sub>2</sub> atmosphere in DMEM high glucose medium supplemented with 1% L-glutamine (2 mM), 100 µg/ml streptomycin, 100 units/ml penicillin, and 10% fetal bovine serum (FBS; Gibco, NY, USA).

### Synthesis of NPs

#### Preparation of OVA, R848, and MPLA-Loaded PLGA NPs

Poly(lactic-co-glycolic) acid nanoparticles containing OVA were prepared by double emulsion-solvent evaporation technique (w/o/w) with some modifications. Briefly, 200 µl OVA (20 mg/ml) was added to 8% w/v PLGA in 1 ml of dichloromethane/acetone mixture (ratio 1:4) under stirring at 1,300 rpm and then the mixture was sonicated (Ultrasonic processor 200H) at 80% amplitude for 1 min on ice. Next, first emulsion was added to 4 ml of an aqueous solution of PVA (5%) under sonication for 10 min on ice to form w/o/w double emulsion. Subsequently, the resulting emulsion (w/o/w) was added to 30 ml of an aqueous solution of 0.1% PVA and vigorously stirred overnight at room temperature to evaporate organic solvent. The PLGA NPs were then centrifuged at 20,000 rpm at 4°C for 20 min and washed three times with deionized water followed by lyophilization (TAITEC Corporation, Japan). NPs were stored at 4°C for later uses. PLGA NPs containing R848 and MPLA were also prepared

as above except that 5% w/v PLGA in organic solvent along with 200 and 70 µg of TLR ligands were used, respectively. Empty PLGA NPs were also prepared as control.

### Preparation of PLGA/PEI<sub>10k</sub> Tripartite Formulation

Polyethylenimine aqueous solution (1 mg/ml) was added to the aforementioned PLGA NPs suspension containing either R848 or MPLA and incubated 30 min at room temperature. After this period, CpG ODN was added and incubated for 20 min at room temperature in order to form the cationic NPs (polyplexes).

## NP Characterization

### Particle Size and Zeta Potential

The hydrodynamic diameter of synthesized NPs was assessed by DLS on a Zetasizer Nano ZS (Malvern Instruments, Malvern, UK). Three independent measurements were performed to generate the intensity-based size distribution profile.

### Polyplex Formation between CpG ODN and Cationic Co-polymer

Polyplexes were prepared by adding various concentrations of PEI in PLGA NP formulations in *N*-(2-hydroxyethyl) piperazine-*N*-(2-ethanesulfonic acid) (HEPES) buffer to equal volume of buffer containing constant amount of 400 ng CpG ODN. After incubating for 20 min at room temperature, polyplexes were formed at a range of carrier/CpG ODN ratios (C/P).

### Agarose Gel Retardation Assay

Retardation of CpG ODN mobility by cationic NPs was evaluated by agarose gel retardation assay. The polyplex solution was first prepared under a predetermined C/P ratio with 400 ng CpG ODN in HEPES buffer. Then, the polyplex solution was loaded onto 1% agarose gel (w/v) containing ethidium bromide (0.5 µg/ml) in TAE buffer (pH 7.4). The naked CpG ODN was used as control. The gel was run under 80 V for 30 min, and CpG ODN migration was recorded on a UV transilluminator system (Uvidoc, Cambridge, UK). DNA ladder (ThermoFisher Scientific, Carlsbad, CA, USA) was used as DNA size marker.

### Determination of Encapsulation Efficiency (EE%) of OVA, R848, and MPLA in PLGA NPs

To determine the amount of encapsulated agents (OVA, MPLA, and R848) in PLGA, PLGA NPs (5 mg) were treated with 0.1 M NaOH solution overnight to break the NPs, followed by neutralizing with 1 M HCl and spinning down at 14,000 rpm for 2 min. After that, supernatant was collected and each sample was assessed in triplicate using BCA assay (562 nm), UV-VIS spectrophotometry (327 nm) and fluorimetry (551–567 nm) for OVA, R848, and MPLA, respectively. EE% and loading content (LC%) of PLGA NPs were calculated by the following equations:

$$\text{EE}(\%) = \frac{\text{Amount of cargo in NPs}}{\text{Amount of cargo used for encapsulation}} \times 100$$

$$\text{LC}(\%) = \frac{\text{Mass of cargo in NPs}}{\text{Mass of NPs}} \times 100.$$

## Structural Characterization

Morphology of PLGA/PEI NPs was examined by field emission scanning electron microscopy (SEM) (FE-SEM, Mira IIIFEG, TESCAN-UK, Ltd). The sample solution in deionized water (1 mg/ml) was dehydrated on a metal stub for FE-SEM analysis. The morphology and bilayer configuration of PLGA/PEI co-polymer were also investigated by transmission electron microscopy (TEM) (Leo 912 AB, Carl Zeiss, Germany).

## In Vitro Study

### In Vitro Release Profile of OVA, R848, and MPLA from PLGA NPs

*In vitro* release of OVA, R848, and MPLA from PLGA NPs in PBS at 37°C was evaluated over a period of 10 days. NPs containing OVA, R848, and/or MPLA (5 mg) were dispersed in 5 ml of PBS (pH 7.4). The samples were incubated at 37°C on shaker (90 rpm) and at predetermined intervals (1, 2, 3, 4, and 5 h and 1, 2, 3, 4, till 10 days), tubes were centrifuged at 3,000 × g for 10 min. In the supernatants, the amount of OVA, R848, and MPLA released from the particles were determined by BCA assay, UV-VIS spectrophotometry, and fluorimetry, respectively. Meanwhile, removed supernatants were replaced with the same amount of fresh PBS to keep the medium volume constant. Release data were expressed as the cumulative percentage of OVA, R848, and MPLA in comparison with the initial content of these molecules in the NPs versus time. Each independent experiment was done in triplicates for each formulation, and experiments were repeated at least thrice.

### Assessment of Vector-CpG ODN Complex Stability

To assess the stability of the vector-oligonucleotide complex, we studied the release of the CpG ODN from the complex for 7 days at 37°C using gel electrophoresis as described in previous step.

### Cytotoxicity Assay

MTT assay was performed with J774 cells for evaluating the cytotoxicity of cationic PLGA/PEI NPs. J774 cells were seeded into a 96-well microplate at 10<sup>4</sup> cells per well, cultured in 37°C, 95% humidity, and 5% CO<sub>2</sub> for 24 h in 100 µl DMEM medium containing high glucose and 10% FBS. Thereafter, PLGA/PEI polyplexes (C/P ratio 2–6) were individually placed into the wells and further incubated for another 48 h. Subsequently, 20 µl of MTT reagent (0.5 mg/ml in phosphate buffer 0.1 M pH 7.4) was added into each well and incubated for 4 h. After removing the medium, DMSO (100 µl/well) was added and shaken for 10 min to dissolve formazan. Each sample with three replicates was analyzed on a microplate reader at wavelengths of A570 and A630 (Infinite NanoQuant M200, Tecan, Switzerland). PEI 25 kDa at C/P 0.8 was used as the reference for the MTT cytotoxicity assay.

## Uptake Study

### Uptake Study on J774 Cells Treated with Cationic NPs Containing CpG ODN

To evaluate the uptake capacity of cationic NPs containing dual adjuvant CpG ODN and either MPLA or R848, the FITC-labeled

PEIs were used. J774 macrophage cells were seeded in 24-well plates at  $4 \times 10^4$  cells/well and cultured overnight. 100  $\mu\text{g}$  of either unmodified PEI/CpG ODN or PLGA/FITC-PEI/CpG ODN NPs were added to each wells containing fresh medium. FITC-PEI 25 kDa at C/P 0.8 and untreated cells were used as positive and negative controls, respectively. Cells were incubated for 48 h and then evaluated by FACS analysis. Propidium iodide gating was used to eliminate dead cells, and 10,000 total events were collected for analysis.

## In Vivo Study

### Immunization of Mice

Female BALB/c mice (8–12 weeks) were purchased from Pasteur Institute (Tehran, Iran) and kept according to the ethical statement. Groups of 14 mice ( $N = 3$ ) (Table 1) were immunized twice (days 0 and 21) by the subcutaneous (S.C.) injection at tail base. For each injection, mice received 200  $\mu\text{l}$  of either sample or physiological saline (as control group). One week after the second vaccination, spleens were taken from mice and splenocytes were isolated and used in ELISpot assay for cytokine detection. The collected sera were kept in  $-80^\circ\text{C}$  for enzyme-linked immunosorbent assay (ELISA) assay.

### Measurement of Antibody Isotypes Titers in Serum

Serum obtained from mice was analyzed for IgG1 and IgG2a antibody titers. All samples were tested by ELISA kits (e-Bioscience, Vienna, Austria) according to the manufacturer's instructions, using 96-well polystyrene plates (Corning costar 9018, flat bottom). Briefly, plates were filled with 100  $\mu\text{l}$  capture antibody diluted in coating buffer at  $4^\circ\text{C}$  overnight and washed twice with Tween 20 (0.05% v/v) containing PBS (pH 7.4). To prevent non-specific binding to the antibody, a blocking step was performed using blocking buffer. The samples diluted in PBS (1/10,000) and added to the plates which were then

incubated for 2 h at room temperature and washed thoroughly as before. HRP-conjugated anti-mouse IgG (subtypes IgG1 and IgG2a) (100  $\mu\text{l}$ ) was then added to each well, and the plates were again incubated for 3 h at room temperature on microplate shaker at 400 rpm, followed by washing as before. Enzyme substrate, tetramethylbenzidine (100  $\mu\text{l}$ ) was added to each well and the reaction was stopped after 15 min with 50  $\mu\text{l}$  2 N  $\text{H}_2\text{SO}_4$ . The optical density at 450 nm using 570 nm filter as a reference wavelength was read in a microplate reader (Infinite NanoQuant M200, Tecan, Switzerland).

### Detection of Cytokines by ELISpot and ELISA

Naive and immunized mice were sacrificed by cervical dislocation at day 7 after secondary immunization. The spleens were removed and placed in RPMI 1640 media (Gibco-BRL, UK) under sterile conditions. Each spleen was chopped, and cells within empirical groups were pooled in one tube. The cellular suspension was centrifuged at  $800 \times g$  for 10 min, supernatant was discarded, and the pellet was washed twice with PBS. Then, the splenocytes were suspended in ACK lysis buffer for 2 min and replenished with RPMI 1640 to stop the erythrocyte elimination reactions. This suspension was centrifuged ( $800 \times g$ , 5 min), and the pellet was resuspended in fresh complete RPMI medium.  $5 \times 10^4$  cells were added to 96-well MultiScreen-IP, clear styrene plates (MAIPS 4510, Millipore, Ireland) along with antigen (10  $\mu\text{g}$ ) added in a final volume 200  $\mu\text{l}$  per well. Negative (wells without antigen) and positive [wells containing ConA (2  $\mu\text{g}/\text{ml}$ )] wells were used as controls. Plates were incubated at  $37^\circ\text{C}$ , 95% humidity, and 5%  $\text{CO}_2$  for 24 h, and IFN- $\gamma$ - and IL-4-producing splenocytes were determined using a commercial ELISpot Ready-SET-Go kit according to the manufacturer's instruction (eBioscience, Vienna, Austria). When spots appeared, counting was done by Kodak 1D image analysis software Version 3.5 (Eastman Kodak, Rochester, NY, USA). IL-1 $\beta$  cytokine titers were measured in the serum by ELISA procedure as described in previous section.

### Statistical Analysis

Statistical analysis was performed with Prism 6.01 (Graphpad, La Jolla, CA, USA) software. Statistical significance was determined using one-way analysis of variance followed by Tukey's and Bunnett's multiple comparison test. The  $P$ -values  $\leq 0.05$  were considered statistically significant.

## RESULTS

### Characterization of NP Formulations

The mean diameters of OVA-loaded, MPLA-loaded, and R848-loaded NPs were 208, 225, and 221 nm, respectively. The zeta potential was negative for NPs varying from  $\sim -13$  to  $-15$  mV. All cationic PLGA-PEI/ODN polyplexes, at all C/P ratios, had effective diameters of less than 180 nm. Zeta potential was in the range of 22–25 mV for all polyplexes (Table 2). The SEM image of PLGA(MPLA)-PEI/ODN polyplex showed smooth surface and spherical shape (Figure 1). Moreover, a core–shell particle structure is envisaged with a PLGA core containing MPLA and a PEI coating. The core–shell structure of the PLGA/PEI NPs was

**TABLE 1 |** *In vivo* immunization of mice by core–shell PLGA/PEI NPs containing either single or dual TLR agonists.

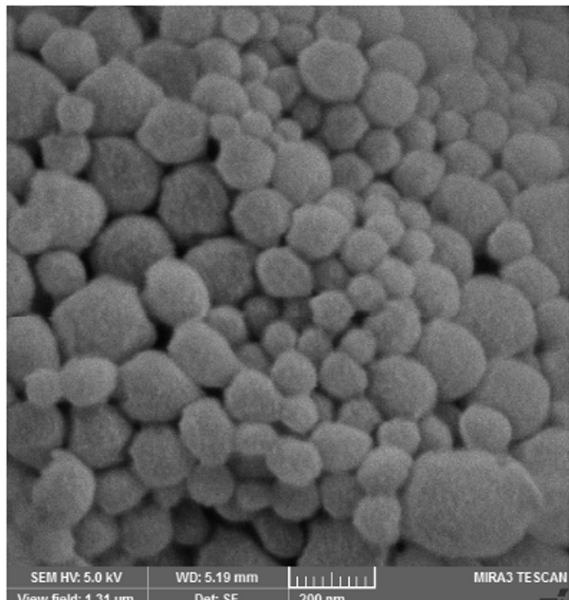
Group	Delivery systems	Antigen ( $\mu\text{g}$ ) (OVA)	Adjuvant ( $\mu\text{g}$ )			
			CpG ODN	MPLA	R848	Alum
1	PEI, PLGA	10	10	—	—	—
2	PEI, PLGA	10	10	3	—	—
3	PEI, PLGA	10	10	—	4	—
4	PLGA	—	—	3	—	—
5	PLGA	—	—	—	4	—
6	PEI	—	10	—	—	—
7	—	—	10	—	—	—
8	—	10	—	—	—	—
9	—	10	—	—	—	100
10	—	—	—	—	—	—
11	PLGA	—	—	—	—	—
12	PLGA	10	—	—	—	—
13	—	—	—	3	—	—
14	—	—	—	—	4	—

Alum, aluminum hydroxide; CpG ODN, cytosine-phosphorothioate–guanine oligodeoxynucleotide; MPLA, monophosphoryl lipid A; NPs, nanoparticles; OVA, ovalbumin; PEI, polyethylenimine; PLGA, poly(lactic-co-glycolic) acid; TLR, toll-like receptor.

**TABLE 2** | Characterization of MPLA-loaded, R848-loaded, and OVA-loaded PLGA/PEI core–shell co-polymer formulations containing CpG ODN.

Formulation	C/P ratio	Size (nm)	Zeta potential (mV)
PLGA (MPLA) NPs	—	225 ± 15	-15 ± 0.7
PLGA(MPLA)-PEI/ODN polyplex	2	180 ± 5	23 ± 0.7
PLGA(MPLA)-PEI/ODN polyplex	4	140 ± 5	25 ± 0.6
PLGA(MPLA)-PEI/ODN polyplex	6	128 ± 2	22 ± 0.2
PLGA (R848) NPs	—	221 ± 2	-15 ± 0.7
PLGA(R848)-PEI/ODN polyplex	2	135 ± 7	20 ± 0.3
PLGA(R848)-PEI/ODN polyplex	4	130 ± 15	25 ± 0.8
PLGA(R848)-PEI/ODN polyplex	6	125 ± 4	26 ± 0.5
PLGA (OVA) NPs	—	208 ± 7	-12.9 ± 2.2

CpG ODN, cytosine–phosphorothioate–guanine oligodeoxynucleotide; MPLA, monophosphoryl lipid A; NPs, nanoparticles; OVA, ovalbumin; PEI, polyethylenimine; PLGA, poly(lactic-co-glycolic) acid; R848, resiquimod.

**FIGURE 1** | Scanning electron microscopy image of poly(lactic-co-glycolic) acid/polyethylenimine structure.

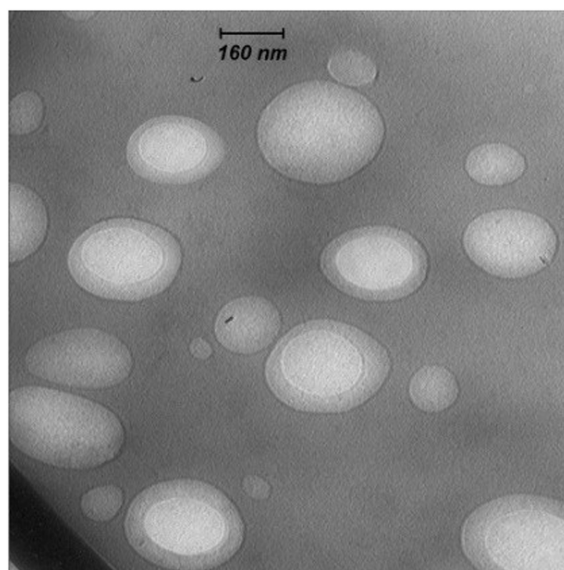
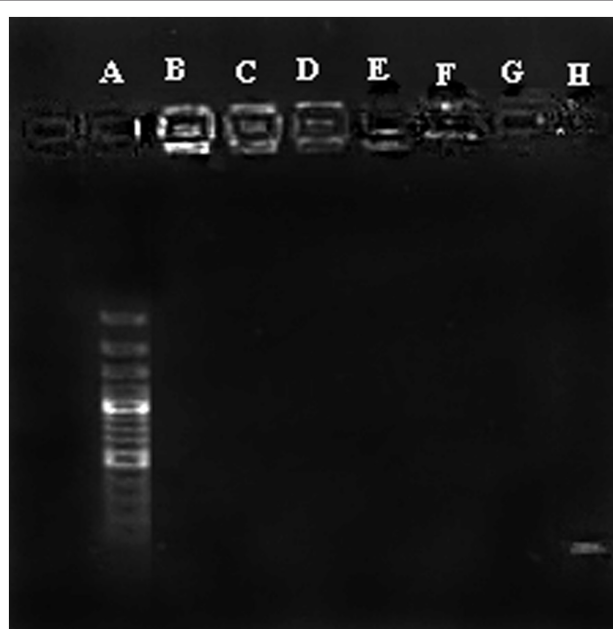
confirmed by TEM analysis (**Figure 2**). Slight size changes were observed following complexes of the PLGA/PEI NPs with ODN as reported in other studies (25).

### Agarose Gel Retardation Assay

Condensation of CpG ODN into nano-sized particles is an essential requirement for efficient delivery of ODN to the cells. Condensation of CpG ODN by PLGA/PEI was evaluated by agarose gel retardation assay. Results indicated that the complex was able to efficiently condense ODN at all C/P ratios (**Figure 3**).

### In Vitro Release Study

*In vitro* release of OVA, R848, and MPLA from PLGA NPs in PBS at 37°C was evaluated over a period of 10 days. As shown in **Figure 5**, about 23% of the total amount of OVA is released

**FIGURE 2** | Transmission electron microscopy image of poly(lactic-co-glycolic) acid/polyethylenimine core–shell structure.**FIGURE 3** | Agarose gel retardation assay of cationic poly(lactic-co-glycolic) acid (PLGA)/polyethylenimine (PEI) nanoparticles. A: Ladder, B–D: PLGA/PEI CP 2-4-6, E–G: PEI CP 2-4-6, H: cytosine–phosphorothioate–guanine oligodeoxynucleotide alone.

from the NPs during the first 5 h. This initial release of OVA is attributed to antigen located near the NPs external surface. This phenomenon is consistent with high amount of OVA reported to reside on the external surface and/or in the pores connected to the surface of PLGA particles. The release profile of the MPLA and R848 was found to be similar to that of OVA

**(Figure 4).** Only a small amount of MPLA (6%) and R848 (9%) was released from the PLGA NPs after 10 days of incubation in PBS at 37°C, and after 7 days, a plateau in release of these adjuvants was reached. Also as shown in **Figure 5**, stable conjugation between the CpG ODN and vector formed as after 7 days it remained condensed in agarose gel electrophoresis.

### EE% of PLGA (OVA), PLGA (R848), and PLGA (MPLA) NPs

The EE% of NPs loaded with OVA, R848, or MPLA were  $96 \pm 3$ ,  $98 \pm 2$ , and  $60 \pm 2.2\%$ , respectively (**Table 3**).

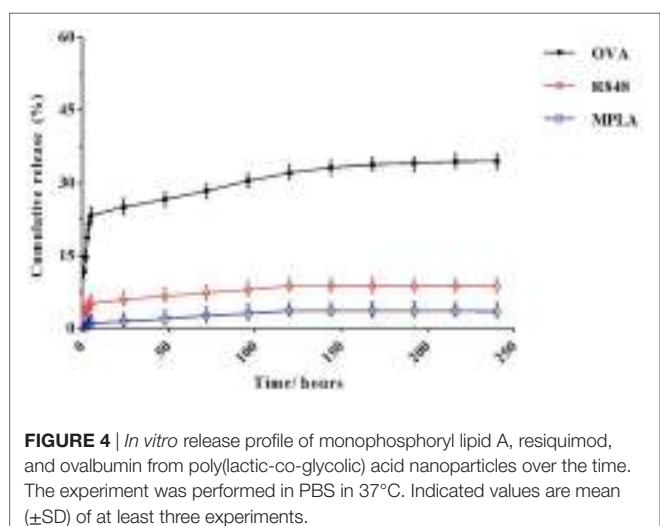


**FIGURE 4 |** *In vitro* release profile of monophosphoryl lipid A, resiquimod, and ovalbumin from poly(lactic-co-glycolic) acid nanoparticles over the time. The experiment was performed in PBS at 37°C. Indicated values are mean ( $\pm$ SD) of at least three experiments.

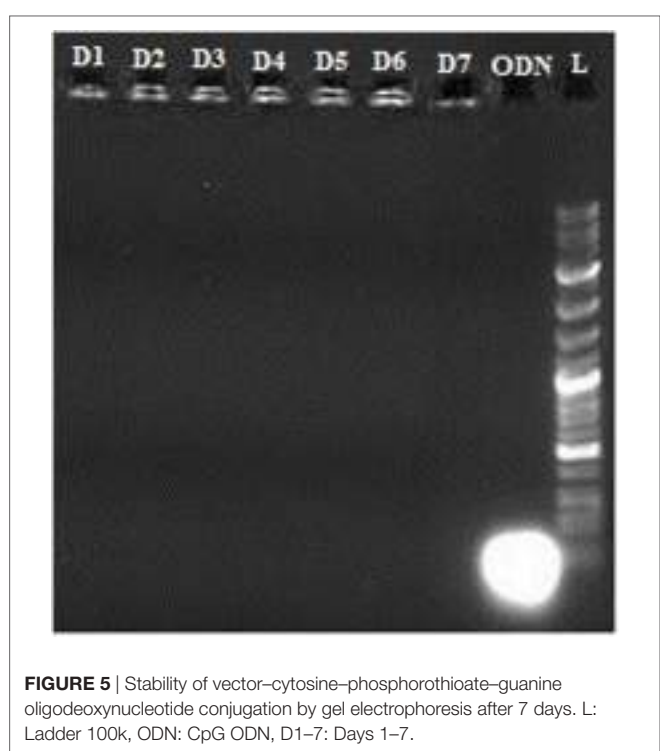


**FIGURE 5 |** Stability of vector–cytosine–phosphorothioate–guanine oligodeoxynucleotide conjugation by gel electrophoresis after 7 days. L: Ladder 100k, ODN: CpG ODN, D1–7: Days 1–7.

### Evaluation of Cytotoxicity Using MTT Assay

*In vitro* cytotoxicity of PEI and PLGA/PEI at C/P 2, 4, and 6 were evaluated in J774 cells. PEI 25 kDa at C/P 0.8 was used as positive control. PEI and PLGA/PEI at C/P 2 and 4 did not exhibit pronounced cytotoxicity and only PEI and PLGA/PEI at C/P 6 showed moderate cytotoxicity in comparison with PEI 25 kDa. However, the results indicated a viability of more than 95% at all C/P ratios tested (**Figure 6**). We should point out that the only material for which cytotoxicity was expected was PEI. As reported, no cytotoxicity test was performed for either MPLA or R848 as these adjuvants were used at very low doses in our study (14, 26).

### Uptake Study on J774 Cells Treated with CpG ODN Complexed Cationic NPs

The uptake efficiency of FITC-labeled NPs prepared from PLGA (MPLA or R848)/PEI complexed with CpG ODN was determined in J774 cells by flow cytometry. As shown in **Figure 7**, PLGA (MPLA or R848)/PEI NPs exhibited significantly more uptake than PEI10-CpG ODN and PEI25-CpG ODN as positive control groups at mass ratio tested (C/P 2).

**TABLE 3 |** The encapsulation efficiency of different formulations.

Formulation	Encapsulation efficiency (%)	
	R848, OVA (UV-Vis)	MPLA (fluorimetry)
PLGA (OVA)	$96 \pm 3$	—
PLGA (R848)	$98 \pm 2$	—
PLGA (MPLA)	—	$60 \pm 2.2$

MPLA, monophosphoryl lipid A; OVA, ovalbumin; PLGA, poly(lactic-co-glycolic) acid; R848, resiquimod.

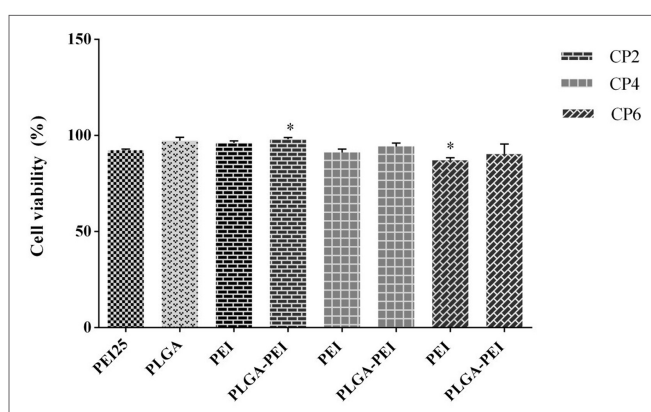
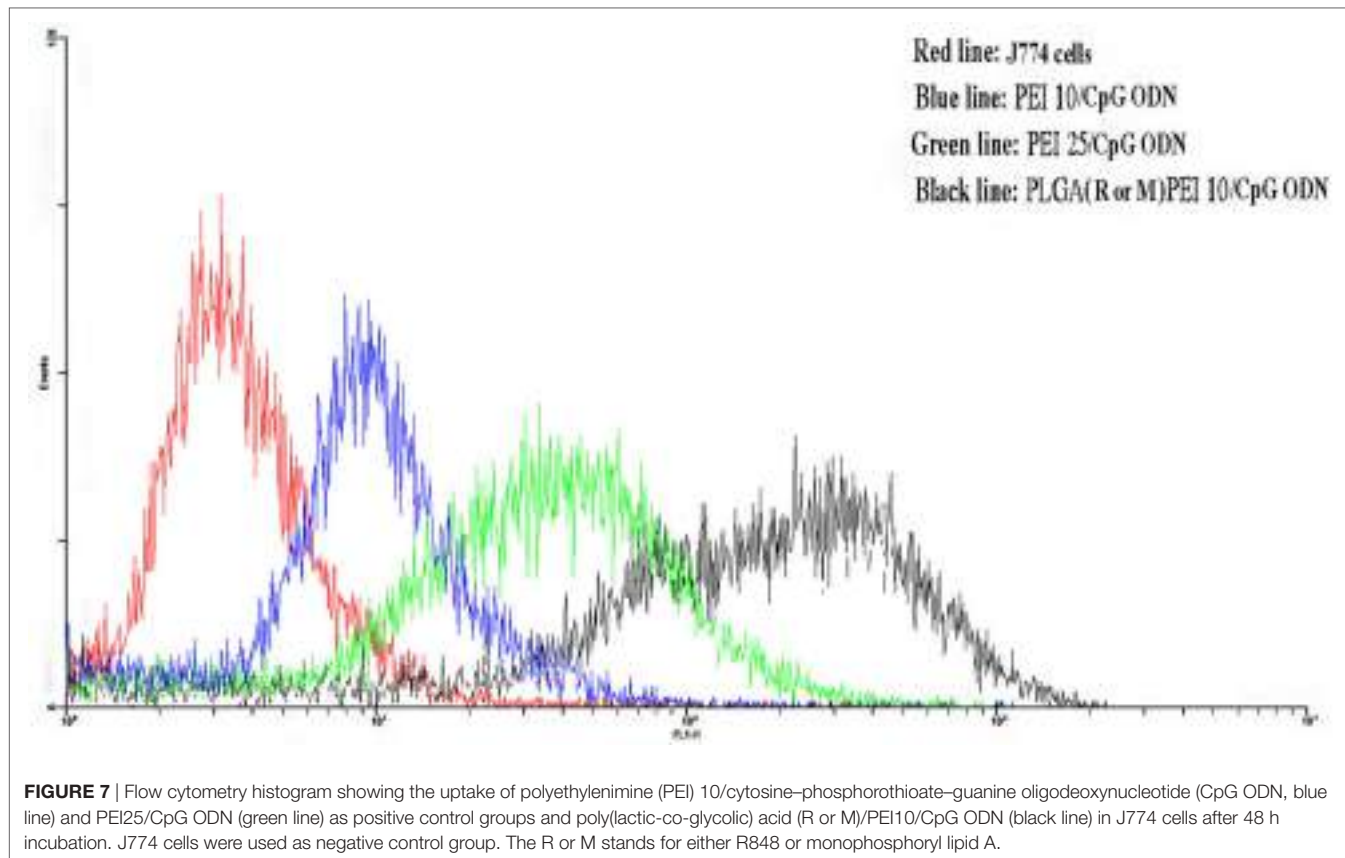


**FIGURE 6 |** Comparison of cellular viability of polyethylenimine (PEI) 25 kDa (C/P 0.8) as control with PEI and cationic poly(lactic-co-glycolic) acid /PEI complexed with cytosine–phosphorothioate–guanine oligodeoxynucleotide up to C/P 6 in J774 cells. Cells were treated for 48 h under the condition used in uptake assay, and then cell viability was assessed using MTT. The results are reported as mean  $\pm$  SD,  $n = 3$ .

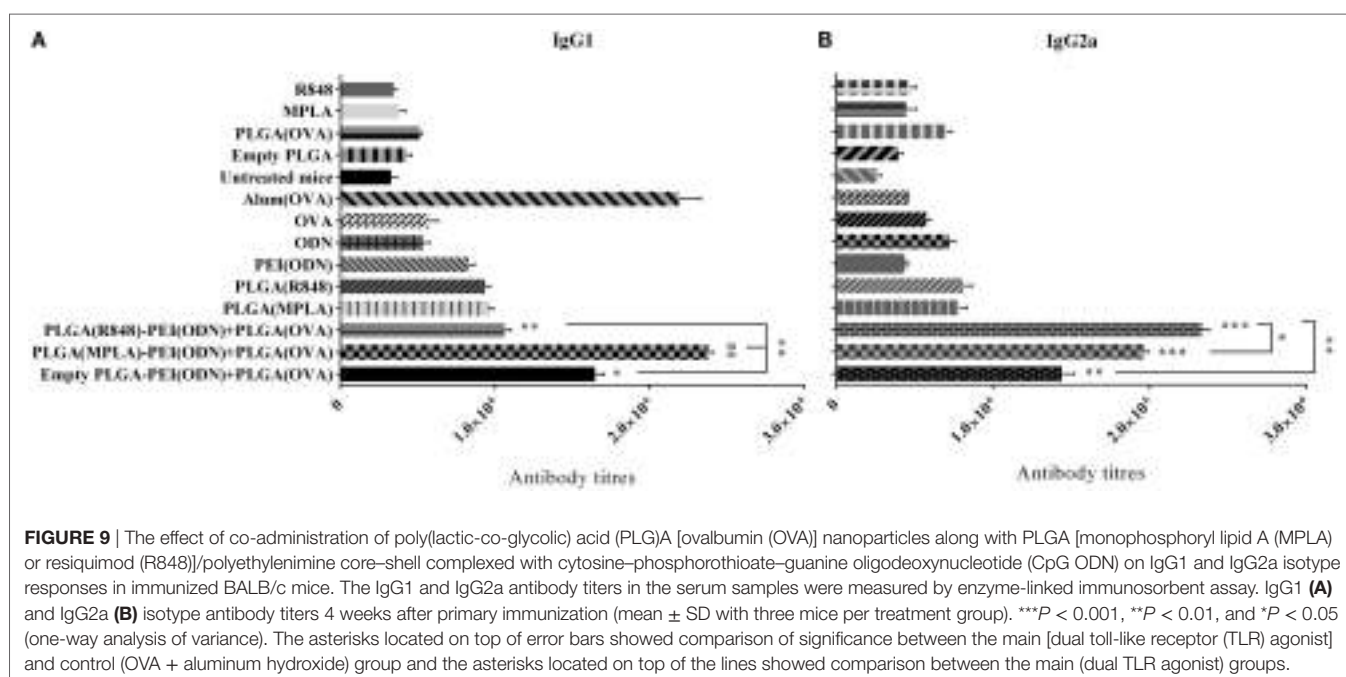
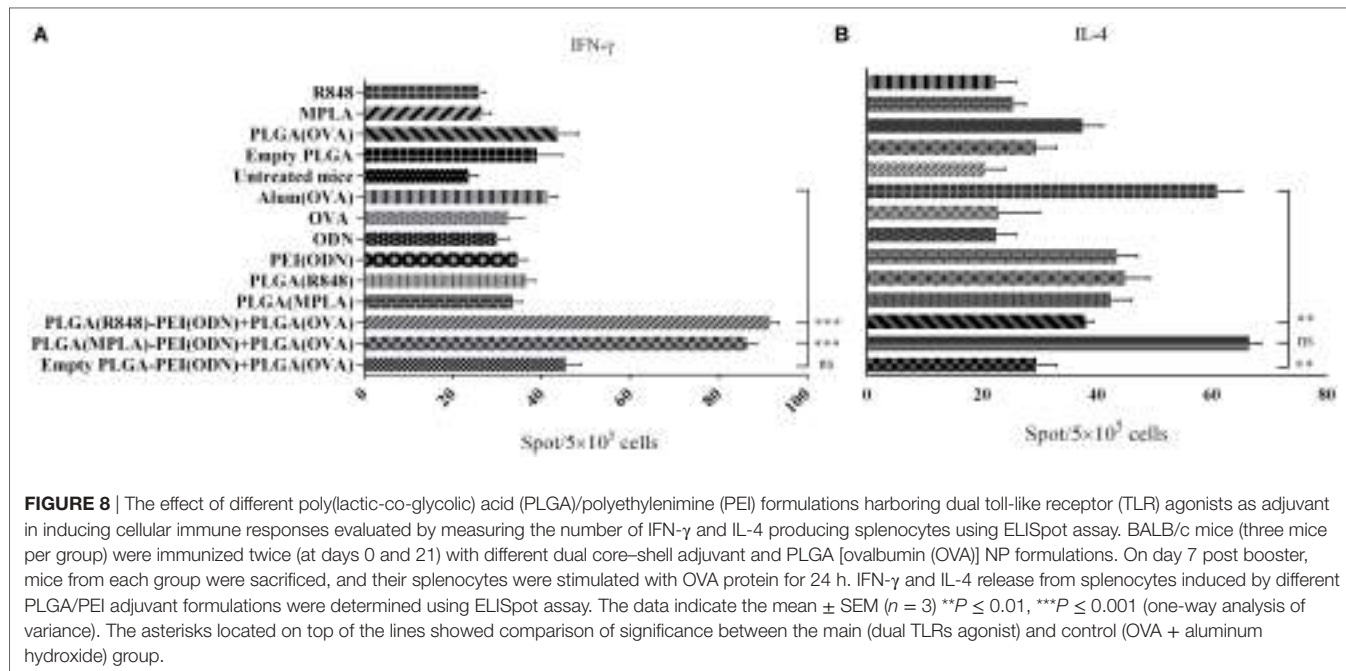


## In Vivo Induction of Immune Responses by Various NP Formulations

To investigate how immune responses is influenced by administration of different tripartite NPs formulation *in vivo*, we used OVA as a model antigen for encapsulation into PLGA NPs along with either PLGA (MPLA)-PEI/(CpG ODN) or PLGA (R848)-PEI/(CpG ODN) NPs. These formulations were injected S.C. either alone or in combination with PEI/CpG ODN into the base of tail of BALB/c mice. Single TLR agonists, either encapsulated in PLGA or in soluble forms, were also used as control. One week after the second immunization, splenocytes were removed and after 24 h of *in vitro* restimulation with antigen, spleen cells were assessed for IL-4 and IFN- $\gamma$  secretion by ELISpot assay. As shown in **Figure 8**, in immunized animals with PLGA (R848)-PEI/(CpG ODN) NPs, IL-4 production significantly diminished while IFN- $\gamma$  production increased to a level higher than the control group (OVA + Alum). Also, there was a significant different ( $P < 0.05$ ) in secretion of IFN- $\gamma$  between immunized animals with PLGA (MPLA)-PEI/(CpG ODN) and control group (OVA + Alum). We also observed significant differences in IFN- $\gamma$  secretion between animal immunized with dual TLR agonist compared to single TLR agonists. In other words, when MPLA as TLR4 ligand or R848 as TLR7/8 agonist is co-delivered with CpG ODN as TLR9 ligand using PLGA/PEI NPs, a significant increase in IFN- $\gamma$  secretion can be observed in comparison to single TLR ligands

(encapsulated in PLGA) and alum-adjuvanted OVA group. As for the IL-4 secretion, while a significant effect of using dual TLR ligands (MPLA + CpG ODN) is observed as compared to PLGA (R848)-PEI/(CpG ODN) NPs as well as PLGA-PEI/(CpG ODN) group, no significant differences in IL-4 secretion can be observed in comparison to alum-adjuvanted OVA group.

To further characterize the immune response generated after immunization of mice with various nanoparticulate adjuvant formulations, we measured IgG1 and IgG2a antibody isotype titers in the serum of immunized animals by ELISA one week after the second immunization. As indicated in **Figure 9**, a strong antibody response in terms of IgG1 and IgG2a isotypes was detected after *in vivo* administration of dual TLR agonist formulations (MPLA or R848 inside and CpG ODN outside PLGA/PEI NPs). Like cytokine detection, a high level of both IgG1 and IgG2a was observed after immunization of animals with dual TLR agonists containing PLGA (MPLA)-PEI/(CpG ODN) (**Figure 9**). A high titer of IgG2a, which correspond to Th1 immune response, was also observed when dual TLR7/8 and TLR9 agonists (R848 + CpG ODN) were delivered by PLGA/PEI NPs. The highest level of IgG1 which correspond to Th2 immune response was achieved after *in vivo* administration of dual TLR4 and TLR9 agonists (MPLA + CpG ODN) co-delivered by PLGA/PEI NPs. This response was comparable to positive control group (alum-adjuvanted OVA).



We also measured the level of IL-1 $\beta$  as a main pro-inflammatory cytokine important in initiating the innate immune responses, in the serum of immunized animals by ELISA one week after the second immunization. As indicated in **Figure 10**. A steady state increased level of IL-1 $\beta$  detected in all adjuvant immunized animals as compared to naive animals (untreated mice) points to the activation of innate responses, which is a pre-requisite of any effective acquired immune responses generated by infection or vaccination.

The relative order of effectiveness of various adjuvant formulations used in this study in inducing IFN- $\gamma$ , IL-4, IgG1, and IgG2a secretion is summarized in **Table 4**.

## DISCUSSION

Recently, we have described a novel delivery vehicle for TLR9 ligand (CpG ODN) based on single-walled carbon nanotube functionalized with PEI and demonstrated its efficacy in

induction of Th1/Th2 immune responses in mice (27). Given the pivotal role of PRRs and specially TLRs in initiating and tuning of immune responses in the context of vaccine-adjuvant development, the present study was conducted to synthesize and evaluate a PLGA NP-based adjuvant delivery platform using multiple TLRs (TLR4, TLR7/8, and TLR9) agonists. MPLA as

TLR4 agonist and R848 as TLR7/8 agonist were encapsulated in PLGA NPs. Subsequently, CpG ODN as TLR9 agonist was physically linked to the core-shell of PLGA (MPLA) or PLGA (R848) using PEI to form a hybrid PLGA NPs containing dual TLR agonists (MPLA + CpG ODN or R848 + CpG ODN). *In vivo* immunization of these dual adjuvant formulations along with OVA-encapsulated PLGA NPs as antigen in mice elicited efficient Th1-skewed cytokine (IFN- $\gamma$ ) and antibody (IgG2a)-mediated responses compared to single TLR agonist (encapsulated in PLGA) and OVA encapsulated PLGA, or OVA with or without alum. Targeting antigens along with TLR agonists encapsulated in PLGA NPs to APCs is a promising approach for generating potent Th1 polarizing immune responses that can be potentially useful in immunotherapy of cancer and intracellular pathogens (28). In this respect, activation of TLR4 by LPS and TLR9 by CpG ODN induces strong Th1 immune responses through the secretion of IL-12p70 (29). Furthermore, it has been reported that, stimulation of IFN- $\alpha$  secretion by TLR3, TLR4, TLR7, and TLR9 is an important driving force of TLR-mediated Th1 immune responses (30). Also, it was shown that multiple TLR activation (TLR3, TLR4, TLR7, TLR8, and TLR9) improved and sustained Th1 immune responses, through the enhancement of IL-12 and IL-23 production in both human and mouse DCs (11). Additionally, we observed a significant Th2 skewing cytokine (IL-4) and antibody (IgG1) responses when the combination of TLR4 and TLR9 agonists along with OVA was delivered by PLGA NPs, suggesting the effects of these TLR agonists on activation of both Th1 and Th2 mediated immune responses. The observed Th2 responses seen in our study were significantly higher than OVA with or without encapsulation in PLGA and comparable to immunization with combination of OVA plus alum, both of them considered to be potent Th2 inducers (1). PEI used in the construction of hybrid PLGA NPs in our study forms a polyplex with CpG ODN (as a shell) on the core of PLGA NPs resulting in enhanced immunogenicity of the polyplexes due to increased antigen uptake by APCs, improved trafficking of DCs to draining lymph nodes, and induction of Th1/Th2 cytokine profiles (31). Potential weakness of PEI is that high molecular PEI is toxic to

**FIGURE 10** | Detection of IL-1 $\beta$  level in the serum in BALB/c mice immunized with various toll-like receptor (TLR) agonist adjuvant formulations along with poly(lactic-co-glycolic) acid (PLGA) [ovalbumin (OVA)] NPs. Serum IL-1 $\beta$  level was determined using enzyme-linked immunosorbent assay. There was no significant difference in IL-1 $\beta$  secretion between different adjuvant formulations in comparison with positive control (OVA + aluminum hydroxide). The asterisks located on top of the lines showed comparison of significance between the main (dual TLRs agonist) and naive (untreated mice) as well as mice immunized with empty PLGA and PLGA (OVA). The data are indicated the mean  $\pm$  SD ( $n = 3$ ).

**TABLE 4** | Summary of *in vivo* antibody isotype as well as cytokine secretions elicited by various PLGA/PEI adjuvant formulations.

Group	Delivery systems	Alum ( $\mu$ g)	OVA ( $\mu$ g)	R848 ( $\mu$ g)	MPLA ( $\mu$ g)	CpG ODN ( $\mu$ g)	IgG1	IgG2a	IFN- $\gamma$	IL-4
1	PEI, PLGA	—	10	—	—	10	+++	++	++	++
2	PEI, PLGA	—	10	—	3	10	++++	+++	+++	++++
3	PEI, PLGA	—	10	4	—	10	++	++++	++++	++
4	PLGA	—	—	—	3	—	++	+	+	++
5	PLGA	—	—	4	—	—	++	+	+	++
6	PEI	—	—	—	—	10	++	+	+	++
7	—	—	—	—	—	10	+	+	+	+
8	—	—	10	—	—	—	+	+	+	+
9	—	100	10	—	—	—	++++	+	++	+++
10	—	—	—	—	—	—	+	+	+	+
11	PLGA	—	—	—	—	—	+	+	+	++
12	PLGA	—	10	—	—	—	+	+	+	+
13	—	—	—	—	3	—	+	+	+	+
14	—	—	—	4	—	—	+	+	+	+

The level of IgG isotypes or cytokine levels in descending order is indicated by ++++, +++, ++, and +. Highest level illustrated by ++++ and lowest level +.

Alum, aluminum hydroxide; CpG ODN, cytosine-phosphorothioate-guanine oligodeoxynucleotide; MPLA, monophosphoryl lipid A; OVA, ovalbumin; PEI, polyethylenimine; PLGA, poly(lactic-co-glycolic) acid.

cells due to plasma membrane and/or lysosomal damage by the proton-sponge effects (32, 33). Thus, PEI with optimal molecular weight (10 kDa) which we used in this study is considered to be safe and effective in the context of adjuvant development and can deliver the adjuvant cargo to the phagosome compartment of APCs efficiently (27).

Arranging TLR ligands on or inside PLGA NPs, which are in the size range of viruses and bacteria, created biomimetic platforms for efficient interactions with APCs, inducing synergistic antibody as well as T cell-mediated immune responses *in vitro* and *in vivo* which is required for efficient vaccine immunogenicity (34).

Given the size ( $180 \pm 5$  and  $135 \pm 7$  nm) of the vehicles constructed in our study which are in the size range of pathogens like viruses and small bacteria and the presence of dual TLR agonists on and inside the NPs, this could be considered as an artificial biomimetic approach to resemble pathogen-like molecules harboring artificial PAMPs. During natural infection, most pathogens present multiple PAMPs to initiate the innate immune responses through multiple stimulation of PRRs, resulting in activation of innate and adoptive immune responses (4, 30). Therefore, pathogen-mimicking NPs hold great potential as vaccine and adjuvant delivery system due to their ability to induce and enhance cytokine secretion and recruitment of professional immune cells at the injection site as well as stronger humoral and cellular immune responses *in vivo* (35, 36). The magnitude and direction of vaccine-adjuvant responses generated by successful vaccination can serve as an ideal model for design and development of novel nanoparticulate vaccine-adjuvant combination. Despite the shortcoming of many traditional vaccines, yellow fever vaccine 17D is one of the safest and efficacious live attenuated vaccines ever developed to date, still controlling outbreaks in modern day (37). Its efficacy likely results from activation of multiple TLRs (TLR2, TLR7, TLR8, and TLR9) on plasmacytoid and myeloid DCs, characterized by a mixed Th1/Th2 cytokine profile and antigen-specific CD8<sup>+</sup> T cells (38), suggesting that synergistic activation of multiple TLRs is a crucial step in promoting effective vaccine immunogenicity (30). Therefore, given the importance of TLRs in linking innate and adaptive immunity by both inducing APC maturation, Th cell activation, and attenuating suppressor functions of regulatory T cells (39), the data presented here provide additional credit to a novel biomimetic approach for induction of robust Th1/Th2 immune responses generated by PLGA-based NPs containing multiple TLRs agonist to enhance the vaccine-adjuvant immunogenicity. Further research is

necessary to reveal whether the NP formulation strategies like this with reduced dose of antigen-adjuvant and the increased effect observed between TLR agonists will still be effective and safe in implementing and orchestrating the optimal and effective *in vivo* vaccine responses.

## ETHICS STATEMENT

Animal care and all animal experiments were performed after approval of the Institutional Ethical Committee and Research Advisory Committee of Mashhad University of Medical Sciences and Ferdowsi University of Mashhad based on the national guidelines from Ministry of Health and Medical Education of Iran, adopted from the 86/609/EEC Directives of European Community. Mice were housed in animal cages before performing the study and were kept with free access to water and food.

## AUTHOR CONTRIBUTIONS

ME performed the experiments, analyzed data, assisted in writing, revision, and edited the paper; MH assisted in analyzing data and edition of the paper; MM, GH, and KA provided reagents; MR provided reagents, designed experiments, assisted in analyzing data, and edition of the paper; and AH conceived the idea, designed experiments, provided reagents, analyzed data, wrote, edited, and revised the entire manuscript.

## ACKNOWLEDGMENTS

We would like to gratefully acknowledge Dr. Amin Reza Nikpoor and Dr. Zahra Gholizadeh at the Department of Immunology of Mashhad University of Medical Sciences for technical assistance during *in vivo* experiment and Dr. Sara Amel Farzad at Pharmaceutical Research Center of Mashhad University of Medical Sciences for her technical assistance. This work was included in part in the Ph.D. thesis of Dr. Mahboubeh Ebrahimian.

## FUNDING

This study was supported by grant number 21021 from Ferdowsi University of Mashhad and Mashhad University of Medical Sciences. Financial support was received from the Iranian Nanotechnology Initiative Council.

## REFERENCES

- Pulendran B, Ahmed R. Immunological mechanisms of vaccination. *Nat Immunol* (2011) 12(6):509–17. doi:10.1038/ni.2039
- Coffman RL, Sher A, Seder RA. Vaccine adjuvants: putting innate immunity to work. *Immunity* (2010) 33(4):492–503. doi:10.1016/j.jimmuni.2010.10.002
- Reed SG, Orr MT, Fox CB. Key roles of adjuvants in modern vaccines. *Nat Med* (2013) 19(12):1597–608. doi:10.1038/nm.3409
- Haghparast A, Zakeri A, Ebrahimian M, Ramezani M. Targeting pattern recognition receptors (PRRs) in nano-adjuvants: current perspectives. *Curr Biomed Technol* (2016) 2(1):47–59. doi:10.2174/2213529402666160601125159
- Qi H, Denning TL, Soong L. Differential induction of interleukin-10 and interleukin-12 in dendritic cells by microbial toll-like receptor activators and skewing of T-cell cytokine profiles. *Infect Immun* (2003) 71:3337–42. doi:10.1128/IAI.71.6.3337-3342.2003
- Netea MG, Van der Meer JWM, Sutmuller RP, Adema GJ, Kullberg B-J. From the Th1/Th2 paradigm towards a toll-like receptor/T-helper bias.

- Antimicrob Agents Chemother* (2005) 49(10):3991–6. doi:10.1128/AAC.49.10.3991-3996.2005
7. Barton GM, Medzhitov R. Control of adaptive immune responses by toll-like receptors. *Curr Opin Immunol* (2002) 14(3):380–3. doi:10.1016/S0952-7915(02)00343-6
  8. Moyer TJ, Zmolek AC, Irvine DJ. Beyond antigens and adjuvants: formulating future vaccines. *J Clin Invest* (2016) 126(3):799–808. doi:10.1172/JCI81083
  9. Zhu M, Wang R, Nie G. Applications of nanomaterials as vaccine adjuvants. *Hum Vaccin Immunother* (2014) 10(9):2761–74. doi:10.4161/hv.29589
  10. Silva AL, Soema PC, Slüter B, Ossendorp F, Jiskoot W. PLGA particulate delivery systems for subunit vaccines: linking particle properties to immunogenicity. *Hum Vaccin Immunother* (2016) 12(4):1056–69. doi:10.1080/21645515.2015.1117714
  11. Napolitani G, Rinaldi A, Bertoni F, Sallusto F, Lanzavecchia A. Selected TLR agonist combinations synergistically trigger a T(H)1 polarizing program in dendritic cells. *Nat Immunol* (2005) 6(8):769–76. doi:10.1038/ni1223
  12. Moody MA, Santra S, Vandergrift NA, Sutherland LL, Gurley TC, Drinker MS, et al. Toll-like receptor 7/8 (TLR7/8) and TLR9 agonists cooperate to enhance HIV-1 envelope antibody responses in rhesus macaques. *J Virol* (2014) 88(6):3329–39. doi:10.1128/JVI.03309-13
  13. Kasturi SP, Kozlowski PA, Nakaya HI, Burger MC, Russo P, Pham M, et al. Adjuvanting a Simian immunodeficiency virus vaccine with toll-like receptor ligands encapsulated in nanoparticles induces persistent antibody responses and enhanced protection in TRIM5α restrictive macaques. *J Virol* (2017) 4(31):91. doi:10.1128/JVI.01844-16
  14. Kasturi SP, Skountzou I, Albrecht RA, Koutsanatos D, Hua T, Nakaya HI, et al. Programming the magnitude and persistence of antibody responses with innate immunity. *Nature* (2011) 470(7335):543–7. doi:10.1038/nature09737
  15. Siebert AL, Ehrlich A, Corral MJ, Goldsmith-Pestana K, McMahon-Pratt D, Fahmy TM. Immunomodulatory nanoparticles ameliorate disease in the *Leishmania (Viannia) panamensis* mouse model. *Biomaterials* (2016) 108:168–76. doi:10.1016/j.biomaterials.2016.09.004
  16. Chong CS, Cao M, Wong WW, Fischer KP, Addison WR, Kwon GS, et al. Enhancement of T helper type 1 immune responses against hepatitis B virus core antigen by PLGA nanoparticle vaccine delivery. *J Control Release* (2005) 102(1):85–99. doi:10.1016/j.jconrel.2004.09.014
  17. Demento SL, Bonafé N, Cui W, Kaech SM, Caplan MJ, Fikrig E, et al. TLR9-targeted biodegradable nanoparticles as immunization vectors protect AGAINST West Nile encephalitis. *J Immunol* (2010) 185(5):2989–97. doi:10.4049/jimmunol.1000768
  18. Singh SM, Alkie TN, Nagy E, Kulkarni RR, Hodgins DC, Sharif S. Delivery of an inactivated avian influenza virus vaccine adjuvanted with poly(D,L-lactic-co-glycolic acid) encapsulated CpG ODN induces protective immune responses in chickens. *Vaccine* (2016) 34(40):4807–13. doi:10.1016/j.vaccine.2016.08.009
  19. Hamdy S, Molavi O, Ma Z, Haddadi A, Alshamsan A, Gobti Z, et al. Co-delivery of cancer-associated antigen and toll-like receptor 4 ligand in PLGA nanoparticles induces potent CD8+ T cell-mediated anti-tumor immunity. *Vaccine* (2008) 26(39):5046–57. doi:10.1016/j.vaccine.2008.07.035
  20. Seth A, Lee H, Cho MY, Park C, Korm S, Lee JY, et al. Combining vasculature disrupting agent and toll-like receptor 7/8 agonist for cancer therapy. *Oncotarget* (2017) 8(3):5371–81. doi:10.18632/oncotarget.14260
  21. Lee Y-R, Lee Y-H, Kim K-H, Im S-A, Lee C-K. Induction of potent antigen-specific cytotoxic T cell response by PLGA-nanoparticles containing antigen and TLR agonist. *Immune Netw* (2013) 13(1):30–3. doi:10.4110/in.2013.13.1.30
  22. Mata-Haro V, Cekic C, Martin M, Chilton PM, Casella CR, Mitchell TC. The vaccine adjuvant monophosphoryl lipid A as a TRIF-biased agonist of TLR4. *Science* (2007) 316(5831):1628. doi:10.1126/science.1138963
  23. Grant EV, Thomas M, Fortune J, Klipanov AM, Letvin NL. Enhancement of plasmid DNA immunogenicity with linear polyethylenimine. *Eur J Immunol* (2012) 42(11):2937–48. doi:10.1002/eji.201242410
  24. Sheppard NC, Brinckmann SA, Gartlan KH, Puthia M, Svanborg C, Krashias G, et al. Polyethylenimine is a potent systemic adjuvant for glycoprotein antigens. *Int Immunol* (2014) 26(10):531–8. doi:10.1093/intimm/dxu055
  25. Liang GF, Zhu YL, Sun B, Hu FH, Tian T, Li SC, et al. PLGA-based gene delivering nanoparticle enhance suppression effect of miRNA in HePG2 cells. *Nanoscale Res Lett* (2011) 6(1):447–447. doi:10.1186/1556-276X-6-447
  26. Sarti F, Perera G, Hintzen F, Kotti K, Karageorgiou V, Kammona O, et al. In vivo evidence of oral vaccination with PLGA nanoparticles containing the immunostimulant monophosphoryl lipid A. *Biomaterials* (2011) 32(16):4052–7. doi:10.1016/j.biomaterials.2011.02.011
  27. Ebrahimian M, Hashemi M, Maleki M, Abnous K, Hashemitarab G, Ramezani M, et al. Induction of a balanced Th1/Th2 immune responses by co-delivery of PLGA/ovalbumin nanospheres and CpG ODNs/PEI-SWCNT nanoparticles as TLR9 agonist in BALB/c mice. *Int J Pharm* (2016) 515(1–2):708–20. doi:10.1016/j.ijpharm.2016.10.065
  28. Elamanchili P, Lutsiak CME, Hamdy S, Diwan M, Samuel J. Pathogen-mimicking nanoparticles for vaccine delivery to dendritic cells. *J Immunother* (2007) 30(4):378–95. doi:10.1097/CJI.0b013e31802cf3e3
  29. Agrawal S, Agrawal A, Doughty B, Gerwitz A, Blenis J, Van Dyke T, et al. Cutting edge: different toll-like receptor agonists instruct dendritic cells to induce distinct Th responses via differential modulation of extracellular signal-regulated kinase-mitogen-activated protein kinase and c-Fos. *J Immunol* (2003) 171(10):4984. doi:10.4049/jimmunol.171.10.4984
  30. Pulendran B. Modulating vaccine responses with dendritic cells and toll-like receptors. *Immunol Rev* (2004) 199(1):227–50. doi:10.1111/j.0105-2896.2004.00144.x
  31. Sun B, Xia T. Nanomaterial-based vaccine adjuvants. *J Mater Chem B* (2016) 4(33):5496–509. doi:10.1039/C6TB01131D
  32. Xia T, Kovochich M, Liang M, Meng H, Kabehie S, Zink JI, et al. Polyethyleneimine coating enhances the cellular uptake of mesoporous silica nanoparticles and allows safe delivery of siRNA and DNA constructs. *ACS Nano* (2009) 3(10):3273–86. doi:10.1021/nn900918w
  33. Zhang H, Xia T, Meng H, Xue M, George S, Ji Z, et al. Differential expression of syndecan-1 mediates cationic nanoparticle toxicity in undifferentiated versus differentiated normal human bronchial epithelial cells. *ACS Nano* (2011) 5(4):2756–69. doi:10.1021/nn200328m
  34. Siebert AL, Caplan MJ, Fahmy TM. Artificial bacterial biomimetic nanoparticles synergize pathogen-associated molecular patterns for vaccine efficacy. *Biomaterials* (2016) 97:85–96. doi:10.1016/j.biomaterials.2016.03.039
  35. Rosenthal JA, Chen L, Baker JL, Putnam D, DeLisa MP. Pathogen-like particles: biomimetic vaccine carriers engineered at the nanoscale. *Curr Opin Biotechnol* (2014) 28:51–8. doi:10.1016/j.copbio.2013.11.005
  36. Demento SL, Siebert AL, Bandyopadhyay A, Sharp FA, Fahmy TM. Pathogen-associated molecular patterns on biomaterials: a paradigm for engineering new vaccines. *Trends Biotechnol* (2011) 29(6):294–306. doi:10.1016/j.tibtech.2011.02.004
  37. Collins ND, Barrett AD. Live attenuated yellow fever 17D vaccine: a legacy vaccine still controlling outbreaks in modern day. *Curr Infect Dis Rep* (2017) 19:4. doi:10.1007/s11908-017-0566-9
  38. Querec T, Bennouna S, Alkan S, Laouar Y, Gorden K, Flavell R, et al. Yellow fever vaccine YF-17D activates multiple dendritic cell subsets via TLR2, 7, 8, and 9 to stimulate polyvalent immunity. *J Exp Med* (2006) 203(2):413–24. doi:10.1084/jem.20051720
  39. Pasare C, Medzhitov R. Toll pathway-dependent blockade of CD4+CD25+ T cell-mediated suppression by dendritic cells. *Science* (2003) 299(5609):1033–6. doi:10.1126/science.1078231

**Conflict of Interest Statement:** The authors declare that the research was conducted in the absence of any commercial or financial relationships that could be construed as a potential conflict of interest.

Copyright © 2017 Ebrahimian, Hashemi, Maleki, Hashemitarab, Abnous, Ramezani and Haghparast. This is an open-access article distributed under the terms of the Creative Commons Attribution License (CC BY). The use, distribution or reproduction in other forums is permitted, provided the original author(s) or licensor are credited and that the original publication in this journal is cited, in accordance with accepted academic practice. No use, distribution or reproduction is permitted which does not comply with these terms.



# Human Scavenger Receptor A1-Mediated Inflammatory Response to Silica Particle Exposure Is Size Specific

## OPEN ACCESS

### Edited by:

Diana Boraschi,  
Consiglio Nazionale Delle Ricerche  
(CNR), Italy

### Reviewed by:

Paolo Decuzzi,  
The Methodist Hospital Research  
Institute, USA  
Albert Duschl,  
University of Salzburg, Austria

### \*Correspondence:

Yasuo Yoshioka  
y-yoshioka@biken.osaka-u.ac.jp;  
Yasuo Tsutsumi  
ytsutsumi@phs.osaka-u.ac.jp

<sup>†</sup>These authors have contributed  
equally to this work.

### #Present address:

Toshiro Hirai,  
Departments of Dermatology and  
Immunology, University of Pittsburgh,  
Pittsburgh, PA, USA

### Specialty section:

This article was submitted  
to Inflammation,  
a section of the journal  
*Frontiers in Immunology*

**Received:** 13 January 2017

**Accepted:** 16 March 2017

**Published:** 03 April 2017

### Citation:

Nishijima N, Hirai T, Misato K,  
Aoyama M, Kuroda E, Ishii KJ,  
Higashisaka K, Yoshioka Y and  
Tsutsumi Y (2017) Human Scavenger  
Receptor A1-Mediated Inflammatory  
Response to Silica Particle Exposure  
Is Size Specific.  
*Front. Immunol.* 8:379.  
doi: 10.3389/fimmu.2017.00379

**Nobuo Nishijima**<sup>††</sup>, **Toshiro Hirai**<sup>††‡</sup>, **Kazuki Misato**<sup>2</sup>, **Michihiko Aoyama**<sup>1</sup>, **Etsushi Kuroda**<sup>3,4</sup>,  
**Ken J. Ishii**<sup>3,4</sup>, **Kazuma Higashisaka**<sup>1</sup>, **Yasuo Yoshioka**<sup>1,2,5\*</sup> and **Yasuo Tsutsumi**<sup>1,6\*</sup>

<sup>1</sup>Laboratory of Toxicology and Safety Science, Graduate School of Pharmaceutical Sciences, Osaka University, Suita, Japan,

<sup>2</sup>Vaccine Creation Project, BIKEN Innovative Vaccine Research Alliance Laboratories, Research Institute for Microbial Diseases, Osaka University, Suita, Japan, <sup>3</sup>Laboratory of Vaccine Science, WPI Immunology Frontier Research Center (iFReC), Osaka University, Suita, Japan, <sup>4</sup>Laboratory of Adjuvant Innovation, National Institutes of Biomedical Innovation, Health and Nutrition (NIBIOHN), Ibaraki, Japan, <sup>5</sup>BIKEN Center for Innovative Vaccine Research and Development, The Research Foundation for Microbial Diseases of Osaka University, Suita, Japan, <sup>6</sup>The Center for Advanced Medical Engineering and Informatics, Osaka University, Suita, Japan

The application of nanotechnology in the health care setting has many potential benefits; however, our understanding of the interactions between nanoparticles and our immune system remains incomplete. Although many of the biological effects of nanoparticles are negatively correlated with particle size, some are clearly size specific and the mechanisms underlying these size-specific biological effects remain unknown. Here, we examined the pro-inflammatory effects of silica particles in THP-1 cells with respect to particle size; a large overall size range with narrow intervals between particle diameters (particle diameter: 10, 30, 50, 70, 100, 300, and 1,000 nm) was used. Secretion of the pro-inflammatory cytokines interleukin (IL)-1 $\beta$  and tumor necrosis factor (TNF)- $\alpha$  induced by exposure to the silica particles had a bell-shaped distribution, where the maximal secretion was induced by silica nanoparticles with a diameter of 50 nm and particles with smaller or larger diameters had progressively less effect. We found that blockade of IL-1 $\beta$  secretion markedly inhibited TNF- $\alpha$  secretion, suggesting that IL-1 $\beta$  is upstream of TNF- $\alpha$  in the inflammatory cascade induced by exposure to silica particles, and that the induction of IL-1 $\beta$  secretion was dependent on both the NLRP3 inflammasome and on uptake of the silica particles into the cells via endocytosis. However, a quantitative analysis of silica particle uptake showed that IL-1 $\beta$  secretion was not correlated with the amount of silica particles taken up by the cells. Further investigation revealed that the induction of IL-1 $\beta$  secretion and uptake of silica nanoparticles with diameters of 50 or 100 nm, but not of 10 or 1,000 nm, was dependent on scavenger receptor (SR) A1. In addition, of the silica particles examined, only those with a diameter of 50 nm induced

**Abbreviations:** nSP10, nSP30, nSP50, nSP70, nSP100, mSP300, and mSP1000, amorphous silica particles with diameters of 10, 30, 50, 70, 100, 300, and 1,000 nm, respectively; silica particles, amorphous silica particles; crystalline silica, crystalline silica particles; PMA, phorbol 12-myristate 13-acetate; poly I, polyinosinic acid potassium salt; ATP, adenosine 5'-triphosphate disodium salt hydrate; ICP-AES, inductively coupled plasma atomic emission spectrometry; FLICA, fluorescent-coupled YVAD inhibitor to the activated form of caspase-1; SR, scavenger receptor; MARCO, macrophage receptor with collagenous structure.

strong IL-1 $\beta$  secretion *via* activation of Mer receptor tyrosine kinase, a signal mediator of SR A1. Together, our results suggest that the SR A1-mediated pro-inflammatory response is dependent on ligand size and that both SR A1-mediated endocytosis and receptor-mediated signaling are required to produce the maximal pro-inflammatory response to exposure to silica particles.

**Keywords:** inflammasome, Mer receptor tyrosine kinase, nanoparticles, nanotoxicity, scavenger receptor, size

## INTRODUCTION

The application of nanotechnology is a promising means of developing novel diagnostic and imaging technologies, photothermal therapies, vaccines, and drug delivery systems (1–3). However, various immune toxicities associated with exposure to nanoparticles have been reported, including inflammation (4), immune suppression (5), IgE-biased immune responses (6), and the induction of metal allergies (7). Therefore, improving our understanding of the interactions between nanoparticles and our immune system is essential to ensure the safe use of nanotechnology in the health care setting.

There are two main factors that make nanoparticles not only more effective but also more hazardous than the bulk material. The first is their ability to cross biological barriers [e.g., blood-brain barrier (8), placental barrier (9), blood-milk barrier (10), and nuclear barrier (11)]. The second is their large surface area per unit mass due to their small particle size. Since biological interactions occur on the surface of nanoparticles, the biological activity of nanoparticles per unit mass increases as particle size decreases (12). Indeed, many studies, both *in vitro* and *in vivo*, have demonstrated that smaller nanoparticles have biological activities of greater strength compared with larger particles (13–16). However, several *in vitro* studies have also shown that nanoparticles with a diameter of 50 nm are more readily taken up by cells and/or have greater cytotoxicity than larger and smaller particles of the same material (17–20). Indeed, we recently identified a size-specific effect in mice, where silica nanoparticles with a diameter of 50 nm induced the most severe hypothermia in the 10–1,000 nm size range (21). In addition, it has been reported that in a comparison of nanoparticle-based antitumor vaccines that differed only with respect to particle diameter (20, 40, 100, 200, 500, 1,000, or 2,000 nm), the vaccine with a particle diameter of 40 nm was the most effective (22). Together, these studies demonstrate not only that size-specific biological effects of nanoparticles exist but also that particles with diameters of around 50 nm induce the strongest biological effects. Further studies are needed to elucidate the mechanisms underlying these size-specific effects.

The pro-inflammatory effects of nanoparticles are well described in the literature and are a major issue for the development of safe nanomedicines (23). In particular, the NLRP3 inflammasome-mediated pro-inflammatory effects of nanoparticles have been reported (4, 24–26). However, the effect of particle size on the pro-inflammatory effects of nanoparticles is poorly understood, most likely because previous studies did not examine a particle size range that included fine enough intervals between particle sizes.

In the present study, we examined the effects of particle size on the pro-inflammatory response of THP-1 cells to exposure to silica particles within a large overall size range (10–1,000 nm) that included narrow intervals between the particle diameters. We also explored the mechanisms underlying this size-specific inflammatory response in our model, although it should be noted that the experimental conditions were not chosen to represent human exposure scenarios.

## MATERIALS AND METHODS

### Silica Particles

Amorphous silica particles (silica particles) with diameters of 10, 30, 50, 70, 100, 300, or 1,000 nm (nSP10, nSP30, nSP50, nSP70, nSP100, mSP300, and mSP1000, respectively) were purchased from Micromod Partikeltechnologie (Rostock/Warnemünde, Germany). Crystalline silica particles (Min-U-Sil-5; crystalline silica in diameter of not bigger than 5  $\mu\text{m}$ ) were purchased from Pennsylvania Sand Glass Corporation (Pittsburgh, PA, USA). The endotoxin level of each size of silica particle (50  $\mu\text{g}/\text{mL}$  in cell culture media) was 0.25, 0.15, 0.11, 14.88, 1.23, 0.01, and <0.01 endotoxin units/mL for nSP10, nSP30, nSP50, nSP70, nSP100, mSP300, and mSP1000, respectively, as determined by a Pyros Kinetix turbidity assay instrument with a limit of detection of 0.001 endotoxin units/mL. Endotoxin testing was performed on our behalf by nanoComposix (San Diego, CA, USA). Immediately prior to use, the dispersions of the particles were sonicated at 400 W for 5 min at 25°C and then vortexed for 1 min.

### Reagents

Phorbol 12-myristate 13-acetate (PMA), polyinosinic acid potassium salt (poly I), cytochalasin D, bafilomycin A1, BMS345541, and adenosine 5'-triphosphate disodium salt hydrate (ATP) were purchased from Sigma Aldrich (St. Louis, MO, USA). zYVAD-fmk and UNC569 were purchased from Merck (Darmstadt, Germany).

### THP-1 Cells

THP-1 cells (human acute monocytic leukemia cell line) were obtained from the American Type Culture Collection (Manassas, VA, USA) and cultured at 37°C (95% room air, 5% CO<sub>2</sub>) in RPMI1640 (Wako Pure Chemical Industries, Osaka, Japan) supplemented with 10% fetal bovine serum, 1% antibiotic cocktail (10,000 U/mL penicillin, 10,000  $\mu\text{g}/\text{mL}$  streptomycin, and 25  $\mu\text{g}/\text{mL}$  amphotericin B; Gibco, BRL, Bethesda, MD, USA), and 2-mercaptoethanol (50  $\mu\text{M}$ ; Gibco).

## Evaluation of the Pro-inflammatory Activity of the Silica Particles

THP-1 cells ( $3.0 \times 10^4$  cells/well) were seeded in flat-bottom 96-well plates (Nunc, Rochester, NY, USA) and then differentiated into macrophages by incubation with 0.5  $\mu$ M PMA at 37°C for 24 h. After incubation, the cells were washed with the cell culture media and treated with the silica particles, crystalline silica, or ATP. After incubation for 6, 12, or 24 h, the supernatants were collected. To determine cell viability after exposure to the test materials, the concentration of lactate dehydrogenase in the supernatants was measured by using a Cytotoxicity LDH Assay Kit (Wako, Osaka, Japan) in accordance with the manufacturer's instructions. To evaluate the pro-inflammatory response to exposure to the test materials, the concentrations of the pro-inflammatory cytokines interleukin (IL)-1 $\beta$  and tumor necrosis factor (TNF)- $\alpha$ , and of the receptor antagonist (RA) IL-1RA, in the supernatants were assessed by ELISA kits (IL-1 $\beta$ , BD Pharmingen, San Diego, CA, USA; TNF- $\alpha$ , eBioscience, San Diego, CA, USA; IL-1RA, R&D Systems, Minneapolis, MN, USA) in accordance with the manufacturers' instructions. In inhibitory and neutralizing antibody assays, cytochalasin D, zYVAD-fmk, BMS345541, baflomycin A1, anti-human scavenger receptor (SR) A1 monoclonal antibody (351620) (R&D Systems) or its mouse IgG1 isotype control (BioLegend, San Diego, CA, USA), anti-human macrophage receptor with collagenous structure (MARCO) antibody (PLK1) (Hycult Biotech, Uden, The Netherlands) (27) or its mouse IgG3 isotype control (BioLegend), recombinant human IL-1RA (R&D systems), or anti-human IL-1 $\beta$ /IL-1F2 (2805) (R&D systems) were added to the wells containing the PMA-differentiated THP-1 cells 30 min before stimulation with the test materials.

## Western Blotting Analysis

THP-1 cells ( $9.0 \times 10^5$  cells/well) were seeded in 6-well plates (Nunc) and then differentiated into macrophages by incubation with 0.5  $\mu$ M PMA at 37°C for 24 h. After incubation, the cells were washed with the cell culture media and treated with the silica particles (50  $\mu$ g/mL), crystalline silica (500  $\mu$ g/mL), or ATP (3 mM). After incubation for 6, 12, or 24 h, the cells were washed twice with phosphate-buffered saline and lysed with Mammalian Protein Extraction Reagent (M-PER; Thermo Fisher Scientific, Rockford, IL, USA). Protein samples (1  $\mu$ g) were loaded on a 20% sodium dodecyl sulfate–polyacrylamide gel. After electrophoresis, proteins were transferred to polyvinylidene difluoride membranes (GE Healthcare, Buckinghamshire, UK). The blots were blocked with 1% BSA in phosphate-buffered saline with 0.02% Tween 20 for 2 h at room temperature. The blots were incubated with monoclonal antibody to human IL-1 $\beta$ /IL-1F2 (8516) (R&D systems) at 1 h. HRP-conjugated goat anti-mouse antibody (SouthernBiotech, Birmingham, AL, USA) was added to the membranes, which were then incubated for 1 h at room temperature. The protein bands on the membrane were visualized with SuperSignal West Femto Maximum Sensitivity Substrate (Thermo Fisher Scientific), and the images were captured by LAS4000 mini (GE Healthcare). The densities of the bands in the captured image were analyzed by using the ImageJ software (version 1.46r, National Institutes of Health).

## Inductively Coupled Plasma Atomic Emission Spectrometry (ICP-AES) Analysis

THP-1 cells ( $1.4 \times 10^7$  cells/dish) were seeded in 150-mm dishes and differentiated into macrophages by incubation with 0.5  $\mu$ M PMA at 37°C for 24 h. After incubation, the cells were washed with phosphate-buffered saline and incubated with 50  $\mu$ g/mL of each test material for 6, 12, or 24 h. In a neutralization assay, PMA-differentiated THP-1 cells were pre-incubated for 30 min with anti-human SR-A1 or its isotype control at a concentration of 0.4  $\mu$ g/mL. After incubation with the test materials, the supernatant was removed and the cells were washed twice with phosphate-buffered saline. The cells were then detached from the dish surface using trypsin, washed with the cell culture media, and collected. After the cells were collected, samples from three dishes were pooled for analysis. The pooled cells were counted, suspended in 1 mL of MilliQ water, and sent to Japan Food Research Laboratories (Osaka, Japan), where the samples were prepared for ICP-AES analysis as follows: the cells were heated to 500°C and ash melted with sodium carbonate. Water was added to the residue and the mixture was heated for 30 min before being passed through filter paper. The filtrates were then brought to a volume of 50 mL with ultrapure water. The mass of silicon in each sample was then measured with a Vista-MPX ICP-AES instrument (Varian, Palo Alto, CA, USA) on our behalf by Kiyokawa Plating Industry Co., Ltd. (Fukui, Japan). Silicon uptake by the cells was calculated as the amount of silicon in silica particle-treated cells minus the silicon level in non-silica-treated cells.

## Statistical Analyses

Statistical analyses were performed by using the Ekuseru-Toukei 2012 software (Social Survey Research Information Co., Ltd., Tokyo, Japan). Data are presented as mean  $\pm$  SD. Significant differences between the control group and experimental group were assessed by using Student's *t*-test. *P* < 0.05 was considered statistically significant.

Methods used in the Supplementary Figures are in the supplementary figures file.

## RESULTS

### Effect of Particle Size on the Pro-inflammatory Effect of Silica Particles in THP-1 Cells

The hydrodynamic diameters of the silica particles dispersed in the cell culture medium (5 mg/mL), as measured by means of dynamic light scattering, were 10.0, 24.3, 48.3, 64.7, 86.0, 285.7, and 1,164.3 nm for nSP10, nSP30, nSP50, nSP70, nSP100, mSP300, and mSP1000, respectively (Table S1 in Supplementary Material). These hydrodynamic diameters suggest that the silica particles were well dispersed in the cell culture medium. Transmission electron microscopy images of the silica particles used in the present study are provided in our previous reports (6, 21, 28).

We first evaluated the cytotoxicity of the silica particles in THP-1 cells by means of a lactate dehydrogenase cytotoxicity

assay (**Figure 1A**). PMA-differentiated THP-1 cells were incubated with the different silica particles (nSP10, nSP30, nSP50, nSP70, nSP100, mSP300, or mSP1000) for 6, 12, or 24 h. We hardly detected cytotoxicity in our dose range at 6 and 12 h. On the other hand, dose-dependent cytotoxicity was observed at a dose greater than 100  $\mu\text{g/mL}$  in all of the silica particle-treated groups at 24 h and the data suggested that larger particles tended

to induce stronger cytotoxicity. In the following assays, 50  $\mu\text{g/mL}$  was the maximum dose of silica particles used to avoid inducing cytotoxicity.

To examine the effect of particle size on the pro-inflammatory effects of the silica particles in THP-1 cells, we measured the concentration of the pro-inflammatory cytokines IL-1 $\beta$  and TNF- $\alpha$  in the culture supernatant after incubation of the cells

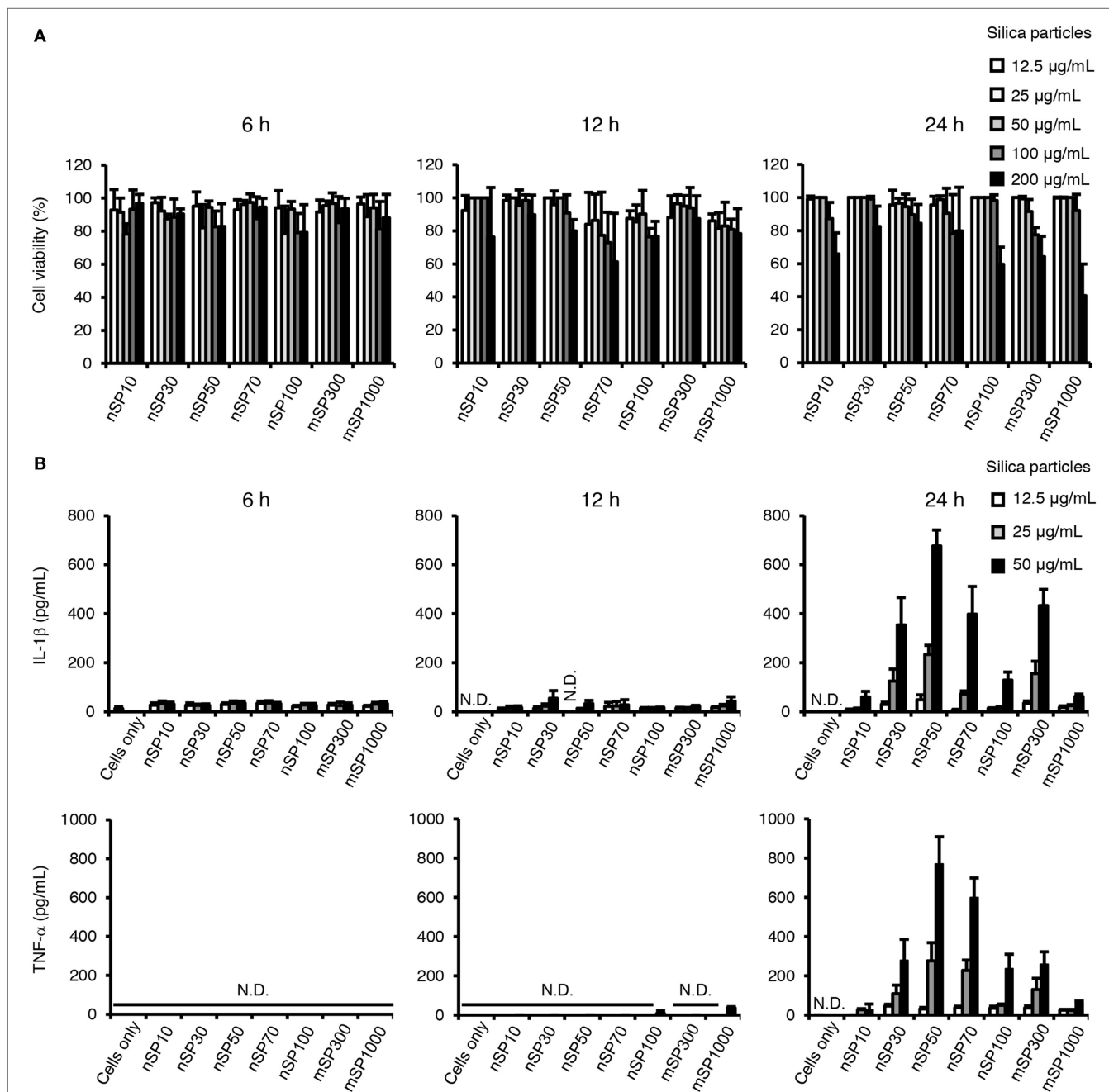


**FIGURE 1 | Effects of silica particles on THP-1 cell viability and pro-inflammatory cytokine secretion.** Phorbol 12-myristate 13-acetate-differentiated THP-1 cells were incubated with silica particles of various concentrations for 6, 12, or 24 h. After incubation, culture supernatants were collected. **(A)** Cell viability was determined by means of a lactate dehydrogenase assay. **(B)** Interleukin (IL)-1 $\beta$  and tumor necrosis factor (TNF)- $\alpha$  concentration in the culture supernatant was measured by ELISA. Data are presented as mean  $\pm$  SD ( $n = 4$  independent cultures/group). N.D., not detected.

with the silica particles for 6, 12, or 24 h (**Figure 1B**). Although incubation with the silica particles for 6 or 12 h had little effect on the secretion of IL-1 $\beta$  and TNF- $\alpha$ , incubation for 24 h resulted in a marked increase in the concentrations of IL-1 $\beta$  and TNF- $\alpha$  in the supernatant in several of the silica particle-treated groups. Furthermore, a bell-shaped size-specific effect was observed, where the silica particles with a diameter of 50 nm induced the greatest secretion of IL-1 $\beta$  and TNF- $\alpha$  and silica particles with smaller or larger diameters had progressively less effect (overall size range, 10–1,000 nm). In addition, the transcript levels of IL-1 $\beta$  and TNF- $\alpha$  were increased 24 h after incubation with nSP50 compared with the control group (Figure S1 in Supplementary Material), which was consistent with the results regarding the secreted proteins. As a positive control, we also exposed the cells to crystalline silica and ATP, which has known pro-inflammatory effects, and found that with this exposure the secretion of IL-1 $\beta$  was increased at the 6, 12, and 24-h time points (Figure S2 in Supplementary Material), which is consistent with a previous report (29). Thus, the size-specific pro-inflammatory effects of silica particles had a relatively slow onset compared with that of crystalline silica as a control particle.

It has been reported that the induction of TNF- $\alpha$  production by crystalline silica is mediated by IL-1 $\beta$  (29), which implies that the observed increase in TNF- $\alpha$  secretion by exposure to the silica particles may also be mediated by IL-1 $\beta$ . We, therefore, examined the effect of inhibiting IL-1 signaling on the silica particle-induced secretion of TNF- $\alpha$ . Co-incubation of the cells with the silica particles (nSP10, nSP50, nSP100, and mSP1000 as representatives of the size effect) and the RA IL-1RA resulted in a marked reduction in the amount of TNF- $\alpha$  secreted by cells incubated with nSP50 (**Figure 2A**, left). Similar results were obtained after co-incubation of the cells with the silica particles and anti-IL-1 $\beta$  (**Figure 2B**). Together, these results suggest that the induction of TNF- $\alpha$  by the silica particles was completely dependent on the production of IL-1 $\beta$ . Furthermore, co-incubation with IL-1RA was found to suppress the secretion of IL-1 $\beta$  in nSP50- or mSP1000-treated cells, but not in nSP10- or nSP100-treated cells, suggesting that a positive feedback loop is created for IL-1 $\beta$  in nSP50- or mSP1000-treated cells (**Figure 2A**, right). We speculated that perhaps nSP50 inhibited endogenous IL-1RA production, which would enhance the effect of IL-1 $\beta$ . However, the concentration of IL-1RA in the culture supernatants of the cells exposed to the silica particles was comparable with that in the supernatants of unstimulated cells (**Figure 2C**).

Two processes are involved in the secretion of mature IL-1 $\beta$ : NF- $\kappa$ B-dependent pro-IL-1 $\beta$  synthesis and NLRP3 inflammasome (caspase-1)-dependent cleavage of pro-IL-1 $\beta$  (30). Therefore, next we evaluated the effect of exposure to the silica particles on these two processes. Blocking the maturation of IL-1 $\beta$  with zYVAD-fmk, a caspase-1 inhibitor, considerably reduced the concentration of IL-1 $\beta$  in the culture supernatants of the silica particle-treated cells and in the crystalline silica- or ATP-treated cells, which were positive controls for activation of the NLRP3 inflammasome (30) (**Figure 3A**). These results suggest that induction of IL-1 $\beta$  by silica particles is dependent on the NLRP3 inflammasome. In addition, flow cytometric evaluation of the binding of a fluorescence-coupled YVAD inhibitor of

caspase-1 activation showed that caspase-1 tended to be activated in cells treated with nSP10, nSP50, nSP100, or mSP1000 (Figure S3A in Supplementary Material).

Particulate matter such as crystalline silica and alum is known to activate the NLRP3 inflammasome *via* lysosomal destabilization, and neutralization of lysosomal pH inhibits this activation pathway (30). In the present study, inhibiting lysosomal acidification by co-incubation with baflomycin A1, an inhibitor of vacuolar-type H<sup>+</sup>-ATPase, reduced the induction of IL-1 $\beta$  by all of the silica particles or crystalline silica, but not that induced by ATP (**Figure 3B**), which is independent of lysosomal destabilization (31). Furthermore, we found that loss of the red acidity-dependent acridine orange signal, which is an index of lysosomal integrity, was significantly increased in nSP50- or crystalline silica-treated cells, but not in ATP-treated cells (Figure S2B in Supplementary Material). The loss of the red acidity-dependent acridine orange signal appeared to be enhanced in nSP10- or nSP100-treated cells (Figure S3B in Supplementary Material). These findings suggest that, like crystalline silica, silica particles activate the NLRP3 inflammasome *via* lysosomal destabilization (32). Thus, the present results show that the silica particles induced the secretion of IL-1 $\beta$  *via* activation of the NLRP3 inflammasome. The results imply that nSP50 activated the NLRP3 inflammasome more than did the other sizes of silica particles *via* stronger induction of lysosomal destabilization (Figure S3 in Supplementary Material).

We next examined the effects of silica particle size on the induction of pro-IL-1 $\beta$ . Since we detected pro-IL-1 $\beta$  in untreated cells, PMA-differentiation has induced a certain amount of pro-IL-1 $\beta$ , which is consistent with a previous report (**Figures 3C,D**) (32). The expression of pro-IL-1 $\beta$  was increased in cells incubated with ATP for 12 or 24 h (**Figures 3C,D**). In addition, nSP50 induced more pro-IL-1 $\beta$  compared with the other silica particles after incubation for 24 h (**Figures 3C,D**). This induction of pro-IL-1 $\beta$  further confirms that a positive feedback loop for IL-1 $\beta$  is created in nSP50-treated cells (**Figure 2A**, 24 h).

## Relationship between Cellular Uptake and the Size-Specific Pro-inflammatory Effect of Silica Particles

It is well known that endocytosis of particulate matter triggers the pro-inflammatory responses. We, therefore, evaluated whether the size-specific pro-inflammatory effect of silica particles was endocytosis dependent. Blocking actin-dependent endocytosis with cytochalasin D, a potent inhibitor of actin polymerization, completely suppressed the induction of IL-1 $\beta$  in the silica particle- or crystalline silica-treated cells (**Figure 4A**). This result suggests that the induction of IL-1 $\beta$  by the silica particles or crystalline silica was dependent on actin-dependent endocytosis. Therefore, we hypothesized that the size-specific pro-inflammatory effects of the silica particles were a result of greater uptake of nSP50 than of the other sizes of silica particles. We, therefore, quantitatively measured by means of ICP-AES the amount of silicon inside cells exposed to the silica particles. A time-dependent increase in the uptake of silica particles was observed in all of the silica particle-treated cells (**Figure 4B**). The greatest concentration of silicon was found in the cells treated with mSP1000, whereas

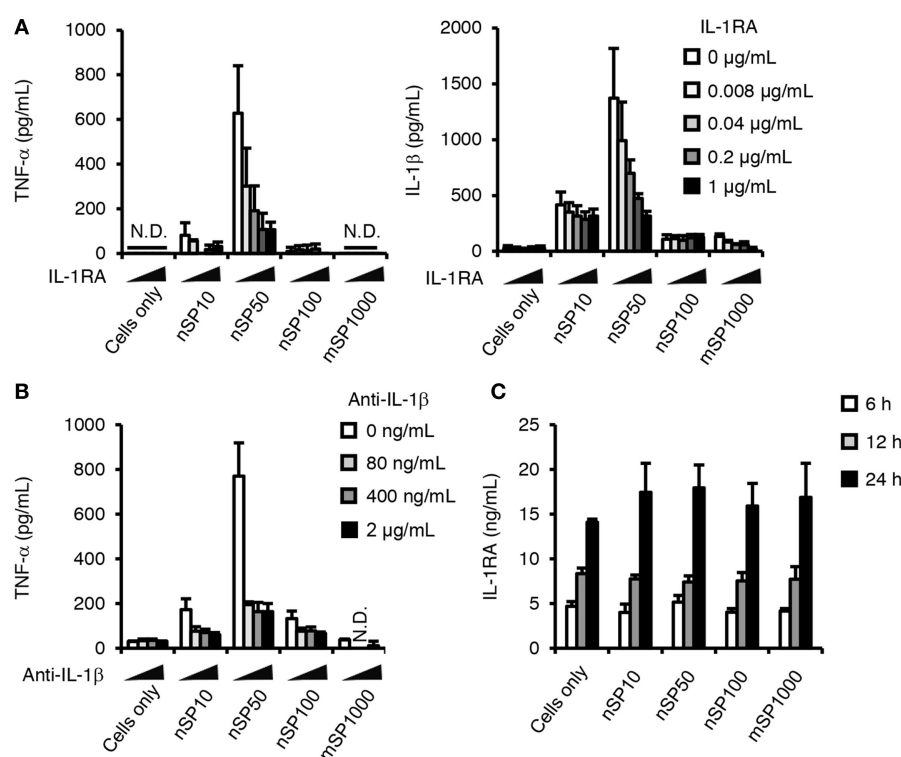


**FIGURE 2 | Role of interleukin (IL)-1 $\beta$  in the pro-inflammatory effects of silica particles.** Phorbol 12-myristate 13-acetate-differentiated THP-1 cells were incubated with IL-1 receptor antagonist (IL-1RA) **(A)** or anti-IL-1 $\beta$  **(B)** 30 min before the addition of silica particles (50  $\mu$ g/mL). After incubation for 24 h, the concentration of IL-1 $\beta$  **(A,B)** and tumor necrosis factor (TNF)- $\alpha$  **(A)** in the culture supernatant was measured by ELISA. **(C)** Phorbol 12-myristate 13-acetate-differentiated THP-1 cells were incubated with silica particles (50  $\mu$ g/mL) for 6, 12, or 24 h. After incubation, IL-1RA concentration in the culture supernatants was determined by ELISA. Data are presented as mean  $\pm$  SD ( $n = 4$  independent cultures/group). N.D., not detected.

the least was found in the cells treated with nSP50 (Figure 4B, left panel). By using the concentration of silicon in the cells to calculate the surface area and number of silica particles taken up, we found that nSP10-treated cells contained the greatest total particle surface area and number of silica particles (Figure 4B, center and right panels). Therefore, the induction of IL-1 $\beta$  by the silica particles was not correlated with the total mass of silicon, the total particle surface area, or the number of silica particles taken up by the cells, even though IL-1 $\beta$  secretion appeared to be completely dependent on the uptake of the silica particles *via* actin-dependent endocytosis. We, therefore, hypothesized that a specific mode of endocytosis that is only used for the uptake of silica particles in a specific size range was responsible for their observed size-specific pro-inflammatory effect.

Class A scavenging receptors (SR-A) are a group of receptors reported to be involved in the uptake into cells of environmental particles, including artificial nanoparticles such as amorphous silica nanoparticles (33, 34). Therefore, we examined the effect of poly I, a scavenging receptor antagonist, on the induction of IL-1 $\beta$ . Poly I treatment enhanced the induction of IL-1 $\beta$  secretion in nSP10-, mSP1000-, or crystalline silica-treated cells, but markedly suppressed it in nSP50- or nSP100-treated cells (Figure 5A). Since poly I is reported to have inflammatory potential as a ligand of toll-like receptor 3 (35), one explanation for this observation

in poly I-treated cells is that the uptake of nSP50 and nSP100 was blocked by poly I, the uptake of nSP10, mSP1000, and crystalline silica was completely independent of SR-A, and the inflammatory potential of poly I enhanced IL-1 $\beta$  by nSP10, mSP1000, and crystalline silica. To confirm this hypothesis, we examined the effect of neutralizing SR-As, namely SR-A1 or MARCO, which is reported to be endocytic receptors for particulate matter, on the size-specific pro-inflammatory effects of the silica particles (33, 34). Neutralization of SR-A1 suppressed the induction of IL-1 $\beta$  in nSP50- or nSP100-, but not in nSP10-, mSP1000-, or crystalline silica-treated cells (Figure 5B). Neutralization of MARCO did not affect the induction of IL-1 $\beta$  by the silica particles or crystalline silica (Figure 5C). Neutralization of SR-A1 also significantly reduced the uptake of nSP50 ( $P < 0.05$ ) and nSP100 ( $P < 0.01$ ), but not of nSP10, mSP1000, or crystalline silica (Figure 5D). Thus, it is likely that the size-specific pro-inflammatory effect of the silica particles was a result of SR-A1-mediated endocytosis of particles in a specific size range.

A remaining question is why exposure to nSP50 had a greater effect on the induction of IL-1 $\beta$  than exposure to nSP100 even though both appeared to be taken up *via* the same receptor. It is known that SR-A1 lacks enzymatic activity and intracellular signaling motifs, and that it induces Mer receptor tyrosine kinase (MerTK) signaling (36). Therefore, we evaluated the contribution

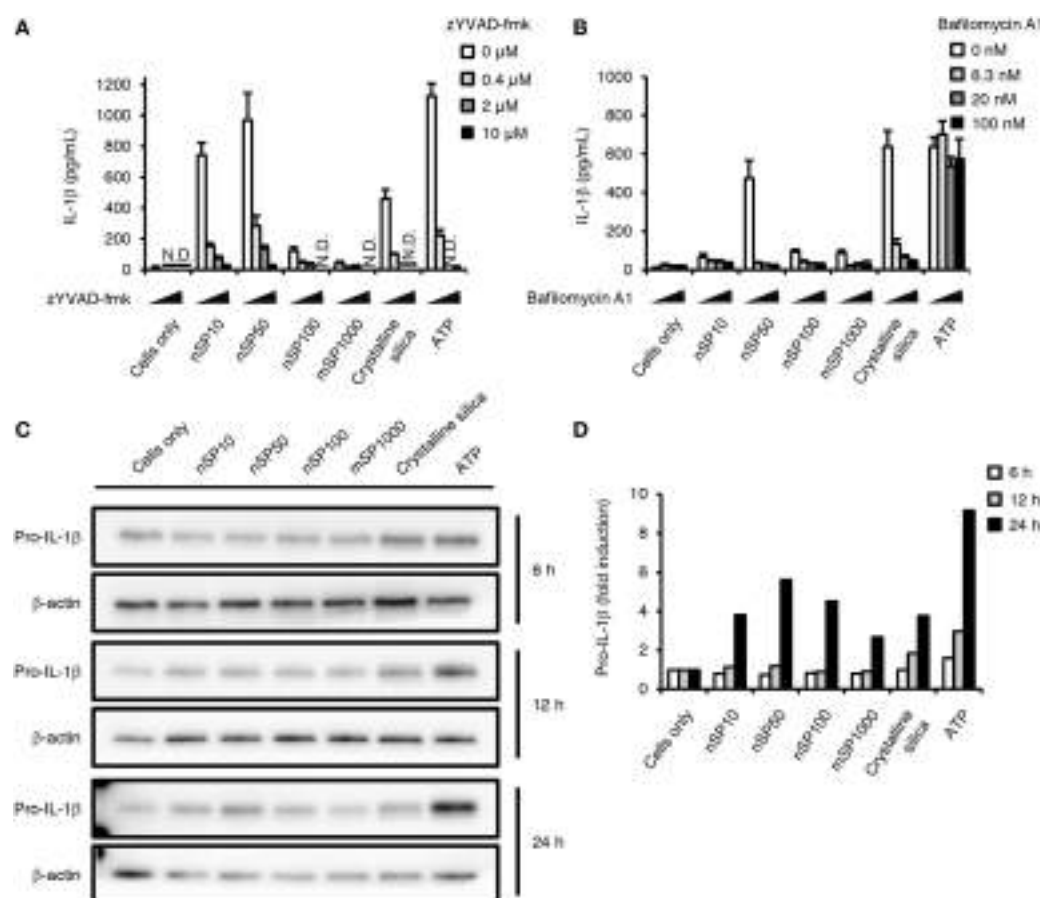


**FIGURE 3 | Effect of silica particles on caspase-1 activation and pro-IL-1 $\beta$  synthesis.** Phorbol 12-myristate 13-acetate-differentiated THP-1 cells were incubated with zYVAD-fmk (**A**) or baflomycin A1 (**B**) 30 min before the addition of silica particles (50  $\mu$ g/mL), crystalline silica (500  $\mu$ g/mL), or adenosine 5'-triphosphate disodium salt hydrate (ATP, 3 mM). Twenty-four hours after incubation, culture supernatants were collected and interleukin (IL)-1 $\beta$  secretion was determined by ELISA. Data are presented as mean  $\pm$  SD ( $n = 4$  independent cultures/group). N.D., not detected. (**C**) Phorbol 12-myristate 13-acetate-differentiated THP-1 cells were incubated with silica particles (50  $\mu$ g/mL), crystalline silica (500  $\mu$ g/mL), or ATP (3 mM) for 6, 12, or 24 h, and pro-IL-1 $\beta$  in the cells was analyzed by means of western blotting. (**D**) The densities of the bands of pro-IL-1 $\beta$  in (**C**) were quantified by using the ImageJ software (version 1.46r, National Institutes of Health). The values of pro-IL-1 $\beta$  were normalized to that of  $\beta$ -actin. Fold induction is relative to the cells only group.

of MerTK to the induction of IL-1 $\beta$  by nSP50 or nSP100 by using UNC569, an inhibitor of the phosphorylation of MerTK (37). Inhibition of MerTK signaling markedly suppressed the induction of IL-1 $\beta$  by nSP50, but not by nSP100 (**Figure 5E**). Consistent with the effect of neutralizing SR-A1, the induction of IL-1 $\beta$  by nSP10-, mSP1000-, or crystalline silica was not blocked by UNC569. Together, these results suggest that although the uptake of both nSP50 and nSP100 was dependent on SR-A1, only nSP50 appeared to induce MerTK signaling, which in turn produced a greater induction of IL-1 $\beta$ .

## DISCUSSION

The present results suggest that SR-A1-mediated endocytosis underlies silica particle-induced IL-1 $\beta$  secretion, and that the size-specific pro-inflammatory effects of silica particles are a result of the ligand size specificity of this SR-A1-mediated endocytosis. The

present results also suggest that silica particles with a diameter of 50 nm induced the strongest pro-inflammatory response. SR-A1 is known to mediate both pro- and anti-inflammatory responses due to its broad ligand specificity (38). However, it remains unknown how different ligands produce opposite responses *via* the same receptor. One report has demonstrated that SR-A1-mediated ligand endocytosis is mediated *via* clathrin-dependent and caveolae-dependent pathways, and that each endocytic mode has distinct functional consequences *via* different signaling cascades (39). Interestingly, clathrin-mediated and caveolae-mediated endocytosis are known to be limited to ligands with sizes of about 120 and 60 nm, respectively (40). Given these size limitations, in the present study, only nSP100 or smaller particles could be taken up *via* clathrin-mediated endocytosis, and only nSP50 (or possibly nSP70) or smaller silica particles could be taken up by caveolae-mediated endocytosis. Therefore, it is possible that the ligand size limit of each endocytic mode contributed to the particle size-specific effects. Further studies are required to

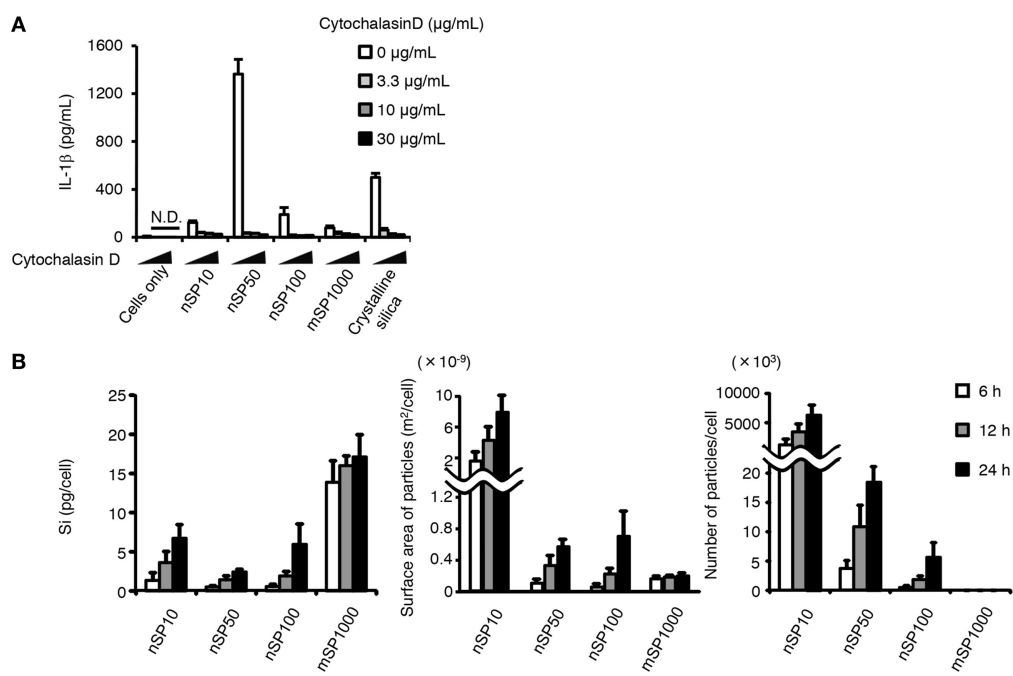


**FIGURE 4 | Relationship between uptake of silica particles and interleukin (IL)-1 $\beta$  secretion. (A)** Phorbol 12-myristate 13-acetate-differentiated THP-1 cells were incubated with cytochalasin D 30 min before the addition of silica particles (50  $\mu$ g/mL) or crystalline silica (500  $\mu$ g/mL). Twenty-four hours after incubation, culture supernatants were collected and IL-1 $\beta$  secretion was determined by ELISA. **(B)** Phorbol 12-myristate 13-acetate-differentiated THP-1 cells were incubated with silica particles (50  $\mu$ g/mL) for 6, 12, or 24 h. The amount of silicon in the cells was then determined by inductively coupled plasma atomic emission spectrometry. Silicon uptake by the cells was calculated as the amount of silicon in silica particle-treated cells minus the amount of silicon in non-treated cells. The total particle surface area and number of particles taken up by cells was calculated from information provided in the manufacturer's data sheet for each type of silica particle. Data are presented as mean  $\pm$  SD ( $n = 4$  independent cultures/group). N.D., not detected.

elucidate the relationship between each endocytic mode of SR-A and the activation of MerTK, which in turn produced the greater pro-inflammatory effects.

The results of the present study also suggest that the uptake of nSP10 is independent of SR-A1-mediated endocytosis (Figure 5D). Small nanoparticles are suggested to be difficult to promote multivalent binding by the receptors and thus smaller nanoparticles dissociate from the receptors before being taken up by cells due to low binding avidity (18). Therefore, it is possible that low avidity of nSP10 to SR-A1 cause the independency of SR-A1-mediated endocytosis. In addition, for silica particles to be ligands of SR-A1 they must be anionic in some extent; therefore, the number of silanol groups on the surface of silica particles will determine whether or not they are ligands of SR-A1. Since, the concentration of silanol groups on the surface of silica nanoparticles increases as particle size decreases (41), the ability of the silica particles to bind to SR-A1 must be changed dependent on the size. Thus it is also possible that nSP10 is not a ligand of SR-A1 due to the too much concentration of silanol groups.

The present results suggest that nSP50-mediated MerTK signaling increased the induction of IL-1 $\beta$ , although MerTK signaling itself is often discussed in an anti-inflammatory, immunosuppressive context mainly due to its relationship to the uptake of apoptotic cells by macrophages (42, 43). It has been reported that MerTK activation leads to inhibition of the mTOR pathway

and SR-A1-mediated activation of macrophages (44). Inhibition of the mTOR pathway enhances the effects of pro-inflammatory cytokines via NF- $\kappa$ B in phagocytic cells after bacterial stimulation (45) and of caspase-1 during endotoxin-mediated shock (46). In addition, phagocytosis of autophagic dying cells is reported to activate the NLRP3 inflammasome rather than inhibit immune reactions (47). Thus, in our model, MerTK signaling may induce pro-IL-1 $\beta$  and caspase-1 activation, which in turn increases silica particle-induced IL-1 $\beta$  secretion. Further studies are required to determine how MerTK signaling led to the inflammatory state in our model and what phenotype the size-specific effects of silica particles result in *in vivo*.

In previous studies, we observed greater induction of IL-1 $\beta$  in THP-1 cells treated with mSP1000 than in those treated with smaller particles (i.e., nSP30, nSP50, nSP70, mSP300, and mSP1000), although higher concentrations of silica particles were used than in the present study (i.e., 100  $\mu$ g/mL; 6 h incubation) (48). However, under the present low-cytotoxic conditions, treatment with mSP1000 induced little IL-1 $\beta$ , even after incubation for 24 h (Figure 1). Furthermore, under the present conditions, IL-1 $\beta$  was detected only at 24 h, irrespective of which silica particle the cells were exposed to. Another group has reported that exposure to high concentrations (125–500  $\mu$ g/mL) of silica nanoparticles with a diameter of 15 nm induced IL-1 $\beta$  after incubation for 6 h, and that active ATP release was the underlying mechanism

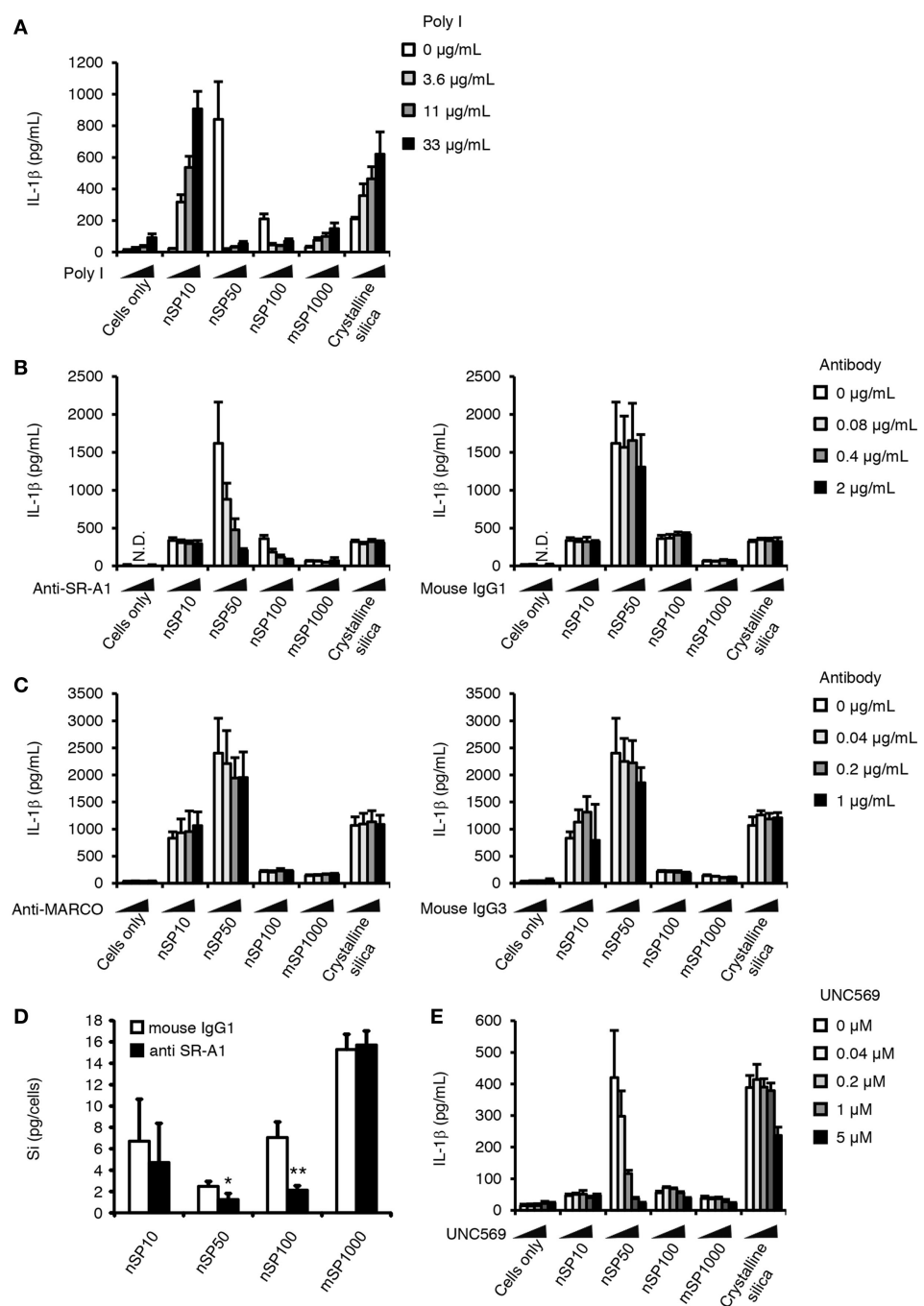


**FIGURE 5 |** Role of scavenger receptor (SR)-A1 and Mer receptor tyrosine kinase (MerTK) in the size-specific pro-inflammatory effects of silica particles. Phorbol 12-myristate 13-acetate-differentiated THP-1 cells were incubated with poly I (A), anti-SR-A1 or its isotype control (mouse IgG1) (B,D),

anti-MARCO antibody or its isotype control (mouse IgG3) (C), or UNC569 (a specific inhibitor of MerTK) (E) 30 min before the addition of silica particles (50 µg/mL) or crystalline silica (500 µg/mL). (A–C,E) Twenty-four hours after incubation, culture supernatants were collected and the concentration of interleukin (IL)-1β was determined by ELISA. (D) The amount of silicon in the cells was determined by inductively coupled plasma atomic emission spectrometry. Silicon uptake by the cells was calculated as the amount of silicon in treated cells minus the amount of silicon in non-treated cells. Data are presented as mean ± SD ( $n = 4$  independent cultures/group). \* $P < 0.05$ , \*\* $P < 0.01$  versus isotype control group. N.D., not detected.

(26). Interestingly, larger silica particles have also been shown to produce greater IL-1 $\beta$  induction (4) that is consistent with the results of our previous study, where we used high doses of silica

particles (48). Therefore, it is possible that larger silica particles induce greater production of IL-1 $\beta$  than do smaller silica particles under high-dose (i.e., high-stress) conditions via an active ATP

release mechanism. Since active ATP release has been shown to be the mechanism underlying the induction of IL-1 $\beta$  by other particles (e.g., uric acid, crystalline silica, alum) (Figure S2 in Supplementary Material, 6 h incubation) (49), it may have evolved to enable cells to rapidly secrete IL-1 $\beta$ . Therefore, it is likely that there are two different mechanisms underlying the induction of IL-1 $\beta$  by silica particles that are activated only during exposure to specific concentrations of silica particles. Further studies are required to elucidate whether the slower SR-A1-mediated IL-1 $\beta$  secretion observed in the present study involves active ATP release.

Scavenger receptors are a potentially useful target for vaccines for vaccine development (50, 51). Although elucidation of the relationship between the SR-A1-mediated size-specific effects of nanoparticles and adjuvanticity is required, optimizing the size of the nanoparticles may be a useful way to maximize the effects of nanoparticle-mediated vaccines. However, the size-specific effects of nanoparticles mean that it is difficult to reliably predict the safety of nanoparticles and so individual safety assessments will likely be required for each new nanoparticle-based product. It is, therefore, important to improve our understanding of the size-specific effects of nanoparticles.

The results of the present study suggest that SR-A1-mediated uptake of nanoparticles led to a size-specific inflammatory response in THP-1 cells. Since nanoparticles also have size-specific effects in non-phagocytic cells (17–19), there are likely additional underlying mechanisms in these cells. Further studies to examine the effects of silica and other nanoparticles on a variety of cell types would improve our understanding of the size-specific effects of nanoparticles. In the present study, nanoparticles with a diameter of around 50 nm were found to have the greatest pro-inflammatory effects, and the size-specific effects of nanoparticles of this size are well reported in the literature. Therefore, further

## REFERENCES

- Bachmann MF, Jennings GT. Vaccine delivery: a matter of size, geometry, kinetics and molecular patterns. *Nat Rev Immunol* (2010) 10(11):787–96. doi:10.1038/nri2868
- Muthu MS, Mei L, Feng SS. Nanotheranostics: advanced nanomedicine for the integration of diagnosis and therapy. *Nanomedicine (Lond)* (2014) 9(9):1277–80. doi:10.2217/nmm.14.83
- Tong R, Kohane DS. New strategies in cancer nanomedicine. *Annu Rev Pharmacol Toxicol* (2016) 56:41–57. doi:10.1146/annurev-pharmtox-010715-103456
- Yazdi AS, Guarda G, Riteau N, Drexler SK, Tardivel A, Couillin I, et al. Nanoparticles activate the NLR pyrin domain containing 3 (Nlrp3) inflammasome and cause pulmonary inflammation through release of IL-1 $\alpha$  and IL-1 $\beta$ . *Proc Natl Acad Sci U S A* (2010) 107(45):19449–54. doi:10.1073/pnas.1008155107
- Mitchell LA, Lauer FT, Burchiel SW, McDonald JD. Mechanisms for how inhaled multiwalled carbon nanotubes suppress systemic immune function in mice. *Nat Nanotechnol* (2009) 4(7):451–6. doi:10.1038/nnano.2009.151
- Hirai T, Yoshioka Y, Takahashi H, Ichihashi K, Ueda A, Mori T, et al. Cutaneous exposure to agglomerates of silica nanoparticles and allergen results in IgE-biased immune response and increased sensitivity to anaphylaxis in mice. *Part Fibre Toxicol* (2015) 12:16. doi:10.1186/s12989-015-0095-3
- Hirai T, Yoshioka Y, Izumi N, Ichihashi K, Handa T, Nishijima N, et al. Metal nanoparticles in the presence of lipopolysaccharides trigger the onset of metal allergy in mice. *Nat Nanotechnol* (2016) 11(9):808–16. doi:10.1038/nnano.2016.88
- Hwang SR, Kim K. Nano-enabled delivery systems across the blood-brain barrier. *Arch Pharm Res* (2014) 37(1):24–30. doi:10.1007/s12272-013-0272-6
- Yamashita K, Yoshioka Y, Higashisaka K, Mimura K, Morishita Y, Nozaki M, et al. Silica and titanium dioxide nanoparticles cause pregnancy complications in mice. *Nat Nanotechnol* (2011) 6(5):321–8. doi:10.1038/nnano.2011.41
- Morishita Y, Yoshioka Y, Takimura Y, Shimizu Y, Namba Y, Nojiri N, et al. Distribution of silver nanoparticles to breast milk and their biological effects on breast-fed offspring mice. *ACS Nano* (2016) 10(9):8180–91. doi:10.1021/acsnano.6b01782
- Huo S, Jin S, Ma X, Xue X, Yang K, Kumar A, et al. Ultrasmall gold nanoparticles as carriers for nucleus-based gene therapy due to size-dependent nuclear entry. *ACS Nano* (2014) 8(6):5852–62. doi:10.1021/nn5008572
- Oberdorster G, Maynard A, Donaldson K, Castranova V, Fitzpatrick J, Ausman K, et al. Principles for characterizing the potential human health effects from exposure to nanomaterials: elements of a screening strategy. *Part Fibre Toxicol* (2005) 2:8. doi:10.1186/1743-8977-2-8
- Park MV, Neigh AM, Vermeulen JP, de la Fonteyne LJ, Verharen HW, Briede JJ, et al. The effect of particle size on the cytotoxicity, inflammation, developmental toxicity and genotoxicity of silver nanoparticles. *Biomaterials* (2011) 32(36):9810–7. doi:10.1016/j.biomaterials.2011.08.085
- Hirai T, Yoshikawa T, Nabeshi H, Yoshida T, Tochigi S, Ichihashi K, et al. Amorphous silica nanoparticles size-dependently aggravate atopic dermatitis-like skin lesions following an intradermal injection. *Part Fibre Toxicol* (2012) 9:3. doi:10.1186/1743-8977-9-3

examination not only of the size-specific effects of nanoparticles but also of the possibility that 50 nm is a size that has special implications in biological systems in general is needed.

## AUTHOR CONTRIBUTIONS

NN, TH, and YY designed the experiments and interpreted the results. NN, TH, KM, and MA performed the experiments and analyzed the data. NN, TH, and YY wrote the manuscript; EK, KI, and KH provided technical support and conceptual advice. YT supervised the project. All authors have read, discussed, and approved the final manuscript.

## ACKNOWLEDGMENTS

The authors thank Ms. Kaori Murayama, Ms. Risako Nagahashi, and Ms. Nobuyo Hashino for supporting them in the lab.

## FUNDING

This study was supported by Grants-in-Aid for Scientific Research from the Japan Society for the Promotion of Science (no. JP16K01437 to KH, no. JP25136712 to YY, no. JP12J00488 to TH, no. JP26242055 to YT, and no. JP15K12540 to YT); by a Health Labour Sciences Research Grant from the Ministry of Health, Labour, and Welfare of Japan (no. H25-kagaku-ippan-005 to YT); and by the Uehara Memorial Foundation (to YY).

## SUPPLEMENTARY MATERIAL

The Supplementary Material for this article can be found online at <http://journal.frontiersin.org/article/10.3389/fimmu.2017.00379/full#supplementary-material>.

15. Akhavan O, Ghaderi E, Akhavan A. Size-dependent genotoxicity of graphene nanoplatelets in human stem cells. *Biomaterials* (2012) 33(32):8017–25. doi:10.1016/j.biomaterials.2012.07.040
16. Yoshida T, Yoshioka Y, Tochigi S, Hirai T, Uji M, Ichihashi K, et al. Intranasal exposure to amorphous nanosilica particles could activate intrinsic coagulation cascade and platelets in mice. *Part Fibre Toxicol* (2013) 10:41. doi:10.1186/1743-8977-10-41
17. Chithrani BD, Ghazani AA, Chan WC. Determining the size and shape dependence of gold nanoparticle uptake into mammalian cells. *Nano Lett* (2006) 6(4):662–8. doi:10.1021/nl052396o
18. Jiang W, Kim BY, Rutka JT, Chan WC. Nanoparticle-mediated cellular response is size-dependent. *Nat Nanotechnol* (2008) 3(3):145–50. doi:10.1038/nnano.2008.30
19. Lu F, Wu SH, Hung Y, Mou CY. Size effect on cell uptake in well-suspended, uniform mesoporous silica nanoparticles. *Small* (2009) 5(12):1408–13. doi:10.1002/smll.200900005
20. Oh WK, Kim S, Choi M, Kim C, Jeong YS, Cho BR, et al. Cellular uptake, cytotoxicity, and innate immune response of silica-titania hollow nanoparticles based on size and surface functionality. *ACS Nano* (2010) 4(9):5301–13. doi:10.1021/nn100561e
21. Handa T, Hirai T, Izumi N, Eto S, Tsunoda S, Nagano K, et al. Identifying a size-specific hazard of silica nanoparticles after intravenous administration and its relationship to the other hazards that have negative correlations with the particle size in mice. *Nanotechnology* (2017) 28(13):135101. doi:10.1088/1361-6528/aa5d7c
22. Fifis T, Gamvrellis A, Crimeen-Irwin B, Pietersz GA, Li J, Mottram PL, et al. Size-dependent immunogenicity: therapeutic and protective properties of nano-vaccines against tumors. *J Immunol* (2004) 173(5):3148–54. doi:10.4049/jimmunol.173.5.3148
23. Haque S, Whittaker MR, McIntosh MP, Pouton CW, Kaminskas LM. Disposition and safety of inhaled biodegradable nanomedicines: opportunities and challenges. *Nanomedicine* (2016) 12(6):1703–24. doi:10.1016/j.nano.2016.03.002
24. Lunov O, Syrovets T, Loos C, Nienhaus GU, Mailander V, Landfester K, et al. Amino-functionalized polystyrene nanoparticles activate the NLRP3 inflammasome in human macrophages. *ACS Nano* (2011) 5(12):9648–57. doi:10.1021/nn203596e
25. Simard JC, Vallieres F, de Liz R, Lavastre V, Girard D. Silver nanoparticles induce degradation of the endoplasmic reticulum stress sensor activating transcription factor-6 leading to activation of the NLRP-3 inflammasome. *J Biol Chem* (2015) 290(9):5926–39. doi:10.1074/jbc.M114.610899
26. Baron L, Gombault A, Fanny M, Villeret B, Savigny F, Guillou N, et al. The NLRP3 inflammasome is activated by nanoparticles through ATP, ADP and adenosine. *Cell Death Dis* (2015) 6:e1629. doi:10.1038/cddis.2014.576
27. Baqir M, Chen CZ, Martin RJ, Thaikoothathil J, Case SR, Minor MN, et al. Cigarette smoke decreases MARCO expression in macrophages: implication in *Mycoplasma pneumoniae* infection. *Respir Med* (2008) 102(11):1604–10. doi:10.1016/j.rmed.2008.05.002
28. Nabeshi H, Yoshikawa T, Matsuyama K, Nakazato Y, Matsuo K, Arimori A, et al. Systemic distribution, nuclear entry and cytotoxicity of amorphous nanosilica following topical application. *Biomaterials* (2011) 32(11):2713–24. doi:10.1016/j.biomaterials.2010.12.042
29. Martinon F, Petrilli V, Mayor A, Tardivel A, Tschopp J. Gout-associated uric acid crystals activate the NALP3 inflammasome. *Nature* (2006) 440(7081):237–41. doi:10.1038/nature04516
30. Jo EK, Kim JK, Shin DM, Sasakawa C. Molecular mechanisms regulating NLRP3 inflammasome activation. *Cell Mol Immunol* (2016) 13(2):148–59. doi:10.1038/cmi.2015.95
31. Munoz-Planillo R, Kuffa P, Martinez-Colon G, Smith BL, Rajendiran TM, Nunez G. K(+) efflux is the common trigger of NLRP3 inflammasome activation by bacterial toxins and particulate matter. *Immunity* (2013) 38(6):1142–53. doi:10.1016/j.immuni.2013.05.016
32. Hornung V, Bauernfeind F, Halle A, Samstad EO, Kono H, Rock KL, et al. Silica crystals and aluminum salts activate the NALP3 inflammasome through phagosomal destabilization. *Nat Immunol* (2008) 9(8):847–56. doi:10.1038/ni.1631
33. Hamilton RF Jr, Thakur SA, Mayfair JK, Holian A. MARCO mediates silica uptake and toxicity in alveolar macrophages from C57BL/6 mice. *J Biol Chem* (2006) 281(45):34218–26. doi:10.1074/jbc.M605229200
34. Orr GA, Chrisler WB, Cassens KJ, Tan R, Tarasevich BJ, Markillie LM, et al. Cellular recognition and trafficking of amorphous silica nanoparticles by macrophage scavenger receptor A. *Nanotoxicology* (2011) 5(3):296–311. doi:10.3109/17435390.2010.513836
35. Mukhopadhyay S, Varin A, Chen Y, Liu B, Tryggvason K, Gordon S, SR-A/MARCO-mediated ligand delivery enhances intracellular TLR and NLR function, but ligand scavenging from cell surface limits TLR4 response to pathogens. *Blood* (2011) 117(4):1319–28. doi:10.1182/blood-2010-03-276733
36. Todt JC, Hu B, Curtis JL. The scavenger receptor SR-A I/II (CD204) signals via the receptor tyrosine kinase Mertk during apoptotic cell uptake by murine macrophages. *J Leukoc Biol* (2008) 84(2):510–8. doi:10.1189/jlb.0307135
37. Liu J, Yang C, Simpson C, Deryckere D, Van Deusen A, Miley MJ, et al. Discovery of novel small molecule Mer kinase inhibitors for the treatment of pediatric acute lymphoblastic leukemia. *ACS Med Chem Lett* (2012) 3(2):129–34. doi:10.1021/ml200239k
38. Canton J, Neculai D, Grinstein S. Scavenger receptors in homeostasis and immunity. *Nat Rev Immunol* (2013) 13(9):621–34. doi:10.1038/nri3515
39. Zhu XD, Zhuang Y, Ben JJ, Qian LL, Huang HP, Bai H, et al. Caveolae-dependent endocytosis is required for class A macrophage scavenger receptor-mediated apoptosis in macrophages. *J Biol Chem* (2011) 286(10):8231–9. doi:10.1074/jbc.M110.145888
40. Petros RA, DeSimone JM. Strategies in the design of nanoparticles for therapeutic applications. *Nat Rev Drug Discov* (2010) 9(8):615–27. doi:10.1038/nrd3591
41. Rahmana IA, Vejayakumarana P, Sipauta CS, Ismaila J, Chee CK. Size-dependent physicochemical and optical properties of silica nanoparticles. *Mater Chem Phys* (2009) 114:328–32. doi:10.1016/j.matchemphys.2008.09.068
42. Zizzo G, Hilliard BA, Monestier M, Cohen PL. Efficient clearance of early apoptotic cells by human macrophages requires M2c polarization and MerTK induction. *J Immunol* (2012) 189(7):3508–20. doi:10.4049/jimmunol.1200662
43. Graham DK, DeRyckere D, Davies KD, Earp HS. The TAM family: phosphatidylserine sensing receptor tyrosine kinases gone awry in cancer. *Nat Rev Cancer* (2014) 14(12):769–85. doi:10.1038/nrc3847
44. Labonte AC, Sung SJ, Jennelle LT, Dandekar AP, Hahn YS. Expression of scavenger receptor-AI promotes alternative activation of murine macrophages to limit hepatic inflammation and fibrosis. *Hepatology* (2017) 65(1):32–43. doi:10.1002/hep.28873
45. Weichhart T, Costantino G, Poglitsch M, Rosner M, Zeyda M, Stuhlmeier KM, et al. The TSC-mTOR signaling pathway regulates the innate inflammatory response. *Immunity* (2008) 29(4):565–77. doi:10.1016/j.immuni.2008.08.012
46. Schmitz F, Heit A, Dreher S, Eisenacher K, Mages J, Haas T, et al. Mammalian target of rapamycin (mTOR) orchestrates the defense program of innate immune cells. *Eur J Immunol* (2008) 38(11):2981–92. doi:10.1002/eji.200838761
47. Ayna G, Krysko DV, Kaczmarek A, Petrovski G, Vandebaele P, Fesus L. ATP release from dying autophagic cells and their phagocytosis are crucial for inflammasome activation in macrophages. *PLoS One* (2012) 7(6):e40069. doi:10.1371/journal.pone.0040069
48. Morishige T, Yoshioka Y, Inakura H, Tanabe A, Yao X, Narimatsu S, et al. The effect of surface modification of amorphous silica particles on NLRP3 inflammasome mediated IL-1beta production, ROS production and endosomal rupture. *Biomaterials* (2010) 31(26):6833–42. doi:10.1016/j.biomaterials.2010.05.036
49. Riteau N, Baron L, Villeret B, Guillou N, Savigny F, Ryffel B, et al. ATP release and purinergic signaling: a common pathway for particle-mediated inflammasome activation. *Cell Death Dis* (2012) 3:e403. doi:10.1038/cddis.2012.144
50. McNulty S, Colaco CA, Blandford LE, Bailey CR, Baschieri S, Todryk S. Heat-shock proteins as dendritic cell-targeting vaccines – getting warmer. *Immunology* (2013) 139(4):407–15. doi:10.1111/immm.12104

51. Apostolopoulos V, Thalhammer T, Tzakos AG, Stojanovska L. Targeting antigens to dendritic cell receptors for vaccine development. *J Drug Deliv* (2013) 2013:869718. doi:10.1155/2013/869718

**Conflict of Interest Statement:** YY is employed by the Research Foundation for Microbial Diseases of Osaka University. All other authors declare no competing financial interests.

Copyright © 2017 Nishijima, Hirai, Misato, Aoyama, Kuroda, Ishii, Higashisaka, Yoshioka and Tsutsumi. This is an open-access article distributed under the terms of the Creative Commons Attribution License (CC BY). The use, distribution or reproduction in other forums is permitted, provided the original author(s) or licensor are credited and that the original publication in this journal is cited, in accordance with accepted academic practice. No use, distribution or reproduction is permitted which does not comply with these terms.



# Induction of Innate Immune Memory by Engineered Nanoparticles: A Hypothesis That May Become True

**Paola Italiani\*** and **Diana Boraschi**

*Institute of Protein Biochemistry, National Research Council, Napoli, Italy*

## OPEN ACCESS

**Edited by:**

Manuela Mengozzi,  
Brighton and Sussex Medical School,  
United Kingdom

**Reviewed by:**

Marc Pallardy,  
Université Paris-Sud, France  
Seyed Moein Moghimi,  
Durham University,  
United Kingdom

**\*Correspondence:**

Paola Italiani  
*italianipaola@gmail.com*,  
*p.italiani@ibp.cnr.it*

**Specialty section:**

This article was submitted  
to Inflammation,  
a section of the journal  
*Frontiers in Immunology*

**Received:** 31 March 2017

**Accepted:** 09 June 2017

**Published:** 26 June 2017

**Citation:**

Italiani P and Boraschi D (2017)  
*Induction of Innate Immune Memory  
by Engineered Nanoparticles:  
A Hypothesis That May  
Become True.*  
*Front. Immunol.* 8:734.  
doi: 10.3389/fimmu.2017.00734

Innate immune memory is the capacity of cells of the innate immune system, such as monocytes and macrophages, to react differently to an inflammatory or infectious challenge if previously exposed to the same or to another agent. Innate immune memory is a protective mechanism, based on epigenetic reprogramming, that ensures effective protection while limiting side effects of tissue damage, by controlling innate/inflammatory responses to repeated stimulations. Engineered nanoparticles (NPs) are novel challenges for our innate immune system, and their ability to induce inflammatory activation, thereby posing health risks, is currently being investigated with controversial results. Besides their putative direct inflammation-inducing effects, we hypothesize that engineered NPs may induce innate memory based on their capacity to induce epigenetic modulation of gene expression. Preliminary results using non-toxic non-inflammatory gold NPs show that in fact NPs can induce memory by modulating in either positive or negative fashion the inflammatory activation of human monocytes to a subsequent bacterial challenge. The possibility of shaping innate/inflammatory reactivity with NPs could open the way to future novel approaches of preventive and therapeutic immunomodulation.

**Keywords:** innate memory, monocytes, macrophages, engineered nanoparticles, inflammation

## INTRODUCTION

The ability of the body of developing immune reactions is strongly influenced by the environment. During its lifetime, each person is exposed to a great number and types of environmental and infectious cues, which shape the immune system in terms of type and extent of reaction. Consequently, the immune system of each individual is unique as it is the result of the individual experience. A recent study based on systems-level analysis of healthy twins has shown that different functional units of immunity (cytokines, chemokines, growth factors, immune cells subsets, and cellular responses to cytokines) vary across individuals primarily as a consequence of extrinsic non-heritable factors (1). This supports the notion that the immune system is shaped by the environmental events encountered during life (in particular microbes) rather than genetics. Environmental factors exert a cumulative influence that overshadows the influence of heritable traits with age (1). The footprints of these exposures are preserved in the immune cells, and each immune system can be considered as a kind of “memory snapshot/fingerprinting.” Consequently, the infection history of a person could explain the different individual patterns of immunodominance and protection and why some individuals mount productive immune responses to vaccines and pathogens and others do not. Until recently, the common belief was that adaptive immunity was the only type of immunity able to maintain a memory of previous infections. Indeed, in every immunology textbook we can find

that memory is one of the hallmarks distinguishing adaptive from innate immunity. However, recent evidence has revived the old concept of innate immune memory, well-known in plants and invertebrates and also observed in mice.

Innate memory is the capacity of innate immune cells such as monocytes and macrophages to mount, upon a second challenge, a lower or higher non-specific response (tolerance vs. trained immunity) compared to the response of naïve cells (2). The innate response is usually measured in terms of production of inflammatory effector molecules (e.g., cytokines and chemokines). Thus, within each individual, innate immune cells such as monocytes are never the same and their reactivity depends on their immunological history of previous encounters and “the tracks that they left.” As long as they live, monocytes may display an altered responsiveness due to previous encounters not only with viral or bacterial infections but also following diseases and exposure to food/dietary components, pollutants, and nanoparticles (NPs).

Engineered NPs have entered the human environment in recent years because of their presence in many common products as additives (e.g., toothpaste, cosmetics, candies, and cigarettes) and in public spaces or workplaces as pollutants. The rapid development of nanotechnologies has also provided new opportunities in medicine mainly through the use of NPs for diagnostic and therapeutic purposes (biomedical imaging, drug delivery, and targeting). A lot of questions are still outstanding regarding the risks associated with exposure to NPs. Monocytes and macrophages are the first line of defense in the innate immune response to foreign materials, by phagocytosing and destroying the dangerous agents and in addition by triggering an inflammatory defensive reaction. An inflammatory reaction may, however, become pathological and lead to tissue destruction if it is excessive and prolonged (3). Over the last decade, a great deal of attention has been devoted to the study of the capacity of NPs to induce inflammation, taken as a sign of pathological risk. The inflammation-inducing effects of NPs are still controversial because of the many problems and challenges in the development and validation of assays that could reliably assess the *bona fide* NP effects, without interference and artifacts due to technical or contamination problems (4). Thus, many NPs do not show direct capacity of triggering an inflammatory reaction in human monocytes in culture when the interaction occurs in real life-mimicking conditions of dose and exposure, and if the NPs are rigorously free of contaminating LPS (bacterial endotoxin) (5, 6). Even if unable to directly initiate an inflammatory reaction, the exposure to NPs might interfere with the effector functions of monocytes and macrophages, including their activation, their polarization, and (as we propose here) their memory. For instance, it has been observed that NPs can provoke morphological changes, proliferation alterations, toxicity, functional phenotype switching, and epigenetic reprogramming (7–11). To date, the epigenetic reprogramming is known to be the main mechanism underlying the capacity of innate immune cells to develop a memory. Here, we would like to discuss the possible influence of NPs on the development of innate memory, in other words if previous exposure to NPs can modulate the responses of monocytes and macrophages to subsequent infections or challenges (**Figure 1**).

## INNATE MEMORY AND UNDERLYING EPIGENETIC MECHANISMS

The immune system has evolved with the increased complexity of living organisms (innate immunity only in plants and invertebrates; innate plus adaptive immunity in vertebrates). More impressively, immunity developed in parallel with the evolution of microorganisms in an equilibrium in which the host develops tools for keeping the microorganisms at bay and avoid damage, and the pathogen devises mechanisms for escaping the host surveillance and ensure its own survival and growth (12). The ability of the adaptive immune system to recognizing different challenges is mainly due to the rearrangement of V(D)J gene segments, aimed to generating a vast array of different specific antibodies and receptors necessary for the recognition of virtually all non-self-molecules, which are then conserved by B and T memory cells throughout lifetime. As a consequence, one of the most potent weapons of adaptive immunity is to implement a faster and more potent defense response upon a second exposure to the same pathogen, due to the ability to “remember” a first encounter. This capacity to remember, considered a distinctive trait of adaptive immunity, can be, however, found also in vertebrate innate immunity, although with different characteristics. Innate memory is already well-known as the protective mechanism against reinfection in organisms lacking adaptive immunity, such as plants and invertebrates (13, 14). Thus, the dogma that innate immunity has no memory should be revised, as the capacity of memory has been described in innate cells belonging to both the lymphoid lineage, such as natural killer (NK) cells, and to myeloid cells such as monocytes and macrophages. For instance, upon human cytomegalovirus infection in mice and macaques, certain NK cell subpopulations display adaptive properties such as longevity, subset expansion, and altered functionality during a secondary response (15). The main differences between innate and adaptive immune memory are summarized in **Table 1**.

Focusing our attention on monocytes and macrophages, the innate immune memory appears as an increase (“trained immunity”) or a decrease (“tolerance”) of their functional program. Thus, primed monocytes or macrophages become more or less capable of producing inflammatory cytokines, as well as phagocytosing and killing microorganisms, in response to a second challenge. It is hypothesized that this altered functional state could persist for weeks to months, rather than years, after the elimination of the initial stimulus (16), although it might persist much longer in bone marrow niches. The main difference between innate and adaptive memory is that innate memory is non-specific. Although this could seem a limitation, it has the advantage of protecting against different kinds of inflammation-inducing challenges, not only microbes and the same microbes. To put it simply, primed monocytes can react or not following a secondary challenge, which can be the same or different from the primary stimulus, conferring a non-specific and broad protection.

The phenomenon of tolerance upon chronic or repeated exposure to microbial agents is well-known and represents a state of refractoriness to additional challenge with microbial molecules such as LPS (17, 18). Tolerance has also been identified as the hyporesponsiveness/immunosuppressive phenotype observed in late sepsis. Indeed, tolerance is viewed as a defense strategy

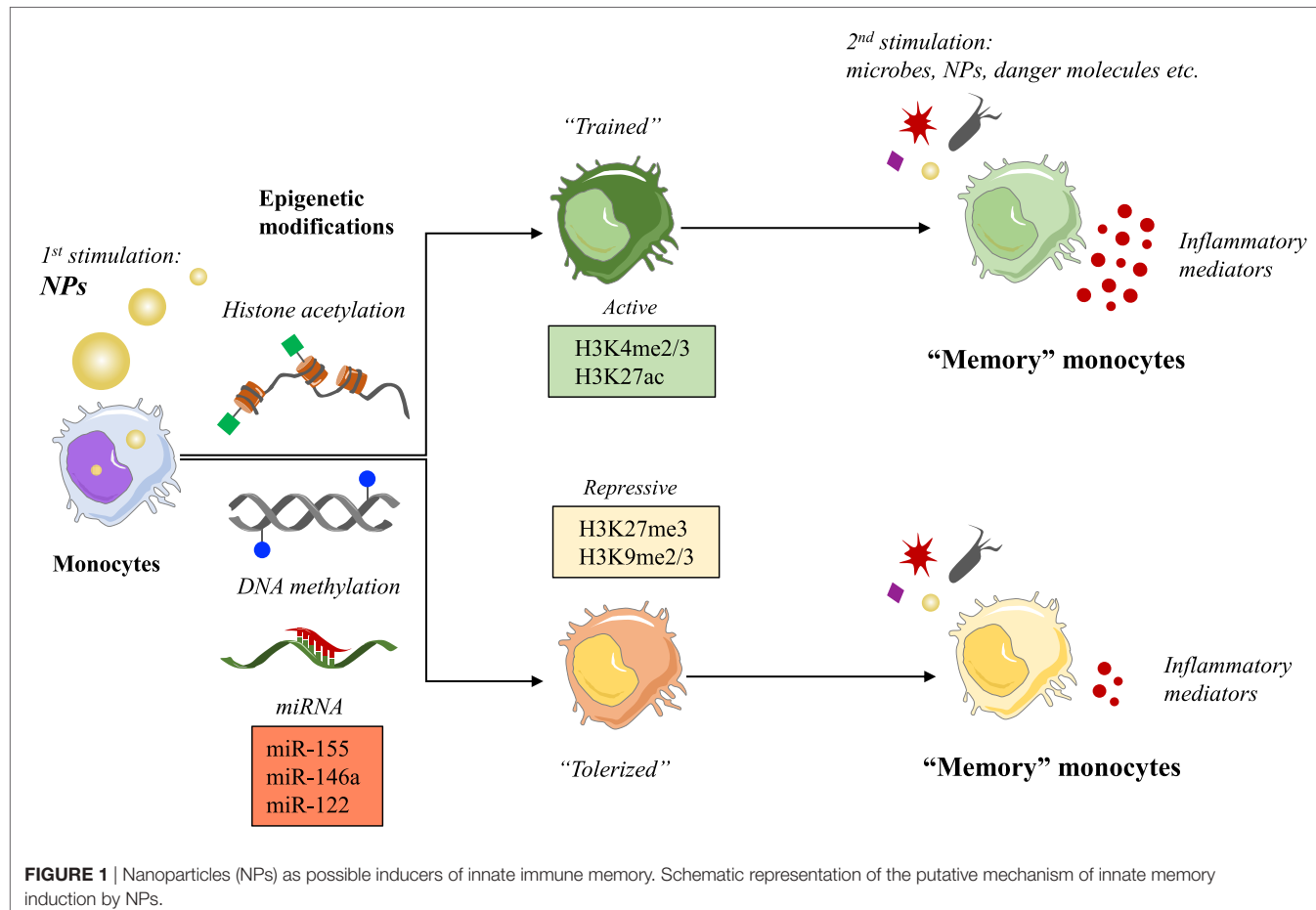


**TABLE 1 |** The main differences between innate and adaptive immune memory.

	Innate memory	Adaptive memory
Effector molecules	Cytokines	Antibodies
Mechanisms	Epigenetic changes (e.g., DNA methylation, histone acetylation)	Gene rearrangement (somatic recombination of gene segments)
Type of response	Rapid (same as primary response), either enhanced ("trained memory") or reduced ("tolerance")	Rapid (much more than primary response), enhanced/more potent
Specificity	Triggered by any molecule or stressful event (e.g., molecules shared by groups of related microbes or produced by damaged host cells, metabolic compounds, pollutants, etc.), upon a second exposure to the same or different agent/event	For a specific antigen, upon a second exposure to the same

to limit inflammation-caused tissue damage (19). Conversely, the newer concept of "trained immunity" arises from a number of epidemiological studies that suggest non-specific beneficial effects of vaccination beyond its target disease (20). For instance, one of the world's most administrated vaccines, the Bacille

Calmette–Guérin (BCG), protects not only against tuberculosis but it also has positive effects on neonatal sepsis and respiratory tract infections (21), and improves resistance and survival of infants (22). These observations have been confirmed by experimental studies in murine models lacking T and B lymphocytes, which proved that BCG vaccination has non-specific effects against pathogens other than mycobacteria, such as *Candida albicans*. In turn, administration of *C. albicans* β-glucan or from subjects vaccinated with BCG have increased capacity to produce inflammatory cytokines, as well as to phagocytose and kill microorganisms (16, 24).

Regarding the molecular mechanisms involved in the development of the innate memory, studies on Systemic Acquired Resistance in plants showed that epigenetic processes are responsible for the resistance to reinfection (13). Other studies have demonstrated that regulation of chromatin states is on the basis of the innate immune tolerance induced by LPS (25). Indeed, both tolerance and trained innate immunity in monocytes and macrophages are dependent on long-term epigenetic changes. These modifications involve both histone methylation and acetylation, such as H3K4 monomethylation and H3K27 acetylation induced by LPS (26, 27), and histone H3K4 trimethylation and H3K27

acetylation caused by  $\beta$ -glucan (24, 27). Moreover, it has been hypothesized that innate memory could involve the modulation of expression of “latent and *de novo*” enhancers, microRNAs, and/or long non-coding RNAs (28). All these epigenetic changes and molecular mechanisms promote higher transcription levels in several genes, such as pathogen recognition receptors, signaling molecules, and cytokines (24), in a short window of time. An accurate description of all these mechanisms and the role of cellular metabolites in shaping the epigenetic program of innate immune memory has been recently published in an excellent review (28).

## THE EFFECTS OF NPs ON THE EPIGENOME

Monocytes and macrophages are not only activated by microorganisms but they can react to any harmful stimulus by initiating an inflammatory reaction. Accordingly, all these agents might prime monocytes and macrophages and reprogram their reactivity against a subsequent stimulation, i.e., they can induce innate memory.

In the last few years, our immune system has become exposed to a new class of agents, i.e., the engineered nanomaterials, which have entered our life because of their successful use in many products, thanks to their physical and chemical properties (size, chemical composition, surface properties, solubility, shape, etc.). Apart from the advantages of such new materials, the possible detrimental effects of exposure to NPs are being actively investigated from a safety point of view. Being the innate immune system the first line of defense of the body, and monocytes and macrophages among the first cells which NPs interact with, assessing the outcomes of such interaction becomes a priority in order to avoid harmful effects that can damage tissues and organs of the body (induction of uncontrolled inflammation) both in the case of NPs for medical use and in the case of occasional or unintentional exposure. Also, knowing the ways of nanoimmune interaction can help us avoiding the immune-mediated rapid elimination of nanomedicines that are detected as possible dangers by the immune system. The consequences of the interaction between NPs and immune system have been extensively discussed (29). Here, we want to focus on the effects of NPs on the epigenome. It is known that the gene expression pattern of a cell is modulated (upregulated or silenced) by epigenetic changes, such as DNA methylation, post-translational modifications of histones, chromatin remodeling, and modulation of non-coding RNAs. Several NPs have shown the capacity of inducing epigenetic effects, which may alter gene expression and in the long run may lead to health risks. For instance, a decrease in global DNA methylation has been observed in human epidermal keratinocytes following exposure to SiO<sub>2</sub> NPs *in vitro* and in the lungs and blood of mice upon inhalation of multiwall carbon nanotubes (30, 31). Regarding the effect of NPs on histone post-translational modifications, little is known so far. A preliminary study showed that exposure to cadmium telluride quantum dots induced global H3 histone hypoacetylation and reduced gene transcription in a breast cancer cell line (32). In another study, silver NPs induced a decrease in methylation of H3K4me3 and H3K79me1 in mouse erythroleukemia cells, causing a reduction in hemoglobin levels (33). NPs can also affect ncRNAs.

The effects of NPs on miRNA expression have been observed both *in vivo* and *in vitro*. Inhaled surface-coated nanoTiO<sub>2</sub> and intravenous doses of silica NPs resulted in an enrichment of miRNA expression in mouse lung (miR-1, miR-49a, and miR-135b) and liver (miR-122), respectively (34, 35). *In vitro* exposure to gold NPs upregulated the expression of miR-155 in human fetal fibroblasts (36), and exposure of the human Jurkat T cell line to silver NPs altered the expression of 63 miRNAs (37). A high-throughput sequencing analysis of a mouse fibroblast cell line exposed to iron oxide, quantum dots, and carbon nanotubes resulted in widely dysregulated miRNA expression profiles depending on the characteristic of nanomaterials (38).

All the known effects of NPs on the epigenome have been recently reviewed in detail elsewhere (9–11). However, the consequences of such changes on cellular functions and the eventual impact on human health are far from being known.

## COULD NPs AFFECT/MODULATE THE INNATE IMMUNE MEMORY?

Since an epigenetic reprogramming is the major molecular mechanism underlying the establishment of innate memory, and the NP exposure could alter the epigenetic program in monocyte-like cell lines (39, 40), it is logical to hypothesize that NPs may be able to induce or modulate innate memory, and therefore, affect the capacity of innate cells to react to dangerous stimuli. The hypothesis that NPs can modulate innate memory adds a new perspective in the evaluation of nanoimmune interactions in terms of functional outputs, both from the point of view of safety and, most interestingly, for its possible medical exploitation in reprogramming innate memory in immunostimulatory and immunosuppressive strategies (vaccination, age- or disease-related immunosuppression, chronic inflammatory and degenerative diseases, etc.). As proof-of-concept, we have preliminarily assessed the role of gold (Au) NPs in the induction of innate memory in an *in vitro* system based on human primary monocytes. Monocytes were incubated with LPS or with endotoxin-free Au NPs for 24 h (priming), then rested for 6 days in the absence of stimuli, and eventually restimulated (challenge) with the same stimulus or cross-stimulated with the other agent. **Figure 2** shows preliminary data obtained by measuring the production of the inflammatory cytokine TNF- $\alpha$  by monocytes from two individual donors. It is important to say (not shown in the figure) that in response to the first stimulation LPS induced a significant response while Au NPs were completely inactive. After 6 days of resting, all cells were fully rested, i.e., they did not produce any measurable amount of the cytokine (not shown). When challenged with LPS, cells primed with LPS showed either a tolerant or a trained response, depending on the donor. When primed with Au NPs, an opposite response to LPS was observed, i.e., cells that were tolerant when primed with LPS were trained if primed with Au NPs and *vice versa*. Notably, not only naïve cells but also primed cells (either with LPS or with Au NPs) could not be stimulated by Au NPs to produce TNF- $\alpha$ . Several important considerations arise from these observations. The first is that NPs, even when unable to directly activate monocytes, could induce a memory that modulates the cell reactivity

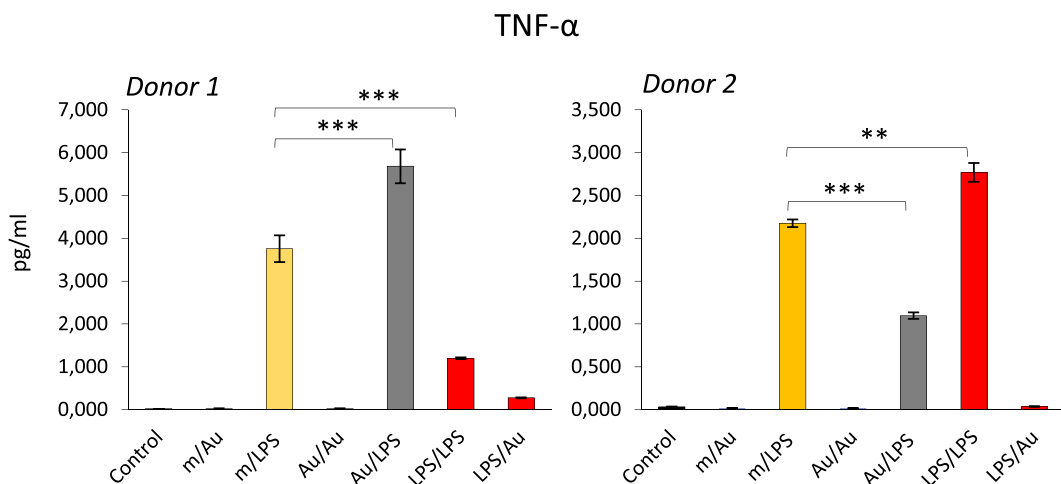


**FIGURE 2 |** Modulation of innate memory by Au nanoparticles (NPs). Freshly isolated human monocytes were exposed to medium alone (m) or containing bacterial LPS (LPS) (0.1 ng/ml) or Au NPs (Au) [40 nm, provided by Prof. Victor F. Puntes, ICN2, Barcelona; 10 ng/ml (4, 5)] for 24 h (priming). After elimination of the stimuli, cells were rested for 6 days, and then challenged for 24 h with either LPS (1 ng/ml) or Au NPs (10 ng/ml). Controls are cells primed with medium, LPS, or Au NPs and challenged with medium alone (m/m, LPS/m, Au/m; control) and were all negative. Production of TNF- $\alpha$  after challenge was measured by ELISA. Data from two different donors are shown. Priming with Au NPs increased the response to an LPS challenge compared to unprimed cells in donor 1, whereas a decrease was observed in donor 2. Conversely, LPS priming decreased the response to an LPS challenge in donor 1 and increased it in donor 2. The characteristics of the Au NPs used in this study are reported in Ref. (5). The contamination with LPS (endotoxin) was assessed by the limulus amebocyte lysate assay and found to be <0.005 EU/ $\mu$ g particles (41). Student's *t*-test was used to analyze statistically significant differences. The differences between controls and treatments are all statistically significant, but the *p*-value is not indicated to avoid overwriting the figure. We indicated only the differences discussed in the text. \*\**p* < 0.01, \*\*\**p* < 0.001.

to a subsequent challenge. The second consideration is that, as expected, each individual subject responds differently not only in quantitative terms (the amount of cytokine produced) but also in terms of type of response (enhanced reaction vs. decreased response). This behavior most likely depends on the past history of exposure of the donor, i.e., age, vaccinations, diseases, etc. Moreover, it is important to note that, since the same stimulus is able to prime for decreased or increased responses in different donors, the innate memory seems to be a complete reprogramming of the reactivity of cells rather than a stimulus-dependent inhibition or enhancement, a reprogramming that, again, most likely depends on the past “history” of the monocytes of each individual.

## CONCLUDING REMARKS AND FUTURE PERSPECTIVES

Although the study of the effect of NPs on human epigenome is still in its infancy, it is possible to speculate that NPs, like all other foreign agents that come in contact with the innate immune system, have the potential of modulating the innate memory in monocytes and macrophages through epigenetic changes. Plants and animals, including human beings, live in an environment that constantly expose them to challenges, including an enormous variety of microorganisms and other parasites, in addition to chemical compounds, pollutants, NPs, and many others. All the agents that confront the innate immune cells can prime them, so that these cells are more ready to mount an adequate protective response upon subsequent challenges. This is a general protective mechanism that aims at maintaining a good protective response

while avoiding, in particular in situation of frequent exposures, excessive damage to the body (as in the case of endotoxin tolerance). Examining the effects of engineered NPs in this context is of great importance. We have seen that innocuous NPs such as Au NPs can induce memory and change the response of monocytes to bacterial compounds (represented by LPS). This means that NPs are in fact behaving like microbial agents in terms of ability to induce innate memory and consequent reprogramming of innate reactivity. The effect of NPs on innate memory, as in the case of microbial compounds, depends both on the physicochemical nature of the NP and on the history of previous exposure of the subject. Thus, NP safety and efficacy studies would need to consider a personalized approach, because we expect each subject to respond differently both from others and in different periods of his/her life. From this perspective, it is exciting that the hypothesis that the manipulation of innate memory with NPs may become an effective immunomodulatory therapeutic option in future approaches of precision medicine.

## AUTHOR CONTRIBUTIONS

PI wrote the article and drew the figures; DB critically revised it.

## FUNDING

This work was supported by the EU Commission FP7 project BioCog (GA 602461), the EU Commission H2020 project PANDORA (GA 671881), by the Italian MIUR projects InterOmics (flagship project) and Medintech (Cluster project).

## REFERENCES

1. Brodin P, Jovic V, Gao T, Bhattacharya S, Lopez Angel CJ, Furman D, et al. Variation in the human Immune system is largely driven by non-heritable influences. *Cell* (2015) 160:37–47. doi:10.1016/j.cell.2014.12.020
2. Arts RJW, Netea MG. Adaptive characteristics of innate immune responses in macrophages. *Microbiol Spectr* (2016) 4: MCHD-0023-2015. doi:10.1128/microbiolspec.MCHD-0023-2015
3. Fullerton JN, Gilroy DW. Resolution of inflammation: a new therapeutic frontier. *Nat Rev Drug Discov* (2016) 15:551–67. doi:10.1038/nrd.2016.39
4. Oostingh GJ, Casals E, Italiani P, Colognato R, Stritzinger R, Ponti J, et al. Problems and challenges in the development and validation of human cell-based assays to determine nanoparticle-induced immunomodulatory effects. *Part Fibre Toxicol* (2011) 8:8. doi:10.1186/1743-8977-8-8
5. Li Y, Italiani P, Casals E, Valkenborg D, Mertens I, Baggerman G, et al. Assessing the immunosafety of engineered nanoparticles with a novel in vitro model based on human primary monocytes. *ACS Appl Mater Interfaces* (2016) 8:28437–47. doi:10.1021/acsmami.6b06278
6. Li Y, Boraschi D. Endotoxin contamination: a key element in the interpretation of nanosafety studies. *Nanomedicine (Lond)* (2016) 11:269–87. doi:10.2217/nmm.15.196
7. Oberdörster G, Oberdörster E, Oberdörster J. Nanotoxicology: an emerging discipline evolving from studies of ultrafine particles. *Environ Health Perspect* (2005) 113:823–39. doi:10.1289/ehp.7339
8. Mytych J, Wnuk M. Nanoparticle technology as a double-edged sword: cytotoxic, genotoxic and epigenetic effects on living cells. *J Biomater Nanobiotechnol* (2013) 4:53–63. doi:10.4236/j.bjnb.2013.41008
9. Sierra MI, Valdés A, Fernández AF, Torrecillas R, Fraga MF. The effect of exposure to nanoparticles and nanomaterials on the mammalian epigenome. *Int J Nanomedicine* (2016) 11:6297–306. doi:10.2147/IJN.S120104
10. Yao Y, Costa M. Genetic and epigenetic effects of nanoparticles. *J Mol Genet Med* (2013) 7:86. doi:10.4172/1747-0862.1000086
11. Stoccoro A, Karlsson HL, Coppedè F, Migliore L. Epigenetic effects of nano-sized materials. *Toxicology* (2013) 313:3–14. doi:10.1016/j.tox.2012.12.002
12. Jack RS. Evolution of immunity and pathogens. *Results Probl Cell Differ* (2015) 57:1–20. doi:10.1007/978-3-319-20819-0\_1
13. Reimer-Michalski EM, Conrath U. Innate immune memory in plants. *Semin Immunol* (2016) 28:319–27. doi:10.1016/j.smim.2016.05.006
14. Milutinović B, Kurtz J. Immune memory in invertebrates. *Semin Immunol* (2016) 28:328–42. doi:10.1016/j.smim.2016.05.004
15. Rolle A, Brodin P. Immune adaption to environment influence: the case of NK cells and HCMV. *Trends Immunol* (2016) 37:233–43. doi:10.1016/j.it.2016.01.005
16. Kleinnijenhuis J, Quintin J, Preijers F, Joosten LA, Ifrim DC, Saeed S, et al. Bacille Calmette-Guerin induces NOD2-dependent nonspecific protection from reinfection via epigenetic reprogramming of monocytes. *Proc Natl Acad Sci U S A* (2012) 109:17537–42. doi:10.1073/pnas.1202870109
17. Dobrovolskaia MA, Vogel SN. Toll receptors, CD14, and macrophage activation and deactivation by LPS. *Microbes Infect* (2002) 4:903–14. doi:10.1016/S1286-4579(02)01613-1
18. Biswas SK, Lopez-Collazo E. Endotoxin tolerance: new mechanisms, molecules and clinical significance. *Trends Immunol* (2009) 30:475–87. doi:10.1016/j.it.2009.07.009
19. Medzhitov R, Schneider DS, Soares MP. Disease tolerance as a defence strategy. *Science* (2012) 335:936–41. doi:10.1126/science.1214935
20. Benn CS, Netea MG, Selin LK, Aaby P. A small jab – a big effect: nonspecific immunomodulation by vaccines. *Trends Immunol* (2013) 34:431–9. doi:10.1016/j.it.2013.04.004
21. Aaby P, Roth A, Ravn H, Napirna BM, Rodrigues A, Lisse IM, et al. Randomized trial of BCG vaccination at birth to low-birth-weight children: beneficial nonspecific effects in the neonatal period? *J Infect Dis* (2011) 204:245–52. doi:10.1093/infdis/jir240
22. Naeslund C. Expérience de vaccination par le BCG dans la province du Norrbotten (Suède). *Rev Tuberc* (1931) 12:617–36.
23. Bistoni F, Vecchiarelli A, Cenci E, Puccetti P, Marconi P, Cassone A. Evidence for macrophage-mediated protection against lethal *Candida albicans* infection. *Infect Immun* (1986) 51:668–74.
24. Quintin J, Saeed S, Martens JH, Giambarellous-Bourboulis EJ, Ifrim DC, Logie C, et al. *Candida albicans* infection affords protection against reinfection via functional reprogramming of monocytes. *Cell Host Microbe* (2012) 12:223–32. doi:10.1016/j.chom.2012.06.006
25. Foster SL, Hargreaves DC, Medzhitov R. Gene-specific control of inflammation by TLR-induced chromatin modifications. *Nature* (2007) 447:972–8. doi:10.1038/nature05836
26. Ostuni R, Piccolo V, Barozzi I, Polletti S, Termanini A, Bonifacio S, et al. Latent enhancers activated by stimulation in differentiated cells. *Cell* (2013) 152:157–71. doi:10.1016/j.cell.2012.12.018
27. Saeed S, Quintin J, Kerstens HH, Rao NA, Aghajanireshah A, Matarese F, et al. Epigenetic programming of monocyte-to-macrophage differentiation and trained innate immunity. *Science* (2014) 345:1251086. doi:10.1126/science.1251086
28. Netea MG, Joosten LAB, Lat E, Mills KH, Natoli G, Stunnenberg HG, et al. Trained immunity: a program of innate immune memory in health and disease. *Science* (2016) 352:427–36. doi:10.1126/science.aaf1098
29. Italiani P, Boraschi D. Engineered nanoparticles and the immune system: interaction and consequences. In: Esser C, editor. *Environmental Influences on the Immune System*. New York: Springer (2016). p. 205–26
30. Gong C, Tao G, Yang L, Liu J, Liu Q, Zuang Z. SiO(2) nanoparticles induce global genomic hypomethylation in HaCaT cells. *Biochem Biophys Res Commun* (2010) 397:397–400. doi:10.1016/j.bbrc.2010.05.076
31. Brown TA, Lee JW, Holian A, Porter V, Fredriksen H, Kim M, et al. Alterations in DNA methylation corresponding with lung inflammation and as a biomarker for disease development after MWCNT exposure. *Nanotoxicology* (2016) 10:453–61. doi:10.3109/17435390.2015.1078852
32. Choi AO, Brown SE, Szyf M, Maysinger D. Quantum dot-induced epigenetic and genotoxic changes in human breast cancer cells. *J Mol Med* (2008) 86:291–302. doi:10.1007/s00109-007-0274-2
33. Qian Y, Zhang J, Hu Q, Xu M, Chen Y, Hu G, et al. Silver nanoparticle-induced hemoglobin decrease involves alteration of histone 3 methylation status. *Biomaterials* (2015) 70:12–22. doi:10.1016/j.biomaterials.2015.08.015
34. Halappanavar S, Jackson P, Williams A, Jensen KA, Hougaard KS, Vogel U, et al. Pulmonary response to surface-coated nanotitanium dioxide particles includes induction of acute phase response genes, inflammatory cascades, and changes in microRNAs: a toxicogenomic study. *Environ Mol Mutagen* (2011) 52:425–39. doi:10.1002/em.20639
35. Nagano T, Higashisaka K, Kunieda A, Iwahara Y, Tanaka K, Nagano K, et al. Liver-specific microRNAs as biomarkers of nanomaterial-induced liver damage. *Nanotechnology* (2013) 24:405102. doi:10.1088/0957-4484/24/40/405102
36. Ng CT, Dheen ST, Yip WCG, Ong CN, Bay BH, Lanry Yung LY. The induction of epigenetic regulation of PROS1 gene in lung fibroblasts by gold nanoparticles and implications for potential lung injury. *Biomaterials* (2011) 32:7609–15. doi:10.1016/j.biomaterials.2011.06.038
37. Eom HJ, Chatterjee N, Lee J, Choi J. Integrated mRNA and micro RNA profiling reveals epigenetic mechanism of differential sensitivity of Jurkat T cells to AgNPs and Ag ions. *Toxicol Lett* (2014) 229:311–8. doi:10.1016/j.toxlet.2014.05.019
38. Li S, Wang H, Qi Y, Tu J, Bai Y, Tian T, et al. Assessment of nanomaterial cytotoxicity with SOLiD sequencing-based microRNA expression profiling. *Biomaterials* (2011) 32:7609–15. doi:10.1016/j.biomaterials.2011.08.033
39. Lu X, Miousse IR, Pirela SV, Melnyk S, Koturbash I, Demokritou P. Short-term exposure to engineered nanomaterials affects cellular epigenome. *Nanotoxicology* (2016) 10:140–50. doi:10.3109/17435390.2015.1025115
40. Connolly J, Byrne SJ, Gun'ko YK, Rakovich YP, Donegan JE, Davies A, et al. CdTe nanoparticles display tropism to core histones and histone-rich cell organelles. *Small* (2008) 4:2006–15. doi:10.1002/smll.200800088
41. Li Y, Italiani P, Casals E, Tran N, Puntes VF, Boraschi D. Optimising the use of commercial LAL assays for the analysis of endotoxin contamination in metal colloids and metal oxide nanoparticles. *Nanotoxicology* (2015) 9:462–73. doi:10.3109/17435390.2014.948090

**Conflict of Interest Statement:** The authors have no financial or non-financial competing interests with the content of the article.

Copyright © 2017 Italiani and Boraschi. This is an open-access article distributed under the terms of the Creative Commons Attribution License (CC BY). The use, distribution or reproduction in other forums is permitted, provided the original author(s) or licensor are credited and that the original publication in this journal is cited, in accordance with accepted academic practice. No use, distribution or reproduction is permitted which does not comply with these terms.

# Advantages of publishing in Frontiers



## OPEN ACCESS

Articles are free to read,  
for greatest visibility



## COLLABORATIVE PEER-REVIEW

Designed to be rigorous  
– yet also collaborative,  
fair and constructive



## FAST PUBLICATION

Average 85 days from  
submission to publication  
(across all journals)



## COPYRIGHT TO AUTHORS

No limit to article  
distribution and re-use



## TRANSPARENT

Editors and reviewers  
acknowledged by name  
on published articles



## SUPPORT

By our Swiss-based  
editorial team



## IMPACT METRICS

Advanced metrics  
track your article's impact



## GLOBAL SPREAD

5'100'000+ monthly  
article views  
and downloads



## LOOP RESEARCH NETWORK

Our network  
increases readership  
for your article

## Frontiers

EPFL Innovation Park, Building I • 1015 Lausanne • Switzerland  
Tel +41 21 510 17 00 • Fax +41 21 510 17 01 • info@frontiersin.org  
[www.frontiersin.org](http://www.frontiersin.org)

## Find us on

